Bioinorganic Chemistry

NATO ASI Series

Advanced Science Institutes Series

A Series presenting the results of activities sponsored by the NATO Science Committee, which aims at the dissemination of advanced scientific and technological knowledge, with a view to strengthening links between scientific communities.

The Series is published by an international board of publishers in conjunction with the NATO Scientific Affairs Division

A Life Sciences	Plenum Publishing Corporation
B Physics	London and New York
C Mathematical and Physical Sciences	Kluwer Academic Publishers
D Behavioural and Social Sciences	Dordrecht, Boston and London
E Applied Sciences	
F Computer and Systems Sciences	Springer-Verlag
G Ecological Sciences	Berlin, Heidelberg, New York, London,
H Cell Biology	Paris and Tokyo
I Global Environmental Change	

PARTNERSHIP SUB-SERIES

1. Disarmament Technologies	Kluwer Academic Publishers
2. Environment	Springer-Verlag
3. High Technology	Kluwer Academic Publishers
4. Science and Technology Policy	Kluwer Academic Publishers
5. Computer Networking	Kluwer Academic Publishers

The Partnership Sub-Series incorporates activities undertaken in collaboration with NATO's Cooperation Partners, the countries of the CIS and Central and Eastern Europe, in Priority Areas of concern to those countries.

NATO-PCO-DATA BASE

The electronic index to the NATO ASI Series provides full bibliographical references (with keywords and/or abstracts) to more than 30000 contributions from international scientists published in all sections of the NATO ASI Series.
Access to the NATO-PCO-DATA BASE is possible in two ways:

– via online FILE 128 (NATO-PCO-DATA BASE) hosted by ESRIN,
Via Galileo Galilei, I-00044 Frascati, Italy.

– via CD-ROM "NATO-PCO-DATA BASE" with user-friendly retrieval software in English, French and German (© WTV GmbH and DATAWARE Technologies Inc. 1989).

The CD-ROM can be ordered through any member of the Board of Publishers or through NATO-PCO, Overijse, Belgium.

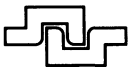

Series C: Mathematical and Physical Sciences – Vol. 459

Bioinorganic Chemistry

An Inorganic Perspective of Life

edited by

Dimitris P. Kessissoglou
Department of General and Inorganic Chemistry,
Aristotle University of Thessaloniki,
Thessaloniki, Greece

Springer-Science+Business Media, B.V.

Proceedings of the NATO Advanced Study Institute on
Bioinorganic Chemistry. An Inorganic Perspective of Life
Rhodes Island, Greece
June 5–17, 1994

A C.I.P. Catalogue record for this book is available from the Library of Congress.

ISBN 978-94-010-4113-3 ISBN 978-94-011-0255-1 (eBook)
DOI 10.1007/978-94-011-0255-1

Printed on acid-free paper

TABLE OF CONTENTS

Modeling Active Sites

PREFACE

During the last decade significant attention has been focused on the role of metal atoms in biology, giving rise to a very active research field of Bioinorganic Chemistry. Many crucial questions arising from the interference of metal ions in our life still remain unanswered. Even though very important structures of metalloenzymes as *MoFeco* of *nitrogenase*, *copper* or *manganese superoxide dismutase* or *plastocyanin* are known, the synthetic routes of modelling these centers are of great interest. Besides, other metalloenzymes, like the manganese center of *Oxygen Evolving Complex(OEC)* of *PSII*, are still in the centre of structural and spectroscopic in-depth examination. The drug-metal interaction and the metal ions antagonism are also an essential area of investigation. The understanding of the chemistry of metal ions in biological systems will be most beneficial to the scientific community because it will make possible the attack on certain difficult problems. Such problems may include biomineralization and the future production of advanced materials by micro-organisms. The NATO ASI, on which this book is based, was organised to promote interactions across these fields, to expose young researchers at an early stage of their careers to the several conceptual frameworks that currently contribute to the area.

Therefore, in June, 1994, about ninety scientists gathered at the Olympic Palace, on the Ixia coast near the City of Rhodes, Rhodes Island of Aegean Sea, Greece, for a two-week Advanced Study Institute dedicated to the theme of Bioinorganic Chemistry. This volume contains most of the invited lectures presented at the NATO ASI on "Bioinorganic Chemistry: An Inorganic Perspective of Life". It was decided not to 'referee' the submitted manuscripts, and therefor the entire responsibility of the content of the lectures rests with the authors.

It was my pleasure to act as the Director of the NATO ASI and I am most grateful to my esteemed colleagues on the Organising committee, Prof. Dimitri Coucouvanis, University of Michigan, USA, Prof. Mercouri Kanatzidis, Michigan State University USA, Dr. Bernard Meunier, CNRS, Toulouse, FRANCE and Prof. Athanassios Coutsolelos, University of Crete, GREECE and the invited lecturers for their enthusiastic support and valuable advice on various matters relating to the ASI. My special heartfelt thanks go to the students without whose interest and participation the ASI would not have been possible.

I sincerely thank Dr. L.V. da Cunha, Director, NATO Advanced Study Institute Programme and his Staff, who helped me throughout the various Stages of the ASI.

Of course the ASI would not have been possible without the financial aid of NATO. We are also grateful for the very important financial support and technical assistance provided by the Greek Secretariat of Research and Technology, the Greek Ministry of Industry, the Greek National Tourist Organisation, the Municipality of Thessaloniki, the Municipality of City of Rhodes, the University of Thessaloniki, the University of Crete, the Center of Solid Fuels Technology & Applications(C.S.F.T.A.), DOW Hellas and Petrola Hellas.

The local arrangements were handled with the cheerful aid of Dr. Catherine Dendrinou-Samara, Ms. Dora Malamatari and Mr. Nasos Papadopoulos. I also express my thanks to Prof. Evangelos Bakalbassis, who has handled many manuscript for this book, reformatting most of the chapters, and skilfully catching slips of the authors' word processors. I cannot fully express my appreciation for the unfailing support and understanding given to me by my wife Mary and my sons Philip and John during my Directorship of the Advanced Study Institute.

Finally I would like to express my best thanks to Professor George Manoussakis for his presentation during the ASI dinner. It was an excellent historical review of the sciences developed in Ancient Aegean Sea, where the Rhodes Island is situated. I believe that the readers of this book will loose the roots of the scientific output of this meeting without having access to this presentation. So it would be a pleasure for me if this preface came along with the following speech of Prof. George Manoussakis.

Dimitris P. Kessissoglou

"Ladies and Gentlemen,

As you know we are in the south part of the Aegean Sea which was the cradle of a great civilisation 25 centuries ago. Several very well known philosophers were born and have developed their ideas in this area.

I will stop at those places which are more important to us as chemists. I will stop to the philosopher who tried to answer most successfully to the question "what is the world made of?". I will focus particularly on the Ionian and Atomic Philosophers.

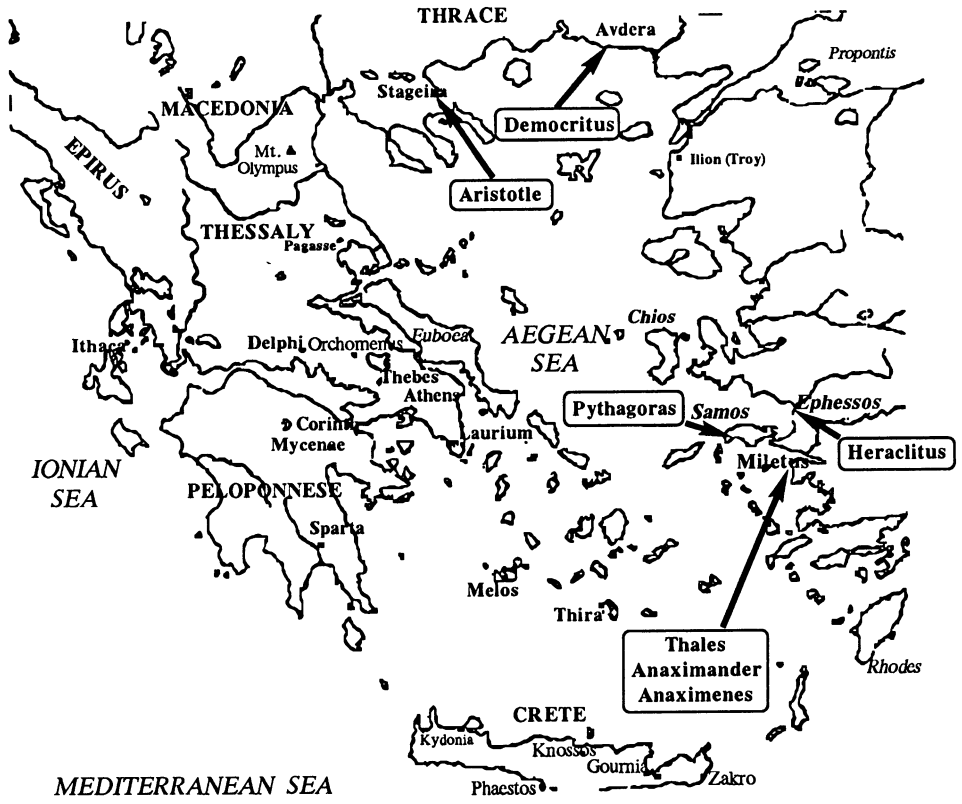

The Ionian or Milesian School is represented by Thales, Anaximander and Anaximanes, all three were from the same prosperous Ionian city of Mellitus. Their time overlapped in the early sixth century B.C.

***Thales** concluded that the world is made of water. The train of thoughts which led him to this conclusion is that water exhibits itself in three forms: solid, liquid and gaseous as ice water and steam. Water is everywhere and is a component almost of everything, alive or not. He also supported the idea that Earth rests on water.*

*The younger fellow-citizen of Thales, **Anaximander** supported the idea that the world is a result of the combination of opposite qualities, of which four were primary, hot and cold, wet and dry. The combination of wet and cold gives water, wet and hot air, hot and dry fire, cold and dry earth. According to Anaximander, and opposite to the Thales suggestion that earth rest on the water, earth rests on nothing and it does not fall because it is situated just on the center of the universe and has no reason for falling in one direction or another.*

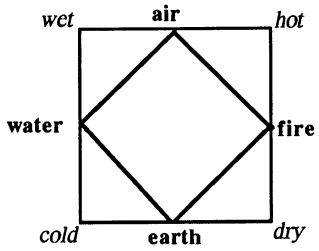

The ideas of Anaximander were adopted later by Aristotle from Stageira in his notation of the four basic "elements" of which the material world consisted of; they emerged from the opposition of and contained the properties proposed by Anaximander, i.e. the combination of wet and cold gives water, wet and hot air, hot and dry fire, cold and dry earth.

***Anaximenes**, another member of the Milesian School, claimed that the primary substance is air (aer, αήρ). According to him, the term air includes mist or fog. Air, surrounds the earth; moreover, air is possible to undergo μάνωση, i.e., condensation. The name manometer is after the word μάνωση. The result of the μάνωση(condensation) is mist, water and further, solid and stones. He also supported that "air is the stuff of life".*

***Pythagoras**, was born in island Samos (550 BC), his main interest was initially mathematical. He used to say that "Things were number and the harmony of sounds and the movement or stars is a matter of mathematical equations". Also he believed that "The number is in the center of matter and adjusts its properties". We know today that the atomic number, the number of protons in atomic nucleus, adjusts the chemical properties of th elements.*

The Pythagorean ideas of a peaceful and harmonic world, were rejected by Heraclitus, another famous Ionian philosopher.

***Heraclitus** (576-480), from Ephessos of Asia Minor, believed that war is the father of all and there is attraction between opposites. His primary substance was fire. According to him everything comes from fire and ends to fire. He said that "fire consists of tiny particles" which he named "ψήγματα" The "fire" of Heraclitus may be regarded as corresponding to energy and in an analogous manner "ψήγματα" to the quanta of energy.*

All these ideas of the Ionian philosophers may sound today as simply-minded, but we have to remember that until their time the theories about the creation of the universe were based entirely on purely magical or theological explanations and the forces of nature were attributed to the actions of the anthropomorphic gods, e.g. Zeus (cloud-gatherer, thunder-striker) and Poseidon (mover of earth, ship-wrecker).

The atomic philosopher ***Democritus,*** *from Avdera of Thrace (460 BC), believed that the smallest particles of matter and therefore of substances are atoms.*

The characteristics of atoms[*] *are the following:*

-solid,
-hard,
-indestructible,
-unsplitable,
-too small to be perceived by senses
-clashing and recoiling in endless motion and
-substantial identical.

Atoms differ in size and shape only as the difference between the letters A and N. The combination in different ways of these letters (atoms) gives the isomers compounds AN or NA. So Democritus had, in a way, predicted the phenomenon of isomerization. Democritus with his Atomic Theory tried to explain many properties of matter.

Hard-soft. *Hard things are made of atoms packed closely together, so the absence of the possibility of compression offers resistance to the touch. Soft things are made of atoms wider apart. They contain more empty space and so are capable of compression thus offering less resistance to the touch.*

Taste. *Sweet things are made of smooth atoms. Bitter taste is caused by sharp atoms which make minute excoriation on the tongue.*

Colour. *The various positions of the atoms on the surface of objects causes the light, which falls upon them, to throw back or reflect in different ways. These differences we perceive as different colours.*

Volatility. *The volatile substances consist of particularly small, fine and round atoms moving quickly because of their smallness and roundness.*

Smell. *Atoms of a certain size and shape, being in the surface of substance, detach from the surface and as they drift through the air to the nose produce the sense of smell.*

We believe today that the atoms of a certain size and shape, being in the surface of a substance, detach from the surface and as they drift through the air to the nose, fill the receptors of the ends of certain nerves stimulate them and produce the sense of smell."

[*] The word atoms comes from the word άτομο which means indivisible. The letter α- preceding greek words has a steretic value corresponding generally to modern *un-* and the verb τέμνω means to split.

LIST OF CONTRIBUTORS

STEPHEN J. LIPPARD
Department of Chemistry Massachusetts Institute of Technology Cambridge, Massachusetts 02139, USA; Tel.:001-(617)-2531892; FAX:001-(617)-2588150 El.Mail: LIPPARD@LIPPARD.MIT.EDU

KENNETH N. RAYMOND
Department of Chemistry University of California, Berkeley, CA 94720, USA; Tel:001-(510)-6427219; FAX:001-(510)-4865283, El.Mail: RAYMOND@GARNET. BERKELEY.EDU

JOHN T. GROVES
Department of Chemistry, Princeton University, Princeton, New Jersey 08544, USA; Tel: 001-(609)-2583900; FAX: 001-(609)-2586746

A.G.SYKES
Department of Chemistry, University of Newcastle, Newcastle upon Tyne, NE1 7RU, UK; Tel: 0044-(91)-222-6700; FAX:0044-91-222-6929

JOAN SELVERSTONE VALENTINE
Department of Chemistry and Biochemistry,University of California, Los Angeles, California 90024, U.S.A.; Te.:001-(310)-825-9835; FAX: 001-(310)-206-7197

IVANO BERTINI
Department of Chemistry - University of Florence Via Gino Capponi 7, 50121 Florence, ITALY Tel.0039-(55)-2757549;FAX: 0039-(55)-2757555 El.Mail; BERTINI@IFICHIM

IRÉNE MORGENSTERN-BADARAU
Laboratoire de Chimie bioorganique et bioinorganiquem Institut de Chimie Molèculaire d'Orsay, Université PARIS-SUD-XI, 91405-Orsay, France; Tel.: (00331)69417440; FAX:(00331)69417281

N. HADJILIADIS
Laboratory of Inorganic and General Chemistry, Department of Chemistry, University of Ioannina, Ioannina 45-110, GREECE; FAX: 0030-(651)-44112; El.Mail: NHADJIL@GRIOANUN. BITNET

EINAR SLETTEN
Department of Chemistry, University of Bergen, N-5007 Bergen, NORWAY; Tel; 0047-(55)-213352;FAX:0047-(55)-329058; El.Mail: EINAR@MVII.KJ. UIB.NO

HELMUT SIGEL
University of Basel, Institute of Inorganic Chemistry, Spitalstrasse 51, CH-4056 Basel, SWITZERLAND; Tel. 0041-61-322-1557, FAX: 0041-61-322-1554 El.Mail:SIGEL@URZ.UNIBAS.CH

BERNHART LIPPERT
Department of Chemistry, University of Dortmund, D-44221 Dortmund, Germany; Tel:0049-(231)-7553840; FAX:0049-231-755-3771; El.Mail: UCH026@UNIDORZ. HRZ.UNI-DORTMUND.DE

T. THEOPHANIDES
National Technical University of Athens, Chemical Engineering Department, Radiation Chemistry and Biospectroscopy, Zografou Campus, Zografou 15780, Athens, Greece; Tel:0030-(1)-8014979

N. KATSAROS
NCSR "Demokritos" Institute of Physical Chemistry, 153 10 Aghia Paraskevi Attikis, Greece; Tel. 0030-(1)-6513111; FAX: 0030-1-6511767

H. HOLDEN THORP
Department of Chemistry, University of North Carolina at Chapel Hill, Chapel Hill, North Carolina 27599-3290; Tel. (001)(919)962-0276, FAX:(001)(919)(962-2388); THORP @GIBBS.OIT.UNC.EDU

DIMITRI COUCOUVANIS
Department of Chemistry, The University of Michigan, Ann Arbor Michigan, 48109-1055 USA; Tel: 001-(313)-764-7339, FAX:001-(313)-747-4865; El.Mail: Dimitri COUCOUVANIS@UM.CC. UMICH.EDU

VINCENT L. PECORARO
Department of Chemistry, University of Michigan, Ann Arbor, MI 48109-1055 USA; Tel:001-(313)-7631519;FAX: 001-(313)-7474865; El.Mail: USERLB4D@UM.CC. UMICH.EDU

B. MEUNIER
Directeur de Recherche, Centre National de la Recharche Scientifique, Laboratoire de Chimie de Coordination du CNRS, 205 route de Narbonne, 31077 Toulouse cedex, FRANCE. Tel.: 0033-(61)333100; FAX: 0033(61)553003

MERCOURI G. KANATZIDIS
Department of Chemistry, Michigan State University, East Lansing MI 48824, USA; Tel: 001-(517)-3534511; FAX: 001-(517)-3531793; El.Mail:KANATZIDIS@MSUCEM. BITNET

A. G. COUTSOLELOS
University of Crete, Department of Chemistry, Laboratory of Bioinorganic Coordination Chemistry University of Crete, P.O.Box 1470, 71409-Heraklion, Crete, GREECE; Tel.0030-(81)-235-014; FAX:0030-(81)-238-468; El.Mail: THANOS @GREARN

BERNT KREBS
Institute of Inorganic Chemistry, University of Münster, Wilhelm-Klemm Strasse 8, D-48149 Münster, GERMANY; Tel.:0049-(251)-833131; FAX:0049-(251)-838366; El.Mail: KREBS VNWZ01@UNI-MUENSTER-DE

DIMITRIS P. KESSISSOGLOU
Department of General & Inorganic Chemistry, Aristotle University of Thessaloniki, Thessaloniki 54006, Greece; Tel:30-(31)-997723, FAX:30-(31)-997723 El.Mail:CCAZ13 @GRTHEUN1.BITNET

LIST OF PARTICIPANTS

ASI STUDENTS

Denmark

Ms. Inge Margrethe JENSEN,
Graduate Student, Dept. of Chemistry, University of Odense, DK-5230 Odense M, DENMARK; Tel.: (66)158600; FAX: (66)158428; El.Mail.: IMJ@OUKEMI.OU.DK

France

Dr. Genevieve BLONDIN,
Lab. de Chimie Inorganique, URA CNRS 420, Universite de Paris-Sud, 91405 Orsay Cedex FRANCE; Tel.: (0033)(1)69417436; FAX: (0033)(1)69855536; El.Mail.:LCI@CTH.U-PSUD.FR

Dr. Anne ROBERT,
Laboratoire de Chimie de Coordination, C.N.R.S., 205 route de Narbonne, 31077 Toulouse cedex,FRANCE; Tel.: (0033)61333146, FAX:(0033) (61553003)

Germany

Ms. Martina HUBER,
Graduate Student. Institute fur Physikalishe Chemie, Technische, Hochschule Darmstadt, Petersen Str. 20, 64287 Darmstadt, GERMANY; Tel.:(0061)(51)163698; FAX:(0061)(51)164298

Dr. Roland KRAMER,
Anorganish-Chemisches Institute, University of Munster, Wilhelm-Klemm-Strasse 8, D-48149 Munster, GERMANY; Te.:(0061)(251)833158; FAX:(0061)(251)838366; E-mail: Kramerr@VNWZ01.UNI-MUENSTER.DE

Mr. Andre SCHREIBER,
Graduate Student, Universitat Dortmund Fachbereich Chemie Anorganische Chemie, Otto-Hahn-Strasse 6, D-4600 Dortmund 50, GERMANY;Tel:0049-(231)-7553840; FAX:0049-231-755-3771; El.Mail: UCH026@UNIDORZ.HRZ.UNI-DORTMUND.DE

Greece

Prof. Evagelos BAKALBASIS,
Aristotle University of Thessaloniki, Dept. of Gen. & Inorg. Chemistry, 54006 Thessaloniki, GREECE; Tel. (30)(31)997815; FAX:(30)(31)997738

Prof. Christos BOLOS,
Aristotle University of Thessaloniki, Dept. of Gen. & Inorg. Chemistry, 54006 Thessaloniki, GREECE; Tel. (30)(31)997705; FAX:(30)(31)997738

Mr. Vagelis DAVORAS,
Graduate Student, University of Crete, Dept. of Chemistry, 71409 Iraklion Crete, GREECE; Tel.:(30)(81)238468; FAX:(30)(81)210951

Ms. Dimitra DAPHNOMILI
Graduate Student, Thenon 45, Heraklion, Crete, GREECE; Tel.:(30)(81)310352; FAX:(30)(81)210951

Dr. Catherine DENDRINOU-SAMARA
Aristotle University of Thessaloniki, Dept. of Gen. & Inorg. Chemistry, 54006 Thessaloniki, Greece; Tel. (30)(31)997738; FAX:(30)(31)997738

Ms. Marietta HADJILIADI-LAMERA,
Hospital "The hope" Trichonidos & Dimitsanis, Ampelokipoi, Athens, GREECE; Tel. 0030-(1)-6444529

Prof. Dimitris KYRIAKIDIS
Aristotle University of Thessaloniki, Dept. of Org. Chemistry & Biochemistry, 54006 Thessaloniki, GREECE; Tel. (30)(31)997771; FAX:(30)(31)997738

Ms. Dora MALAMATARI
Graduate Student, Aristotle University of Thessaloniki, Dept. of Gen. & Inorg. Chemistry, 54006 Thessaloniki, GREECE; Tel. (30)(31)997739; FAX:(30)(31)997723

Prof. George MANOUSSAKIS,
Aristotle University of Thessaloniki, Dept. of Gen. & Inorg. Chemistry, 54006 Thessaloniki, GREECE; Tel. (30)(31)997781; FAX:(30)(31)997738

Mr. Athanassios PAPADOPOULOS,
Graduate Student, Aristotle University of Thessaloniki, Dept. of Gen. & Inorg. Chemistry, 54006 Thessaloniki, GREECE; Tel. (30)(31)997739; FAX:(30)(31)997738

Prof. Raphael RAPTIS,
University of Crete, Dept. of Chemistry, 71409 Iraklion Crete, GREECE; Tel.:0030-(81)-238400; FAX:(30)(81)210951

Dr. Cathernine RAPTOPOULOU,
Institute of Material Science, N.R.C. Demokritos,Ag. Paraskevi, 15310 Athens, GREECE, Tel.:(30)(31)6513111; FAX:(30)(31)6519430

Mr. Spyros SERVES,
Graduate Student, Department of Chemistry, University of Patras, GREECE; home address: Stravonos 20, 25100 Aigion, GREECE; Tel. 0030-(61)27031

Mr. George SPYROULIAS,
Graduate Student, University of Crete, Dept. of Chemistry, 71409 Iraklion Crete, GREECE; Tel.:(30)(81)238468; FAX:(30)(81)210951; El.Mail.: Spyroulias@talos.cc.uch.gr

Dr. Hariklia STASSINOPOULOU,
Institute Of Biology, NRCPS "Demokritos", 15310 Agia Paraskevi Attikis, GREECE; Tel. 0030-(1)-6513111; FAX: 0030-1-6511767

Dr. Leandros TZAVELLAS
Aristotle University of Thessaloniki, Dept. of Gen. & Inorg. Chemistry, 54006 Thessaloniki, Greece; Tel. (30)(31)997786; FAX:(30)(31)997738

Italy

Dr. Giuseppe Enrico ARENA,
Dipartimento di Chimica Inorganica, Analytica E. Struttura Molecolare Universita delgi Studi di Messina Salita sperone 31, Villagio S. Agata 98166 Messina, ITALY; Tel.: 0039-90-392901; FAX:0039-90-393756

Mr. Gianantonio BATTISTUZZI,
Graduate Student. Dept. of Chemistry, University of Modena, via Campi, 183, 41100 Modena, ITALY;Tel.: (0039)(59)378421, FAX:(0039)(59) 373543

Dr. Giulia GRASSO,
Dipartimento di scienze Chimiche, Universita di Catania V.le A.Doria 8, 95125 Catania, ITALY; Tel: 0039-95-337678; FAX: 0039-95-580138

Dr. Graziella VECCHIO,
Dipartimento di scienze Chimiche, Universita di Catania V.le A.Doria 8, 95125 Catania, ITALY; Tel: 0039-95-337678; FAX: 0039-95-580138

The Netherlands

Prof. Jan REEDIJK
Leiden Institute of Chemistry, Gorlaeus Laboratories, Leiden University, P.O.Box 95502, 2300 RA Leiden, THE NETHERLANDS; Tel. 0031-71-274459; FAX; 0031-71-274451; El.Mail: Reedijk@rulgca.Leidenuniv.nl

Norway

Prof. Jorum AMBJORG-SLETTEN,
Department of Chemistry, University of Bergen, N-5007 Bergen, NORWAY; Tel; 0047-(55)-213352;FAX:0047-(55)-329058; El.Mail: EINAR@MVII.KJ. UIB.NO

Prof. Willy NERDAL,
Dept. of Chemistry, University of BergenAllegt. 41, N5007 Bergen, NORWAY; Tel.:(47)55213353; FAX: (47)55329058; El.Mail.: Willy.nerdal@kj.uib.no

Ms. Signe STEINKOPF,
Graduate Student, Kjemisk Institutt, Universitetet i Bergen, Allegt. 41, N-5007 Bergen, NORWAY; Tel.:(55)213359; FAX: (55)3229058; El. Mail: Signe.Steinkopf@kj.uib.no

Portugal

Ms. Maria Marise Simoes de ALMEIDA,
faculdade de Ciencias de Lisboa, Dept. of Chemistry, Campo Grande, 1700 Lisboa, PORTUGAL

Ms. Maria Jose FEIO,
Graduate Student, Centro de Tecnologia Quimica e Biologica(CTQB), Rua da Quinta Grande, 6, Apartado 127, 2780 OEIRAS PORTUGAL; (00351)(01)4426146; FAX: (00351)(01)4428766

Prof. Antonio V. XAVIER,
Centro de Tecnologia Quimica e Biologica(CTQB) Rua da Quinta Grande, 6, Apartado 127, 2780 OEIRAS PORTUGAL, Tel:00351-(1)-4426146; FAX:00351-1-4428766

Spain

Prof. Juan Antonio Rodriguez RENUNCIO,
J.A.R., Professor, Facultad de Quimica Universidad Complutense, E-28040 Madrid, SPAIN; Tel.: (341)3944120; FAX: (341)3944135; El.Mail: mendu@quim.ucm.es

Turkey

Ms. Meray BASTURKMEN,
Ortadogu Teknik Universitesi Fen Edebiyat Fakultesi Kimya Bolumu 06531 Ankara, TURKEY; TEL.: 0090-312-2101000; FAX: 0090-312-2101280

Ms Guller GOZEL,
Graduate Student, Middle East Technical University
Chemistry Dept. 06531 Ankara, TURKEY; Tel: (0090)(4210)10003210; El.Mail.: A09984@TR METIS

Prof. Renat ZHDANOV,
Orta Dogu Teknik Universitesi, Middle East Technical University, Dept. of Biology, 06531 Ankara, Turkey; Tel: (0090)(4)2101000/3105; FAX:(0090)(4)2101289; El.Mail.: Zhdanov@vm.cc.metu.edu.tr

United Kingdom

Mr. Nadeem AURANGZEB,
Graduate Student, Dept. of Chemistry, UMIST, Sackvill Street, Manchester, M601QD, United Kingdom;Tel. (0044)(61)2363311; FAX:(0044)(61)2287040

Dr. Elisabeth A. MARSEGLIA,
Univeristy of Cambridge, Dept. of Physics, Cavendish Laboratory, Madingley Road, Cambridge, CB3OHE, U.K.. Tel.: 0044-(223)- 337277; FAX: 0044-(223)-353397; El.Mail.: EM10@PHY.CAM.AC.UK

Mr. Michael WATKINSON,
Graduate Student, 80 Philip Street, Eccles, Manchester M30 OWE, United Kingdom; Tel.: (0044)(61)7894048

U.S.A.

Prof. Peggy CARVER,
College of Pharmacy, University of Michigan, 428 Church St., Ann Arbor, MI 48109-1065, USA; Tel:(001)(313)764-9384, FAX:(001)(313)763-2022: El.Mail: USERGDEL@ UMICH.UM.EDU

Mr. Kostas DEMADIS,
Draduate Student,Dept. of Chemistry, University of Michigan, Ann Arbor, Michigan 48109-1055, USA; Tel: 001-(313)-764-7339, FAX:001-(313)-747-4865; El.Mail: Dimitri Coucouvanis@um.cc. umich.edu

Mr. Andrew FEIG,
Graduate Student,Department of Chemistry, Room 18-290, Massachusetts Institute of Technology, Cambridge, MA 02139,USA Tel.:001-(617)253-1892; FAX:001-(617)-258-8150 El.Mail: LIPPARD@LIPPARD.MIT.EDU

Mr. Brian GIBNEY,
Graduate Student,Dept. of Chemistry, University of Michigan, Ann Arbor, Michigan 48109-1055, USA, Tel:001-(313)-7631519;FAX: 001-(313)-747-4865; El.Mail: USERLB4D@UM.CC.UMICH.EDU

Prof. Martin L. KIRK,
Dept. of Chemistry, University of New Mexico
Albuquerque, New Mexico 87131-1096, USA; Tel:(001)(505)277-5992; FAX:(001)(505)277-2609; El.Mail. mkirk@hydra.unm.edu

Dr. Helen PAPPA,
Dept. of Molecular Biology & Biochemistry, University of California, Irvine, California 92717, USA;FAX:(001)(714)856-8540; El..mail: poulos@uci.edu

Ms. Di QIU,
Graduate Student, Dept. of Chemistry, Princeton University, Princeton, NJ 08544, USA;Tel.:(001)(609)258-3908; FAX:(001)(609)258-6746; El.Mail:Qiu@Chemvax.Princeton.edu

Mr. M. SCOTT,
Graduate Student, Dept. of Chemistry, Harvard University, Cambridge, Massachusetts 02138, USA, FAX:(001)(617)496-9289, El.Mail.:HOLM@FEMOCO. HARVARD.EDU

Prof. Michael J. THERIEN,
Dept. Of Chemistry, University of Pennsylvania, Philadelphia, PA 19104-6323, USA

Mr. Jason TELFORD,
Graduate Student, Dept. of Chemistry, University of California, Berkeley, Berkeley, CA 94720,USA; Tel. (001)(510)642-5589; FAX(001)(510)486-5283; El.Mail.: KNRGROUP@GARNET.BERKELEY.EDU

Austria

Mr. Erwin HERLINGER
Graduate Student, Dept. of Inorg Chemistry, Technical University Estreidemarkt 9/153, A-1060 Vienna, AUSTRIA; Tel.: (0043)(1)58801-4623; FAX: (0043)(1)5874835

Bulgaria

Prof. Stoyan SHISHKOV,
Faculty of Biology, University of Sofia, 8 Dragan Tzankov Str, 1421 Sofia, BULGARIA; Tel.: 63301(293); FAX: (00359)(2)463589

Czech Republic

Dr. Jana ZACHOVA,
Institute of Physics of the Charles University, Ke Karlovu 5, CZ-121 16 Prague 2, CZECH REPUBLIC; Tel.:(0042)(2)292544; FAX: (0042)(2)296764; El.Mail.: Florian@CSPGUK11

Hungary

Mr. Jozsef KAIZER,
Dept. of Organic Chemistry, University of Veszprem, 8201 Veszprem,
HUNGARY; Tel.: (0036)(88)422022; FAX: (0036)(88)426016; El.Mail.: H2107SPE@HUELLA.BITNET

Mr. Istuan LIPPAI,
Graduate Student, H-8201 Veszprem, P.O.Box 158 HUNGARY, Tel.: (0036)(88)422022; FAX: (0036)(88)426016; El.Mail: H2107SPE@ HUELLA.BITNET

Prof. Laszlo NAGY,
A. Jozsef University, Dept of Inorg. & Analytical Chemistry, 6720 Szeged, Dom ter 7, Hungary, Tel. (0036)(62)311622; FAX: (0036)(62)312505

Poland

Dr. Justyn OCHOCKI,
Medical University of Lodz, Dept. of Pharmacy Pl 90-151 Lodz, Muszynskkiego 1, Poland; Tel.: (0048)(42)785570; FAX: (0048)(42) 322347; El. Mail; PHARMACY@PLUNLO51.BITNET

Mr. Krzysztof SLOWINSKI,
Graduate Student, Dept. of Chemistry, University of Warsaw, 02093 Warsaw, Pasteura 1, Poland; Tel.: (0048)(22)220211; FAX: (0048)(22)225996; El.Mail.: SLOWIK@CHEM.UW.EDU.PL

Rumania

Prof. Claudia SUPURAN,
University of Bucharest, Dept of Chemistry Bd. Carul 1(Republicia) 13, Bucharest, Roumania; Tel: (0040)(1)6163449 FAX: (0040)(1)6130296

Russian Federation

Dr. Lyudmila OREKHOVA,
Institute of Biorganic Chem. ul. Miklukho-Maklaya 16/10, Moscow 117871, RUSSIA. FAX: 007095(00359)3357103; El. Mail.: ORL@BCH.SIOBO.MSK.SU

Ukraine

Dr. Igor FRITSKY,
Institute of Chemistry, University of Wroclaw, 50383, Wroclaw, Poland; Tel: (0048)(71)204313; FAX: (0048)(71)222348; El.Mail.: Arka@ Plwruw11.Bitnet

Metalloenzymes

METHANE MONOOXYGENASE

STEPHEN J. LIPPARD
Department of Chemistry
Massachusetts Institute of Technology
Cambridge, Massachusetts 02139 USA

ABSTRACT. The X-ray crystal structure determination of the resting state of the hydroxylase enzyme of methane monooxygenase from the organism *Methylococcus capsulatus* (Bath) reveals a dinuclear iron center bridged by a hydroxide ion, an acetate ligand from the crystallization buffer, and the carboxylate group of a glutamate residue. The terminal positions of this diiron(III) unit are occupied by three additional glutamates, two histidines, and a water molecule. Residues adjacent to this bioinorganic active site form a hydrophobic pocket for methane binding. The reaction cycle of the enzyme begins with reduction to the diiron(II) state in the presence of substrate and two other protein components, a reductase and a small molecular weight coupling protein, also known as protein B. Reaction of the reduced hydroxylase with dioxygen proceeds through several intermediates prior to hydroxylation of alkane to yield the product alcohol, water, and the resting diiron(III) form of the enzyme. The rate of the reaction, regioselectivity of hydroxylation, and ability to detect the intermediates spectroscopically depends upon the presence of the coupling protein. Freeze-quench Mössbauer and low temperature stopped-flow optical spectroscopic experiments have identified two key intermediates in the reaction cycle, designated L and Q, the properties of which are discussed. Experiments with radical clock substrate probes revealed no evidence for substrate radical intermediates. Mechanisms are proposed to account for these observations.

1. Introduction

Methane monooxygenase is an enzymatic system comprised of three proteins, a hydroxylase (H), a reductase (R), and a coupling protein, also known as protein B, which selectively and efficiently converts methane to methanol in the methanotrophic bacterium *Methylococcus capsulatus* (Bath).[1-3] A diagrammatic representation of these components and the overall reaction catalyzed by this system are presented in Fig. 1. The catalytic unit responsible for hydroxylation is a non-heme dinuclear iron center housed in the a subunit of the hydroxylase. It resembles carboxylate-bridged diiron centers in other dioxygen-utilizing proteins such as hemerythrin and

D.P. Kessissoglou (ed.), Bioinorganic Chemistry, 1-12

ribonucleotide reductase.[4-6] Our laboratory has engaged in a broad program to investigate both the MMO system and model compounds for the dinuclear center in the hydroxylase enzyme.

$$CH_4 + NADH + H^+ + O_2 \longrightarrow CH_3OH + NAD^+ + H_2O$$

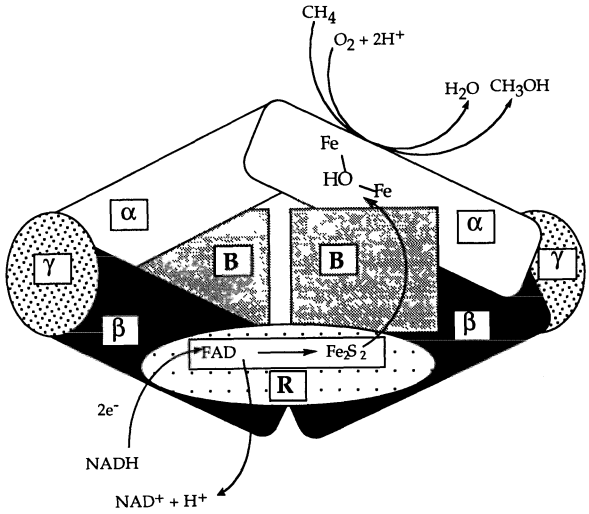

Hydroxylase (H)	Reductase (R)	Coupling protein (B)
251 kDa	38.6 kDa	15.5 kDa

Fig. 1. Proteins of the methane monooxygenase system from *M. capsulatus* (Bath). The relative positions of the α, β, and γ subunits of the hydroxylase protein are as determined in the X-ray crystal structure. The binding sites of the B and R proteins on H are unknown. Reprinted with permission from ref. 7. Copyright 1994, American Chemical Society.

Our goals have been to determine the structure of the hydroxylase enzyme and its interactions with the other components; to measure and understand the physical properties of the dinuclear iron center in relation to the structure; to elucidate the chemical properties of the non-heme diiron center of the hydroxylase, including its redox states, substrate binding, and dioxygen reaction chemistry; and to unravel a detailed mechanism for the hydroxylation of alkanes, particularly methane. The present article describes recent progress made in determining the structure of the hydroxylase by single crystal X-ray diffraction and the use of spectroscopic and chemical probes to gain insight into the reaction cycle. A more general, in-depth summary, including a broad discussion of the reactions of diiron(II) model systems and proteins with dioxygen, may be found elsewhere.[7]

2. X-ray Structure of MMO Hydroxylase from *M. capsulatus* (Bath)

The X-ray crystal structure of the MMO hydroxylase in its resting, diiron(III) state has recently been determined to 2.2 Å resolution.[8] The results provide detailed information about the coordination environment of the dinuclear iron center; interactions among the a, b, and g subunits of this component; possible pathways by which methane might access and methanol might depart from the active site; the hydrophobic pocket for methane binding; and possible positions on the iron atoms where dioxygen and species derived therefrom might coordinate. Fig. 2 presents the overall structure of the hydroxylase, which has a non-crystallographically required twofold symmetry axis running through it vertically, in the plane of the page.

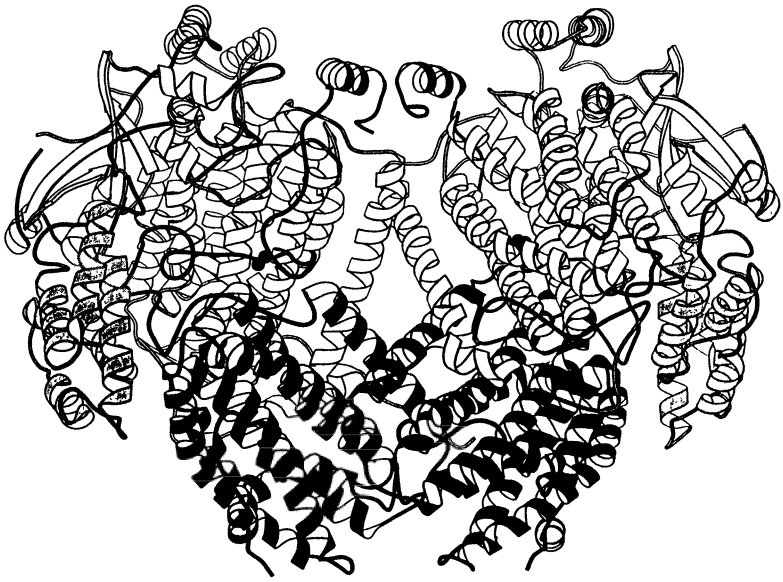

Fig. 2. MOLSCRIPT (Kraulis, P. *J. Appl. Crystallogr.* **1991**, *24*, 946) representation of the structure of the hydroxylase protein of *Methylococcus capsulatus* (Bath). Reprinted with permission from ref. 7. Copyright 1994, American Chemical Society.

The a subunit is rendered in white, the b subunit in black, and the g subunit in gray. As can be seen, the protein fold is almost entirely comprised of a helices, with only a small region of b structure in the a subunits. The fold of the b subunit is remarkably similar to that of a large domain in the a subunit, and the relative positioning of a and b subunits strongly resembles the interaction of the two halves of the protein dimer in the R2 protein of ribonucleotide reductase.[8-10] A region in the center of the hydroxylase, a large canyon lined by several long helices of the a subunit, has been identified as a putative binding site for the other two components, the coupling

protein and the reductase. The dinuclear iron centers are located in the two a subunits at a distance of 45 Å from one another.

As indicated in Fig. 3, the dinuclear centers are bridged by an exogenous hydroxide ion, a semi-bridging glutamate (Glu 144), and a bidentate acetate from the crystallization buffer. The terminal coordination positions are occupied by histidine side chains, one on each iron, three monodentate glutamates, and a water molecule, which is hydrogen bonded to Glu 114 and Glu 243. The solvent-derived exogenous ligands, the bridging hydroxide ion and terminal water molecule, had been previously identified for the *M. capsulatus* (Bath) hydroxylase from proton ENDOR studies on the paramagnetic, mixed-valent form of the protein.[11] The Fe◊◊◊Fe distance of 3.4 Å and overall coordination geometry are in accord with expectations based on extensive EXAFS and other spectroscopic properties of the protein.[12] The inventory of charges results in a neutral active site, consistent with its ability to bind methane and other non-polar hydrocarbon substrates.

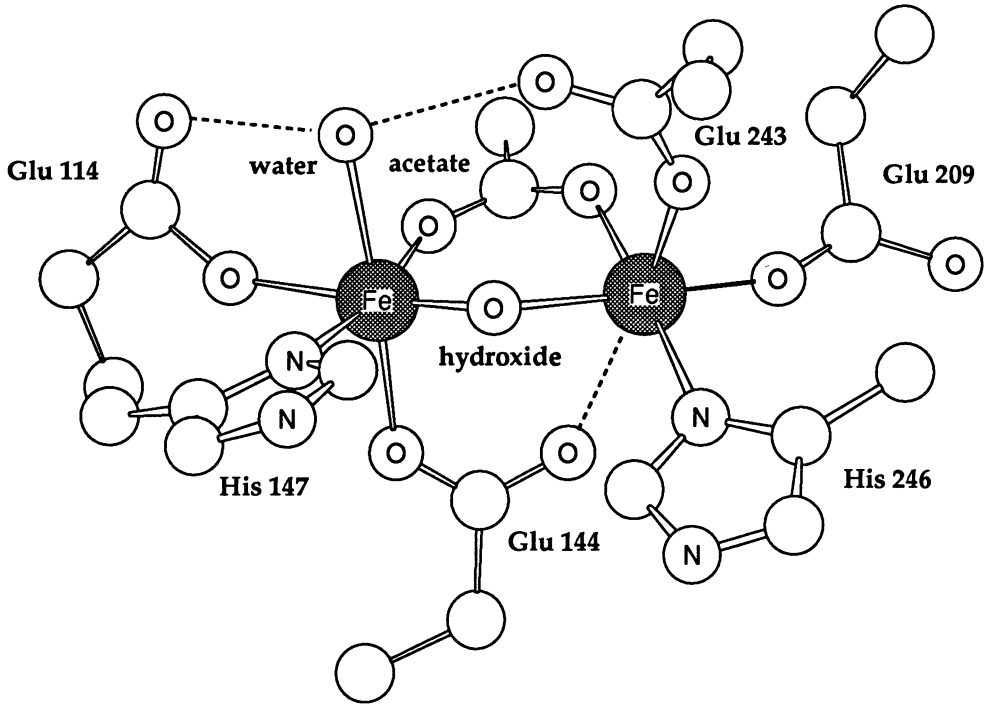

Fig. 3. Structure of the dinuclear iron center at the active site of the hydroxylase protein of *Methylococcus capsulatus* (Bath). Reprinted with permission from ref. 7. Copyright 1994, American Chemical Society.

The positions of the exogenous acetate and water ligands in the oxidized hydroxylase crystal structure suggest possible sites of binding and activation of dioxygen, substrate, and product during the catalytic cycle. For example, the site occupied by

the acetate may delineate where the product methoxide might bind prior to its release from the enzyme. These ligands protrude into an adjacenthydrophobic cavity lined by side chains from non-polar amino acids glycine, leucine, isoleucine, and phenylalanine. A stereo view of this cavity is presented in Fig. 4. Also present in the cavity is the side chain of Thr 213, which resides at a p-turn in a very long helix. A similar feature is found in cytochromes P-450, as discussed elsewhere.[8] Examination of the a subunit revealed a series of hydrophobic pockets extending 30 Å from the surface through the protein and leading to the active site cavity, thus delineating a possible pathway by which methane and other substrates might access the catalytic iron center. Entrance to the hydrophobic cavity of the active site at the end of this pathway could occur by slight rotation of Phe 188 and/or Thr 213 side chains (Fig. 4). Also present in the active site cavity is a cysteine residue, Cys 151, the sulfur atom of which was the binding site for mercury in one of the derivatives used to solve the crystal structure of the hydroxylase.[8] This amino acid occupies virtually the same position with respect to the dinuclear iron center as does the tyrosine residue in the structurally related R2 protein of ribonucleotide reductase,[10,13] a tyrosine that gets oxidized to a functionally important tyrosyl radical.

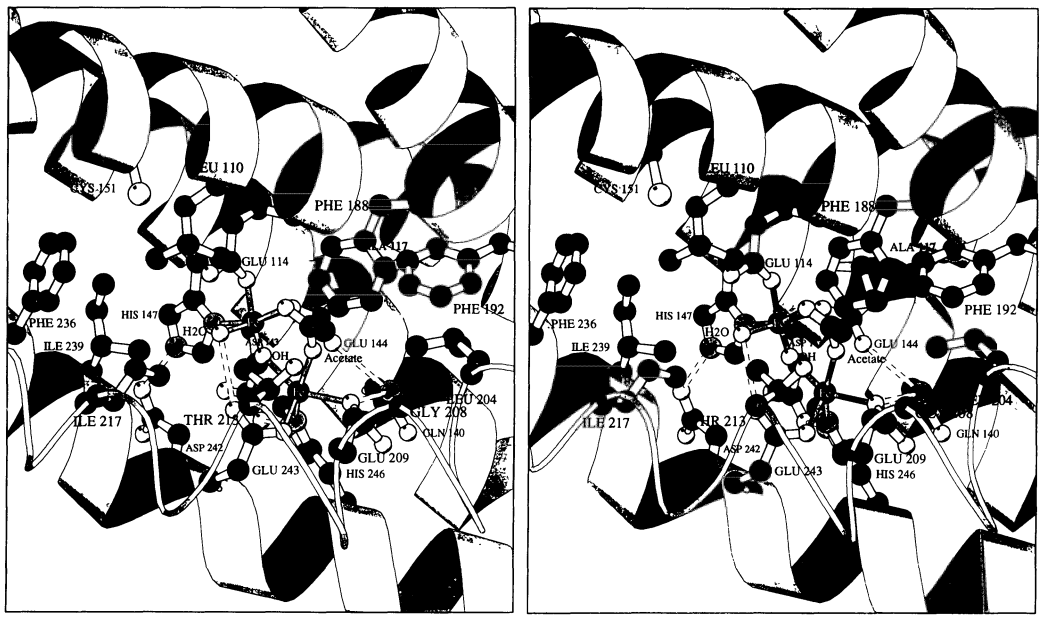

Fig. 4. MOLSCRIPT (Kraulis, P. *J. Appl. Crystallogr.* **1991**, *24*, 946) stereo representation of the active site structure of the hydroxylase protein of *Methylococcus capsulatus* (Bath). Reprinted with permission from ref. 8. Copyright 1993, Macmillan Magazines Limited.

The occurrence of Cys 151 in the MMO hydroxylase at this location suggests the

possible involvement of a cysteinyl radical in the catalytic mechanism of the enzyme. We shall return to this point later.

3. Spectroscopic Evidence for Intermediates in the Reaction Cycle of the MMO Hydroxylase from *M. capsulatus* (Bath)

The reaction cycle of methane monooxygenase has frequently been written by analogy to the more extensively studied cytochrome P-450 enzyme systems.[14-17] Several variations on this chemistry are possible for a non-heme dinuclear center, as presented in considerable detail elsewhere.[7,18] Low-temperature stopped-flow spectroscopic and freeze quench Mössbauer studies of the reaction of dioxygen with the reduced hydroxylase from *M. trichosporium* OB3b have revealed the presence of intermediates in the reaction cycle of the MMO hydroxylase,[19,20] and parallel studies on the enzyme from *M. capsulatus* (Bath) have augmented this work.[21] In the latter experiments, the hydroxylase enzyme was first reduced in an anaerobic chamber with dithionite and a suitable electron-transfer mediator. After

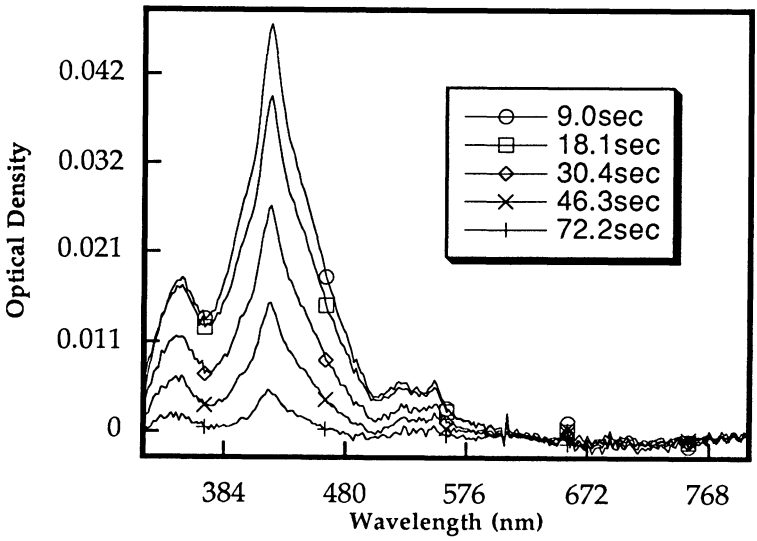

Fig. 5. Spectoscopic evidence for intermediates in the reaction of H_{red} from *M. capsulatus* (Bath) with dioxygen in the presence of 2 equiv of protein B.

removal of the mediator by dialysis, the reduced hydroxylase (H_{red}) was loaded into one syringe of a rapid stopped flow mixing apparatus while a solution of buffer, saturated with dioxygen, was loaded into the other syringe. The solutions and apparatus were then cooled to 4 °C and rapidly mixed. Optical spectroscopic studies revealed the buildup and decay of three absorption bands at 350, 420, and520 nm, as illustrated in Fig. 5. Kinetic analysis of the exponential buildup and decay of these

signals at single wavelength showed that they could be fit well with two rate constants, one for the formation ($k_f = 0.31 \pm 0.02\ s^{-1}$) and one for the decay ($k_d = 0.065 \pm 0.017\ s^{-1}$). The data and fits are shown in Fig. 6. Addition of methane abolished the signal, suggesting that it might be on the reaction pathway for hydroxylation, and failure to add the coupling protein substantially diminished the rate at which the color of the intermediate developed.

Freeze-quench Mössbauer experiments significantly extended insights offered by these optical studies.[19,21] In these investigations, the solution was

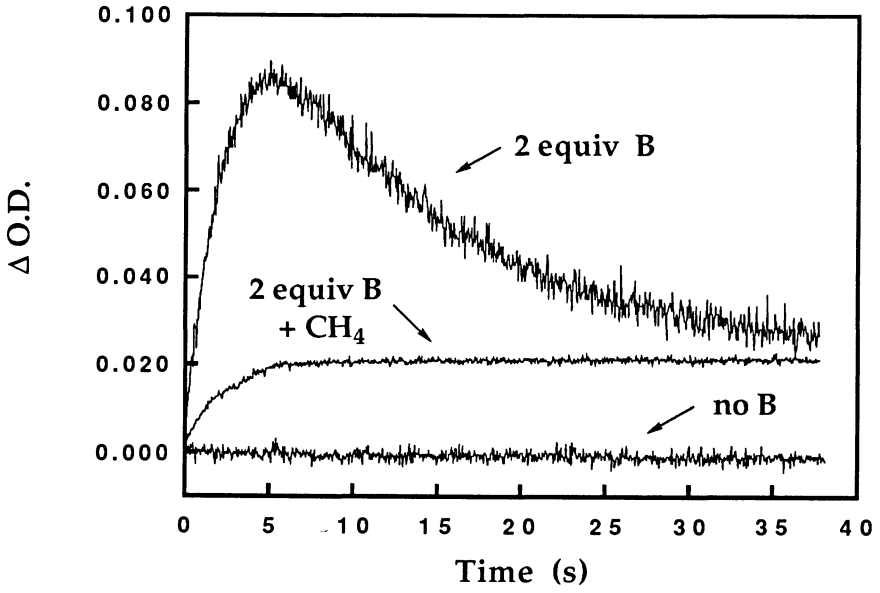

Fig. 6. Buildup and decay of the 420 nm absorption observed in the reaction of H_{red} with dioxygen at 4 °C. As can be seen, this intermediate required protein B to be observed and is rapidly quenched in the presence of substrate.

passed through the mixing chamber at 4 °C and then allowed to flow through a tube of variable length which opened into a nozzle that sprayed the mixed solution into liquid isopentane at - 140 °C. The frozen mixture was then packaged into a Mössbauer sample cell and its spectrum recorded. By changing the length of the tube, the time after mixing was varied from 0.025 - 60 sec. These experiments required growing the organism on ^{57}Fe-enriched iron and long exposure times (days) in the Mössbauer spectrometer in order to achieve the appropriate signal-to-noise

ratio. The reward was worth the effort, however, since the growth and decay of two spectroscopic intermediates, designated L and Q, were detected by this methodology.[21] The properties of these species are given in Table 1, from which it can be seen that Q corresponds to the transient detected by optical spectroscopy, whereas L is kinetically competent to be the precursor of Q in the reaction cycle. Analogous results were obtained for the *M. trichosporium* hydroxylase,[19] with the following exceptions: L was not observed; Q was assigned as having two equivalent rather than slightly different iron atoms; and the kinetic constants differed slightly from those found for the *M. capsulatus* enzyme.

From the spectroscopic properties of L and Q in Table 1 it is not possible to make a definitive assignment of the structures of the two species based on any known inorganic model complexes.[4,5,22] The most reasonable supposition

Table 1. Summary of Mössbauer Parameters (mm/sec) and Kinetic Rate Constants (sec^{-1}) for Intermediates in the Reaction of Reduced MMO Hydroxylase with Dioxygen

Organism	d, L	DE_Q, L	d, Q	DE_Q, Q	k_f, L	k_d, L	k_f, Q	k_d, Q
M. capsulatus	0.66	1.51	0.14	0.55	~25	~0.2	~0.4	
			0.21	0.68			0.31[a]	0.065[a]
M. trichosporium	ND[b]	ND[b]	0.17	0.53			1.0[a]	0.05[a]

[a]From optical spectroscopic studies.
[b]Not detected.

at this time is that L corresponds to a (m-peroxo)diiron(III) species and that Q is either a pair of low-spin ferric ions coordinated to an oxyl anion (see below) or a pair of high valent, iron(IV) centers. It should be emphasized that these formulations are very preliminary and that it is not even certain whether the O-O bond is cleaved in either L or Q. The synthesis and X-ray structural characterization of inorganic analogues of these interesting intermediates may be necessary in order to assign their structures definitively. A reaction cycle illustrating the catalytic mechanism of the MMO hydroxylase is depicted in Fig. 7.

4. Radical Clock Substrate Probe Studies and a Working Hypothesis for the Catalytic Mechanism of MMO

Since the spectroscopic intermediate Q decays more rapidly in the presence of substrates such as nitrobenzene,[20,23] it is reasonable to speculate that Q is the

species responsible for the hydroxylation step. Although experiments on the *M. trichosporium* system with chiral ethane (CH_3CHDT) have been interpreted as evidence for substrate radical intermediates,[24] attempts to use radical clock

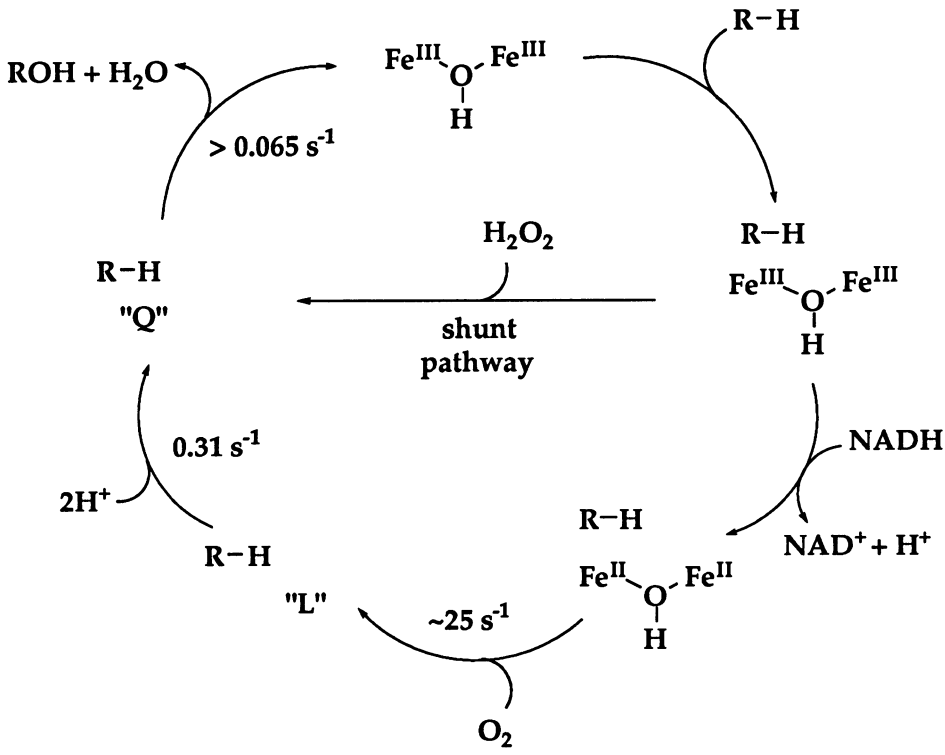

Fig. 7. Hypothetical reaction cycle for the MMO hydroxylase. Intermediates labeled L and Q were detected by stopped-flow spectroscopic and freeze-quench Mössbauer experiments. Rate constants depicted are for the *M. capsulatus* (Bath) enzyme.

substrate probes to measure the rate of rebound from a putative radical species failed in the case of MMO hydroxylase from *M. capsulatus* (Bath) to provide any evidence for the existence of radicals.[18,23] In particular, when *trans*-phenylmethylcyclopropane and methylcubane were assayed with the reconstituted MMO hydroxylase, coupling protein, and reductase system, the only products observed were *trans*-phenylcyclopropylmethanol and the cubyl methanol, respectively. Since these substrate probes would ring-open to afford other product alcohols if a carbinyl radical were generated during the course of the reaction, it was concluded that either radicals do not form in the reaction or that, if they do form, their rate of rebound to form the product alcohol would have to be in excess of 4×10^{13} s^{-1}. In the case of MMO from *M. trichosporium*, a small amount of ring-opened radical was observed with the substrate probe *trans*-phenylmethylcyclopropane,[18] leading to an estimate for the

rebound rate that is consistent with that cited above for the chiral ethane study with enzyme from this organism.[25]

These and other results lead to the following working hypothesis for the reaction mechanism.[7] The diiron(III) center in the resting state of the hydroxylase is reduced by two electrons in the presence of substrate and the other components, the reductase and coupling protein (Fig. 7). This reduction may lead to a rearrangement in the coordination spheres of the iron atoms, perhaps by extrusion of solvent-derived ligands and/or carboxylate shifts.[26] In such reactions, one or more of the glutamates might alter its binding mode, for example, from bridging to terminal or from monodentate to bidendate. Such chemistry may be required in order to make sites available on one or both of the iron(II) centers for binding of dioxygen. Detailed temperature-dependent kinetic studies of sterically hindered diiron(II) model complexes indicate the need for an open coordination site for binding of dioxygen in the reaction to form peroxide-bridged diiron(III) complexes.[27] As in these model complexes, it is likely that dioxygen coordinates to the iron center in H_{red} and is reduced by an inner sphere pathway to form a bridged diiron(III) peroxide intermediate, possibly compound L (Fig. 7).

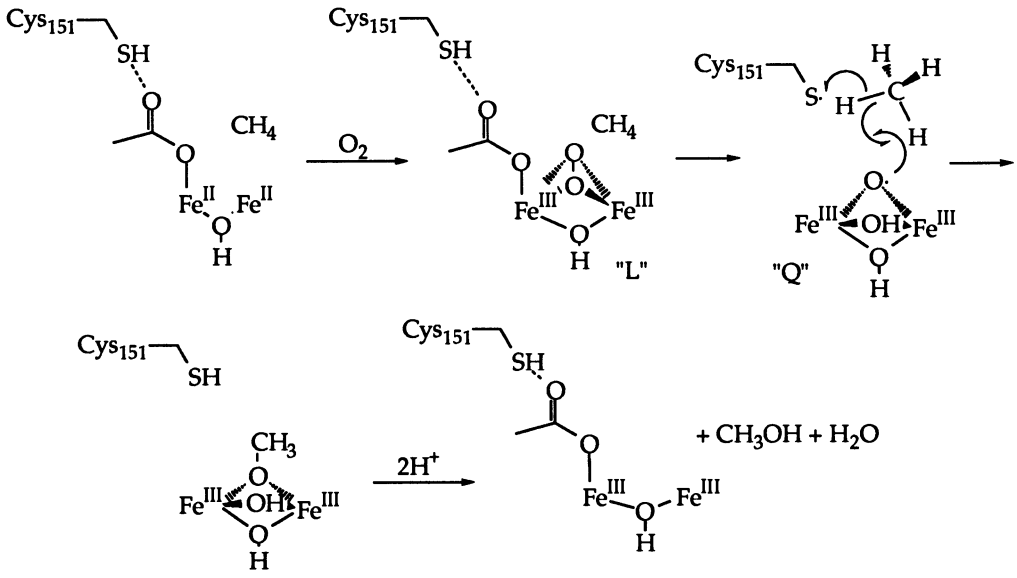

Fig. 8. Hypothetical mechanism for the reductive activation of dioxygen by Cys 151 in MMO hydroxylase.

As shown in Fig. 8, we propose as a working hypothesis that this species is further activated reductively by electron transfer from the nearby cysteine residue, Cys 151 in the active site (Fig. 4). This reductive activation step cleaves the O-O bond to form a metallooxyl residue, formally an analogue of the hydroxyl radical, a seven-electron $O^{\cdot}\Diamond$ species (Fig. 8). This species may correspond to intermediate Q (Fig. 7), the

Mössbauer isomer shift of which would be accounted for if the two iron(III) centers were low spin. The metallooxyl and cysteinyl radical formed in this step could then attack the C-H bond in a concerted fashion, restoring the cysteine residue and leading to coordinated methoxide which is protonated and departs as methanol. There is presently no definitive evidence to support or refute such a mechanism, further consequences and nuances of which are discussed elsewhere.[7]

5. Acknowledgments

This work was supported by a grant from the National Institute of General Medical Sciences. I am grateful to my co-workers, collaborators, and colleagues cited in the individual references for their inspired contributions to this research.

6. References

(1) Colby, J.; Stirling, D. I.; Dalton, H. *Biochem. J.* **1977**, *165*, 395.
(2) Patel, R. N.; Hou, C. T.; Laskin, A. I.; Felix, A. *Applied and Environmental Microbiology* **1982**, *44*, 1130.
(3) Fox, B. G.; Lipscomb, J. D. *Biochem. Biophys. Res. Comm.* **1988**, *154*, 165.
(4) Lippard, S. J. *Angew. Chem. Int. Ed. Engl.* **1988**, *27*, 344.
(5) Que, L., Jr.; True, A. E. *Prog. Inorg. Chem.* **1990**, *38*, 97.
(6) Vincent, J. B.; Olivier-Lilley, G. L.; Averill, B. A. *Chem. Rev.* **1990**, *90*, 1447.
(7) Feig, A. L.; Lippard, S. J. *Chem. Rev.* **1994**, *94*, 759.
(8) Rosenzweig, A. C.; Frederick, C. A.; Lippard, S. J.; Nordlund, P. *Nature* **1993**, *366*, 537.
(9) Nordlund, P.; Sjöberg, B.-M.; Eklund, H. *Nature* **1990**, *345*, 593.
(10) Nordlund, P.; Dalton, H.; Eklund, H. *FEBS Lett.* **1992**, *307*, 257.
(11) DeRose, V.; Liu, K. E.; Lippard, S. J.; Hoffman, B. *J. Am. Chem. Soc.* **1993**, *115*, 6440.
(12) DeWitt, J. G.; Bentsen, J. G.; Rosenzweig, A. C.; Hedman, B.; Green, J.; Pilkington, S.; Papaefthymiou, G. C.; Dalton, H.; Hodgson, K. O.; Lippard, S. J. *J. Am. Chem. Soc.* **1991**, *113*, 9219.
(13) Nordlund, P.; Eklund, H. *J. Mol. Biol.* **1993**, *231*, 123.
(14) *Cytochrome P-450: Structure, Mechanism, and Biochemistry*; Ortiz de Montellano, P. R., Ed.; Plenum Press: New York, 1986.
(15) Green, J.; Dalton, H. *J. Biol. Chem.* **1989**, *264*, 17698.
(16) Andersson, K. K.; Froland, W. A.; Lee, S.-K.; Lipscomb, J. D. *New J. Chem.* **1991**, *15*, 411.
(17) Wilkins, P.; Dalton, H.; Podmore, I. D.; Deighton, N.; Symons, M. C. R. *Eur. J. Biochem.* **1992**, *210*, 67.
(18) Liu, K. E.; Johnson, C. C.; Newcomb, M.; Lippard, S. J. *J. Am. Chem. Soc.* **1993**, *115*, 939.

(19) Lee, S.-K.; Fox, B. G.; Froland, W. A.; Lipscomb, J. D.; Münck, E. *J. Am. Chem. Soc.* **1993**, *115*, 6450.
(20) Lee, S.-K.; Nesheim, J. C.; Lipscomb, J. D. *J. Biol. Chem.* **1993**, *268*, 21569.
(21) Liu, K. E.; Wang, D.; Huynh, B. H.; Edmondson, D. E.; Salifoglou, A.; Lippard, S. J. **1994**, submitted for publication.
(22) Kurtz, D. M. *Chem. Rev.* **1990**, *90*, 585.
(23) Liu, K. E.; Lippard, S. J., unpublished results.
(24) Priestley, N. D.; Floss, H. G.; Froland, W. A.; Lipscomb, J. D.; Williams, P. G.; Morimoto, H. *J. Am. Chem. Soc.* **1992**, *114*, 7561.
(25) Newcomb, M. private communication.
(26) Rardin, R. L.; Tolman, W. B.; Lippard, S. J. *New. J. Chem.* **1991**, *15*, 417.
(27) Feig, A. L.; Lippard, S. J. *J. Am. Chem. Soc.* **1994**, in press.

THE COORDINATION CHEMISTRY OF IRON IN BIOLOGICAL TRANSPORT AND STORAGE; IRON REMOVAL *IN VIVO*

KENNETH N. RAYMOND and BARBARA L. BRYAN
Department of Chemistry
University of California
Berkeley, CA 94720

ABSTRACT. Serum transferrin is the iron transport agent of mammals. Its function and structure are increasingly well understood, particularly because of the relatively recent protein crystal structure information. Transferrin not only acts as a transport agent but also functions as an iron buffer, maintaining free ferric ion concentrations in the body at a very low but constant value. This role of transferrin, and our understanding of the mechanisms of iron binding and release by the protein, are important in four areas of medical science. First, iron storage and transport are critical to understanding the molecular basis of anemias. [Iron uptake by the gut involves the eventual complexation by transferrin.] Second, iron overload occurs in several disorders, the most common due to long-term transfusion therapy of ίβ-thalassemia (Cooley's anemia). [Iron is only regulated by uptake; there is no mechanism for spontaneous removal of iron.] Chelation therapy of iron overload has long used desferrioxamine B (Desferal®). There is a continuing search for new sequestering agents that would have improved properties, particularly oral activity. · One issue thus raised is the thermodynamic and kinetic ability of such sequestering agents to remove iron from transferrin. Third, the release of iron, the reductive generation of Fe^{2+}, and subsequent free radical generation from reaction with O_2 (Fenton chemistry) are now thought to be the major cause of tissue damage following myocardial infarction. The use of iron chelating agents may provide a way to block such damage by keeping free ferric ion at low levels - a function of transferrin in circulating serum that is disrupted by the heart attack. Finally, the fourth area of medical relevance for transferrin iron binding and release is related to bacterial infection. The role of iron in the pathogenicity of bacterial infections is now well established. Iron availability to the invading bacterium is known to be directly connected to the virulence of infections that cause infantile enteritis, leprosy, cholera, and tuberculosis, as major examples. Several siderophores of pathogenic microorganisms are capable of removing iron from serum transferrin. Hence the mechanism(s) by which iron is released from transferrin to such ligands is of medical, as well as general biochemical, significance.

Transferrin is a bilobal protein of molecular weight 78,000 that is apparently the result of the fusion of two units of an ancestral protein. Each of the two lobes contain one metal binding site that has a very high affinity for high-spin Fe^{3+}. Single crystal structures of rabbit diferric and human monoferric transferrins and lactoferrin establish that the iron binding sites of these closely related proteins are essentially identical, composed of a bidentate carbonate, 2 phenolate groups (tyrosine), 1 nitrogen (histidine) and a carboxylate oxygen (aspartate). The stable form of metal-free, apotransferrin has an "open" conformation in which the iron binding site is in an open cleft near the protein surface and is accessible to the surrounding solution. In contrast, the stable form of the iron complex has the cleft closed so that the metal binding site is buried under the surface of the protein, thus making the metal inaccessible to competing ligands. The kinetic behavior of iron removal

D.P. Kessissoglou (ed.), Bioinorganic Chemistry, 13-24

by several different types of ligands is examined with the view of new ligand design for ligands of use in human iron decorporation therapy.

1. Introduction

All plant and animal life (and essentially all microbial life) has an absolute requirement for iron. As shown in Table 1, even though iron is quite abundant on the surface of the planet, it frequently is a growth limiting nutrient. The versatility of iron, with respect to its remarkable changes in redox and reactivity behavior as a function of its ligand field environment, made it a maleable component of the chemical constituents of early evolution. For example, the redox potentials of iron-containing metalloenzymes range from -400 to +400 millivolts.

Table 1: The terrestial distribution and bioavailability of iron [1-3]

Approximately one-third Earth's mass; most abundant element by weight	
Fourth most abundant element in Earth's crust.	
Typical Distributions:	
Crustal rocks (weight %):	
igneous	5.6
shale	4.7
sandstone	1.0
limestone	0.4
Ocean (70% of Earth's surface):	
0.003 - 0.1 ppb, increasing with depth; limiting factor in plankton growth	
Rivers:	
0.07 - 7 ppm	
Bioavailability:	
K_{sp} $(Fe(OH)_3$ is approximately 10^{-39}	
In absence of chelating agents, pH 7, $[Fe^{3+}]$ is approximately 10^{-18} M	
Typical iron content of living cells : 10^{-5} to 10^{-8} M	

The effect of iron complexing agents as inhibitors of infection has been known since long before the modern understanding of microorganisms and their role in disease[4]. As Shakespeare has an aide say to the Earl of Gloucester (who has just had his eyes gouged out) "I'll fetch some flax, and whites of eggs/To apply to his bleeding face".[5] In mammals iron transport is carried out by serum transferrin. This is one in a family of closely related proteins that act as iron complexing agents *in vivo*.[6] Transferrin not only acts as a transport agent but also functions as an iron buffer, maintaining free ferric ion concentrations in our bodies at a very low but constant value. This role of transferrin, and our understanding of the mechanisms of iron binding and release by the protein, are important in four areas of medical science: First, iron storage and transport are critical to understanding the molecular basis of anemias. Iron uptake occurs in the upper intestine, although the details of the intervening steps between that transport and its appearance in serum transferrin are still being characterized.[7] Second, iron overload occurs in several disorders, the most common due to long-term transfusion therapy of β-thalassemia (Cooley's anemia). Since iron is only regulated by uptake, with no mechanism for spontaneous removal of iron, any long-term

increase in iron storage results in iron overload.[8] That this NATO workshop is in Greece is particularly significant, given the major health problem represented by β-thalassemia in this country. Patients with Cooley's anemia require long-term blood transfusions with the result of large increases in iron. Chelation therapy of iron overload has long used desferrioxamine B or Desferal® (Figure 1).

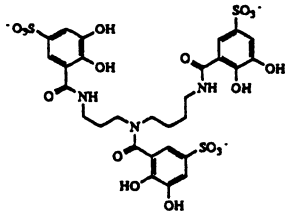

3,4-LICAMS

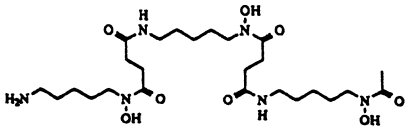

Desferrioxamine B

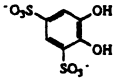

Tiron

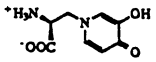

L-mimosine

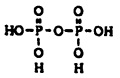

Pyrophosphate

Figure 1: Structures of typical iron chelators: the catecholates, 3,4-LICAMS and Tiron, a hydroxypyridinone, L-mimosine, and a hydroxamate, desferrioximine B (Desferal®). Pyrophosphate is not thermodynamically capable of removing iron from transferrin, but can serve as a mediator to increase the rate of iron removal by other chelators.

However there are a number of problems with this chelating agent and there has been a long-standing search for new sequestering agents that would have improved properties, particularly oral activity. One issue that is raised is the thermodynamic and kinetic ability of such sequestering agents to remove iron from transferrin. That will be a particular focus of this paper. A series of different kinds of ligands, and their kinetics of iron removal from transferrin, will be examined both to characterize the mechanism of iron release by this protein and to provide a fundamental design basis for new ligand syntheses.

The third area of medical science of relevance involves the release of iron, the reductive generation of Fe^{2+}, and subsequent free radical generation from reaction with O_2 (Fenton Chemistry). This is now thought to be the major cause of tissue damage following myocardial infarction. The use of iron chelating agents may provide a way to block such damage by keeping free ferric ion at low levels - a function of transferrin and circulating serum that is disrupted in the heart attack.[9] It

has been estimated that as much as 20% of the adult male population is at risk of oxidative cellular damage due to elevated serum iron levels.[10] The fourth area of medical relevance is related to bacterial infection. The role of iron in the pathogenicity of bacterial infections is now well established.[8] Iron availability to the invading bacterium is known to be directly connected to the virulence of infections that cause infantile enteritis, leprosy, cholera, and tuberculosis, as major examples. Several siderophores of pathogenic microorganisms are capable of removing iron from serum transferrin.

Although iron is an essential element for humans and required in large amounts (3 to 5 grams normally), it is also very toxic when in excess. The most common iron overload is due to regular blood-transfusions, particularly in the treatment of β-thalassemia. The toxicity of excess iron in the body can be ameliorated by administration of an iron chelating agent which is able to remove iron *in vivo* from transferrin, ferritin, and other iron stores. The current drug of choice for chelation therapy is the methane sulfonate salt of desferrioxamine B (Desferal®). While Desferal has been shown to increase iron excretion and to reduce liver iron in β-thalassemic patients, its drawbacks include a lack of oral activity and a short body retention time, which necessitates its administration by one of the cumbersome and expensive methods of slow subcutaneous or intravenous infusion. More serious is the lack of patient compliance that results from the inconvenience and discomfort of this therapy. For the last two decades considerable effort has been invested in developing a more effective iron removal agent; however, the treatment has remained essentially unchanged.

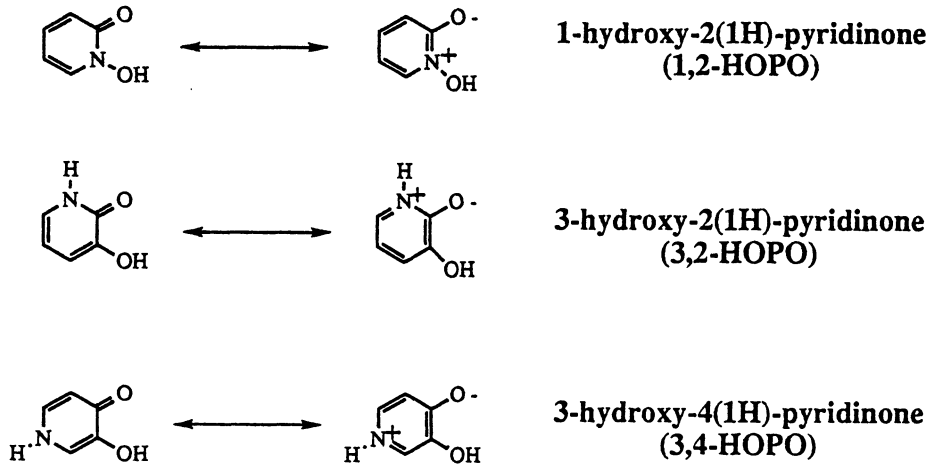

Figure 2: The simple chelating hydroxypyridinones and their abbreviations.

Many different approaches have been taken in the development of new iron sequestering agents of potential use as therapeutic agents. One approach is developing iron chelating agents based on hydroxypyridinones. Although not as common a functional group as either the hydroxamate or catecholate moieties, the hydroxypyridonate functional groups are found in siderophores. These compounds can be viewed as either an aromatic hydroxamic acid (for the 1,2 isomer) or as a catechol analogue (the hydroxypyridonate and catecholate anions are isoelectronic and isostructural). With varying positions of the nitrogen in the ring, there are three unsubstituted chelating hydroxypyridinones. Their abbreviations and structures are shown in Figure 2.

Transferrin constitutes 3.5% of human plasma proteins. It carries iron to and from storage sites in cells (where it is stored in ferritin). Normally only about 30% of the iron sites are occupied, so that the protein has a large buffering capacity to respond to iron addition. With infection or neoplasia, the empty binding sites can increase up to 90%. Because of its high binding, the standard reduction potential of transferrin is -0.5 volts vs. hydrogen electrode,[12] which blocks Fe^{2+} production and hence Fenton Chemistry.

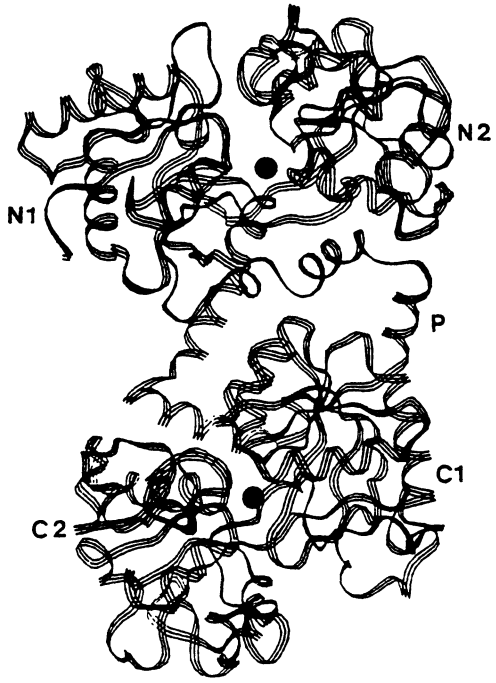

Figure 3: A ribbon diagram showing the characteristic folding of transferrins into N-terminal and C-terminal lobes, each with a type I and a type II domain. Iron atoms are shown as filled circles. The peptide connecting the lobes (P), is helical in lactoferrin, but irregular in serum transferrin. (Figure from reference 13, used with permission.)

A ribbon structure of diferric transferrin is shown in Figure 3.[13] The protein is composed of two domains which are essentially the same with regard to their iron coordination chemistry and general structure. Both iron binding sites contain one bidentate carbonate (which is hydrogen bonded within the pocket and whose binding to the protein is a prerequisite for iron complexation), two oxygens from tyrosines,

one oxygen from aspartate and one histidine nitrogen. Both the *N*-terminal and *C*-terminal lobes each contain two domains, which form a kind of clam shell structure. This structure can close where it is hinged so that the iron binding site is either open, and exposed to the solution environment,or closed and buried about 12 or 13 Å under the surface of the protein. This is shown in cartoon form in Figure 4.[14]:

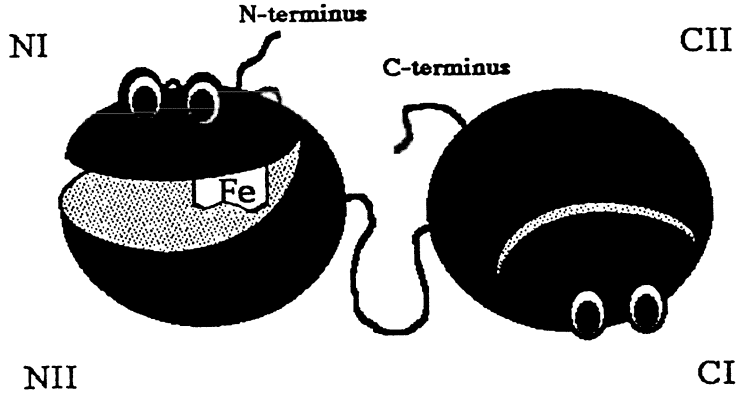

Figure 4: A cartoon representation of diferric transferrin. The iron-binding site in each lobe is located in the cleft between type I and type II domains; the two lobes of the protein are homologous, but not identical.

The iron-binding cleft at the N-terminal site is shown here still in the "open" conformation, while the iron at the C-terminal end is hidden in the "closed" conformation. In those crystal stuctures reported to date, however, all iron-containing sites are in the closed conformation. (Cartoon concept: H. J. Zuccola, reference 14)

This is particularly important in understanding and interpreting the kinetic results for the many different ligands that have been investigated with regard to the iron removal capability from transferrin.

Other proteins in the transferrin family also play defensive roles by securely sequestering free iron. Ovotransferrin, which constitutes 12% by weight of egg white solids, is an 80 kD protein belonging to this family. It is the major reason why eggs, which are laid in a very non-sterile environment, are not subject to bacterial infection and spoilage for a very long period of time. Egg white has a pH of 9.5, which is also where ovotransferrin best complexes ferric ion. Ovotransferrin shows antimicrobial activity, which is neutralized when the protein is saturated with iron.[15].

Similarly, milk constitutes an ideal culture medium and yet infants fed on mothers milk are known to be much less susceptible to gastric enteritis than those fed on prepared substitutes. Breast infections within nursing mothers are also relatively uncommon. Both of these phenomena are primarily due to lactoferrin, which comprises 20% of total protein in human milk (about 1 gram per liter) and up to seven times this amount in colostrum, the secretion first produced by nursing mothers. Unlike transferrin, which releases iron at pH 4, lactoferrin retains its iron binding capability at this acid pH. [This is quite important, since sepsis lowers pH.] Lactoferrin is found in exocrine solutions of bronchial, nasal, lachrymal and genitourinary passages — everywhere the inside of the body meets the outside world. In addition to iron-related bacteriostasis, lactoferrin is thought to be involved in

bacteriocide by another mechanism. Thus, lactoferrin has both a defensive role and a role in safely transporting iron from mother to infant.[16]

It has long been known that strong chelating agents remove ferric transferrin at rates that initially increase as the ligand concentration increases. However virtually all these rates saturate at some concentration of chelating agent. Shortly after the catechol-containing siderophore enterobactin was found to be such a powerful chelating agent, synthetic analogs were prepared and investigated for their iron removal characteristics. Unlike more common ligands such as EDTA, ligands such as 3,4-LICAMS[17] (Figure 1) could be used at relatively low concentrations and still get significant rates of iron removal from the protein. This is highly significant because most other chelating agents can only remove iron at comparable rates when the ligand concentration is so high that one needs to be concerned about other changes of the protein or solution environment. To explain the saturation behavior seen in the iron removal behavior of 3,4-LICAMS, Carrano and Raymond proposed a pseudo-enzyme mechanism that involved complexation of the protein by the ligand as shown in Equation 1. This generates a ligand concentration dependence for the pseudo first order rate constant (found when the ligand is in large excess with respect to the protein concentration) as shown below in Equation 2.

$$FeTf + L \underset{k-1}{\overset{k1}{\rightleftarrows}} LFeTf \xrightarrow{k2} FeL + Tf \tag{1}$$

$$k_{obsd} = \frac{k_2[L]K_{eq}}{2.3 + 2.3K_{eq}[L]} \tag{2}$$

However subsequent evidence for a conformation change of the protein was first proposed by Cowart and Bates,[18] who presented a reaction mechanism as shown in the equation below.

$$FeTf \underset{k-1}{\overset{k_1}{\rightleftarrows}} FeTf^* \qquad LFeTf^* \xrightarrow{k_3} FeL + Tf^*$$

$$FeTf^* + L \underset{k-2}{\overset{k_2}{\rightleftarrows}} LFeTf^* \qquad k_{obsd} = \frac{k_1 k_2 k_3 [L]}{k_{-1}(k_{-2} + k_3) + k_2 k_3 [L]} \tag{3}$$

where * = "open conformation", Tf = bicarbonate complex of ferric transferrin, and L = a chelating agent.. This then leads to the same overall dependence of the observed first order rate constant on ligand concentration, but for completely different reasons as shown by the equation that relates the microscopic rate constants to the macroscopic observed rates. One key prediction of the Cowart, Kojima and Bates mechanism is that the limiting rate of all ligands should be essentially the same, since this is due to the conformation change of the protein. It has been clear for some time that these limiting rates vary dramatically from ligand to ligand. As will be seen, in light of the now available structural information about the protein and new kinetic

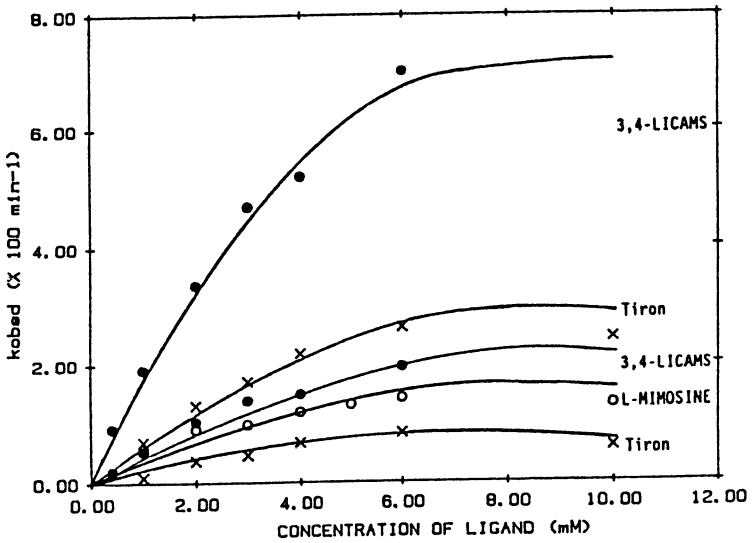

Figure 5: Iron removal from diferric transferrin by chelators: The dependence of observed rate constants on chelator concentration. Legend: ●, 3,4-LICAMS (biphasic kinetics); O, L-mimonsine (monophasic kinetics); and ✕, Tiron (biphasic kinetics). Conditions: 0.1 mM diferric transferrin, 50 mM HEPES buffer, pH 7.4, 25 °C, $\mu = 0.026$.

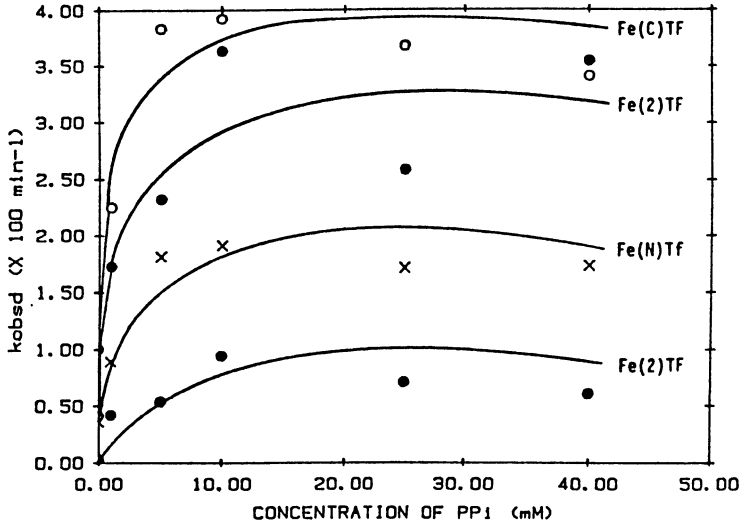

Figure 6: Iron removal from ferric transferrins by desferrioxamine B: The dependence of observed rate constants on the concentration of pyrophosphate. Legend: ●, removal from diferric transferrin (biphasic); O, removal from Fe_CTf; and ✕, removal from Fe_NTf. Conditions: 0.1 mM transferrin, 50 mM HEPES buffer, pH 7.4, 25 °C, $\mu = 0.026$.

studies, the actual mechanism for iron removal from serum transferrin by strong chelating agents is nearly a linear combination of the two early proposals.

Iron removal from serum transferrin actually involves three different forms of the protein: Diferric transferrin, monoferric (*N*-terminal) transferrin, and monoferric (*C*-terminal) transferrin. The *N*-terminal iron binding site forms a weaker complex than does the *C*-terminal and, in general, releases its iron more quickly. Hence in many cases iron removal from diferric transferrin conforms to a double exponential rate law.[19,20] For catechol ligands the rate of iron removal for diferric transferrin correlates very closely with the individual microscopic rate constants seen for the *C*-terminal and *N*-terminal sites, implying that there is little or no interaction between the two different lobes affecting the kinetics of iron release.[21]

Iron removal from transfer has been studied using many different iron chelators, some representatives appear in Figure 1. While catechol ligands such as 3,4-LICAMS or the simple commercially-available chelating agent Tiron show two-component rates of iron removal, with a clear distinction seen between the *N*-terminal and *C*-terminal sites, the hydroxypyridonate L-mimocine shows no such behavior. Mimosine does show saturation behavior, as shown in Figure 5 but a comparison shows that it is a much less effective ligand with respect to rate of iron removal than the catechol ligands. Shown in this figure are different microscopic rate constants seen for the rate of iron removal from the *N*-terminal and *C*-terminal sites for the catechol ligands, a distinction not seen in the slower mimosine kinetics.

Carbonate, the binding of which is an absolute prerequisite for iron binding to the protein, has been called a "synergistic anion." Other ligands, including oxalate, malonate and salicylate can take its place.[22] Disruption of the binding and of the synergistic ion to Fe^{3+} is a kinetically important step.

At low concentrations, pyrophosphate is not thermodynamically capable of taking iron out of transferrin. However, as shown in Figure 6, the rate of iron removal from transferrin by DFO (desferrioxamine B) is substantially increased in the presence of pyrophosphate. In other words, Desferral is capable of removing iron thermodynamically but is kinetically incompetent to do so. Its ability to remove iron increases dramatically in the presence of pyrophosphate. There is an even more dramatic effect upon the addition of catechol ligands such as 3,4-dihydroxybenzoic acid.[23] In contrast to instances in which pyrophosphate is the mediator, iron removal by 20 millimolar DFO mediated by 3,4-dihydroxybenzoic acid is linearly dependent on the added ligand. It also shows identical rates of iron removal from diferric and either *C*-terminal or *N*-terminal monoferric transferrin. This catechol ligand is present at concentrations below the concentration that would be required for iron complex formation in competition with transferrin or DFO. There is no spectroscopic evidence for any binding of the catechol to the metal ion. As might be expected from this result, conjugation of catechol substituents to DFO generate a substantial rate of enhancement for iron removal.[24]

Studies investigating the dependence of ionic strength on rates of iron removal from transferrin have shown an absolute dependence on ionic strength for iron removal; as the ionic strength goes to zero the extrapolated first order rate constant also goes to zero in every case.[25] This conforms closely to the structural information now available: anion binding to the protein substantially stabilizes the "open" conformation. That binding then triggers the conformation change that is a prerequisite for ion site accessibility for an attacking ligand. For monoferric serum transferrin, the unoccupied site is in the "open" conformation,[14] the more stable form when iron has not yet been complexed by the protein. In contrast, the diferric form

of the protein as seen in diferric lactoferrin[26]; and diferric rabbit serum transferrin[27]; has both lobes in the "closed" conformation. In this regard it is most interesting that the crystal structure of apolactoferrin[28] shows only one site in the "open" conformation and that the lobe of the protein seems to have anions bound to it. The other site is in the "closed" conformation, consistent with details of the structure differences between lactoferrin and transferrin that establish the compared stability of the closed conformation is greater for lactoferrin relative to transferrin. The structural data and the iron removal kinetics indicate that iron removal from transferrin to chelators occurs in three steps: 1) Rapid equilibrium binding of cooperative anions to the ferric protein. 2) Concomitant conformational change of the iron binding lobe of the protein from the stable "closed" form to the "open" form, which exposes the site to ligands in the surrounding solution. 3) Binding of the metal ion by the attacking ligand and removal of the synergistic carbonate at the ferric binding site.

These results have also been used to explain the observation that lactoferrin forms a much more stable complex than does transferrin.[29]. Shown below are the effect of differences in conformation stability on the stability constants and differences in pM values for these two proteins.[30] For an observed macroscopic rate constant as shown below the individual components of those rates are tabulated in Table 2. For the reaction scheme shown in Equation 3 above the ratio of k_1 to k_{-1} the unimolecular rate constant for the conformational change of the protein from the "closed" to "open" form should be the maximum achievable microscopic rate constant k_{obs}. At 37 °C this corresponds to half life for iron removal from transferrin of 8.4 minutes, compared to a half life of 1,100 minutes for lactoferrin! In short, lactoferrin gains most of its extra stability by making iron removal comparatively more difficult than from serum transferrin. This in turn is due to the greater stability of the closed form of the protein and is entirely consistent with its function as a bacteriostatic agent that substantially inhibits iron availability to an invading microorganism. As has been described,[30] "lactoferrin locks up iron and throws away the key."

Table 2: Comparison of stability and iron release rates of transferrins[a]

	pM[b]	Maximum k_{obs} for iron removal (3,4-LICAMS)[c]	$t_{1/2}$
Human Serum Transferrin	21.6	6×10^{-2} min^{-1}	8.4 min
Human Lactoferrin	24.9	6×10^{-4} min^{-1}	1,100 min

[a] Reference 30

[b] pM = -log[$Fe(H_2O)_6^{3+}$] , when $[Fe^{3+}]_{total}$ = 1 μM, $[L]_{total}$ = 10 μM, pH 7.4, 25 °C, and, in this Table, $[HCO_3^-]$ = 0.23 M (CO_2-saturated).

[b] Compared at 37 °C, pH 7.4, 0.0625 mM protein.

In summary, the relatively recent structural information on the transferrins now allows the assembly of a coherent picture of the kinetics of iron removal from these

proteins by strong chelating agents. Anion binding to the protein (which may be by the attacking ligand itself) triggers a conformational change to the open form of the protein in which the iron binding site of an individual lobe of the protein is exposed. Attack of the iron site shows a great variability among ligands: catechols are particularly effective in disrupting the iron coordination site for the first step in the subsequently rapid decomplexation of iron by the protein and complexation by the attacking chelating ligand. If new iron chelating agents for human therapy are to be effective, they must be able to compete with transferrin for iron complexation at concentrations that are not toxic. While the total amount of iron in transferrin is very low, it remains the major shuttle to the iron in storage sites and hence it is a rational target for new sequestering agents. Ligands that are kinetically competent for the removal of iron from transferrin should be designed so that they incorporate at least one functional group that shows an enhanced kinetic capability for iron removal. This does not include hydroxamate or most hydroxypyridonate ligands but does include catechol ligands. These features need to be kept in mind by those seeking to design new iron sequestering agents for human iron decorporation therapy.

2. Acknowledgment

We are pleased to acknowledge our many past research coworkers who have contributed to this subject, as cited in the references. This research was supported by NIH Grant DK32999.

3. References:

(1) Martin, J. H.; Gordon, R. M., *Deep Sea Research* **1988**, *35*, 177.
(2) Fox, L. L. *Geochim. Cosmochim. Acta* **1988**, *52,* 771
(3) Theil, E. C.; Raymond, K. N. ,"Transition-Metal Storage, Transport, and Biomineralization" in *Bioinorganic Chemistry,* I. Bertini, H. Gray, S. Lippard and J. Valentine Eds., University Science Books: Mill Valley, CA, **1994**, pp. 1-37.
(4) .Weinberg, E., *Biol. & Med.* **1993**, *36*, 215.
(5) Shakespeare, W. "Act III, Scene 7," in *King Lear*
(6) Baker, E. N., , **1994**, (in press).
(7) Conrad, M. E.; Umbreit, J. N., *Am. J. Hematology* **1993**, *42*, 67.
(8) Borgna-Pignatti, C.; Castriota-Scanderbeg, A., *Haematologica* **1991**, *76*, 409.
(9) Wolfe, L.; Olivieri, N.; Sallan, D.; Colan, S.; Rose, V.; Propper, R.; Freedman, M. H.; Nathan, D. G., *New England Journal of Medicine* **1985**, *312*, 1600.
(10) Herbert, V.; Shaw, S.; Jayatilleke, E.; Stopler-Kasdan, T., *Stem Cells* **1994**, *12*, 289.
(11) Otto, B. R.; Verweij-van Vught, A. M. J. J.; MacLaren, D. M.*Critical Revs. Microbiol.* , **1992**, *18*, 217.
(12) Kretchmar, S. A.; Reyes, Z. E.; Raymond, K. N., *Biochim. et Biophys. Acta* **1988**, *956*, 85.
(13) Baker, E. N.; Lindley, P. F., *J. Inorg. Biochem.* **1992**, *47*, 147.
(14) Zuccula, H. J. The Crystal Structure of Monoferric Human Serum Transferrin Ph.D. Dissertation Thesis, Georgia Institute of Technology, 1993.
(15) a) Alderton, G.; Ward, W. H.; Fevold, H. L., *Archives of Biochemistry* **1946**, *11*, 9-13. b) Schade, A. L.; Caroline, L., *Science* **1946**, *104,* 340.
(16) Iyer, S.; Lφnnerdal, B., *Eur. J. Clin. Nut.* ,**1993**, *47*, 232.
(17) Carrano, C. J.; Raymond, K. N., *J. Am. Chem. Soc.* **1979**, *101*, 5401.

(18) Cowart, R. E.; Kojima, N.; Bates, G. W., *J. Biol. Chem.* , **1982**, *257*, 7560.
(19) Baldwin, D. A., *Biochim. Biophys. Acta* **1980**, *623*, 183.
(20) Kretchmar, S. A.; Raymond, K. N., *J. Am. Chem. Soc.* **1986,** *108*, 6212.
(21) Kretchmar, S. A.; Raymond, K. N., *Biol. Metals* **1989,** *2*, 65-68.
(22) Harris, D. C.; Aisen, P. in *Iron Carriers and Iron Proteins*; T. M. Loehr, Ed.; VCH Publishers: New York; pp 239-352, **1989**.
(23) Kretchmar Nguyen, S. A.; Craig, A.; Raymond, K. N., *J. Am. Chem. Soc.* **1993,** *115*, 6758.
(24) Rodgers, S. J.; Raymond, K. N., *J. Med. Chem.* ,**1983,** *26*, 439.
(25) Kretchmar, S. A.; Raymond, K. N., *Inorg. Chem.* **1988**, *27*, 1436.
(26) Baker, E. N.; Anderson, B. F.; Baker, H. M.; Haridas, M.; Norris, G. E.; Rumball, S. V.; Smith, C. A., *Pure & Appl. Chem.* **1990,** *62*, 1067.
(27) Bailey, S.; Evans, R. W.; Garrett, R. C.; Gorinsky, B.; Hasnain, S.; Horsburgh, C.; Jhoti, H.; Lindley, P. F.; Mydin, A.; Sarra, R.; Watson, J. L., *Biochemistry,* **1988**, *27, 5804.*
(28) Anderson, B. F.; Baker, H. M.; Norris, G. E.; Rumball, S. V.; Baker, E. N., *Nature* **1990**, *344*, 784.
(29) Aisen, P.; Leibman, A., *Biochim. Biophys. Acta* **1972,** *257*, 314.
(30) Chung, T. D. Y.; Raymond, K. N., *J. Am. Chem. Soc.* **1993**, *115*, 6765..

SIDEROPHORE-MEDIATED IRON TRANSPORT IN MICROBES

KENNETH N. RAYMOND and JASON R. TELFORD
Department of Chemistry, University of California, Berkeley, CA 94720, U.S.A.

ABSTRACT. Iron is an essential element for all living things (with the exception perhaps of a few bacteria in specialized environments). Incorporation of iron into biochemistry certainly occurred in the very earliest evolution of life on this planet. By changing the global surface chemistry, life also changed the availability of iron on the planet since the ferric ion present in an aerobic environment is much less readily available than the ferrous ion largely present on the surface of primordial earth. A brief review of the availability of iron, its storage and transport, is presented. The focus is especially on transport and storage systems as pertains to the virulence of microorganisms. Most aerobic and anaerobic bacteria synthesize and excrete low molecular weight compounds (siderophores) for the solubilization and transport of iron. Since the iron supply is often a limiting factor in the growth of these microbes, siderophores and their corresponding transport systems play an important role in bacterial virulence.

1. Introduction

Iron, generally in large quantities, is absolutely required for growth in all but a few microorganisms. This requires mechanisms by which organisms can ingest, transport and store the metal. For organisms in an aerobic environment, which includes most organisms, this task is complicated by the extreme insolubility of ferric hydroxide. A K_{sp} of 10^{-39}, limits the free iron concentration to 10^{-18} M. The solubilization and transport of iron has been addressed by microorganisms by producing low molecular weight, virtually iron-specific complexing agents called siderophores.[1]

In mammals, the proteins transferrin and lactoferrin are responsible for iron transport and storage. These systems have a two pronged effectiveness: not only do they perform the necessary transport roles, but also form an efficient iron buffer system, lowering the free iron concentration to even lower than *in aquo*. The storage of iron is accomplished the protein ferritin. Most of the iron in the body is intracellular in the proteins hemoglobin, myoglobin, ferritin, and cyochrome c.[2] Hemoglobin released by the destruction of erythrocytes is quickly complexed by haptoglobin and removed from circulation. Serum iron is scavenged by transferrin, and iron concentrations in secretions are kept extremely low by lactoferrin. Yet, iron availability is increasingly implicated as a determinant in a number of disease states.[3,4] When the above-mentioned mammalian systems are stressed beyond their native abilities, either by iron overload or parasitic competition, the results are dramatic and often catastrophic.

D.P. Kessissoglou (ed.), Bioinorganic Chemistry, 25-37

One of the functions of iron that makes it a particularly useful cofactor in proteins is the catalysis of free radical based reactions. In cases where the normal iron withholding defenses are overwhelmed, the catalytic activity of iron can be manifested in the formation of radicals which can damage cells via autooxidative (Fenton) processes such as oxidation of sulfhydryl groups or addition of oxygen at double bonds.[5]. A practical consequence of this action is the release of iron into the plasma during ishchemic insult, leading to oxidative damage of the vascular compartment on reperfusion. Desferrioxamine and its derivitives, siderophores from *Streptomyces pilosus*, are being examined to determine if iron chelation following 'ishaemic insult' can reduce reperfusive injury.[6,7].

The relationship between iron and microbial virulence is rapidly becoming clear. Several recent papers illustrate the signals which control virulence expression in bacteria; iron is a common theme.[3-5,8-11]. A microbial infection exists as an intricate relationship between the host and a pathogen, dependant on a number of characteristics of the host and the microbe. We will focus on bacterial infections, though analogies can be made to fungal infections.

During the course of an infection, the invader must obtain all of its nutrients, including iron, from the host. The host, in turn, is obligated to deny these nutrients to the invader such that only those pathogens able to successfully compete for nutrients can survive. Iron has been shown to play a significant role in this interaction. The ability to acquire iron from a host, against a strong free energy bias, confers a distinct advantage to an invading organism. In normal sera, the concentration of iron is far too low to support the pathogen (*vida supra*). The addition of iron to tissues during or concommitant with infection is dramatic. If the iron binding proteins of the host are saturated, either by induced or natural iron overload, the serum loses its ability to inhibit bacterial growth.

The virulence of organisms diverse as *Escherichia*,[12]. *Klebsiella*, [13]. *Listeria*,[10]. *Neisseria*;[14,15]. *Pasteurella*,[16]. *Shigella*, [17]. *Vibrio*,[18]. and *Yersinia* [19]. are all enhanced by available iron. Iron dextran injections in children, originally designed to prevent iron deficiencies, enhanced *E. coli* bacteremia and menningitis.[20,21]. It was found that non-lethal injections of *E. coli* in mice could be converted into lethal infections by the addition of either heme or enough iron to saturate the transferrin.[22,23]. *Y. enterocolitica* , normally unable to cause disease, can cause a fatal bacteremia if iron is freely available. *Y. enterocolitica* is unable to grow in normal human serum nor is it able to utilize transferrin as an iron source, rendering it unable to grow in the presence of unsaturated transferrin. These bacteriostatic effects are abrogated if iron or a siderophore (desferrioxamine) is added. In one study on the virulence of *Y enterocolitica*, the LD_{50} of the organism was reduced from 10^8 to 10 organisms by the peritoneal injection of iron and desferrioxamine.[19]. A similar effect is seen if desferrioxamine is supplied during infections of *Klebsiella* and *Salmonella*.[24].

A number of pathogenic bacteria express iron regulated outer membrane proteins, IROMPS, which bind either transferrin, lactoferrin, or heme compounds. *Neiseria sp.* [25]. including the gonococcal variety, *Haemophilus sp.* [26]. and *Aeromonas sp.*[27]. are all known to express receptors for the host heam compounds. Certain *Shigella* species also express these receptors but for a rather different reason. Shigella are enteroinvasive with part of their life cycle spent inside host epithellial cells. *Shigella sp.* are unable to utilize either transferrin or lactoferrin but are able to utilize heam compounds and they express large amounts of plasmid encoded receptors for heme on the cell surface. Although *Shigellae* are able to utilize heme as the sole iron source, it does not appear that expression of this receptor is primarily for utilization of heme, but it is necessary for the cells to become enteroinvasive. It has been suggested that *Shigella* bind and coat themselves with heme compounds at the cell surface making themselves more palatable to the host, and invading

via the host's heme receptors. Once the host cell has taken up this Trojan horse, the bacterium is free to acquire iron intracellularly.[17]

Hemolysins appear as part of bacterial virulence repertoirs.[9] Hemolysins lyse mamalian erythrocytes and other cells, and in some cases have been shown to be iron regulated. Expression of hemolysins and subsequent lysis of erythrocytes releases hemoglobin and raises local iron concentrations, enhancing growth of the invading organism or any other that would be present.

Another method for obtaining iron is the production of iron reducing compounds. *Listeria monocytogenes* produces a peptide reductase which reduces Fe^{3+} to Fe^{2+}.[28] This favors the release of the ferrous ion from transferrin. *Streptococcus mutans,* which causes plaque (not plague), expresses a cell surface reductase.[29] *E. coli,* while not possessing any relevant reductases, does have a high affinity uptake system for ferrous ion which is induced during anaerobic growth under iron restrictive conditions.[30]

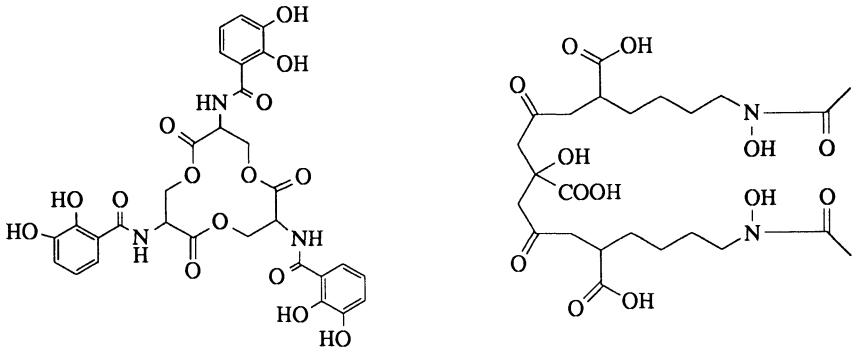

Figure 1. Enterobactin and Aerobactin

Perhaps the most well studied method of iron acquisition is by siderophores. Of the approximately 200 siderophores now discovered, enterobactin, produced by enteric bacteria such as *Escherichia coli,* has received considerable attention. Since its discovery in 1970, the synthesis, biosynthesis, microbial transport, and solution thermodynamics of enterobactin have been investigated. The thermodynamic studies have shown that enterobactin forms the most stable Fe^{III} complex known, with a formal stability constant of 10^{49}. The enterobactin molecule (Figure 1) is 3-fold symmetric and is comprised of three catecholate groups suspended from a trilactone backbone; metal coordination at neutral pH occurs through the six catecholate oxygens

Enterobactin (ent) and aerobactin are employed by members of the Enterobacteriacea, but have not yet been found outside that family and the siderophore systems of non-enteric bacteria have not enjoyed as much study.

In addition to enterobactin and aerobactin, the enteric bacteria utilize exogenous siderophores, ferricitrate, and a ferrous iron uptake system. Enterobactin is thermodynamically capable of removing iron from transferrin and it has been shown that it is kinetically competent to do this as well.

Aerobactin is a linear citrate/hydroxamic acid siderophore, first isolated from *Aerobacter aerogenes*.[31] It too is able to remove iron from transferrin, albeit slower than enterobactin. The genes encoding production of aerobactin and receptors reside most often on the

pCoIV plasmid, although the genes have been located chromasomally and on other plasmids encoding multidrug resistance as well.

On the basis of their ability to remove iron from transferrin alone, one might be tempted to conclude that enterobactin is a much more effective iron chelator *in vivo*. However, nature is often more sublime, and it turns out that a few other factors must be taken into consideration. Enterobactin is hydrolytically unstable in vivo, and while the rate of iron removal by enterobactin versus aerobactin from transferrin is greater in HEPES buffer, the rates are reversed in serum.[32]. This is due to the enterobactin molecule binding to seroalbumin, effectively removing it from solution. Enterobactin is a hapten as well, and stimulates antibody production.[33].

Aerobactin is in some ways a more efficient siderophore. Production of the siderophore and excretion into solution is more rapid than enterobactin in response to iron stress[34]. and aerobactin is recycled.[35]. Once aerobactin delivers iron to the cell, the aerobactin molecule is re-excreted. Experimental evidence corroborates that it is the production of aerobactin, and not enterobactin, that enhances virulence.[36,37].

Aeromonas hydrophila produces one of two siderophores, either enterobactin or amonabactin, but not both.[38]. The amonabactins have also been detected in isolates of *A. caviae*, and to a lesser extent *A. sobria*. These siderophores have recently been structurally characterized in our laboratories and shown to be four distinct peptide based siderophores. Amonabactin may be involved in the virulence of *Aeromonas*.[27]. *Aeromonas* isolates which produce amonabactin are able to grow in serum, where enterobactin producing isolates are not. An amonabactin production mutant was able to grow in serum only if supplemented with amonabactin, suggesting a role for the siderophore in iron removal from transferrin.

2. Solution Studies of Siderophores, Transport, Sterochemistry & Thermodynamics

Iron transport by siderophores has many practical implications to understanding the basic bioorganic, bioinorganic and coordination chemistry of these compounds. To this end, considerable research has studied these molecules using a number of techniques. Substitution of Cr^{3+} for Fe^{3+} in a siderophore complex gives a molecule which retains its coordination geometry but has quite different ligand exchange kinetics and electronic soectra. All iron siderophore complexes incorporate high-spin Fe^{3+}. The iron complexes, with five unpaired electrons, have no allowed d-d transitions, nor is there any ligand field stabilization of the complexes. Still, these complexes are highly colored due to charge transfer processes which we have only recently begun to understand.[39]. The chromic complexes, on the other hand, have well characterized d-d transitions which generate the characteristic VIS/UV and circular dichroism (CD) spectra shown in Figure 2, and are kinetically inert. Figure 2 also shows desferriferrichrome, a siderophore produced by *Ustilago sphaerogena* which was one of the first siderophores (or family of siderophores) to be characterized.

If the same substitution of Cr^{3+} for Fe^{3+} is made in enterobactin (Figure 3), again very characteristic VIS/UV and CD spectra are obtained. By comparing the CD spectrum of the Cr^{3+}ent with that of Cr^{3+}desferriferrichrome (Figure 3), it is evident that the Cr^{3+}ent is the opposite chirality(at the metal center) of Cr^{3+}desferriferrichrome. Since the chirality in ferrichrome A was established by a crystal structure analysis is L, the enterobactin chirality is[41].. This is now confirmed by the crystal structure of [V(ent)].

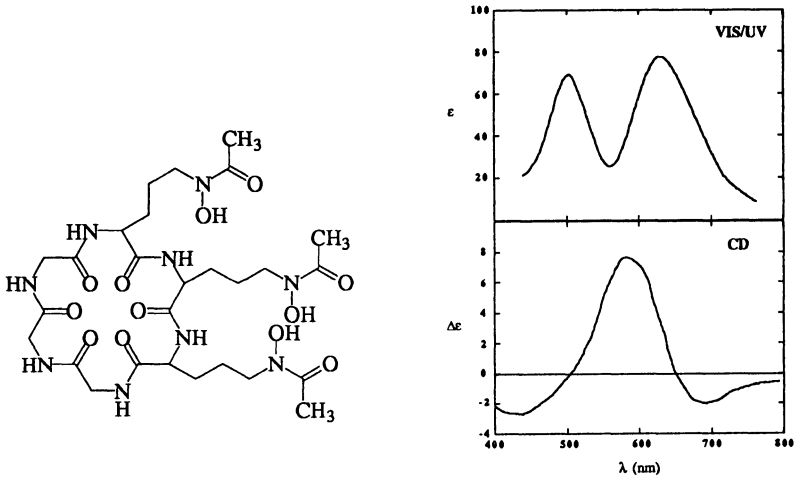

Figure 2. The first synthesis of a kinetically inert siderophore complex. The VIS/UV and CD spectra of the chromic complex of desferriferrichrome is shown. This established the L cis coordination environment of the metal center in this complex[40].

The kinetic inertness of the chromic siderophore complexes has been used to monitor siderophore mediated iron uptake in microorganisms. Ordinarily, radioactively labeled iron complexes have been used to measure rates of uptake (Figure 4) but since these are labile complexes, it was not known whether the ligand accompanied the metal in uptake. In transport experiments utilizing Cr^{3+} substituted siderophores, it was established that the complex was taken up at the same rate.[42] In fact, under a microscope, one can visually observe the microorganisms turning green! This was the first use of a kinetically inert metal complex to probe siderophore mediated iron transport. The results of this and other experiments has established some general patterns. Iron uptake mediated by siderophores involves highly specific proteins located on the outer membrane of the microorganism. These proteins actively transport the metal-siderophore complex and are sensitive to both key structural features of the siderophore and the chirality of the metal-siderophore complex.[1]

Another substitution, by gallium, has been used to probe the mechanism of iron realease in siderophores. Removal of the metal from the siderophore is, of course, important to metabolize this nutrient. One possible mechanism would be through a redox process at the time of uptake, and thus substitution of iron by a redox inactive metal would give quite different transport kinetics. It was suggested early on that since Ga^{3+} is an analog to Fe^{3+} and has no accessible Ga^{2+} oxidation state, it could be used for this purpose. Tom Emery and coworkers examined this in an early experiment.[44]

Later, more extensive experiments involving transport of ferrioxamine B by *Ustilago sphaerogena* (Figure 5) established that uptake rates were the same for ferric or gallium substituted siderophore complexes.[43] This demonstrated that the uptake process does not involve a reduction. Reduction of the iron, and subsequent release from the siderophore complex, is an event that occurs after active transport into the cell. Several studies have shown that the chirality of the metal center is of primary importance to recognition of the siderophore complex.

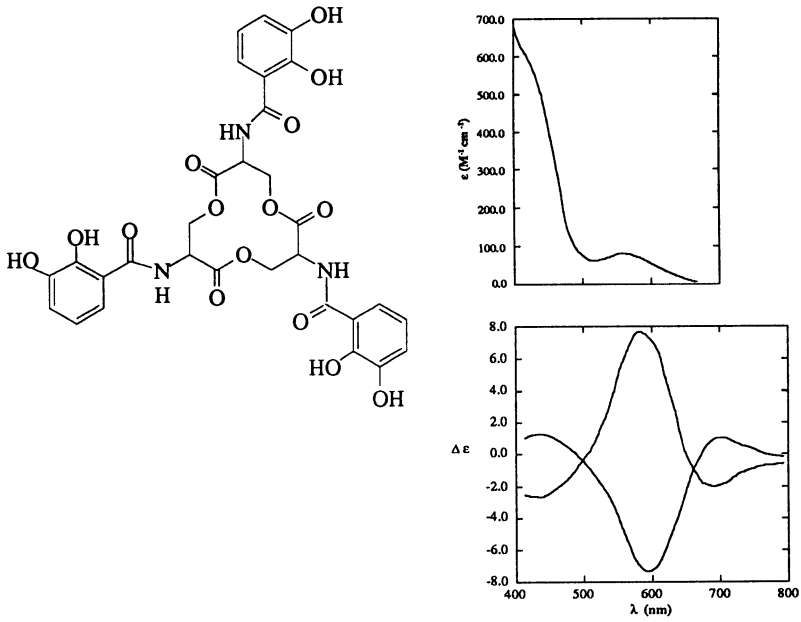

Figure 3. The first use of CD and VIS/UV spectra to determine the chirality of a metal-siderophore complex: $[Cr^{III}(enterobactin)]^{3-}$. VIS/UV spectrum (top) and CD spectrum (bottom) of $[NH_4]_3[Cr(enterobactin)]$ (negative at 600 cm) and Cr(desferriferrichrome) (positive at 600 nm) [41]

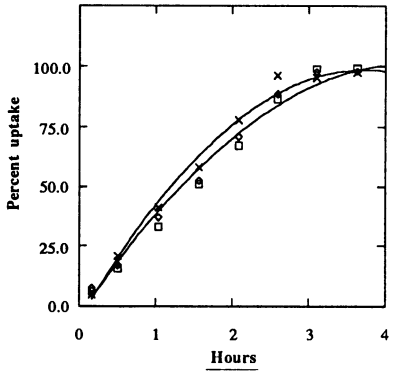

Figure 4. The uptake of the natural Fe^{3+} (X) and kinetically inert Cr^{3+} complexes of $[^{14}C]$ ferrichrome in the microorganism Ustilago sphaerogena (14C, ≠_), (Cr, Δ_)[42].

An early example of this is a series of uptake experiments with rhodotorulic acid, shown in Figure 6.[45]. Rhodotorulic acid is a dihydroxamic acid, produced by Rhodotorula pilminia. Since rhodotorulic acid is a dihydroxamic acid, it accomplishes full octahedral coordination of iron by forming a 3:2 ligand:metal complex. The absolute configuration at the metal centers is D, opposite that of ferrichrome.

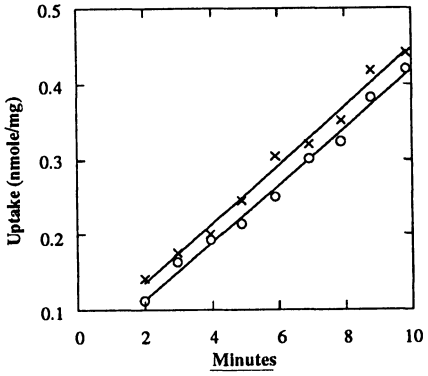

Figure 5. The use of Ga^{3+} (O) substitution for Fe^{3+} (X) to probe the role of reduction in siderophore-mediated microbial iron transport[43] ..

The mirror image rhodotorulic acid, produced synthetically, has a L configuration at the metal centers.

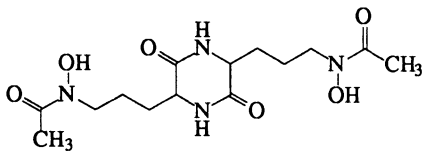

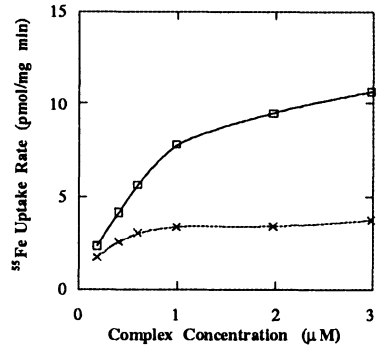

Figure 6. The role of the stereochemistry at the metal center in siderophore recognition and transport. Shown is the uptake into E. coli. of radioactive Fe as mediated by natural rhodotorulic acid (o) versus its unnatural enantiomer (x)

Ferrichrome, as mentioned earlier, is a trihydroxamic acid which forms a 1:1 ligand:metal complex with a preferred L geometry. *E. coli*, while it does not produce ferrichrome, does have receptors for ferrichrome which recognize and transport the complex. It was demonstrated (Figure 6) that it is the unnatural rhodotorulic acid which was most effective

at mediating iron uptake. This is because the receptor protein on *E. coli* preferentially recognizes the L tris-hydroxamate complex.

This geometry exists in the enantio-rhodotorulic acid complex which to the protein, looks like the iron coordination center in ferrichrome. This and other experiments demonstrated a new kind of chiral recognition in biology: one based on a metal center rather than a carbon center.

3. Enterobactin - Structure and Stability

Enterobactin has been known for almost two decades, but still enjoys the title of the most powerful iron complexing agent. There have been several synthetic mimics (Figure 7) of enterobactin but in every case they are about 10^6 weaker in complexing ability.

Also given in Figure 7 is the formal stability constant, a measure of the formation constant of the fully deprotonated ligand, and the pM value, analogous to the pH value.[46]. The pM value is a direct measure of the relative free energy under specific conditions. For a total metal concentration of one micromolar and a total ligand concentration of ten micromolar at pH 7.4 (physiologic pH), the negative log of the free ferric ion concentration is the pM. One of our goals has been to explain the remarkable stability of the enterobactin complex with regard to TRENCAM and MECAM. One might think they should be similar since the ligating groups are the same: three pendant catechol amide groups. A major contribution to the stability of enterobactin is the backbone size of enterobactin.

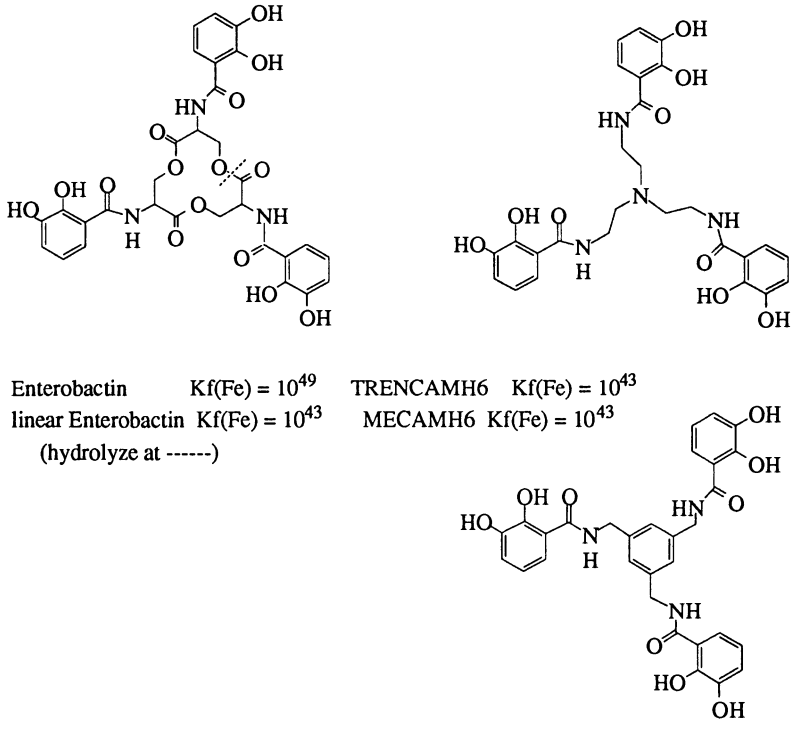

Figure 7. The relative stability of enterobactin and model compounds[46]

Hydrolysis of the backbone reduces the binding efficiency of enterobactin by 6 orders of magnitude. Direct calorimetric measurements (Figure 8) have established that about two-thirds of this loss is entropic and one-third enthalpic in origin.[46] Only recently have we been able to report the three dimensional structure of the enterobactin complex as provided by a single crystal structural analysis.[47] The V(enterobactin) complex anion is shown in Figure 9 and includes some of the important features of this molecule. The catechol to amide-proton hydrogen bond is an important feature, not only to the stability of the complex, but is also involved in the rapid formation of the metal complex. Structural analyses of enterobactin analogs have shown a hydrogen bond between the protonated ortho hydroxyl and amide oxygen. On metal complexation, the catechol moiety swings 180° around the CN vector so the ortho oxygen then hydrogen bonds to the amide proton. This structural change, from the catechols 'pointing out' of the cavity in the free ligand to 'in' the cavity on metal complexation represent one degree of freedom for each catechol.

Thermodynamic Contributions to the Formation of Ferric Enterobactin

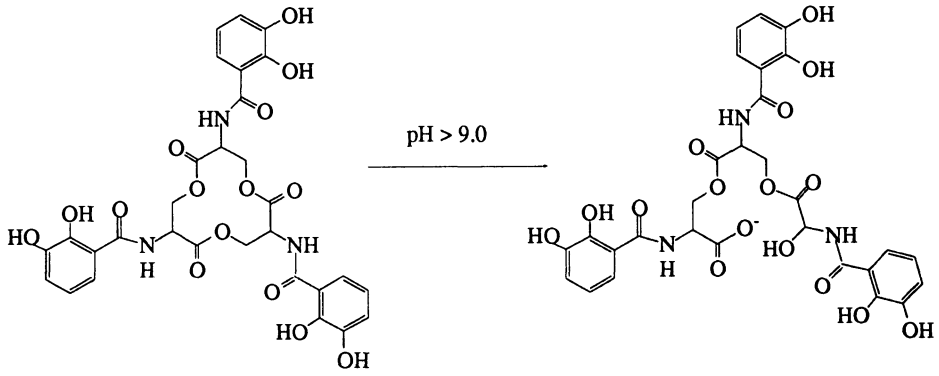

Enterobactin

Linear Enterobactin Trimer

$$H_3L^{q-} + Fe^{3+} \longrightarrow FeL^{q-} + 3H^+$$

	Log K	ΔG (Kcal/mol)	ΔH (Kcal/mol)	TΔS @ 297 K (Kcal/mol)
Enterobactin	12.3	-16.8	-6.5	10.3
Linear Enterobactin Trimer	6.5	-8.9	-3.4	5.5

Figure 8. The loss of stability of the ferric enterobactin complex due to hydrolysis of one ester bond of the ligand skeleton.[46]

If one compares the backbone of enterobactin to comparable trilactones synthesized by Shanzer and coworkers[48], and Seebach and coworkers,[49], it is evident that there is very little reorganization of the backbone on metal complexation (Figure 10). A least squares analysis of the overlay of the enterobactin backbone and Seebach's trilactone give an RMS deviation of atoms of only 0.1 Å. Although the single crystal structure of the enterobactin free ligand is not yet available, the crystal structure analyses of several enterobactin analogs (including one which forces a static gearing of the pendant catechol groups) are available[50], and together with this analysis suggests that the ground state of the backbone of enterobactin is essentially the same in the free ligand and metal complex and that the only degree of freedom is rotation of each of the catechol groups. We have concluded that the enterobacin molecule is thus predisposed for complexation and that the entropic advantage of enterobactin over linear enterobactin and other analogs is derived from the backbone architecture.

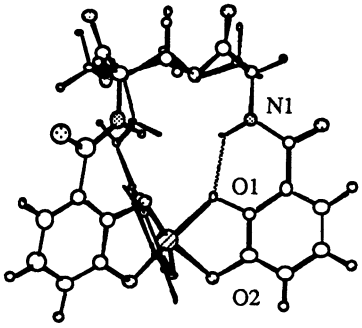

Figure 9. The structure of the vanadium (IV) enterobactin complex[47]

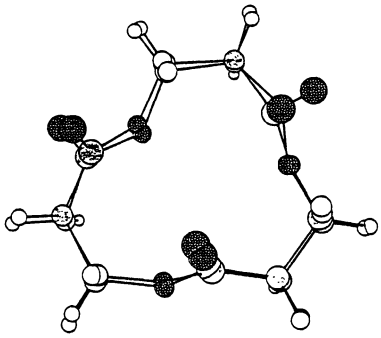

Fig. 10. A comparison of the skeleton of enterobactin and a synthetic trilactone by Seebach et al[49]

The characterization of novel siderophores continues. A series of siderophores from Aeromonas hydrophila has proven to be a provocative area of research.

The aeromonads are mesophilic, gram negative, fresh water, opportunistic pathogens causing a wide range of diseases in poikilothermic and homeothermic animals. These range from red leg and furunculosis in frogs and fish, to septicemia and soft tissue infections in mammals. They produce a hemolysin under iron stress,[27], which is important

to virulence, and most produce one of two siderophores; either enterobactin or amonabactin.[51]. The amonabactins were originally isolated, and given their trivial name, by Barghouthi et al.[38]. Their early characterization of these siderophores indicated two compounds, containing glycine, lysine, either tryptophan or phenylalanine, and catechol.

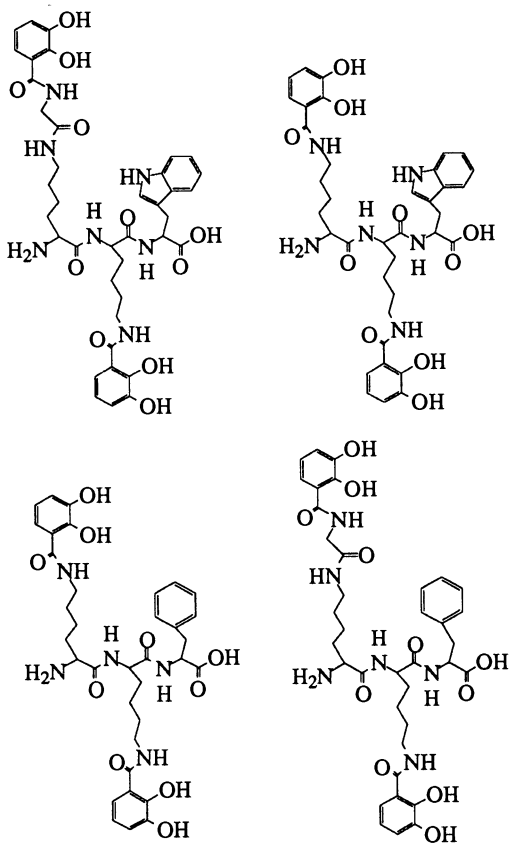

Figure 11. Structures of the amonabactin siderophores. Top left to right: amonabactin T 789 (AmoT 789), amonabactin T 732 (AmoT 732); Bottom left to right: amonabactin P 750 (AmoP 750), amonabactin P 693 (AmoP 693) [52].

The full structures of the amonabactins (Figure 11) have been deduced using amino acid analysis, tandem mass spectroscopy, chiral GC-MS, and 2-D NMR.[52]. As a further proof, each of the four amonabactins were synthesized and their spectral properties compared with that of the natural product.

While it is not yet known whether the production of amonabactin is significant in the virulence of the Aeromonads, there is evidence that the amonabactin producing isolates of *Aeromonas* are able to remove iron from transferrin and show greater resistance to the complement activity of serum.[27]. Whether amonabactin is a cause or consequence of this is a question that remains to be answered.

4. Acknowledgements

We thank our many past and present coworkers, who are cited in the references. This research is supported by the National Institutes of Health through grant AI 11744.

5. References

(1) Matzanke, B. F.; Móller-Matzanke, G.; Raymond, K. N. *Siderophore Mediated Iron Transport*; VCH: New York, 1989, pp 1-121.
(2) Otto, B. R.; Verweij-van Vught, A. M. J. J.; MacLaren, D. M. *Crit. Rev. Microbiol.* **1992**, *18*, 217-233.
(3) Bullen, J. J.; Ward, C. G.; Rogers, H. J. *Eur. J. Microbiol. Infect. Dis.* **1991**, *10*, 613-617.
(4) Expert, D.; Gill, P. R. *Iron: A Modulator in Bacterial Virulence and Symbiotic Nitrogen-Fixation*; CRC Press: Boca Raton, 1992, pp 229-245.
(5) Weinberg, E. D. *ASM News* **1993**, *59*, 559-562.
(6) Wolfe, L.; al, e. *Am. J. Physiol.* **1985**, *253*, 1372-1380.
(7) Hedlund, B. E.; Hallaway, P. E. *Biochem. Soc. Trans.* **1993**, *21*, 340-343.
(8) Gross, R. *FEMS Microbiol. Rev.* **1993**, *104*, 301-326.
(9) Wooldridge, K. G.; Williams, P. H. *FEMS Microbiol. Rev.* **1993**, *12*, 325-348.
(10) Martvnez, J. L.; Delgado-Iribarren, A.; Baquero, F. *FEMS Microbiol. Rev.* **1990**, *75*, 45-56.
(11) Griffiths, E. *J. Biosci.* **1990**, *15*, 173-177.
(12) Bullen, J. J.; Rogers, H. J. *Nature* **1969**, *224*, 380-382.
(13) Ward, C. G.; Hammond, J. S.; Bullen, J. J. *Infect. and Immun.* **1986**, *51*, 723-730.
(14) Holbein, B. E.; Jericho, K. W. F.; Likes, G. C. *Infect. Immun.* **1979**, *24*, 545-551.
(15) Holbein, B. E. *Infect. Immun.* **1980**, *29*, 886-891.
(16) Bullen, J. J.; Rogers, H. J.; Lewin, J. E. *Immunology* **1971**, *20*, 391-406.
(17) Payne, S. M. *Molec. Microbiol.* **1989**, *3*, 1301-1306.
(18) Chart, H.; Griffiths, E. *FEMS Microbiol. Lett.* **1985**, *26*, 227-231.
(19) Robins-Browne, R. M.; Prpic, J. K. *Infect. Immun.* **1985**, *47*, 774-779.
(20) Weinberg, E. D. *Physiol. Rev.* **1984**, *64*, 65-102.
(21) Barry, D. M. J.; Reeve, A. W. *Pediatrics* **1977**, *60*, 17-28.
(22) Bullen, J. J.; Leigh, L. C.; Rogers, H. J. *Immunology* **1968**, *15*, 581-588.
(23) Bornside, G. H.; Bouis, P. J.; Cohn, I. *Surgery* **1970**, *68*, 41-45.
(24) Griffiths, E. In *Iron and Infection: Molecular, Physiological and Clinical Aspects*; J. J. a. G. Bullen E., Eds.; John Wiley & Sons: Chichester, U.K., 1987.
(25) Michelsen, A.; Sparling, P. F. *Infect. Immun.* **1981**, *36*, 107.
(26) Coulton, J. W.; Pang, J. C. S. *Curr. Microbiol.* **1983**, *29*, 121.
(27) Massad, G.; Arceneaux, J. E. L.; Byers, B. R. *J. Gen. Microbiol.* **1991**, *137*, 237-241.
(28) Cowart, R. E.; Foster, B. G. *J. Infect. Dis.* **1985**, *151*, 721-730.
(29) Evans, S. L.; Arceneaux, J. E. L.; Byers, B. R.; Martin, M. E.; Aranha, N. *J. Bacteriol.* **1986**, *168*, 1096-99.
(30) Lodge, J. S.; Emery, T. *J. Bacteriol.* **1984**, *160*, 801-804.
(31) Gibson, F.; Magrath, D. J. *Biochim. Biophys. Acta* **1969**, *192*, 175-187.
(32) Konopka, K.; Neilands, J. B. *Biochemistry* **1984**, *23*, 2122-2127.
(33) Moore, D. G.; Earhart, C. F. *Infect. Immun.* **1981**, *31*, 631-635.

(34) Der Vartanian, M. *Infect. Immun.* **1988**, *56*, 413-418.
(35) Braun, V.; Brazel-Faisst, C.; Schneider, R. *FEMS Microbiol. Lett.* **1984**, *21*, 99-103.
(36) Williams, P. H.; Warner, P. J. *Infect. Immun* **1980**, *29*, 411-416.
(37) Nassif, X.; Sansonetti, P. J.; 1986 *Infect. Immun.* **1986**, *54*, 603-608.
(38) Barghouthi, S.; Young, R.; Olson, M. O. J.; Arceneaux, J. E. L.; Clem, L. W.; Byers, B. R. *J. Bacteriol.* **1989**, *171*, 1811-1816.
(39) Karpishin, T. B.; Gebhard, M. S.; Solomon, E. I.; Raymond, K. N. *J. Am. Chem. Soc.* **1991**, *113*, 2977-2984.
(40) Leong, J.; Raymond, K. N. *J. Am. Chem. Soc.* **1974**, *96*, 6628-6630.
(41) Isied, S. S.; Kuo, G.; Raymond, K. N. *J. Am. Chem. Soc.* **1976**, *98*, 1763-1767.
(42) Leong, J.; Neilands, J. B.; Raymond, K. N. *Biochem. Biophys. Soc. Trans.* **1974**, *60*, 1066-71.
(43) Müller, G.; Raymond, K. N. *J. Bacteriol.* **1984**, *160*, 304-312.
(44) Emery, T.; Hoffer, P. B. *J. Nucl. Med.* **1980**, *21*, 935.
(45) Muller, G.; Matzanke, B. F.; Raymond, K. N. *J. Bacteriol.* **1984**, *160*, 313-318.
(46) Scarrow, R. C.; Ecker, D. J.; Ng, C.; Liu, S.; Raymond, K. N. *Inorg. Chem.* **1991**, *30*, 900-906.
(47) Karpishin, T. B.; Raymond, K. N. *Angew. Chem. Int. Ed.* **1992**, *31*, 466-468.
(48) Shanzer, A.; Libman, J.; Frolow, F. *J. Am. Chem. Soc.* **1981**, *103*, 7739-7740.
(49) Seebach, D.; Muller, H.-M.; Burger, H. M.; Plattner, D. A. *Angew. Chem. Int. Ed. Engl.* **1992**, *31*, 434-435.
(50) Stack, T. D. P.; Z., H.; Raymond, K. N. *J. Am. Chem. Soc.* **1993**, *115*, 6466-6467.
(51) Zywno, S. R.; Arceneaux, J. E. L.; Altwegg, M.; Byers, B. R. *J. Clin. Microbiol.* **1992**, *30*, 619-622.
(52) Telford, J. R.; Leary, J. A.; Tunstad, L. M. G.; Byers, B. R.; Raymond, K. N. *J. Am. Chem. Soc.* **1994**, *116*, 4499-4500..

ON THE MECHANISM OF EPOXIDATION AND HYDROXYLATION CATALYZED BY IRON PORPHYRINS. EVIDENCE FOR NON-INTERSECTING REACTION PATHWAYS

JOHN T. GROVES AND ZEEV GROSS
Department of Chemistry
Princeton University
Princeton, New Jersey 08544, USA

ABSTRACT: The oxygenation of cyclohexene to cyclohexene oxide and cyclohexen-3-ol by $(O)Fe^{IV}TMP^{\cdot+}(X)$ (**1**) at various temperatures was compared with the iodosylbenzene mediated reaction catalyzed by chloro-5,10,15,20-tetramesitylporphyrinatoiron(III) [Fe^{III}(TMP)Cl]. The product ratios were found to depend on the axial ligand X in **1** and on the temperature in an unusual way. The results demonstrate that at least one reaction intermediate must be produced and further, that while the epoxidation proceeds via the formation of a complex between **1** and the olefin, the hydroxylation reaction proceeds by a non-intersecting reaction pathway not involving this complex.

The elucidation of the mechanisms of metalloporphyrin catalyzed oxygenation of hydrocarbons and the relationships of these reactions to the catalytic functions of cytochrome P-450 continue to pose significant challenges.[1,2,3,4,5] Of particular interest are probes of the nature of reactive iron-oxo and iron-peroxo intermediates which have been indicated in the action of both heme and non-heme iron-containing enzymes.[6] The catalytic cycle currently accepted for cytochrome P-450 is outlined in Scheme I. The structure of the suspected but still unobserved reactive iron -oxo intermediate is shown in Figure 1.

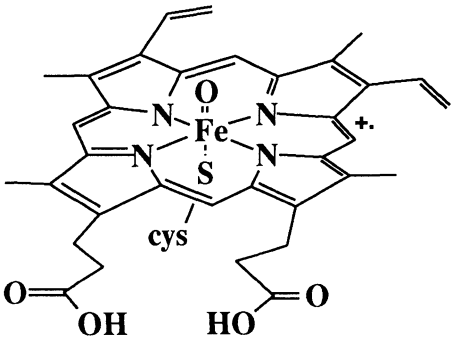

Figure 1. Proposed reactive species of cytochrome P-450

D.P. Kessissoglou (ed.), Bioinorganic Chemistry, 39-47

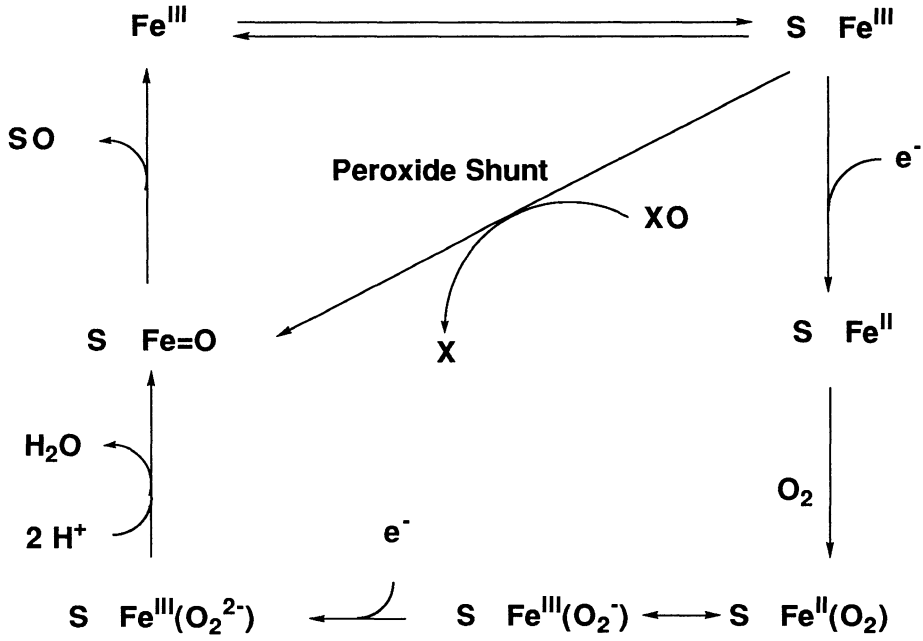

Scheme I. Catalytic cycle for cytochrome P-450

The characterization of a synthetic oxoiron(IV) porphyrin cation radical [(O)$Fe^{IV}TMP^{\cdot+}$(X), **1**] derived from the reaction of peroxyacids with chloro-5,10,15,20-tetramesitylporphyrinatoiron(III) [Fe^{III}(TMP)Cl] and the ability of this complex to epoxidize and hydroxylate appropriate substrates[7] provides an opportunity to compare these two reactions. Although we have shown that the mechanism of olefin epoxidation varies with changes in reaction conditions[8], the oxidizing species has been assumed to be structurally related to **1** in a variety of different oxidation systems.[9]

There is abundant evidence that the hydroxylation of hydrocarbons catalyzed by cytochrome P-450 occurs by a mechanism involving hydrogen atom abstraction from the substrate (R-H) followed by rapid transfer of the metal-bound hydroxy radical to an intermediate alkyl radical (R·) (Scheme II). This so-called oxygen rebound mechanism

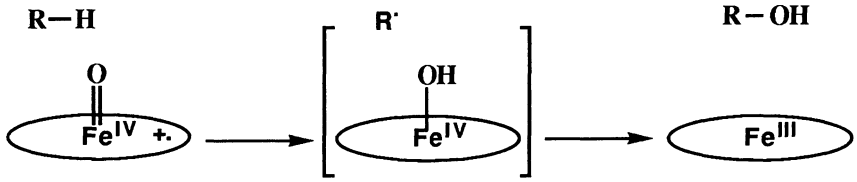

Scheme II. Rebound mechanism for the hydroxylations by cytochrome P-450.

is consistent with the stereochemical, regiochemical and allylic scrambling results observed in the oxidation of norbornane, camphor and cyclohexene by cytochrome P-450. The hydroxylation of a saturated methylene (CH_2) in norbornane was accompanied by a

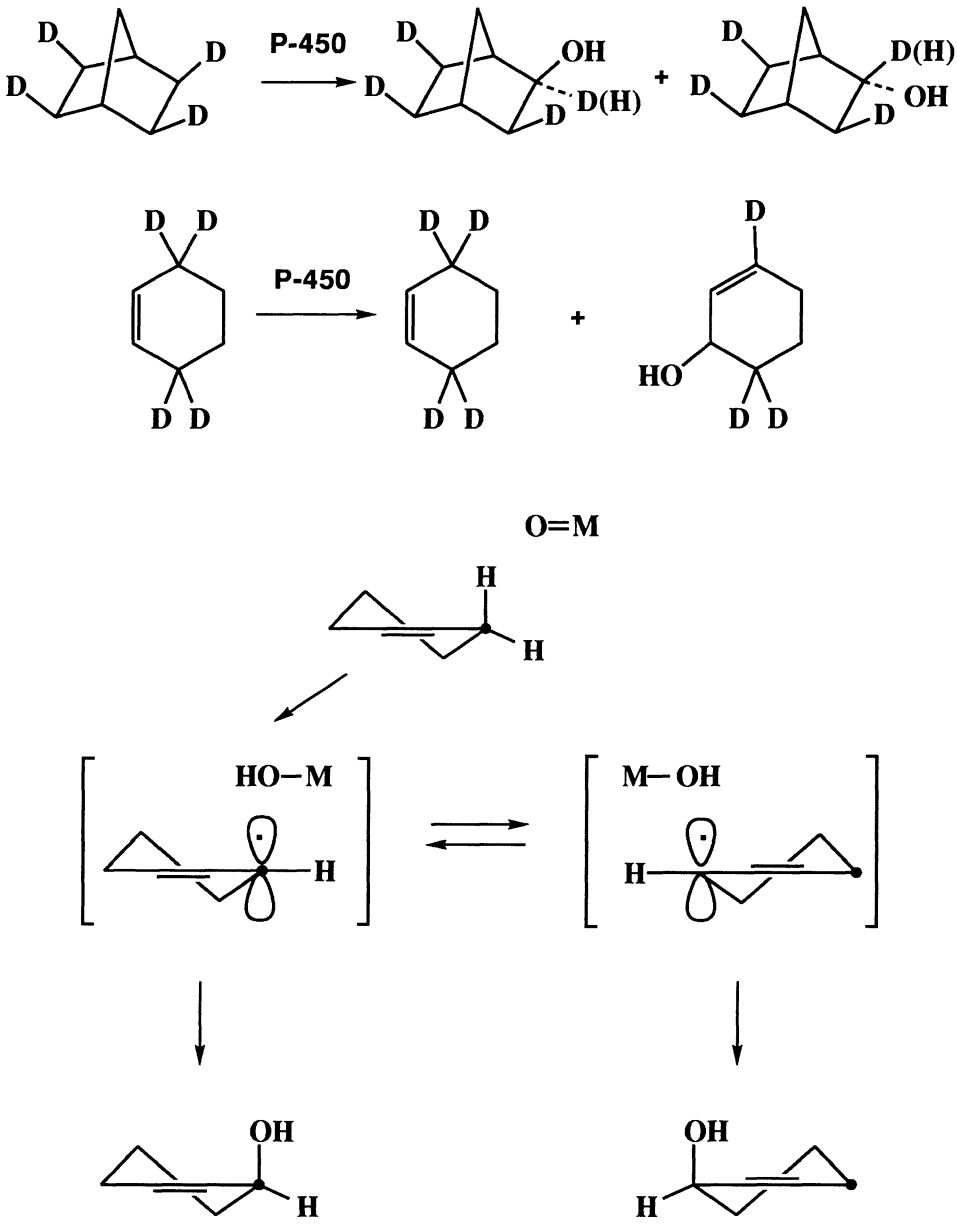

Scheme III. Epimerization and allylic scrambling observed for cytochrome P-450 catalyzed hydroxylation.

significant amount of epimerization at the carbon center. Thus, the hydroxylation of *exo-exo-exo-exo*-tetadeuterionorbornane by P-450$_{LM}$ and in the hydroxylation of camphor by P-450$_{cam}$ gave *exo*-alcohol with the retention of the *exo*-deuterium label (Scheme III). The hydroxylation of selectively deuterated cyclohexene proceeded with substantial allylic scrambling (Scheme III).[10] The intrinsic isotope effects for the oxygen insertion into a C-H bond are very large[11]: (1) k_H/k_D = 11.5 ± 1.0 for the hydroxylation of tetra-*exo*-deuterated norbornane. (2) k_H/k_D = 11 for the benzylic hydroxylation of [1,1-D]-1,3-diphenylpropane, (3) k_H/k_D = 10 for the O-demethylation of *p*-trideuteriomethoxyanisole, and (4) k_H/k_D = 13.5 for the demethylation of 7-methoxycumarin. These large isotope effects are inconsistent with an insertion process and indicate that the C-H bond is essentially half-broken in a linear [O···H···C] transition state and thus provide strong evidence for a nonconcerted mechanism.

The existence of a complex between the ferryl species **1** and olefins as an intermediate on the epoxidation pathway is supported by several lines of evidence.[8] It is clear from the variety of data that more than one type of intermediate can intervene depending upon the nature of the substrate olefin and the structure of the porphyrin. Several of the proposed intermediates are shown in Figure 2.

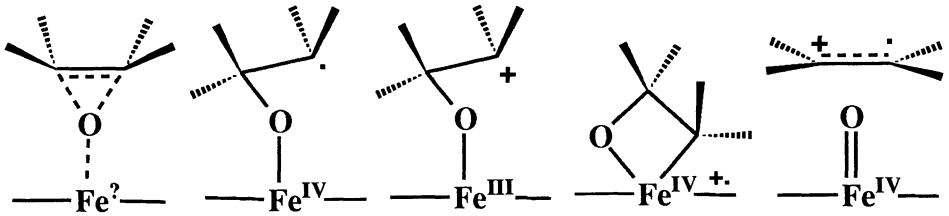

Figure 2. Proposed intermediates in epoxidations by cytochrome P-450 and metalloporphyrins.

Cyclohexene has been shown to be a revealing substrate for the nature of reactive metalloporphyrin intermediates in both model and enzyme regimes[12]. In this paper we demonstrate that while the epoxidation of cyclohexene by the oxoiron porphyrins such as **1** passes through an intermediate complex, the competing allylic hydroxylation does not proceed from this complex.

The oxygenation of cyclohexene by **1** with different axial ligands was compared with that of an iodosylbenzene-mediated reaction catalyzed by Fe^{III}(TMP)Cl. The reactions were performed in CH_2Cl_2 at various temperatures with MCPBA/Fe(TMP)Cl, PhIO/Fe(TMP)Cl and with MCPBA/Fe(TMP)Cl in 5% MeOH and the ratio of epoxidation to hydroxylation was determined in each case (eq. 1).

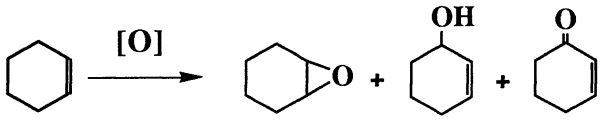

$$\text{ratio} = \frac{[3]}{[4]+[5]} \qquad (1)$$

2 **3** **4** **5**

The results presented in Figure 3 show that although the observed product ratios for all reactions were similar at room temperature, the changes observed upon varying the temperature differed markedly. The response of the iodosylbenzene reaction to lower temperature (curve b) was to produce more epoxide, while for the MCPBA reaction (curve a) allylic hydroxylation increased and eventually became the major product. For the same reaction in 5% MeOH (curve c) a more complicated behavior was observed. The reaction of cyclohexene with MCPBA /Fe(TMP)OH was examined at -78°C as well and the epoxidation/hydroxylation product ratios obtained from **1** prepared from Fe(TMP)OH, Fe(TMP)Cl and Fe(TMP)Cl in 5 % MeOH/CH_2Cl_2 were found to be 0.44, 0.8 and 2.4, respectively.

That the trend observed for the MCPBA-initiated reaction eventually reversed the major and minor products (Fig. 3, curve a) rules out *any* mechanism in which one common intermediate (or transition state) leads to all products. Similarly, two simple, independent pathways cannot be accommodated by these results. In both cases the relative amount of the minor product is expected to decrease with temperature due to its larger activation energy, as was the case for the iodosylbenzene catalyzed reaction (Fig. 3, curve b).

The different temperature behavior of the PhIO and MCPBA mediated reactions can be accommodated by assuming that only epoxide is formed from a reversibly formed complex between (O)Fe(IV)TMP^+ (**1**) and cyclohexene . This mechanism is outlined in Scheme IV and is based on the following observations. Formation of a complex between **1** and olefins has been shown by us to be fast and reversible under conditions for which epoxide formation is slow,[8] whereas hydrogen abstraction leading to **4** should be irreversible.

The general kinetic expression for the epoxide/alcohol ratio for this situation is $k_1k_2/k_3(k_{-1}+k_2)$, which predicts that under conditions for which complex formation is reversible, the epoxide/alcohol ratio is governed by K_1k_2/k_3, whereas for irreversible, rate-determining complex formation, the product ratio is k_1/k_3. Since at low temperature $k_{-1}>>k_2$, increasing the temperature should indeed decrease the difference between these constants, but never to the extent as to change the relative order of k_{-1} and k_2. For this to happen there must be an additional variable which is suggested by the results with various catalysts to be the axial ligand.

We have shown that the reversible formation of a complex between **1** and styrene was made irreversible and rate determining by the addition of methanol[8]. A similar trend toward irreversibility of the formation of **6** in methanol-containing solutions should be reflected in a higher epoxide/alcohol ratio as was indeed observed. The fact that **1** prepared in 5% MeOH containing CD_2Cl_2[13] or toluene-d_8[14] has been identified as $[(O)Fe^{IV}TMP^{\cdot+}(HOCH_3)]^+X^-$ rather than $(O)Fe^{IV}TMP^{\cdot+}(X)$ and the different product ratios obtained with Fe(TMP)OH and Fe(TMP)Cl leads one to conclude that *at the complex formation step between 1 and cyclohexene, the ligand (X in 6) is still bound and involved in the rate determining step* .

Another indication of the difference between the various $(O)Fe^{IV}TMP^{\cdot+}(X)$ species is the observation that for samples of **1** prepared by the MCPBA oxidation of Fe(TMP)Cl and Fe(TMP)OH in CD_2Cl_2, only broad, unresolved ^{1}H-NMR resonances were observed. Addition of 5% CD_3OD to the former solution resulted in the characteristic ^{1}H NMR spectrum of $[(O)Fe^{IV}TMP^{\cdot+}(HOCH_3)]^+X^-$ [7] whereas $Fe^{IV}TMP(OCH_3)_2$ was formed from CD_3OD addition to the latter solution[15]. Significantly, when solutions of **1** were prepared at -78°C and subjected to temperature excursions prior to olefin addition, the product selectivity observed was characteristic of the final temperature.[16]

We conclude that allylic hydroxylation and epoxidation of cyclohexene by **1** proceed via independent pathways one of which involves an intermediate. This is consistent with the formation of a complex (**6**) between the high valent iron oxo species (**1**) and the olefin on the pathway to epoxide formation, which under normal catalytic conditions is rate

determining. However, at low temperatures and/or with strongly bound sixth ligands, formation of the complex **6** must be a reversible and non-rate limiting step.

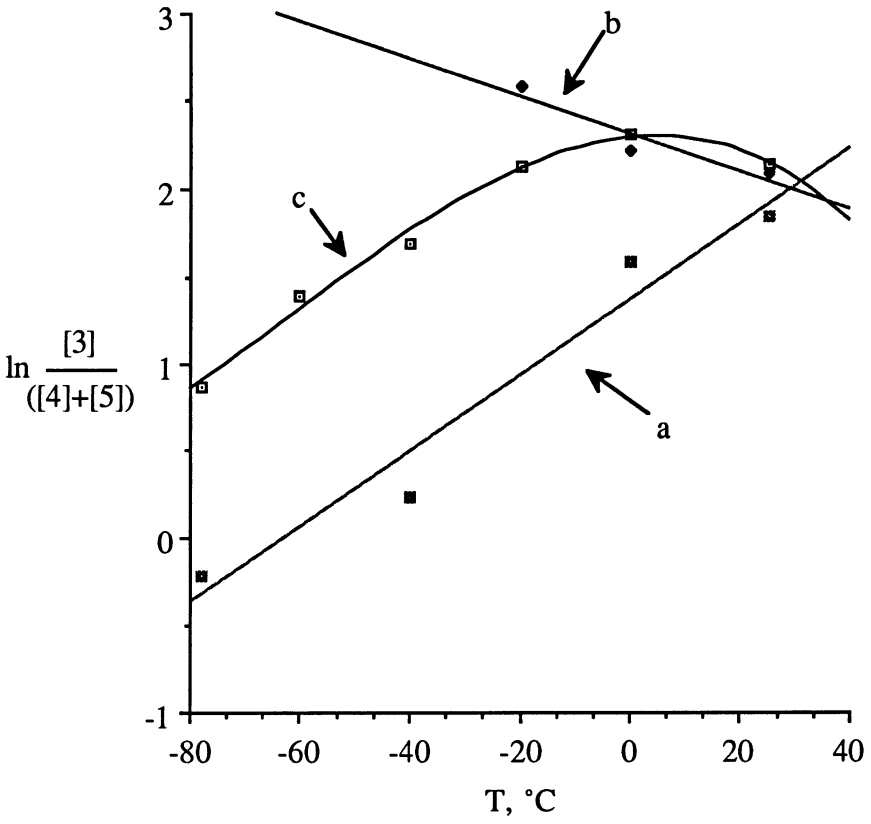

Figure 3. Product ratios (cyclohexene oxide/(cyclohexen-3-ol + cyclohexen-3-one, [**3**]/([**4**] + [**5**])) for Fe(TMP)Cl catalyzed oxidation[a-c] of cyclohexene at various temperatures.[d] [a] MCPBA mediated reactions; at T ≥ -20°C addition of 0.95 equiv MCPBA to a solution of 2.5 μmol Fe(TMP)Cl and 18 equiv cyclohexene in 150 μL CH_2Cl_2 and for T≤ -40°C 10 μL of 1.2 eq. MCPBA solution were added to 2.5 μmol Fe(TMP)Cl in 150 μL CH_2Cl_2 to observe the characteristic green color of **1** and then 18 eq. cyclohexene were added. The product ratios at RT, 0, -40 and -78 °C were 6.3, 4.9, 1.27 and 0.8, respectively. [b] PhIO mediated; 250 μmol cyclohexene, 100 μmol PhIO and 0.6 μmol Fe(TMP)Cl in 1 mL CH_2Cl_2 for 1 hr; The product ratio at RT, 0 and -20 °C were 8.1, 9.2 and 13.2 respectively. [c] The same reaction conditions as for a, but in 5 % MeOH/CH_2Cl_2. The product ratio at RT, 0, -20, -40, -60 and -78 °C were 8.55, 10.1, 8.4, 5.4, 4.0 and 2.4 respectively. [d] Determined by glpc by comparison to authentic samples.

The ligand effect described here may be helpful in understanding the role of the axial ligand in determining the reactivity and selectivity of metalloporphyrin catalysts and in controlling the range of reactivities of heme enzymes[17]. It also illuminates the surprising richness and complexity of these oxygenation reactions which continue to be under investigation in this laboratory.

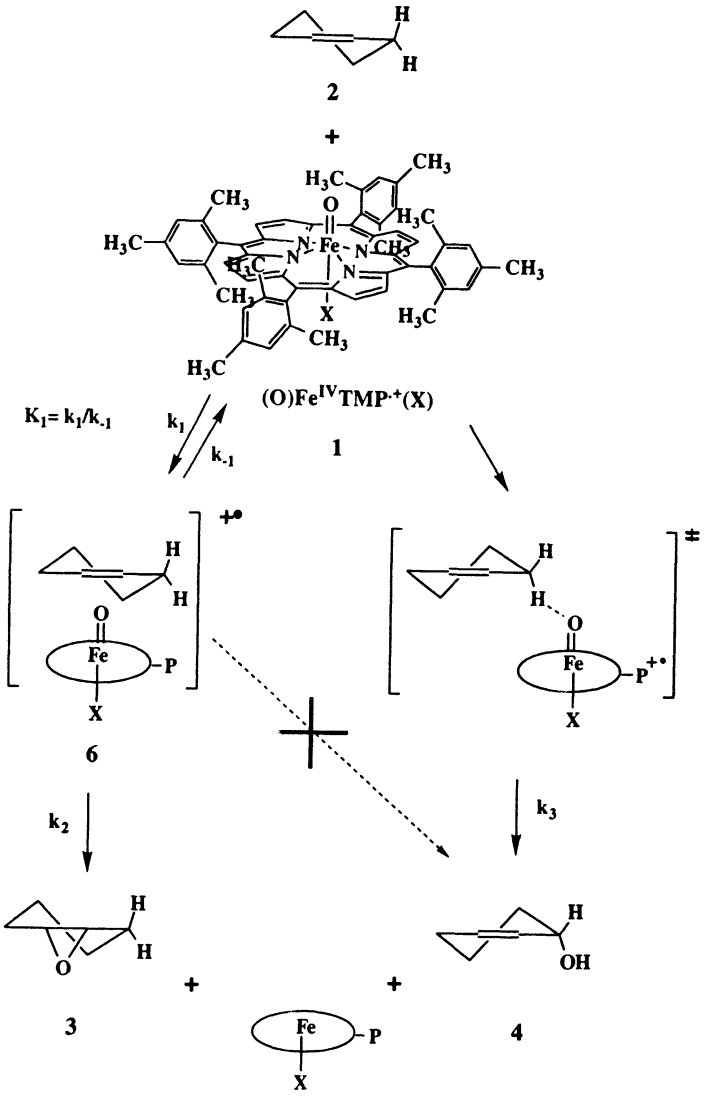

Scheme IV

Acknowledgments

Financial support of this research by the National Institutes of Health (GM-36298) is gratefully acknowledged. Postdoctoral fellowship support for Z.G. from the CIES (Fulbright) is gratefully acknowledged as well.

References

†Present address: Department of Chemistry, Technion, Israel Institute of Science, Technion City, Haifa 3200, Israel.

(1) (a) Groves, J. T.; McClusky, G. A. in *Biochemical and Clinical Aspects of Oxygen*, Caughey, W. S. Ed., Academic Press: New York, 1979, p. 227. (b) Guengrich, F. P.; MacDonald, T. L. *Acc. Chem. Res.* **1984**, *17*, 9. (c) McMurry, T. J.; Groves, J. T. in Cytochrome P-450, Ortiz de Montellano, P. R. Ed., Plenum Press: NY 1986, pp. 1-28. (d) Watanabe, Y. and Groves, J. T. "Molecular Mechanism of Oxygen Activation by Cytochrome P-450" in *The Enzymes*, 3rd edition, Vol XX, "Mechanisms of Catalysis", D. Sigman, Ed., Academic Press, San Diego, 1992, pp 406-453.

(2) (a) Traylor, T. G.; Miksztal, A. R *J. Am. Chem. Soc.* **1989**, *111*, 7443. (b) Traylor, T. G.; Nakano, T.; Dunlap, B. E.; Traylor, P.S.; Dolphin, D.*J. Am. Chem. Soc.* **1986**, *108*, 2782. (c) Traylor, T. G.; Xu, F. *J. Am. Chem. Soc.* **1988**,*110*, 1953. (d) Traylor, T. G.; Miksztal, A. R. *J. Am. Chem. Soc.* **1987**, *109*, 2770.

(3) (a) Ostovic, D.; Bruice, T. C. *J. Am. Chem. Soc.* **1989**, *111*, 6511. (b) Garrison, J. M.; Ostovic, D.; Bruice, T. C. *J. Am. Chem. Soc.* **1989**, *111*, 4960. (c) Garrison, J. M.; Bruice, T. C. *J. Am. Chem. Soc.* **1989**, *111*, 191. (d) Ostovic, D.; Bruice, T. C. *J. Am. Chem. Soc.* **1988**, *110*, 6906. (e) Castellino, A. J.; Bruice, T. C. *J. Am. Chem. Soc.* **1988**, *110*, 1313. (f) Castellino, A. J.; Bruice, T. C. *J. Am. Chem. Soc.* **1988**, *110*, 158.

(4) (a) Collman, J. P.; Kodadek, T.; Brauman, J. I. *J. Am. Chem. Soc.* **1986**, *108*, 2588. (b) Kodadek, T.; Raybuck, S. A.; Collman, J. P.; Brauman, J. I.; Papazian, L. M. *J. Am. Chem. Soc.* **1985**, *107*, 4343. (c) Collman, J. P.; Brauman, J. I.; Meunier, B.; Hayashi, T.; Kodadek, T.; Raybuck, S. A. *J. Am. Chem. Soc.* **1985**, *107*, 2000. (d) Collman, J. P.; Brauman, J. I.; Meunier, B.; Raybuck, S. A.; Kodadek, T. *Proc. Natl. Acad. Sci. U. S. A.* **1984**, *81*, 3245.

(5) (a) Weber, L., Hommel, R., Behling, J., Haufe, G., Hennig, H. *J. Am. Chem. Soc.*, **1994**, *116*, 2400. (b) Centeno, F., Gutierrez-Merino, C. *Biochemistry*, **1992**, *31*, 8473. (c) Adachi, S., Nagano, S., Ishimori, K., Watanabe, Y., Morishima, I., Egawa, T., Kitigawa, T., Makino, R. *Biochemistry*, **1993**, *32*, 241. (d) Roberts, E. S., Vaz, A. D. N., Coon, M. J. *Proc. Nat. Acad. Sci. USA*, **1991**, *88*, 8963. (e) Patzelt, H., Woggon, W. *Helv. Chim. Acta*, **1992**, *75*, 523.

(6) (a) Hanzlik, R. P.; Ling, K.-H. J. *J. Org. Chem.* **1990**, *55*, 3992. (b) Leising, R. A.; Brennan, B. A.; Que, L. *J. Am. Chem. Soc.* **1991**, *113*, 3988. (c) Baldwin, J. E. *J. Heterocyclic Chem.* **1990**, *27*, 71. (d) Groves, J. T., McClusky, G. A. *J. Am. Chem. Soc.*, **1976**, *98*, 859. (d) Aikens, J., Sligar, S. G. *J. Am. Chem. Soc.*, **1994**, *116*, 1143.

(7) (a) Groves, J.T.; Haushalter, R.C.; Nakamura, M.; Nemo, T.E.; Evans, B.J. *J. Am. Chem. Soc.*, **1981**, *103*, 2884. (b) Groves, J.T.; Watanabe, Y. *J. Am. Chem. Soc.* **1988**, *110*, 8443.

(8) Groves, J. T.; Watanabe, Y. *J. Am. Chem. Soc.* **1986**, *108*, 507.

(9) Traylor, T.G.; Fann, W.P.; Bandyopadhyay, D. *J. Am. Chem. Soc.*, **1989**, *111*, 8009.

(10) (a) Groves, J. T.; McClusky, G. A.; White, R. E.; Coon, M. J. *Biochem. Biophys. Res. Commun.* **1978**, *81*, 154. (b) Groves, J. T.; Subramanian, D. V. *J. Am. Chem. Soc.* **1984**, *106*, 2177.

(11) (a) Hjelmeland, L. M.; Aronow, L.; Trudell, J. *Biochem. Biophys. Res. Commun.* **1977**, *76*, 541. (b) Foster, A. B.; Jarman, M.; Stevens, J. D.; Thomas, P.; Westwood, J. H. *Chem. Biol. Interact.* **1974**, *9*, 327. (c) Miwa, G. T.; Walsh, J. S.; Lu, A. Y. *J. Biol. Chem.* **1984**, *259*, 3000.

(12) Groves, J.T.; Avaria-Neisser, G.E.; Fish, K. M.; Imachi, M.; Kuczkowski, R.L. *J. Am. Chem. Soc.*, **1986**, *108*, 3837.

(13) (a) McMurry, T.J. Ph.D. Thesis, The University of Michigan, Ann Arbor, 1984. (b) Groves, J.T.; McMurry, T.J. *Revista Portuguesa de Quimica* **1989**, *27*, 102.

(14) Balch, A.L.; Latos-Grazynsky, L.; Renner, M.W. *J. Am. Chem. Soc.*, **1985**, *107*, 2983.

(15) (a) Groves, J.T.; Quinn, R.; McMurry, T.J.; Lang, G.; Boso, B. *J. Chem. Soc., Chem. Commun.* **1984**, 1455. (b) Groves, J.T.; Quinn, R.; McMurry, T.J.; Nakamura, M.; Lang, G.; Boso, B. *J. Am. Chem. Soc.*, **1985**, *107*, 354.

(16) Results for the iodosylbenzene mediated reaction suggest that in this case the intermediate **1** is formed without a sixth axial ligand, however reaction could not be studied in 5% MeOH/CH_2Cl_2 due to the formation of $(O)Fe^{IV}TMP$ which also reacts with cyclohexene; Groves, J.T.; Gross, Z.; Stern, M., *Inorg. Chem.*, **1994**, *in press.*

(17) (a) Hanson, L.K.; Chang, C.K.; Davis, M.S.; Fajer, J. *J. Am. Chem. Soc.* **1981**, *103*, 663. (b) Belal, R.; Momenteau, M.; Meunier, B. *J. Chem. Soc., Chem. Commun.* **1989**, 412. (c) Groves, J.T.; Krishnan, S.; Avaria, G. E.; Nemo, T.E.; in "Advances in Chemistry", Series 191, **1980**.

SELF-ASSEMBLY, CATALYSIS AND ELECTRON TRANSFER WITH METALLOPORPHYRINS IN PHOSPHOLIPID MEMBRANES

RONALD M. KIM, GWENDOLYN D. FATE, JESUS E. GONZALES, JOYDEEP LAHIRI, SOLOMON B. UNGASHE & JOHN T. GROVES
Department of Chemistry
Princeton University
Princeton, New Jersey 08544, USA

ABSTRACT: The design and assembly of synthetic hemes in a model membrane is described. A synthetic porphyrin with four steroidal appendages has been designed to bind to phospholipid membranes. The iron and manganese derivatives of this porphyrin are selective catalysts for the epoxidation of olefins and the hydroxylation of saturated carbon centers. Regioselectivity is imposed by the restricted motion of the substrates and catalyst in the lipid environment. Electron transfer reactions to and from this membrane-embedded porphyrin have also been explored. It is shown that ferricytochrome *c* is recruited to the membrane surface through ionic interactions with the anionic zinc porphyrin to form a protein-molecule complex. Electron transfer among various components in this membrane ensemble suggest a medium-mediated process through multiple pathways over a distance of ca. 23 Å.

The biological importance of processes catalyzed by membrane associated multienzyme systems has stimulated intensive research aimed at understanding the chemical nature of these transformations. Yet the sheer complexity of these natural systems, and the lack of information regarding the structure and topology of the enzymes and enzyme complexes, especially of membrane-bound proteins, has made investigation of these systems difficult. As a result, a great deal of effort has been put forth creating relatively simple enzyme models which allow for the systematic variation of factors which dictate the reactivity of the natural systems[1]. One approach involves synthesizing elaborately arranged molecules in which the reactive centers are covalently linked, often by rigid spacers. An alternative approach, which will be reviewed in this chapter, involves compartmentalizing relatively simple components in membrane bilayers and non-biological organized media, forming supramolecular arrays capable of biomimetic activity. While some of these self-assembling systems attempt to closely approximate the structural and topological features of the natural enzyme complexes, others invoke completely abiological components to affect the desired transformations. In either case, a major role of the host matrix is to serve as a scaffolding for arrangement of the individual components into functional arrays. Furthermore, the microenvironment provided by the host (hydrophobic, electrostatic, amphipathic, etc.) may alter the reactivity of the catalysts, potentially leading to novel reactivity[1b, 2]. Because the self-assembling systems typically make use of non-covalent forces to organize relatively simple individual components, synthesis is often facilitated in comparison to covalently-linked models. The supramolecular systems require, however, that close attention be paid to the spatial disposition of the individual groups relative to the host matrix and to each other, as well as to their mobility in, and their affect on, the organizing medium. Because of the variety of transformations catalyzed by porphyrins and metalloporphyrins, in addition to their prominence in biological systems, incorporation of porphyrins into ordered host matrices has been invoked in the development of such materials as photoconversion and photostorage devices, conductors and semiconductors, non-linear optical materials,

D.P. Kessissoglou (ed.), Bioinorganic Chemistry, 49-56

oxidative catalysts, and oxygen transport agents. This chapter will present a brief description of biological membranes, and artificial bilayers which serve as biomembrane models, and review some of the efforts to assemble artificial heme-containing systems in membrane bilayers and in non-biological matrices.

The membrane-spanning porphyrin H_2ChP, **1**, was designed and synthesized and demonstrated to insert in a highly ordered microenvironment within phosphatidylcholine bilayers[3].

The C_2-symmetric porphyrin was designed to reside at the core of bilayer membranes, anchored by the steroid appendages located on the *meso* phenyl rings. This orientation was corroborated by EPR spectroscopy of metallo derivatives[3b]. Oriented EPR spectra of Cu^{II}ChP incorporated in phospholipid multibilayers indicated that the heme plane lay parallel with the membrane surface. The depth of the macrocycle in the membrane was probed using a "plum bob" experiment, in which α–ω alkyl imidazole acids of varying chain length were added to membrane-intercalated CoChP, and coordination of the imidazole to Co(II) was determined by EPR spectroscopy. Ligation was only observed with a carbon chain-length $n \geq 8$, which is consistent with localization of the heme at the middle of the bilayer. The fluorescence spectrum of the ZnChP in DPPC membranes was also indicative of a hydrophobic environment[4]. The location of the porphyrin ring in the membrane interior, oriented parallel to the membrane surface, offers good topological mimicry of the P-450 heme cofactor in the inner mitochondrial membrane[5]. In addition, the hydrophobic pocket formed above the heme plane by the steroid appendages and lipid chains serves as a good model for the hydrophobic active site of P-450$_{cam}$ determined from the crystal structure[6], and for P-450 liver hydroxylase enzymes, whose active sites are also believed to be hydrophobic clefts[7].

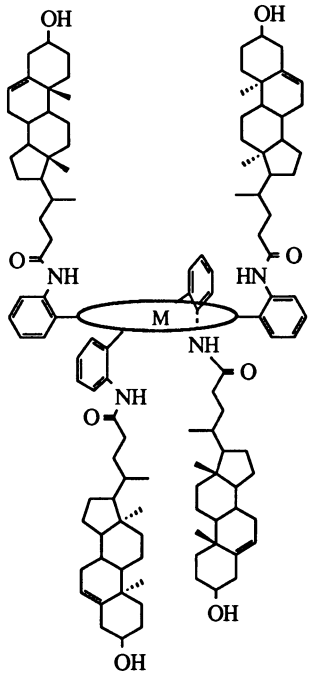

1 MChP, M = Fe^{III}, Co^{II}, Mn^{III}, Cu^{II}

We have utilized the highly ordered microenvironment of liposome-intercalated FeChP, **1-Fe**, and MnChP, **1-Mn**, to catalyze highly regioselective oxidations of amphiphilic substrates[3]. The ordered microenvironment was indeed shown to direct regioselectivity in the hydroxylation and epoxidation of amphiphilic steroid and fatty acid substrates. For example the membrane assembly catalyzed exclusive epoxidation of the side-chain double bond of desmosterol, even though oxidations in homogeneous solution showed the B-ring double bond to be more susceptible toward epoxidation. Similarly, cholesterol was selectively hydroxylated at the C-25 side chain position. An idealized depiction of the orientation of desmosterol and the leading to the observed product is shown in **Figure 1.**

We have extended this work, creating a biocompatible assembly depicted in Figure 2 which utilizes molecular oxygen to oxidize lipophilic substrates[8]. The zwitterionic flavin AmFl, **2**, was shown to catalyze reduction of Mn^{III}ChP by flavoenzyme pyruvate oxidase (PO) in the aqueous phase, which itself received electrons from pyruvate. In the presence of oxygen, the pyruvate

oxidase/AmFl/MnChP system catalyzed the oxidation of ethyl benzene to methylphenylketone. No oxidation of substrate was measured upon omission of any of the components.

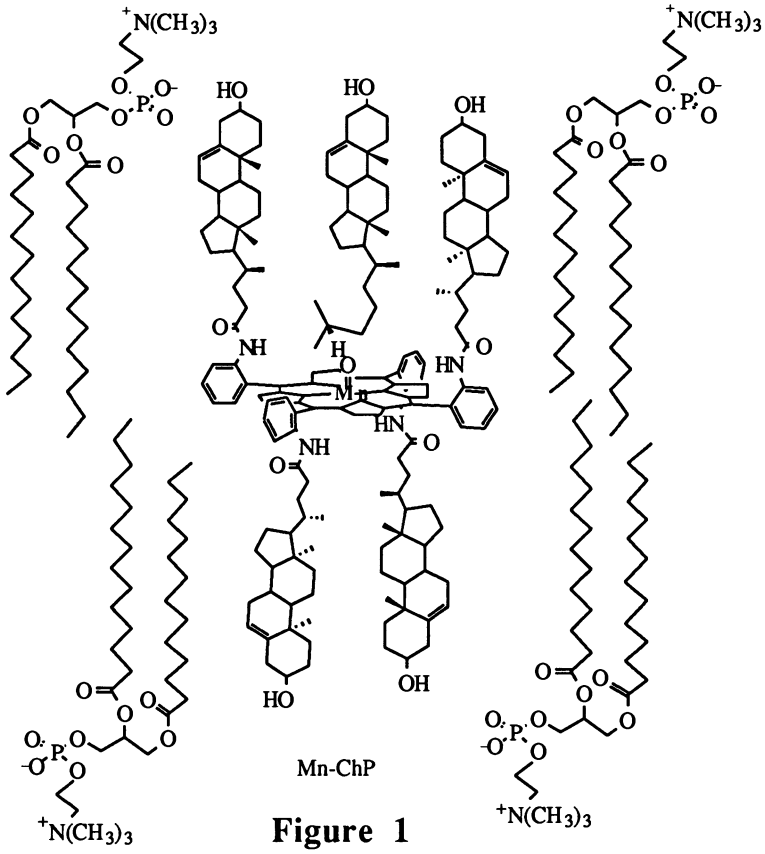

Figure 1

The proposed mechanism of oxidation involves AmFl-mediated reduction of $Mn^{III}ChP$ by PO, oxygen ligation to Mn(II), and oxygen activation upon introduction of a second reducing equivalent, analogous to the P-450 catalytic. The AmFl/MnChP redox couple is believed to be a good topological model for the P-450 reductase/P-450 binary complex.

A multi-component electron transfer chain which closely models the topological arrangement of redox partners in the liver microsomal hydroxylase system has been assembled[4]. During its catalytic cycle, $P\text{-}450_{LM}$ receives two reducing equivalents from cytosolic NAD(P)H via an associated two-electron/one-electron shuttle cytochrome P-450 reductase, which contains an FAD and FMN cofactor. A schematic depiction of the possible arrangement of redox sites is shown in **Figure 3**. The artificial assembly, which consists of NADPH, zwitterionic flavin AmFl, **2**, and MnChP **1-Mn**, mimics the spatial disposition of the natural redox sites in the membrane.

Figure 2

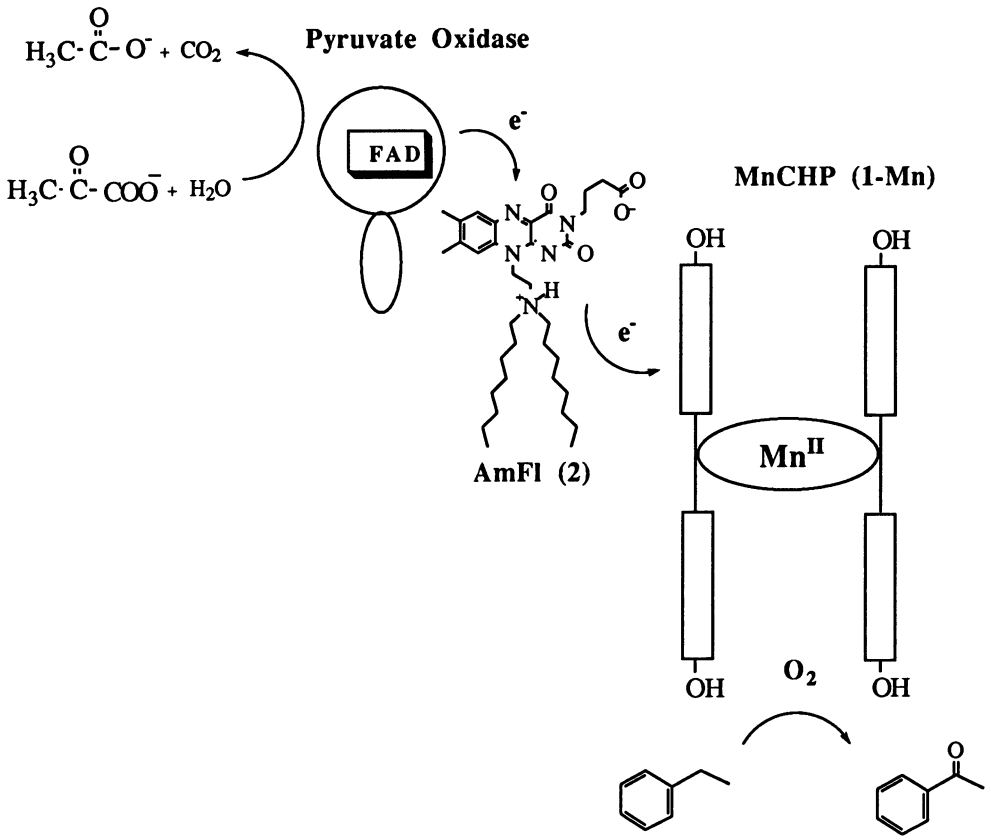

Kinetic studies revealed that the mechanism of electron transfer from NADPH to vesicular $Mn^{III}ChP$ was analogous to P-450 reductase-catalyzed reduction of ferric P-450 by NADPH[9], and thus entailed rapid reduction of the flavin by NADPH, followed by rate-limiting electron transfer from the dihydroflavin to Mn(III). The rate of $Mn^{III}ChP$ reduction was slower than P-450 reduction by ca. two orders of magnitude, and may reflect the lack of complexation between the flavin and heme centers.

In addition to supramolecular assemblies which shuttle electrons from aqueous reductants to liposome-intercalated MnChP, we have demonstrated that $Mn^{II}ChP$, **1-Mn**, can transfer electrons to ferricytochrome c, docked to the membrane surface by a tricationic porphyrin amphiphiles, ZnTCAP **3**[4] and ZnTCImAP, **4**[10]. The infusion of the amphiphilic zinc porphyrin **4** into vesicular solutions of **1-Mn** were shown to form the 1:1 adduct **5**. Binding of cyt c to **5** to produce the termolecular ensemble **6** was shown to be stoichiometric with a binding constant of ca. 10^7.

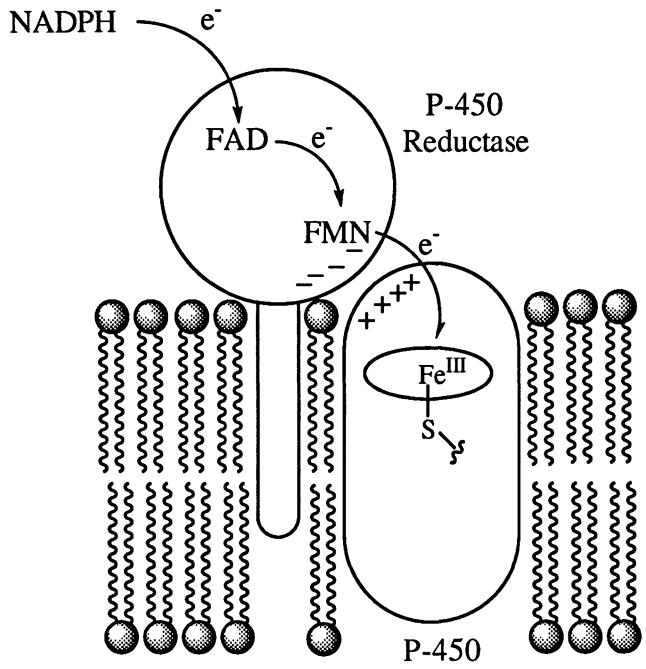

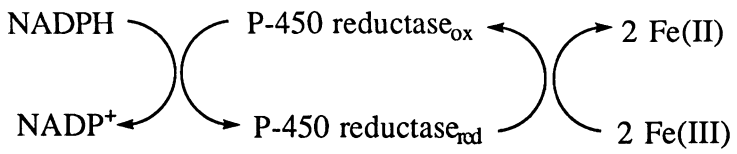

Addition of cytochrome c to mixed DMPC/DPPC vesicles containing Mn^{II}ChP and ZnTCAP resulted in reduction to ferrocytochrome c with concomitant formation of Mn(III). Reduction was first order in the Mn^{II}ChP-zinc amphiporporphyrin **4**-ferricytochrome c assembly, indicating that cyt c and MnChP were complexed. By contrast, vesicles containing cyt c with MnChP, ZnTCAP lacking the imidazole ligand showed second order kinetic behavior. Thus, the reduction kinetics for the ternary species **6** was *consistent with electron transfer from MnIIIChP to Fe(III) in a single three-component complex.* By comparing the rate of electron transfer with other similar systems of known distance, the electron transfer rate was used to estimate the distance between the Fe and Mn in the three-component assembly. Factors such as reorganizational energy and the decay constant were assumed to be similar with other systems. The distance thus estimated from the electron transfer rate was ca. 23 Å, which is remarkably similar to that anticipated from models.

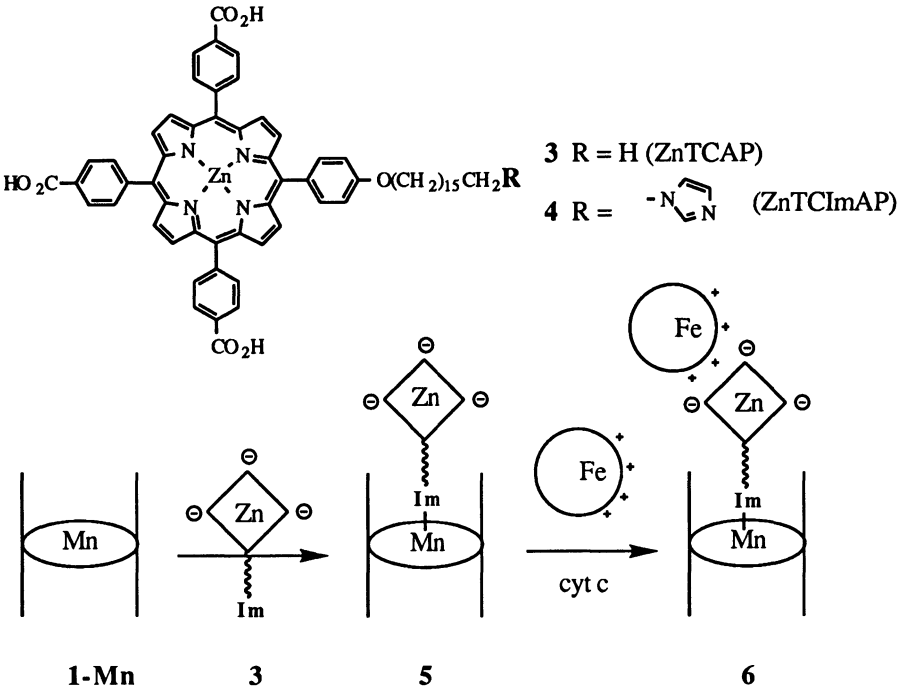

We have recently reported the formation of a proton-selective ion channel consisting of porphyrin-templated peptide helices[11]. Previous work by DeGrado demonstrated that in the presence of an electric potential, amphiphilic peptide helices lined with hydroxyl groups on one helical face and hydrophobic groups on the other face formed proton-selective ion channels[12]. From molecular modeling studies, and by analogy with natural ionophores composed of amphiphilic helices, it was predicted that the conducting state consisted of a parallel four-helix bundle. In order to verify the tetrameric nature of the ionophores, and to create more stable pore structures, four peptide units were linked via amide linkages to tetrakis(*m*-carboxyphenyl)porphyrin, affording tetraphilin **5**, shown in Figure **4**. Computer modeling indicated that the *meta* linkages were well-oriented to allow for tetramer formation, and would also permit rotation of the *meso* phenyl groups, thereby allowing the helices to "seek out" favorable conformations. Insertion of tetraphilin into BLM's indicated that the porphyrin-templated peptides indeed formed ion channels through the membrane which were proton-selective, confirming the four-helix bundle structure of the ionophores. Both the frequency and the length of the conducting state were enhanced in **5** vs. untemplated helices, demonstrating that templating of the peptide units to the porphyrin enhanced formation of the conducting state. Additionally, the low voltage dependence of the conducting state suggests that, unlike the unmodified peptides, the peptide units of the tetraphilin predominantly span the bilayer, even in the absence of an applied potential.

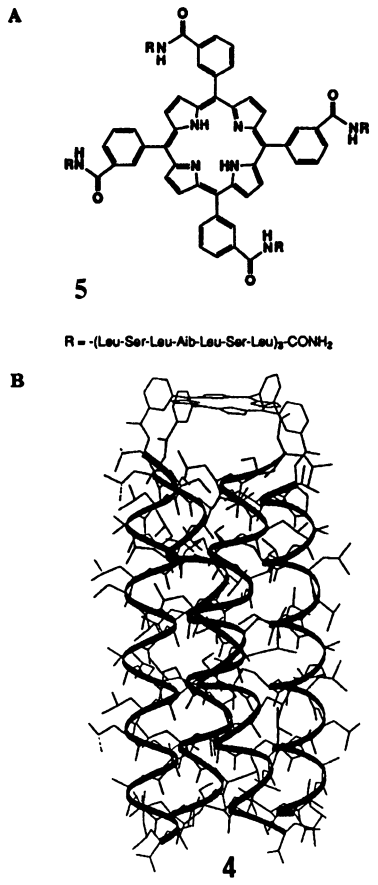

Figure 4. Structure of tetraphilin **5**. (Top) Chemical structure showing the peptide attachment sites to the porphyrin template, (bottom) energy-minimized computer model of the proposed proton-conducting state.

Acknowledgments

Financial support of this research by the National Institutes of Health (GM-36298) and the National Science Foundation is gratefully acknowledged.

References

(1) (a) Ungashe,S. B. and Groves,J. T. "Porphyrins and Metalloporphyrins in Synthetic Bilayer Membranes", in *Advances in Inorganic Biochemistry*, Vol. 9, L. G. Marzilli, Ed., Academic Press, **1993**, 318-351. (b) Balzani, V.; Moggi, L.; Scandola, F., in *Supramolecular Photochemistry*, Balzani, V. Ed.; D. Reidel Publishing Co.: Dordrecht, Holland 1987, p. 1-28. (b) Hurst, J.K., in *Kinetics and Catalysis in Microhetrogeneous Systems*; Gratzel, M.; Kalyanasundaram, Eds.; Marcel Dekker, Inc.: New York, 1991; p. 183-226. (c) Fendler, J.H., *Membrane Mimetic Chemistry*, John Wiley & Sons: New York, 1982.

(2) Fendler, J.H. *Chem. Rev.* **1987**, *87*, 877.

(3) (a) Groves, J.T.; Neumann, R. *J. Am. Chem. Soc.* **1987**, *109*, 5045. (b) Groves, J.T.; Neumann, R. *J. Am. Chem. Soc.* **1989**, *111*, 2900. (c) Groves, J.T.; Neumann, R. *J. Org. Chem.* **1988**, *53*, 3891.

(4) Ungashe, S.B. Ph.D. Dissertation, Princeton University, 1991.

(5) (a) Watanabe, Y. and Groves,J. T. "The Molecular Mechanism of Oxygen Activation by Cytochrome P-450. *The Enzymes*, 3rd edition, D. Sigman, Ed., Academic Press, (1992) p 405-452. (b) Cytochrome P-450,: *Structure, Mechanism and Biochemistry*, Ortiz de Montellano, P.R., Ed.; Plenum Press: New York, 1986. (c) Rich, P.R.; Tiede, D.M.; Bonner, W.D., Jr. *Biochim. Biophys. Acta* **1978**, *546*, 307.

(6) (a) Poulos, T.L.; Finzel, B.C.; Howard, A.J. *Biochemistry* **1986**, *25*, 5314. (b) Poulos, T.L.; Finzel, B.C.; Howard, A.J. *J. Mol. Biol.* **1987**, *195*, 687.

(7) White, R.E.; Coon, M.J. *Ann. Rev. Biochem.* **1980**, *49*, 315.

(8) Groves, J.T.; Ungashe, S.B. *J. Am. Chem. Soc.* **1990**, *112*, 7796.

(9) (a) Vermilion, J.L.; Coon, M.J. *J. Biol. Chem.* **1978**, *253*, 8812. (b) Vermilion, J.L.; Ballou, D.P.; Massey, V.; Coon, M.J. *J. Biol. Chem.* **1981**, *256*, 266.

(10) Groves, J. T., Fate, G. D., Lahiri, J. *J. Am. Chem. Soc.*, **1994**, *116*, *in press*.

(11) Åkerfeldt, K.S.; Kim, R.M.; Camac, D.; Groves, J.T.; Lear, J.D.; DeGrado, W.F. *J. Am. Chem. Soc.* **1992**, *114*, 9656.

(12) Lear, J.D.; Wasserman, Z.R.; DeGrado, W.F. *Science* **1988**, *240*, 1177.

MECHANISTIC STUDIES ON THE BINUCLEAR Fe ENZYMES RIBONUCLEOTIDE REDUCTASE AND PURPLE ACID PHOSPHATASE

M.A.S. AQUINO, J.-Y. HAN,
J.C. SWARTS & A. G. SYKES
Department of Chemistry,
University of Newcastle,
Newcastle upon Tyne, NE1 7RU, UK

1. Introduction

The enzymes ribonucleotide reductase (ribonucleotides → deoxyribonucleotides), purple acid phosphatase (hydrolysis of phosphate esters), methane monooxygenase ($CH_4 \rightarrow CH_3OH$), along with the O_2-carrier hemerythrin are a diverse and important category of metalloproteins containing binuclear iron centres.[1] The active site structures of three of these (RNR,[2] MMO[3] and Hr[4]) are known from X-ray diffraction studies, and from physical measurements a structure for PAP has been proposed.[5] The active form of RNR has a tyrosyl radical (Tyr·) close to (5.3 Å) but not coordinated to the $Fe(III)_2$ centre as illustrated, Figure 1. In the case of PAP

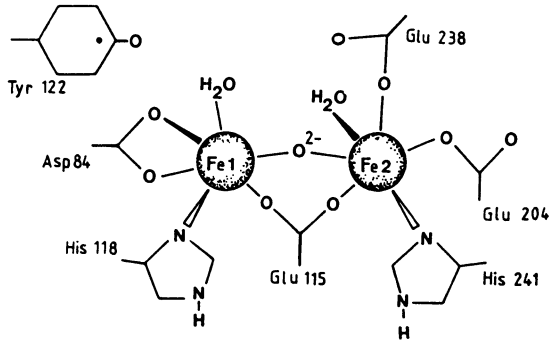

Figure 1

and MMO the active form of the enzyme is in the mixed-valent Fe(II)Fe(III) state. From physical measurements the most recently proposed PAP structures are as in Figure 2 for the

D.P. Kessissoglou (ed.), Bioinorganic Chemistry, 57-65

rest state Fe(II)Fe(III) form, and a related phosphate bound product.[5] Professor Krebs has presented the latest information on the structures of the Zn(II)Fe(III) kidney bean phosphatase.[6] There are however as yet no details from the crystallography of the amino acids which coordinate the active site. Hemerythrin in the deoxy $Fe(II)_2$ state coordinates O_2 at the vacant coordination site to give a peroxo-bound $Fe(III)_2$ product, oxyHr.[7] The structure of the hydroxylase protein of MMO has many similarities to RNR, and is at an advanced stage as reported by Professor Lippard.[3]

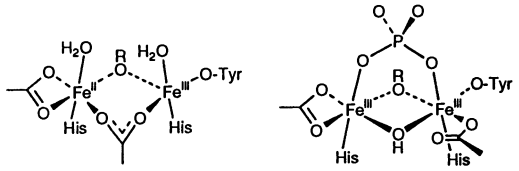

Figure 2

2. Reactivity of RNR

This enzyme from *E.coli* consists of R1 and R2 subunits each of which is a homodimer M_r 2 x 86.0 and 2 x 43.5 kDa respectively[8], Figure 3. The R1 subunit contains the binding sites for substrate and allosteric effectors and also has redox active cysteines, while R2 has the Tyr which is stabilised by a μ-oxo bridged $Fe(III)_2$ centre. The secondary alcohol at the 2'-carbon of the ribose is reduced as in (1). The first step in

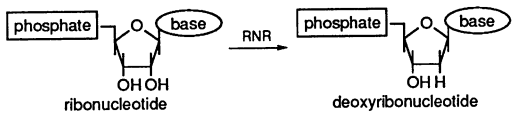

(1)

the Stubbe mechanism is the abstraction of a hydrogen atom at the 3' position.[9] The Tyr· radical of the R2 subunit is believed to be involved in this process. Later the same hydrogen is returned to the 3' position. However the radical is ~10Å buried from the hydrophobic surface of R2 which is believed to bind R1. The manner in which it is accessed and/or becomes involved in redox processes is of considerable interest therefore. A possible route for ET involves Trp48 at the proposed R1 binding surface to a hydrogen bonded Asp-237, which also forms a hydrogen bond to the Fe coordinated His-118,[2] and hence presumably to the Tyr` at 122, Figure 4.

The buried nature of the Tyr· and $Fe(III)_2$ makes it more difficult to understand the mechanism of redox processes. In addition to electron transfer from the surface, H-atom transfer with or without penetration of the protein matrix has to be considered for reactions of R2 with different reductants.[10] Although dithionite is a strong reductant, it is not able to

reduce either components of the *E.coli* R2 active centre.[11] Also reactions of R2 with inorganic complexes are generally very slow even when there is a high driving force.[12] Charge appears to bring about a significant inhibition.

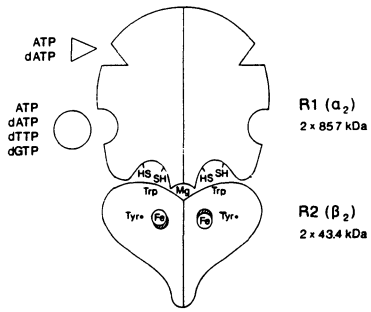

Figure 3

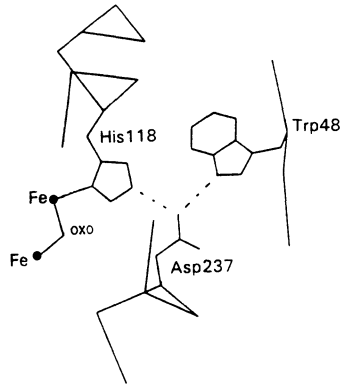

Figure 4

A number of redox studies of the *E.coli* R2 subunit of RNR have been carried out. Redox changes are generally monitored at the Tyr· peak at 410nm, or at 370nm which emphasises more the decay of the $Fe(III)_2$. Five categories of reaction of the *E.coli* R2 protein of ribonucleotide reductase (RNR) are defined from mechanistic studies with reagents of the kind hydroxyurea, methylhydroxylamine, hydroxamic acid derivatives, long-lived organic radicals of which methyl viologen $MV^{\cdot+}$ is a good example, hydrazine, catechol and its derivatives.[10]

Attention is focused on whether a particular reagent reduces only the tyrosyl radical (Tyr·) giving metR2, or the Tyr· and $Fe(III)_2$ in consecutive steps to give fully reduced R2. In the case of hydrazine (N_2H_4) reduction of the Tyr· and $Fe(III)_2$ occurs in a uniphasic process, while with di-imide (N_2H_2) it has already been demonstrated that the Tyr· is reduced and that Fe(II)Fe(III) semi-metR2 is formed.[13] A further mechanism is observed with catechol and catechol-like derivatives (in this work 3,4-dihydroxybenzo-hydroxamic here abbreviated to Didox), in which there is reduction of the Tyr· in the first stage followed by removal of the $Fe(III)_2$ in the second. The latter offers a more permanent inactivation of R2 meriting more extensive study in the context of cancer drug therapy.

The following observations can be made on the reactions described. First N_2H_4 in view of the multi-electron nature of the uniphasic reaction reported,[14] and O_2 (identification of intermediates),[15] must both react by accessing the active centre. Protonation equilibria taking place in the pH range 6.4-8.4 and which give e.g. $N_2H_5^+$ and $CH_3NH_2^+OH$ have little or no reactivity compared to the uncharged reagent. Although methylhydroxylamine (CH_3NHOH) is a better reductant than hydroxyurea ($NH_2CONHOH$) the two are about the same size and give similar rate constants $0.41M^{-1}s^{-1}$ and $0.46M^{-1}s^{-1}$ respectively. Penetration is therefore a strong possibility. Consistent with this the slightly bulkier reagents $CH_3CONHOH$ ($0.020M^{-1}s^{-1}$) and $C_6H_5CONHOH$ ($0.040M^{-1}s^{-1}$), with a hydrophobic rather than non-polar component, are less reactive. Moreover in the case of catechol, $C_6H_4(OH)_2$, and Didox,

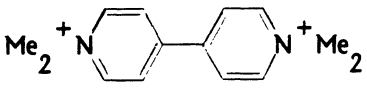

Methyl Viologen

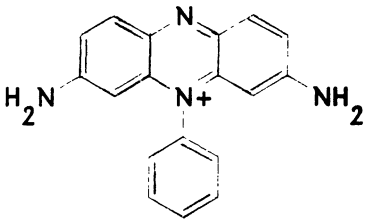

Phenosafranin

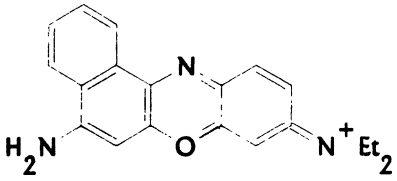

Nile Blue

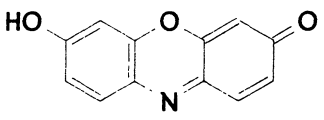

Resorufin

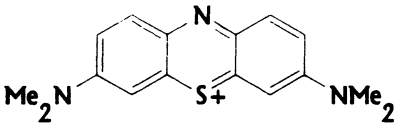

Methylene Blue

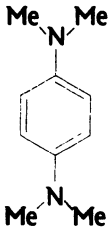

N,N,N',N'-p-Tetramethyl-phenylenediamine
(TMPD)

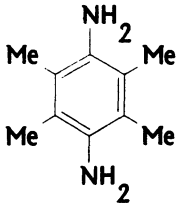

2,3,5,6-Tetramethyl-phenylenediamine
(DAD)

Figure 5

$(OH)_2C_6H_3CONHOH$, the efficient removal of the two Fe(III)'s is likely to require a mechanism of the reagent accessing the $Fe(III)_2$ site.[10]

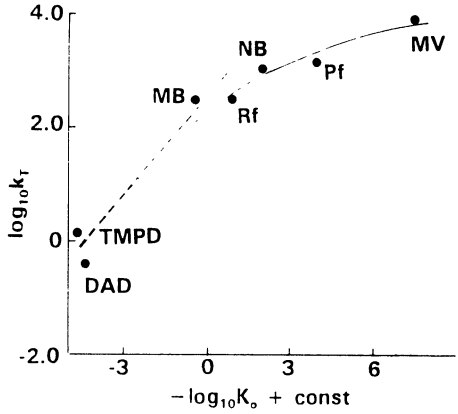

Figure 6

Reagents likely to reduce Tyr· and Fe(III), from the hydrophobic surface have also been studied, Figure 5. A feature of these reagents is that one-electron reduction potentials can be determined (as indicated). In all but the two cases phenylenediamine reagents the approach is to generate the Long-Lived Organic Radical (LLOR) with dithionite. Since the latter does not react with R2,[11] and the LLOR is generated in a rapid step, the concentration of the LLOR reagents remains constant and need not be in >10-fold excess of R2 to observe first-order kinetics. The reactions can also be adjusted to a conventional time range of study and monitored at 370nm and/or 410nm. Thus solutions of MV^{2+} for example are made up with an ~1000-fold excess of dithionite to generate the LLOR written as $MV^{\cdot+}$. Rate constants were determined in all cases for reduction of the tyrosyl radical (k_T). The free-energy plot, Figure 6, with an initial slope 0.5 is consistent with electron-transfer from the surface. Indeed penetration of such large (and in the main hydrophobic) molecules is unlikely, added to which H-atom transfer is only conceivable in those cases in which an NH_2 group is present. At high driving force the reactions appear to become diffusion controlled with a resultant levelling out of the free-energy plot.

3. Reactivity of PAP

The active mammalian Fe(II)Fe(III) form (PAP_r) has a characteristic pink colour with a peak at 510mn (ε = 4000 $M^{-1}cm^{-1}$), and the inactive Fe(III)Fe(III) form (PAP_o) a purple colour with peak at 550nm (ε = 4000 $M^{-1}cm^{-1}$).[1,16] The absorption originates from the tyrosine → Fe(III) ligand-to-metal charge transfer (LMCT) at the normally redox-inactive Fe(III) centre.[17]

Reactions of different phosphates (represented here as PO_4) with the Fe(II)Fe(III) form of purple acid phosphatase (PAP_r) from porcine uteri (uteroferrin) have been studied by

monitoring absorbance changes for the iron(III) chromophore at 620nm.[18] Reagents studied include $H_2PO_4^-$(as prototype) (•), phenylphosphate (and the *p*-nitro derivative) (+), pyrophosphate (*), tripolyphosphate (•), and adenosine 5'-triphosphate (ATP) (♦). In all cases stopped-flow rate constants are independent of total [PO_4] (10-50mM), Figure 7, and decrease with increasing pH (2.5-6.5), Figure 8.

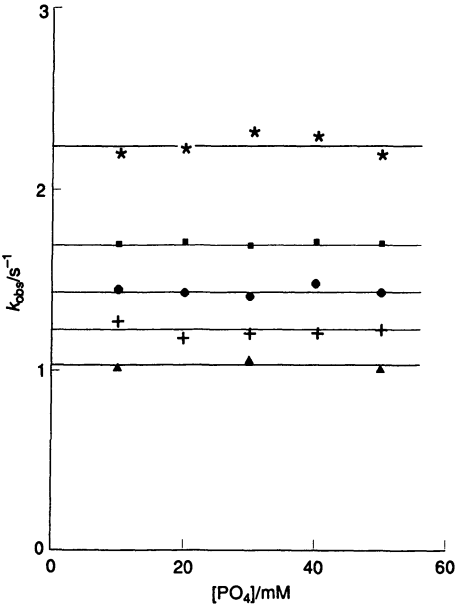

Figure 7

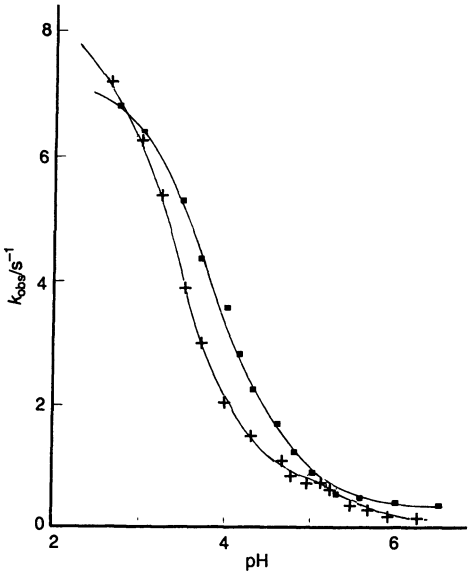

Figure 8

At the lower pH's a mechanism of rapid PO_4 binding to the Fe(II) followed by rate-controlling [PO_4]-independent bridging to the Fe(III) with displacement of a coordinated H_2O is proposed. From Figure 3 it is noted that rate constants vary little with the size and charge on the phosphate reactant.

Further information comes from experiments on the hydrolysis activity of PAP_r monitored by the release of _α-naphthol (323nm) from _α-naphthyl phosphate, which maximises at pH 4.9. The full mechanism illustrated in Figure 9 requires participation of Fe(III)-OH, which substitutes into the phosphate moiety thus bringing about hydrolysis.

The faster phosphate displacement of H_2O on the Fe(III) does not lead to hydrolysis and in such instances the reverse bridge cleavage process followed by reformation presumably occurs until Fe(III)-OH participation results in hydrolysis. Other evidence in support of this proposed mechanism are the EXAFS demonstration that phosphate bridges the two Fe's,[5] that inversion occurs at the phosphate,[19] and that there is indeed Fe(III)-OH participation.[20] An

essential part of the reaction steps proposed is the replacement of H_2O ligands one to each metal.[20]

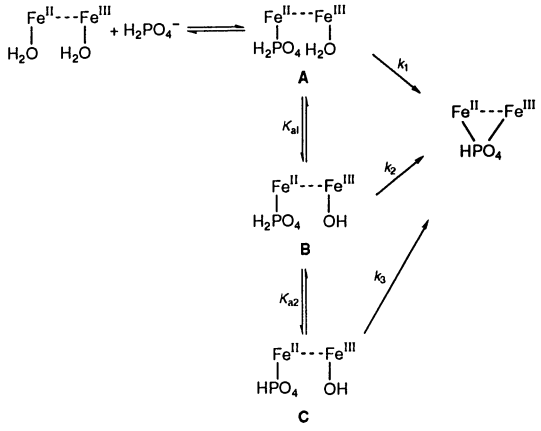

Figure 9

Equation (2) summarises the principal step in

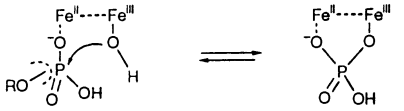

(2)

the hydrolysis, where again the existence of an equilibration process has to be stressed, i.e. the reaction does not proceed to 100% and the amount of μ-phosphato product increases as the total phosphate increases. One problem is that the equilibration makes it difficult to explain the independence of rate constants on $[PO_4]$. If coordination of PO_4 to Fe(III) involves an equilibrium process then binding of PO_4 to the less charged Fe(II) is likely to behave similarly. If however the polypeptide is also implicated in binding of PO_4 to Fe(II), then ~100% binding may result. An important observation is that PAP has an isoelectric pI of >9.6, so that at pH _7 it will retain a substantial positive charge.[21]

The presence of a positively charged region near to the binuclear Fe active centre is clearly a requirement of redox studies with negatively charged inorganic complexes as will now be described. First of all with the one-equivalent reagent $[Co(phen)_3]^{3+}$ (370mV) oxidation of PAP_r (367mV),[22] Fe(III)Fe(II) _ $Fe(III)_2$, gives simple first-order kinetics ($k = 1.26M^{-1}s^{-1}$) at pH 5.0. However with $[Fe(CN)_6]^{3-}$ (410mV) as oxidant, saturation kinetics are observed, and indicate an association process $K_{Fe} = 540M^{-1}$ prior to electron transfer, $k = 1.0s^{-1}$, as in (3)-(4).

$$PAP_r + [Fe(CN)_6]^{3-} \overset{K_{Fe}}{\Leftrightarrow} PAP_r, [Fe(CN)_6]^{3-} \qquad (3)$$

$$PAP_r, [Fe(CN)_6]^{3-} \xrightarrow{k} PAP_o + [Fe(CN)_6]^{4-} \qquad (4)$$

Furthermore the redox inactive complexes $[Cr(CN)_6]^{3-}$ ($550M^{-1}$) and $[Mo(CN)_8]^{4-}$ (1580 M^{-1}) inhibit the $[Fe(CN)_6]^{3-}$ reaction, and give association constants as indicated for interaction with PAP_r, presumably the result of an interaction at the same site.[23] This behaviour and the magnitude of values suggests a positively charged region of ~+4,[24] close to the surface of PAP_r.

The ability of Zn(II) to replace Fe(II) in plant PAP_r,[25] and initiate the same chemistry has been noted. The lability and redox inactivity of zinc supports such a functional role.

4. Acknowledgement

We thank NATO/Natural Sciences and Engineering Research Council of Canada for a Fellowship (MASA), the UK Science and Engineering Research Council for a Research Grant, the University of the Orange Free State in Bloemfontein for sabbatical leave (JCS), and the British Council and N.E. of England Cancer Research Campaign (J-YH) for their generous support of this work.

5. References

(1) (a) Wilkins, R.G., *Chem.Soc.Rev.*, **1992**, *21*, 171, (b) Vincent, J.B.; Olivier-Lilley, G.L. and Averill, B.A., *Chem.Rev.*, **1990**, *90*, 1447.

(2) (a) Nordlund, P.; Sjoberg, B.-M. and Eklund, H., *Nature*, **1990**, *345*, 593; (b) Nordlund, P. and Eklund, H., *J.Mol.Biol.*, **1993**, *232*, 126.

(3) Rosenzwig, A.C.; Frederick, C.A.; Lippard, S.J. and Nordlund, P., *Nature*, **1993**, *366*, 537, and this volume.

(4) (a) Stenkamp, R.E.; Sieker, L.C. and Jensen, L.H., *J.Am.Chem.Soc.*, **1984**, *106*, 618, (b) Sheriff, S.; Hendrickson, W.A. and Smith, J.L., *J.Mol.Biol.*, **1987**, *197*, 273, (c) Holmes, M.A.; Trong, I.L.; Turley, S.; Sieker, L.C. and Stenkamp, R.E., *J.Mol.Biol.*, **1991**, *218*, 583.

(5) True, A.E.; Scarrow, R.C.; Randell, C.R.; Holz, R.C. and Que, L., jun., *J.Am.Chem.Soc.*, **1993**, *115*, 4246.

(6) Strater, N.; Frolich, R.; Schiemann, A.; Krebs, B.; Kormer, M.; Suerbaum, H. and Witzel H., *J.Mol.Biol.*, **1992**, *224*, 511, and this volume.

(7) (a) Stenkamp, R.E.; Sieker, L.C.; Jensen, L.H.; McCallum, J.D. and Sanders-Loehr, J., *Proc.Natl.Acad.Sci., USA*, **1985**, *82*, 713, (b) McCormick, J.M.; Reem, R.C. and Solomon, E.I., *J.Am.Chem.Soc.*, 1991, 9066.

(8) (a) Carlson, J.; Fucks, J.A. and Messing, J., *Proc.Nat.Acad.Sci., USA*, 1984, 81, 4294; (b) Nilsson, O.; Eberg, A.; Lundqvist, T. and Sjoberg, B.-M., *Nucl. Acids. Res.*, **1988**, *16*, 4174

(9) (a) Stubbe, J., *Adv.Enzymol.*, **1990**, *63*, 349, (b) Stubbe, *Ann.Rev.Biochem.*, **1989**, *58*, 257.
(10) (a) Swarts, J.C. and Sykes, A.G., *Anti-Cancer Drug Design.*, **1994**, *9*, 41, (b) Swarts, J.C.; Aquino, M.A.S.; Lam, K.-Y. and Sykes, A.G., to be published.
(11) Sahlin, M.; Graslund, A.; Petersson, L.; Ehrenberg, A. and Sjoberg, B.-M., *Biochemistry*, **1989**, *28*, 2618.
(12) Lam, K.-Y.; Fortier, D.G. and Sykes, A.G., *J.Chem.Soc., Chem. Commun.*, **1990**, 1019.
(13) Gerez, C.; Gaillard, J.; Latour, J.-M. and Fontecave, M., *Ange.Chem. Int., Ed. Engl.*, **1991**, *30*, 1135.
(14) Gerez, C. and Fontecave, M., *Biochemistry*, **1992**, *31*, 780.
(15) (a) Bolinger, J.M., Jr.; Edmondson, D.E.; Huynh. B.H.; Filley, J.; Norton, J.R. and Stubbe, J., *Science*, **1991**, *253*, 292, (b) Ling, J.; Sahlin, M.; Sjoberg, B.-M.; Loehr, T.M. and Sanders-Loehr, J., *J.Biol.Chem.*, **1994**, *269*, 5595.
(16) Pyrz, J.W.; Sage, J.T.; Debrunner, P.G. and Que, L., jun., *J.Biol.Chem.*, **1986**, *261*, 11015.
(17) (a) Davis, J.C. and Averill, B.A., *Proc.Natl.Acad.Sci., USA.*, **1982**, *79*, 4623, (b) Beck, J.L.; Keough, D.T.; de Jersey, J. and Zerner, B., *Biochim.Biophys. Acta*, **1984**, *791*, 357.
(18) Aquino, M.A.S.; Lim, J.-S. and Sykes, A.G., *J.Chem.Soc., Dalton Trans.*, **1994**, 429.
(19) Mueller, E.G.; Crowder, M.W.; Averill, B.A.; Knowles, J.R., *J.Am.Chem.Soc.*, **1993**, *115*, 2974.
(20) Dietrich, M.; Munstermann, D.; Suerburn, H.; Witzel, H., *Eur.J.Chem.*, **1991**, *199*, 105.
(21) Antanaitis, B.C. and Arsen, P., *Adv.Inorg.Biochem.*, **1983**, *5*, 111.
(22) Wang, D.L.; Holz, R.C.; David, S.S.; Que, L., jun., and Stankovich, M.T., *Biochemistry*, **1991**, *30*, 8187.
(23) Aquino, M.A.S.; Lim, J.-S. and Sykes, A.G., *J.Chem.Soc., Dalton Trans.*, **1994**, 683.
(24) Chapman, S.K.; Sinclair-Day, J.D.; Sykes, A.G.; Tam, S.-C. and Williams, R.J.P., *J.Chem.Soc., Chem.Commun.*, **1983**, 1152.
(25) Beck, J.L.; McConachie, L.A.; Summers, A.C.; Arnold, W.N.; Jersey, J. de.;

STRUCTURE AND REACTIVITY OF THE BLUE COPPER PROTEINS

P. KYRITSIS, C. DENNISON & A.G.SYKES
Department of Chemistry, University of Newcastle
Newcastle upon Tyne, NE1 7RU, UK

1. Introduction

The blue copper proteins are involved in electron transport and have a single type 1 copper centre which makes use of the Cu(II) and Cu(I) oxidation states.[1] The Cu(II) proteins have two very striking non-separable properties, an intense S(Cys)→Cu(II) charge-transfer band at ~600nm, giving rise to the blue colour, and an EPR spectrum which in the parallel region gives unusually narrow hyperfine splitting[1] (3.5-6.3)x10^{-3} cm^{-1}. To date probably the best synthetic analogue which has modelled these properties is that with hydrotris(3,5-diisopropyl-1-pyrazolyl)borate and a thiolate as ligands, [{HB(3,5-ipr$_2$pZ$_3$)}Cu(SR)], where R is e.g. t-butyl.[2] This type of molecule has N_3S rather than the normally N_2S_2 donor atoms of the proteins. Properties of eight different proteins to be considered are listed in Table 1.

Protein	Source	Amino acids	pI	E^{m} (mV)	λ_{max} (nm)	ε (M^{-1} cm^{-1})
Plastocyanin	Higher plants/green algae	99	4.2	375	597	4500
Azurin	Denitrifying bacteria	128	5.4	305	625	5200
Pseudoazurin	Denitrifying bacteria	123	7 65	—	593	2900
CBP	Cucumber	96	10.5	317	597	3400
Amicyanin	Methylotropic bacteria	106	4 7	260	596	3900
Rusticyanin	*Thiobacillus ferrooxidans* bacteria	144	9.1	680	597	2240
Stellacyanin	Lacquer tree	107	9 9	184	608	4080
Umecyanin	Horseradish roots	125	5.8	283	610	3400

Structurally the proteins are very well documented from X-ray crystallography and NMR studies, Table 2. The first structure information, which was for plastocyanin from poplar leaves, appeared in Nature[3] (1978), Figure 1. While there has been extensive use of physical techniques to understand properties of the proteins, knowledge of the structures has been of particular importance. The Cu is coordinated by N(His-37), S(Cys-84), N(His-87) and S(Met-92) in a distorted tetrahedral arrangement. The imidazole ring of His-87 separates the Cu from the solvent by 6 Å. An unusually long Cu-S(Met92) bond, Figure 2, and two bond angles differing by >20° from a regular tetrahedron are features of the active site.

D.P. Kessissoglou (ed.), Bioinorganic Chemistry, 67-76

Table 2. X-ray and NMR Structures of Type 1 Cu Proteins

Plastocyanin				
Poplar leaves	Cu(II)	Freeman	1978/83	Nature/J.Mol.Biol
	Cu(I)	Freeman	1986	J.Mol.Biol.
	Apo	Freeman	1984	J.Biol.Chem.
	Hg(II)	Freeman	1986	J.Biol.Chem.
Enteromorpha prolifera	Cu(II)	Freeman	1990	J.Mol.Biol.
Oleander leaves	Cu(II)	Freeman	1991	Ph.D.Thesis
Chlamydo' reinhardtii	Cu(II)	Yeates	1993	Biochemistry
Anabaena variabilis	Cu(II)	Freeman	1994	Ph.D.Thesis
Scenedesmus obliquus	Cu(I)	Wright	1988(NMR)	Biochemistry
French bean leaves	Cu(I)	Wright	1991(NMR)	J.Mol.Biol.
Azurin				
Pseudomonas aeruginosa	Cu(II)	Adman	1978/81	Isr.J.Chem.
	Cu(II)	Huber	1991	J.Mol.Biol.
	mutants	Huber	1991/3	J.Mol.Biol.
Alcaligenes denitrificans	Zn(II)	Huber	1992	Eur.J.Biochem.
	Cu(II)	Baker	1988	J.Mol.Biol.
	Cu(I)	Baker	1990	J.A.C.S.
	Apo	Baker	1993	Acta Cryst.
	Cd(II)	Baker	1994	Acta Cryst.
Pseudoazurin				
Alcaligenes faecalis	Cu(II)	Adman/petratos	1989	J.Biol.Chem.
	mutants	Adman	1991994	Prot.Eng.
Methylobacterium AMI	Cu(II)	Kai		Acta Cryst.
Amicyanin				
Paracoccus denitrificans	Cu(II)/apo	Mathews	1993	Prot.Sci.
Thiobacillus versutus	Cu(II)	Messerschmidt	1994	J.Mol.Biol.
	Cu(I)	Canters	1994(NMR)	in press
Cucumber Basic Protein	Cu(II)	Freeman	1988	Science
Ascorbate Oxidase (squash)	Cu(II)	Messerschmidt	1989/92	J.Mol.Biol.
Nitrite Reductase				
A. cycloclastes	Cu(II)	Adman	1991	Science
A. faecalis	Cu(II)/ mutants	Adman	1994	Biochemistry

With minor differences the same active site structure is observed for other type 1 proteins, but in the case of stellacyanin, umecyanin and cucumber peeling cupredoxin (CPC - not listed in Table 1),[4] Gln replaces Met as the fourth ligand.

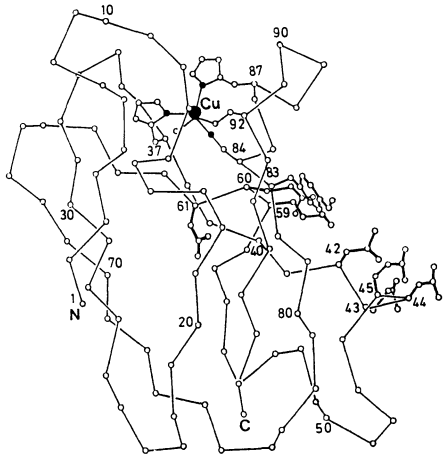

Figure 1

One difference in the case of the active site of azurin from *Alcaligenes denitrificans* is the coordination of the O-atom of the carbonyl of Gly-45 as a fifth ligand in an approximately trigonal bipyrimid arrangement, Figure 3.

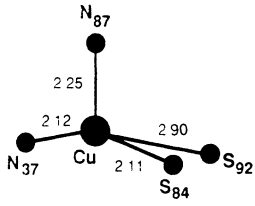

Figure 2

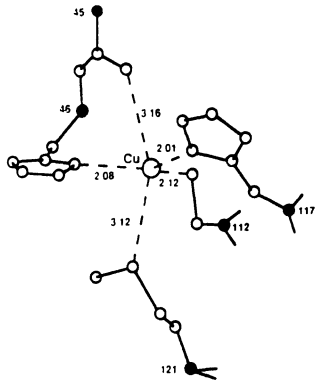

Figure 3

The axial bonds, Cu-O (3.16Å), and Cu-S(Met-121) of 3.12 Å are both long. The structure has therefore features acceptable to Cu(II) (5-coordination), and Cu(I) (trigonal 3-coordination). Whereas in the case of plastocyanin the Cu(II) is ~0.3 Å out of the plane defined by N(His-37), S(Cys-84), S(Met-92), with azurin the Cu(II) is only ~0.1 Å out of the corresponding plane. The pronounced β-sandwich structure gives a barrel

shape to the plastocyanin molecule of dimensions approximately 40 x 32 x 28 A.[5] Plastocyanin in the Cu(I) state normally has a charge balance of -9 ± 1. Notably there is a negatively charged region resulting from highly conserved acidic residues at 42-45 and 59-61 either side of an exposed Tyr-83, Figure 1. From extensive studies using inorganic complexes as redox partners, evidence has been obtained for the involvement of this **remote** site as well as the **adjacent** hydrophobic region as a site for electron transfer(ET). In particular, use has been made of the $[Fe(CN)_6]^{3}/[Fe(CN)_6]^{4-}$ (410mV) and $[Co(phen)_3]^{3+}/[Co(phen)_3]^{2+}$ (370mV) redox couples.

2. Two-Site Reactivity of Plastocyanin

As has been well documented[1], the first indications that the remote site can be used for ET came from the observation of saturation kinetic behaviour in the oxidation of PCu(I) with $[Co(phen)_3]^{3+}$ (reactant in >10-fold excess) at pH 7.5.[6] Further competitive inhibition is observed with redox inactive complexes of high positive charge such as $[Cr(phen)_3]^{3+}$, $[Pt(NH_3)_6]^{4+}$ and $[(NH_3)_5CoNH_2Co(NH_3)_5]^{5+}$, which by associating at the remote site inhibit oxidation by $[Co(phen)_3]^{3+}$.[1] An additional detail demonstrated in the course of such studies was that $[Co(phen)_3]^{3+}$ reacts _50% at this site, and in some part at a second site (most likely the adjacent site). Other support for two-site reactivity comes from ^1H NMR line-broadening of the PCu(I) protein brought about by paramagnetic redox inactive analogue complexes $[Cr(phen)_3]^{3+}$ (Tyr-83) and $[Cr(CN)_6]^{3-}$ (His-87).[7] These studies provide support for $[Fe(CN)_6]^{3-}$ reacting at the adjacent site.

Azurin on the other hand has no charged regions, and an insert of ~25 residues gives a flap in the region of the acidic patch of plastocyanin. It is possible therefore that azurin uses only one site for ET. The possibility that other type 1 proteins exhibit two-site reactivity has now been examined and will form a part of this report. Amicyanin for example with a positively charged remote site has properties appropriate for two-site reactivity. On the other hand plastocyanin from *Anabaena variabilis* has much less negative charge than other plastocyanins, with a charge balance of +1 and no negative patch. This is reflected in the behaviour observed with $[Fe(CN)_6]^{3-}$ and $[Co(phen)_3]^{3+}$ as oxidants for the PCu(I) form.

In photosynthesis plastocyanin (a solute in the inner thylakoid) transports an electron from membrane bound cytochrome f to the P700 component of photosystem I. From *in vitro* studies cytochrome f reacts at the acidic patch, and P700 at the adjacent hydrophobic surface of plastocyanin.[8] The evidence for two-site reactivity is a particularly unique aspect of plastocyanin reactivity. The structure of cytochrome f,[9] has demonstrated that there is a region of positively charged residues Lys-58, Lys-65, Lys-66, Lys-187 and Arg-209, which could be relevant in docking the protein at the remote site of PCu(II).

3. Effects of pH on Reactivity

On decreasing the pH from 7.5 to values in the 4-5 region (as low as it is possible to go without protein denaturation), plastocyanin Cu(I), but not the Cu(II) form, approaches a state of redox inactivity. Thus in the case of the $[Fe(CN)_6]^{3-}$ (reactant in >10-fold

excess) oxidation of PCu(I), rate constants of ~8 x $10^4 M^{-1}s^{-1}$ at pH 7.5 decrease to values at or close to zero.[6] X-ray crystallography has established this as a process involving protonation and dissociation of the coordinated N-atom of His-87.[10] Active site pK_a's for the different plastocyanins, which can also be determined by NMR, and are in the range 4.7-5.1, can be as high as 5.4-5.9 when there are deletions at positions 57 and 58 in the polypeptide chain.[1] There are various changes accompanying the protonation which result in the Cu(I) becoming trigonal-planar coordinated.[1b] Since Cu(II) does not exhibit trigonal coordination in any of its known chemistry, a barrier to Cu(I) _ Cu(II) change is created. Such inactivity fits the requirements of plastocyanin in photosynthetic electron transport. As soon as the PCu(II) receives an electron from cytochrome f, it is rapidly converted to inactive PCu(I) since the inner thylakoid is at a pH <5.0. The PCu(I) is therefore inactive until it is required to reduce P700. How the P700 reactivates PCu(I) and becomes reduced at this stage is not yet clear.

When PCu(I) is oxidised by cationic oxidants such as $[Co(phen)_3]^{3+}$ protonation at the acidic patch occurs as well as active-site protonation. From a two pK_a fit it can be concluded that the remote site has pK_a's in the range 5.3-5.8. Such values are high for single carboxylates. It has also been observed that for the reduction of PCu(II) by cationic reductants, there is a decrease in rate constants with pH, giving single pK_a fits in the range 4.8-5.1. The latter is also assigned to the remote acidic patch. It is interesting that at a distance of 15-20 Å from the Cu the oxidation state of the Cu appears relevant. A possible explanation is that some small movement is transmitted to the remote site so that two of the carboxylates, which in the Cu(I) state share a proton, are not able to do so in the Cu(II) state.[11] There is some crystallographic evidence in support of this.[12] The effect might constitute (or contribute to) a mechanism for dissociating the cytochrome f and plastocyanin components after ET between the two.

Two other proteins in Table 1 exhibit active-site protonation and dissociation of the exposed active site C-terminus His in the accessible range of pH. In all three cases satisfactory agreement is observed for pK_a's determined by NMR and from kinetic studies. In the case of *T.versutus* amicyanin the acid dissociation constant pK_a (6.7),[13] is higher than the range of values (4.7-5.1) observed for the plastocyanin. The value determined for *A.cycloclastes* pseudoazurin (4.7) is similar to that of plastocyanin.[14] The number of amino acids between the C-terminus Cys and His residues co-ordinating the active site for these three proteins is 2, whereas other proteins listed in Table 1 have 3 or 4.[14] Similarly there is a small loop of 2 residues between the C-terminus His and Met of amicyanin, which may explain the higher pK_a in this case. The need for a higher pK_a in the case of amicyanin may relate to the physiological pH of ~7.0. We note also that as the one-electron amicyanin reduction of the tryptophan-tryptophylquinone cofactor of the MADH protein occurs the latter has to lose a proton, and amicyanin may be required to bring about both changes.[13b] Pseudoazurin is involved in ET to nitrite reductase. The newly identified blue copper protein halocyanin,[15] also has 2 amino-acids between the coordinated C-terminus Cys and His residues, and it will be of interest whether active site protonation is observed here also.

4. Electron Self-Exchange Rate Constants

Self-exchange rate constants at 25°C, pH 7.0, e.g. for plastocyanin, are as defined in (1).

$$PCu(I) + PCu(II) \rightarrow PCu(II) + PCu(I) \qquad (1)$$

Table 3. Self-Exchange Rate Constants Type 1 Cu Proteins

Protein	$k_{ESE}/M^{-1}s^{-1}$	pH	Method	Charge Cu(I)	Ref
Azurin (*P.a.*)	9.6×10^5	4.5	NMR	-1	28
	7.0×10^5	9.0	NMR		28
	2.4×10^6	5.0	EPR		29
Azurin (*A.d*)	4.0×10^5	6.7	NMR		30
Plastocyanin (*A.v.*)	3.2×10^5	7.5	NMR	+1	31
	5.9×10^5	7.5	Marcus		32
(Parsley)	3.3×10^3	7.5	Marcus-8		32
(Spinach)	$\sim 4 \times 10^3$	6.0	NMR	-9	33
(French bean)	$<<2 \times 10^4$	7.4	NMR	-9	34
Stellacyanin	1.2×10^5	7.0	EPR	+7	19
Amicyanin (*T.v.*)	1.3×10^5	8.6	NMR	-4	13a
Pseudoazurin (*A.c.*)	2.9×10^3	7.5	NMR	+1	35
	2.7×10^3	7.5	Marcus		35
Umecyanin	5.8×10^3	7.5	NMR	-4	20
	7.9 and 26	7.0	Marcus		20
Rusticyanin	$\sim 10^4$	5.7	NMR	-3	36

25°C; I = 0.100M (NaCl)

These can be determined by ^{1}H NMR and EPR methods, and by cross-reaction studies using the Marcus Equations (2) - (3),[16]

$$k_{12} = (k_{11}\, k_{22}\, K_{12}\, f)^{1/2}$$

$$f = \log (K_{12})^2/4 \log (k_{11}\, k_{22}/Z^2) \qquad (3)$$

where k_{11} and k_{22} are self-exchange rate constants for the respective couples involved in the cross reaction, K_{12} is the equilibrium constant, k_{12} is the rate constant for the cross reaction, and Z is the frequency factor $10^{11} M^{-1}s^{-1}$. Such rate constants k_{11} and k_{22}, listed in Table 3 as k_{ESE} values, are a measure of the intrinsic ET properties of the protein. A comparison of recently determined values with those from previous studies is given in Table 3. The approach in the case of the cross-reaction studies has been to use *P.aeruginosa* azurin, Table 3, and in some cases cytochrome c_{551}, $k_{ESE} = 4.6 \times 10^6$ M^{-1} s^{-1}, as redox partners, where the k_{ESE} values are known from earlier studies.[17] The prime advantage is that these proteins have little overall charge, and there is less likelihood therefore that work terms need to be allowed for. Values of k_{ESE} listed are in the range 10^3-10^6 $M^{-1}s^{-1}$, which confirms a much more favourable rate constant than is observed for Cu(I)/Cu(II) self-exchange reactions in which two different geometries apply.[18]

Points to make about the values in Table 3 are the good agreement of rate constants determined by the NMR and ESR methods, the inhibiting effect of high overall charge in the case of plant plastocyanins, the good agreement of the NMR and Marcus values for *A. variabilis* plastocyanin and pseudoazurin, and the smaller inhibiting effect of charge in the case of stellacyanin (carbohydrate attachments contribute ~40% to the mass and may

be relevant).[19] The less good agreement of NMR and Marcus k_{ESE} values for umecyanin is also noted, where both azurin and cytochrome c_{551} were used in the cross-reaction studies.[20] A possible explanation is that a different protein site is used in the umecyanin cross-reactions. Also from current work the NMR k_{ESE} value of $\sim 10^4$ M^{-1} s^{-1} for rusticyanin is of interest in view of the very hydrophobic surrounding of the Cu active site.[21] In all instances an ESE process via hydrophobic adjacent surface is believed to occur. Involvement of two remote charged regions, or of one charged and one hydrophobic region are regarded as energetically unfavourable processes.

The effect of introducing charged residues on the adjacent hydrophobic surface of plastocyanin and azurin by site directed mutagenesis has been explored. Thus Leu12Glu at the higher pH's when the Glu residue is negatively charged, retards the oxidation of PCu(I) by $[Fe(CN)_6]^{3-}$ by 10-fold.[22] Similarly in the case of azurin the Met44Lys mutant produces a 200-fold effect on the self-exchange rate constant at low pH values.[23]

Results for $[Cr(CN)_6]^{3-}$ line-broadening of ^1H peaks in the NMR spectrum of amicyanin indicate three sites for interaction.[20] That occurring to the lower part of the molecule at Ile-38 is not regarded as relevant to ET. An effect is also observed at the exposed His-96 at the hydrophobic surface. However the most effective site is that corresponding to the acidic patch of plastocyanin. From known sequences this site has an exposed Phe or His at position 92 (corresponding to Tyr-83 in plastocyanin), and is attached to the active site Cys-93. It is moreover surrounded by positively charged residues Lys-59, Lys-60, Lys-69 and Arg-100. The latter two sites are candidates therefore for consideration in biologically relevant ET processes.

The ET route which has been identified involving the remote site of plastocyanin (Cu-Cys-Tyr/Phe), and is here suggested for amicyanin (Cu-Cys-Phe/His), is also relevant in the intramolecular ET processes occurring in the case of ascorbate oxidase (Cu-Cys-His-Cu_3) and nitrite reductase (Cu-Cys-His-Cu). The existence of the latter two intramolecular ET routes provides additional support for the involvement of remote sites in the reactions of plastocyanin and amicyanin.

5. Other Studies

In collaborative studies the full amino-acid sequence of umecyanin prepared by a literature procedure has been investigated.[4b] The full amino-acid sequence has been determined. Not only are there iso-forms from the Val → Ile change at position 48, but considerable heterogeneity is observed from the retention of different lengths of carbohydrate at Asn-76. In addition cleavage of the polypeptide occurs during procedures carried out at a number of points between residues 103 to 115, the latter being the longest chain length observed. Protein purchased from the Sigma Chemical Co was found to give similar behaviour. The most common chain length is 106 residues. In addition to this heterogeneity, there are sequence homologies with stellacyanin (which has no Met residues) as well as CBP (structure available),[24] and CPC. It can be concluded that umecyanin, stellacyanin and CPC have Gln and not Met as the fourth coordinating residue, Figure 4.[4b] In solution studies it has been noted that umecyanin and stellacyanin give colour changes at pH >8 corresponding to an isomerisation process.[25] This behaviour is consistent with Gln instead of Met coordination. Thus a reasonable explanation is that at low pH the O-atom and at high pH the N-atom of the Gln side

chain is coordinated to the Cu(II). In a further elaboration it is possible that two sequential processes may be occurring with involvement of the lysine residue nearby.[4b]

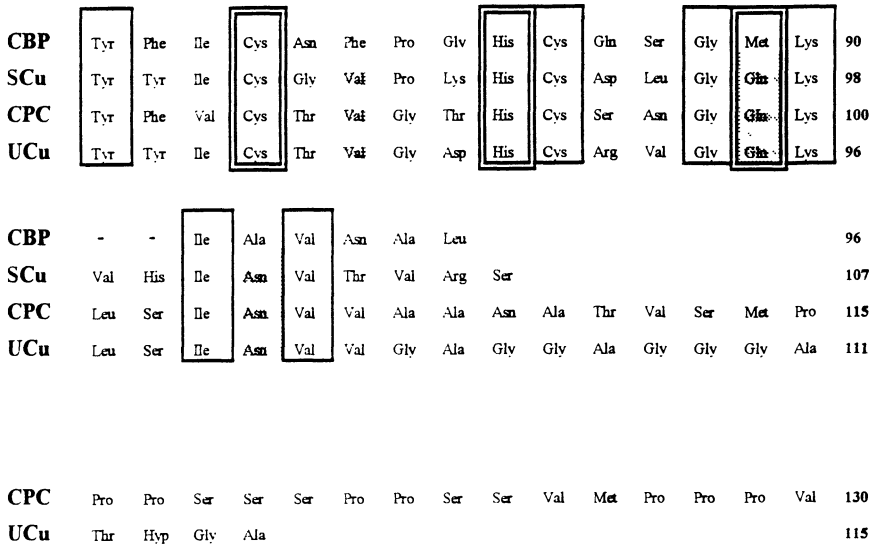

Figure 4

Finally it should be noted that some of the above mentioned blue copper proteins, as well as others not so far mentioned, have been little studied. These include halocyanin,[15] CPC,[4c] auracyanin,[26] CBP,[24] along with the protein from mung beans and mavicyanin, which have been the subject of earlier reports.[27] From the behaviour of different proteins already observed, and further subtle changes that will no doubt be revealed, these are worthwhile subjects for further study.

6. Acknowledgements

We thank the UK Science and Engineering Research Council (CD), and the European Commission under a Human Capital and Mobility Network Programme (PK) for financial support.

7. References

(1) (a) Sykes, A.G., *Adv.Inorg.Chem.*, **1991**,*36*,377, (b) Sykes, A.G., *Struct.Bonding (Berlin)*, **1990**, *75*, 175, (c) Solomon, E.I.; Baldwin, M.J.; Lowery, M.D., *Chem.Rev.*, **1992**, *92*, 521.

(2) Kitajima, N., *Adv.Inorg.Chem.*, **1992**, *39*, 3-20.

(3) Colman, P.M.; Freeman, H.C.; Guss, J.M.; Murata, M.; Norris, V.A.; Ramshaw, J.A.M.; Venkatappa, M.P., *Nature (London),* **1978**, *272,* 319.
(4) (a) Fields, B.A.; Guss, J.M.; Freeman, H.C., *J.Mol.Biol.,* **1991**, *272,* 1053; (b) Van Driessche, G.; Dennison, C.; Sykes, A.G.; Van Beeuman, J., to be published, (c) Mann, K.; Schafer, W.; Thoenes, V.; Messerschmidt, A.; Mehrabian, Z.; Nalbandyan, R., *FEBS Lett.,* **1992**, *314*, 220.
(5) Guss, J.M.; Freeman, H.C., *J.Mol.Biol.*, **1983**, *169,* 521.
(6) Segal, M.G.; Sykes, A.G., *J.Am.Chem.Soc.*, **1978**, *100*, 4585.
(7) Cookson, D.J.; Hayes, M.T.; Wright,P.E., *Biochim.Biophys.Acta.*,**1980**,*591*, 162
(8) Beoku-Betts, D.; Chapman, S.K.; Knox, C.V.; Sykes, A.G., *Inorg.Chem.,* **1985**, *24*,1677.
(9) Martinez, S.E.; Huang, D.; Szczepaniak, A.; Cramer, W.A.; Smith, J.L., *Structure,* **1994**, *2*, 95.
(10) Guss, J.M.; Harrowell, P.R.; Murata, M.; Norris, V.A.; Freeman, H.C., *J.Mol.Biol.,* **1986**, *192,* 361.
(11) McGinnis, J.; Sinclair-Day, J.D.; Sykes, A.G., *J.Chem.Soc., Dalton Trans.,* **1986**, 2011.
(12) Collyer, C.A.; Guss, J.M.; Sugimura, F.; Yoshizaki, F.; Freeman, H.C.,*J.Mol. Biol.*, **1990**, *211,* 617.
(13) (a) Lommen, A.; Canters, G.W., *J.Biol.Chem.,* **1990**, *265*, 2768, (b) Kyritsis, P.; Dennison, D.; Kalverda, A.P.; Canters, G.W.; Sykes, A.G., submitted.
(14) Dennison, C.; Kohzuma, T.; McFarlane, W.; Suzuki, S.; Sykes, A.G., *J.Chem.Soc., Chem.Commun.*, **1994**, 581.
(15) Scharf, B.; Engelhard, M., *Biochemistry.*, **1993**, *32,* 12894.
(16) Marcus, R.A.; Sutin, N., *Biochim.Biophys.Acta.*, **1985**, *811*, 265.
(17) Timkovich, R.; Cai, M.L.; Dixon, D.W., *Biochem.Biophys.Res.Commun.*, **1988**, *150,* 1044.
(18) Karlin, K.D.; Yandell, J.K., *Inorg.Chem.,* **1984**, *23,* 1184.
(19) Dahlin, S.; Reinhammer, B.; Wilson, M.T., *Biochem.J.,* **1984**, *218*, 609.
(20) Dennison, C., Ph.D. Thesis, University of Newcastle, **1994**, and unpublished work.
(21) Hunt, A.; Toy-Palmer, A.; Assa-Munt, N.; Cavanagh, J.; Blake, R.C.; Dyson, H.J., *J.Mol.Biol.,* to be published.
(22) Kyritsis, P.; Dennison, C.; McFarlane, W.; Nordling, M.; Vanngard, T.; Young, S.; Sykes, A.G., *J.Chem.Soc., Dalton Trans*, **1993**, 2289.
(23) Van de Kamp, M.; Canters, G.W.; Andrew, C.R.; Sanders-Loehr, J.; Bender, C.J.; Peisach, J., *Eur.J.Biochem.*, **1993**, *218,* 229.
(24) Guss, J.M.; Merrit, E.A.; Phizackerley, R.P.; Hedman, B.; Murata, M.;Hodgson, K.D.; Freeman, H.C., *Science,* **1988**, *241*, 806.
(25) Chapman, S.K.; Orme-Johnson, W.H.; McGinnis, J.; Sinclair-Day, J.D.; Sykes, A.G.; Ohlsson, P.-I.; Paul, K.-G., *J.Chem.Soc., Dalton Trans.,* 1986, 2063.
(26) Frost, J.T.; McManus, J.D.; Freeman, J.C.; Ramakrishna, B.L.; Blankeship, R.E., *Biochemistry,* **1988**, *27,* 7858.
(27) Fee, J., *Struct.Bonding,* **1975**, *23,* 1.
(28) Groeneveld, C.M.; Canters, G.W., *J.Biol.Chem.,* **1988**, *203,* 167.
(29) Groeneveld, C.M.; Dahlin, S.; Reinhammer, B.; Canters, G.W., *J.Am.Chem. Soc.,* **1987**, *109,* 3247.

(30) Groeneveld, C.M.; Ouwerling, M.C.; Erkelens, C.; Canters, G.W., *J.Mol.Biol.,* **1988,** *200.* 189.
(31) Dennison.; Kyritsis, P.; McFarlane, W.; Sykes, A.G., *J.Chem.Soc., Dalton Trans.,* **1993**, 1959.
(32) de Silva, D.G.A.H.; Beoku-Betts, D.; Kyritsis, P.; Govindaraju, K.; Powls, R.; Tomkinson, N.; Sykes, A.G., *J.Chem.Soc., Dalton Trans.,* **1992,** 2145.
(33) Armstrong, F.A.; Driscoll, D.C.; Hill, H.A.O., *FEBS Lett.,* **1985,** *190,* 942.
(34) Beattie, J.K.; Fenson, D.J.; Freeman, H.C.; Woodcock, E.; Hill, H.A.O.; Stokes, A.M., *Biochim.Biophys.Acta.*, **1975**, *405,* 109.
(35) Dennison, C.; Kohzuma, T.; McFarlane, W.; Suzuki, S.; Sykes, A.G., *J.Chem. Soc., Dalton Trans.,* **1994**, 437.
(36) Kyritsis, P.; Dennison, C.; Ingledew, W.J.; McFarlane, W.; Sykes, A.G., to be published.

COPPER-ZINC SUPEROXIDE DISMUTASE: MECHANISTIC AND BIOLOGICAL STUDIES

JOAN SELVERSTONE VALENTINE, LISA M. ELLERBY,
JANET A. GRADEN, CLINTON R. NISHIDA,
& EDITH BUTLER GRALLA
Department of Chemistry and Biochemistry
University of California,
Los Angeles, California 90024, U.S.A.

ABSTRACT. Copper-zinc superoxide dismutase (CuZnSOD) is one of a class of enzymes known to be excellent catalysts of the disproportionation of superoxide ($2\ O_2^- + 2\ H^+ \rightarrow O_2 + H_2O_2$). An unusual aspect of the structure of this enzyme is the occurrence of a bridging imidazolate ligand, which holds the copper and zinc ions in each subunit 6.3 Å apart. The mechanism of CuZnSOD-catalyzed superoxide disproportionation is understood in broad outline, but only relatively recently has it been possible to address several important aspects of the structure-function relationships in this enzyme. Of particular interest are the pH independence of both the spectroscopic and catalytic properties of this enzyme over a wide range of pH and the function of the zinc-imidazolate ligand to the copper in the catalytic mechanism. Recently, there have been several intriguing results concerning the physiological role played by CuZnSOD *in vivo*. There is a growing body of evidence indicating that oxidative damage in mammalian cells is associated with aging, carcinogenesis, and induction of other serious disease states and that toxic metabolites derived from the metabolism of O_2 may be responsible for such damage. Superoxide dismutases have been proposed to act as antioxidant enzymes by lowering the steady state concentration of superoxide *in vivo*. Mutations in this enzyme have also been reported to be associated with the familial form of amyotrophic lateral sclerosis (ALS), frequently termed Lou Gehrig's Disease, but the mechanism by which these mutations cause the disease is as yet unknown.

1. Background

Superoxide dismutases, found in virtually all areobic organisms, catalyze the disproportionation of superoxide ($2\ O_2^- + 2\ H^+ \rightarrow O_2 + H_2O_2$). Copper-zinc superoxide dismutase (CuZnSOD) is an enzyme found in relatively high concentration in the cytoplasm of all or nearly all eukaryotic cells.[1] CuZnSODs from different organisms are very similar, particularly in the regions of their metal-binding sites, as judged from a high degree of homology in their amino acid sequences and the resemblance of the spectral properties of the native enzymes and metal-substituted derivatives from different organisms.[2-4] Several CuZnSODs have been extensively studied, most notably bovine, human, and yeast. Eukaryotic cells also have a mitochondrial Mn-containing SOD, and prokaryotes often have Fe- and Mn-containing SODs. The Fe and Mn enzymes are structurally related to each other. Neither the Mn- nor the Fe-containing SOD is structurally related to CuZnSOD. All of the SODs are believed to function as intracellular antioxidant enzymes by reducing the steady-state level of superoxide present in the cell.

D.P. Kessissoglou (ed.), Bioinorganic Chemistry, 77-91

2. Relationship between the Structure and the Enzymatic Mechanism

2.1 STRUCTURE OF CuZnSOD

The x-ray crystal structures of the oxidized form of CuZnSOD show it to consist of two identical subunits held together almost entirely by hydrophobic interactions. Each subunit consists of a flattened cylindrical barrel of β-pleated sheet from which three external loops of irregular structure extend.[5-8]

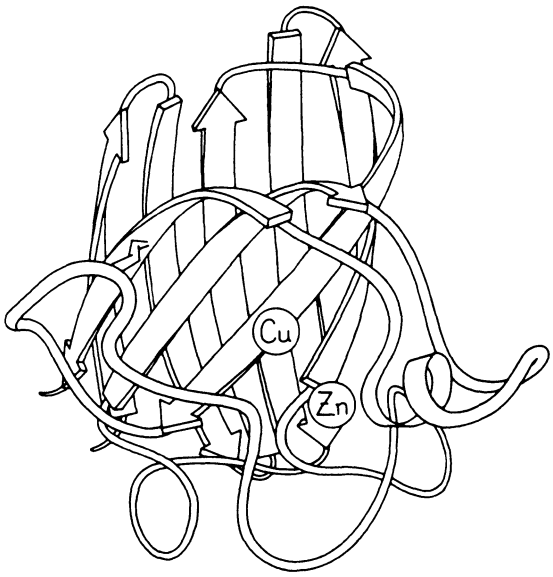

Figure 1. Schematic backbone drawing of the CuZnSOD subunit (from ref. 6).

The metal-binding region of the protein binds Cu^{2+} and Zn^{2+} in close proximity to each other, bridged by the imidazolate ring of a histidyl side chain. The Cu^{2+} ion is coordinated to four histidyl imidazoles and a water in a distorted square pyramidal geometry. The Zn^{2+} ion is coordinated to three histidyl imidazoles (including the one shared with copper) and an aspartyl carboxylate group, forming a distorted tetrahedral geometry around the metal ion.

One of the most unusual aspects of the structure of this enzyme is the occurrence of the bridging imidazolate ligand, which holds the copper and zinc ions 6.3 Å apart. Such a configuration is not unusual for imidazole complexes of metal ions, which sometimes form long polymeric imidazolate-bridged structures. However, no other imidazolate-bridged bi- or poly-metallic metalloprotein has yet been identified.

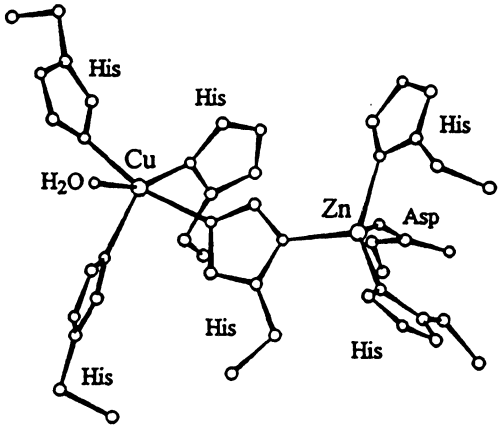

Figure 2. Schematic drawing of the metal-binding sites of CuZnSOD.

The role of the zinc ion in CuZnSOD appears to be primarily structural. There is no evidence that water or other ligands can bind to the zinc, and it is therefore highly unlikely that superoxide would interact with that site. The copper site is clearly the site of primary interaction of superoxide with the protein. The x-ray structure shows that the copper ion lies at the bottom of a narrow channel which is large enough to admit only water, small anions, and similarly small ligands. In the lining of the channel is found the positively charged side chain of an arginine residue, 5 Å away from the copper ion and situated in such a position that it could interact with superoxide and other anions when they bind to copper. Near the mouth of the channel at the surface of the protein, are located two positively charged lysine residues, which are believed to play a role in attracting anions and guiding them into the channel.

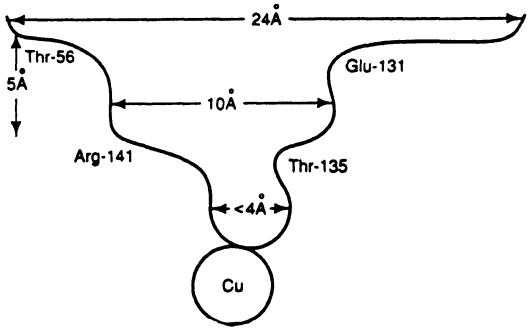

Figure 3. Schematic diagram of a cross section of the active-site channel in CuZnSOD (from ref. 38).

2.2. CATALYTIC MECHANISM OF CuZnSOD

The uncatalyzed disproportionation of superoxide proceeds spontaneously in water with a rate that is strongly pH dependent due to the fact that the fastest pathway is reduction of the protonated form, HO_2, by O_2^-. Thus the maximum in the rate occurs at pH 4.8, where the pH equals the pK_a, i.e. the pH at which superoxide is half protonated.[9]

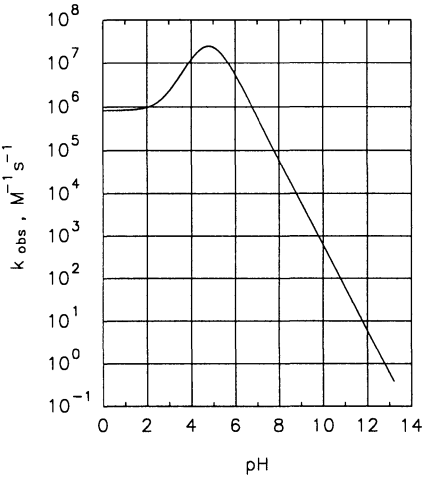

Figure 4. The rate of HO_2/O_2^- disproportionation as a function of pH.

Catalysis of superoxide disproportionation by metal complexes and metalloenzymes has been proposed to go by either of two mechanisms.[10]

Mechanism A:

$$M^{n+} + O_2^- \longrightarrow M^{(n-1)+} + O_2$$

$$M^{(n-1)+} + O_2^- \longrightarrow M^{n+}(O_2^{2-}) \xrightarrow{2\,H^+} M^{n+} + H_2O_2$$

Mechanism B:

$$M^{n+} + O_2^- \longrightarrow M^{n+}(O_2^-)$$

$$M^{n+}(O_2^-) + O_2^- \longrightarrow Mn+(O_2^{2-}) \xrightarrow{2\,H^+} M^{n+} + H_2O_2 + O_2$$

Mechanism A involves reduction by superoxide of the oxidized metal ion to its reduced state accompanied by the release of dioxygen, followed by reoxidation by a second superoxide of the reduced metal ion to its oxidized state with the release of HO_2^- or H_2O_2. In mechanism B, the metal ion is never reduced but instead forms a superoxo complex which is reduced to a peroxo complex by a second superoxide ion. For both mechanisms A and B, the peroxo ligands are protonated and dissociate to give hydrogen peroxide. If a metal ion or complex can be reduced by superoxide and if its reduced form can be oxidized by superoxide, both at rates competitive with superoxide disproportionation, the complex can probably act as an SOD by mechanism A. Mechanism B has been proposed to account for the apparent catalysis of superoxide disproportionation by Lewis acidic non-redox active metal ions under certain conditions, but could apply to other cases as well. The mechanism of superoxide disproportionation catalyzed by CuZnSOD is generally believed to go by mechanism A.

In both mechanisms A and B, the protonation of peroxide dianion, O_2^{2-}, prior to its release from the metal ion is required because peroxide dianion is highly basic and thus too unstable to be released free in its unprotonated form. Thus both mechanisms A and B would ordinarily be expected to lead to pH-dependent rates for superoxide disproportionation, with the rate being slower at high pH. In fact, the rates of superoxide disproportionation, either catalyzed or uncatalyzed, to our knowledge are always pH dependent, giving faster rates at low pH, *except* in the case of the superoxide dismutase enzymes.

In the case of CuZnSOD, mechanism A is believed to be operating, with the copper center undergoing changes in redox state.

$$O_2^- + Cu^{II}SOD \rightarrow O_2 + Cu^{I}SOD$$

$$O_2^- + 2\,H^+ + Cu^{I}SOD \rightarrow H_2O_2 + Cu^{II}SOD$$

The rates of the individual steps in this mechanism have been measured and the rate constants found to be identical, i.e. $k_1 = k_2 = 2 \times 10^9\ M^{-1}\ sec^{-1}$, and pH independent over the range pH 5 - 9.5.[3] The pH independence of the catalytic rate constants for CuZnSOD is a striking characteristic that needs to be explained in any mechanistic proposal (see below).

The source of the proton(s) that protonates peroxide in the catalytic mechanism of CuZnSOD is the subject of some interest. Reduction of the oxidized protein has been shown to be accompanied by the uptake of one proton per subunit. That proton is believed to protonate the bridging imidazolate in association with the breaking of the bridge upon reduction of the copper. The same proton is thus an attractive possibility for protonation of peroxide as it is formed in the enzymatic mechanism.

Attractive as this mechanism appears, there are some problems with it. For example, it has been pointed out that, at higher concentrations of superoxide, the turnover of the enzyme is too fast for this protonation and deprotonation cycle of the bridging histidine to be occurring.[11] It therefore appears that the catalysis under such conditions may proceed without breaking of the imidazolate bridge.

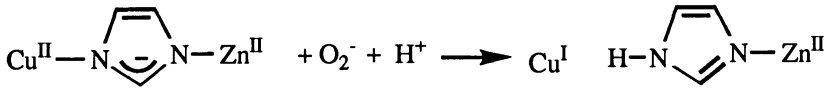

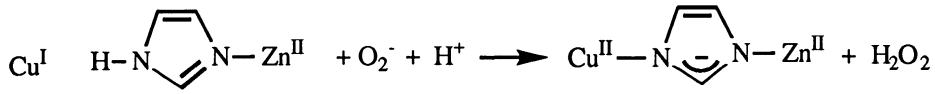

Electrostatic calculations of the charges on the CuZnSOD protein suggest that superoxide and other anions entering into the vicinity of the protein will be drawn toward and into the channel leading down to the copper site by the distribution of positive charges on the surface of the protein, the positively charged lysines at the mouth of the active site cavity, and the positively charged arginine and copper ion within the active site region.[5] Several of the anions studied have been shown to inhibit the SOD activity of the enzyme. The source of the inhibition is generally assumed to be competition with superoxide for binding to the copper, but it may also be due in some cases to a shift in the redox potential of copper known to occur in some instances upon binding of an anion to copper.

Studies of the VIS-UV, ESR, and NMR spectroscopic properties of CuZnSOD and its metal-substituted derivatives have been particularly valuable in providing detailed information about the nature of the metal-binding sites. These properties have been reviewed in detail in other publications and will not be reviewed here.[2-4] With respect to the catalytic mechanism, however, it is important to note that the spectroscopic properties of CuZnSOD are unchanged over the same pH range wherein the rate of superoxide dismutation is unchanged by pH, i.e. pH 5 - 9.5. This property is unusual because the oxidized form of CuZnSOD contains a water molecule bound to Cu^{II} and water molecules bound to Cu^{II} either in a protein or in a coordination complex generally ionize well below pH 9.5 to give Cu^{II}-hydroxide complexes. The implications of this unusual property are discussed below.

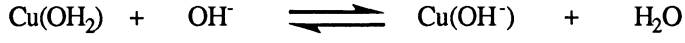

2.3 SITE-DIRECTED MUTANT CuZnSODs

Much of the valuable recent information that has been obtained concerning the mechanism of CuZnSOD comes from studies of mutant human CuZnSOD proteins prepared by site-directed mutagenesis. Examples of some of these studies are given in Table 1.

Arg143 is located in the channel that leads from the exterior of the protein to the copper ion. Either chemical modification or mutation of this residue resulted in a large decrease in its SOD activity, thus implicating that positively-charged residue as a key factor in drawing the anionic substrate into the channel.[12] Thr137 is also located in the channel leading to the copper. Mutation of this residue to Ile decreases the dismutation rate by 25%, leading to the conclusion that this residue plays a role in maintaining the hydrophilicity of the channel.[14-16] Mutation of the same residue to Arg decreased the rate by a factor of 3 despite the fact that the anion binding affinity of the mutant was dramatically increased. These results imply that a precise positioning of the positive charges in the channel is required for high catalytic rates.[13] Mutation of the negatively-charged residues Glu133 and

Glu132 on the exterior of the protein either with neutral or positively-charged residues has been shown to enhance the catalytic rate of superoxide dismutation relative to wild-type, presumably through enhancement of the electrostatic guidance of superoxide toward and into the channel leading to the copper center.[17]

Table 1. Some Examples of Site-Directed Mutants of Human CuZnSOD

Residue	Mutant Proteins	Reference
Arg143	Lys, Ile, Glu, Asp, Ala	12
Thr137	Ile, Ser, Ala, Arg, and Arg143/Ala137	13-16
Glu 132, Glu133	Gln132, Gln 133, Gln132/Gln133, and Gln132/Lys133	17
Asp124	Asn, Gly, and Asn124/Asn125	18

The mutations in the first three entries of Table 1 all appear to influence the electrostatic guidance of the superoxide anion into and through the channel leading to the copper. The fourth, however, by contrast, influences the metal-binding site directly. In the crystal structure of the wild-type protein, it can be seen that Asp124 forms a secondary bridge between the copper and the zinc site by hydrogen bonding to the zinc ligand His71 and the copper ligand His46. Mutations of this residue produce zinc-deficient proteins which have substantially reduced SOD activities. More importantly for our discussion here, the SOD activities of these mutants are markedly pH dependent.[18] This characteristic will be discussed further below.

Recently we have been preparing and characterizing site-directed mutants of CuZnSOD from the yeast *Saccharomyces cerevisiae*.[19-21] We have concentrated in particular on replacement of the ligands to the copper and zinc ions. In order to investigate the role of the bridging imidazolate in this protein, we have prepared and characterized the His63Ala mutant of SOD. We find that the metal-binding behavior of the copper site of this mutant protein is remarkably similar to that of the wild-type protein, despite the absence of the bridging histidyl imidazolate from His63. Furthermore, we find that the spectroscopic properties of the copper site of the mutant and the SOD activity are markedly pH-dependent.

A histidine-to-alanine mutant (H63A) was prepared using oligonucleotide-directed mutagenesis on the cloned CuZnSOD gene from *Saccharomyces cerevisiae*. The mutant gene was sequenced and expressed in *Escherichia coli* in the T7 RNA polymerase expression system, the protein was purified to homogeneity, and apoprotein was prepared.

Addition of one equivalent each of Cu^{2+} and Zn^{2+} per subunit to apo-H63ASOD gave a derivative whose visible absorption spectrum showed a d-d transition with $\lambda_{max} = 670$ nm, remarkably similar to Cu^{II} in the copper site of wild-type CuZnSOD. Binding of Cu^{2+} was stoichiometric, indicating that the binding constant is high. In striking contrast to wild-type SOD whose visible-UV and ESR spectral properties are invariant with pH over the range $5 < pH < 10.5$, the spectroscopic properties of H63ASOD show reversible pH-dependent behavior, with a pK_a of 9.3. Reversible, pH-dependent changes in the ESR spectrum were also observed. We conclude from these results that His63 plays a crucial role in

maintaining the pH-independence of the copper site of wild-type CuZnSOD.

The visible-UV and ESR spectra for H63ASOD at pH > 9.5 indicate that copper(II) in that site has an approximately square-planar geometry. The pH-dependent changes in the ESR spectra are analogous to those observed for copper-substituted carbonic anhydrase[22] and met apo hemocyanin.[23] The pK_a of the pH-dependent transition is also similar to the pK_a for ionizing water bound to Cu^{2+} complexes.[24] Thus the Cu^{2+} ion in H63ASOD is behaving in a fashion normal for small Cu^{II} complexes or copper-containing proteins. An abnormally high pK_a, such as is found in wild-type SOD, is strong evidence that the water ligand remains in an axial position on the Cu^{II} center even at relatively high pH, since the interaction between the copper center and its axial ligands is much weaker than that with its equatorial ligands. The changes observed at high pH resemble those occurring when cyanide binds to CuZnSOD suggesting that the binding of OH^- and CN^- occur in a similar fashion. It is believed that CN^- binding to the Cu^{II} in SOD causes the axes of the copper to reorient placing the CN^- in an equatorial position on the copper and creating a square planar geometry.[2]

As might be expected from the pH-dependence of the spectroscopic properties, the SOD activity of the H63A mutant is also pH-dependent, with higher SOD activity at lower pH. However, we find the pK_a for the pH-dependence of the SOD activity to be considerably lower than that for the ionization of the bound water in H63ASOD. There are several possible steps in the catalytic mechanism that might lead to a pH-dependence.

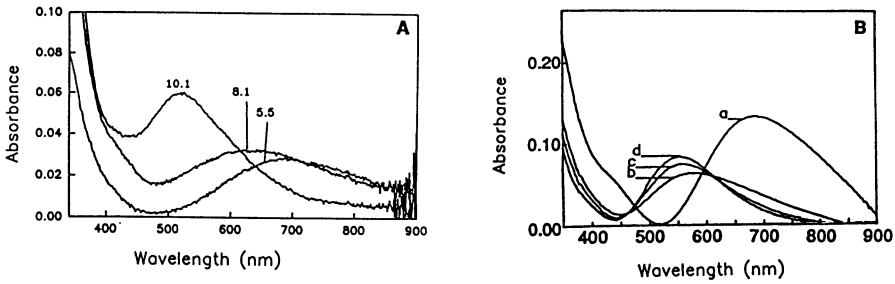

Figure 5. Visible absorption spectra of (A) a pH-titration of H63ACuZnSOD and (B) titration of wild-type CuZnSOD with added cyanide (from ref. 25).

The first of these, ionization of water on Cu^{II} leading to inhibition by bound hydroxide, is a very plausible mechanism for inhibition of the first step of the catalytic mechanism, i.e. reduction of Cu^{II} by superoxide, but cannot account for the low pK_a for the SOD activity. A second possible mechanism, oxidation of Cu^{I} by HO_2 rather than O_2^- in the second step of the catalytic mechanism, is also feasible, but the pH-dependence of the catalytic rate does not match that expected for protonation of O_2^- either. The third possibility, and the one that we believe most likely, is that the pH-dependence of the catalytic rate is caused by slow product release, i.e. that the dissociation of the peroxide formed in the second step of the mechanism from the Cu^{II} center becomes rate limiting in H63ASOD.

Why would the dissociation of peroxide from Cu^{II} in the absence of the zinc-imidazolate moiety in H63ASOD be slower than in wild-type CuZnSOD? The argument goes as follows. We know that the pK_a of water bound to Cu^{II} in wild-type CuZnSOD is abnormally high. We conclude, as described above, that this is due to the fact that the hydroxide ligand, when it is formed by deprotonation of the bound water at high pH cannot move into a more strongly bonded, equatorial position in the Cu^{II} coordination sphere. In H63ASOD, the pK_a of the water ligand to the Cu^{II} is normal, and we therefore conclude that the hydroxide ligand can move into an equatorial position, just as cyanide does when it binds to the wild-type protein. It therefore appears likely that peroxide, O_2^{2-}, or more likely hydroperoxide, HO_2^-, binds in an equatorial position in H63ASOD but in wild-type CuZnSOD is restricted to a more weakly-binding, rapidly-exchanging axial position. The peroxide-dissociation step for H63ASOD and wild-type CuZnSOD are illustrated below.

H63ASOD

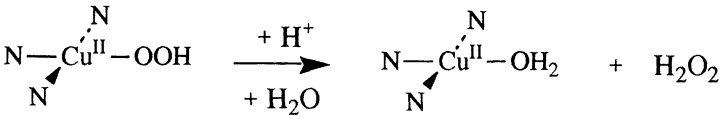

Wild-type CuZnSOD

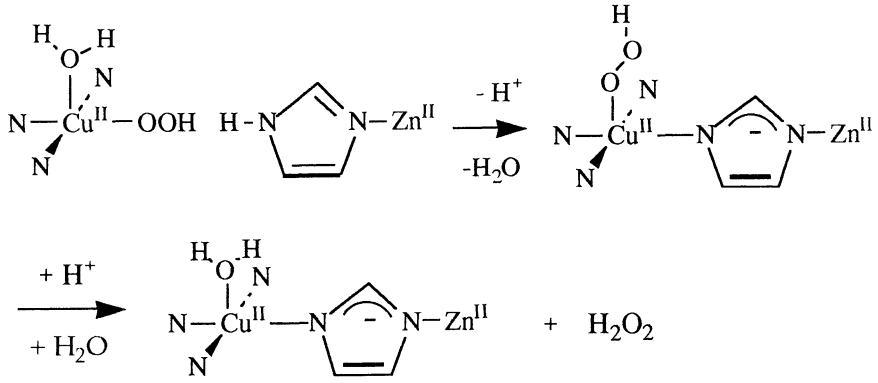

It is our conclusion that the zinc-imidazolate moiety plays a very significant role in the catalytic mechanism of CuZnSOD by ensuring that peroxide leaves rapidly from the coordination sphere of the Cu^{II} ion in the final step of the mechanism. It does so by an internal displacement reaction in which the zinc-imidazolate rebinds to Cu^{II}, forcing the peroxide ligand into an axial position, thus ensuring that it will leave rapidly from the

coordination sphere of the copper ion. In the mutant lacking the zinc-imidazolate moiety, the rate is presumably pH-dependent due to a requirement that the peroxide ligand be protonated to make it a better leaving group so that it can leave more rapidly from the equatorial position of the Cu^{II} ion. This mechanistic proposal can explain catalysis under conditions where the concentration of superoxide is saturating and the turnover of the enzyme is too fast for the histidine bridge breaking and reformation to occur.[11] In this case the bridge remains intact in CuZnSOD and the peroxide ligand remains in the rapidly exchanging axial position. The pH dependence of the SOD activities of the zinc-deficient Asp124 mutants described above[18] suggests that both the zinc and the bridging histidine are required to maintain a copper(II) coordination sphere configuration that will give a pH-independent SOD activity and therefore a very high SOD activity at physiological pH.

3. Physiological Studies of CuZnSOD

3.1. YEAST AS A MODEL SYSTEM FOR STUDIES OF CuZnSOD *IN VIVO*

CuZnSOD is one of the antioxidant enzymes found in eukaryotic cells. There is a growing body of evidence that it, along with catalases, peroxidases, and small molecule antioxidants such as glutathione, ascorbate, ubihydroquinone, and α-tocopherol, plays an important role in defending against oxidative stress in aerobic living systems.[26]

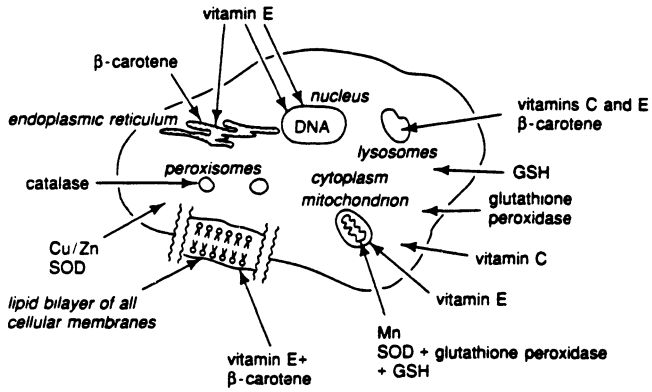

Figure 6. Cartoon showing some of the antioxidant agents inside the cell (from ref. 39).

Oxidative stress in mammalian cells has been implicated in the aging process and several disease states including cancer, Down's syndrome, and, very recently, the familial form of amyotrophic lateral sclerosis (Lou Gehrig's Disease).[27] The cell appears to have a natural balance of antioxidants to cope with oxidative stress, and degenerative states, such as those mentioned above, can arise when this balance is disrupted. However, it is not yet known on a molecular level how reactive oxidizing species derived from oxygen exert their toxic effects nor is it understood in detail precisely how the cells' antioxidants work together to protect against oxidative damage. To understand how cells defend against oxidative stress, we are currently studying the role of CuZnSOD and other known naturally occurring antioxidant proteins in a simple eukaryotic system, the yeast *Saccharomyces*

cerevisiae.

The yeast *Saccharomyces cerevisiae* provides an excellent model system for molecular studies of oxidative stress.[28] In the yeast system, in contrast to mammalian systems, genetic manipulations are very straightforward. It is easy to remove systematically the genes for the relevant proteins and to study the effects of each null mutant separately, or in combination with others. The genes for the major antioxidant proteins in yeast have been cloned, and strains lacking these genes have been constructed. In addition, *Saccharomyces cerevisiae* and some other yeasts do not require respiratory O_2 metabolism for growth since they prefer to grow by glycolysis (fermentation) with glucose as the carbon source, even when O_2 is present. If glucose is not available, mitochondrial respiration is turned on to utilize other (non-fermentable) carbon sources such as ethanol or lactate. Wild-type yeast also have a wide range of O_2 tolerance and grow well in conditions ranging from 100% O_2 to totally anaerobic. These characteristics allow the researcher to grow yeast under conditions that vary with respect to the rate of O_2 metabolism and presumably therefore the rate of oxygen radical production.

Our laboratory originally cloned the gene for CuZnSOD of *Saccharomyces cerevisiae*.[29] Since that time, we have been studying its regulation[30] and the phenotype of mutant yeast strains lacking this gene (*sod1*$^-$).[28,31,32] The importance of cytoplasmic SOD is illustrated by the fact that mutants of yeast lacking CuZnSOD exhibit a very distinct phenotype which includes extreme sensitivity to redox-cycling drugs such as paraquat, poor growth in air, sensitivity to 100% oxygen, and requirements for lysine and methionine or cysteine when grown aerobically.[28] We have also shown that *sod1*$^-$ mutants exhibit higher aerobic mutation rates than wild-type cells.[31] More recently, we constructed yeast strains lacking MnSOD and double mutants lacking both SODs. The latter are only slightly worse off than the single mutants lacking CuZnSOD only, in spite of the fact that the major source of superoxide radicals is believed to be mitochondrial respiration.

We have studied the regulation of the *SOD1* gene of yeast by copper, and found that it is regulated in response to copper by the same copper-binding transcription factor, ACE1, that controls the metallothionein gene response to copper. There is a single binding site in the SOD1 promoter where this factor binds to stimulate transcription two- to three-fold.[30]

We have continued the work on the relationship between copper and SOD by showing that copper can rescue the *sod1*$^-$ mutant yeast for growth on lactate and improve their growth on other carbon sources. The rescue can be attributed to the antioxidant activity of the metallothionein that is induced by the excess copper, as mutants lacking *CUP1* or *ACE1* genes are not rescued. In addition, oxygen stress was shown to induce *CUP1*.[32]

The *sod1*$^-$ mutant yeast strains have thus provided an experimental system in which to probe the role of CuZnSOD in general, and recently we have been using this same approach to develop a model for FALS (familial amyotrophic lateral sclerosis), a disease that has been shown to be associated with mutations in CuZnSOD in some instances (see below).

3.2. THE ROLE OF CuZnSOD IN FALS

Amyotrophic lateral sclerosis (ALS), commonly termed Lou Gehrig's Disease, is a neurodegenerative disease characterized by late onset, degeneration of motor neurons, and death, almost invariably within six years. Approximately 10% of cases are "familial" (FALS), and genetic linkage studies have therefore been possible. A recent collaborative effort succeeded in tracing the FALS locus to the gene coding for CuZnSOD[27] making this disease the major neurodegenerative disease with the most direct link to oxidative damage. One of the surprising aspects of the linkage of CuZnSOD with FALS mutations is that SOD is a ubiquitous enzyme within the organism while ALS is a highly cell-specific disease. CuZnSOD has always been thought of as a simple, straightforward, constitutively

expressed, housekeeping protein. Its importance is generally ascribed to its antioxidant, protective function. It is found in substantial quantities in every organ of the body and, indeed, in every eukaryotic organism. Motor neurons, the specific site of damage in ALS, on the other hand, are a highly specialized cell type which contains high levels of CuZnSOD.

The most obvious explanation for the link between the FALS mutations in SOD and the disease itself is that insufficient SOD activity allows excess oxidative damage to a particularly vulnerable target to occur. However, this explanation does not appear to us to be entirely satisfactory from a genetic standpoint. FALS is a dominant trait, but with late penetrance, meaning that one defective copy of the gene is enough to cause the disease, but it only manifests itself relatively late in life. In most dominant mutations, the mutated protein has new or altered function. For example, it may interact with other proteins improperly, have a new enzymatic activity, or be placed in the wrong cellular compartment. We have taken a two-pronged approach to the investigation of possible causes of FALS by (1) preparing mutant yeast strains with mutations in CuZnSOD that are analogous to those found in human FALS and investigating the phenotype of these mutations *in vivo* and (2) expressing, isolating, and characterizing *in vitro* the mutant CuZnSOD proteins with these same FALS mutations.

Our own structural analysis and prediction of the effects of the FALS mutations on the CuZnSOD structure using computer graphics agree with the published analysis[33] and indicate that most of the mutations are remote from the active site and are likely to cause alterations in the structure and/or stability of the enzyme. Using the mutagenesis and expression system that we developed for the active site mutants in yeast, we constructed three ALS-equivalent yeast SODs (yALS-SOD mutations). Two mutations, Gly85Arg (G85R) and Gly93Ala (G93A), were chosen in regions where yeast and human CuZnSOD have nearly identical structures. Gly85 is involved in hydrogen bonding to another β-strand and in forming the β-bulge which holds the zinc-binding Asp83 in position; Gly93 is located at the tight turn of a β-strand. Both residues are conserved in almost all known CuZnSODs.[34] Based on their positions in the 3-dimensional structure, we anticipated that the addition of bulky residues at either of these positions would destabilize the protein relative to wild-type. A third mutation, Lys100Gly (K100G), was also constructed. This residue is not itself conserved between yeast and human wild-type proteins (it is Glu in human CuZnSOD), but the structure of the region is conserved,[35,36] and we expected that substitution of a glycine for this residue would introduce flexibility into this region of either the yeast or human proteins.

The yeast FALS *SOD1* mutant genes were expressed in yeast lacking CuZnSOD (*sod1*) in order to test the ability of the mutant CuZnSODs to provide SOD activity in the native host. Expression plasmids containing wild-type or mutant CuZnSOD genes under the control of the native CuZnSOD promoter were constructed and transformed into *sod1*$^-$ yeast and tested for oxygen sensitivity, paraquat sensitivity and growth in air. Transformation with the plasmid containing the wild-type gene restored resistance to both oxygen and paraquat, as well as growth in air. Surprisingly, the G93A and K100G CuZnSOD mutants were able to rescue completely the *sod1*$^-$ yeast for growth under oxidative conditions, while the G85R mutant protein was not.

SOD activity was measured in soluble protein extracts for each of the strains. Little or no SOD activity was found in the strain carrying the G85R mutant protein. By contrast, a significant level of SOD activity was found in the strains expressing the G93A and K100G proteins, although the wild-type strain showed a higher level of activity. The vector-only control showed no activity. In order to determine if the lack of SOD activity was due to the absence of the mutant CuZnSOD protein, western blot analysis was carried out. This analysis demonstrated that the concentrations of the G85R, G93A, and K100G mutant proteins were similar, although somewhat reduced relative to the level of the wild-type

CuZnSOD protein in the strain carrying the wild-type CuZnSOD gene. The fact that the CuZnSOD protein levels in the three mutant strains were not noticeably different from each other indicates that the loss of SOD activity in the G85R strain was due to the presence of an inactive CuZnSOD protein rather than to the total absence of the protein. We concluded, therefore, that the SOD activities of the mutant CuZnSOD proteins were markedly different, i.e. that the G85R protein had a significantly lower SOD activity than G93A or K100G CuZnSOD.

In order to investigate the reasons for the markedly different abilities of G85R and G93ACuZnSOD to function *in vivo*, we purified these proteins to homogeneity[36] and characterized their SOD activity, thermal stability, and spectroscopic and metal-binding properties *in vitro*. The UV-vis spectra of wild-type CuZnSOD and G85RCuZnSOD are strongly similar indicating that the metal-binding regions are very similar in geometry when the native metals are used. However, substituting other metals in place of Zn^{2+} gave quite different results. For example, putting copper in the zinc site did not produce the 810 nm band characteristic of the derivative of wild-type CuZnSOD containing copper in the both the copper and the zinc sites. Instead, a further increase in the 700 nm d-d band was observed, indicating that the site is more flexible and adjusts to the more nearly tetragonal geometry preferred by Cu^{2+}. In sharp contrast, the G93A protein, in which the mutation is farther from the active site, bound metals in a manner indistinguishable from wild-type.

We assayed the activity of the isolated mutant CuZnSOD proteins using three different SOD assays. As isolated from our expression system, G85RCuZnSOD did not contain its full complement of Cu^{2+} and Zn^{2+} and had an SOD activity about 20% of that of the native protein at pH 7.4 or 7.8. Reconstituted (fully metallated) G85RCuZnSOD, prepared from the apoprotein, had 40% of the SOD activity of native CuZnSOD. The activity of reconstituted G85RCuZnSOD was sensitive to EDTA, losing activity with less than one equivalent of EDTA, while native CuZnSOD was resistant to more than a 2000-fold excess of EDTA at pH 7.8. By contrast, reconstituted G93ACuZnSOD possessed 80% native activity and retained this activity even in the presence of a 2000-fold excess of EDTA.

A prediction had been made, based on analysis of the x-ray crystal structure of the wild-type human protein, that the FALS mutations would destabilize the protein and result in lowered SOD activity in persons carrying one of these genes. In support of this prediction, CuZnSOD isolated from red cells of FALS patients using the relatively harsh conditions that are commonly used for wild-type CuZnSODs gave preparations with substantially reduced SOD activities relative to that of wild-type.[33] Our yeast system has enabled us to assess the ability of the yeast FALS mutant SODs to function in an *in vivo* system without exposing the protein to the harsh conditions of protein isolation. We are able to compare the properties of the mutant proteins *in vivo* with those of the isolated, purified proteins *in vitro*. The G85R mutation, for example, clearly resulted in a structurally altered CuZnSOD protein. However, the protein was stable enough to be expressed and purified in high yield and retained considerable SOD activity when fully metallated. On the other hand, expression of the G85R mutant protein under physiological conditions in its native host did not rescue *sod1*$^-$ yeast. The defect in its *in vivo* activity and the partial defect in its *in vitro* activity may well be due to its altered metal-binding abilities. By contrast, G93ASOD is spectroscopically indistinguishable from wild-type and, like wild-type, successfully restores the SOD$^+$ phenotype to *sod1*$^-$ yeast. The fully metallated form possessed 80% of the activity of wild-type.

The most obvious possible explanation for the association of mutations in CuZnSOD with FALS is that FALS is caused in some fashion by lowered SOD activity,[33] and, in support of this hypothesis, we find that the SOD activities measured in crude extracts of all three of our strains are somewhat reduced relative to strains containing the wild-type gene. However, only one of the mutations, G85R, failed to reverse the *sod1*$^-$ phenotype *in vivo*. By contrast, the other two mutant SODs, G93A and K100G, reversed the oxygen-sensitive

sod1⁻ phenotype *in vivo*, and significant levels of SOD activity could be measured in their cell extracts. These results suggest that some of the human FALS mutant CuZnSODs probably retain significant levels of SOD activity *in vivo* and that it is therefore premature to conclude that FALS is caused simply by a large decrease in SOD activity, or indeed that SOD activity is always reduced in cases of FALS.

It should be noted that we have also co-expressed FALS mutant CuZnSOD and wild-type CuZnSOD in yeast, a situation that more closely approximates the conditions found in FALS patients who carry a wild-type CuZnSOD gene in addition to the mutant gene. We find such strains to be phenotypically indistinguishable from wild-type, so far as we have been able to determine to date, with respect to their growth rates and resistance to 100% oxygen or paraquat. We are currently expanding our characterization of representative FALS mutations in yeast in an effort to find common features or trends. It is our hope that full characterization of the various mutants will help to identify the disease-causing aspect(s) of these mutant proteins.

4. Acknowledgments

The authors would like to thank Dr. Diane Cabelli for interesting discussions and collaborative studies. Financial support from the NIH (GM28222 and DK46828) and the ALS Association is also gratefully acknowledged.

5. References

(1) Fridovich, I. *J. Biol. Chem.* **1989**, *264*, 7761.
(2) Bertini, I.; Banci, L.; Piccioli, M.; Luchinat, C. *Coord. Chem. Rev.* **1990**, *100*, 67.
(3) Bannister, J. V.; Bannister, W. H.; Rotilio, G. *CRC Crit. Rev. Biochem.* **1987**, *22*, 111.
(4) Valentine, J. S.; Pantoliano, M. W. In *Copper Proteins*; T. G. Spiro, Ed.; John Wiley and Sons, Inc.: 1981; pp 292.
(5) Getzoff, E. D.; Tainer, J. A.; Weiner, P. K.; Kollman, P. A.; Richardson, J. S.; Richardson, D. C. *Nature* **1983**, *306*, 287.
(6) Tainer, J. A.; Getzoff, E. D.; Beem, K. M.; Richardson, J. S.; Richardson, D. C. *J. Mol. Biol.* **1982**, *160*, 181.
(7) Tainer, J. A.; Getzoff, E. D.; Richardson, J. S.; Richardson, D. C. *Nature* **1983**, *306*, 284.
(8) Fisher, C. L.; Hallewell, R. A.; Roberts, V. A.; Tainer, J. A.; Getzoff, E. D. *Free Rad. Res. Commun.* **1991**, *12-13*, 287.
(9) Bielski, B. H. J.; Cabelli, D. E. *Int. J. Radiat. Biol.* **1991**, *59*, 291.
(10) Sawyer, D. T.; Valentine, J. S. *Acc. Chem. Res.* **1981**, *14*, 393.
(11) Fee, J. A.; Bull, C. *J. Biol. Chem.* **1986**, *261*, 13000.
(12) Banci, L.; Bertini, I.; Luchinat, C.; Hallewell, R. A. *J. Am. Chem. Soc.* **1988**, *110*, 3629.
(13) Banci, L.; Bertini, I.; Bauer, D.; Hallewell, R. A.; Viezzoli, M. S. *Biochemistry* **1993**, *32*, 4384.
(14) Bertini, I.; Banci, L.; Luchinat, C.; Bielski, B. H. J.; Cabelli, D. E.; Mullenbach, G. T.; Hallewell, R. A. *J. Am. Chem. Soc.* **1989**, *111*, 714.
(15) Banci, L.; Bertini, I.; Turano, P. *Eur. Biophys. J.* **1991**, *19*, 141.
(16) Banci, L.; Bertini, I.; Cabelli, D.; Hallewell, R. A.; Luchinat, C.; Viezzoli, M. S. *Inorg. Chem.* **1990**, *29*, 2398.

(17) Getzoff, E. D.; Cabelli, D. E.; Fisher, C. L.; Parge, H. E.; Viezzoli, M. S.; Banci, L.; Hallewell, R. A. *Nature* **1992**, *358*, 347.
(18) Banci, L.; Bertini, I.; Cabelli, D. E.; Hallewell, R. A.; Tung, J. W.; Viezzoli, M. S. *Eur. J. Biochem.* **1991**, *196*, 123.
(19) Lu, Y.; Gralla, E. B.; Valentine, J. S. In *Bioinorganic Chemistry of Copper;* K. D. Karlin and Z. Tyeklár, Ed.; Chapman & Hall: 1993; pp 64.
(20) Lu, Y.; Gralla, E. B.; Roe, J. A.; Valentine, J. S. *J. Am. Chem. Soc.* **1992**, *114*, 3560.
(21) Lu, Y.; Lacroix, L. B.; Lowery, M. D.; Solomon, E. I.; Bender, C. J.; Peisach, J.; Roe, J. A.; Gralla, E. B.; Valentine, J. S. *J. Am. Chem. Soc.* **1993**, *115*, 5907.
(22) Taylor, J. S.; Coleman, J. E. *J. Biol. Chem.* **1971**, *246*, 7058.
(23) Himmelwright, R. S.; Eickman, N. C.; Solomon, E. I. *Biochem. Biophys. Res. Commun.* **1978**, *81*, 243.
(24) Allison, J. W.; Angelici, R. J. *Inorg. Chem.* **1971**, *10*, 2233.
(25) Ellerby, L. M.; Nishida, C. R.; Nishida, F.; Yamanaka, S. A.; Dunn, B.; Valentine, J. S.; Zink, J. I. *Science* **1992**, *255*, 1041.
(26) Halliwell, B.; Gutteridge, J. M. C. *Free Radicals in Biology and Medicine;* 2nd ed.; Oxford University Press: London, **1989**.
(27) Rosen, D. R.; Siddique, T.; Patterson, D.; Figlewicz, D. A.; Sapp, P.; Hentati, A.; Donaldson, D.; Goto, J.; O'Regan, J. P.; Deng, H.-X.; Rahmani, Z.; Krizus, A.; McKenna-Yasek, D.; Cayabyab, A.; Gaston, S. M.; Berger, R.; Tanzi, R. E.; Halperin, J. J.; Herzfeldt, B.; Van den Bergh, R.; Hung, W.-Y.; Bird, T.; Deng, G.; Mulder, D. W.; Smyth, C.; Laing, N. G.; Soriano, E.; Pericak-Vance, M. A.; Haines, J.; Rouleau, G. A.; Gusella, J. S.; Horvitz, H. R.; Brown, Jr., R. H. *Nature* **1993**, *362*, 59.
(28) Gralla, E. B.; Kosman, D. J. *Adv. Genet.* **1992**, *30*, 251.
(29) Bermingham-McDonogh, O.; Gralla, E. B.; Valentine, J. S. *Proc. Natl. Acad. Sci. USA* **1988**, *85*, 4789.
(30) Gralla, E. B.; Thiele, D. J.; Silar, P.; Valentine, J. S. *Proc. Natl. Acad. Sci. USA* **1991**, *88*, 8558.
(31) Gralla, E. B.; Valentine, J. S. *J. Bacteriol.* **1991**, *173*, 5918.
(32) Tamai, K. T.; Gralla, E. B.; Ellerby, L. M.; Valentine, J. S.; Thiele, D. J. *Proc. Natl. Acad. Sci. USA* **1993**, *90*, 8013.
(33) Deng, H.-X.; Hentati, A.; Tainer, J. A.; Iqbal, Z.; Cayabyab, A.; Hung, W.-Y.; Getzoff, E. D.; Hu, P.; Herzfeldt, B.; Roos, R. P.; Warner, C.; Deng, G.; Soriano, E.; Smyth, C.; Parge, H. E.; Ahmed, A.; Roses, A. D.; Hallewell, R. A.; Pericak-Vance, M. A.; Siddique, T. *Science* **1993**, *261*, 1047.
(34) Frei, B.; Kim, M. C.; Ames, B. N. *Proc. Natl. Acad. Sci.USA* **1990**, *87*, 4879.
(35) Kim, K.; Guarente, L. *Nature* **1989**, *342*, 200.
(36) Parge, H. E.; Getzoff, E. D.; Scandella, C. S.; Hallewell, R. A.; Tainer, J. A. *J. Biol. Chem.* **1986**, *261*, 16215.
(37) Han, J.; Loehr, T. M.; Lu, Y.; Valentine, J. S.; Averill, B. A.; Sanders-Loehr, J. *J. Am. Chem. Soc.* **1993**, *115*, 4256.
(38) Roberts, V. A.; Fisher, C. L.; Redford, S. M.; McRee, D. E.; Parge, H. E.; Getzoff, E. D.; Tainer, J. A. *Free Radical Res. Comms.* **1991**;*12-13*; 269.
(39) Machlin, L. J.; Bendich, A. *FASEB J.* **1987**, *1*, 441.

NMR OF PARAMAGNETIC MOLECULES: A CONTRIBUTION TO THE UNDERSTANDING OF ENZYMATIC MECHANISMS

IVANO BERTINI and MARIA SILVIA VIEZZOLI
Department of Chemistry - University of Florence
Via Gino Capponi 7, 50121 Florence, Italy

ABSTRACT. The presence of a metal ion with unpaired electrons is not a drawback for NMR as long as the electron nucleus correlation time is short enough. Actually, the hyperfine coupling allows the investigaton of metalloproteins as large as 50,000 MW which otherwise are difficult to investigate. We here report the achievements obtained in the case of Cu_2Co_2superoxide dismutase (MW 32,000), peroxidases (MW 34,000-46,000), cytochrome P450 (MW 45,000). The systems with inhibitors or pseudosubstrates are also discussed.

1. Introduction

In paramagnetic systems the presence of unpaired electrons broadens the NMR lines of the nuclei sensing the paramagnetic center. However, the interaction between unpaired electrons and protons may provide a hyperfine shift which often leads to signals outside the diamagnetic region of the ^1H NMR spectrum [1-4]. Through saturation of the shifted signals, Nuclear Overhauser Effects are obtained on other signals, which on their turn can be independently assigned, and a sound assignment can be carried out [5,6].

When the signals of the protons nearby the paramagnetic centers are assigned, precious structural information can be obtained which allows us to investigate also the interactions with inhibitors and pseudosubstrates. When the protein is small, a complete tridimensional structure in solution can be obtained[7]; the tedious procedure of obtaining the structure can be avoided if we limit our interest to local information in the vicinity of the metal ion. This procedure is the unique approach for paramagnetic proteins larger than 20,000 MW.

We report here some examples of investigaton of enzymatic systems like Cu,Zn superoxide dismutase, peroxidases and cytochrome $P450_{cam}$.

2. Superoxide Dismutase

Copper, zinc superoxide dismutase (Cu_2Zn_2SOD) and the copper,cobalt derivative (Cu_2Co_2SOD) represent a typical and extensively investigated example of application of Nuclear Magnetic Resonance tecnique to paramagnetic macromolecules in order to elucidate the enzymatic mechanism.

D.P. Kessissoglou (ed.), Bioinorganic Chemistry, 93-104

The native enzyme, a dimer of molecular weight 32,000, in its oxidized state contains two zinc(II) and two copper(II) ions (Figure 1). The copper ion is bound to four His nitrogens whereas the zinc ion is bound to three His nitrogens and to an oxygen of an Asp residue. The two metal ions are bridges by an imidazole ion provided by a His residue[8,9]. The long electronic relaxation time of copper(II) (10^{-8}-10^{-9} s) prevents the application of high resolution NMR tecnique[4]. This relaxation time can be shortened when zinc(II) is substituted by metal ions with short electronic relaxation time, like cobalt(II), or nickel(II)[10,11]. This happens as a consequence of the magnetic interaction between the two metal sites, that are bridged by a histine residue (Figure 1): the unpaired electron of copper behaves like those of cobalt, as far as electron relaxation is concerned[12]. Furthermore, the presence of the paramagnetic ions induce a hyperfine shift on all the ligand protons that are observed outside the diamagnetic region where most of the protons usually fall. In the case of Cu_2Co_2SOD, it has been possible to detect all the ligand protons of both cobalt and copper domains[13].

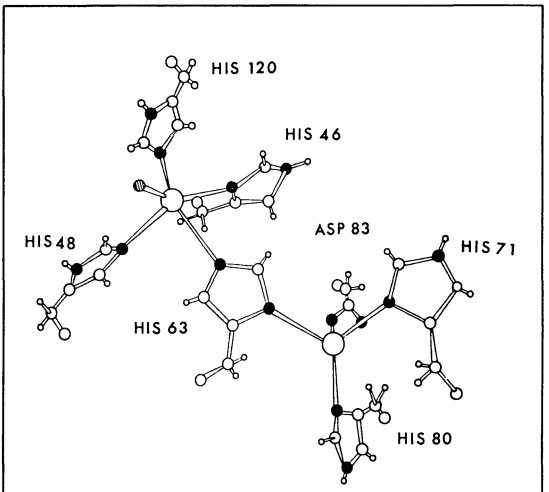

Figure 1. Schematic view of the active site of SOD

Since 1985 our group is engaged in the investigation of SOD through ^1H NMR of Cu_2Co_2SOD[13]. The spectrum, reported in Figure 2, shows 21 resonances, most of them well-resolved, in the region of the hyperfine shifted signals. Five of them disappear when the spectrum is recorded in D_2O. A first assignment of the spectrum was based on the attribution of the exchangeable signals as histidines NH's of residues coordinated to the metal ions (the signals which disappear in D_2O), on the dependence of linewidth from magnetic field and on the calculation of the metal-to-proton distance from T_1 values[13]. However, a significant contribution to the complete assignment of the spectrum was given in 1989 by NOE experiments[14]. At that time the observation of Nuclear Overhauser Effects in a paramagnetic metalloprotein with proton T_1's shorter than 10 ms, represented a significative step forward in the evolution of the NMR technique. The systematic saturation of all the hyperfine shifted signals in both H_2O and in D_2O provided a network of connectivities that allowed us to firmly establish the assignment of the hyperfine shifted signals.

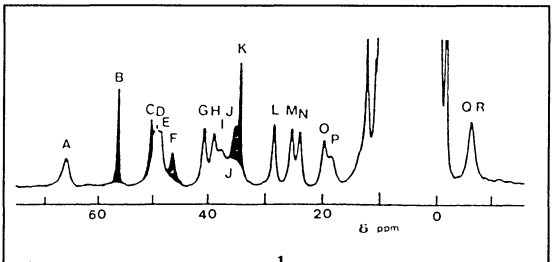

Figure 2. 300 MHz ^1H NMR spectrum of Cu_2Co_2SOD. The shaded signals disappear in D_2O

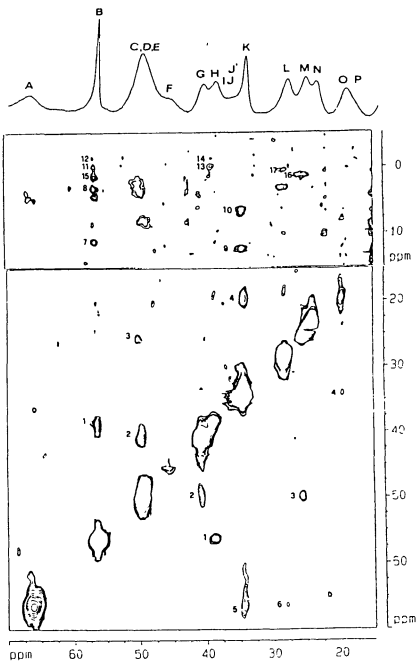

Figure 3. 600 MHz NOESY spectrum of Cu_2Co_2SOD.

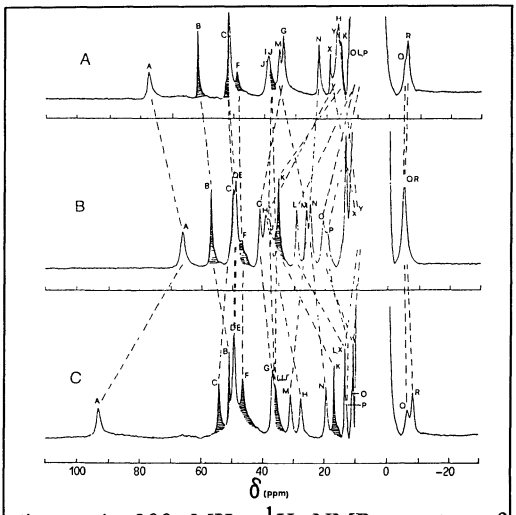

Figure 4. 300 MHz ^1H NMR spectra of Cu_2Co_2SOD in the presence of saturating amount of (A) CN^- and (C) N_3^-. The spectrum without anions is reported in Figure (B).

Nowadays, in 2D experiments, through the optimizaton of the experimental conditions, it has been possible to detect dipolar and scalar connectivities between protons with short T_1 and T_2. In the case of Cu_2Co_2SOD NOESY and COSY experiments have recently shown cross-peaks between fast relaxing protons. From the NOESY spectrum reported in Figure 3, with a single experiment, it was possible to obtain all the information that were obtained from a long series of NOE experiments[15]. Furthermore it has been possible to extend the assignment around the active site by taking into account connectivities between the hyperfine-shifted signals and the signals belonging to residues present in the active cavity but not directly coordinated to the metal ion.

The interaction of SOD with small inorganic anions has been matter of investigation and debate. Indeed, anions like N_3^-, CN^-, NCS^-, NCO^-, F^- may be taken as models of superoxide, the natural substrate of SOD and, with respect to superoxide, have the advantage to form stable adducts. For this reason their behavior with SOD is instructive as far as the interaction of superoxide with the enzyme is concerned. In the past they have been studied through a large variety of spectroscopic techniques (electronic and CD spectroscopy, EPR and NMR etheronuclear)[16-24]. These anions are reported to bind copper. Some of them are competitive inhibitors (CN^-, N_3^-, F^-).

The Cu_2Co_2-derivative is suitable for the ^1H NMR investigation of SOD in the presence of anions[13,25-30]. In all the cases, but CN^-, the exchange between the anions and the protein is fast on the NMR time scale. Therefore it is possible to monitor the shifts of all the signals as a function of anion concentration, to assign the spectrum of the anion adduct and to calculate the

affinity constant of the anion for the protein. With CN^- we observe the appearance of the signals of the CN^--enzyme species, whereas the signals of free enzyme disappear (Figure 4).

All the anions cause a decrease in the shifts of the His 48 ring protons, but to a different extent (Table 1).

Table 1. 200 MHz ^1H NMR shifts of His-48 ring protons.

Cu_2Co_2SOD derivatives	δ(ppm) signal K(Hδ1)	δ(ppm) signal L(Hδ2)	δ(ppm) signal O(Hε1)
BSOD	34.5	28.4	19.6
BSOD + F^-	31.3	25.6	18.2
BSOD + NCS^-	27.7	23.8	16.4
BSOD + NCO^-	19.8	15.6	14.3
BSOD + N_3^-	15.9	12.5	10.5
BSOD + CN^-	13.0	9.1	<11

The following order of increasing effect is observed: $F^- < NCS^- < NCO^- < N_3^- < CN^-$. In order to obtain structural information and to monitor geometric variations of the histidine ligands upon anion binding we have performed NOE experiments on the N_3^- adduct of Cu_2Co_2SOD (N_3^- is the anion that has higher affinity constant, among anions in fast exchange). An accurate optimization of experimental conditions allowed us to monitor NOE values as small as 0.2 %, with estimated errors of 10-30%. The Nuclear Overhauser Effects observed in the azide-bound enzyme provided a map of proton-proton distances that have been compared with the azide-free enzyme[31].

Table 2. T_1, NOE values and proton-proton distances calculated from ^1H NOE measurements on native and azide-bound bovine Cu_2Co_2SOD, at 200 MHz.

Saturated signal	Observed signal	T_1(ms) (nat.)	T_1(ms) ($+N_3^-$)	NOE (%) (nat.)	NOE (%) ($+N_3^-$)	calc. dist. nat.	calc. dist. ($+N_3^-$)
A Hε 2His63	L Hδ2His48	4.3	8.2	0.9±0.1	1.1±0.2	2.7±0.2	2.9 ±0.2
A Hε 2His63	K Hδ1His48	8.0	17.5	0.6±0.2	1.1±0.2	3.2±0.3	3.3±0.2
A Hε 2His63	R Hβ2His48	2.4	4.5	0.2±0.1	0.3±0.1	3.3±0.3	3.2±0.3
B Hδ 1His120	H Hε 1His120	1.8	2.6	1.0±0.2	0.9±0.2	2.3±0.2	2.5±0.2
C Hε2His46	G Hδ2His46	3.5	3.8	1.4±0.2	2.1±0.2	2.4±0.2	2.3±0.2
C Hε2His46	M Hε1His46	2.7	2.9	0.9±0.1	0.8±0.2	2.5±0.2	2.5±0.2
G Hδ 2His46	C Hε2His46	4.2	4.4	1.7±0.4	1.4±0.2	2.4±0.2	2.5±0.2
M Hε 1His46	C Hε2His46	4.2	4.4	2.2±0.2	1.5±0.1	2.4±0.2	2.3±0.2
M Hε 1His46	N Hδ 2His120	2.9	3.7		0.5±0.1		2.9±0.3
R Hβ 2His48	G Hδ2His46	3.5	3.8	0.6±0.2	0.6±0.2	2.8±0.3	2.8±0.3

Table 2 continuation

Q Hβ 1His71	D Hδ2His71	3.8	5.1	1.4±0.2	1.2±0.1	2.4±0.2	2.6±0.2
L Hδ2His48	γCH$_3$Val118	70	120	33±6	48±9	2.8±0.3	2.9±0.3
N Hδ 2His120	P"Hβ 2His120			9±1	4±0.5		
R Hβ 2His48	P Hβ1His46	1.6	5.5	5.4±0.8	5.9±1.0	1.7±0.2	2.0±0.2
P Hβ1His46	R Hβ2His48	2.4	4.5	9.0±1.0		1.7±0.2	
L Hδ2His48	P Hβ1His46	1.6	5.5	1.3±0.3		2.2±0.2	
P Hβ1His46	L Hδ2His48	4.3	8.2	5.5±1.0		2.0±0.2	2.0±0.2
L Hδ2His48	R Hβ2His48	2.4	4.5	0.5±0.1	1.3±0.3	2.6±0.3	2.6±0.2
R Hβ 2His48	L Hδ2His48	4.3	8.2	2.3±0.2	4.0±0.8	2.3±0.2	2.3±0.2

A similar trend is observed for superoxide dismutation and affinity for N_3^- and seems to be strongly modulated by the charge of the residues in the active cavity.

The results, shown in Table 2, indicate that the overall relative spatial disposition of the hystidines coordinating copper does not change significantly upon interaction with azide, despite the sizeable effects observed in the electronic and EPR spectra. These data have been interpretated in terms of a movement of the copper ion, as a consequence of the binding of a strong ligand. This movement determines the lengthening of His 48 and then the decrease of the hyperfine coupling between the protons of His 48 and the unpaired electrons on copper. The proposed mechanism is supported by theoretical calculatons[31].

In order to study the mechanism of electron transfer between O_2^- and copper(II) we have investigated the electron transfer process between hexacyanoferrate(II) and copper(II) in wild type SOD and in some mutants in which residues of the active cavity have been substituted[32]. The electron transfer rate has been measured for the mutants and compared with the wild type enzyme. We have observed that i) substitution of the positive charge on Arg 143 with a neutral group decreases the overall electron transfer rate; ii) mutation of Thr 137 has little influence; iii) substitution of Glu 133 with neutral groups increases the rate (Table 3).

Table 3. Reduction rate constants, affinity constant for N_3^- and activity for O_2^- dismutation of human wild type SOD and some of its mutant

	k_{obs} (M^{-1} s^{-1})	K(M^{-1}) for N_3^- (Cu_2Co_2SOD)	activity (%)
WT	2.88	94±5	100
Ile 143	0.018	16±1	11
Ser 137	1.44	90±7	70
Gln 133	108	534±42	222

We have proposed that the $Fe(CN)_6^{4-}$ anion approaches the copper ion at the entrance of the cavity. This hypothesis has been confirmed by ^{13}C NMR data on SOD titrated with ^{13}C-enriched $Co(CN)_6^{3-}$, a structural analog of $Fe(CN)_6^{4-}$. From the measurements we calculate a Cu-N distance of 3.9 Å. This value indicates the the $Fe(CN)_6^{4-}$ ion enters the cavity, approaches the copper ion and a direct electron transfer between nitrogen and

copper occurs. The rate of the approach depends on the presence of positive charged residues in the active cavity. These charged residues may also modulate the copper-nitrogen distance. The parallelism that we have observed in various mutants between the activity towards superoxide and the electron transfer rate supports the hypothesis that also in the case of dismutation of superoxide, the rate constant for the approach of O_2^-, k_{on}, should have a determinant role.

3. Peroxidases

Peroxidases are hemoproteins containing iron(III) which is further bound to a proximal histidine[33-36]. These systems have been investigated by a variety of techniques; however ^1H NMR spectroscopy has been particularly useful for the cyanide derivative which provides a six-coordinated low spin iron with S=1/2 ground state[37-48]. The atoms numbering is reported in Figure 5. In this case electron relaxation times are very short and NMR lines are sharp. The studied protein include horseradish Peroxidase (HRP, MW 42000), Ligninase (LiP, MW 42,000), Mn-peroxidase (MnP, MW 46,000) and Cytochrome c Peroxidase (CcP, MW 34,000).

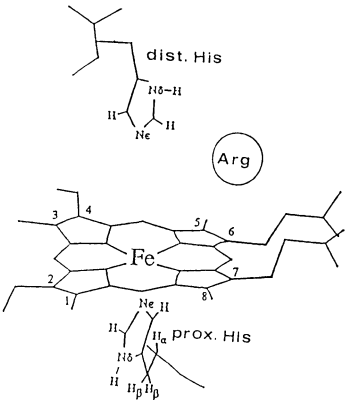

Figure 5. Active site of yeast cytochrome c peroxidase

The X-ray structure is available for CcP and LiP[49-52]. The assignment of the heme protons and of the proximal and distal histidines, as reported in Table 4, shows the similarity of the active centers of these peroxidases. The large variations occur at the proximal histidine protons[53].

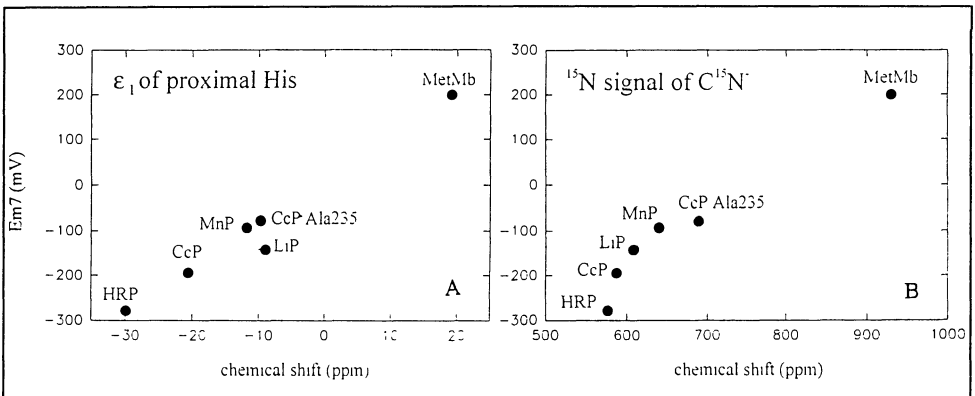

Figure 6. Relationship of the redox potential $E_{m7}(Fe^{3+}/Fe^{2+})$ to chemical shift of A) H ε1 of the proximal His and B) ^{15}N signal of $C^{15}N^-$ for HRP, CcP, LiP, CcPAla235, metmyoglobin.

If we plot the chemical shift of any of the proximal histidine protons, for example of the ε_1 proton, versus Fe^{3+}/Fe^{2+} redox potential we obtain the plot of Figure 6A, where CcP and Ala 235 CcP mutant are also reported[54,55].It is believed that the upfield shift of the ε_1 proton of the proximal histidine is largely due to a strong Fe-imidazole bond, due to the imidazolate character of the proximal histidine.

Table 4. Chemical shift values for the hyperfine shifted resonances in the cyanide derivatives of HRP, CcP, LiP, MnP, and Asp235Ala CcP.

	shift(ppm)				
Assignment	HRP-CN^-	CcP-CN^-	LiP-CN^-	MnP-CN^-	Asp235Ala CcP-CN^-
heme					
2-Hα	5.3	7.1	8.5	8.6	8.7
2-Hβcis	-1.6	-3.7	-3.6	-3.4	-4.1
2-Hβtrans	-2.7	-3.0	-4.1	-3.2	-3.3
α-meso	1.9		1.1	-1.1	
3-CH_3	26.0	30.6	31.0	30.7	24.0
4-Hα	20.1	16.0	14.2	12.7	13.8
4-Hβcis	-3.3	-3.8	-3.2	-2.8	-1.9
4-Hβtrans	-2.2	-2.1	-2.0	-1.8	-3.7
7-Hα	19.6	18.3	13.0	12.5	10.5
7-Hα'	9.7	6.4	9.2	8.0	6.2
8-CH_3	31.0	27.6	20.4	20.4	28.2
δ-meso	6.3		7.6	7.0	
proximal His					
NHp	12.9	12.9	11.6	12.4	
Hβ	23.7	19.4	17.4	19.5	12.3
Hβ'	15.6	14.8	17.0	16.9	11.4
Hδ1	9.9	10.2	14.0	15.1	11.8
Hε1	-29.9	-20.6	-9.0	-11.8	-9.7
Hδ2	23.1	15.8	13.3	20.3	14.6
distal His					
Hδ1	16.3	16.5	17.0	17.0	16.3
Hε1	13.3	14.0	13.6	12.8	13.9
Hδ2	9.8		13.1	13.9	8.7
Hε2	31.0	28.4	35.2	34.2	27.1

The degree of the histidinate character depends on the strength of the hydrogen bond with Asp 235 (Figure 7). An imidazolate ligand favors iron(III) and stabilizes the formal iron(V) oxidation state which is obtained after reaction with H_2O_2. The experimental correlation between the shift of the above mentioned ε_1 proton and the redox potential is consistent with the above hypothesis. On this light the iron-imidazole bond in myoglobin would appear quite weak and inconsistent with the relative strength of hydrogen bonds of histidine NH.

In fact the proximal His is H-bonded to CO of Asp 235, whereas the CcP Ala 235 mutant does not form any H-bond. It is possible that the different pseudocontact contribution to the ε1 shift between peroxidases and myoglobin partly accounts for this inconsistency.

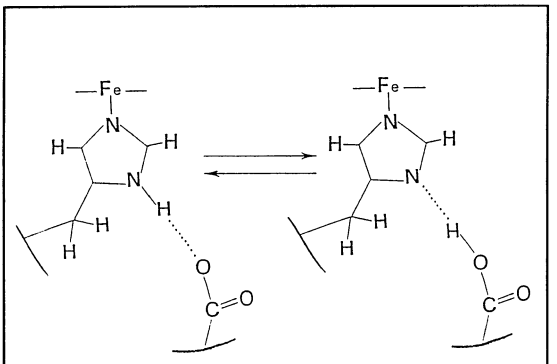

Figure 7. Scheme of the H-bond between proximal His and Asp 235

The strength of the iron(III)-imidazole bond is inversely related to the strength of the cyanide bond which in its turn is monitored through the ^{15}N NMR shifts. Indeed, the shifts of ^{15}N follow a similar pattern as the ε1 shifts (Figure 6B). The pseudo-contact contributions does not significantly contribute to the ^{15}N hyperfine shifts which are very large. In such a case contributions to ^{15}N hyperfine shifts arise from H-bonding and solvation.

It should be noted that all of the above information have been obtained on relatively large proteins and by starting the NMR analysis from protons shifted outside the diamagnetic region.

In the case of Mn-peroxidase it has been possible to obtain information on the Mn binding site, from the broadening of the hyperfine shifted signals[56]. Mn(II) has five unpaired electrons and long relaxation time which causes broadening of the signals depending on the sixth power of the Mn-protons distances (Figure 8).

From the dipolar connectivity of p-cresol and HRP-CN, it has been possible to propose a binding site of small aromatic molecules in HRP (Figure 9).

4. Cytochrome $P450_{cam}$

Cytochrome $P450_{cam}$, without substrate, is in the low spin state; it contains an iron(III) ion with an S=1/2 in its ground state[57]. The iron is bound, besides the heme, to a cystein and a solvent molecule[58-65]. The two axial ligands are weaker than in the case of histidine and cyanide, discussed in the previous section. This "tetragonal elongation" leads to long electron relaxation times and the NMR signals are broad[66-69]. If we consider that the protein has a MW of 45,000, it is not difficult to figure out that the NMR information were scarce. However, when the protein is treated with aromatic bases like pyridine, imidazole and N-methylimidazole, 2 molecules of base enter the cavity, one binding the metal and one interacting with the hydrophobic pocket[70]. In this case, the NMR lines can be a little sharper and some assignments have been proposed. The two bases exchange slowly on the

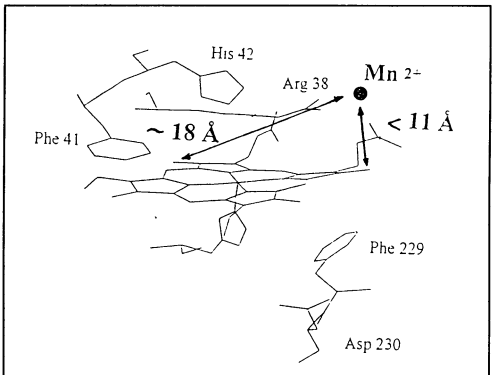

Figure 8. The binding of Mn(II) to Manganese Peroxidase

NMR time scale. Figure 10 shows the NMR spectra obtained through titration with pyridine (A) and imidazole (B) with the assignment which has been obtained through NOEs and some bidimensional NOESY experiments. The information obtained in this case is that of revealing two different species.

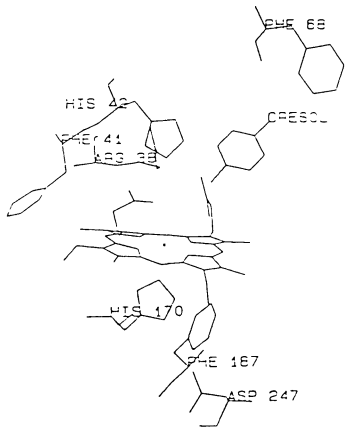

Figure 9. The binding site of p-cresol in HRP

5. Concluding Remarks

The field of NMR of paramagnetic metalloproteins has grown to the level which allows NOEs detection under many circumstances and to obtain local information on the surrounding of the paramagnetic centers even in proteins with molecular weight of about 50,000.

The detailed assignment of all the protons of histidine bound to both copper and cobalt in Cu_2Co_2SOD has provided a precious tool to monitor the reactivity with inhibitors and substrate analogs.

In peroxidases NMR has proven the similarity of the various proteins and has provided unique information about the strength of the proximal imidazole-iron bond. Such piece of information is relevant with respect to the mechanism of action.

Even in the case of Cyt P450, which is the most difficult to investigate by means of

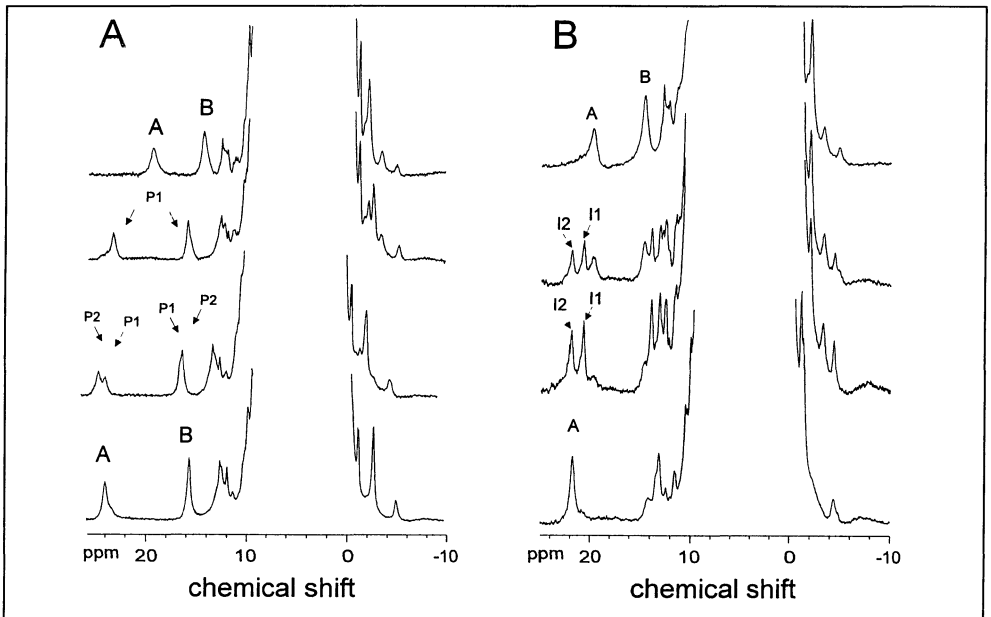

Figure 10. A) 600 MHz ^1H NMR titration of P450 with pyridine: (a) P450; (b) P450 + 1.3 eq of pyridine; (c) P450 + 5 eq of pyridine; (d) P450 + 18 eq of pyridine. B) 600 MHz ^1H NMR titration of P450 with imidazole: (a) P450; (b) P450 + 1.0 eq of imidazole; (c) P450 + 2.0 eq of imidazole; (d) final adduct (0.15 M imidazole). Signals A and B have been assigned as 8-CH_3 and 3-CH_3 protons, respectively.

NMR, detailed structural and kinetics parameters are obtained on organic molecules interacting with the protein.

Other systems like Co-substituted Zn-enzymes, iron-sulfur proteins and cytochromes have been under extensive investigation for a long time[53] *and references therein*.

The 2D and 3D spectra, the latter including heteronuclear spectroscopy, have been optimized to such an extent that the structure in solution of paramagnetic proteins is nowaday affordable[7].

6. References

(1) *NMR of Paramagnetic Molecules*, Academic Press, New York, **1973**

(2) Dwek, R.A. *Nuclear Magnetic Resonance in Biochemistry: Applications to Enzyme Systems*, Oxford University Press, London, **1973**

(3) Banci, L., Bertini, I., Luchinat, C. & Piccioli, M. in *NMR and biomolecular structure* (Bertini, I., Molinari, H. & Niccolai, N. eds.) pp. 31-60, VCH, **1991**

(4) Bertini, I. & Luchinat, C. *NMR of paramagnetic molecules in biological systems*, Benjamin/Cummings, Menlo Park, CA,**1986**

(5) Noggle, J.H. & Schirmer, R.E. *The nuclear Overhauser effect*, Academic Press, New York, **1971**

(6) Neuhaus, D. & Williamson, M. *The nuclear Overhauser effect in structural and conformational analysis*, VCH, New York,**1989**

(7) Banci, L., Bertini, I., Felli, I., Kastrau, D., Luchinat, C., Piccioli, M.& Pierattelli, R.(submitted)

(8) Tainer, J.A., Getzoff, E.D., Beem, K.M., Richardson, J.S. & Richardson, D.C. *J. Mol. Biol.* **1982,** *160*, 181.

(9) Parge, H.E., Hallewell, R.A. & Tainer, J. () *Proc. Natl. Acad. Sci. USA* **1992,** *89*, 6109.

(10) Owens, C., Drago, R.S., Bertini, I., Luchinat, C. & Banci, L., *J. Am. Chem. Soc.* **1986,***108*, 3298.

(11) Bertini, I., Luchinat, C., Owens, C. & Drago, R.S., *J. Am. Chem. Soc.* **1987,***109*, 5208.

(12) Banci, L., Bertini, I. & Luchinat, C. *Nuclear and electron relaxation. The magnetic nucleus-unpaired electron coupling in solution*, VCH, Weinheim,**1991.**

(13) Bertini, I., Lanini, G., Luchinat, C., Messori, L., Monnanni, R. & Scozzafava, A., *J. Am. Chem. Soc.* **1985,** *107*, 4391.

(14) Banci, L., Bertini, I., Luchinat, C., Piccioli, M., Scozzafava, A. & Turano, P., *Inorg. Chem.* **1989,***28*, 4650.

(15) Banci, L., Bertini, I., Luchinat, C., Piccioli, M. & Scozzafava, A. *Gazz. Chim. Ital.*, **1993,** *123*, 95.

(16) Blackburn, N.J., Hasnain, S.S., Binsted, N., Diakun, G.P., Garner, C.D. & Knowles, P.F., *Biochem. J.*,**1984,** *219*, 985.

(17) Fee, J.A. & Gaber, B.P. (1972) *J. Biol. Chem.*,**1972,** *247*, 60.

(18) Pantoliano, M.W., Valentine, J.S. & Nafie, L.A., *J. Am. Chem. Soc.*,**1982,** *104*, 6310.

(19) Rotilio, G., Calabrese, L., Bossa, F., Barra, D., Finazzi Agro', A. & Mondovi, B. *Biochemistry* ,**1972,** *11*, 2182.

(20) Liebermann, R.A., Sands, R.H. & Fee, J.A., *J. Biol. Chem.*, **1982,** *257*, 336.

(21) Van Camp, H.L., Sands, R.H. & Fee, J.A., *Biochim. Biophys. Acta*, **1982,***704*, 75.
(22) Huettermann, J., Kappl, R., Banci, L. & Bertini, I., *Biochim. Biophys. Acta* **1988,***956*, 173.
(23) Fee, J.A., Peisach, J. & Mims, W.B., *J. Biol. Chem.* **1981,***256*, 1910.
(24) Blackburn, N.J., Strange, R.W., McFadden, L.M. & Hasnain, S.S., *J. Am. Chem. Soc.* **1987,** *109*, 7162.
(25) Banci, L., Bencini, A., Bertini, I., Luchinat, C. & Viezzoli, M.S., *Gazz. Chim. Ital.* **1990,** *120*, 179.
(26) Ming, L.J., Banci, L., Luchinat, C., Bertini, I. & Valentine, J.S., *Inorg. Chem.* **1988,** *27*, 728.
(27) Banci, L., Bertini, I., Luchinat, C., Monnanni, R. & Scozzafava, A., *Inorg. Chem.* **1988,** *27*, 107.
(28) Banci, L., Bertini, I., Luchinat, C., Scozzafava, A. & Turano, P., *Inorg. Chem.* **1989,** *28*, 2377.
(29) Banci, L., Bertini, I., Luchinat, C. & Scozzafava, A., *J. Biol. Chem.* **1989,** *264*, 9742.
(30) Paci, M., Desideri, A. & Rotilio, G., *J. Biol. Chem.* **1988,** *263*, 162.
(31) Banci, L., Bencini, A., Bertini, I., Luchinat, C. & Piccioli, M., *Inorg. Chem.* **1990,** *29*, 4867.
(32) Bertini, I., Hiromi, K., Hirose, J., Sola, M. & Viezzoli, M.S., *Inorg. Chem.* **1993,** *32*, 1106.
(33) Dunford, H.B. in *Peroxidases in Chemistry and Biology* (Everse, J., Everse, K.E. & Grisham, M.B. eds.) pp. 51-84, CRC Press, Boca Raton, FL, **1991.**
(34) Bosshard, H.R., Anni, H. & Yonetani, T., in *Peroxidases in Chemistry and Biology* (Everse, J., Everse, K.E. & Grisham, M.B. eds.) pp. 51-84, CRC Press, Boca Raton,FL, **1991.**
(35) Poulos, T.L. & Kraut, J., *J. Biol. Chem.* ,**1980,** *255*, 8199.
(36) Finzel, B.C., Poulos, T.L. & Kraut, J., *J. Biol. Chem.* **1984,** *259*, 13027.
(37) de Ropp, J.S, Yu, L.P. & La Mar G.N., *J. Biomol. NMR*, **1991,** *1*, 175.,
(38) de Ropp, J.S, La Mar, G.N., Smith, K.M. & Langry, K.C., *J. Am. Chem. Soc.* **1984,** *106*, 4438.
(39) Thanabal, V., de Ropp, J.S & La Mar, G.N., *J. Am. Chem. Soc.* **1987,** *109*, 7516.
(40) Thanabal, V., de Ropp, J.S & La Mar, G.N., *J. Am. Chem. Soc.* **1986,** *108*, 4244.
(41) Thanabal, V., de Ropp, J.S & La Mar, G.N., *J. Am. Chem. Soc.* **1987,** *109*, 265.
(42) Thanabal, V., de Ropp, J.S & La Mar, G.N., *J. Am. Chem. Soc.* **1988,** *110*, 3027.
(43) Satterlee, J.D., Erman, J.E., La Mar, G.N., Smith, K.M. & Langry, K.C., *Biochim. Biophys. Acta* **1983,** *743*, 246.
(44) Satterlee, J.D., Erman, J.E. & de Ropp, J.S., *J. Biol. Chem.* **1987,** *262*, 11578.
(45) Satterlee, J.D., Erman, J.E., La Mar, G.N., Smith, K.M. & Langry, K.C., *J. Am. Chem. Soc.* **1983,** *105*, 2099.
(46) Satterlee, J.D., Erman, J.E., Mauro, J.M. & Kraut, J. , *Biochemistry* **1990,** *29*, 8797.
(47) Banci, L., Bertini, I., Turano, P., Ferrer, J.C. & Mauk, A.G.,*Inorg. Chem.* **1991,** *30*, 4510.
(48) Banci, L., Bertini, I., Kuan, I-C., Tien, M., Turano, P. & Vila, A.J., *Biochemistry* **1993,** *32*, 13483.
(49) Wang, J., Mauro, J.M., Edwards, S.L., Oatley, S.J., Fishel, L.A., Ashford, V.A., Xuong, N. & Kraut, J., *Biochemistry* **1990,** *29*, 7160.

(50) Edwards, S.L., Raag, R., Wariishi, H., Gold, M.H. & Poulos, T.L., *Proc. Natl. Acad. Sci. USA* **,1993,** *90*, 750.
(51) Piontek, K., Glumoff, T. & Winterhalter, K., *FEBS Lett.* **1993,** *315*, 119.
(52) Poulos, T.L., Edwards, S.L., Wariishi, H. & Gold, M.H., *J. Biol. Chem.* **1993,** *268*, 4429.
(53) Bertini, I., Turano, P. & Vila, A.J. , *Chem. Rev.* **1993,** *93*, 2833.
(54) Banci, L., Bertini, I., Turano, P., Tien, M. & Kirk, T.K., *Proc. Natl. Acad. Sci. USA* **1991,** *88*, 6956.
(55) Ferrer, J.C., Turano, P., Banci, L., Bertini, I., Mauk, A.G. & Smith, K.M., *Biochemistry* **1994**(In Press)
(56) Banci, L., Bertini, I., Bini, T., Tien, M. & Turano, P., *Biochemistry* **1993,** *32*, 5825.
(57) Weiner, L.M., *CRC Crit. Rev. Biochem.* **1986,** *20*, 139.
(58) Poulos, T.L., Finzel, B.C. & Howard, A.J. , *J. Mol. Biol.* **1987,** *195*, 687.
(59) Poulos, T.L., Finzel, B.C. & Howard, A.J., *Biochemistry* **1986,** *25*, 5314.
(60) Poulos, T.L., Finzel, B.C., Gunsalus, I.C., Wagner, G. & Kraut, J., *J. Biol. Chem.* **1985,** *260*, 16122.
(61) Collman, J.P., Sorrell, Th.N. & Hoffmann, B.M., *J. Am. Chem. Soc.* **1975,** *97*, 913.
(62) Tang, S.C., Koch, S., Papaefthyomyou, G.C., Foner, S., Frankel, R.B., Ibers, J.A. & Holm, R.H., *J. Am. Chem. Soc.* **1976,** *98*, 2414.
(63) Collman, J.P., Sorrell, Th.N., Hodgson, K.O., Kulshrestha, A.K. & Strouse, C.E., *J. Am. Chem. Soc.* **1977,** *99*, 5180.
(64) Griffin, B.W. & Peterson, J.A., *J. Biol. Chem.* **1975,** *250*, 6445.
(65) Philson, S.B., Debrunner, P.G., Schmidt, P.G. & Gunsalus, I.C., *J. Biol. Chem.* **1979,** *254*, 10173.
(66) Lukat, G.S. & Goff, H.M., *Biochim. Biophys. Acta* **1990,** *1037*, 351.
(67) Keller, R.M., Wóthrich, K.J. & Debrunner, P.G., *Proc. Natl. Acad. Sci. USA* **1972,** *69*, 2073.
(68) Sato, R. & Omura, T., *Cytochrome P450*, Academic Press, New York, **1978**.
(69) Banci, L., Bertini, I., Eltis, L.D. & Pierattelli, R., *Biophys. J.* **1993,** *65*, 806.
(70) Banci, L., Bertini, I., Marconi, S., Pierattelli, R. & Sligar, S.G. (1994) *J. Am. Chem. Soc.***1994** (In Press).

MAGNETIC AND EPR STUDIES OF SUPEROXIDE DISMUTASES (SOD): ELECTRONIC STRUCTURE OF THE ACTIVE SITES FOR THE (COPPER-ZINC)SOD, ITS COBALT SUBSTITUTED DERIVATIVE AND THE IRON(III)SOD FROM *E. COLI*

IRENE MORGENSTERN-BADARAU
Laboratoire de Chimie bioorganique et bioinorganique
Institut de Chimie Moléculaire d'Orsay
Université PARIS-SUD-XI, 91405-Orsay, France

1. Introduction

There are three types of superoxide dismutases (SOD), based on the metal involved in the catalysis {Cu(II), Fe(III) or Mn(III) in the native enzymes}. The most intensively studied protein is the copper-zinc superoxide dismutase (Cu-Zn)SOD and its metal substituted derivatives[1] : an imidazolate bridging the two metal ions is the characteristic feature of the active site[2]. Manganese or iron SOD are a different class of proteins: X-ray crystallographic data indicate that they are structural homologs characterized by a trigonal bipyramidal arrangement around the metal ion with four protein ligands and possibly a water molecule[3].

Magnetic susceptibility (or magnetization) and EPR studies are efficient in probing electronic structure and especially the ground state structure which is important with respect to the possible mechanisms. In order to get a consistent description of the results, we have developed a protocol based on the two complementary techniques. We have applied this protocol to study various problems. We present here our approach, focussing on the following examples:

(i) the Co subsituted (Cu-Zn)SOD with the cobalt at the tetrahedral zinc site[4] in order to determine the exchange interaction between cobalt and copper which provides insight into the bridging imidazolate ligand

(ii) the Fe(III)SOD from *E. Coli* in order to evaluate the ground state zero-field splitting which is strongly related to the symmetry of the metal center and its chemical environment.

2. Experimental protocol

For many years, EPR spectroscopy has been used to study metalloproteins. It is an important tool in the case of odd spin systems.Currently, many different problems can be considered, as listed below in a non exhaustive way. For example, the EPR utility is found to indicate the site symmetries of the paramagnetic centers, to independently identify each Kramers doublet, to evaluate their relative energy positions and their associated effective g factors, to show the possible hyperfine interactions and to study saturation phenomena. Experiments are usually performed on glassy samples, according to well known procedures.

In addition to odd spin systems, magnetic susceptibility measurements can also be used for integer systems and therefore is one of the most powerful techniques to study the

D.P. Kessissoglou (ed.), Bioinorganic Chemistry, 105-111

electronic structure of these systems. Spin states, their relative energy positions, mean g values and zero-field splittings are usually obtained. In the case of exchange coupling in polynuclear molecules, magnetization and magnetic susceptibility studies as a function of the temperature are of prime importance to determine the nature and the magnitude of metal ion interaction .

The use of magnetic techniques for the case of metalloproteins needs the solution of several serious problems in order to get reliable results[5]. Due to their large molecular weight and the small amount of paramagnetic centers, the proteins are essentially diamagnetic. The difficulties are firstly, to extract a very small paramagnetic effect from an high diamagnetic signal overall, and secondly, to precisely determine the amount of metal ions in order to obtain the molecular magnetic properties. Therefore, to resolve the contribution of interest, we have perfected a protocol based on the following points:

- high degree of purity and homogeneity of the proteins;
- precise analysis of the metal content;
- high sensitivity and accuracy of the susceptometers as those built on quantum flux detection methods;
- direct and independent measurement of the diamagnetic susceptibility of the apoproteins which is crucial for getting absolute values of susceptibilities.

In order to get a consistent set of data, all the experiments have to be run on same samples.

3. The copper-zinc superoxide dismutase and its cobalt substituted derivatives

In the native enzyme, the active site contains one copper(II) ion in a square pyramidal arrangement, and a zinc(II) ion in a tetrahedral symmetry with an imidazolate group bridging the two metal ions. A cobalt(II) ion can replace the zinc in its site. The resulting copper(II)-cobalt(II) pair interacting through the imidazolate bridge characterized the cobalt substituted protein. Two apo proteins are also available, the apoSOD with no metal, and the (apoCo)SOD with only the cobalt present in the zinc site. These four proteins, the native (Cu-Zn)SOD, the (Cu-Co)SOD, the apoSOD and the (apoCo)SOD have been studied. They have been prepared from the same source, according to established procedures[4]. They provide an unique set for testing the perfected protocol for the study of exchange coupling in proteins.

From the apoprotein, a reasonable value of the diamagnetism of the four studied proteins has been obtained, since they differ only in their metal contents. The diamagnetic susceptibility was found to be equal to -1.43×10^{-6} cm^3g^{-1}.

From the (Cu-Zn)SOD and the (apoCo)SOD, the properties of the isolated Cu and Co chromophores are deduced from both magnetic and EPR experiments and can be compared to the ones in the coupled systems. Figure 1 shows the temperature dependence of the effective magnetic moment (in Bohr magnetons μ_B). (Cu-Zn)SOD follows a Curie law as expected for a S=1/2 system (μ_{eff}=1.73 μ_B and g=2.06). From EPR, axial symmetry is revealed with the corresponding $g_\perp$=2.26 and $g_\parallel$ =2. (apoCo)SOD has a magnetic moment varying from 4.27 μ_B at high temperature to 3.8 μ_B at 6 K, in good agreement with a S=3/2 state (Figure 1). The zero field splitting obtained from the fit of the magnetic data to the susceptibility equation was found to be equal to 10.8cm^{-1}, very close to the value of 11.5 cm^{-1} obtained from the temperature dependence of the EPR spectrum[6].

The copper-cobalt interaction in the cobalt substituted derivative (Cu-Co)SOD has been studied by using magnetic susceptiblity measurements which in this case were particularly challenging as this derivative is a non Kramers system and does not show any EPR signal[7].

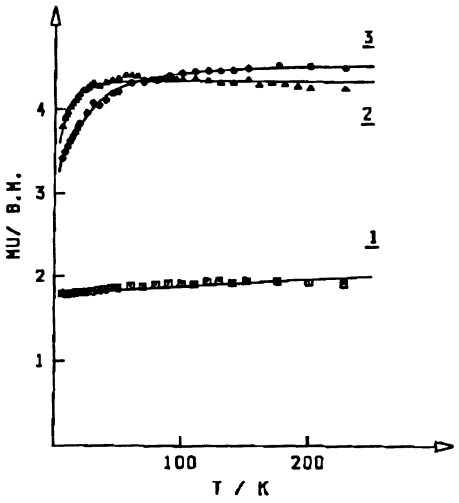

Figure 1. Magnetic moment data for **1** (Cu-Zn)SOD, **2** (apoCo)SOD, **3** (Cu-Co)SOD.

The comparison of the magnetic behavior of the three paramagnetic proteins as displayed in Figure 1, clearly shows an antiferromagnetic interaction between the cobalt and the copper ions since, under 100K, its moment is lower than the moment of the (apoCo)SOD. The copper-cobalt antiferromagnetic coupling[8] has been made quantitative. The spin Hamiltonion parameters describing the energy levels arising from the interaction are collected in Figure 2. The energy gap between the two states S=1 and S=2 is found to be equal to 33 cm^{-1}.

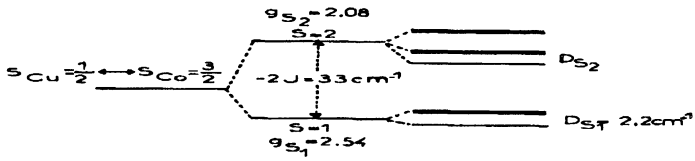

Figure 2. Electronic structure of the (Cu-Co)SOD active site. Spin Hamiltonian parameters associated with the energy levels.

These results unambiguously indicate that the imidazolate bridge propagates the electronic effects. They can also predict that the efficient pathway is essentially a "σ" pathway in agreement with the results found for the copper-copper interaction in the copper substituted[9] (Cu-Cu)SOD. Indeed, only one electron pair, with one unpaired electron on each copper center is active in the (Cu-Cu)SOD. It corresponds to the "σ" pathway through

the imidazolate bridge. In the case of the cobalt derivative, three electron pairs have to be considered. From the comparison of the magnitude of the coupling found in both enzymes, it can be deduced that only one electron pair is active in the cobalt substituted enzyme, which implies that the same pathway is used for propagating the electronic effects.

In other respects, the effect of this coupling on NMR parameters has been intensively investigated[10].

4. The Fe(III)superoxide dismutase from *E. Coli*

The studies have been carried out by using both EPR and magnetic techniques , in solution and lyophilized forms, after purification according to published procedures[11]. The experimental approach is the same as described above.

The diamagnetic contribution measured on the apoenzyme is equal to -0.5×10^{-6} cm^3g^{-1}. It is in good agreement with the calculated diamagnetic atomic susceptibilities obtained from the primary structure of the protein.The effective magnetic moment has a constant value of 5.85 μ_B over a large temperature range which is an indication of a S=5/2 ground state with small spin quantum mixing. The fit to the data of the susceptibility equation for high spin iron(III) gives the spin hamiltonian parameters g and zero-field splitting D: from the high temperature range, the g value is found to be equal to 1.98; from the low temperature rang, a reasonable estimation of the Dparameter is obtained D=2.5 cm^{-1} (the degree of rhombicity and the sign of D can't be reached).

The X-band EPR spectrum for the native enzyme at liquid helium temperature reveals three intense signals in the 1500 gauss region with the corresponding effective g values equal to 4.7, 4, 3.7, and two weak signals at low field with effective g values equal to 9.8 and 9.4, which have been assigned to the three different Kramers doublets arising from the S=5/2 ground state (Figure 3).

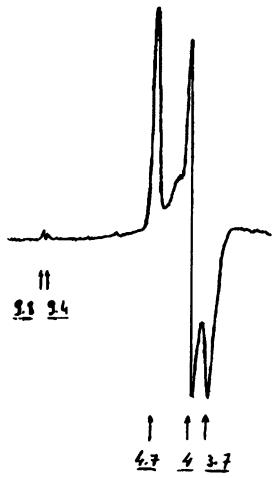

Figure 3. X-band EPR spectrum of the iron(III)SOD active site recorded at 4.2K. Effective g values.

The three intense resonances are typical of the transitions within the intermediate Kramers doublet of the 5/2 spin system in rhombic symmetry[12]: a maximum of the intensity for the three signals has been observed at 9K. The fit of the corresponding effective g values to theoretical equations[13] gives an estimation of the degree of rhombicity E/D= 0.25. The "9.8" resonance shows an intensity that decreases when the temperature increases and therefore has been assigned to the ground Kramers doublet; the experimental effective g value is in good agreement with the calculated one (9.83) from the evaluation of the rhombicity factor. The intensity of the "9.4" signal reaches a maximum at 18 K and then the corresponding transition was assigned to the second excited doublet; the observed effective g value agrees with the calculated one (9.39).

The consistency of the effective g values, associated with the observed temperature dependence of the intensities leads to the identification of the ground Kramers doublet as $|\pm 5/2\rangle$ and therefore to a negative zero-field splitting parameter. From the variation of the intensities and using the following approximate equation

$$F = 1 / \{T(1+\exp 3D/kT+\exp 6.6D/kT)\}$$

the energy gaps 3.6D and 3D within the three doublets have been calculated. They correspond to the value of the zero field splitting parameter $D = -2\ cm^{-1}$ (Figure 4).

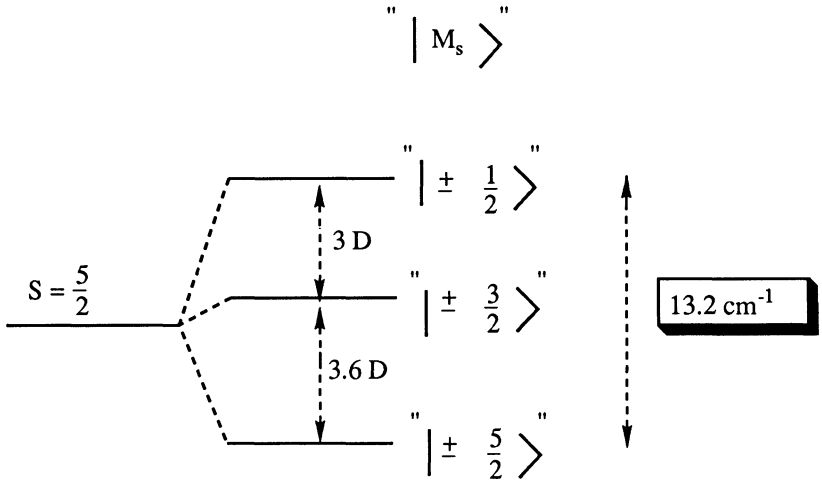

Figure 4. Electronic structure of the ground state for the Iron(III) SOD. Energy gaps between the Kramers doublets associated with a negative zero-field splitting parameter.

These properties have been interpreted in terms of ligand field theory. We have developed a ligand field model for d^5 configuration , in the case of five coordinated ions in trigonal symmetry[14]. We have defined the position of the metal ion relative to the equatorial plane by the angle ϕ, as shown in Figure 5.

In order to simulate the ground state zero-field splitting, the calculations have been done for the value of ϕ equal to the value in the protein[3] ϕ=83°. The energy level positions, and the quantum admixtures have been calculated as a function of the ratio Δ/ζ, with Δ and ζ as ligand field and spin-orbit coupling parameters respectively, and taking into account the covalency effect. The simulation reproduces a negative zerofield splitting associated

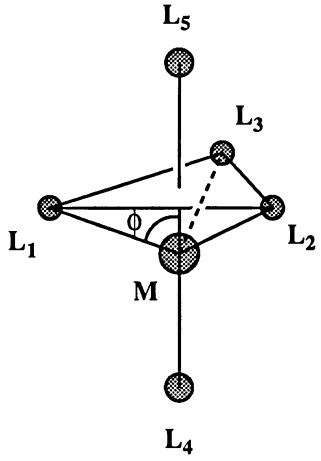

Figure 5. Bipyramidal trigonal site. The metal ion M is located at a position defined by the ϕ angle.

with a "Ms=5/2" ground Kramers doublet, with the quartet ^4E as the lowest excited intermediate spin state. For the value $\Delta/\zeta \cong -20$, the total energy gap between the Kramers doublets has been evaluated to 10.5 cm-1, which, compared to the experimental one, is reasonable owing to the overparametrization of the model. It corresponds to a quantum mixing of approximately 2% of the quartet state and 98% of the sextet, for the ground doublet.

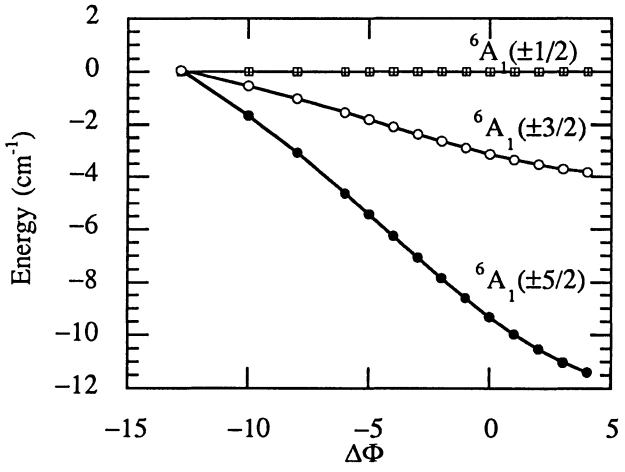

Figure 6. Ligand field simulation of the zero field splitting as a function of the position of the metal ion.

It is also shown in Figure 6 that varying the relative position of the metal ion with respect to the equatorial plane as $\Delta\phi$ induces sensitive changes in the ground state essentially due to a change in the position of the first excited intermediate spin state ^4E. In other words, moving the metal in the direction of the fifth axial position would drive the system towards a larger stabilization of the intermediate state, a point which may be relevant to the possible mechanism of the enzyme.

6. References

(1) For review, see, for example: (a) J.A.Fee, *Metal ions in biological systems*, Ed. H. Sigel, p.259, Marcel Dekker, Inc. New York **1981**. (b) J.S.Valentine, M.W.Pantoliano, *Copper proteins*, Ed. T.G.Spiro, p. 291, Wiley, New-York **1981**. (c) I.Bertini, L.Banci, C.Luchinat, M.Piccioli, *Coord. Chem. Rev.* **1990**, *100*, 67.

(2) J.A.Tainer, E.D.Getzoff, K.M.Beem, J.S.Richardson , D.C.Richardson, *J. Mol. Biol.* **1981**, *160*, 181.

(3) (a) W.C.Stallings, T.B.Powers, K.A.Pattridge, J.A.Fee , M. Ludwig, *Proc. Natl. Acad. Sci USA* **1983**, *80*, 3884. (b) B.L.Stoddard, P.L.Howell, D.Ringe, G.A.Petsko, *Biochemistry* **1990**, *29*, 8885.

(4) (a) L.Calabrese, G. Rotilio, B. Mondovi, *Biochim. Biophys. Acta* **1972**, *263*, 827. (b) L.Calabrese, D.Cocco, L.Morpurgo, B. Mondovi, G. Rotilio, *Eur. J. Biochem.* **1976**, *64*, 465. (c) J.A.Fee, *J. Biol. Chem.* .**1973**, *248*, 4229.

(5) E.P. Day, T.A. Kent, P.A. Lindahl, E. Münck, W.H. Orme-Johnson, H. Roder, A. Roy, *Biophys. J.* **1987**, *52*, 837.

(6) G.Rotilio, L.Calabrese, B.Mondovi, W.E.Blumberg, *J. Biol. Chem.* **1974**, *249*, 3157.

(7) J.A. Fee, *J. Biol. Chem.*, **1978**, *248*, 4229.

(8) I. Morgenstern-Badarau, D.Cocco, A.Desideri, G.Rotilio, J.Jordanov, N.Dupré, *J. Am. Chem. Soc.* **1986**, *108*, 300.

(9) J.A. Fee, R.G. Briggs, *Biochim Biophys. Acta*, **1975**, *400*, 439.

(10) I.Bertini, C.Luchinat, M.Piccioli, *Progress in NMR Spectroscopy*, **1994**, *26*, 91. ref.within

(11) F.J.Yost, I.Fridovich, *J. Biol. Chem.* **1973**, *248*, 4905.

(12) (a) K.Puget, A.M.Michelson, *Biochimie* **1974**, *56*, 1255. (b) T.O.Slykhouse, J.A.Fee, *J. Biol. Chem.* **1976**, *251*, 5472.

(13) H.H.Wickman, M.P.Klein, D.A.Shirley, *J. Chem. Phys.* **1965**, *42*, 2113.

(14) X.Y.Kuang, I.Morgenstern-Badarau, M.C.Rodriguez, *Phys.Rev.* **1993**, *B 48*, 6676-6679.

MECHANISM OF ACTION OF THIAMIN ENZYMES ROLE OF METAL IONS

N. HADJILIADIS, K. DODI & M. LOULOUDI
University of Ioannina, Department of Chemistry, Laboratory of Inorganic and General Chemistry, Ioannina 45-110, Greece

ABSTRACT: The mechanism of action of thiamin enzymes involving bivalent metal ions is examined in this paper.

1. Introduction

1.1. HISTORICAL BACKGROUND

In 1926 Jansen and Donath[1], with a series of experiments, succeeded in the isolation of Vitamin B_1 (thiamin) in the form of crystalline hydrochloride 1, from rice bran.

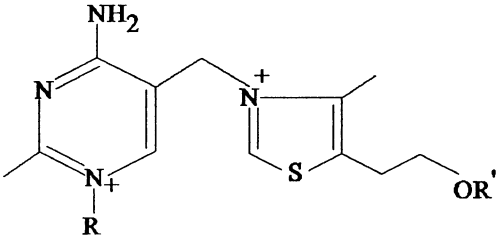

1 R=H, Thiamin
2 R=P2O63-, Thiamin pyrophosphate
3 R=HX, Thiaminium salts

Williams and his collaborators[2,3] succeeded in proving its chemical structure. By first treating vitamin B_1 in neutral sulfite solution at room temperature, the molecule was cleaved into two halves, as follows,

D.P. Kessissoglou (ed.), Bioinorganic Chemistry, 113-128

$C_{12}H_{13}N_4SOCl_2+Na_2SO_3 \rightarrow C_6H_4N_3SO_3+C_6H_9NSO+2Nacl$ (1)

Compound $C_6H_4N_3SO_3$ (4) was proved to be a pyrimidin derivative, while compound C_6H_9NSO (5) was proved to be a thiazole derivative.

The first structure however published by Williams for thiamin was incorrect lacking the methylenic bridge[2]. The correct formula 1 was finally proposed again by Williams[4] a little later. Williams[5] succeeded also to its first laboratory synthesis.

1.2. CHEMICAL PROPERTIES

The structure of thiamin is strongly pH dependent. In acidic aqueous solutions the predominant structure is 3. At pH 11 however it is converted to dihydrothiochrome 6, by the addition of the 4-amino group to the thiazole ring, followed by the formation of the yellow thiol form 7.

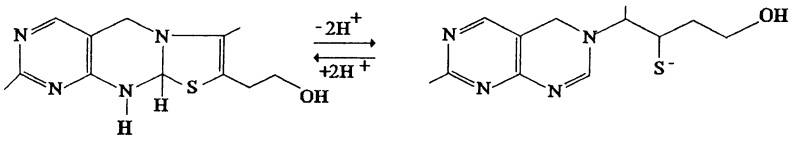

6 7

This reversible transformation has an apparent pKa of 11.6. From the yellow thiol form, thiochrome is formed, 8.

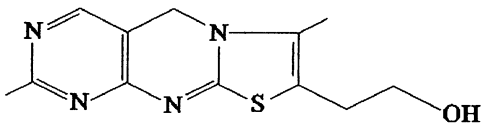

8

The colorless thiolate 9 is produced with hydrolysis of 7 with an apparent pKa of 9.3 or by hydrolysis of thiamin through the formation of a pseudobase with a pKa of the thiol of 7.9.

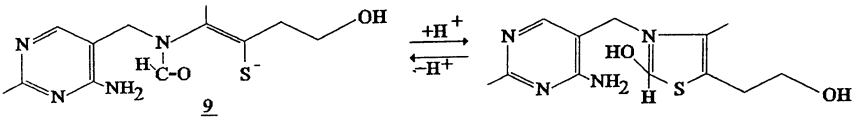

9 10

The thiolate form 9 is readily reduced to a disulfide 11 which in turn is easily reduced back to the vitamin. It is

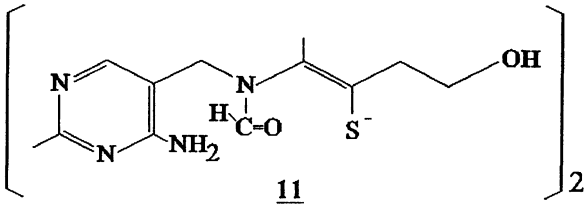

11

for this reason that it was used as a vitamin substitute, because the neutral form passes through membranes more readily than the ionic material.

Compound 12 can finally be obtained from 6 in basic alcoholic solutions and can be converted back to the vitamin by the action of an acid.

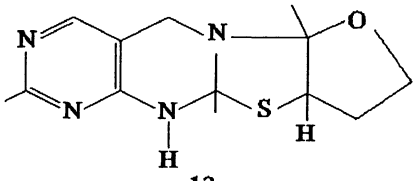

12

1.3. BIOLOGICAL ACTION

Vitamin B_1 deficiency accumulates pyrouvic acid in the blood and produces the disease beri-beri. In modern societies however, alcoholism produces a dietary deficiency giving rise to neurological (Wermicke's disease) and heart disease (Korsakoff disease).

The biologically active form of thiamin is its pyrophosphate ester 2, thiamin pyrophosphate or TPP. This was first isolated by Lohmann and Schuster[6].

TPP is the coenzyme of many enzymes like carboxylase, pyrouvic dehydrogenase, transketolase, phosphoketalase, etc. It was first named cocarboxylase, believed to be the coenzyme of only carboxylase[7]. For its action bivalent metal ions like Mg^{2+} are required[7]. Other bivalent metal ions such as Co^{2+},Zn^{2+},Cd^{2+}, Mn^{2+} etc can also catalyze the reactions of TPP *in vitro*. The reactions catalyzed by TPP are the decarboxylation of α-ketoacids and the formation or degradation of α-ketols. Both imply the breaking of a C-C bond near a $\rangle C = O$ group and the creation of an acyl carbanion R-CO .

2. Mechanism Of Action Of Thiamin Enzymes

2.1. INTRODUCTION

Since TPP was first thought as the coenzyme of only carboxylase, the early investigations were referring to the mechanism of decarboxylation of pyruvic acid, known to be catalyzed by the enzyme. Cocarboxylase has a molecular weight of about 150,000 (apoenzyme) and contains also TPP and Mg^{2+} ions in the ratio (1:1:5) respectively[7].
Pyruvic acid oxidation to acetic acid and CO_2 was believed to be catalysed by TPP.

$$CH_3COCOOH + |O| \rightarrow CH_3COOH + CO_2 \qquad (4)$$

TPP on the other hand was catalyzing the anaerobic decarboxylation of pyruvic acid to acetaldehyde and CO_2, according to Lohmann and Schuster[6,8].

$$CH_3COCOOH \rightarrow CH_3CH{=}O + CO_2 \qquad (5)$$

Pyruvic acid can also dismutate[7],

$$2CH_3COCOOH \rightarrow CH_3CHOHCOOH + CH_3COOH + CO_2 \qquad (6)$$

It could also be reduced to lactic acid and carboxylized to oxaloacetic acid[7]. All these reactions were due to an activation of pyruvic acid caused by TPP, according to Barron et al[9],

$$CH_3COCOOH \xrightarrow{TPP} CH_3C(O^+)COOH$$

Later it was shown that TPP as an integral part of many other enzymes except carboxylase, could take part in various reactions.

2.2. THIAMIN AS A REVERSIBLE REDOX SYSTEM

After showing that TPP can be hydrogenated[10] in the presence of Pt black or sodium dithionate to dihydrothiamin pyrophosphate (8), Lipmann[7,10] proposed that cocarboxylase must act as a reversible redox system.

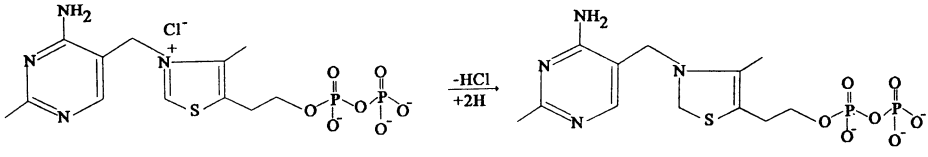

Based on the fact that thiamin decomposes to products 7 and 9 which are then converted to disulfate 11, that can subsequently be reduced back to thiamin, Zima and Williams[11] also

suggested that thiamin may act as an oxidation-reduction enzyme, similar to the cysteine-cystine system[12]. All these were subsequently proved to be incorrect[7].

2.3. FORMATION OF A SCHIFF-BASE

A mechanism involving the formation of a Schiff-base intermediate with the amino group of the pyrimidin moiety of thiamin was later proposed by Langebeck[13] and later by Wisner and Valenta[14] (Scheme I). It was based on the fact that primary amines were able to decarboxylize pyrouvic acid through the formation of such bases. Since thiamin itself was not able to form Schiff bases involving the amino group, due to the poor basic properties of the latter, the lone pair of electrons of which take part to the pyrimidine ring resonance,this model was also abandoned later, as well.

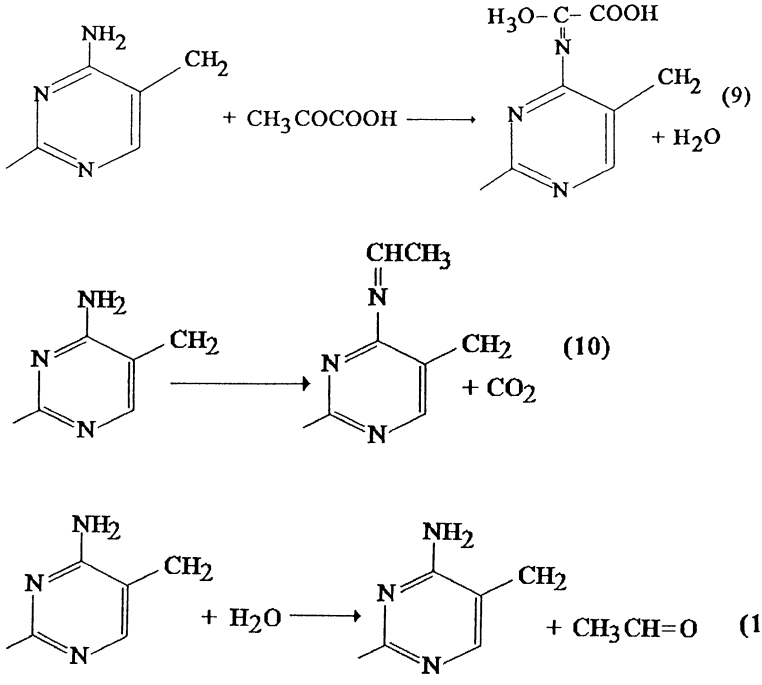

Scheme I

2.4. CATALYSIS BY THIAMIN IN NON ENZYMATIC MODELS

Based on the known procedure of formation of condensation products of pyrimidin compounds to form adducts to the α-position of the quaternary nitrogen atom (12), Ugai et

al[13,14] found that the similar to pyridinium, thiazolium nitrogen of thiamin was catalyzing acyloin condensation. These findings allowed Mizuhara et al[17,18] to show that thiamin at room temperature

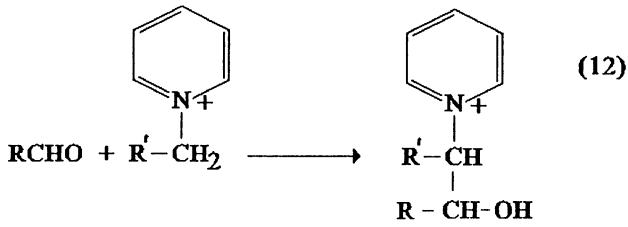

(12)

(pH = 8.4), could decarboxylate pyrouric acid, catalyze the formation of acetoine and the reactions of diacetyl and acetaldehyde to acetic acid and acetoine. They proposed that these could be achieved by the attack of the carbonyl carbon atom of the substrate to the tertiary nitrogen atom of the pseudo base (13).

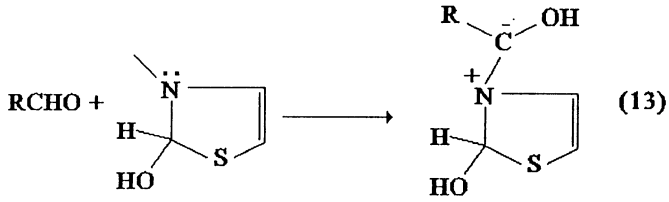

(13)

However, since no appreciable amounts of a pseudobase was present in solution at any pH[19], this mechanism was also abandoned. Based on these nonenzymatic models, Breslow[20] modified this mechanism by proposing the combination of pyrouvic acid with the methylenic bridging group of thiamin, prior to its loss of CO_2 and production of acetaldehyde and thiamin. Deuteration experiments however[21], showed that the methylenic protons are not readily exchanged with deuterium, a requirement for supporting this mechanism. Breslow confirmed this lack of exchanges of the protons of the methylenic bridging group, but found instead that the C(2) proton of the thiazolium ring exchanged readily with deuterium. Following these findings, Breslow proposed the nowadays generally accepted mechanism for the catalysis of thiamin, by analogy between cyanide ion 13 and the thiamin C(2) carbanion 14, adopting a similar to the benzoin condensation one, mechanism

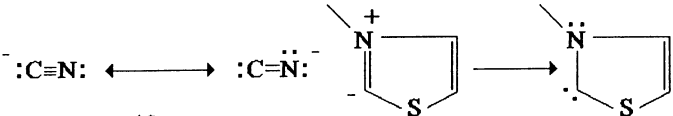

13 14

A general form for the decarboxylation of pyruvic acid by thiamin is presented in Scheme II.

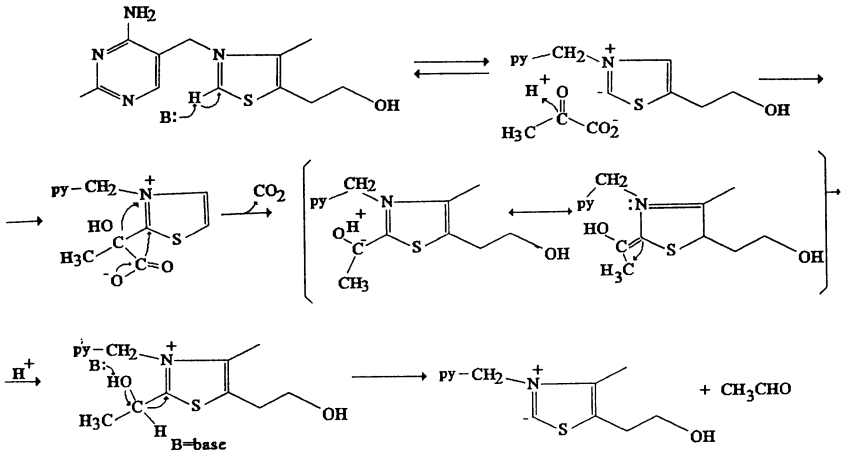

Scheme II

This mechanism was confirmed later by many other works in both enzymatic and non enzymatic systems. These included among others the synthesis of 2-(α-hydroxyethyl)thiamin PP (HET-PP) and the proof for its chemical competence in many enzymatic systems[23]. The similar to HET=PP compounds were named "active aldehyde" derivatives of thiamin 15.

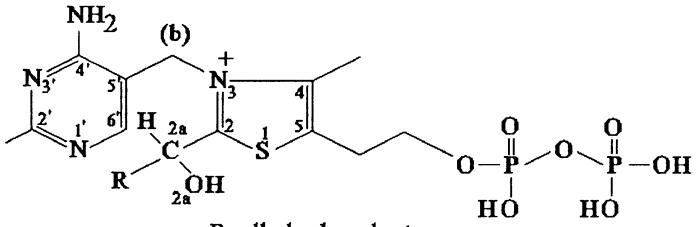

15

Despite the general acceptance of the Breslow mechanism, there are many unknown details on it[24], concerning the role that the various parts of TPP may play during the enzymatic action, as well as the role of the bivalent metal ions, which are required both *in vivo* (Mg^{2+}) or *in vitro* (Mg^{2+},Co^{2+},Zn^{2+},Ni^{2+},Cd^{2+} etc.). These will be examined here.

2.5. ROLE OF PYRIMIDIN AND THE METHYLENIC BRIDGING GROUP

Schellenberger[25], based on enzymatic and model studies, concluded that the N(1') site of the pyrimidin moiety of TPP should be the binding site with the substrate, through the intervention of bivalent metal ions. He also proposed that the role of the 4'-NH_2 group of pyrimidin is to act as a proton acceptor, e.g. to act as a Brensted base, accepting the liberated protons in the mechanisms of Breslow (Scheme II), despite its low basicity, which according to Schellenberger could be enhanced by its interaction with the substrate. The 4'-NH_2 group could however act as a proton donor rather than a proton acceptor, according to the theoretical calculations of Jordan and Mariam[26] (Scheme II).
Later Schellenberger[27] proposed that the 4'-NH_2 group takes part in both the binding of the molecule to the substrate and to the liberation of the aldehyde through the formation of a hydrogen bonding (NH·····O). For such roles however, to be played by the 4'-NH_2 group, the pyrmidin and thiazole orientation relative to each other should bring this group near the C(2) of thiazole.
The orientation of these two rings depends upon the torsional angles φ_p=N(3)-C(b)-C(5')-C(4') and φ_T=C(5')-C(b)-N(3)-C(2), 16, defined by Pletcher and Sax[28], based on crystallographic studies. Both angles have positive values in the clockwise direction. Thiamin and its derivatives are found in three possible conformations, depending on the values of φ_p and φ_T. The S conformation with $\varphi_T = \pm 100$, $\varphi_p = \pm 150$ usually found in the C-2 substituted derivatives of thiamin, the more common F conformation, $\varphi_T = 0^o$, $\varphi_p = \pm 90^o$ usually found in free thiamin derivatives and the V conformation $\varphi_T = \pm 90^o$, $\varphi_p = \pm 90^o$, found only rarely[24]. The V conformation is the one that allows the 4'-NH_2 group to play the role of either a proton acceptor or donor during the enzymatic action, bringing it near the C(2) site of thiazole.

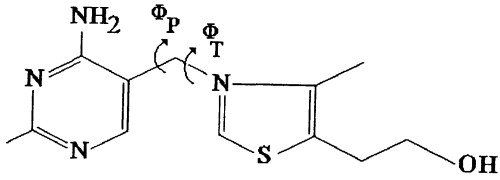

16

This however is very rarely found[24] and it was the reason for the non acceptance of the Schellenberger's proposal[24,29]. More recently however, Shin et al[30] based on results of molecular mechanics calculations and the known X-ray structures of enzymic systems[31,34] containing thiamin in the V conformation, emphasized again the importance of this form in the formation of hydrogen bonds between the 4'-NH_2 group and pyrouvic acid, during the enzymatic action.

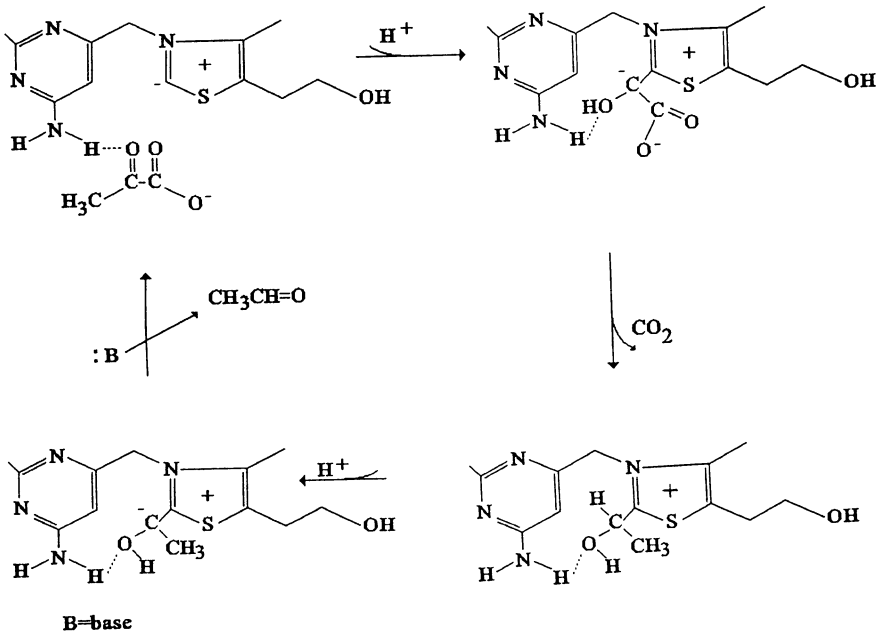

Scheme III

Witorf and Gubler[35] assigned a stabilization role of the coenzyme-apoenzyme binding being played by the 2'-CH_3 group of pyrimidin with hydrophobic interaction. Finally, the methylenic bridging group -CH_2- is important in the enzymatic action of thiamin, regulating the distance between the two rings. Its lengthening resulted to the destruction of the enzymatic activity[36].

2.6. ROLE OF THIAZOLE AND THE PYROPHOSPHATE GROUP

The C(2) position's importance in the mechanism of action of TPP has already been emphasized (Schemes II,III). According to Schellenberger[27] the _α-carbanion 17, represents better the intermediates of the various enzymatic processes, than enamin 18 or the enol forms 19.

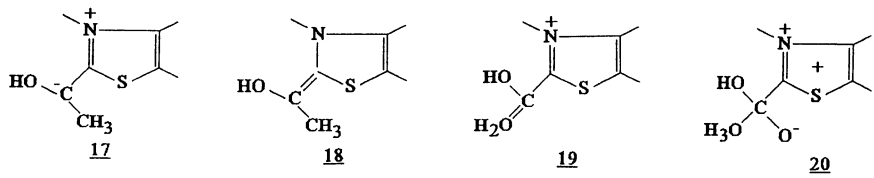

17 18 19 20

The transition state intermediate 20, producing 17, is stabilized by the use of the 3d orbitals of sulfur of TPP, according to Hogg[37].The crystal structure determination of several C(2) substituted derivatives of thiamin on the other hand[24], show a strong electrostatic interaction between the S atom of thiazole and the carbonyl O atom of the substituent at the C(2) position. These results together with other data[24], led Hogg[37] to propose a mechanism that emphasizes the electrostatic interaction $S^{+}_{(1)}\cdots O_{(2a)}^{-}$ (Scheme IV).

Supporting evidence for this mechanism was also given by the crystal structure of Zn(2-α-(hydroxy-α-cyclohexyl)thiamin)Cl_3 and Hg(2-α-(hydroxybenzyl)thiamin)Cl_3[38], but this will be discussed in the chapter 3 of this article.

The 4-CH_3 group of thiamin interacts with the substrate by hydrophobic interactions, as the 2'-CH_3 group of pyrimidin does. Finally the pyrophosphate ester group of TPP is believed to be the binding site of the coenzyme with the apoenzyme through Mg^{2+} or other metal ions[24,31-34].

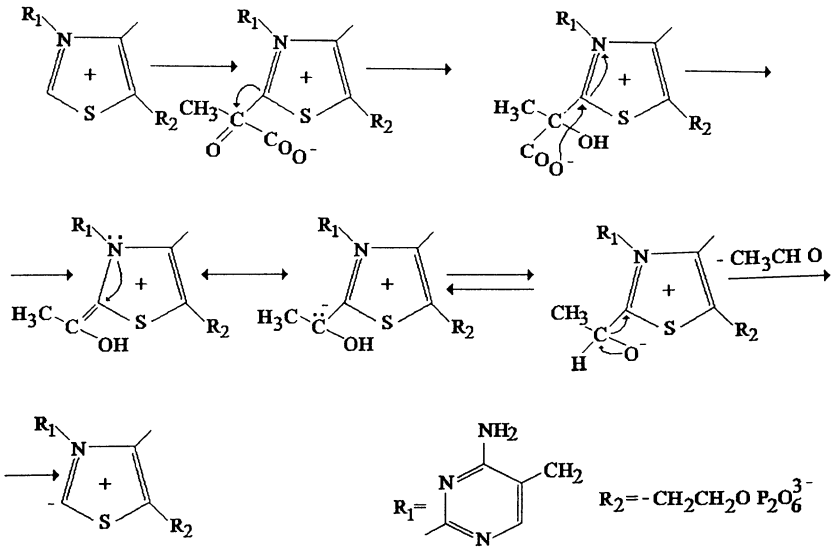

Scheme IV

3. Role of the Bivalent Metal Ions in the Enzymatic Action of Thiamin

3.1. GENERAL CONSIDERATION

As already mentioned, bivalent metal ions are essential for the enzymatic action of thiamin enzymes. Their activity varies and the most active are Mg^{2+} ions. Thus for the decarboxylation of pyruvic acid with carboxylase isolated from wheat germ, the activity follows the order[7]:

support Schellenberger's mechanism (Scheme III), except of course the recent crystal structure of the enzymatic systems[31-34]. Instead and especially in the structures of all the C(2) substituted derivatives of thiamin, either free or metal complexed, the ligands are always found in the S conformation, always stabilized with an $S^+\cdots O^-$ type electrostatic interaction[24],15. This strong interaction led us to the hypothesis that metal complexes would be easier formed than ionic salts, if the "active aldehyde" derivatives of thiamin than thiamin itself, since in the former an internal neutralization of the thiazole charge occurs through the $S^+\cdots O^-$ electrostatic interaction[24]. This was proved to be the case[38,41-44] for all the complexes with Co^{2+}, Ni^{2+}, Zn^{2+}, Cd^{2+} and Hg^{2+}, with the ligand always being in the S conformation both in solution and the solid state and retaining the $S^+\cdots O^-$ interaction. These findings are in support of the mechanism proposed by Hogg[37] (Scheme IV).

More recent results also show that Zn^{2+} ions bind with both N(1') site and the monophosphate group of TMP (thiamin monophosphate), depending on pH.

3.2. DISCUSSION OF CRYSTALLOGRAPHIC DATA

3.2.1. *Pyrimidin.* The high basicity of the N(1') site of pyrimidin seems to play the major role for the metal ions binding in thiamin[24]. On the other hand, the role of the 4'-NH_2 group of thiamin in the enzymatic reactions (e.g. its basicity and ability to take part to hydrogen bonds) depend upon the bond length C(4')-N(4'α).This in turn, depends upon the protonation and metallation at the N(1') site causing shortening or lengthening of its correspondingly[24],with subsequent reduction to its ability to act as a proton donor in the latter case. Also, the size of the C(2')-N(1')-C(6') angle is influenced by protonation or complexation at N(1') increasing with protonation and decreasing with complexation. This angle increases however systematically in the series of metals $Zn^{2+} < Cu^+ < Cd^{2+} < Hg^{2+}$. The increase of the C(4')-N(4'α) bond length on the other hand, follows the order $Cu^+ < Zn^{2+} < Cd^{2+} < Hg^{2+}$

3.2.2. *Thiazole and the Pyrophospate Group.* The torsional angles $\varphi_{5\alpha}$=S(1)-C(5)-C(5α)-C(5β), $\varphi_{5\beta}$=C(5)-C(5α)-C(5β)-O(5γ), $\varphi_{5\gamma}$=C(5α)-C(5β)-O(5γ)-P(5δ), $\varphi_{5\delta}$=C(5β)-O(5γ)-P(5δ)-O(5ε) and $\varphi_{5\varepsilon}$=O(5γ)-P(5δ)-O(5ε)-P(5ζ), 21 determine the relative orientations of the hydroxyethyl and pyrophosphate side chain of thiazole in TPP, 21.

When $\varphi_{5\beta}=\pm 60^0$ a strong $S_{(1)}\cdots O_{(5\gamma)}$ electrostatic interaction is taking place. This is favored by metal complexation at N(1'), which may be transferring some additional small positive charge on the S(1) atom[24]. This interaction may have some importance in the enzymatic action.

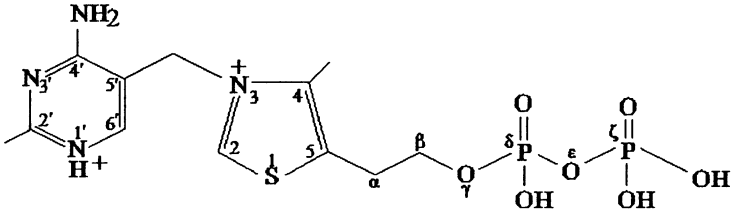

21

The pyrophosphate side chain is flexible and it may be folded over the thiazole ring (structure of TPP.HCl) or extended away (structure of neutral TPP, 21). (See Newman projection 22,23 respectively).

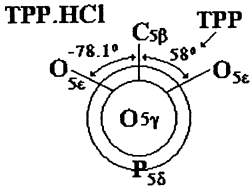

22

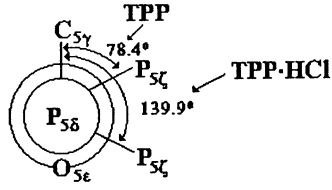

23

The electrostatic interaction $S_{(1)}^{+}\cdots O_{(2\alpha)}^{-}$ observed in all the C(2) substituted derivatives of thiamin 15, strongly influences the side chain conformation at this site. The values of the torsional angle S(1)-C(2)-C(2α)- O(2α) and the corresponding $S^{+}_{(1)}$ - $O_{(2\alpha)}^{-}$ distances of the structures of four C(2) substituted derivatives of thiamin, 15 are given in Table 1.

The strong $S_{(1)}^{+}\cdots O_{(2\alpha)}^{-}$ interaction lowers the pKa of the $O_{(2\alpha)}$-H proton and its liberation is facilitated in support of the Hogg's mechanism[37], as already mentioned. This interaction also facilitates the formation of metal complexes through N(1') once the C(2)"active aldehyde" derivatives of thiamin are formed[38,41-44].

Substituted derivatives of thiamin, 15 are given in Table 1.

Such a $S_{(1)}^{+}\cdots O_{(2\alpha)}^{-}$ electrostatic interaction was not observed only in the case of the crystal structure of the methyl-acetyl-phosphonic acid derivative at C(2) of thiamin, which however is a strong inhibitor of the enzyme pyruvic dehydrogenase[24].

Table 1

Compound	Angle in °C S(1)-C(2)-C(2α)-O(2α)	Distance $S_1^{+}\cdots O_{2\alpha}^{-}$
HET.HCl 2-(α-hydroxyethyl)thiamin HCl	20.6	2.901
HBT.HCl 2-(α-hydroxybenzyl)thiamin HCl	8.4	2.764
HBOT.HCl 2-(α-hydroxybenzyl)oxythiamin HCl	11.7	2.749
$Hg(HBT)Cl_3$	10.5	2.790

3.2.3. *Stabilization of the F, S and V conformations of thiamin.* As already mentioned, the F,S and V conformations of thiamin are defined by the values of the torsional angles φ_p= N(3)-C(6)-C(5')-C(4') and φ_T= C(5')-C(b)-N(3)-C(2) of φ_p=±90°, φ_T=0° for the F, φ_p= ±150°, φ_T=± 100° for the S and φ_p= ±90°, φ_T = ±90° for the V conformation[24].

The two forms F and S do not differ significantly energetically. The following factors

$$Mg^{2+} > Co^{2+} > Zn^{2+} > Fe^{2+} > Mn^{2+} > Ni^{2+} > Cd^{2+}$$

The order for carboxylase taken from yeast, becomes;

$$Mg^{2+} > Mn^{2+} > Co^{2+} > Ca^{2+} > Fe^{2+} > Cd^{2+} > Zn^{2+}$$

and for transketalase from yeast,

$$Mn^{2+} > Mg^{2+} > Fe^{2+} > Ni^{2+} > Zn^{2+} > Co^{2+} > Ca^{2+}$$

Later, Schellenberger[25] found with kinetic methods that Mg^{2+} ions are required for the apoenzyme binding with TPP, (14),

$$\text{apoenzyme} + Mg^{2+} + \text{TAP} \Leftrightarrow \text{holoenzyme} \quad (14)$$

This is achieved with Mg^{2+} ions binding to the N(1') position of pyrimidin and to the pyrophosphate group[25].

Subsequent studies were concentrated in determining the coordination sites of thiamin and its derivatives with various spectroscopic and other techniques, including X-ray structure determinations. Early ^{1}HNMR solution studies showed that M^{2+} ions bind either through the pyrophosphate ester group or/and through the N(1') site of pyrimidin, directly or through a water molecule [7,24]. Studies in the solid state however, were leading for many years to the isolation of ionic solid adducts, without any direct metal-ligand bonding. They corresponded to formulae $[MX_4]^{2-}[Th]^{2+}$, $[MX_4]^{2-}[Th]_2^{+}$, $[MX_3]_2^{-}[Th]^{2+}$, with M = Co^{2+},Ni^{2+}, Cu^{2+}, Zn^{2+}, U^{4+}, Cd^{2+}, Hg^{2+} and X = Cl, Br. Thus, no conclusion on the metal site bonding with thiamin could be made, during the enzymatic action. This was due to the net positive charge on thiazole and the pKa of about 5, of the N(1') site of pyrimidin, making thiamin to exist as a dication at pH <5 and a monoanion at pH = 5.7, at pH > 7 being unstable. The complexes MLX_3, with M = Pd $^{2+}$, Pt^{2+}, L = Th(thiamin), TMP and TPP monocations and X = Cl, Br were the first solid adducts reported to present a direct M-L bond in the solid state[39]. Later the proposed structure[39] for the $Pt(Th)Cl_3$ complex was confirmed with X-rays[40]. Today the known structures of thiamin and derivatives that contain a direct metal-ligand bonding include[24], $Cd(Th)Cl_3$. H_2O, $Cu(Th)Cl_2$, $Rh_2(CH_3COO)_4(TMP)_2$ $1.5H_2O$, $Zn(Th)Cl_3.4H_2O$, $Cu(Th)Br_2$, $Hg(HBT)Cl_3.H_2O$, (HBT=2-(α-hydroxybenzyl)thiamin), $Zn(HCMT)Cl_3$ (HCMT=2-(α-hydroxy-α-cyclohexyl-methyl)thiamin), $Co(Th)Cl_3.0.4H_2O$, $Zn(Th)Br_3.0.2H_2O$ and $Zn(Th)(SCN)_3$. In all cases the metals are bound to the N(1')site of pyrimidin, except the Cu^{2+} complex with the metal bound to the pyrophosphate group of TPP, the complex $Cd(Th)(SCN)_3$ with Cd^{2+} bound to O(5γ) of the side hydroxy-ethyl group and the complex $[Mn(Th)Cl_2(H_2O)]_2$ $[Th]_2Cl_4.2H_2O$, with Mn^{2+} binding simultaneously the N(1') site and the O(5) site.

Also in all the enzyme structures known today[31-34],Mg^{2+} and Ca^{2+} ions are bound to pyrophosphate group, making the binding of the apoenzyme with the coenzyme.

Except the determination of the bonding sites, the conformation (F,S, or V), of thiamin or its derivatives after metal complexation is also of interest and importance, to conclude for the enzymatic action of thiamin. In this aspect, it should be noted that in none of the known structures of thiamin metal complexes the molecule was found in the V conformation, to

have been proposed to influence the F or S conformation:
a. In thiamin complexes with polychlorometallic anions the F form is favored by small metallic ions and smaller non bonding Cl····Cl distances of about 3.4 A, while the S form requires a 3.9 A distance. This suggestion however was not confirmed since it has many exceptions (Table 2).
b. When thiamin is in the F form, the two rings of thiazole and pyrimidin are connected with the so called "one point" anion bridge of the type $HN_{(4'\alpha)}$···X···thiazole, while in the S form this connection is achieved with the "two points" anion bridge, $HN_{(4'\alpha)}$-H···X_1M-X_2···thiazole[24]. The first bridge obviously brings the two rings closer than the latter. It was proposed that carboxylic anions like aspartic and glutamic acids etc., should play an important role in the recognition and stabilization of one of the F and S forms.

Table 2

Complex	X ···X in A	Conformation
(ThH)($PtCl_4$)	3.247	F
(ThH) ($PtCl_4$)Cl_2	3.262	F
Pt(Th)Cl_3	3.270	F
(ThH)($CuCl_4$)	3.420	F
Zn(Th)Cl_3	3.700	S
Cu(Th)Cl_2	3.867	F
(ThH)($CdCl_4$)	4.000	S
Cd(Th)(Cl_3)	4.000	S
Hg(HBT)Cl_3	3.857	S
Cu(Th)Br_2	3.995	F
(ThH)($CoCl_4$)	3.720	S
Zn(Th)Br_3	3.900	S
Co(Th)Cl_3	3.710	S

c. The F conformation may be stabilized by a C(2)- H···X···pyrimidin bonding[24]. The F conformation is also protecting the C(2)-H protons through an electrostatic interaction with the aromatic electron density of the pyrimidin ring. In the S conformation this position is exposed to reaction with the substrate. Therefore pyruvic acid will rather attack the C(2) position, when the molecule is in the S conformation[24].
d. When a bulky tetrahedral metal complex (X···X > 3.7 A) is approaching the thiazole ring with a trigonal plane, thiamin undertakes the S conformation to reduce steric hindrance between its two rings. Thus when the complex anion is not bulky, the F conformation is preferred.
e. Steric hindrance between the substituents at C(2) and C(4'), and C(4) and C(6') should favor an S over an F conformation, since with the former they achieve their maximum separation distance.
f. The only structures of thiamin known in the V conformation were the ones of oxythiamin and thiamin thiazolone, prior to the strucures of the enzymes, pyruvate decarboxylase, apotransketalase, pyruvate oxidase and transketolase[31-34], all containing TPP in this

conformation.

It was proposed that this conformation might be adopted whenever the repulsions and the sizes of the substituents at C(2) and C(4') are minimized.

3.2.4. *Metal Complexes of HBT and HCMT.* These were prepared very easily from aqueous and/or alcoholic solutions of the ligands with the metals[38,41-44], Co^{2+}, Ni^{2+}, Zn^{2+}, Cd^{2+} and Hg^{2+}. They correspond to the general formula $MLCl_3$. Cu^{2+} on the other hand oxidized both ligands to thiochrome, forming complexes with the latter (L'), of the type $CuL'(H_2O)Cl_2$ containing Cu^{2+} and $Cu_2(L'H)Cl_4$,MeOH containing both Cu^{1+} and Cu^{2+}. Various techniques including X-ray structure determinations, vibrational IR-Raman, 1-D, ^1H, ^{13}C, ^{31}P and $^{199}HgNMR$, 2-D ^1HNMR and solid state $^{13}CNMR$, electronic UV-Vis and mass spectra were used to determine the structures of the various complexes in solution and in the solid state[41-45]. The results that will be presented in detail, showed that the metals coordinate preferentially at N(1') of pyrimidin. The pyrophosphate group[45] of TMP may also be a coordination site at pH ~ 5.5 with Zn^{2+}. The ligand conformation is always kept S both in solution and in the solid state. These studies allowed us to conclude that the S conformation must be important besides the V, in the enzymatic action and possibly the metal ions coordinate to N(1'), if such an interaction is finally taking place, after the formation of the "active aldehyde" intermediates at the C(2) position of thiamin.

3.2.5. *Concluding Remarks.* From the above discussion it is obvious that all the steps followed in the enzymatic action of thiamin enzymes using metal complexes are not yet known in detail. Two main mechanisms, (i) the one involving the V conformation of thiamin (Scheme III), where the 4'-NH2 group approaches the C(2) site of thiazole and (ii) the one involving the S conformation and emphasizing the importance of the $S_{(1)}{}^{+}\cdots O_{(2a)}{}^{-}$ electrostatic interaction (Scheme IV) exist.

The recent X-ray structures of the enzymes[31-34] containing Ca^{2+} or Mg^{2+} seem to favor the first (i) mechanism.

According to Shin[30] even the C(2) "active aldehyde" derivatives of thiamin assume the V conformation in the enzymatic systems. To our opinion, both the V and the S conformation of thiamin may be important during the enzymatic action and may succeed each other in the various steps. Thus the V conformation may facilitate the - ylid formation in the first step, while the S conformation may be formed once the "active aldehyde" intermediate is formed. The metal ions may be bound to N(1') of pyrimidin and the substrate, after the formation of the C(2) substituted derivatives. There remain a crystal structure of an enzyme containing a C(2) substituted derivative of thiamin to be solved, to substantiate or not this hypothesis.

4. References

(1) B.S.P. Jansen & W.F. Donath, Proc. K. Aad. Watensch, Amsterdam, **1926**,*29*,1390
(2) R.R. Williams, *J. Am. Chem. Soc.*, **1935**,*57*, 229
(3) R.R. Williams, "Vitamin B_1 and its use in Medicine", McMillan, **1938**
(4) R.R. Williams, *J. Am.Chem. Soc.*, **1936**,*58*,1063
(5) R.R. Williams and J.K. Cline, *J. Am.Chem.Soc.*, **1936**,*58*,1504
(6) K. Lohmann & P. Schuster, *Biochem Z.*,**1937**,*294*, 188

(7) N. Hadjiliadis & J. Markopoulos, *Chim. Chron, New Ser.* ,**1981,***10*,1
(8) K. Lohmann & P. Schuster, *Naturwiss*, **1937,***25*,26
(9) E.S.G. Barron, C.M. Lyman, M.A. Lipton & J.M. Goldinger,*J.Biol.Chem.*, **1941**,*140*,11
(10) F. Lipmann, *Nature,* 1936,*138*,1097
(11) O. Zima & R.R. Williams, *Ber.*, **1940,***73*,941
(12) O. Zima, K. Ritsert & T. Moll, Z. Physiol. Chem., **1941,***267*,210
(13) W. Langebeck, "Die Organischen Katalysatoren" Julius Springer,Berlin,**1935,** p.55
(14) K. Wiesner & Z. Valenta, *Experientia,* **1956,***12*,192
(15) T. Ugai, S. Tanaka & S. Dokawa, J. Pharm. Soc. Jpn., **1943,***63*, 269
(16) T. Ugai, S. Dokawa & S. Tsubokawa, *J. Pharm. Soc.Jpn.*, **1944,***64*,3
(17) S. Mizuhara, R. Tamura & H. Arata, *Proc.Japan Acad.*, **1951,***27*,302
(18) S. Mizuhara & P. Handler, *J.Am.Chem.Soc.*, **1954,***76*,571
(19) J.M. Duclos & P. Haake, *Biochemistry*, **1974,***13*,5358
(20) R. Breslow, *Chem & Ind.* (London), **1956,**28
(21) L.L. Ingraham & F.H. Westheimer, *Chem & Ind.* (London),**1956,**846
(22) R. Breslow, *J.Am.Chem.Soc.*,**1958,***80*,3719
(23) L.O. Krampitz, G. Gruell, C.S. Miller, J.B. Bicking, H.R. Skeggs & J.M. Sprague, *J.Am.Chem.Soc.*, **1957,***80*,5893
(24) M. Louloudi & N. Hadjiliadis, *Coord. Chem. Revs*, in the press.
(25) A. Schellenberger, *Angew.Chem.Inter.Ed.*, **1967,***6*,1024
(26) F. Jordan & Y. Marian, *J.Am.Chem.Soc.*, **1978,***100*,2534
(27) A. Schellenberger, *Ann.N.Y,Acad,Sci.*, **1982,***378*,51
(28) J. Pletcher & M. Sax, *J.Am.Chem.Soc.*,**1972,***94*,3998
(29) M. Washabaugh & W. Jencks, *Biochemistry,* **1976,***27*,2564
(30) W. Shin, D.G. Oh, C.H. Chae & T.S. Yoon, *J.Am.Chem.Soc.*, **1993,***115*,12238
(31) Y. Lindqvist, G. Schneider, V. Ermler & M. Sundstrom, EMBO J,**1992,***11*, 2373
(32) Y. Lindqvist, G. Schneider, *FEBS Lett.,* **1992,***313*, 229
(33) Y.A. Muller and G.E. Schulz, Science, **1993,***259*,965
(34) F. Dyda, W. Furey, S. Swaminathan, M. Sax, B. Farrenkopf & F. Jordan
(35) J. Wittorf & C. Gubler, *Eur.J.Biochem.*, **1971,***22*,544
(36) A. Schellenberger & G. Huber, *Angew.Chem.Int.Ed.*, **1968,***7*,68
(37) J. Hogg, *Bioorgan,. Chem*, **1981,***10*,233
(38) M. Louloudi, N. Hadjiliadis, J.P. Laussac & R. Bau, Metal Based Drugs, in the press.
(39) N. Hadjiliadis, J. Markopoulos, G. Pneumatikakis, D. Katakis & T. Theophanides, *Inorg.Chim Acta,* **1977,***25*,21
(40) R. Cramer, R. Kirkup & M. Carrie, *Inorg.Chem.,* **1988,***27*,123
(41) M. Louloudi, N. Hadjiliadis, J.A. Feng, S. Sukumar & R. Bau, *J.Am.Chem.Soc.*, **1990,***112*,7233
(42) M. Louloudi & N. Hadjiliadis, *J.Chem.Soc.Dalton,* **1991**,1635
(43) N. Hadjiliadis, M. Louloudi & I.S. Butler, *Spectrochim. Acta* 1991,*47A*,445
(44) M. Louloudi, N. Hadjiliadis & I.S. Butler, *J.Chem.Soc.,Dalton,* **1992**,1401
(45) K. Dodi & N. Hadjiliadis manuscript in preparation.

Metal-DNA Interaction

PLATINUM ANTICANCER DRUGS

STEPHEN J. LIPPARD
Department of Chemistry
Massachusetts Institute of Technology
Cambridge, Massachusetts 02139 USA

ABSTRACT. Cisplatin, *cis*-diamminedichloroplatinum(II), is a simple inorganic complex widely used in cancer chemotherapy and especially effective against testicular tumors. The trans isomer is biologically inactive. A principal target of cisplatin in the cancer cell is DNA. The major adducts of cisplatin with DNA, accounting for 90% of platinum on the duplex, are intrastrand cross-links in which adjacent guanine or adenine/guanine bases are coordinated in the cis positions originally occupied by chloride ions. The resulting platinated DNA unwinds by ~ 13° and is bent by ~ 34° toward the major groove. Details of this structural distortion were obtained by gel electrophoretic and X-ray crystallographic studies of DNA containing intrastrand *cis*-diammineplatinum(II) d(GpG) or d(ApG) cross-links. Both gel-electrophoretic mobility shift assays and expression library screening of human cells with cisplatin-modified DNA revealed the existence of proteins that bind specifically to the major DNA adducts of the drug. These proteins, designated structure-specific recognition proteins, or SSRPs, have in common a 75 amino acid sequence known as the HMG domain which is the source of specificity for platinated DNA. Deletion of a non-essential HMG-domain SSRP in yeast desensitized the cells by twofold to cisplatin but not to the inactive analogue *trans*-DDP. When DNA containing the major adducts of cisplatin was added to a mammalian cell extract, the damage was excised by the excinuclease excision repair system. Specifically, the platinated strand was cleaved ~ 5 nucleotides to the 3' side and ~22-24 nucleotides to the 5' side of the damage. This process was selectively inhibited by addition of HMG1. Adding the HMG-domain protein human mitochondrial transcription factor mtTFA gave similar results. This shielding phenomenon was selective for the major d(GpG) intrastrand cross-link of the drug and not the less abundant long-range cross-links such as the 1,3-adduct, d(GpTpG). The latter was repaired but not shielded. These results suggest that the molecular mechanism of cisplatin might involved shielding of its adducts by HMG-domain proteins in the cancer cell, protecting them from repair and thereby preserving their ability to block replication of DNA required for tumor cell proliferation. Thus new anticancer platinum drugs might be developed based upon the ability of their DNA adducts to be recognized and shielded by HMG1 and related proteins.

1. Introduction

Cisplatin, known also as *cis*-DDP or *cis*-diamminedichloroplatinum(II), is an effective

D.P. Kessissoglou (ed.), Bioinorganic Chemistry, 131-140

anticancer drug with demonstrated activity against head and neck, ovarian, and especially testicular cancer.[1] The trans isomer is inactive. A compound having fewer toxic side effects, carboplatin, has also been approved for use. Cisplatin and carboplatin are administered by intravenous injection, but recently platinum(IV) complexes having activity following oral administration have been introduced.[2] Fig. 1 summarizes these developments.

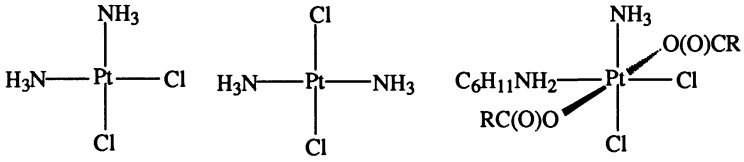

cis-[Pt(NH$_3$)$_2$Cl$_2$] active drug

trans-[Pt(NH$_3$)$_2$Cl$_2$] inactive analogue

cis-[Pt(CyNH$_2$)(NH$_3$)Cl$_2$(OAc)$_2$] oral analogue

Discovery of Anticancer Activity: Rosenberg, 1969
Approval of *cis*-[Pt(NH$_3$)$_2$Cl$_2$] (cisplatin) by FDA, 1979
Approval of [Pt(NH$_3$)$_2$(1,1-{O$_2$C}$_2$C$_4$H$_6$)] (carboplatin) by FDA, 1990

Figure 1. Platinum anticancer drugs. Summary of developments.

When cisplatin and related compounds diffuse across the cell membrane, they encounter a much diminished chloride ion concentration compared to blood serum. As a consequence, the complexes hydrolyze in a stepwise manner forming positively charged, aquated species that ultimately migrate to and bind nucleobases on DNA.[3]

Table 1. Percentage of Various Adducts for Cisplatin, [Pt(en)Cl$_2$], and [Pt(NH$_3$)(C$_6$H$_{11}$NH$_2$)(OH$_2$)$_2$]$^{2+}$ on DNA.

Cisplatin			[Pt(en)Cl$_2$]	*cis*-[Pt(NH$_3$)(C$_6$H$_{11}$NH$_2$)(OH$_2$)$_2$]$^{2+}$
GpG	55-65%	GpG	57-62%	40%, 20%*
ApG	25-35%	ApG	5-10%	5-10%, 0%*
GpNpG	6%	GpNpG or	13-18%	
G-Pt-G	<5%	G-Pt-G	<5%	

*The two values correspond to orientational isomers (see ref. 10).

The DNA molecule may itself to promote this covalent reaction[4] by serving as a one dimensional template upon which cationic platinum complexes aggregate before migrating to their thermodynamically preferred binding sites, the purine nucleobases guanine and adenine. Table 1 summarizes the binding site preferences for cisplatin and its active analogues, from which it can be seen that intrastrand d(GpG) and d(ApG)

comprise the major targets. The molecular structure of one such adduct, the intrastrand d(GpG) cross-link formed by *cis*-$\{Pt(NH_3)_2\}^{2+}$, as revealed in a single crystal X-ray structure determination,[5,6] is depicted in Fig. 2. The structure reveals that the two guanine ring planes, which in normal, B-form DNA are parallel to one another, are tilted at an angle of ~ 80° in order to optimize binding of the N(7) atoms with platinum. This structural distortion, detected for the binding to a simple dinucleotide, takes on a slightly different form in double-stranded DNA platinated with cisplatin. From gel electrophoresis studies of DNA duplex oligonucleotides modified site-specifically with cisplatin it was deduced that platinum bends the DNA by ~32-34° while unwinding it locally by ~ 13°.[7-9] Similar experiments were performed on a variety of site-specifically modified DNAs, the results of which are summarized in Table 2. Also shown in the table is the extent to which specific platinum adducts can inhibit the replication of DNA on a template containing a single, site-specific adduct.[10] From the data it is apparent that both clinically active and inactive platinum complexes damage DNA differently, but all bifunctional adducts are capable of blocking replication.

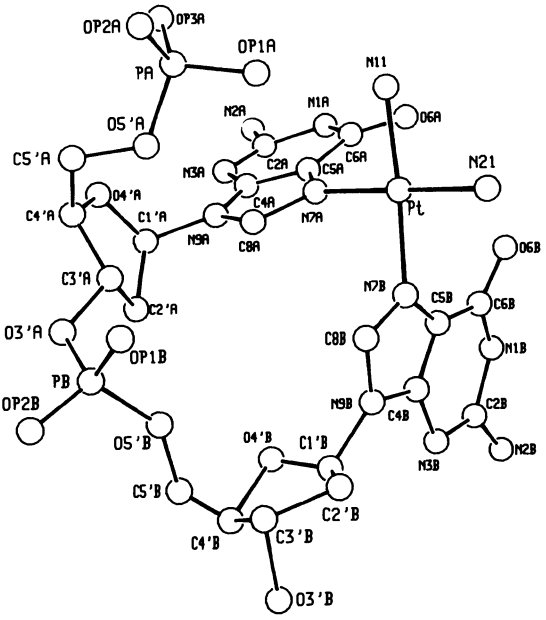

Figure 2. Molecular structure of the major cisplatin adduct on DNA *cis*-[$Pt(NH_3)_2${d(pGpG)}]. Reprinted with permission from ref. 5. Copyright 1985, American Association for the Advancement of Science.

Thus the differential activity of the compounds must arise from some other cellular processing event(s). With this information in hand, a search was undertaken to identify proteins that might recognize and bind specifically to DNA adducts of active, but not inactive, platinum complexes with the goal of determining whether such interactions might be important in the molecular mechanism of the drug. Two approaches were taken, one biochemical and one genetic, both of which revealed the presence of a class of proteins, designated as structure specific recognition proteins or SSRPs, which displayed the desired property of binding specifically to platinum complexes exhibiting anticancer activity.

2. Identification and Properties of Structure-Specific Recognition Proteins which Bind Selectively to Cisplatin-DNA Major Adducts

When radiolabeled DNA restriction fragments modified with cisplatin were incubated with human or other mammalian cell extracts, their electrophoretic mobility shifted dramatically as a result of the binding of specific proteins.[11] Further work revealed that this behavior was selective for the major adducts of cisplatin, intrastrand d(GpG) and d(ApG) cross-links (Table 1). When proteins from the cell extract were separated by gel electrophoresis and identified by staining with radiolabeled, cisplatin-modified DNA in a Southwestern blot assay,[12] it was determined that they belonged to two classes according to whether they had high (80 < MW < 100 kDa) or low (<30 kDa) molecular weights.

Table 2. Properties of Platinum-DNA Adducts.

cis-DDP Adduct	Unwinding Angle	Bending Angle	Translesion Synthesis
GpG intrastrand	13°	32-34°	3 - 5%
ApG intrastrand	13°	32-34°	6 - 14%
GNG intrastrand	23°	32-34°	25%
trans-DDP Adduct			
GTG intrastrand	6-13°	hinge joint	N/A
globally modified	9°		good block

In parallel work, an expression cDNA library was screened with platinated DNA[12] and a gene fragment was identified that encoded a protein with cisplatin-modified DNA binding capability. Further human library screening ultimately produced a full length gene encoding an 81 kDa protein, designated human SSRP1, which bound specifically to the major cisplatin-DNA intrastrand cross-links.[13] Examination of the sequence revealed

several domains, one of which bore a remarkable similarity to the high mobility proteins HMG1 and HMG2. This HMG domain is shared by a variety of eukaryotic proteins, most of which are transcription factors, as shown in Fig. 3.

Once it was realized that HMG1-domain proteins bound specifically to DNA modified by cisplatin, studies quickly revealed that HMG1 itself was such a cisplatin-damaged DNA-binding protein.[14] This conclusion was independently reached when HMG1 and HMG2 were found to bind to DNA modified with cisplatin.[15] Investigations with site-specifically platinated DNAs further proved that, as with hSSRP1, only the intrastrand d(ApG) and d(GpG) cross-links were recognized.[14] These conclusions were reached on the basis of gel electrophoretic mobility shift assays, in which bands corresponding to radiolabeled, platinated DNAs exhibited retarded mobilities in the presence of HMG1. Subsequent work revealed that most proteins containing an HMG domain share the property of selective binding to the major adducts of cisplatin on DNA. The specificity of binding over unmodified, sequence-neutral DNA is on the order of 10^2.[14]

3. Models for How Structure Specific Recognition Proteins Might Promote the Anticancer Activity of Cisplatin-Modified DNA

Fig. 4 summarizes several models to explain how the SSRPs might effect the antitumor activity of cisplatin.[11] One possibility is that DNA repair in eukaryotes involves one or more proteins containing an HMG domain. This feature would account for the selective binding of HMG-domain proteins for cisplatin-DNA adducts. Diminished levels or activity of such a protein would sensitize cells to cisplatin. Since no other DNA damaging agent, for example photo-crosslinking, produces a lesion that is recognized by the SSRPs, however, this possibility seems unlikely.

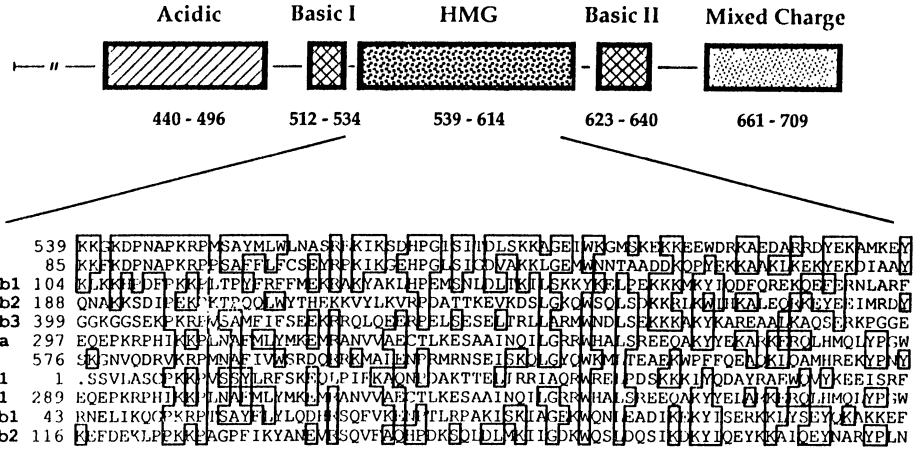

Figure 3. Comparison between the HMG box of human SSRP1 and various other eukaryotic DNA bonding proteins.

Isolation and purification of the components of DNA excision repair[16] should enable this conclusion to be tested. If none of the damage-recognition components contains an HMG domain, this model can be eliminated.

A second possibility is that HMG1 or a related protein facilitates the binding of cisplatin to DNA, perhaps by bending or otherwise distorting the duplex. In addition, the ternary complex between platinum, DNA, and HMG-domain protein might better disrupt gene function. Both events could lead to anticancer activity if the levels of the SSRP were elevated in cisplatin-sensitive tumor cells. Although the features of this model have not yet been experimentally tested, it seems unlikely that the rate of DNA platination could be accelerated by the protein. As indicated previously, the rate-determining step in platinum binding to DNA is hydrolytic loss of chloride ion, followed by relatively rapid binding to the nucleobases. Such a mechanism would not be significantly affected by acceleration of the DNA-binding step.

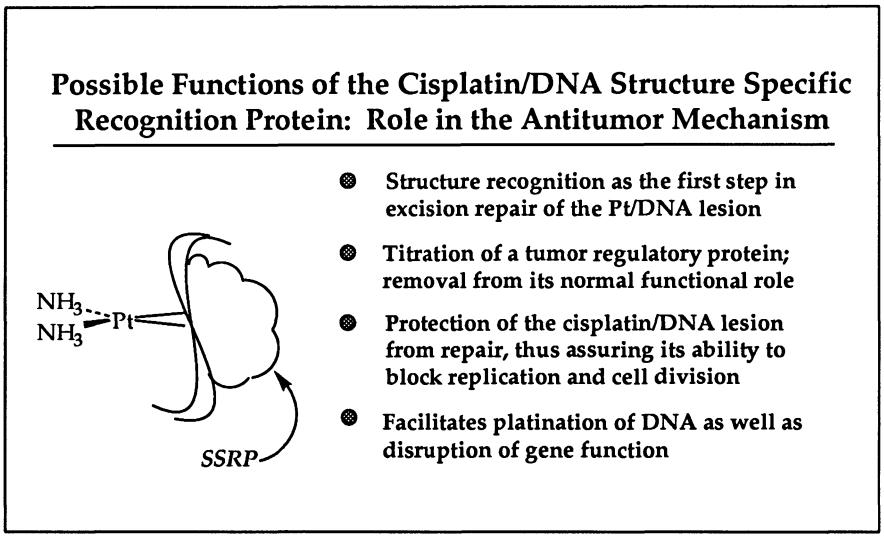

Figure 4. Models for how SSRPs might potentiate the action of cisplatin.

A third model for how SSRPs might potentiate the action of cisplatin is that one or more of the proteins controls the transcription of a gene that is critical to the survival of the tumor cell. Binding of the protein to platinum adducts would divert, or "hijack",[17] the SSRP from its natural site on the genome, diverting it from its natural role. Such a mechanism would sensitize the cell to the drug if the function destroyed in this manner were critical to survival. This model has also not been tested in vivo, but recently it was determined indirectly that the HMG-domain protein hUBF, a factor which controls the transcription of ribosomal RNA, could be competed away from its natural binding sequence by a site-specifically platinated 100-bp duplex DNA containing a single

intrastrand *cis*-[Pt(NH3)2[d(GpG)}] cross-link.[17] Thus, in principle, this mechanism could contribute to the selective cytotoxicity of cisplatin.

The fourth model depicted in Fig. 4 proposes that binding of the HMG-domain proteins to cisplatin 1,2-cross-links on DNA masks their presence and renders them unable to be repaired. According to this model, elevation of SSRP levels would sensitize cells to the drug by shielding adducts from repair. The irreparable platinum lesions would kill cells by blocking gene function and/or by induction of apoptosis.[18] Recently, evidence has come from several directions that supports this model, as described in the next section.

4. HMG-Domain Proteins Can Potentiate Cisplatin Cytotoxicity by Shielding the Major Intrastrand d(GpG) Cross-links from Excision Repair

When a yeast *Saccharomyces cerevisiae* expression cDNA library was screened with cisplatin-modified DNA, a gene encoding a SSRP was identified and sequenced.[19] Not surprisingly, the translated 68 kDa protein sequence had two tandem HMG domains. The expressed protein was able to bind specifically to cisplatin-modified DNA in a gel mobility shift assay, in much the same manner as HMG1.[20] Interruption of the non-essential gene, designated *IXR* (for "intrastrand cross-link recognition"), for this yeast SSRP afforded the

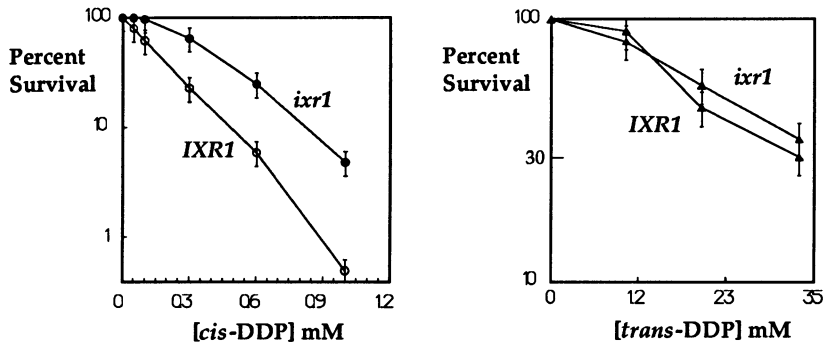

Figure 5. Survival of wild type (*IXR1*) and mutant *ixr1* cells in the presence of *cis*- or *trans*-DDP

interesting result shown in Fig. 5. The mutant cells were desensitized to the drug. When similar "knockout" experiments were attempted with repair-deficient yeast cells, no desensitization was observed.[21] The phenomenon thus seems to involve DNA repair protection. This conclusion was supported by the finding of substantially lower levels of platinum on DNA isolated from the mutant compared to the wild type yeast cells

following treatment with cisplatin. Direct evidence that HMG-domain proteins can protect the major cisplatin-DNA adducts from repair was provided by in vitro experiments in which excision repair was monitored in human cell extracts.[22]

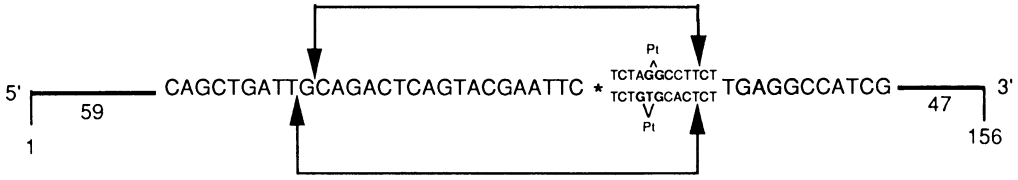

Figure 6. Partial sequences of site-specifically modified DNAs used to study excision repair in human cell extract. The oligonucleotides were prepared by annealing and ligating seven fragments, one of which contained a specific cis-diammineplatinum(II) intrastrand 1,2-d(GpG) or 1,3-d(GpTpG) cross-link.

First (Fig. 6) an oligonucleotide containing a site-specific cisplatin adduct was prepared and characterized. This material was then allowed to incubate in a cell extract from normal or excision-repair deficient human cells.

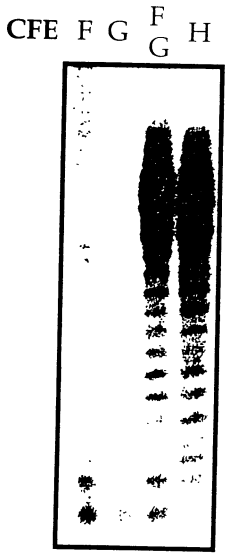

Fig. 7. Repair of *cis*-$\{Pt(NH_3)_2\}^{2+}$ intrastrand cross-links by human cell extract excinuclease. Cell free extracts (CFE) were prepared from *Xerodemra pigmentosum* (XP) cells F or G, lanes 1 and 2, respectively. Lane 3 shows results for a mixture of XPF and XPG lanes and lane 4, results for human HeLa cell extracts.

Only the former were capable of removing the adducts, which they did as 29-base oligonucleotides terminating 22-24 bp to the 5' side and 5 nucleotides to the 3' side of the damage (Fig. 7). Both intrastrand 1,2-d(GpG) and 1,3-d(GpTpG) cisplatin cross-links were repaired, the latter slightly more efficiently.

When these experiments were repeated in the presence of increasing amounts of HMG1, excision repair in the extract could be blocked. This shielding phenomenon was selective for the major 1,2-d(GpG) intrastrand cross-links of the drug and not the less abundant long-range 1,3-d(GpTpG) cross-link (Fig. 8).[22] Only the former adduct reacts specifically with HMG-domain proteins, indicating that it is the specific recognition of the major cisplatin adducts that is responsible for the shielding effect. Similar results were obtained when the human mitochondrial transcription factor mtTFA, which contains an HMG domain, was employed. These results suggest that the molecular mechanism of cisplatin might involve recognition of its major adducts by HMG-domain proteins in the cancer cell, protecting them from repair and thereby preserving their ability to block replication of DNA required for tumor cell proliferation. Thus new anticancer platinum drugs might be developed based upon the ability of their DNA adducts to be recognized and shielded by HMG1 and related proteins.

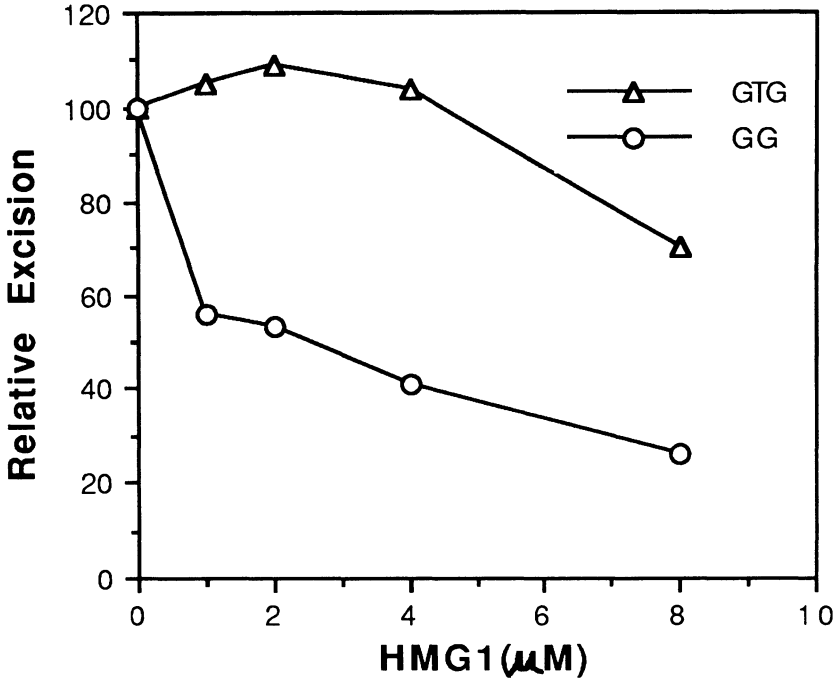

Fig. 8. Plot of excisiont repair of site-specific cisplatin 1,2-d(GpG) and 1,3-d(GpTpG) cross-links, assayed as indicated in Fig. 7. The more efficient blocking of the former adducts is clearly apparent.

5. Acknowledgments

This work was supported by a grant from the National Cancer Institute. I am grateful to my co-workers, collaborators, and colleagues cited in the individual references for their inspired contributions to this research.

6. References

(1) Loehrer, P. J.; Einhorn, L. H. *Ann. of Inter. Med.* **1984**, *100*, 704.
(2) Kelland, L. R.; Murrer, B. A.; Abel, G.; Giandomenico, C. M.; Mistry, P.; Harrap, K. R. *Cancer Res.* **1992**, *52*, 822.
(3) Sundquist, W. I.; Lippard, S. J. *Coord. Chem. Rev.* **1990**, *100*, 293.
(4) Elmroth, S. K. C.; Lippard, S. J. *J. Am. Chem. Soc.* **1994**, *116*, 3633.
(5) Sherman, S. E.; Gibson, D.; Wang, A. H.-J.; Lippard, S. J. *Science* **1985**, *230*, 412.
(6) Sherman, S. E.; Lippard, S. J. *Chem. Rev.* **1989**, *87*, 1153.
(7) Rice, J. A.; Crothers, D. M.; Pinto, A. L.; Lippard, S. J. *Proc. Natl. Acad. Sci. USA* **1988**, *85*, 4158.
(8) Bellon, S. F.; Lippard, S. J. *Biophys. Chem.* **1990**, *35*, 179.
(9) Bellon, S. F.; Coleman, J. H.; Lippard, S. J. *Biochemistry* **1991**, *30*, 8027.
(10) Hartwig, J. F.; Lippard, S. J. *J. Am. Chem. Soc.* **1992**, *114*, 5646.
(11) Donahue, B. A.; Augot, M.; Bellon, S. F.; Treiber, D. K.; Toney, J. H.; S. J. Lippard; Essigmann, J. M. *Biochemistry* **1990**, *29*, 5872.
(12) Toney, J. H.; Donahue, B. A.; Kellett, P. J.; Bruhn, S. L.; Essigmann, J. M.; Lippard, S. J. *Proc. Natl. Acad. Sci. USA* **1989**, *86*, 8328.
(13) Bruhn, S. L.; Pil, P. M.; Essigmann, J. M.; Housman, D. E.; Lippard, S. J. *Proc. Natl. Acad. Sci. USA* **1992**, *89*, 2307.
(14) Pil, P. M.; Lippard, S. J. *Science* **1992**, *256*, 234.
(15) Hughes, E. N.; Engelsberg, B. N.; Billings, P. C. *J. Biol. Chem.* **1992**, *267*, 13520.
(16) Sancar, A.; Tang, M.-S. *Photochem. Photobiol.* **1993**, *57*, 905.
(17) Treiber, D. K.; Zhai, X.; Jantzen, H.-M.; Essigmann, J. M. *Proc. Natl. Acad. Sci, USA* **1994**, in press.
(18) Eastman, A. *Cancer Cells* **1990**, *2*, 275.
(19) Brown, S. J.; Kellett, P. J.; Lippard, S. J. *Science* **1993**, *261*, 603.
(20) Whitehead, J. P.; Lippard, S. J. **1994**, unpublished results.
(21) McA'Nulty, M. M.; Lippard, S. J. **1994**, to be submitted for publication.
(22) Huang, J.-C.; Zamble, D. B.; Reardon, J. T.; Lippard, S. J.; Sancar, A. **1994**, to be submitted for publication.

NMR SPECTROSCOPIC STRUCTURE DETERMINATION OF METAL ION - OLIGONUCLEOTIDE COMPLEXES - THE RESULTS OF SEQUENCE-SELECTIVE BINDING STUDIES

EINAR SLETTEN and NILS ÅGE FRØYSTEIN
Department of Chemistry, University of Bergen, N-5007 Bergen, Norway.

ABSTRACT. This overview will address the current state-of-the-art in characterising metal ion - oligonucleotide interaction by NMR spectroscopy. First the methodology of structure determination of oligonucleotides - metal ion complexes in solution will be discussed. In the second part recent results on sequence-selective metal ion binding to DNA oligonucleotides by NMR methods will be presented. Metal ion titrations of several dodecamer duplexes have been carried out using Mn(II), Zn(II), Hg(II) and Pd(II) salts. The selectivity is shown to be determined by the sequential variation in molecular electrostatic potential along the chain and also to a certain degree by the preferred coordination geometry of the metal ion.

1. Introduction

A large amount of data have been published on structures of metal ion complexes of nucleic acid monomers both in solution and in the solid state. Especially, NMR methods have been shown to be very effective in elucidating the bonding pattern in solution. Application of these methods to structure determination of complexes of oligonucleotides has proved to be considerably more difficult than for proteins. This is partly because DNA, with only four different bases in a generally linear structure, require a different assignment strategy and most importantly, are lacking the long-range structure information found in a folded protein.

A large variety of experimental techniques have been shown to yield valuable, indirect information on metal ion - nucleic acid interactions; e.g. gel-electrophoretic mobility studies suggest that the anti-tumor agent $Pt(NH_3)_2Cl_2$ induces "kinks" and/or bending of DNA[1]; circular dichroism spectroscopy has been used to monitor metal ion induced B- to Z-DNA transition[2]. UV spectroscopic studies on the melting and renaturing behaviour of native DNA in the presence of rather high concentrations of various divalent metal ions showed an interesting variation through the series of metals[3]. These observations could be explained in terms of a varying degree of affinity towards the phosphate backbone and the base nitrogens.

In order to distinguish between inherent sequence-dependent bending of duplex DNA and metal ion induced distortion one needs to know the molecular structure of the unperturbed system. The method of choice for determining the structure of biomolecules in the solid state is X-ray crystallography and in solution NMR spectroscopy. The latter method is often used in combination with Molecular Dynamics calculations[4].

D.P. Kessissoglou (ed.), Bioinorganic Chemistry, 141-153

2. The Structure of Oligonucleotide Ligands

Two-dimensional nuclear resonance spectroscopy (2D NMR) in combination with distance geometry (DG) calculation has the potential for quantitative structure determination of intermediate-sized biological polymers in solution. At present, the size of palindromic DNA oligomers conveniently handled by this technique is limited by spectral resolution to approximately 20 base pairs. For a particular oligomer the amount of overlap in 2D maps is also dependent on sequence heterogeneity.

The method is based on the NOESY experiment measuring through-space dipolar coupling (cross-relaxation) between protons. The NOE build-up rate are equal to the rate of magnetisation transfer (R_{ij}) between nuclear spins ($i\,j$) (initial rate approximation) and given by the simplified expression:

$$R_{1(ij)} = \frac{\gamma^4 \cdot h^2 \cdot \tau_c}{10 r_{ij}^{\,6}} \qquad \text{when } \omega t_c >> 1$$

The NOE build-up rates ($R_{1(ij)}$) are seen to be proportional to the correlation time, t_c and the sixth power of the inter-nuclear distance between nuclei, r_{ij}. The strong dependence upon inter-nuclear distances makes it difficult to observe a direct (two-spin) off-diagonal cross-peak in the NOESY map for proton pairs less than 5Å apart. A typical example of the spectral resolution in a NOESY map recorded for a palindromic 12-base pair deoxyoligonucleotide is shown in Fig.1.

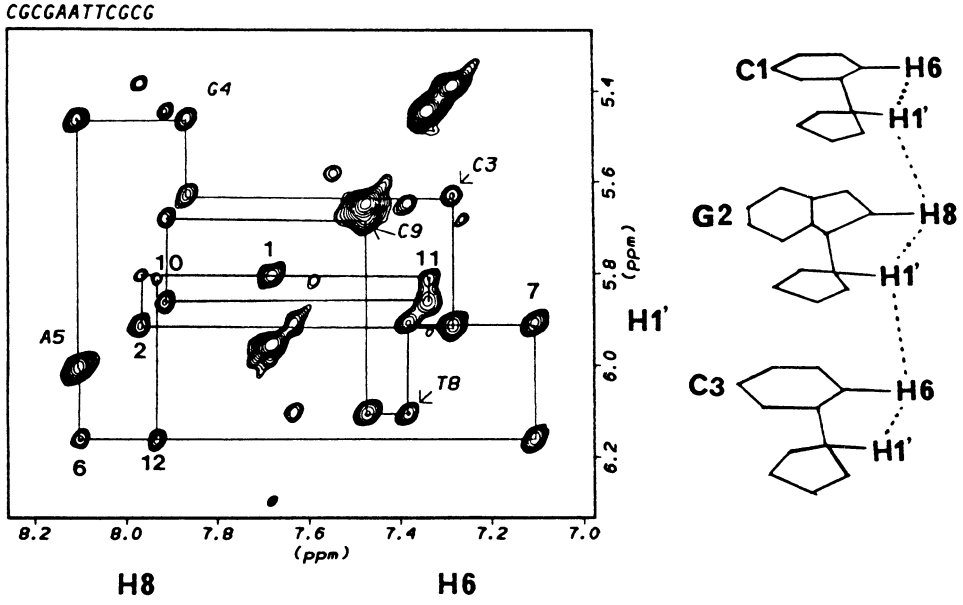

Figure 1. Contour plots of the H8/H6 *vs* H1′ region in the 500 MHz NOESY spectra of the dodecamer d[CGCGAATTCGCG]$_2$. The sequential connectivities are indicated.

The sequential cross-peak pattern corresponding to inter nuclear dipolar coupling between the base protons (H8/H6) and the anomeric protons H1′ is also shown. Both the intra residue and the inter residue base - sugar distances give rise to cross-peaks. The four largest peaks in the map correspond to the cytosine H5 - H6 distances of 2.45 Å.

If all the inter-nuclear vectors have the same correlation time t_c (i.e. assuming no internal motion) it is possible to relate relaxation rates of unknown distances to that of a known fixed reference distance:

$$\frac{R(ij)}{R(kl)} = \frac{r^6(kl)}{r^6(ij)}$$

The use of such scaling to a reference distance is only valid if the unknown proton pair has the same correlation time as the reference proton pair. If the molecule under study exhibits internal motion in addition to the global motion in solution it is important to choose a proper reference.

The two-spin approximation is only an approximation for a real multispin system in which relaxation through multiple pathways occurs simultaneously. To circumvent this problem several NOESY spectra are recorded at different mixing times. The spin-diffusion effects from intervening spins are progressively reduced at shorter and shorter mixing times and the initial rate two-spin approximation approaches that for the true interproton distance. In practice, the ability to sample the true initial cross-relaxation rates is limited by the signal-to-noise ratio at very short mixing times.

In summary the NMR structure analysis is based on the following assumptions:

1. The molecule tumbles isotropically in solution
2. All pairs of protons have the same correlation time t_c
3. The two-spin approximation is valid in multi-spin systems
4. Only one conformation is present in the solution

The dimensions of a hydrated DNA dodecamer (diameter = 20.5 Å, length = 41 Å) implies that this molecule has anisotropic tumbling in solution. However, a distance error of less than 3% is introduced by ignoring the effect of anisotropy[5]. The second assumption is also found to be valid within the level of precision of measuring cross-peak intensities.

The validity of the two-spin approximation depends on how well the initial rates are obtained from a series of NOESY spectra. Usually, a better approach is to match the experimental spectra with simulated (back-calculated) spectra where the spin-diffusion present in a multi-spin system has been taken into account. An example of visual comparison of experimental and simulated spectra is shown in Fig.2.

A more convenient way of monitoring the fit of the simulated intensity V_{ij} to the experimental NOE intensity is to calculate a residual R factor analogous to the one used for X-ray structures:

$$R = \frac{1}{N} \Sigma \frac{V_{ij}^e - V_{ij}^s}{V_{ij}^s}$$

The problem with this type of R-factor is the r^{-6} dependency. Unlike the X-ray crystallographic R-factor the corresponding NMR factor can be quite misleading -

especially for long global distances in the range 4-5 Å. R factors calculated for several different bond regions may be used to monitor the refinement procedure.

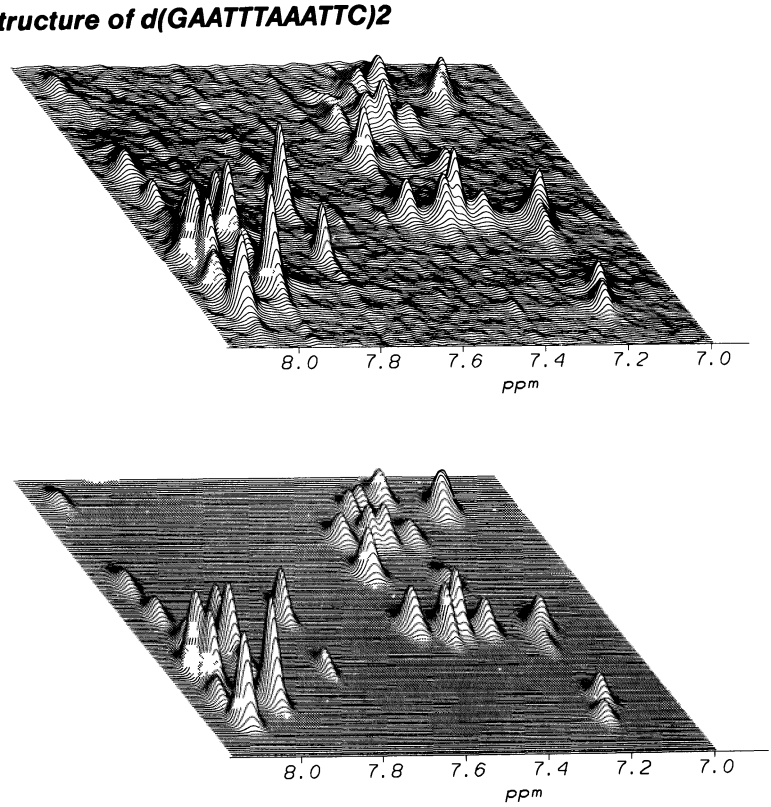

Figure 2. Stacked plots of the H6/H8 ·H2′/H2′′ region for the experimental (upper) and calculated (lower) NOESY spectra for the structure of d[GAATTTAAATTC]$_2$ obtained after visual refinement (from ref.4).

The conclusion based on several NMR studies of DNA oligomers is as follows: i) It is relatively easy to distinguish between A, B, and Z-forms of DNA, ii) the determination of glycosidic angles converge to within 10° variability, iii) the pseudorotation phase angles of the individual sugars and the local helical parameters tilt, roll, twist and slide appear to be rather well-determined. However, the degree of helix bending is difficult to assess[4].

3. Metal Ion - Oligonucleotide Complexes.

DNA and RNA oligonucleotides offer a wide range of potential binding sites for metal ions; the most important are: i) Backbone phosphate, ii) nitrogen atoms of the heterocyclic rings, and iii) exocyclic amino- and oxogroups of nucleobases. When elucidating the bonding pattern in these systems by ^{1}H NMR spectroscopic methods it is convenient to distinguish between two distinct type of complexes: i) diamagnetic and ii) paramagnetic.

In the former chemical shifts may be monitored at stoichiometric metal ion - ligand ratios while in the latter strong paramagnetic proton broadening and shifts allows only systems with large excess of ligands to be studied.

3.1 DIAMAGNETIC COMPLEXES

Interactions between diamagnetic metal ions and oligonucleotides may be detected by monitoring chemical shifts for constituent nuclei (^{1}H, ^{13}C, ^{15}N, ^{31}P). The interpretation of observed chemical shift changes in terms of binding pattern is not always straightforward. Protonation or the establishment of a chemical bond to a metal ion may cause changes in the chemical shifts of ^{1}H resonances of hydrogens in the proximity of the binding site. However, the intrinsic shift changes induced by certain metal ions are found to be rather small for nucleobase monomers; e.g. for Hg^{2+} complexes of DNA or its constituents, intrinsic ^{1}H shifts due to covalent binding to nucleobases are rather insignificant, as shown for thymidine and guanosine[6]. Metal binding induced changes in nucleobase stacking pattern, which in turn alter the ring current shifts, are probably the major source of the observed shifts in proton resonances.

The chemical shifts of nuclei of heavier atoms than hydrogen are increasingly dominated by intrinsic electronic effects. The ^{15}N chemical shifts of pyridine-like nitrogens of nucleobases change markedly in the *up-field* direction upon protonation[7] , or binding to *cis*-$[Pt(NH_3)_2Cl_2]$ [8], Zn^{2+}, Hg^{2+} [9]. These changes can largely be attributed to reduced local paramagnetic deshielding at the ligand nitrogen[8].

In order to determine quantitatively the effect of metal ion complexation a complete set of 2D NOESY spectra may be recorded at stoichiometric ratios. A set of integrated cross-peak intensities are used as input to distance geometry calculations to obtain gross structural features. A less elaborate procedure involving the measurement of rotational correlation time may be followed in order to distinguish between a "bulged" duplex and a single stranded hair-pin structures[10].

3.2 PARAMAGNETIC COMPLEXES

Paramagnetic relaxation phenomena arise in NMR spectroscopy whenever an unpaired electron spin interacts with a nuclear spin. A large magnetogyric ratio of the electron compared to that of the proton or any other nucleus makes dipolar coupling to the electron spin a very effective means of relaxation for the nuclear spin. Scalar interaction between the electron and nuclear spins have similar effects[11]. In the simplest possible case, a ligand molecule exchanges between a paramagnetic environment (e.g. bound to Mn^{2+}, S = 5/2) and a "free" state. However, due to very effective paramagnetic line-broadening it is necessary to use a large excess of ligand (10^2 - 10^4) in order to observe the affected signals.

A strong scalar effect requires that a chemical bond is established. In other words, if such an effect is observed, there must be a bond between the paramagnetic centre and a site in the neighbourhood of the affected resonance. However, even this qualitative interpretation may not always be straightforward when for instance a water molecule is bridging a metal ion and a nucleobase nitrogen atom.

The fast exchange observed in a paramagnetic system preclude quantitative structure determination in solution except in special cases where rapid sampling of NOESY data may give important information on paramagnetic shifted signals. On the other hand, the presence of small amounts of paramagnetic impurities in samples of biomolecules may have detrimental effect on a NMR structure based on integrated NOESY maps. The

published 3D solution structure of the duplex, $[d(CGCGAATTCGCG)]_2$ was determined based on NOESY intensities[12]. However, we now show that critical cross-peak intensities in the NOESY map involving G4-H8 was drastically affected by paramagnetic impurities in the sample. This obviously introduce large errors in the integrated interproton cross-peak intensities, and consequently produced serious structural artefacts.

4. Sequence-Selective Metal Ion - Oligonucleotide Interaction

Metal ions play an important part in regulating enzyme-DNA interaction; e.g. in the presence of Mg^{2+} ions the EcoRV restriction endonuclease cleaves DNA at one particular recognition sequence, 5′-G-A-T-A-T-C- 3′, at least one million times more readily than any other sequence. If Mg^{2+} is replaced by Mn^{2+} both activity and specificity are drastically reduced[13]. How does metal binding influence the recognition mechanism ?

The nucleic acid monomers, guanine (G), adenine (A), thymine (T), cytosine (C), have different metal ion affinities. The order of stability of 3d transition metal ion - nucleobase complexes are: G > A , C > T. [14] For other metal ions e.g. Hg^{2+} ions the relative affinities have been found to decrease in the order : T > G > >A, C [14] . At physiological pH the preferred binding sites on the nucleobases are: guanine N7, adenine N1 and/or N7, cytosine N3 , thymine O4. A typical example of mononucleotide - metal ion binding is the polymeric Cu^{2+} complex of guanosinemonophosphate (GMP) where the metal ion is bridging the GMP ligands through alternating N7 - Cu - phosphate bonds[15].

The nucleobase affinities towards metal ions are modified when incorporated into a duplex DNA matrix. It has been shown that several divalent metal ions like Mn^{2+}, Cu^{2+}, Pt^{2+} prefer GC-rich regions while e.g. Hg^{2+} prefer AT-rich regions. However, the most important question to ask concerning the recognition mechanism is whether or not metal binding to base residues is sequence-dependent, i.e. will all guanines in a particular sequence show identical affinity towards a specific type of metal ion ?

Another aspect of metals in biological systems is the increased flux of metals in the environment through the last decades. An assessment of the toxic effect of an unnatural metal ion concentration must include information on the processes in which the metal can participate. The metal ions Cd^{2+}, Ni^{2+}, Zn^{2+} and Co^{2+} are known to be carcinogenic[16], however, the mechanisms involved are not understood.

In this second lecture NMR studies of the interaction between metal ions and short oligodeoxyribonucleotides are presented. We will focus our attention on certain transition metal ions which are expected to interact with DNA in a site-specific manner and concentrate on the following problems:

1. Determination of the preferred binding sites of single metal ions on DNA
2. How metal binding may affect the structure of duplex DNA, possible local variation as well as overall changes in secondary structure.
3. How the base composition of DNA may affect the interaction between a certain metal ion and DNA.
4. Elucidate differences in binding mode between various metal ions.

4.1. METAL ION TITRATIONS

The effect of adding paramagnetic metal ions to an aqueous solution of DNA fragments are monitored by observing the differential line-broadening of specific resonances in the ^1H NMR spectrum. Often, in 1D spectra of oligonucleotide molecules containing 10 base pairs or more key ^1H resonances may be severely overlapped, preventing an accurate

assessment of the influence of the added metal ions. In these cases 2D NOESY experiments may provide improved resolution and valuable information.

Table 1. Paramagnetically broadened and/or diamagnetically shifted guanine H8 resonances (marked in bold) in a series of duplex deoxyoligonucleotide sequences[a].

DNA oligomer sequences	
1. 5′-CGC**G**AATTCGCG *	7. 5′-GCCGTGCAC**G**GC
2. 5′-GCCGATATC**G**GC *	8. 5′-GCCGTTAAC**G**GC
3. 5′-GCCGTATAC**G**GC *	9. 5′-GCCT**G**ATCA**G**GC
4. 5′-GCCA**G**ATCT**G**GC *	10. 5′-CCAAGCTT**G**G
5. 5′-**G**AATTTAAATTC	11. 5′-GCC**G**AATTC**G**GC
6. 5′-CGC**G**TATACGCG *	12. 5′-AT**GG**GTACCCAT *[b]

[a]The line broadening is induced by paramagnetic impurities. Sequences marked with an asterisk(*) have also been subjected to EDTA treatment , purified and subsequently titrated with $MnCl_2$ and /or $ZnCl_2$ and /or $Hg(ClO_4)_2$. [b] Ref. 19.

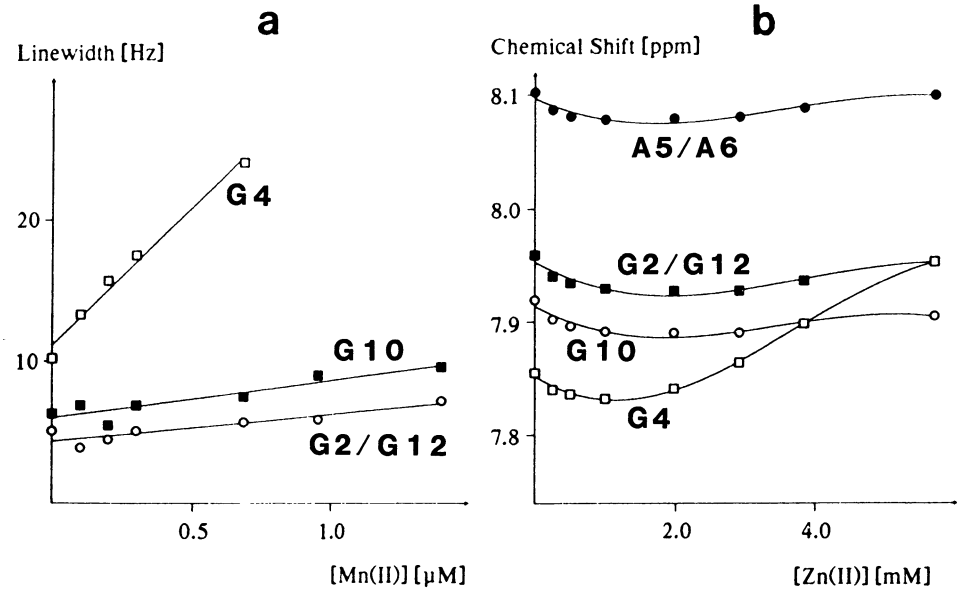

Figure 3. (a). The line widths of the four guanosine H8 resonances *vs* manganese(II) concentration. (b) The chemical shifts of the H8 resonances of the four guanosine and the two adenosine residues. *vs* zinc(II) concentration.

The sequences studied (Table 1) are divided into two groups according to the type of experiments carried out; duplexes subjected to controlled titration by metal salts, and duplexes where selective line-broadening was observed both in 1D ^1H NMR spectra and/or 2D NOESY spectra, owing to the presence of small amounts of non-specific paramagnetic impurities. To confirm that the line-broadening was caused by traces of

paramagnetic metal ions EDTA was added to these samples in order to chelate the metal ions and eliminate the line-broadening of the affected resonances.

4.1.1. *Mn(II)-Titration* . The first metal ion titration experiment of this type was carried out on the oligonucleotide duplex d[CGCGAATTCGCG]$_2$ which contains the EcoRI recognition sequence -GAATTC- [17]. In this sequence, most base proton signals are well resolved in the 1D spectrum enabling us to observe the effect of added metal salts .

Substantial line-broadening was observed for the G4-H8 proton when aliquots of $MnCl_2$ solution were added while much smaller effects were observed for the other proton resonances in the duplex. The observed preference for guanine residues by 3d transition metals is not surprising, considering the differences in thermodynamic stability of the corresponding nucleoside and nucleotide monomer complexes[14]. However, the sequence-dependent metal binding pattern manifested through the apparent preference for G4-N7 rather than N7 of residues G2, G10, or G12 , was unexpected (Fig. 3,a)

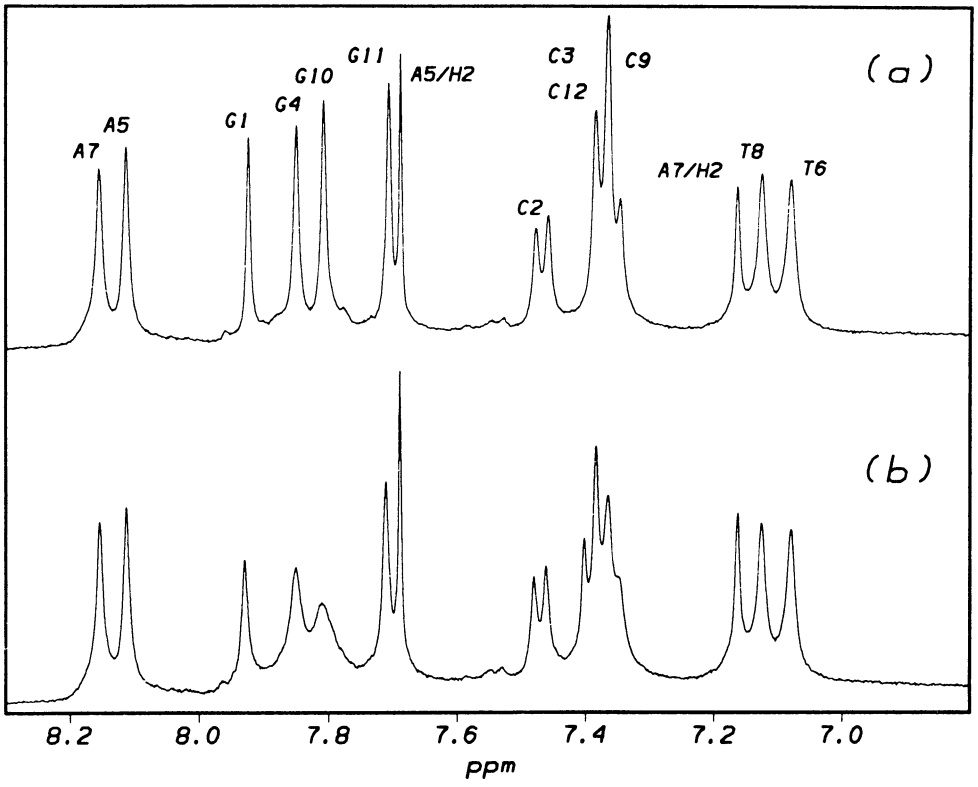

Figure 4. 500 MHz ^{1}H NMR spectra, the aromatic region, of the dodecamer duplex d[GCCAGATCTGGC]$_2$. (a) Mn(II) - free solution and (b) with 81 mM $MnCl_2$. The H6/H8 proton resonances are labelled according to assignment from ref. 18.

In order to elucidate the rules for this apparent sequence-selectivity several different oligonucleotides were studied (Table 1)[18]. The duplex helix d[GCCGTATACGGC]$_2$

contains the recognition site, -GTATAC- for the restriction enzyme AccI. Titration with Mn^{2+} salt causes G10-H8 broadening, leaving H8 of G1, G4, and G11 unperturbed. A common bonding pattern emerges from a comparison of the oligonucleotides 1-3; Guanines in the context 5′-py-G-pu- seem to be the preferred binding sites.

To test this hypothesis the duplex d[GCCAGATCTGGC]$_2$, containing BglII restriction fragment ,-AGATCT-, was titrated. In this sequence we can compare the affinity of G in the context 5′-pu-G-pu- and 5′-py-G-pu, respectively. We find that both G5-H8 and G10-H8 are selectively broadened by Mn^{2+}, whereas H8 of G1 and G11 are relatively unaffected (Fig.4, a, b).

Significant line-broadening, although far less severe than that found for G5/G10, is observed for the base protons of the 5′- preceding residues A4-H8 and T9-H6, while broadening effects were not detected for the neighbouring residues on the 3′side.The 5′lead-in residue (pyrimidine or purine) does not seem to influence the metal ion affinity of the subsequent guanine residue. Evidently, the sufficient requirement for G-binding is the presence of a purine residue (G or A) on the 3′side.

A support for this hypothesis is the observed drastic paramagnetic broadening of the G1-H8 signal for the duplex d[GAATTTAAATTC]$_2$. For the other oligomers with a terminal 5′-G-py- step, there is no apparent G1-H8 line-broadening, neither in controlled titration experiments nor as a result of paramagnetic impurities in the samples. This leads to the conclusion that 5′-Gs are susceptible to manganese binding whenever the sequence contains 5′-GG or 5′-GA steps.

In Table 1 where all the duplexes studied so far, are listed, one may notice one exception to the proposed rule, sequence nr 6, where G4-H8 in a 5′-GT step is broadened by Mn^{2+} ions. However, the discrepancy may be explained by the fact that in this particular duplex there is no 5′-G-pu- step present to compete with 5′-GT step for metal ions.

4.1.2. *Zn(II)Titration.* The use of diamagnetic metal ions requires the addition of equimolecular amounts of salt. The first of these diamagnetic selectivity experiments was the titration of the duplex d[CGCGAATTCGCG]$_2$ by $ZnCl_2$ up to a 4:1 metal ion - dodecamer ratio[17]. The most pronounced changes in the aromatic/anomeric region of the ^{1}H spectrum induced by Zn(II) are the down-field shift of G4-H8 (0.10 ppm) and the up-field shift of G4-H1′(-0.19 ppm) (Fig. 3, a, b). These diamagnetic shift effects are most likely due to a combination of the slight Zn(II) induced alterations of the local geometry of the DNA helix and intrinsic electroninc perturbation brought about by direct metal binding at or close to G4. Another interesting effect of the titration is observed in the base-pairing imino region where the G4 imino signal has disappeared. Thus the Zn(II) binding seems to cause an opening of the Watson-Crick base-pair G4····C9.

In one other binding study, involving Zn(II)-ions and the duplex oligonucleotide d[ATGGGTACCCAT]$_2$, H8 of G3 and G4 are reported to show the largest chemical shift effects while G5 is left almost unaffected[19]. Thus the results of this study and the one above corroborate the hypothesis that guanine in the context 5′-G-pu- is the preferred 3d metal ion binding site in duplex DNA oligonucleotides.

4.2. THEORETICAL BASES FOR THE POSTULATED SELECTIVITY RULE

It has been suggested that the magnitude of the partial negative charge on the potential binding sites of the nucleobases themselves is a major factor which determines the preferred metal ion binding site[19]. Theoretical calculations of the molecular electrostatic potentials (MEPs) along the double helix show marked sequence-dependent variations[20]. Calculations carried out for several combinations of base triplet have shown that the magnitude of D(MEP) on N7 of 5′-G residues in 5′-GG and 5′-GA steps are larger than

for N7 in 5′-GC and 5′-GT steps indicating that the former is more susceptible to metal binding.

The flanking residues, as expected, modify the MEP to a certain degree. More realistic theoretical MEP values may be obtained by using experimentally determined coordinates for the oligonucleotides based on X-ray or NMR data rather than regular B-DNA geometry. Fluctuation in nucleophilicity of G-N7 sites as a consequence of subtle sequence-dependent conformational changes that alter base stacking could account for the 3d metal ion binding pattern.

Selective methylation reactions on DNA oligomers have been reported[21], where positively charged groups attack specific G-residues at N7 in a manner analogous to the sequence-selectivity observed for metal ion interaction. The methylation intensities between different guanines in DNA fragments show six-to eight-fold variation suggesting the possibility of sequence-dependent G-N7 nucleophilicity. Indeed, for small alkylating groups there seem to be a positive correlation between reactivity at certain sites and MEP[22].

4.3. Hg(II) - TITRATIONS

Hg^{2+} ions have been found by UV and potentiometric methods to interact most strongly with AT-rich DNA[23]. The exposure of native calf thymus DNA to increasing amounts of $Hg(ClO_4)_2$ produces profound changes in its CD spectrum as well as decrease in endonucleolytic DNA cleavage rate[24]. The changes (inversions) in the CD spectrum are explained by a transition of the secondary structure of DNA from B-form ($r<0.01$) to Z-form ($0.12<r<1.0$). These observations are explained by inter-strand cross-linking of DNA bases by Hg(II)-ions, thus assisting the complete renaturation of DNA when Hg is removed by NaCN.

We have carried out Hg(II)-ion titration of two different duplex deoxyoligonucleotides, 5′-CGCGAATTCGCG (1) [25] and 5′-GCCGATATCGGC (2), monitoring the complexation process by ^{1}H and ^{15}N NMR. The expected binding sites, the AT-regions, appear in distinctly different environment in the two sequences, and the question is: will the mercury ion bind in a sequence-selective manner? Also, it is of interest to check if the Hg(II) induced B -> Z transition, proposed based on CD spectra[24], takes place in the titration of the duplex helix.

The titrations of (1) were carried out by successive addition of aliquots of $Hg(ClO_4)_2$ to the oligomer dissolved in phosphate buffer[25]. The thymine imino hydrogens as well as the guanine imino protons G4-NH1 and G10-NH1 disappear while, simultaneously, new strong signals emerge at 13.07 ppm and 12.93 ppm.(Fig. 5,A) In the intermediate titration range an equilibrium exists between the native and the mercurated oligomer.

The conformational transition is most clearly illustrated for the thymine methyl resonances which are gradually reduced at the native positions (1.26 ppm and 1.52 ppm) and a concomitant build-up at 1.05 ppm and 1.80 ppm (Fig. 5, B). The complete transition requires about one Hg(II)- ion per thymine in the duplex. The results indicate that the normal B-form of the duplex (I) has adopted a new well-defined form interacting specifically with mercury at the thymines. The NOESY maps of the new form show that the molecule has retained its duplex structure (Fig. 6). A complete "walk" of sequential NOE connectivities can be completed indicating that the dodecamer remains in a right-handed double-helical conformation after the addition of Hg(II) salt. All characteristic inter-strand cross-peaks involving A5/A6 H2 of one strand and the H1′ proton on the opposite strand are observed as well.

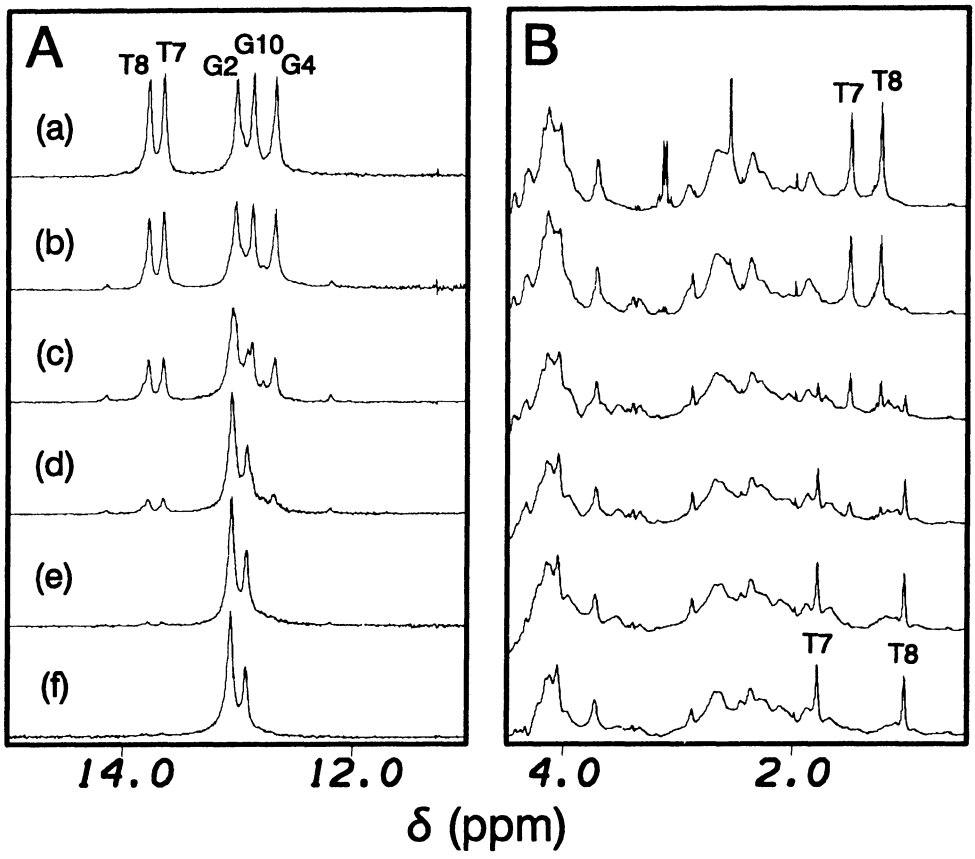

Figure 5. The effect upon the ^1H imino resonances (A) and methyl resonances (B) of adding successive amounts of $Hg(ClO_4)_2$ to a 4.8 mM solution of the duplex form of the dodecamer d[CGCGAATTCGCG]$_2$. The Hg(II)- concentrations were as follows: (a) 0, (b) 6, (c) 13, (d) 19, (e) 25, and (f) 28 mM.

The ^{15}N chemical shift data (not shown) suggest that no chemical bond is established between Hg(II) and A5/A6 N1 in the duplex. We propose the formation of a complex where each of four Hg(II) ions are forming a bond to (i) a NH6 (A NH_2) through a release of a proton and (ii) to an enolic T O4 on the opposite strand, thus cross-linking all A·T base pairs. The way Hg(II) ions are inserted into the A·T base pairs may also explain why the chemical shifts of, e.g. T7 CH_3 and T8 CH_3 changes differently upon incorporation of Hg(II). During the opening and slight stretching of all A·T base pairs the reorientation of the nucleobases may cause changes in the ring-current induced chemical shifts, and therefore their chemical shifts move differently.

The titration of sequence (2) , 5′-GCCGATATCGGC, where the two thymines, T6 and T8, have different environments, indicate differential binding. In this sequence all the imino protons involved in Watson-Crick base pairs remain intact.

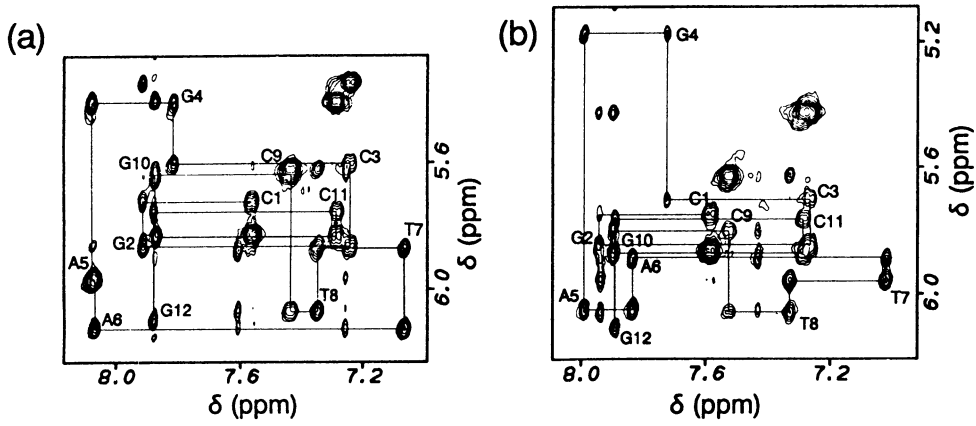

Figure 6. Contour plots of the aromatic/anomeric region from NOESY of the dodecamer duplex d[CGCGAATTCGCG]$_2$. The sequential connectivities are indicated with continuous lines. (a) without Hg(II) added, (b) with $Hg(ClO_4)_2$ / duplex ratio of 5.8:1.

However, large shifts are observed for the T8 and G4 imino signals, but not for the T imino.signal. Furthermore, the methyl signal of T8 shift to a new position while no effect i observed for T6 CH_3. Clearly, in this sequence T8 is the preferred binding site rather than T6 At present, the data is not sufficient to present a consistent model for the binding of Hg(II ions to the two sequences studied. A complete 2D NOESY data set will be collected for th mercurated species in order to carry out a complete structure determination

5. Concluding Remarks

The sequence-selective metal ion binding described above may be rationalised in terms of nucleophilicity and steric factors. The selectivity for Mn(II)/Zn(II) ions seems to be primarily determined by variation in the molecular electrostatic potential along the oligonucleotide sequence. For Hg(II) ions the preference for linear coordination geometry is obviously an important factor in addition to variation in nucleophilicity.

Several reports on the interaction between different platinum species and oligonucleotides using NMR spectroscopy have appeared in the literature[26-28]. The platinum studies, so far, have not dealt with the question of sequence-selectivity, but mainly trying to elucidate structural alteration as a function of metal binding. We are presently carrying out a series of sequence-selectivity experiments involving different Pd(II)- species analogous to the well known anti cancer compounds of platinum[29]

6. References

(1) Sip, M., Schwartz, A., Vovelle, F., Ptak, M. and Leng, M. *Biochemistry,* **1992**, *31*, 2508.
(2) Narasimhan, V. and Bryan, A. M. *Inorg. Chim. Acta* , **1984**, *91*, L39.
(3) Eichhorn, G. L. and Shin, Y. A., *J. Am. Chem. Soc.*, **1968**, *90*, 7323.
(4) Chuprina, V.P., Sletten, E., and Fedoroff, O.Y. *J.Biomol.Struct. Dyn.,* **1993**, *10*, 693.
(5) Wang, A. C., Kim, S. G., Flynn, P. F., Sletten, E., and Reid, B. R. *J. Magn. Reson.*, **1992**,*100*, 358.
(6) Young, P. R., Nandi, U. S. and Kallenback, N., R. *Biochemistry,* **1982**, *21*, 62
(7) Buchner, P., Maurer, W. and Ruterjans, H. *J. Magn. Reson.*, **1978**, *29*, 45.
(8) Nee, M. and Roberts, J. D. *Biochemistry,* **1982**, *21*, 4929.
(9) Buchanan, G. W. and Bell, M. J. *Can. J. Chem.*, **1983**, *61*, 2445.
(10) Frøystein, N. Å. and Sletten, E. *J. Am. Chem. Soc.* (in press)
(11) Kowalewski, J., Nordenskiøld, L., Benetis, N and Westlund, P. O. **1985** *Prog. NMR Spectroscopy 17*, 141.
(12) Nerdal, W., Hare, D. R. and Reid, B. R. *Biochemistry,* **1989**, *28*, 10008.
(13) Taylor, J. D. and Halford, S. E., *Biochemistry* , **1989**,*28*, 6198.
(14) Eichhorn, G. L. In: Eichhorn, G. L., Ed. *Inorganic Bioshemistry*, Elsevier, Amsterdam, **1973**, Vol. 2, Chap. 33-34.
(15) Sletten, E. and Lie, B. *Acta. Cryst.*, **1976**, *B32*, 3301.
(16) Furst, A., *Environ. Health Persp.*, **1981**, *40*, 83.
(17) Frøystein, N. Å. and Sletten, E. *Acta Chem. Scand.*, **1991**,*45*, 219.
(18) Frøystein, N. Å., Davis, J. T., Reid, B. R. and Sletten, E. *Acta Chem. Scand.*, **1993**,*47*, 649.
(19) Jia, X, Zon, G., and Marzilli, G. L. *Inorg. Chem.*, **1991**,*30*, 228.
(20) Pullman, A. and Pullman, B. *Q. Rev. Biopfys.*, **1981**,*14*, 289.
(21) Wurdeman, R. L., Church, K. M., and Gold, B. *J. Am. Chem. Soc.*, **1989**,*111*, 6408.
(22) Kohn, K. W., Hartley, J. A., and Mattes, W. B. *Nucl. Acid Res.* **1987**, *15*, 10531.
(23) Yamane, T. and Davidson, N. *J. Am. Chem. Soc.* **1961**, *83*, 2599.
(24) Gruenwedel, D.W. and Cruikshank, M. K. *Biochemistry,* **1990**, *29*, 2110.
(25) Frøystein, N. Å. and Sletten, E. *J. Am. Chem. Soc.*, **1994**,*116*, 3240.
(26) Sherman, S. E. and Lippard, S. J. *Chem. Rev.*, **1987**,*87*, 1153.
(27) Reedijk, J. *Inorg. Chim. Acta* , **1992**,*198-200*, 873.
(28) Kozelka, J., Fouchet, M. H. and Chottard, J.C. *Eur. J. Biochem.*, **1992**, *205*, 895.
(29) Garoufis, A., Frøystein, N. Å. and Sletten, E. (to be submitted)

METAL ION-COORDINATING PROPERTIES IN SOLUTION OF PURINE-NUCLEOSIDE 5'-MONOPHOSPHATES AND SOME ANALOGUES

HELMUT SIGEL
University of Basel
Institute of Inorganic Chemistry
Spitalstrasse 51
CH-4056 Basel, Switzerland

ABSTRACT. The stability constants of the 1:1 complexes formed between Mg^{2+}, Ca^{2+}, Sr^{2+}, Ba^{2+}, Mn^{2+}, Co^{2+}, Ni^{2+}, Cu^{2+}, Zn^{2+}, or Cd^{2+} and adenosine 5'-monophosphate (AMP^{2-}), inosine 5'-monophosphate (IMP^{2-}), or guanosine 5'- monophosphate (GMP^{2-}) as well as the AMP analogue 9-[2-(phosphonomethoxy)ethyl)]adenine ($PMEA^{2-}$), which owns antiviral properties, are analyzed with regard to the structures of the complexes formed in solution. Based on log $K^{M}_{M(R\text{-}PO_3)}$ versus $pK^{H}_{H(R\text{-}PO_3)}$ straight-line plots, where $R\text{-}PO_3^{2-}$ represents simple phosphate monoester or phosphonate ligands that can only undergo a $\text{-}PO_3^{2-}\text{-}M^{2+}$ coordination, the stabilities of the M(AMP), M(IMP), M(GMP), and M(PMEA) complexes are evaluated. By including tubercidin 5'-monophosphate (= 7-deaza-AMP^{2-}; i.e., N-7 is replaced by a CH unit) into the study it is proven that an increased stability of the M(AMP) complexes is due to macrochelate formation of a phosphate-coordinated metal ion with N-7 of the adenine residue. This macrochelate formation is quantified for the M(AMP), M(IMP), and M(GMP) complexes. Plots of the log stability increases versus the negative log of the micro acidity constants of the H^{+}(N-7) site of the *mono*protonated nucleosides reveal that the extent of macrochelate formation is mainly determined by the basicity of N-7. In the case of the M(PMEA) complexes the also observed stability increase has to be attributed to the formation of five-membered chelates involving the ether oxygen present in the $\text{-}CH_2\text{-}O\text{-}CH_2\text{-}PO_3^{2-}$ residue of PMEA for the complexes with Mg^{2+}, Ca^{2+}, Sr^{2+}, Ba^{2+}, Mn^{2+}, Co^{2+}, Zn^{2+}, and Cd^{2+}; only in the case of Cu^{2+}, and possibly also Ni^{2+}, an interaction with the adenine residue (probably with N-3) occurs in addition. The equilibrium scheme for the three isomers of Cu(PMEA) is elaborated and the formation degree of the various isomers is quantified. Finally, the properties of the M(PMEA) and M(AMP) complexes are compared and it is emphasized that the ether oxygen, which influences so much the stability and structure of the M(PMEA) complexes in solution, is also crucial for the antiviral properties of PMEA.

1. Introduction

The biological activity of nucleotides depends in general on the presence of metal ions;[1] this and the fact that nucleotides are among the most widely used substrates in cell metabolism[2-4] explain and also justify why nucleotide metal binding is receiving considerable attention.[5-8] Indeed, the ambivalent properties of nucleotides and their derivatives present a true challenge to coordination chemists[9] and much effort has been devoted to describe the structure of nucleotide-metal ion complexes in solution,[10-13] since Szent-Györgyi[14] proposed a structure for the Mg^{2+} complex of adenosine 5'-triphosphate (ATP^{4-}) (see also ref 13a).

D.P. Kessissoglou (ed.), Bioinorganic Chemistry, 155-178

In Section 2 of this presentation the focus is on metal ion complexes of some purine-nucleoside 5'-monophosphates (NMP^{2-}) occurring in nature, i.e., adenosine 5'-monophosphate (AMP^{2-}), inosine 5'-monophosphate (IMP^{2-}), and guanosine 5'-monophosphate (GMP^{2-}). The structures of these nucleotides[11a,15] are shown in Figure 1 together with that of tubercidin 5'-monophosphate ($TuMP^{2-}$). Tubercidin is synthesized by molds and fungi;[16] this nucleoside and its derivatives are antibacterial and antiviral agents, which are also active against some forms of cancer.[17] TuMP differs from AMP in the replacement of N-7 by a CH unit (see Figure 1) and is therefore also known as 7-deaza-AMP. A comparison of the coordinating properties of AMP^{2-} and $TuMP^{2-}$ should thus allow an evaluation of the influence of N-7 on the metal ion-binding properties of AMP^{2-}.

In Section 3 the complex-forming properties of an AMP analogue, i.e., 9-[2-(phosphonomethoxy)ethyl]adenine (PMEA), will be considered together with those of some related phosphonate derivatives (Figure 6, vide infra). PMEA shows antiviral properties[18] against DNA viruses, like herpes viruses, and also against retroviruses including human immuno deficiency viruses (HIV). The advantage of such phosphonate derivatives is that they are converted by cellular nucleotide kinases into their diphosphates, and as such they inhibit viral and, to a lesser extent, cellular DNA synthesis,[18,19] whereas base- or sugar-modified nucleotide analogues with monophosphate-ester residues undergo enzyme-catalyzed dephosphorylation,[20] rendering therapeutic application of such antimetabolites inefficient. One may add that the metal ion-binding properties of $PMEA^{2-}$ are complicated by the presence of the ether oxygen in the $-CH_2-O-CH_2-PO_3^{2-}$ residue;[21] participation of this oxygen in metal ion

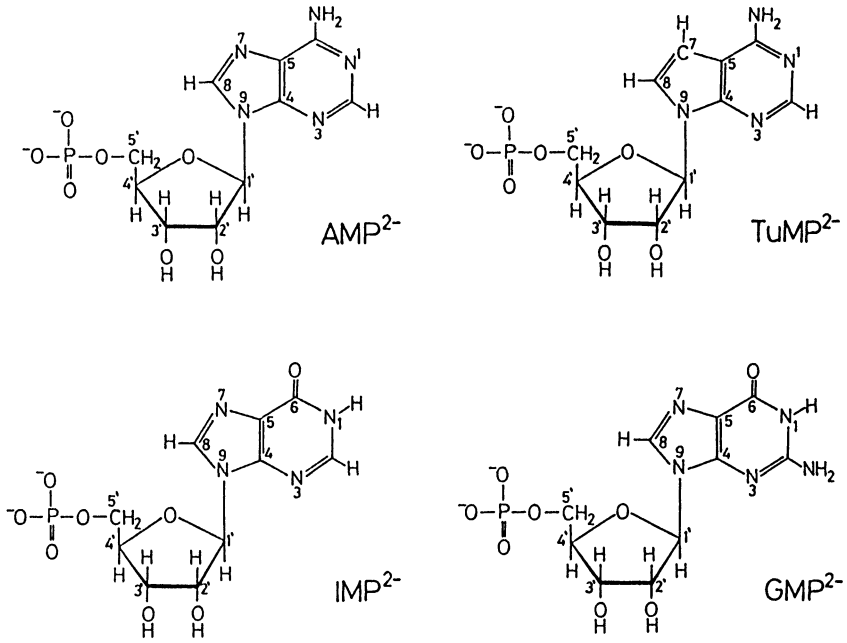

Figure 1. Chemical structures of the nucleoside monophosphates (NMP^{2-}) adenosine 5'-monophosphate (AMP^{2-}), tubercidin 5'-monophosphate ($TuMP^{2-}$ = 7-deaza-AMP^{2-}), inosine 5'-monophosphate (IMP^{2-}), and guanosine 5'-monophosphate (GMP^{2-}) in their dominating *anti* conformation.[11a,15]

binding gives rise to various isomeric equilibria (see Section 3).

It may be emphasized that all the equilibrium constants discussed below were obtained under experimental conditions (usually [NMP] $\leqslant 3 \times 10^{-4}$ M) where self-association is negligible.[21-23] Indeed, purine derivatives are well known to undergo self-association via stacking of their nucleic-base-ring systems;[24] a property promoted by metal ion coordination.[25] All the results presented below apply to monomeric species.

2. Extent of Macrochelate Formation in Complexes of AMP^{2-}, IMP^{2-}, and GMP^{2-}

2.1. ESTABLISHMENT OF RELATIONS BETWEEN COMPLEX STABILITY AND PHOSPHATE GROUP BASICITY

On the one hand it is long known that the number of phosphate groups determines to a large part the stability of metal ion complexes of nucleotides;[26,27] this is also true for the NMP^{2-} complexes formed with Mg^{2+}, Ca^{2+}, Sr^{2+}, Ba^{2+}, Mn^{2+}, Co^{2+}, Ni^{2+}, Cu^{2+}, Zn^{2+}, or Cd^{2+} (= M^{2+}).[28] On the other hand there are indications, for a similarly long time, that purine-NMPs may undergo macrochelate formation with certain metal ions,[10-12,28-31] and indeed, recently this has been proven by various methods.[22,32,33]

Considerations on equilibria and the way they are connected with each other show that any stability increase of a complex that goes beyond the stability expected on the basis of the basicity of a certain ligating site in a family of structurally related ligands proves that a further metal ion interaction must occur.[34] Of course, this general conclusion must also apply to the stabilities of M(NMP) complexes and their dependency on the basicities of the corresponding phosphate groups. With these reasonings in mind the properties of several simple phosphate monoesters, like phenyl phosphate or *n*-butyl phosphate (= $R\text{-}PO_3^{2-}$), were studied.[35] $R\text{-}PO_3^{2-}$ species are dibasic and may accept two protons; therefore, the following deprotonation equilibria need to be considered:

$$H_2(R\text{-}PO_3) \rightleftharpoons H(R\text{-}PO_3)^- + H^+ \qquad (1a)$$

$$K^H_{H_2(R\text{-}PO_3)} = [H(R\text{-}PO_3)^-][H^+]/[H_2(R\text{-}PO_3)] \qquad (1b)$$

$$H(R\text{-}PO_3)^- \rightleftharpoons R\text{-}PO_3^{2-} + H^+ \qquad (2a)$$

$$K^H_{H(R\text{-}PO_3)} = [R\text{-}PO_3^{2-}][H^+]/[H(R\text{-}PO_3)^-] \qquad (2b)$$

The release of the first proton from monoesterified derivatives of phosphoric acid, i.e., from $H_2(R\text{-}PO_3)$ species, occurs at a very low pH: usually $pK_a \lesssim 1$ (eq 1).[35] This means, the first proton from the phosphoric acid residue in $H_2(R\text{-}PO_3)$ species is completely released at pH $\geqslant 3$ and does therefore not affect the equilibrium $H(R\text{-}PO_3)^-/R\text{-}PO_3^{2-}$ (eq 2), the pK_a values of which are usually[35] between 5 and 7, and the complex formation between M^{2+} and $R\text{-}PO_3^{2-}$; the last two reactions occur only at pH > 3.

Indeed, under experimental conditions with a large excess of M^{2+} regarding the concentration of $R\text{-}PO_3^{2-}$, the experimental data of potentiometric pH titrations may be completely described[35] by considering equilibria 2 and 3:

$$M^{2+} + R\text{-}PO_3^{2-} \rightleftharpoons M(R\text{-}PO_3) \qquad (3a)$$

$$K^M_{M(R\text{-}PO_3)} = [M(R\text{-}PO_3)]/([M^{2+}][R\text{-}PO_3^{2-}]) \qquad (3b)$$

As expected, there is a correlation between complex stability and phosphate group basicity, i.e., there is a linear relationship between log $K^{M}_{M(R\text{-}PO_3)}$ and $pK^{H}_{H(R\text{-}PO_3)}$ as is evident from Figure 2, where the corresponding data for the Mg^{2+}, Zn^{2+}, and Cu^{2+} complexes are plotted as an example.[35]

It is clear from Figure 2 that for a given metal ion the complexes with 4-nitrophenyl phosphate ($NPhP^{2-}$), phenyl phosphate (PhP^{2-}), and *n*-butyl phosphate (BuP^{2-}) fit within experimental error on a straight line; furthermore, the value for *D*-ribose 5-monophosphate also fits on this line, indicating that $RibMP^{2-}$ behaves like a simple phosphate monoester with a non-coordinating organic residue.[35] Moreover, the equilibrium data available from the literature for hydrogen phosphate (HPO_4^{2-})[28] and methyl phosphate ($CH_3OPO_3^{2-}$),[36] the simplest phosphate ligands to be thought of, also fit excellently on the base lines.

Today we know that uridine 5'-monophosphate (UMP^{2-}) and thymidine (= 2'-deoxyribosyl thymine) 5'-monophosphate (TMP^{2-})[35] as well as methanephosphonate (MeP^{2-}) and ethanephosphonate (EtP^{2-})[21] also excellently fit on these correlation lines. The corresponding straight line equations, each based on eight simple $R\text{-}PO_3^{2-}$ ligands, for the above mentioned ten metal ions are listed in ref 21.

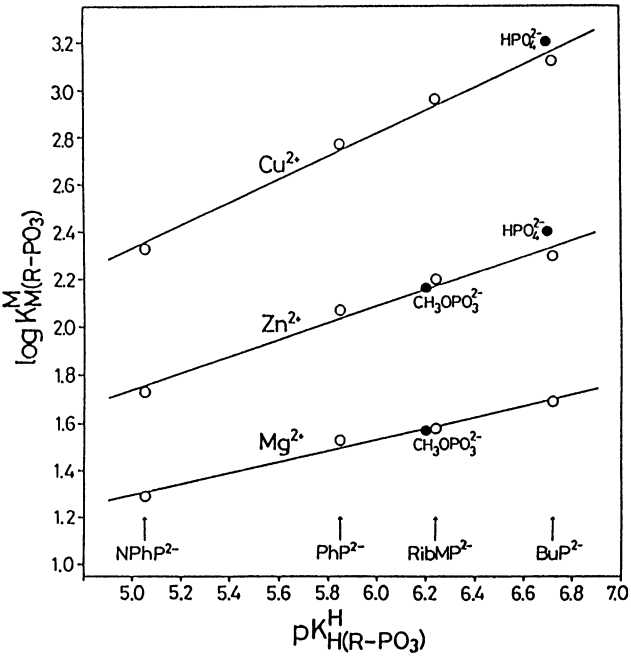

Figure 2. Relationship between log $K^{M}_{M(R\text{-}PO_3)}$ and $pK^{H}_{H(R\text{-}PO_3)}$ for the Mg^{2+}, Zn^{2+}, and Cu^{2+} 1:1 complexes of 4-nitrophenyl phosphate ($NPhP^{2-}$), phenyl phosphate (PhP^{2-}), *D*-ribose 5-monophosphate ($RibMP^{2-}$), and *n*-butyl phosphate (BuP^{2-}) (from left to right, ○). The least-squares lines are drawn through these data (25°C; I = 0.1 M, $NaNO_3$).[35] The points due to the complexes formed with methyl phosphate ($CH_3OPO_3^{2-}$)[36] and hydrogen phosphate (HPO_4^{2-})[28] (●) are inserted for comparison. This figure is a slightly altered version of Figure 2 from ref 35; it is redrawn by permission of the American Chemical Society.

2.2. ENHANCED STABILITY OF COMPLEXES FORMED WITH PURINE-NMPs AND PROOF THAT N-7 IS ITS CAUSE

Reference lines such as those shown in Figure 2 can now be used to decide whether or not a further metal ion interaction occurs in nucleoside monophosphate complexes. It has to be emphasized that any stability increase must be due to a metal ion-nucleic base interaction because the data for *D*-ribose 5-monophosphate complexes fit on the reference lines (Section 2.1).[35] That there is a stability increase, at least in some instances, in purine-NMP^{2-} complexes is seen from the three examples for plots of log $K^{M}_{M(R\text{-}PO_3)}$ versus $pK^{H}_{H(R\text{-}PO_3)}$ shown in Figure 3.[23] The values for Zn(AMP) and Cu(AMP) are clearly above the reference lines.[22] This is also true for all the M(IMP) and M(GMP) complexes with Mg^{2+}, Zn^{2+}, and Cu^{2+}, nicely proving the enhanced complex stability of these M(NMP) species.[23] In each case the vertical distance between the point due to a certain M(NMP) complex and the base line is a reflection of its increased stability (cf. also eq 4, vide infra).

Of course, this increased stability can be clearly defined by calculating the expected stability of a M(NMP) complex by using the corresponding acidity constant of $H(NMP)^{-}$, i.e., $pK^{H}_{H(NMP)}$, and the straight line equations of the various correlations.[21] The stability increase follows then from the difference between the experimentally determined (exper) and calculated (calc) stabilities as defined in equation 4.

$$\log \Delta_{M(NMP)} = \log K^{M}_{M(NMP)exper} - \log K^{M}_{M(NMP)calc} \qquad (4)$$

The experimentally determined and calculated stability constants for the M(AMP), M(IMP), and M(GMP) complexes with the mentioned metal ions are summarized in Table 1. Comparison of these data confirms the observations made in Figure 3 that in many instances the stability of the M(NMP) complexes is larger than that expected for a sole M^{2+}-phosphate group coordination.[23]

That the mentioned stability increases must be due to an interaction of the phosphate-coordinated metal ion with N-7 of the purine moiety follows from studies with $TuMP^{2-}$. $TuMP^{2-}$ differs from AMP^{2-} only by the absence of N-7, which is replaced by a CH unit (see Figure 1). Indeed, the measured stabilities of all M(TuMP) complexes are identical with the calculated values, i.e., they fit on the reference lines, proving that $TuMP^{2-}$ has the coordinating properties of a simple phosphate monoester.[22] In contrast, the complexes of Mn^{2+}, Co^{2+}, Ni^{2+}, Cu^{2+}, Zn^{2+}, and Cd^{2+} with AMP^{2-} show increased complex stabilities (see Figure 3 and Table 1), which prove that macrochelates involving N-7 are formed;[22,23] hence, the question about the position of the following intramolecular equilibrium arises:

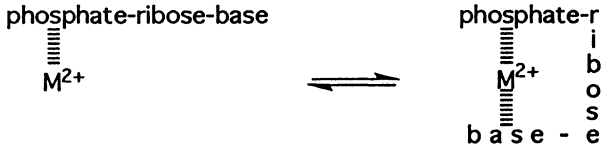

(5)

As the three purine-NMPs, i.e., AMP^{2-}, IMP^{2-}, and GMP^{2-}, are structurally closely related (Figure 1), one expects that the increased complex stabilities (Figure 3 and Table 1) and consequently also the position of equilibrium 5 depend on the basicity of N-7. In other words, one is also expecting a correlation between log $\Delta_{M(NMP)}$ (eq 4) and $pK_{a/N\text{-}7}$.

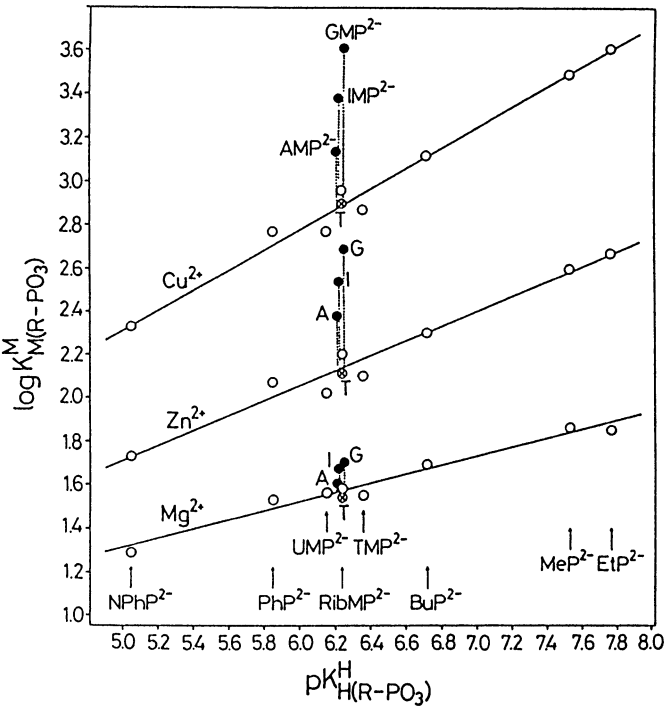

Figure 3. Evidence for an enhanced stability of several M(AMP), M(IMP), and M(GMP) complexes (●), based on the relationship between log $K^{M}_{M(R\text{-}PO_3)}$ and $pK^{H}_{H(R\text{-}PO_3)}$ for the 1:1 complexes of Mg^{2+}, Zn^{2+}, and Cu^{2+} with some simple phosphate monoester or phosphonate ligands ($R\text{-}PO_3^{2-}$): 4-nitrophenyl phosphate ($NPhP^{2-}$), phenyl phosphate (PhP^{2-}), uridine 5'-monophosphate (UMP^{2-}), *D*-ribose 5-monophosphate ($RibMP^{2-}$), thymidine (= 2'-deoxyribosyl thymine) 5'-monophosphate (TMP^{2-}), *n*-butyl phosphate (BuP^{2-}), methanephosphonate (MeP^{2-}), and ethanephosphonate (EtP^{2-}) (from left to right) (○). The least-squares lines are drawn through the corresponding eight data sets, which are taken for the phosphate monoesters from ref 35 and for the phosphonates from ref 21; the equations for these base lines are given in refs 21 and 23. The points due to the equilibrium constants for the NMP systems (●) (AMP^{2-} = A; IMP^{2-} = I; GMP^{2-} = G) are based on the data listed in Table 1. The vertical dotted lines emphasize the stability differences to the corresponding reference lines; these differences equal log $\Delta_{M(NMP)}$ as defined in Section 2.2 by eq 4. All points for the complexes with $TuMP^{2-}$ (= T) (⊗) fall within the error limits on the reference lines; the log stability constants of the M(TuMP) complexes are plotted versus the microconstant $pk^{TuMP}_{TuMP\cdot H}$ = 6.24 and these data are taken from Table III and Figure 2 of ref 22, respectively. All the plotted equilibrium constant values refer to aqueous solutions at 25°C and I = 0.1 M ($NaNO_3$). This figure is a slightly altered version of Figure 3 from ref 23; it is redrawn by permission of the American Chemical Society.

2.3. BASICITY OF THE N-7 SITE IN THE ADENOSINE, INOSINE, AND GUANOSINE RESIDUES

The difficulty in carrying out the indicated evaluation is that the most basic site of the adenine moiety in $H(AMP)^-$ is N-1 and *not* N-7. This means, the protonation reaction of the N-7

Table 1. Evidence for an Increased Stability of Various M(NMP) Complexes by Comparison of the Measured (exper) Stability, $K^{M}_{M(NMP)}$ (Eqs 3,13), with the Calculated (calc) Stability for an Isomer with a Sole M^{2+}-Phosphate Group Coordination in Aqueous Solution at 25°C and I = 0.1 M ($NaNO_3$)[a,b]

M^{2+}	log $K^{M}_{M(AMP)}$		log $K^{M}_{M(IMP)}$		log $K^{M}_{M(GMP)}$	
	exper[c]	calc[e]	exper[d]	calc[e]	exper[d]	calc[e]
Mg^{2+}	1.60±0.02	1.56±0.03	1.67±0.02	1.57±0.03	1.70±0.02	1.57±0.03
Ca^{2+}	1.46±0.01	1.45±0.05	1.50±0.01	1.45±0.05	1.53±0.01	1.45±0.05
Sr^{2+}	1.24±0.01	1.24±0.04	1.32±0.02	1.24±0.04	1.36±0.02	1.24±0.04
Ba^{2+}	1.17±0.02	1.16±0.04	1.28±0.02	1.16±0.04	1.32±0.02	1.17±0.04
Mn^{2+}	2.23±0.01	2.16±0.05	2.31±0.02	2.16±0.05	2.39±0.02	2.17±0.05
Co^{2+}	2.23±0.02	1.94±0.06	2.59±0.01	1.94±0.06	2.72±0.02	1.95±0.06
Ni^{2+}	2.49±0.02	1.94±0.05	2.91±0.03	1.95±0.05	3.13±0.03	1.95±0.05
Cu^{2+}	3.14±0.01	2.87±0.06	3.38±0.02	2.88±0.06	3.61±0.04	2.89±0.06
Zn^{2+}	2.38±0.07	2.13±0.06	2.54±0.02	2.13±0.06	2.69±0.02	2.14±0.06
Cd^{2+}	2.86±0.02	2.44±0.05	2.88±0.02	2.45±0.05	2.98±0.02	2.46±0.05

[a] Acidity constants of the $H_2(NMP)^{\pm}$ species: $pK^{H}_{H_2(AMP)}$ = 3.84 ± 0.02, $pK^{H}_{H(AMP)}$ = 6.21 ± 0.01,[22] $pK^{H}_{H_2(IMP)}$ = 1.30 ± 0.10, $pK^{H}_{H(IMP)}$ = 6.22 ± 0.01;[23] $pK^{H}_{H_2(GMP)}$ = 2.48 ± 0.04, $pK^{H}_{H(GMP)}$ = 6.25 ± 0.02.[23,b] [b] The range of error given with the constants is *three times* the standard error of the mean value or the sum of the probable systematic errors, whichever is larger. [c] From ref 22. [d] From ref 23. Some of these values may actually be slightly larger due to difficulties in the determination of the stability of the M(H·IMP) and M(H·GMP) complexes; for details see Section 1.6 ("A Caveat") in ref 23. However, if so, this would only mean that the effects described in Sections 2.4 and 2.5 are in some instances even somewhat more pronounced. [e] Calculated[23] with $pK^{H}_{H(NMP)}$ (see[a]) and the reference-line equations of Table 3 in ref 23 or in Tables 5 and 6 of ref 21.

site in the presence of an unprotonated, and hence neutral, N-1 site cannot directly be measured. However, recently we have succeeded in estimating in an indirect way, via the complicated procedure summarized below, the micro acidity constant for the H^{+}(N-7) site of *mono*protonated adenosine.[37]

The overall stability constant measured in solution for a complex formed between a metal ion and adenosine (Ado) is defined by eq 6:

$$M^{2+} + Ado \rightleftharpoons M(Ado)^{2+} \tag{6a}$$

$$K^{M}_{M(Ado)} = [M(Ado)^{2+}]/([M^{2+}][Ado]) \tag{6b}$$

Considering that $M(Ado)^{2+}$ may exist in two isomeric forms,[38,39] i.e., one species with N-1 binding and a second one with N-7 binding, one may rewrite eq 6b in the form of eq 7:

$$K^{M}_{M(Ado)} = \frac{([M(N\text{-}1/Ado)^{2+}]+[M(N\text{-}7/Ado)^{2+}])}{[M^{2+}][Ado]} \tag{7a}$$

$$K^{M}_{M(Ado)} = \frac{[M(N\text{-}1/Ado)^{2+}]}{[M^{2+}][Ado]} + \frac{[M(N\text{-}7/Ado)^{2+}]}{[M^{2+}][Ado]} \quad (7b)$$

$$K^{M}_{M(Ado)} = K^{M}_{M(N\text{-}1/Ado)} + K^{M}_{M(N\text{-}7/Ado)} \quad (7c)$$

It becomes thus apparent that the basicity of N-1 *and* of N-7 governs metal ion binding of adenosine.[37]

From all adenosine-metal ion systems studied the information regarding Cu^{2+} is certainly most complete.[37] For this metal ion the interactions with a purine residue have been detailed; i.e., the correlation line for an imidazole-like or purine N-7 type coordination of Cu^{2+} has been given.[39] Similarly, a correlation line for a pyridine-like or N-1 type binding has also been determined[39] and more important, the corresponding correlation line for pyridine-like or N-1 type ligands with an *ortho* amino substituent, i.e., for the adenine residue, has also been elaborated.[40] These results are summarized in Figure 4, where also the steric inhibitory effect of the *ortho* amino group on N-1 binding is nicely seen. Moreover, the stability constant for $Cu(Ado)^{2+}$ has also been independently determined in several laboratories with a satisfactory agreement.[26,41]

In using an average value for the stability of $Cu(Ado)^{2+}$, i.e., $\log K^{Cu}_{Cu(Ado)} = 0.8$ (cf.[37]), the overall stability constant of eq 7c is defined. Furthermore, because N-1 of adenosine is much more basic than N-7,[37] the acidity constant determined by potentiometric pH titration[15] equals the intrinsic $pk^{H}_{H(N\text{-}1/Ado)}$ value, i.e., $pK^{H}_{H(Ado)} = pk^{H}_{H(N\text{-}1/Ado)} = 3.61 \pm 0.03$. By using this acidity constant and the reference line[40] given in eq 8

$$\log K^{Cu}_{Cu(N\text{-}1/ortho)} = (0.456 \pm 0.029)\cdot pK_a - (1.428 \pm 0.175) \quad (8)$$

for N-1 coordination in the presence of an *ortho* amino group, a value for $\log K^{Cu}_{Cu(N\text{-}1/Ado)}$ may be calculated: $\log K^{Cu}_{Cu(N\text{-}1/Ado)} = 0.22 \pm 0.07$. With this constant, the mentioned overall value for $\log K^{Cu}_{Cu(Ado)}$, and eq 7c one may calculate a value for $\log K^{Cu}_{Cu(N\text{-}7/Ado)}$ and one obtains: $\log K^{Cu}_{Cu(N\text{-}7/Ado)} = 0.67$.

With this log stability constant and the correlation line for N-7 binding[39] given in eq 9,

$$\log K^{Cu}_{Cu(N\text{-}7)} = (0.499 \pm 0.019)\cdot pK_a + (0.766 \pm 0.084) \quad (9)$$

we have now the possibility to calculate a value for $pk^{H}_{H(N\text{-}7/Ado)}$ (see also the arrow on the log K axis in Figure 4). Application of $\log K^{Cu}_{Cu(N\text{-}7/Ado)} = 0.67$ to eq 9 gives $pk^{H}_{H(N\text{-}7/Ado)} = -0.19$. The average result given in ref 37, which is based on several experimentally determined values for $\log K^{Cu}_{Cu(Ado)}$, is

$$pk^{H}_{H(N\text{-}7/Ado)} = -0.2 \pm 0.3.$$

To obtain the above given micro acidity constant for the H^{+}(N-7) site of *mono*protonated adenosine was the difficult part. In inosine and guanosine no competition between the proton affinity of N-7 and another site exists; i.e., the measured macroconstants[23,24c] are identical with the corresponding microconstants:

$$pK^{H}_{H(Ino)} = pk^{H}_{H(N\text{-}7/Ino)} = 1.06 \pm 0.06 \quad \text{(ref 24c)}$$

$$pK^{H}_{H(Guo)} = pk^{H}_{H(N\text{-}7/Guo)} = 2.11 \pm 0.04 \quad \text{(ref 23)}$$

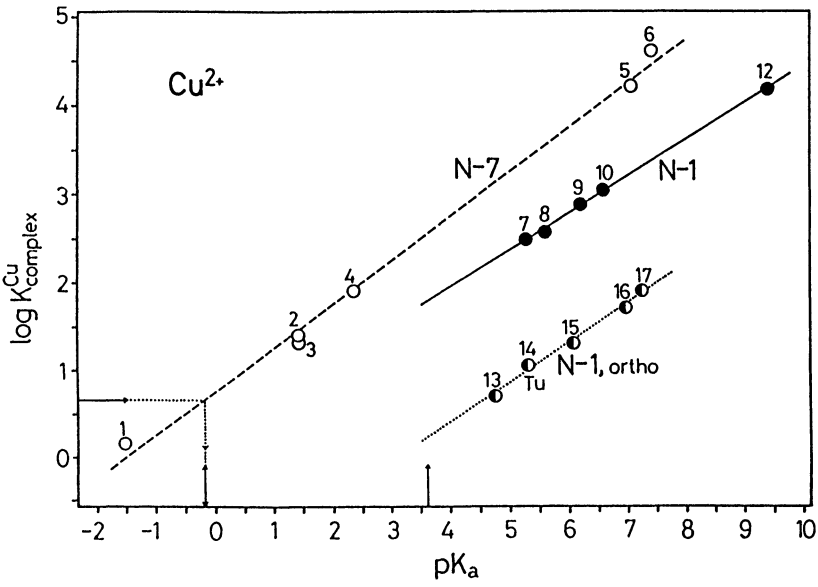

Figure 4. Relationship[37] between log $K^{Cu}_{complex}$ and pK_a for the 1:1 complexes of Cu^{2+} with imidazole-like or purine N-7 type ligands (○, broken line),[39] pyridine-like or N-1 type ligands (●, full line),[39] and pyridine-like or N-1 type ligands with an *ortho* amino substitutent (◐, dotted line).[40] The least-squares lines are drawn according to the equations given in refs 39 and 40, respectively. The inserted numbers correspond to the following ligands (for details see refs 39 and 40): H(adenosine)$^+$ (1), 1-methylinosine (2), inosine (3), guanosine (4), imidazole (5), and 1-methylimidazole (6); pyridine (7), 4-(2-thienyl)pyridine (8), 4-methylpyridine (9), 7-methylinosine (10), inosine (11; for Cu^{2+} no value is available), and ammonia (12; see ref 39 and also Section 2 of ref 37); 2-phenylpyridine (13), tubercidin = 7-deaza-adenosine (14; this point is in addition identified by "Tu"), 2-methylpyridine (15), 2-amino-pyridine (16), and 2-amino-3-methylpyridine (17).[40] The two arrows placed on the pK_a axis correspond to the acidity constants of *mono*protonated adenosine; i.e., $pk^{H}_{H(N\text{-}7/Ado)} = -0.2 \pm 0.3$ and $pk^{H}_{H(N\text{-}1/Ado)} = 3.61 \pm 0.03 = pK^{H}_{H(Ado)}$ (cf. [15]); regarding the arrow on the log K axis see text in Section 2.3.

2.4. INTERRELATION BETWEEN THE OBSERVED STABILITY INCREASE FOR M(NMP) COMPLEXES AND THE BASICITY OF N-7 IN THE CORRESPONDING PURINE RESIDUES

The above given $pk^{H}_{H(N\text{-}7/Ns)}$ values for the H^+(N-7) site in the three nucleosides (Ns), Ado, Ino, and Guo, reflect in a relative sense also the basicity of the N-7 site in AMP^{2-}, IMP^{2-} (regarding the microconstants see Section 2.4 in ref 23), and GMP^{2-} because in all three cases the distance between the phosphate group and N-7 is identical (see Figure 1). As pointed out before in Section 2.2, the extent of macrochelate formation (eq 5) in the complexes of the purine-NMPs is expected to depend on the basicity of N-7 in the corresponding purine residues. Therefore, a plot of the stability increase log $\Delta_{M(NMP)}$ (eq 4), which reflects the extent of macrochelation, versus the pk_a values of the H^+(N-7) site in the nucleosides should result in a straight line. From the data listed in Table 1 the values for the

stability increases log $\Delta_{M(NMP)}$ can be calculated according to equation 4; these results are listed in the second column of Table 2 (*vide infra*). For six representative metal ion systems the values of log $\Delta_{M(NMP)}$ versus the three $pk^{H}_{H(N\text{-}7/Ns)}$ values are plotted in Figure 5.

Indeed, for all ten metal ion systems studied in a first approximation within the error limits of the data straight lines are observed, unequivocally proving that the formation degree of the macrochelates (equilibrium 5) as summarized in Table 2 (*vide infra*) depends on the basicity of the N-7 site. This indicates further that the (C-6)=O group of IMP^{2-} and GMP^{2-} (see Figure 1), if at all, only plays a marginal role.

For some metal ions, like Co^{2+} and Ni^{2+}, the log $\Delta_{M(NMP)}$ versus $pk^{H}_{H(N\text{-}7/Ns)}$ plots might also be drawn as indicated by the broken lines in Figure 5 and this could then be taken as an indication[23] for an additional (outer-sphere) coordination to O-6. These finer details, in

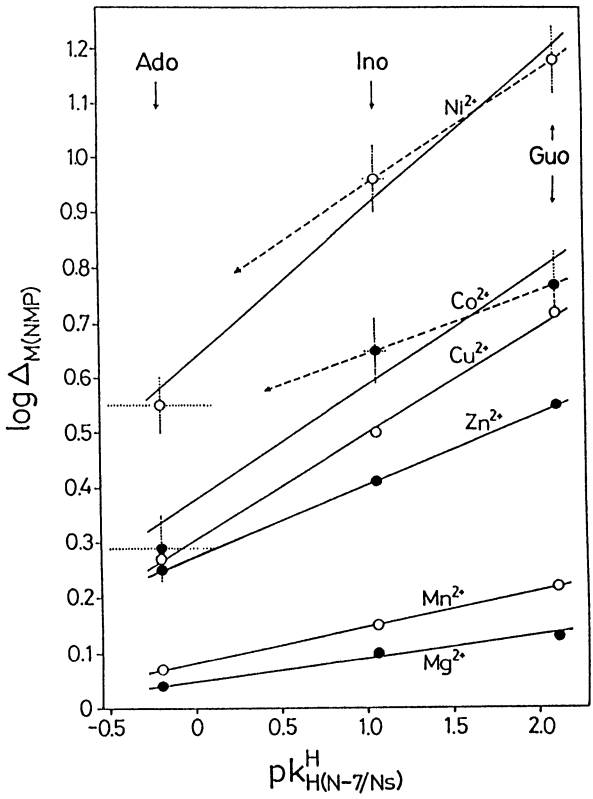

Figure 5. Relationship between log $\Delta_{M(NMP)}$ for the Ni^{2+}(○), Co^{2+} (●), Cu^{2+} (○), Zn^{2+} (●), Mn^{2+} (○), or Mg^{2+} (●) [from top to bottom] 1:1 complexes of AMP^{2-}, IMP^{2-}, or GMP^{2-} and $pk^{H}_{H(N\text{-}7/Ns)}$ of the corresponding nucleosides (Ns), adenosine (Ado), inosine (Ino), and guanosine (Guo). The values for log $\Delta_{M(NMP)}$ are from Table 2 and those for $pk^{H}_{H(N\text{-}7/Ns)}$ are given in the text of Section 2.3 (25°C; I = 0.1 M, $NaNO_3$). With the data points for the Ni^{2+} and Co^{2+} systems also error bars (dotted lines) corresponding to the error limits (3σ; Table 2) are inserted. The straight broken lines for the Ni^{2+} and Co^{2+} systems are based in each case only on the two data points for Ino and Guo; their relevance is shortly indicated in the text of Section 2.4 (for further details ref 23 should be consulted).

connection with X-ray crystal structure data, have been comprehensively discussed in ref 23, which should be consulted regarding these aspects.

2.5. EXTENT OF MACROCHELATE FORMATION IN THE M(NMP) COMPLEXES

The important point in the present context is that the increased complex stabilities prove that macrochelates are formed and, as Figure 5 demonstrates, that the extent of their formation depends on the basicity of N-7 in AMP^{2-}, IMP^{2-}, and GMP^{2-}. However, the actual formation degree of these macrochelates remains to be determined, in other words, the position of the intramolecular equilibrium 5. If we designate the macrochelated or 'closed' species as $M(NMP)_{cl}$ and the 'open' isomer as $M(NMP)_{op}$ the dimension-less equilibrium constant K_I of equilibrium 5 can be defined (eq 10):

$$K_I = [M(NMP)_{cl}]/[M(NMP)_{op}] \tag{10}$$

The reaction between a metal ion and one of the mentioned nucleoside 5'-monophosphates (NMP^{2-}) thus produces equilibrium 11 (which can also be considered as a rewriting of eq 3):[22,34]

$$M^{2+} + NMP^{2-} \rightleftharpoons M(NMP)_{op} \rightleftharpoons M(NMP)_{cl} \tag{11}$$

The equilibrium constant, $K^M_{M(NMP)_{op}}$, for the formation of the open complex is given by eq 12,

$$K^M_{M(NMP)_{op}} = [M(NMP)_{op}]/[M^{2+}][NMP^{2-}]) \tag{12}$$

and the overall equilibrium constant, $K^M_{M(NMP)}$, which is directly accessible by experiments (see Table 1), covering both, open and closed, species, is defined by eq 13:

$$K^M_{M(NMP)} = \frac{[M(NMP)]}{[M^{2+}][NMP^{2-}]} = \frac{([M(NMP)_{op}]+[M(NMP)_{cl}])}{[M^{2+}][NMP^{2-}]}$$
$$= K^M_{M(NMP)_{op}} + K_I \cdot K^M_{M(NMP)_{op}} = K^M_{M(NMP)_{op}} \cdot (1 + K_I) \tag{13}$$

The intramolecular and dimension-less equilibrium constant K_I may now be calculated according to eq 14,

$$K_I = \frac{K^M_{M(NMP)}}{K^M_{M(NMP)_{op}}} - 1 = 10^{\log\Delta} - 1 \tag{14}$$

provided that values for $K^M_{M(NMP)_{op}}$ are obtainable.

From the discussion in Section 2.2 it follows that $K^M_{M(NMP)_{op}}$ is identical with $K^M_{M(NMP)_{calc}}$; i.e., these values reflecting solely a phosphate-metal ion binding can be calculated via the straight-line equations[21] and the $pK^H_{H(NMP)}$ values of the $H(NMP)^-$ species (Table 1). In fact, the results are listed in columns 3, 5, and 7 of Table 1. Hence, the crucial difference log Δ, which appears in the second term of eq 14, is identical with the stability enhancement, log $\Delta_{M(NMP)}$, as defined in equation 4 (Section 2.2). Consequently, this equation 4 can now be rewritten as given in eq 15:

$$\log\Delta = \log\Delta_{M(NMP)} = \log K^M_{M(NMP)} - \log K^M_{M(NMP)_{op}} \tag{15}$$

Obviously the reliability of any calculations for K_I (eq 14) depends on the accuracy of the difference given in eq 15, i.e., on the error of the constants, which becomes more important the more similar the constants are. Therefore, only well defined error limits allow a quantitative evaluation of the extent of a possibly formed macrochelate (eqs 10,14). Finally, if K_I is known, the percentage of the closed or macrochelated species occurring in equilibrium 5 follows from eq 16:

$$\% \, M(NMP)_{cl} = 100 \cdot K_I / (1+K_I) \qquad (16)$$

Application of this procedure[22,34] yields the results of Table 2. The values in column 2 for log $\Delta_{M(NMP)}$ confirm that the stability increase follows the series M(AMP) < M(IMP) < M(GMP) for the ten metal ions studied (see also Figure 3) and this is again reflected from the formation degrees for $M(NMP)_{cl}$ listed in column 4. Substantial percentages of macrochelates are formed for all the M(IMP) and M(GMP) species, including the complexes of the alkaline earth ions.[23] This latter point is remarkable and the most apparent difference to the M(AMP) complexes where, if at all, only traces of macrochelates are formed. It has been concluded[23] that for the Cu^{2+}, Co^{2+}, Ni^{2+}, Zn^{2+}, and Cd^{2+} systems inner-sphere interactions with N-7 are dominating, while for the M(NMP) macrochelates of the alkaline earth ions outer-sphere interactions are suggested (for details ref 23 should be consulted).

2.6. SOME GENERAL CONCLUSIONS

The presented evaluations clearly demonstrate the ambivalent properties of AMP^{2-}, IMP^{2-}, and GMP^{2-} in interactions with metal ions. It is evident that intramolecular equilibria between isomers (cf. also ref 23) are an inherent property of their complexes in solution. These complexes should never be viewed as being of a static, rigid structure! In many instances the energy differences, $\Delta G°$, between isomers are in the order of about 1 kJ/mol or even below.[7,34]

For AMP, IMP, and GMP the metal ion recognition of the N-7 site depends strongly on its basicity (Figure 5). This result is of a general nature and applies also to polynucleotides and nucleic acids. The described evaluations suggest further that the wellknown[42] preferred binding of the *cis*-$Pt(NH_3)_2^{2+}$ drug to the N-7 of guanine over that of adenine in DNA is largely a basicity effect. Furthermore, the high affinity of the N-7 of guanine in DNA does not only hold for Pt^{2+}, but -- not surprising because the basicity is crucial -- is also true for other, especially labile, metal ions,[9] like Mn^{2+} (ref 43), Co^{2+} (ref 44), Cu^{2+} (ref 44), or Zn^{2+} (refs 43,45). That Mg^{2+} interacts with double-stranded poly(dG-dC) electrostatically as a mobile outer-sphere cloud whereas Ni^{2+} coordinates to more than one binding site at the polynucleotide, presumably to guanine-(N-7) and a phosphate group,[46] is also in line with the expectations based on the presented evaluations.

3. Isomeric Equilibria of the Metal Ion Complexes of $PMEA^{2-}$

3.1. CONSIDERATIONS ON THE VARIOUS POTENTIAL BINDING SITES OF $PMEA^{2-}$ AND ON THE CONNECTED EQUILIBRIA

9-[2-(Phosphonomethoxy)ethyl]adenine (PMEA), an AMP analogue with antiviral properties as shortly indicated already in Section 1, is shown in Figure 6 together with related phospho-

Table 2. Increased Complex Stability, log $\Delta_{M(NMP)}$ (Eqs 4,15), and Extent of the Intramolecular Macrochelate Formation (Eq 5) in M(NMP) Complexes as Quantified by the Dimension-less Equilibrium Constant K_I (Eqs 10,14) and the Percentage of $M(NMP)_{cl}$ (Eq 16) in Aqueous Solution at 25°C and I = 0.1 M ($NaNO_3$)[a]

M(NMP)	log $\Delta_{M(NMP)}$	K_I	% $M(NMP)_{cl}$
Mg(AMP)	0.04 ± 0.04	0.10 ± 0.09	0 (9 ± 8/<19)
Ca(AMP)	0.01 ± 0.05	0.02 ± 0.12	0 (2 ±11/<15)
Sr(AMP)	0.00 ± 0.04	0.00 ± 0.09	0 (0 ± 9/<11)
Ba(AMP)	0.01 ± 0.04	0.02 ± 0.11	0 (2 ±10/<15)
Mn(AMP)	0.07 ± 0.05	0.17 ± 0.14	15 ± 10
Co(AMP)	0.29 ± 0.06	0.95 ± 0.28	49 ± 7
Ni(AMP)	0.55 ± 0.05	2.55 ± 0.44	72 ± 3
Cu(AMP)	0.27 ± 0.06	0.86 ± 0.26	46 ± 8
Zn(AMP)	0.25 ± 0.09	0.78 ± 0.38	44 ± 12
Cd(AMP)	0.24 ± 0.05	0.74 ± 0.22	42 ± 7
Mg(IMP)	0.10 ± 0.04	0.26 ± 0.10	21 ± 7
Ca(IMP)	0.05 ± 0.05	0.12 ± 0.13	11 ± 10
Sr(IMP)	0.08 ± 0.04	0.20 ± 0.12	17 ± 9
Ba(IMP)	0.12 ± 0.04	0.32 ± 0.14	24 ± 8
Mn(IMP)	0.15 ± 0.05	0.41 ± 0.18	29 ± 9
Co(IMP)	0.65 ± 0.06	3.47 ± 0.63	78 ± 3
Ni(IMP)	0.96 ± 0.06	8.12 ± 1.22	89 ± 1
Cu(IMP)	0.50 ± 0.06	2.16 ± 0.46	68 ± 5
Zn(IMP)	0.41 ± 0.06	1.57 ± 0.37	61 ± 6
Cd(IMP)	0.43 ± 0.05	1.69 ± 0.33	63 ± 5
Mg(GMP)	0.13 ± 0.04	0.35 ± 0.11	26 ± 6
Ca(GMP)	0.08 ± 0.05	0.20 ± 0.14	17 ± 10
Sr(GMP)	0.12 ± 0.04	0.32 ± 0.14	24 ± 8
Ba(GMP)	0.15 ± 0.04	0.41 ± 0.15	29 ± 7
Mn(GMP)	0.22 ± 0.05	0.66 ± 0.21	40 ± 7
Co(GMP)	0.77 ± 0.06	4.89 ± 0.86	83 ± 2
Ni(GMP)	1.18 ± 0.06	14.14 ± 2.03	93 ± 1
Cu(GMP)	0.72 ± 0.07	4.25 ± 0.87	81 ± 3
Zn(GMP)	0.55 ± 0.06	2.55 ± 0.52	72 ± 4
Cd(GMP)	0.52 ± 0.05	2.31 ± 0.41	70 ± 4

[a] The values are from refs 22 and 23. See also footnote *b* in Table 1.

nate derivatives. The dianion of PMEA itself is an interesting ambivalent ligand; its coordination chemistry was revealed to a large part[21,47-49] by showing that simple phosphonate ligands, like methanephosphonate or ethanephosphonate (Figure 6), form complexes of a stability that is exactly satisfied by the log $K^{M}_{M(R\text{-}PO_3)}$ versus $pK^{H}_{H(R\text{-}PO_3)}$ relations already discussed in Section 2.1 and by taking also into account the metal ion-binding properties of the dianion of (phosphonomethoxy)ethane (PME^{2-} = ethoxymethanephosphonate; see Figure

6). PME^{2-} is closely related to $PMEA^{2-}$; it has the same $-CH_2-O-CH_2-PO_3^{2-}$ residue, which contains aside from the phosphonate group the ether oxygen as a further potential ligating site, but it lacks the adenine moiety. Hence, a comparison of the stabilities of the M(PME) and M(PMEA) complexes should reveal any effect, i.e., participation in metal ion binding, of the adenine residue.

In analogy to nucleotides one expects that the phosphonate group of $PMEA^{2-}$ determines to a large part the stability for most metal ion complexes. Should the adenine moiety interact with a metal ion already coordinated to the phosphonate group this could occur either via N-3 or N-7; N-1 cannot be reached and can therefore be ignored. However, the following two equilibrium schemes have to be considered; in each case three different isomeric species occur:

$$M^{2+} + PMEA^{2-} \overset{K^{M}_{M(PMEA)_{op}}}{\rightleftharpoons} M(PMEA)_{op} \begin{cases} \overset{K_{I/O}}{\rightleftharpoons} M(PMEA)_{cl/O} \\ \overset{K_{I/N7}}{\rightleftharpoons} M(PMEA)_{cl/N7} \end{cases} \quad (17)$$

$$M^{2+} + PMEA^{2-} \overset{K^{M}_{M(PMEA)_{op}}}{\rightleftharpoons} M(PMEA)_{op} \begin{cases} \overset{K_{I/O}}{\rightleftharpoons} M(PMEA)_{cl/O} \\ \overset{K_{I/O/N3}}{\rightleftharpoons} M(PMEA)_{cl/O/N3} \end{cases} \quad (18)$$

Both schemes 17 and 18 have in common the existence of solely phosphonate-coordinated species, i.e., an 'open' isomer designated as $M(PMEA)_{op}$ which can form a five-membered chelate with the ether O-atom of the $-CH_2-O-CH_2-PO_3^{2-}$ residue. Indeed, the ether O-atom is

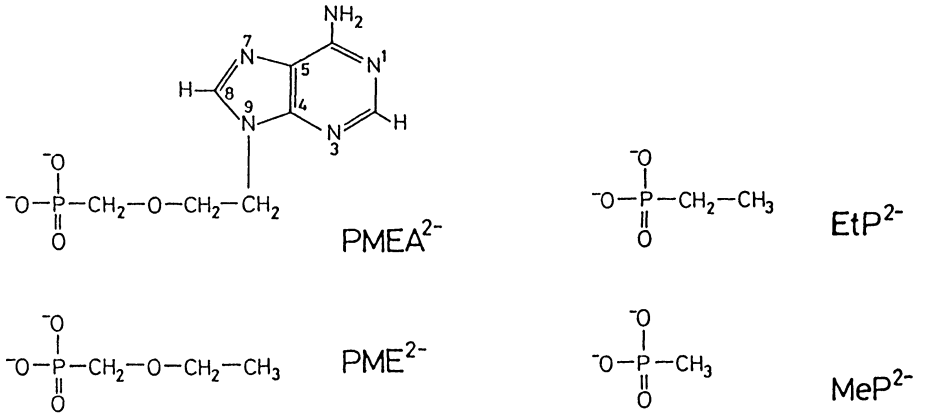

Figure 6. Chemical structure of the dianion of 9-[2-(phosphonomethoxy)ethyl]adenine ($PMEA^{2-}$) in comparison with the structures of the dianion of (phosphonomethoxy)ethane (PME^{2-}), ethanephosphonate (EtP^{2-}), and methanephosphonate (MeP^{2-}), which are also employed in Figure 7.

known[34] to be able to participate in complex formation provided it is located in a suitable position within a ligand. This is for $PMEA^{2-}$ clearly the case; the corresponding species is designated as $M(PMEA)_{cl/O}$ and the connected intramolecular equilibrium with its structural details is shown below:

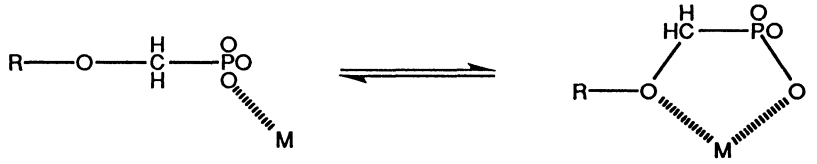

(19)

The crucial difference between the two equilibrium schemes 17 and 18 is that the $M(PMEA)_{cl/O}$ isomer may also interact with N-3 of the adenine residue by forming a seven-membered chelate without disrupting the ether O-M^{2+} bond; hence, the formation of a macrochelate involving only the phosphonate group and N-3 is highly unlikely -- the result is thus scheme 18. This contrasts with the fact that N-7 can only be reached from a phosphonate-coordinated metal ion in a $PMEA^{2-}$ complex if *no* five-membered chelate with the ether O-atom is formed. This means, the open isomer, $M(PMEA)_{op}$, may either transform into a macrochelate with N-7 or into a five-membered chelate with the ether O-atom, but both interactions can *not* occur at the same time in the same complex species -- this leads then to scheme 17.

From schemes 17 and 18 the definitions 20 through 23 follow:

$$K^{M}_{M(PMEA)_{op}} = [M(PMEA)_{op}]/([M^{2+}][PMEA^{2-}]) \quad (20)$$

$$K_{I/O} = [M(PMEA)_{cl/O}]/[M(PMEA)_{op}] \quad (21)$$

$$K_{I/N7} = [M(PMEA)_{cl/N7}]/[M(PMEA)_{op}] \quad (22)$$

$$K_{I/O/N3} = [M(PMEA)_{cl/O/N3}]/[M(PMEA)_{cl/O}] \quad (23)$$

Based on the equilibrium scheme 17 and the above definitions equation 24 follows for the experimentally accessible stability constant:

$$K^{M}_{M(PMEA)} = \frac{[M(PMEA)]}{[M^{2+}][PMEA^{2-}]} \quad (24a)$$

$$= \frac{([M(PMEA)_{op}]+[M(PMEA)_{cl/O}]+[M(PMEA)_{cl/N7}])}{[M^{2+}][PMEA^{2-}]} \quad (24b)$$

$$= K^{M}_{M(PMEA)_{op}} + K_{I/O} \cdot K^{M}_{M(PMEA)_{op}} + K_{I/N7} \cdot K^{M}_{M(PMEA)_{op}} \quad (24c)$$

$$= K^{M}_{M(PMEA)_{op}} (1 + K_{I/O} + K_{I/N7}) \quad (24d)$$

In analogy to eqs 10 and 14 one arrives easily[22,34] at the following eq 25:

$$K_I = K_{I/tot} = \frac{K^{M}_{M(PMEA)}}{K^{M}_{M(PMEA)_{op}}} - 1 = 10^{\log \Delta} - 1 \quad (25a)$$

$$= \frac{[M(PMEA)_{cl/tot}]}{[M(PMEA)_{op}]} = \frac{([M(PMEA)_{cl/O}]+[M(PMEA)_{cl/N7}])}{[M(PMEA)_{op}]} \quad (25b)$$

$$= K_{I/O} + K_{I/N7} \quad (25c)$$

Based on the equilibrium scheme 18 one may derive the following equations by proceeding in the way indicated for scheme 17:

$$K^{M}_{M(PMEA)} = \frac{[M(PMEA)]}{[M^{2+}][PMEA^{2-}]} \quad (26a)$$

$$= \frac{([M(PMEA)_{op}]+[M(PMEA)_{cl/O}]+[M(PMEA)_{cl/O/N3}])}{[M^{2+}][PMEA^{2-}]} \quad (26b)$$

$$= K^{M}_{M(PMEA)_{op}} + K_{I/O} \cdot K^{M}_{M(PMEA)_{op}} + K_{I/O} \cdot K_{I/O/N3} \cdot K^{M}_{M(PMEA)_{op}} \quad (26c)$$

$$= K^{M}_{M(PMEA)_{op}} (1 + K_{I/O} + K_{I/O} \cdot K_{I/O/N3}) \quad (26d)$$

$$K_I = K_{I/tot} = \frac{K^{M}_{M(PMEA)}}{K^{M}_{M(PMEA)_{op}}} - 1 = 10^{\log \Delta} - 1 \quad (27a)$$

$$= \frac{[M(PMEA)_{cl/tot}]}{[M(PMEA)_{op}]} = \frac{([M(PMEA)_{cl/O}]+[M(PMEA)_{cl/O/N3}])}{[M(PMEA)_{op}]} \quad (27b)$$

$$= K_{I/O} + K_{I/O} \cdot K_{I/O/N3} = K_{I/O} (1 + K_{I/O/N3}) \quad (27c)$$

It should be noted that the differences between equations 25c and 27c originate in the different order of the successive equilibria in schemes 17 and 18. This leads to different definitions for some of the intramolecular equilibria (eqs 22 and 23) and hence, to different dependencies of K_I (= $K_{I/tot}$; see eqs 25c and 27c), which is sometimes also addressed as the total stability enhancement E.[34] Of course, if the species $M(PMEA)_{cl/N7}$ and $M(PMEA)_{cl/O/N3}$ of schemes 17 and 18, respectively, are not formed, then equations 25c and 27c reduce to $K_I = K_{I/O}$; i.e., then only equilibrium 19 is operating.

3.2. COMPARISON OF THE STABILITIES OF THE M(PME) AND M(PMEA) COMPLEXES

Based on the experience with the metal ion complexes of AMP^{2-} (Section 2) one may also expect at least for some of the complexes of the AMP^{2-} analogue, $PMEA^{2-}$, an increased stability. To consider this possibility further, plots of log $K^{M}_{M(R\text{-}PO_3)}$ versus $pK^{H}_{H(R\text{-}PO_3)}$ are given in Figure 7 for the 1:1 complexes of Ca^{2+} and Cd^{2+}, as examples, with simple $R\text{-}PO_3^{2-}$ ligands (see also Section 2.1), allowing only a $-PO_3^{2-}$-metal ion binding. The two solid points in Figure 7 which refer to Ca(PMEA) and Cd(PMEA) are, especially for the Cd^{2+} complex, considerably above the reference lines, thus proving an increased stability for these complexes.

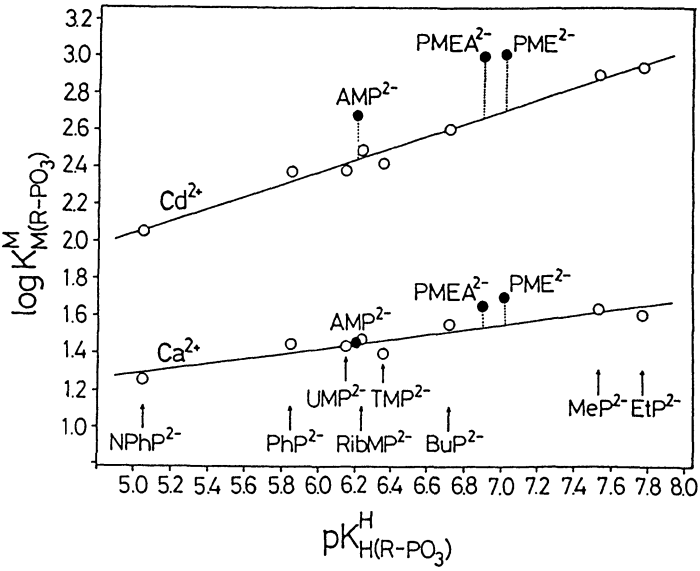

Figure 7. Evidence for an enhanced stability of several M(PME), M(PMEA), and M(AMP) complexes (●), based on the relationship between log $K^{M}_{M(R\text{-}PO_3)}$ and $pK^{H}_{H(R\text{-}PO_3)}$ for the 1:1 complexes of Ca^{2+} and Cd^{2+} with some simple phosphate monoester or phosphonate ligands ($R\text{-}PO_3^{2-}$); the abbreviations used above for these ligands (○) are defined in the legend of Figure 3. The least-squares lines are drawn through the data sets of these eight ligands; they are taken for the phosphate monoesters from ref 35 and for the phosphonates from ref 21; the equations for the base lines are given in ref 21. The data for the points due to the AMP or PMEA and PME systems (●) are taken from refs 22 and 21, respectively (see also Tables 1 and 3). The vertical dotted lines emphasize the stability differences to the corresponding reference lines. All the plotted equilibrium constant values refer to aqueous solutions at 25°C and I = 0.1 M ($NaNO_3$).

From Figure 7 two conclusions are immediately evident by comparing the data points of the corresponding complexes of AMP^{2-}, $PMEA^{2-}$ and PME^{2-}: (i) The M(PME) and M(PMEA) complexes show a very similar stability increase and (ii) such a stability increase is seen only for Cd(AMP), but *not* for Ca(AMP). These observations are thus a first hint that in certain instances $PMEA^{2-}$ and PME^{2-} behave quite alike in their metal ion-binding properties, while AMP^{2-} differs.

A quantitative evaluation of the situation reflected in Figure 7 is possible by calculating with the value of $pK^{H}_{H(PMEA)}$ (= 6.90) and the mentioned straight-line equations (Sections 2.1 and 2.2) the stabilities for M(PMEA) complexes having solely a phosphonate-metal ion coordination (= calc). The corresponding results are listed in column 3 of Table 3; their comparison according to equation 28,

$$\log \Delta_{M(PMEA)} = \log K^{M}_{M(PMEA)_{exper}} - \log K^{M}_{M(PMEA)_{calc}} \quad (28a)$$

$$= \log K^{M}_{M(PMEA)} - \log K^{M}_{M(PMEA)_{op}} \quad (28b)$$

Table 3. Stability-Constant Comparisons for the M(PMEA) and M(PME) Complexes between the Stability Constants (Eqs 3,24,26) Measured (exper) by Potentiometric pH Titrations and the Stability Constants Calculated (calc) for a Pure Phosphonate-M^{2+} Coordination (analogous to Eq 12), Together with the Increased Stabilities, log $\Delta_{M(PMEA)}$ (Eq 28) and log $\Delta_{M(PME)}$ (Eq 29), for Aqueous Solutions at 25°C and I = 0.1 M ($NaNO_3$)[a,b]

M^{2+}	log $K^{M}_{M(PMEA)}$		log$\Delta_{M(PMEA)}$	log $K^{M}_{M(PME)}$		log$\Delta_{M(PME)}$
	exper[c]	calc[e]		exper[d]	calc[e]	
Mg^{2+}	1.87±0.04	1.71±0.03	0.16±0.05	1.95±0.01	1.73±0.03	0.22±0.03
Ca^{2+}	1.65±0.05	1.54±0.05	0.11±0.07	1.70±0.01	1.56±0.05	0.14±0.05
Sr^{2+}	1.37±0.03	1.30±0.04	0.07±0.05	1.38±0.03	1.31±0.04	0.07±0.05
Ba^{2+}	1.30±0.05	1.22±0.04	0.08±0.06	1.33±0.03	1.23±0.04	0.10±0.05
Mn^{2+}	2.54±0.06	2.33±0.05	0.21±0.08	2.62±0.02	2.35±0.05	0.27±0.05
Co^{2+}	2.37±0.03	2.09±0.06	0.28±0.07	2.41±0.02	2.12±0.06	0.29±0.06
Ni^{2+}	2.41±0.05	2.11±0.05	0.30±0.07	2.33±0.02	2.14±0.05	0.19±0.05
Cu^{2+}	3.96±0.04	3.19±0.06	0.77±0.07	3.73±0.03	3.25±0.06	0.48±0.07
Zn^{2+}	-[f]	2.36±0.06	0.30±0.10[g]	2.74±0.02	2.40±0.06	0.34±0.06
Cd^{2+}	3.00±0.04	2.67±0.05	0.33±0.06	3.01±0.02	2.71±0.05	0.30±0.05

[a] Acidity constants[21] for $H_2(PMEA)^{\pm}$, i.e. $pK^{H}_{H_2(PMEA)}$ = 4.16 ± 0.02 and $pK^{H}_{H(PMEA)}$ = 6.90 ± 0.01, and for $H(PME)^{-}$, i.e. $pK^{H}_{H(PME)}$ = 7.02 ± 0.01. [b] Regarding the error limits see footnote *b* in Table 1. [c] From ref 21, where also the stability constants for the $M(H{\cdot}PMEA)^{+}$ complexes are given. [d] From ref 21. [e] Calculated[21] with $pK^{H}_{H(R\text{-}PO_3)}$ (see [a]) and the reference-line equations given in ref 21. [f] Due to precipitation no stability constant could be determined.[21] [g] Estimated value; see ref 21.

i.e., analogous to eqs 4 and 15, with the measured (exper) stability constants leads to the stability differences given in the fourth column of Table 3. Evidently all the M(PMEA) complexes are more stable than expected on the basis of the basicity of the PMEA-phosphonate group, though in some instances the increase is close to its error limit.

With these results in mind the analogous evaluation, based on equation 29,

$$\log \Delta_{M(PME)} = \log K^{M}_{M(PME)_{exper}} - \log K^{M}_{M(PME)_{calc}} \quad (29a)$$

$$= \log K^{M}_{M(PME)} - \log K^{M}_{M(PME)_{op}} \quad (29b)$$

was carried out with the M(PME) complexes; the corresponding data are listed in columns 5 to 7 of Table 3. As PME^{2-} contains, aside from the phosphonate group, only the ether O-atom, the observed increased stabilities must here be due to a metal ion interaction with this site; in other words, equilibrium 19 is definitely operating in the case of the M(PME) complexes.

It is evident that the stability difference, log $\Delta_{M(PMEA)}$, for the M(PMEA) complexes as defined in eq 28 corresponds to the definition given in eq 29 for the M(PME) complexes. Hence, the increased stabilities observed for these two kinds of complexes may be compared with each other; this is best done by equation 30:

$$\Delta \log \Delta_{M} = \log \Delta_{M(PMEA)} - \log \Delta_{M(PME)} \quad (30)$$

Indeed, comparison of the values in columns 4 and 7 of Table 3 shows that the values for $\Delta \log \Delta_M$ are zero within the error limits for most cases. The only exceptions are the Ni^{2+} and Cu^{2+} systems for which one calculates the following differences:

$$\Delta \log \Delta_{Ni} = 0.11 \pm 0.09 \quad (31)$$

$$\Delta \log \Delta_{Cu} = 0.29 \pm 0.10 \quad (32)$$

In other words, for all the other metal ions the stability increases of the M(PME) and M(PMEA) complexes are the same and consequently their structures must also be alike.

3.3. EXTENT OF CHELATE FORMATION IN THE COMPLEXES OF PME^{2-} AND $PMEA^{2-}$

From the results described in the preceding Section 3.2 it follows that for the metal ions Mg^{2+}, Ca^{2+}, Sr^{2+}, Ba^{2+}, Mn^{2+}, Co^{2+}, Zn^{2+}, and Cd^{2+} the measured increased stability of their M(PMEA) complexes can solely be explained by the formation of the five-membered chelate shown in equilibrium 19, there is no remarkable influence of the adenine residue. Indeed, the calculations for the corresponding intramolecular equilibrium constants K_I and for the percentages of $M(PME)_{cl/O}$ and $M(PMEA)_{cl/O}$, which are given in Table 4, confirm that the formation degrees for $M(PMEA)_{cl/O}$ and $M(PME)_{cl/O}$ are identical within the error limits for the mentioned eight metal ion systems and that consequently these chelates own the same structure.

The only clear exception (see Section 3.2) with a *positive* deviation is the Cu(PMEA) complex (eq 32). In this case $\Delta \log \Delta_{Cu} = 0.29$; in other words, the $\log \Delta_{Cu(PMEA)}$ value is by about 0.3 log unit larger than the corresponding one for the Cu(PME) system. This means, the adenine residue in the Cu(PMEA) complex has a stability enhancing effect, beyond that of the ether group discussed above. In the case of Ni(PMEA) the effect is much smaller, i.e. $\Delta \log \Delta_{Ni} = 0.11 \pm 0.09$ (eq 31), but probably still real. Consequently, for Cu(PMEA) and Ni(PMEA) further analysis according to schemes 17 and 18 is necessary by considering the additional possible intramolecular equilibria.

With regard to scheme 18 by taking into account eq 27a it is evident that the values of K_I ($= K_{I/tot}$) are already known (Table 4, column 4), and, therefore, also the concentrations of the open isomers, $M(PMEA)_{op}$. With the justified assumption that $M(PME)_{cl/O}$ and $M(PMEA)_{cl/O}$ have the same stability, and hence identical $K_{I/O}$ values (cf. also the other systems in Table 4), one can calculate the formation degree of the species that forms the five-membered chelate with the ether O-atom, i.e., $M(PMEA)_{cl/O}$ (eq 21). With K_I ($= K_{I/tot}$) and $K_{I/O}$ one can now calculate $K_{I/O/N3}$ from equation 27c and thus the formation degree of the $M(PMEA)_{cl/O/N3}$ species; of course, the difference between 100 and the sum of the percentages for $M(PMEA)_{op}$ and $M(PMEA)_{cl/O}$ will also result in % $M(PMEA)_{cl/O/N3}$ and, hence, in $K_{I/O/N3}$. The results are (for details see ref 21) for

Cu(PMEA):	% $Cu(PMEA)_{op}$	$= 17 \pm 3$		
	% $Cu(PMEA)_{cl/O}$	$= 34 \pm 10$;	$K_{I/O}$	$= 2.02 \pm 0.47$ (eq 21)
	% $Cu(PMEA)_{cl/O/N3}$	$= 49 \pm 10$;	$K_{I/O/N3}$	$= 1.42 \pm 0.74$ (eqs 23,27c)
Ni(PMEA):	% $Ni(PMEA)_{op}$	$= 50 \pm 8$		
	% $Ni(PMEA)_{cl/O}$	$= 28 \pm 10$;	$K_{I/O}$	$= 0.55 \pm 0.19$ (eq 21)
	% $Ni(PMEA)_{cl/O/N3}$	$= 22 \pm 13$;	$K_{I/O/N3}$	$= 0.82 \pm 0.86$ (eqs 23,27c)

Table 4. Extent of Chelate Formation (Eq 19) in M(PME) and M(PMEA) Complexes as Quantified by the Dimension-less Equilibrium Constant K_I and the Percentage of the Chelated Species in Aqueous Solution at 25°C and I = 0.1 M ($NaNO_3$)[a]

M^{2+}	M(PME)		M(PMEA)[b]	
	$K_I = K_{I/O}$ (analog. eqs 10,14)	% $M(PME)_{cl/O}$ (analog. eq 16)	$K_I = K_{I/tot}$ (= $K_{I/O}$)[c] (eqs 25,27)	% $M(PMEA)_{cl/O}$ (analog. eq 16)
Mg^{2+}	0.66 ± 0.12	40 ± 4	0.45 ± 0.17	31 ± 8
Ca^{2+}	0.38 ± 0.16	28 ± 9	0.29 ± 0.21	22 ± 13
Sr^{2+}	0.17 ± 0.14	15 ± 10	0.17 ± 0.14	15 ± 10
Ba^{2+}	0.26 ± 0.14	21 ± 9	0.20 ± 0.18	17 ± 12
Mn^{2+}	0.86 ± 0.23	46 ± 7	0.62 ± 0.29	38 ± 11
Co^{2+}	0.95 ± 0.28	49 ± 7	0.91 ± 0.29	48 ± 8
Ni^{2+}	0.55 ± 0.19	35 ± 8	*1.00 ± 0.32*	*50 ± 8*
Cu^{2+}	2.02 ± 0.47	67 ± 5	*4.89 ± 0.98*	*83 ± 3*
Zn^{2+}	1.19 ± 0.32	54 ± 7	1.00 ± 0.46	50 ± 12
Cd^{2+}	1.00 ± 0.25	50 ± 6	1.14 ± 0.32	53 ± 7

[a] The values are from ref 21. See also footnote *b* in Table 1. -- The above results are based on the values given for log $\Delta_{M(PME)}$ and log $\Delta_{M(PMEA)}$ in Table 3. [b] It should be noted that the results given for Zn(PMEA) are only estimates (see footnotes *f* and *g* in Table 3) and those for Ni(PMEA) and Cu(PMEA) are only *apparent* results, and these are, therefore, printed in *italics* as they refer to variously chelated species (see Section 3.3). [c] $K_I = K_{I/tot} = K_{I/O}$ is valid for all the systems except those containing Ni^{2+} or Cu^{2+} (see text in Section 3.3).

Analysis of the equilibrium scheme 17, again under the assumption that the values of $K_{I/O}$ for $M(PME)_{cl/O}$ and $M(PMEA)_{cl/O}$ are identical, leads to the same results as above, but

$$\% \ Cu(PMEA)_{cl/N7} = 49 + 10; \quad K_{I/N7} = 2.87 \pm 1.09 \text{ (eqs 22,25c) and}$$
$$\% \ Ni(PMEA)_{cl/N7} = 22 \pm 13; \quad K_{I/N7} = 0.45 \pm 0.37 \text{ (eqs 22,25c).}$$

The formation degrees of the $M(PMEA)_{cl/O/N3}$ (eq 18) and $M(PMEA)_{cl/N7}$ isomers (eq 17) are also identical, yet naturally the values of $K_{I/O/N3}$ and $K_{I/N7}$ are different, as they refer to different intramolecular equilibria.

At this point the question arises: Which of the adenine-bound isomers, $M(PMEA)_{cl/O/N3}$ or $M(PMEA)_{cl/N7}$, is actually formed? Or, are even both isomers present at the same time? With the information available, these questions cannot unequivocally be answered. However, careful considerations, including the use of molecular models, have led to the suggestion that the equilibrium scheme 18 is the pertinent one. This suggestion may appear as surprising because N-7 is a very well known binding site for metal ions in complexes of purine-nucleotides (Sections 2.2 and 2.4), in contrast to N-3, yet I feel that for steric reasons N-3 is the preferred site in the M(PMEA) complexes. Indeed, the interaction of metal ions also with N-3 of a purine residue has become apparent in the past few years from various X-ray crystal structure studies[50] and also from studies in solution.[51] Clearly, a final answer is not yet possible, but hopefully studies of the 3-deaza and 7-deaza analogues of $PMEA^{2-}$ will allow to resolve this ambiguity. However, what is certain in any case, is that at the very least in the case of Cu^{2+} the adenine moiety of $PMEA^{2-}$ is also involved in metal ion binding.

3.4. CONCLUSION AND OUTLOOK

The analyses presented in the preceding sections have shown that the ether linkage has a crucial role in the complexing properties of $PMEA^{2-}$. Hence, it is most remarkable that exactly the same ether O-atom is important for the antiviral activity of PMEA. Deletion of this O-atom or replacement by other groups leads to a loss or at least to a considerable reduction of the biological activity.[18,20,52]

Another point that warrants emphasis is the described Cu^{2+}-adenine recognition; as it turns out, this interaction is solvent-dependent:[47] It is quite pronounced in water and in water containing 50% 1,4-dioxane, but not so in water containing 30% 1,4-dioxane. Furthermore, isomeric equilibria, in a way similar to those described herein, also occur in mixed ligand complexes:[48,49] e.g., for Cu(1,10-phenanthroline)(PMEA), next to other species, also one with an intramolecular stack could be quantified.[48] Finally, it may be added that (*S*)-9-[3-hydroxy-2-(phosphonomethoxy)propyl]adenine ($HPMPA^{2-}$), which differs from $PMEA^{2-}$ (Figure 6) by the additional presence of a $-CH_2OH$ group in its residue, i.e. $-CH_2-CH(CH_2OH)-O-CH_2-PO_3^{2-}$, is one of the few compounds which show comparable biological activity[18,53] and indeed, $HPMPA^{2-}$ owns also similar metal ion coordinating properties.[54]

4. Some Closing Remarks

The analysis of the stability data, obtained via potentiometric pH titrations for the complexes of purine-nucleoside 5'-monophosphates and of $PMEA^{2-}$ in Sections 2 and 3, respectively, demonstrates the wealth of information that may in this way be gained about the structures of isomeric complexes in solution as well as about their formation degree. Both, AMP and PMEA (Figures 1 and 6), are in their own rights fascinating molecules. In fact, $PMEA^{2-}$ and AMP^{2-} resemble each other in many respects and those properties which depend only on the qualities of the adenine moiety, like stacking interactions, hydrogen bonding, or metal ion coordination are expected to be very similar or even identical, as long as no sites different from those of the adenine residue are involved.

The length of the *D*-ribose 5-monophosphate residue and of the (phosphonomethoxy)ethane residue are also very similar. Thus, a metal ion coordinated at the phosphate group of AMP^{2-} or at the phosphonate group of $PMEA^{2-}$ is placed at about the same distance from the adenine moiety, at least as long as no further interaction occurs and the complexes are present in their open form (equilibria 5 and 19). Of course, these equal distances could be of importance in various aspects of the biological action of both compounds and not only regarding their metal ion coordination.

However, there are crucial differences between AMP^{2-} and $PMEA^{2-}$ with regard to the structures of the metal ion complexes formed: With AMP^{2-} alkaline earth ions only bind to the phosphate group, while divalent 3d ions and Zn^{2+} or Cd^{2+} form macrochelates involving N-7 of the adenine moiety (Section 2.5). In contrast, with $PMEA^{2-}$ *all* the metal ions studied interact not only with the phosphonate group, but to a remarkable extent also with the neighboring ether O-atom (Section 3.3.), forming five-membered chelates (equilibrium 19). The adenine residue of $PMEA^{2-}$ is only exceptionally involved in metal ion binding, as e.g. with Cu^{2+}, and if so, most probably via N-3 (see Section 3.3.).

In other words, all enhanced complex stabilities observed so far for M(AMP) complexes could always be attributed to an interaction with N-7 (Section 2.2.),[22,23] while the enhanced complex stability of the M(PMEA) complexes has to the largest part to be attributed to the interaction with the ether O-atom. This means, the structures of the complexes having only a phosphate or phosphonate metal ion interaction are similar, yet those isomers, which contain chelates, are very different for AMP^{2-} and $PMEA^{2-}$.

Considering further that the enzymes responsible for DNA synthesis, in fact practically all enzymes which involve nucleotides as substrates, are metal ion-dependent, one wonders if the biological action of $PMEA^{2-}$ has its origin in its metal ion-coordinating properties. It seems quite possible that the formation of the five-membered chelates involving the ether O-atom is responsible for the inhibitory effects of PMEA on the growth of viruses; this chelate formation leads of course to a different orientation in space of the adenine residue than would be the case, e.g., with Mg(AMP) or Zn(AMP) as substrates.

5. Acknowledgements

The competent technical assistance of Mrs. *Rita Baumbusch* in the preparation of the manuscript, the support of this research over the years by the *Swiss National Science Foundation*, and recently in part by the *Swiss Federal Office for Education and Science* (Human Capital and Mobility) are gratefully acknowledged.

6. References

(1) J. J. R. Fraústo da Silva and R. J. P. Williams, '*The Biological Chemistry of the Elements*', Clarendon Press, Oxford, **1991**.
(2) P. D. Boyer, *Biochemistry*, **1987**, *26*, 8503.
(3) F. H. Westheimer, *Science*, **1987**, *235*, 1173.
(4) H. Sigel and A. Sigel, eds., '*Interrelations among Metal Ions, Enzymes, and Gene Expression*', Vol. 25 of *Metal Ions in Biological Systems*, Dekker, New York & Basel, **1989**.
(5) L. G. Marzilli, *Prog. Inorg. Chem.*, **1977**, *23*, 255.
(6) H. Sigel, ed., '*Nucleotides and Derivatives: Their Ligating Ambivalency*', Vol. 8 of *Metal Ions in Biological Systems*, Dekker, New York & Basel, **1979**.
(7) H. Sigel, *ACS Symp. Ser.*, **1989**, *402*, 159.
(8) (a) B. Lippert, *Prog. Inorg. Chem.*, **1989**, *37*, 1-97. (b) B. Lippert, *Biometals*, **1992**, *5*, 195.
(9) H. Sigel, *Chem. Soc. Reviews*, **1993**, *22*, 255.
(10) C. M. Frey and J. Stuehr, *Met. Ions Biol. Syst.*, **1974**, *1*, 51.
(11) (a) R. B. Martin and Y. H. Mariam, *Met. Ions Biol. Syst.*, **1979**, *8*, 57. (b) R. B. Martin, *Met. Ions Biol. Syst.*, **1988**, *23*, 315.
(12) H. Diebler, *J. Mol. Catal.*, **1984**, *23*, 209.
(13) (a) H. Sigel, *Eur. J. Biochem.*, **1987**, *165*, 65. (b) H. Sigel, *Chimia*, **1987**, *41*, 11.
(14) A. Szent-Györgyi in '*Enzymes: Units of Biological Structure and Function*'; O. H. Gaebler, ed.; Academic Press, New York, 1956, pp 393-397.
(15) R. Tribolet and H. Sigel, *Eur. J. Biochem.*, **1987**, *163*, 353.

(16) H. R. Mahler and E. H. Cordes, *'Biological Chemistry'*, Harper and Row, New York, 1966.
(17) (a) A. Bloch, R. J. Leonard, and C. A. Nichol, *Biochim. Biophys. Acta*, **1967**, *138*, 10. (b) T. B. Grage, D. B. Rochlin, A. J. Weiss, and W. L. Wilson, *Cancer Res.*, **1970**, *30*, 79. (c) C. G. Smith, L. M. Reineke, M. R. Burch, A. M. Shefner, and E. E. Muirhead, *Cancer Res.*, **1970**, *30*, 69. (d) F. E. Evans and R. H. Sarma, *Cancer Res.*, **1975**, *35*, 1458.
(18) A. Holý, E. De Clercq, and I. Votruba, *ACS Symp. Series*, **1989**, *401*, 51.
(19) S. A. Foster, J. Černý, and Y.-c. Cheng, *J. Biol. Chem.*, **1991**, *266*, 238.
(20) A. Holý, *Il Farmaco*, 46 (Suppl. 1), **1991**, 141.
(21) H. Sigel, D. Chen, N. A. Corfù, F. Gregáň, A. Holý, and M. Straš̌ák, *Helv. Chim. Acta*, **1992**, *75*, 2634.
(22) H. Sigel, S. S. Massoud, and R. Tribolet, *J. Am. Chem. Soc.*, **1988**, *110*, 6857.
(23) H. Sigel, S. S. Massoud, and N. A. Corfù, *J. Am. Chem. Soc.*, **1994**, *116*, 2958.
(24) (a) H. Sigel, *Biol. Trace Elem. Res.*, **1989**, *21*, 49. (b) N. A. Corfù, R. Tribolet , and H. Sigel, *Eur. J. Biochem.*, **1990**, *191*, 721. (c) N. A. Corfù and H. Sigel, *Eur. J. Biochem.*, **1991**, *199*, 659.
(25) (a) K. H. Scheller, F. Hofstetter, P. R. Mitchell, B. Prijs, and H. Sigel, *J. Am. Chem. Soc.*, **1981**, *103*, 247. (b) K. H. Scheller and H. Sigel, *J. Am. Chem. Soc.*, **1983**, *105*, 5891. (c) H. Sigel and N. A. Corfù, submitted for publication.
(26) P. W. Schneider, H. Brintzinger, and H. Erlenmeyer, *Helv. Chim. Acta*, **1964**, *47*, 992.
(27) H. Sigel and D. B. McCormick, *Acc. Chem. Res.* **1970**, *3*, 201.
(28) H. Sigel, K. Becker, and D. B. McCormick, *Biochim. Biophys. Acta*, **1967**, *148*, 655.
(29) (a) H. Sigel, *Experientia*, **1966**, *22*, 497. (b) H. Sigel and H. Erlenmeyer, *Helv. Chim. Acta*, **1966**, *49*, 1266. (c) H. Sigel and K. H. Scheller, *Eur. J. Biochem.* **1984**, *138*, 291.
(30) (a) R. S. Taylor and H. Diebler, *Bioinorg. Chem.*, **1976**, *6*, 247. (b) A. Peguy and H. Diebler, *J. Phys. Chem.*, **1977**, *81*, 1355. (c) A. Nagasawa and H. Diebler, *J. Phys. Chem.*, **1981**, *85*, 3523.
(31) Y. H. Mariam and R. B. Martin, *Inorg. Chim. Acta*, **1979**, *35*, 23.
(32) (a) M. D. Reily, T. W. Hambley, and L. G. Marzilli, *J. Am. Chem. Soc.*, **1988**, *110*, 2999. (b) L. M. Torres and L. G. Marzilli, *J. Am. Chem. Soc.*, **1991**, *113*, 4678.
(33) (a) M. Green and J. M. Miller, *J. Chem. Soc., Chem. Commun.*, **1987**, 1864; correction: *ibid.*, **1988**, 404. (b) D. M. Orton and M. J. Green, *J. Chem. Soc., Chem. Commun.*, **1991**, 1612.
(34) R. B. Martin and H. Sigel, *Comments Inorg. Chem.*, **1988**, *6*, 285.
(35) S. S. Massoud and H. Sigel, *Inorg. Chem.*, **1988**, *27*, 1447.
(36) (a) H. Brintzinger, *Helv. Chim. Acta*, **1965**, *48*, 47. (b) H. Brintzinger and G. G. Hammes, *Inorg. Chem.*, **1966**, *5*, 1286.
(37) H. Sigel, N. A. Corfù, L.-n. Ji, and R. B. Martin, *Comments Inorg. Chem.*, **1992**, *13*, 35.
(38) R. B. Martin, *Acc. Chem. Res.*, **1985**, *18*, 32.
(39) Y. Kinjo, R. Tribolet, N. A. Corfù, and H. Sigel, *Inorg. Chem.*, **1989**, *28*, 1480.
(40) L.-n. Ji, N. A. Corfù, and H. Sigel, *J. Chem. Soc., Dalton Trans.*, **1991**, 1367.

(41) (a) A. M. Fiskin and M. Beer, *Biochemistry*, **1965**, *4*, 1289. (b) S.-H. Kim and R. B. Martin, see ref 19 and page 42, both in ref 37. (c) H. Lönnberg and J. Arpalahti, *Inorg. Chim. Acta*, **1981**, *55*, 39.

(42) (a) C. A. Lepre and S. J. Lippard in '*Nucleic Acids and Molecular Biology*'; F. Eckstein and D. M. J. Lilley, eds.; Springer Verlag, Berlin & Heidelberg, **1990**; Vol. 4. (b) S. J. Lippard, *Pure Appl. Chem.*, **1987**, *59*, 731. (c) J. Reedijk, *Inorg. Chim. Acta*, **1992**, *198-200*, 873.

(43) N. A. Frøystein, J. T. Davis, B. R. Reid, and E. Sletten, *Acta Chem. Scand.*, **1993**, *47*, 649.

(44) Y.-G. Gao, M. Sriram, and A. H.-J. Wang, *Nucleic Acids Res.*, **1993**, *21*, 4093.

(45) X. Jia, G. Zon, and L. G. Marzilli, *Inorg. Chem.*, **1991**, *30*, 228.

(46) T. Schoenknecht and H. Diebler, *J. Inorg. Biochem.*, **1993**, *50*, 283.

(47) D. Chen, F. Gregáň, A. Holý, and H. Sigel, *Inorg. Chem.*, **1993**, *32*, 5377.

(48) D. Chen, M. Bastian, F. Gregáň, A. Holý, and H. Sigel, J. *Chem. Soc., Dalton Trans.*, **1993**, 1537.

(49) M. Bastian, D. Chen, F. Gregáň, G. Liang, and H. Sigel, *Z. Naturforsch.*, **1993**, *48b*, 1279.

(50) (a) G. Raudaschl-Sieber, H. Schöllhorn, U. Thewalt, and B. Lippert, *J. Am. Chem. Soc.*, **1985**, *107*, 3591. (b) W. S. Sheldrick, and B. Günther, *Inorg. Chim. Acta*, **1988**, *152*, 223. (c) A. Ciccarese, D. A. Clemente, A. Marzotto, M. Rosa, and G. Valle, *J. Inorg. Biochem.*, **1991**, *43*, 470.

(51) S. S. Massoud and H. Sigel, *Eur. J. Biochem.*, **1989**, *179*, 451.

(52) A. Holý, I. Votruba, A. Merta, J. Černý, J. Veselý, J. Vlach, K. Šedivá, I. Rosenberg, M. Otmar, H. Hřebabecký, M. Trávníček, V. Vonka, R. Snoeck, and E. De Clercq, *Antiviral Res.*, **1990**, *13*, 295.

(53) A. Holý, *Adv. Antiviral Drug Design*, **1993**, *1*, 179.

(54) B. Song, A. Holý, and H. Sigel, *Gazz. Chim. Italiana*, submitted for publication.

METAL-NUCLEOBASE CHEMISTRY: COORDINATION, REACTIVITY, AND BASE PAIRING

B. LIPPERT
Fachbereich Chemie
Universität Dortmund
D-44221 Dortmund
Germany

ABSTRACT. The lecture is intended to provide a basis for the understanding of principles of metal-nucleic acid interactions. It will focus on topics such as the relevance of metal-nucleic acid interactions in biology, molecular biology and medicine, coordination patterns of metal species with nucleobases, effects of metal binding on isolated nucleobases as well as oligonucleotides, with particular attention to base pairing.

1. Significance of Metal-Nucleic Acid Interactions

Nucleic acids are biopolymers built up of a ribose (RNA) or 2'-deoxyribose (DNA) phosphate backbone, to which heterocyclic purine or pyrimidine bases are added via the 1'-position of the sugar (Figure 1). The common bases are guanine, adenine, cytosine, and thymine (uracil in RNA). In general, DNA is present in a double-helical arrangement with more or less strict H bonding between complementary bases guanine,cytosine and adenine,thymine whereas RNAs form rather complex structures, with single stranded, double stranded and looped segments possible and coexisting[1].

The chemistry of nucleic acids- their formation, function and degradation - is interrelated with metal ion chemistry at many stages. Examples refer to the biosynthesis of the heterocyclic bases (role of Zn-dependent aspartate carbamylase), the formation of activated nucleoside triphosphates (Mg^{2+} as catalyst), the reduction of the ribonucleotides to the deoxyribonucleotides (various ribonucleotide reductases, dependent on either Fe, Mn, or Co), the oligomerization to RNA and DNA (Zn containing polymerases), the replication and transcription (Mg^{2+}), RNA processing (metal-dependent "ribozymes"), and nucleic acid degradation via metal assisted hydrolysis.

Moreover, at various stages of these processes, regulatory metalloproteins (e.g. "zincfinger proteins") come into play to interact with nucleic acids.

In the following, some of these as well as other aspects will be dealt with in somewhat more detail.

1.1. STRUCTURAL ROLE OF METAL SPECIES

Nucleic acids are polyanions at physiological pH and require for this reason cations for charge neutralization. Apart from protonated oligoamines (e.g. spermidine^{3+}, spermine^{4+}) and protonated amino acid side chains (lysine, arginine) of histone proteins, metal cations play a major role in this respect. Intracellularly, it is in particular K^+ and Mg^{2+} that are

D.P. Kessissoglou (ed.), Bioinorganic Chemistry, 179-199

associated with nucleic acids. These interactions range from mainly electrostatic attraction (K^+) to marked covalency (Mg^{2+}).

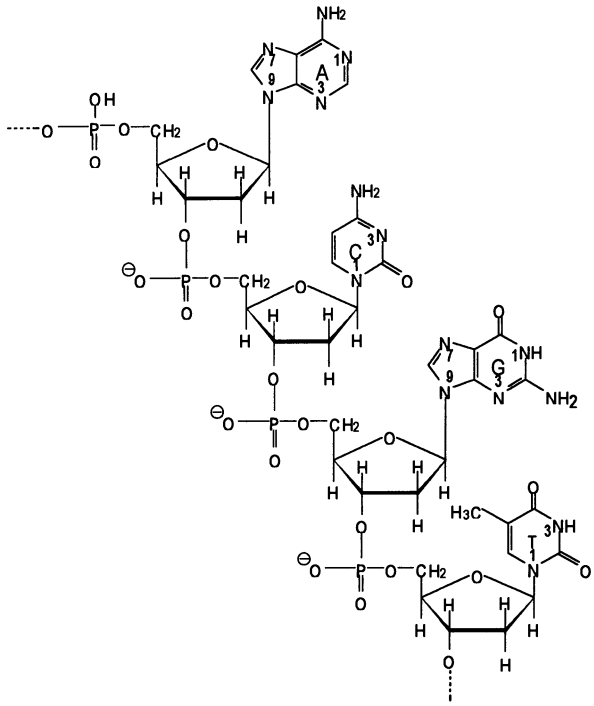

Figure 1. Section of a single strand of DNA with the four common nucleobases guanine (G), adenine (A), cytosine (C), and thymine (T). In RNA, the ribose carries an OH group at the 2'-position instead of H, and the methyl group of T is replaced by a H to give uracil.

DNA condensation and aggregation, respectively, as occurring in the chromosomes or in virus particles, is likewise associated with charge neutralization, e.g. by Mg^{2+}. Exogenous cations, e.g. Cr(III), also show this effect, a phenomenon possibly related with chromium carcinogenicity.

DNA is polymorphic[1] with many unusual structures possible. Apart from the "classical" right-handed A and B double-helical forms, and the left-handed Z-DNA, quite a number of structural variations have been recognized in recent years. Examples are triplex and quadruplex structures, hairpins, cruciforms, and supercoils. In some of these cases, the involvement of metal ions in stabilizing such structures has been clearly established, and it is likely that more examples will be discovered in the future. E.g., potassium ions are integral components of guanine quartets in telomeric DNA[2] and Mg^{2+} ions of four-way DNA junctions ("Holliday junctions"), which are considered central intermediates of genetic recombination[3]. The B $\rightarrow$ Z transition of duplex DNA is accomplished by a variety of cationic metal species, including[4] $[Co(NH_3)_6]^{3+}$ and various Zn complexes[5].

Under physiological conditions, it is probably $[Mg(H_2O)_6]^{2+}$ which contributes to the stabilization of the Z form[6]. Recently it has been shown that a number of bivalent cations and in particular Zn(II) stabilize pyrimidine,purine,purine triples in DNA triplexes[7]. In tRNAs, X-ray crystal structure analysis, in combination with other physico-chemical measurements, has established a number of strong Mg^{2+} binding sites (K up to 10^5 M^{-1}) which appear to be essential for the proper and characteristic folding of these nucleic acids and hence for biological function[8]. Very little is presently known about the role of metal ions with regard to RNA structures. However, considering the heterogeneous folding patterns of RNAs, it is to be predicted that metal ion binding is an essential feature for these nucleic acids as well.

The effect of a metal ion on nucleic acid structure and/or stability strongly varies with the *nature* of the metal and *additional ligands* bound to it (see also 2.3.). Thus DNA melting depends on whether the metal entity favors phosphate binding (usually thermal stabilization) or coordination to the heterocycle of a nucleobase (usually thermal destabilization). Very often a single metal, e.g. Cu(II) or Cd(II), can achieve both effects, depending on concentration[9]. Although probably not relevant to biology, kinetically inert complex cations such as $[Co(NH_3)_6]^{3+}$, $[Co(en)_3]^{3+}$ or $[Pt(NH_3)_4]^{2+}$ very effectively stabilize RNA and DNA duplexes against thermal denaturation by electrostatic attraction and H bonding interactions[10].

1.2. NUCLEIC ACID PROCESSING AND REGULATION

The fundamental processes involving nucleic acids - DNA synthesis during replication, DNA transcription to RNA, RNA translation to protein with the help of tRNAs, nucleic acid degradation - require proteins (polymerases, cofactors, nucleases), which in many cases contain metal ions[11] . The function of metal ions in these proteins is either a catalytic one (e.g. polymerases) or a structural one (e.g. zincfinger proteins) or even both. In addition, metal ions have been demonstrated in a number of cases of exercising a regulatory function in gene expression[12]. It appears that in all cases studied thus far, a metal-responsive gene activation or inactivation involves a primary interaction between the metal ion and a regulatory protein, which in turn interacts with the nucleic acid (DNA). An alternative way - regulation via a direct metal-DNA contact - seems not to have been verified (as yet?). This probably has something to do with the potential threat that a redox or hydrolytically active metal species or a metal that forms kinetically inert adduct with DNA, poses.

With RNA and RNA nucleotides, e.g. ATP, metal complexation to either phosphate oxygens and/or ring atoms, is more common or even desirable: ATP cleavage *requires* metal ions (Mg^{2+})[13] and the ribozymes, a recently discovered class of metalloenzymes on RNA basis, also need metal ions for catalytic activity (in addition to metals required for structural stabilization) [14].

1.3. BIOLOGICAL EFFECTS: MUTAGENICITY, CARCINOGENICITY, AND ANTITUMOR ACTIVITY

As known from epidemiological and animal studies, metal species can be mutagenic, carcinogenic and cytotoxic. Occasionally, cytotoxicity can be exploited for antitumor activity[15]. It is widely accepted that a direct interaction of a metal with DNA or the production of highly reactive oxygen species via metal redox chemistry can lead to DNA errors which, if not repaired, may turn out to be mutagenic or eventually even carcinogenic. The carcinogenicity of Cr(VI) compounds is an example for the first case

and is generally attributed to cross-linking reactions of Cr(III) (formed upon intracellular reduction of Cr(VI)) with DNA or between DNA and proteins[16].

Even though metal binding to DNA always takes place with the risk of introducing errors into DNA, considerable efforts have been put into research aimed at the developments of antitumor metal drugs that directly bind to DNA, following the enormous success of Cisplatin in cancer chemotherapy[17]. Much is known now on the effects of Pt coordination on DNA structure and function[18], even though a comprehensive picture of the mode of action of this drug has not emerged as yet.

Of all the metal compounds that have been demonstrated to be active against various forms of tumors[19], DNA binding as the cause of activity seems to be likely also for a number of these, e.g. Ti(IV) or $[Rh(II)]_2$. Metal binding antibiotics such as the bleomycins represent another class of DNA binders which damage DNA oxidatively via oxygen radical formation catalyzed by redox active metal ions bound in the periphery of the drug[20]

1.4. APPLICATION IN MOLECULAR BIOLOGY AND RELATED AREAS

Metal coordination compounds have become major tools for molecular biologists in recent years. Applications refer in particular to the probing of nucleic acid structures and to the use of metal compounds as artificial chemical nucleases[11,21].

1.4.1. *Covalent Attachment.* The use of OsO_4 modification of exposed thymines in DNA via addition to the 5,6 double bond has a relatively long history[22]. Both directly by electron microscopy and, following sequencing methods after piperidine treatment (leading to strand cleavage) or S1 nuclease treatment (cleavage of opposite strand), allow location of such sites. (For potential thymine probes on the basis of N3 coordination, see 2.3..)

More recently, there have been attempts to covalently bind coordinatively *un*saturated complexes of types $[Rh(phen)_2(H_2O)_2]^{3+}$ or $[Ru(phen)_2(py)(H_2O)]^{2+}$ to DNA as a means to discriminate either DNAs (right handed B form *vs* left handed Z form) and/or the enantiomers (Λ *vs* Δ) of these complexes. Indeed, a pronounced stereoselectivity in DNA binding is observed[23,24] (c.f. also 1.4.5.).

Covalent attachment (to guanine-N7) probably is also involved in cleavage reactions that occur (upon piperidine treatment) at exposed guanines with tetraazamacrocyclic Ni complexes in the presence of the oxidant $KHSO_3$, as demonstrated by Burrows and coworkers[25].

1.4.2. *Base Oxidation.* Unlike OsO_4, in the presence of pyridine, the *anionic* MnO_4^- does not form a stable metal adduct with thymine but rather produces thymine glycol and barbituric acid derivatives[26]. Since piperidine treatment causes strand breaks at the site of oxidation, MnO_4^- can be applied as a chemical probe for thymine. Originally interpreted on the basis of steric effects only (unpaired and solvent accessible thymines), recent experiments indicate that primarily electrostatic effects determine MnO_4^- reactivity[27]. For additional oxidation reactions, see also 3.3.1..

1.4.3. *Cleavage on Basis of Sugar Oxidation.* Oxidative cleavage of nucleic acids is brought about by a variety of agents such as hydroxyl radicals[28], singlet oxygen[29], organic radicals (produced from a metal complex in the presence of O_2, H_2O_2, or light)[30] or directly from a metal (oxo) complex with the metal in a high oxidation state[31]. Depending on the binding properties of the metal species, selective or indiscriminant cleavage takes place. The latter agents are useful for footprinting. $[Fe(EDTA)]^{2-}$, an anion that does not attach to nucleic acids but rather produces $OH^{\cdot}$ radicals in the presence of H_2O_2, is an

example. The radicals react with any sugar proton that is accessible[28]. Likewise, uranyl cations (UO_2^{2+}) produce singlet oxygen upon irridation with little or no discrimination of sequence[29], and methyl radicals generated by photolysis from $[Co(cyclam)(H_2O)(CH_3)]^{2+}$ seem to behave like $OH^{\cdot}$ [30]. On the other hand, $[Cu(phen)_2]^+$ with O_2 or H_2O_2, does not cleave DNA randomly but with some selectivity[32], and photocleavage of $tRNA^{Phe}$ by means of $[Rh(phen)_2(phi)]^{3+}$ occurs at few selected site[33].

To improve sequence or site specificity in nucleic acid cleavage reactions is a major goal, pursued by conjugating metal entities with nucleic acid binding entities (groove binders such as netropsin[34], DNA binding proteins[35], or oligonucleotides in antigene or antisense approaches[36,37]. Specificity reached at present on the basis of DNA triplex formation is enormous[36].

1.4.4. *Hydrolytic Cleavage.* A convenient route to RNA mono and oligonucleotides is still the hydrolysis of natural RNA by metal hydroxides[38]. The mechanism of phosphodiester hydrolysis is reasonably well understood, last but not least as a result of X-ray work on Pb(II) modified[39] $tRNA^{Phe}$. There have been a number of strategies to develop site-specific artificial nucleases[11] for nucleic acids. A major advantage of hydrolytic cleavage over redox cleavage of nucleic acids is the generation of fragment viable to subsequent routine enzymatic reactions. While considerable progress has been made with RNA cleavage, DNA phosphodiester backbone cleavage still represents a great challenge. Lanthanide ions, together with O_2 or H_2O_2, seem to have the potential to hydrolytically cleave DNA as they cleave DNA dinucleotides[40].

1.4.5. *Spectroscopy.* Chiral discrimination of coordinatively saturated octahedral metal complexes containing polypyridyl ligands has been widely studied employing a variety of spectroscopic techniques (UV-vis, fluorescence, NMR, linear and circular dichroism), in particular by the groups of Barton[21a] and others[41]. Binding of the metal compound occurs in these cases through electrostatic, hydrophobic, and possibly H bonding forces, but the exact binding patterns are still controversial[42].

1.4.6. *Miscellaneous.* The method of multiple isomorphous replacements, that is formation of several different heavy-atom isomorphous derivatives is *instrumental* in solving X-ray structures of large biomolecules, including tRNAs or nucleosomes[43]. Heavy metal compounds have also been employed as stains in electron microscopy of DNA and DNA/protein complexes and in studies on ultrastructural effects of drugs (Cisplatin) on whole cells and specifically cell nuclei[44]. Finally, the fractionation of DNAs of different base composition via preferential heavy metal derivatization has been pursued.

2. Metal Binding Patterns

2.1. OVERVIEW

Metal species bind to nucleic acids in a variety of ways (Figure 2). Non-covalent binding modes are those that are (i) purely electrostatic, (ii) involve π-π-interactions between aromatic ligands of the metal and nucleobases (intercalation[45], shape-selective groove-binding[21a,23]) and (iii) hydrogens bonding (e.g. $[Co(NH_3)_6]^{3+}$, c.f. 1.1.)

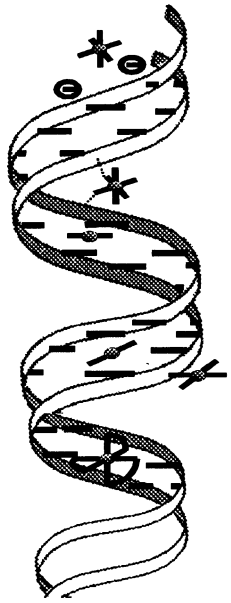

Figure 2. Schematic representation of possible metal binding models to DNA

Covalent metal binding to an isolated nucleobase or a nucleotide incorporated into an oligonucleotide can, in principle, occur (iv) at the phosphate oxygens, (v) at the sugar, (vi) at the heterocyclic purine or pyrimidine ring, or (vii) in a combined fashion.

In general, the various components, e.g. electrostatic attraction, hydrogen bonding, and direct coordination contribute to the overall metal binding energy. Depending upon the metal species, one or more components dominate[46].

Among the various possibilities of direct coordination to a nucleobase (v - vii), binding to sugar oxygens is least likely and restricted to very few established cases with Os and Cd[47]. Phosphate binding is the usual way how hard metal ions bind to nucleobases[47,48]. Binding patterns are particularly versatile for soft metals in that they usually prefer the heterocyclic bases. Although in duplex DNA the number of possible metal binding sites is reduced due to partial involvement in H bonding, in single stranded DNA and RNA many of these possibilities are real. Moreover, metal species may accomplish strand separation (c.f. 4.3.).

It is probably not overexaggerated to state that there is hardly any site in a nucleobase that is not capable of binding a metal. For example, with N1 substituted uracil, X-ray structurally characterized metal binding sites are O2, N3, O4, and C5[49]. A η^2 binding fashion to C5,C6 has been proven spectroscopically[50]. Frequently combinations of phopshate *and* base binding are seen, for example in the solid state of metal nucleotide complexes (intermolecularly), but also occasionally in solution ("macrochelate"[51]). Depending on additional ligands the metal ion is carrying, binding sites can be influenced considerably for steric reasons or favorable ligand-nucleobase interactions[52].

Favorable chelate formation, as seen with oxygens in nucleoside di- and triphosphates, may even lead to a switch in binding preference. The soft Pt in *cis*-$(NH_3)_2Pt(II)$, for example, forms pure phosphato chelates with CTP and CDP[53] rather than binding to the heterocyclic N3 position, as usually seen in CMP, model cytosine bases or cytosine in DNA.

2.2. EXAMPLE: METAL BINDING TO GUANINE

It is beyond the scope of the lecture to review all established metal binding patterns to the common nucleobases or closely related ligands. These have been reviewed[47,49,54]. Only binding patterns to 6-oxopurine ligands will be considered in the following, with particular emphasis on verification by X-ray crystal structure analysis.

2.2.1. *N7 Binding.* The N7 position probably is *the* most common metal binding site in DNA for simple metal aqua ions. However, it is important to recognize that with kinetically inert species, additional ligands carried by the metal may change the picture dramatically (c.f. 2.3.) and that molecular electrostatic potentials of guanine N7 sites in DNA are not uniform but display a marked sequence-dependence[55]. A recurring feature of metal complexes of guanine nucleotides is H bonding between a metal ligand (e.g. H_2O or NH_3) and/or O6 and/or a phosphate oxygen of the same molecule[56]. In the case of the antitumor agent Cisplatin, a similar H bonding interaction is discussed in terms of stabilizing the DNA distortion[57].

2.2.2. *N7,N1 Bridging.* Established in a number of Pt(II) compounds[58], this pattern appears to be quite common in Pt(II) chemistry. Although deprotonation at the N1 site is required, neither high pH nor a large excess of metal is necessary to accomplish this pattern. Even the 1:1 complexes of both *cis*- and *trans*-$[(NH_3)_2Pt(guanine\text{-}N7)(H_2O)]^{2+}$ spontaneously associate to N1,N7 bridged aggregates at neutral pH[59]. The possibility of Cisplatin interacting with DNA in this fashion, following initial N7 binding and strand dissociation, has been proposed[60].

2.2.3. *N7,N1,N3 Binding.* Binding of three metal entities to these sites is a consequence of N1 deprotonation and has been observed with the model nucleobase 9-ethylguanine and $(NH_3)_3Pt(II)$[61].

2.2.4. *N1 Binding.* Unlike N7 binding, which takes place in acidic medium, N1 binding requires neutral or alkaline conditions, depending on the pK_a of the $M(OH_2)$ unit. For preparative purposes, a feasible way of isolating N1 bound guaninato complexes is via a transient blocking of the kinetically preferred N7 position[58b]. Thermodynamically, the N1 linkage isomer is clearly favored over N7 coordination[62].

2.2.5. *N7,O6 Binding.* There has been much discussion on the involvement of this site in the coordination of the antitumor agent Cisplatin ("N7,O6 chelate hypothesis"). Although never proven by X-ray analysis for *cis*-$(NH_3)_2Pt(II)$, in related systems (Pt(IV)/theophylline[63]; $(Cp)_2Ti(IV)$/xanthine[64]) N7,O6 chelates have been verified. N7,O6 bridging with a 6-oxopurine ligand (IMP) has first been observed by Bau and coworkers in a tetranuclear Cu(II) complex[65] and recently also in dirhodium(II) complexes containing anionic and neutral 9-ethylguanine ligands[66].

2.2.6. *N1,O6 Binding.* A heterotrinuclear complex containing the *cis*-$(NH_3)_2Pt(II)$ entity bound to the deprotonated N1 position of a guanine model nucleobase and a Cu(II) at the O6 position has been isolated and X-ray structurally characterized[67]. Again, binding of a metal to O6 is a consequence of deprotonation at N1.

2.2.7. *N1,N7,O6,Phosphate-O Binding.* The tetranuclear complex $[Cu_4(5'\text{-IMPH})_2(phen)_4(H_2O)_4]^{2+}$ already mentioned[65] is a demonstration that even four sites of a 6-oxopurine ligand may be involved in metal binding.

2.2.8. *C8 Binding.* Finally, with 6-oxopurine ligands containing N-blocked positions (e.g. xanthine) formation of organometallic complexes having metal-carbon bonds to C8 have been reported[68].

2.2.9. *Metal Migration.* For kinetically labile metal compounds, a complication arises from the fact that metal migration, e.g. from the kinetically favored N7 position to the thermodynamically favored N1 position, is possible. Such processes have been verified for Pd(II) and Pt(II)[69,70]. It has been proposed[70] that intramolecular migration of (dien)Pt(II) involves temporary O6 binding.

In summary, it appears that with the exception of the amino group at the 2-position, metal binding has now been verified for all the other positions. Considering long-standing statements that N7 is the only likely metal binding site at 6-oxopurine nucleobases, these findings convincingly demonstrate the importance of model studies.

2.3. ROLE OF SPECTATOR LIGANDS

When talking about metal binding selectively to a certain nucleobase, one has to have in mind that generalizations in many cases are inadequate and may lead to wrong conclusions. It is necessary to also consider additional ligands bound to the metal. Zn(II) is a good example in this respect: When $[Zn(H_2O)_x]^{2+}$ reacts with duplex DNA in weakly acidic medium, it binds to guanine-N7 positions (even though not uniformly to all of them, c.f. 2.2.1.)[71,72]. From work with isolated nucleosides it is evident, that binding to this position, is rather weak, logK being ca. 0.8 - 0.9 for the 1:1 complex[73,74]. For N1 binding (deprotonation required, only at alkaline pH relevant), a logK of 2.6 has been calculated[73]. Binding to deprotonated thymine (N3 position) is expected to be considerably stronger (c.f. logK = 4.75 for 1:1 complex with uridine-*N3* [75]), but at acidic pH not yet sufficiently high to compete with guanine-*N7* binding which does not require deprotonation. When introduced into a macrocyclic ring such as 1,4,7,10-tetraazacyclododecane, [12]aneN4, Zn(II) binds even more strongly to uracil and thymine, with logK values now around 5.2 - 5.6[76]. Binding constants for the other nucleobases are considerably lower (<3). The thermodynamic preference of $[Zn(H_2O)([12]aneN_4)]^{2+}$has been attributed to favorable H bonding interactions between the two exocyclic oxygens of the pyrimidine-2,4-dione nucleobases and the amine protons of the $[12]aneN_4$ ring. This "threepoint recognition" model has meanwhile been extended to a "fourpoint recognition" model by introducing an additional pendant aromatic ring (acridine) which, by costacking with the nucleobase, enhances complex stability further (logK for dT, 7.2)[77]. It is now high enough to successfully compete with other binding sites even at physiological pH.

A similar preference for uracil and thymine N3 sites has previously been reported by ourselves for (dien)Au(III)[78], logK being around 8 for the complex with 1-methyluracil. The high selectivity for these positions has been attributed to H bonding between O4 and

O2 oxygens and dien amine protons, as seen in the crystal structure analyses of two complexes of 1-methyluracil, and to the facts that Au(III) carries its own base OH^- to deprotonate the neutral uracil(thymine) bases. Our findings have meanwhile been extended to a variety of oligonucleotides[78b], and include also mixed metal (Pt(II), Au(III)) sequences such as d(TGT).

The effects of additional ligands at the metal on complex stability with a particular nucleobase has been studied by us in more detail in the case of Pd(II). From this work it is evident that H bonding by itself appears not to be sufficient to account for differences in complex stability which, in the case of 1-methyluracil (or uridine), differ by as much as 3 log units[79].

2.4. MULTINUCLEAR, OLIGO- AND POLYMERIC COMPLEXES

It is generally considered likely that under physiological conditions metal binding to nucleobases in nucleic acids take place with the latter being present in a large excess. Consequently, stoichiometries of ML_n ($n \geq 1$) are more likely than M_nL ($n > 1$). Formation of the bis(guanine) adduct of *cis*-$(NH_3)_2Pt(II)$ is an example. On the other hand, from model studies it is quite clear, that formation of M_nL compounds is not uncommon at all. In fact, with single stranded nucleic acids (denaturated DNA; RNA) this situation may be quite relevant. Multiple metal binding to a single nucleobase is facilitated if the complex formation is associated with nucleobase deprotonation[49,80]. This phenomenon has most convincingly been demonstrated for guanine (N7,N1; N7,N1,N3; N1,O6; c.f. 2.2.) and uracil (thymine) (N3,O4; N3,O4,O2[49]), but is also seen in cytosine complexes (N3,N4)[81,82] and includes both homo- and heteronuclear metal systems. With adenine, deprotonation is not a prerequisite in that this nucleobase has two unprotonated binding sites, N1 and N7, at physiological pH. However, if the exocyclic amino group is involved as a binding site together with N1, it is deprotonated as well[83].

Polynuclear arrangements form when metal ions are shared between nucleobases. Polymeric $Ag(9\text{-MeA})(NO_3)\cdot H_2O$ is an example[84]. From the stoichiometry it is frequently not possible to predict the solid state structure. Thus *trans*-$[(NH_3)_2Pt(1\text{-MeU})_2Ag_2]^{2+}$ is polymeric[85] whereas a *trans*-$[(NH_3)_2Pt(1\text{-MeC}^-)_2\ Ag_2]^{2+}$ forms discrete trinuclear cations[86]. This difference probably arises from the more pronounced differences in basicity of the secondary binding sites between 1-MeC^- (N4,O2) as compared to 1-MeU (O4,O2). Oligo or polymeric complexes may also arise when small entities, e.g. dinuclear complexes are used as building blocks. Both metal cation complexation[87], anion bridging[88], H bonding[89], metal-metal bond formation (reinforced by H bonding)[90], as well as bridging by small entities such as H_2O and NO_3^- in combinations with cations[91] has been observed. A special case of oligo- or polymeric metal nucleobase complexes is realized if the metal centers are bridged by anions such as Cl^- or OH^- to form a "backbone", to which nucleobases are added in a regular manner. Two types of complexes of this kind are presently known: Polymeric Hg(II) compounds with a $(HgCl)_\infty$ backbone and guanine ligands[92], and a trinuclear Zn complex having a linear Zn(OH)Zn(OH)Zn backbone with eight 1-methylcytosine bases bound to the three metals[93] (see also 4.3.3.).

Finally, cyclic nucleobase complexes have been prepared in a number of cases[45,63,83b,94]. Even though these compounds are not necessarily biologically relevant, they are a new facette within the field of supramolecular chemistry and definitely of interest with respect to their receptor properties.

2.5. TERNARY COMPLEXES

Ternary complex formation between metal ions, nucleic acids (or nucleobases), and proteins (or peptides and amino acids) in biology can, in principle, take place in three different ways: (i) Direct cross-linking between a nucleobase and an amino acid of the protein via the metal, (ii) metal ion binding to protein, which triggers binding of the protein to the nucleic acid, and (iii) metal binding to the nucleic acid, which causes a protein to associate with the nucleic acids. An example for (ii) are regulatory metalloproteins[12], one for (iii) is the "damage recognition protein" that binds to DNA when it is kinked and partially unwound as a consequence of Cisplatin coordination to two adjacent purines[95]. The biological significance of type (i) is not fully understood, but are there examples of this kind (c.f. literature cited in ref. 96). One refers to suggestions that Cisplatin toxicity[97] and likewise its inactivation[98] is related to cross-link formation of this type. Recently, there have been attempts to exploit such a possibility with regard to cancer chemotherapy applying dinuclear metal complexes[99]. It seems possible to develop highly selective probes for either nucleic acids or proteins on the basis of ternary complex formation, provided binding principles are well understood.

3. Effects of Metal Binding to Nucleobases

3.1. ELECTRONIC EFFECTS

The major electronic effect of metal binding to a nucleobase (heterocyclic part) is on the acidity/basicity of groups. With the exception of metal species capable to act as strong π-back donors (e.g. $(NH_3)_5Ru(II)$), the normal way of metal cations is to acidify NH protons and to reduce the basicity of endocyclic N and exocyclic O sites. Usually aromatic C-H protons are also effected, as demonstrated by a facilitated isotopic exchange. The magnitudes of these effects depend both on the charge of the metal and the distance between the metal and the respective proton. Typically, N7 guanine binding of a dipositive metal increases the N(1)H acidity by 1 - 2 log units[100]. In the case of N3 cytosine binding, an increase by 3 - 4 log units is observed for the exocyclic amino protons by the same metal. Conversely, metal binding to an anionic nucleobase, viz. proton displaced by metal, usually increases the basicity of other sites in the heterocycle as compared to the neutral ligand[101]. As a consequence, primary metal binding to a *deprotonated* nucleobase leads to an increased affinity for additional metal ions (multinuclear complexes, c.f. 2.4.). In the absence of additional ligands, these effects have consequences for H bonding patterns and stability of base pairs as well as base stacking.

3.2. STRUCTURAL ASPECTS

As demonstrated in many examples of X-ray structurally characterized metal nucleobase complexes, the effect of metal complexation on the ring geometry of the base is marginally only. Despite this fact, the metalated base(s) in a nucleic acid fragment respond(s) markedly to metal binding. The changes associated with metal binding have been, for obvious reasons, most intensively studied for the major adduct of Cisplatin with DNA, the intrastrand GG cross-link. The principal methods applied were high resolution NMR spectroscopy[102], molecular mechanics calculations[103] as well as sophisticated biochemical techniques which allow the kinking and unwinding of DNA to be measured[104]. While drastic effects on DNA structure can be expected from bifunctional metal binding (such as

Cisplatin), it is important to realize that even monofunctional binding at the DNA periphery, e.g. the N7 position of a purine in the major groove has remarkable effects on stability *and* geometry of DNA. This conclusion has been reached not only on the basis of solution studies, as in the case of (dien)Pt(II)[105], but also by soaking experiments carried out with crystals of a double stranded DNA dodecamer and Cisplatin[106]. This aspect is also relevant to the question of ligand rotation processes, e.g. of a monofunctionally bound *cis*-$(NH_3)_2PtX$ entity about a Pt-N(nucleobase) bond in DNA prior to completion of the final bis(nucleobase) adduct. Model studies on isolated bis(nucleobase) complexes[107] as well as a molecular mechanics analysis[108] point toward interactions between Pt amine ligands and the substituent at the purine position 6 as a major determining factor for the ease of rotation.

3.3. IRREVERSIBLE BASE MODIFICATIONS

Covalent metal binding to a nucleobase in most cases is reversed by the action of a stronger nucleophile which displaces the metal. Occasionally, however, metal nucleobase bonds can display a remarkable inertness toward substitution, which is of kinetic origin[109]. Irreversible alternations of nucleobases as a consequence of the presence of a metal species have occasionally been observed, as outlined below.

3.3.1. *Nucleobase Oxidation.* Examples of oxidative sugar damage brought about by metal ions have already been referred to in the context of artificial nucleases (c.f. 1.4.). As far as oxidative reactions at the heterocyclic part of the bases are concerned, a number of these have been observed, e.g. oxidative halogenation at the C5 positions of uracil and cytosine bases, including subsequent H_2O addition to the C5,C6 double bond, brought about by $[AuX_4]^-$ (X = Cl, Br)[110], or oxidative dimerization of uracil ligands to bis(uracil-C5,C5), likewise accomplished[111] by $[AuCl_4]^-$. Hydroxymethylation of 1.3-dimethyluracil in the presence of $EuCl_3$ and upon irradiation is another example[112], and $Tl(NO_3)_3$ oxidizes 5-aminouracil to an imidazolone[113]. Finally, C8 oxygenation of 6-oxopurines (inosine; 1-methylinosine) by $(NH_3)_5Ru(III)$ has been observed with the metal entity coordinated to the 7-position[114].

3.3.2. *Nucleotide Hydrolysis.* Hydrolysis of the glycosidic bond is an important reaction in particular in purine nucleobase chemistry. Depurination is usually accomplished by purine protonation. Binding of kinetically inert species, e.g. of Pt(II), thus can have a protective effect in that protonation is delayed. On the other hand, (dien)M(II) (M = Pt, Pd) has clearly been shown to exhibit significant spontaneous hydrolysis[115] and $[PdCl_4]^{2-}$ selectively depurinates adenine residues[116]. Studies with cyclometallated Pd(II) compounds have shown similar results and led to the isolation of a dinuclear Pd complex with coordination to both N3 and N9 of the adenine[117].

3.3.3. *Synthetic Aspects.* Pyrimidine nucleosides and nucleotides with substituents at the C5 position are of substantial interest due to their applications as antiviral agents and probes in nucleic acid chemistry. Synthesis of these compounds in many cases is via organomercury and metastable organopalladium complexes with C5-metal bonds to the pyrimidine bases[118].

4. Metals and Base Pairing

4.1. H BONDING PATTERNS

Hydrogen bond formation between the complementary nucleobases guanine and cytosine as well as adenine and thymine (uracil), according to the Watson-Crick scheme (or occasionally according to Hoogsteen) is of key importance to all processes involving base pairing steps, namely DNA replication and transcription, RNA translation, and reverse transcription. In tRNAs there is no need to conform to these strict pairing patterns and consequently many variations are possible. Likewise the wobble pair between guanine and uracil, which can occur during protein synthesis in the ribosomal mashinery, does not affect conservation of genetic information. It is well established now that a number of additional H bonding motifs involving protonated bases (cytosine[119], adenine[120]), triple-stranded structures (pyrimidine,purine,pyrimidine[121] or purine,purine,pyrimidine[7]), as well as tetraplex structures[2,119,122] are possible in DNA structures.

Mismatches between bases as a consequence of the existence of rare tautomeric structures of nucleobases and/or an *anti* → *syn* switch of a nucleobase[123] are generally considered causes of spontaneous mutations. From model studies it is evident, that inclusion of solvent molecules, e.g. H_2O, in a base pair can also prevent correct pairing[124]. Mismatches, introduced on purpose in duplex oligonucleotides in a number of cases, have been studied by ^1H NMR spectroscopy[125] or X-ray crystal structure analysis[126].

4.2. METAL BINDING TO SITES NOT INVOLVED IN H-BONDING

As pointed out in section 1.1., metal ions in many cases are essential for stabilization of normal or odd base pairing schemes by neutralizing the repulsion between negatively charged polynucleotide strands. However, pushing it to the extreme, metal phosphate binding during a base pairing step (e.g. protein synthesis) can lead to indiscriminate pairing and consequently to errors.

As far as metal coordination to the heterocyclic part of a nucleobase or a base pair is concerned, theoretical calculations strongly suggest that electronic complementary between nucleobases is disturbed[127]. However, no uniform picture has emerged from this work as yet as a consequence of different approaches and in part due to different views on the relative contributions of the various effects to be considered (potential role of water molecules, importance of polarization effects etc.)[128].

Experimental work on the effects of metal coordination to sites not involved in Watson-Crick pairing schemes (e.g. N7 or N3 of purine; C5 and C6 of pyrimidines; O2 of thymine) has provided some insight. For N7 platinated guanine model nucleobases, a pK_a shift (acidification of N1 proton normally involved in H bonding)[129], a loss in base pairing specificity[130] and, as a consequence, the formation of a base pair between a neutral and an anionic guanine[131] have clearly been demonstrated. An effect on the tautomer equilibrium of N7 platinated adenine model bases (increase of imino form) has not explicitly been proven, even though it is likely to take place[132]. In principle, this way the mutagenic potency of the ApG cross-link of Cisplatin, which leads mainly to A → T transversions, could be explained. The principal possibility of stabilizing a rare nucleobase tautomer through metal binding (albeit at sites normally involved in H bonding, e.g. cytosine-N4, thymine-N3, uracil-N3 has been shown[101,133,134]. These model studies point out feasible ways of nucleobase tautomerization which appear to be relevant in particular for kinetically labile systems.

Apart from electronic effects that influence proper H bonding, severe steric constraints can likewise lead to changes in H bonding patterns and, in the extreme, to mispairing. Detailed work on the GG cross-link of Cisplatin with DNA has established that H bonding to cytosines in the opposite strand is, at least for one of the two guanines, altered[102b]. Similarly, the mutagenic potential of the ApG cross-link of Cisplatin mentioned above might simply be a consequence of steric distortion only, with an adenine inserted across the lesion which does not hydrogen bond at all to the platinated A[135]. To complicate things even further, solvent (H_2O) accessibility in a severely distorted DNA sequence may alter the dielectric constant of the medium sufficiently to influence the tautomers equilibrium (for a discussion on adenine see ref. 136) and/or participate in the H bonding scheme, thereby permitting non-complementary pairing[124,137].

4.3. METAL BINDING TO HYDROGEN BONDING SITES

At first glance it might seem unlikely that metal ions are capable of binding to sites normally in the interior of double stranded DNA and involved in H bonding (e.g. N1 of purines; N3 of pyrimidines; exocyclic groups). However, with DNA being a dynamic molecule capable of "breathing", insertion of metal species into a duplex structure is possible. Ways for getting a metal inside the duplex could be (i) insertion from either the major or the minor groove, or (ii) initial binding to a purine N7 position followed by rotation of the metalated base about the glycosidic bond from *anti* to *syn*. Metal binding can (iii), of course, also take place when the nucleic acid is temporarily in a single stranded form. Interstrand cross-linking of a GC base pair by *trans*-$(NH_3)_2PtCl_2$[138,139] most likely occurs via pathway (ii), whereas insertion of Hg(II) into a AT pair[140] could conceivably take place via the major groove. In the first case, no nucleobase deprotonation is required, whereas deprotonation of a base is necessary in the case of Hg(II) binding.

For obvious reasons, metal cross-linking within an essentially planar base pair restricts the metal coordination geometries to a few possibilities (linear; trigonal-planar; in certain cases (c.f. 4.3.3.) tetrahedral). The metal complex formed can be considered a "metal-modified base pair"[141] since the feature of (near-) coplanarity of the bases is maintained. The principle of a suitable metal entity substituting a proton in a H bonded nucleobase associate can be extended from complementary bases to identical or non-complementary ones and can be varied to include also triples and quartets.

As briefly pointed out in ref. 141, the binding patterns seen in "metal-modified base pairs" might be of use in antisense and antigene approaches when applied to oligonucleotides.

4.3.1. *Linear Metal Geometry.* Bis(nucleobase) complexes of Hg(II), Ag(I) or *trans*-$X_2M(II)$ (X = amine or halogen, M = Pt or Pd) typically represent metal-modified base pairs with the two bases in respective *trans*-positions and essentially coplanar. Coplanarity of bases is frequently supported by H bonding between the two bases, or by insertion of a solvent molecule (Figure 3). Moreover, in the case of *trans*-$X_2M(II)$, the X ligands, which are more or less perpendicular to the nucleobases, prevent any large propeller twist of the bases anyway. Formally, bis(nucleobases) complexes of octahedral metal complexes with the two bases in *trans*-position, also can be considered this way. The steric restraints imposed by the four other ligands forces the two heterocyclic bases even more into a coplanar orientation[133a,142].

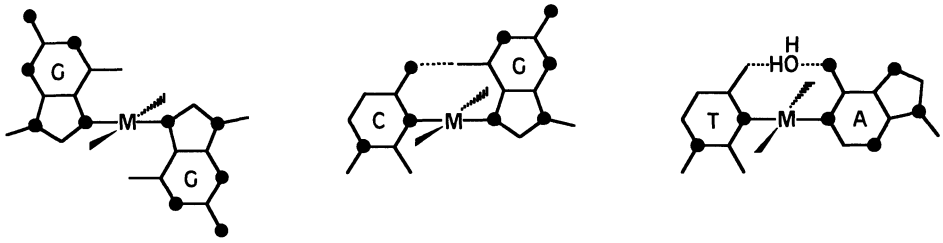

(a) (b) (c)

Figure 3. Coplanarity of two nucleobases in metalated base pairs (a) in the absence of intramolecular H bonding, (b) with intramolecular H bonding, (c) with H_2O mediating H bonding between bases. All three patterns have been established by X-ray analysis (c.f. text). (• denote N atoms)

Depending on the choice and combination of nucleobases, the following situation can be differentiated: (i) Two identical bases. The bis(nucleobase) complexes can then be considered metal analogues of hemiprotonated cytosine, hemiprotonated guanine, protonated guanine(s), or of the (hypothetical) hemi*de*protonated thymine. As in the (hemi) protonated forms, the two nucleobases are oriented *head-tail* in the solid state of the metal analogues[59b,143]. In solution, the *head-head* orientation coexists. In favorable cases it is possible to crystallize also the *head-head* rotational isomer. (ii) Complementary base. Crystallographically characterized examples are the AT complexes of *trans*-a_2Pt(II) in both Hoogsteen and Watson-Crick arrangement and the corresponding GC compound with Hoogsteen-oriented bases[141,144]. H bonding schemes are schematically depicted in Figure 3 b and c. (iii) Non-complementary base. Any combination of linkage isomers of non-complementary bases is possible. Characterized by X-ray crystallography are two examples, again of *trans*-a_2Pt(II), with A-*N7*, C-*N3* [145] and A-*N7*, G-*N7* [143c]. (iv) Triples. Metalated nucleobase triples, containing a metalated base pair and a H bonded third base[146] or three nucleobases connected by two metal entities[147] have been prepared and studied. Work on compounds containing a central purine, metalated at both the N1 and the N7 position has revealed a unique structural feature, namely orthogonality of M-N7 and M-N1 vectors[147]. This fact permits favorable H bonding interactions in tris(purine)M_2 triples of type $(pu_1)M(pu_2)M(pu_1)$, as demonstrated by ^{1}H NMR spectroscopy. It also suggests that it should be possible to synthesize cyclic purine quartets with all four bases coplanar and connected via N1,N7 bridges.

4.3.2. *Trigonal-planar Metal Geometry.* The mixed nucleobase complex [Ag(1-MeC-*N3*)(9-MeA-*N7*) $(H_2O)]NO_3$ is the only example of this kind presently known[148]. It has a (albeit strongly distorted) trigonal-planar coordination geometry about the metal. The most interesting feature of this compound is the H_2O ligand which is clearly involved in the H bonding pattern between the two nucleobases (Figure 4a).

4.3.3. *Tetrahedral Metal Geometry.* As long as binding of two nucleobases to a metal of tetrahedral coordination geometry occurs through endocyclic sites of nucleobases, a coplanar arrangement is excluded for steric reasons. With either both bases bound via exocyclic donor atoms or alternatively via *one* endo- and *one* exocyclic donor atom it is,

however, possible to accommodate two nucleobases in a coplanar fashion about the metal (even with one or more H bonds maintained).

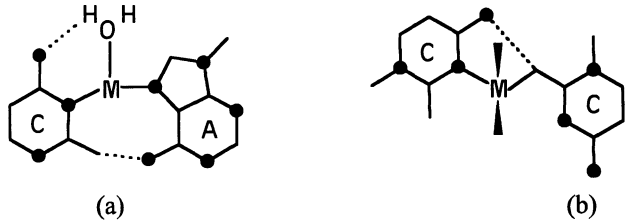

Figure 4. Planar nucleobases in (a) mixed CA complex of Ag^+ with H_2O involved in H bonding, (b) ZnC_2 entity with N3 and O2 bound nucleobase. (• denote N atoms)

This latter possibility is realized in a trinuclear Zn(II) complex containing N3 *and* O2 bond 1-methylcytosines (Figure 4b)[9]. Nucleobase deprotonation is not required. It is also possible to construct Zn-modified pairs containing the complementary bases applying the same principles. It is tempting to speculate, in this context, on the unique role of Zn ions in the reversible unwinding of DNA[9].

5. Abbreviations

A	adenine, unspecified
C	cytosine, unspecified
G	guanine, unspecified
T	thymine, unspecified
U	uracil, unspecified
1-MeC	1-methylcytosine, neutral form
1-MeC$^-$	1-methylcytosine, deprotonated at N4
1-MeU	1-methyluracil, monoanion
9-MeA	9-methyladenine
CMP	cytidine monophosphate
CDP	cytidine diphosphate
CTP	cytidine triphosphate
5'-IMPH	5'-inosine monophosphate
pu	purine
phen	*o*-phenanthroline
phi	phenanthrenequinonediimine
dien	diethylenetriamine

6. Acknowledgement

The author wishes to thank Dr. A. Schreiber, A. Erxleben and M. Gatz for their help in the technical preparation of this contribution.

7. References

(1) (a) Saenger, W. *Principles of Nucleic Acid Structures*; Springer: New York, **1984**.(b) For speciel topics, see also: *Nucl. Acids Mol. Biol.*, Eckstein, F.; Lilley, D. M. L. (eds); Springer: Heidelberg, Volumes 1 - present.
(2) Kang, C.; Zhang, X.; Ratliff, R.; Moyzis, R.; Rich, A. *Nature*,**1992**, *356*, 126.
(3) See, e.g.: Lilley, D. M. J. in ref. 1 b, **1990**,Vol. *4*, p. 55.
(4) Gessner, R. V.; Quigley, G. J.; Wang, A. H.-J.; van der Marel, G. A.; van Boom, J. H.; Rich, A. *Biochemistry*, **1985**, *24*, 237.
(5) See, e.g.: Shinoya, M.; Kimura, E.; Hayashida, H.; Petho, G.; Marzilli, L. G. *Supramol. Chem.*,**1993**, *2*, 173.
(6) van de Sande, J. H.; Jovin, T. M. *EMBO J.*, **1982**, *1*, 115.
(7) Beltran, R.; Martinez-Balbas, A.; Bernues, J.; Bowater, R.; Azorin, F. *J. Mol. Biol.*,**1993**, *230*, 966.
(8) Bina-Stein, M.; Stein, A. *Biochemistry*, **1976**, *15*, 3912.
(9) Eichhorn, G. L.; Shin, Y. A. *J. Am. Chem. Soc.*, **1968**, *90*, 7323.
(10) Karpel, R. L.; Bertelsen, A. H.; Fresco, J. R. *Biochemistry*, **1980**, *19*, 504
(11) Basile, L. A.; Barton, J. K. *Met. Ions Biol. Syst.*, **1989**, *25*, 31.
(12) (a) O'Halloran, T. V. *Science*, 261, 715 (1993). (b) Various articles in: *Met. Ions Biol. Syst.*, **1989**, *25*.
(13) Sigel, H. *Inorg. Chim. Acta*, **1992**, *198 - 200*, 1 and references cited.
(14) (a) Pyle, A. M. *Science*, **1993**, *261*, 709. (b) Piccirilli, J. A.; Vyle, J. S.; Caruthers, M. H.; Cech, T. R. *Nature*, **1993**, *361*, 85.
(15) (a) Flessel, C. P. *Met. Ions Biol. Syst.* **1979**, *10*, 23. (b) Flessel, C. P. *Adv. Med. Biol.*, **1978**, *91*, 117. (c) Loeb, L. A.; Zakour, R. A. in: *Nucleic Acid-Metal Ion Interactions*, Spiro, T. G. (ed); Wiley: New York, **1980**, p. 155. (d) Downey, K. M.; So, A. G. *Met. Ions Biol. Syst.*,**1989**, *25*, 1.
(16) (a) Snow, E. T.; Xu, L.-S. *Biochemistry*, **191**, *30*, 11238; (b) De Floro, S.; Wetterhahn, K. E. *Life Chem. Rep.*, **1989**, *7*, 169 (1989).
(17) See various articles in: *Platinum and Other Metal Coordinations Compounds in Cancer Chemotherapy*, Howell, S. B. (ed); Plenum Press: New York **1991**.
(18) See, e.g.: Sundquist, W. I.; Lippard, S. J. *Coord. Chem. Rev.*, **1990**, *100*, 293.
(19) See various articles in: *Metal Compounds in Cancer Chemotherapy*, Keppler, B. K. (ed); VCH: Weinheim, **1993**.
(20) (a) Stubbe, J.; Kozarich J. W. *Chem. Rev.*,**1987**, *87*, 1007. (b) McGall, G. H.; Raboyw, L. E.; Ashley, G. W.; Wu, S. H.; Kozarich, J. W.; Stubbe, J. *J. Am. Chem. Soc.*, **1992**, *114*, 4958 and references cited.
(21) For reviews on this topic see also: (a) Pyle, A. M.; Barton, J. K. *Prog. Inorg. Chem.*, **1990**, *38*, 413. (b) Sigman, D. S. *Biochemistry*, **1990**, *29*, 9097. (c) Sigman, D. S.; Mazumder, A.; Perrin, D. M. *Chem. Rev.*,**1993**, *93*, 2295.
(22) See, e.g.: (a) Beer, M.; Stern, S.; Carmalt, D.; Mohlenrich, K. H. *Biochemistry*, **1966**, *5*, 2283. (b) Glikin, G. C.; Vojtiskova, M.; Rena-Descalzi, L.; Palacek, E. *Nucl. Acids Res.*, **1984**, *12*, 1725.
(23) (a) Barton, J. K. *Science*, **1986**, *233*, 727. (b) Pyle, A. M.; Rehmann, J. P.; Meshoyrer, R.; Kumar, C. V.; Turro, N. J.; Barton, J. K. *J. Am. Chem. Soc.*, **1989**, *111*, 3051.
(24) Grover, N.; Gupta, N.; Thorp, H. H. *J. Am. Chem. Soc.*, **1992**, *114*, 3390.
(25) (a) Muller, J. G.; Chen, X.; Dadiz, A. C.; Rokita, S. E.; Burrows, C. J. *Pure & Appl. Chem.*, **1993**, *65*, 545. (b) Chen, X.; Woodson, S. A.; Burrows, C. J.; Rokita, S. E. *Biochemistry*, **1993**, *32*, 7610.

(26) Iida, S.; Hayatsu, H. *Biochim. Biophys. Acta*, **1971,** *228*, 1.
(27) Hänsler, U.; Rokita, S. E. *J. Am. Chem. Soc.*,**1993,** *115*, 8554.
(28) Tullius, T. D. *Trends Biochem. Sci.*, **1987,** *12*, 297.
(29) Nielsen, P. E.; Jeppesen, C.; Burchardt, O. *FEBS Lett.*, **1988,** *235*, 122.
(30) Riordan, C. G.; Wei, P. *J. Am. Chem. Soc.*, **1994,** *116*, 2189.
(31) (a) Grover, N.; Thorp, H. H. *J. Am. Chem. Soc.*, **1991,** *113*, 7030. (b) Neyhardt, G. A.; Grover, N.; Smith, S. R.; Kalsbeck, W. A.; Fairley, T. A.; Cory, M.; Thorp, H. H. *J. Am. Chem. Soc.*, **1993,** *115*, 4423.
(32) Sigman, D. S.; Chen, C.-h. B. in: *Metal-DNA Chemistry*, Tullius, T. D. (ed); ACS Symp. Ser. 402; ACS: Washington, D.C., 1989, p. 24.
(33) Chow, C. S.; Behlen, L. S.; Uhlenbeck, O. C.; Barton, J. K. *Biochemistry*, **1992,** *31*, 972.
(34) Bailly, C.; Sun, S. J.; Colson, P.; Houssier, C.; Hélène, C.; Waring, M. J.; Hunichart, J.-P. *Bioconjugate Chem.*, **1992,** *3*, 100.
(35) (a) Chen, C. H. B.; Sigman, D. S. *Science*, **1987,** *237*, 1197. (b) Mack, D. P.; Iverson, B. L.; Dervan, P. B., **1988,** *J. Am. Chem. Soc.*, *110*, 7572. (c) Mack, D. P.; Dervan, P. B. **1990,** *J. Am. Chem. Soc.*, *112*, 4604. (d) Mack, D. P.; Dervan, P. B. *Biochemistry*, **1992,** *31*, 9399.
(36) Strobel, S. A.; Dervan, P. B. *Science*, **1990,** *249*, 73.
(37) (a) Meunier, B. *Chem. Rev.*, **1992,** *92*, 1411. (b) Pitié, M.; Casas, C.; Lacey, C. J.; Pratviel, G.; Bernadou, J.; Meunier, B. *Angew. Chem., Int. Ed. Engl.*, **1993,** *32*, 557.
(38) Dimroth, K.; Witzel, H.; Hülsen, W.; Mirbach, H. *Hoppe-Seyler's Z. Physiol. Chem.*,**1959,** *620*, 94.
(39) Brown, R. S.; Hingerty, B. E.; Dewan, J. C.; Klug, A. *Nature*, **1983,** *303*, 543.
(40) Takasaki, B. K.; Chin, J. *J. Am. Chem. Soc.*, **1994,** *116*, 1121.
(41) (a) Eriksson, M.; Leijon, M.; Hiort, C.; Norden, B.; Gräslund, A. *J. Am. Chem. Soc.*, **1992,** *114*, 4933. (b) Satyanarayana, S.; Dabrowiak, J. C.; Chaires, J. B. *Biochemistry*, **1992,** *31*, 9321.
(42) (a) Hiort, C.; Norden, B.; Rodger, A. *J. Am. Chem. Soc.*, **1990,** *112*, 1971. (b) Satyanarayana, S.; Dabrowiak, J. C.; Chaires J. B. *Biochemiestry*, **1992,** *31*, 9321.
(43) O'Halloran, T. V.; Lippard, S. J.; Richmond, T. J.; Klug, A. *J. Mol. Biol.*, **1987,** *194*, 705.
(44) Aggarwal, S. K.; Whitehouse, M. W.; Ramachandran, C. in: *Cisplatin-Current Status and New Developments,* Prestayko, A. W.; Crooke, S. T.; Carter, S. K., (eds); Academic Press: London, **1980**, p. 79.
(45) (a) Wang, A. H. J.; Nathans, J.; van der Marel, G.; van Boom, J. A.; Rich, A. *Nature*, **1978,** *276*, 471. (b) Marzilli, L. G. *New J. Chem.*, **1990,** *14*, 409.
(46) Black, C. B.; Cowan, J. A. *J. Am. Chem. Soc.*, **1994,** *116*, 1174.
(47) Gellert, R.; Bau, R. *Met. Ions. Biol. Syst.*, **1979,** *8*, 1 and references cited.
(48) Martin, R. B.; Mariam, Y. H. *Met. Ions Biol. Syst.*, **1979,** *8*, 57.
(49) Lippert, B. *Prog. Inorg. Chem.*, **1989,** *37*, 1.
(50) Shepherd, R. E.; Zhang, S.; Lin, F.-T.; Kortes, R. A. *Inorg. Chem.*, **1992,** *31*, 1457 and references cited.
(51) (a) Reily, M. D.; Marzilli, L. G. *J. Am. Chem. Soc.*, **1986,** *108*, 8299. (b) Green, M.; Miller, J. *J. Chem. Soc., Chem. Commun.*, **1987,** 124 and 1864.
(52) See, e.g.: Aoki, K. *J. Chem. Soc., Chem. Commun.*, **1979,** 589.
(53) Slavin, L. L.; Bose, R. N. *J. Chem. Soc., Chem. Commun.*, **1990,** 1256.

(54) (a) Lusty, J. R. *Handbook of Nucleobase Complexes*; CRC Press: Boca Raton, Vol. I, **1990**. (b) Lusty, J. R.; Wearden, R.; Moreno, V. *Handbook of Nucleobase Complexes*; CRC Press: Boca Raton, Vol. II, **1992**. (c) Terron, A. *Comments Inorg. Chem.*,**1993**, *14*, 63. (d) Marzilli, L. G.; Kistenmacher, T. J.; Eichhorn, G. L. in: *Nucleic Acid-Metal Ion Interactions*; Spiro, T. G., (ed); Wiley: New York, **1980**, p. 179. (e) Swaminathan, V.; Sundaralingam, M. *CRC Crit. Rev. Biochem.*, **1979**, *6*, 245.
(55) Pullman, A.; Pullman, B. *Q. Rev. Biophys.*, **1981**, *14*, 289.
(56) See, e.g.: Sherman, S. E.; Gibson, D.; Wang, A. H.-J.; Lippard, S. J. *J. Am. Chem. Soc.*, **1988**, *230*, 412.
(57) See, e.g.: Reedijk, J. *Inorg. Chim. Acta*, **1992**, *198 - 200*, 873.
(58) (a) Frommer, G.; Schöllhorn, H.; Thewalt, U.; Lippert, B. *Inorg. Chem.*,**1990**, *29*, 1417. (b) Frommer, G.; Mutikainen, I.; Pesch, F. J.; Hillgeris, E. C.; Preut, H.; Lippert, B. *Inorg. Chem.*, **1992**, *31*, 2429.
(59) (a) Raudaschl-Sieber, G.; Marzilli, L. G.; Lippert, B.; Shinozuka, K. *Inorg. Chem.*, **1985**, *24*, 989. (b) Pesch, F. J.; Wienken, M.; Preut, H.; Tenten, A.; Lippert, B. *Inorg. Chim. Acta*, **1992**, *197*, 243.
(60) Kelman, A. D.; Peresie, H. J.; Stone, P. J. *J. Clin. Hemat. Oncol.*, **1977**, *7*, 440.
(61) Raudaschl-Sieber, G.; Schöllhorn, H.; Thewalt, U.; Lippert, B. *J. Am. Chem. Soc.*,**1985**, *107*, 3591.
(62) Martin, R. B. *Acc. Chem. Res.*, **1985**, *18*, 32.
(63) Lorberth, J.; El-Essawi, M.; Massa, W.; Labib, L. *Angew. Chem., Int. Ed. Engl.* **1988**, *27*, 1160.
(64) Beauchamp, A. L.; Bélanger-Gariépy, F.; Mardhy, A.; Cozak, D. *Inorg. Chim. Acta*, **1986**, *124*, L 23.
(65) Gellert, R. W.; Fischer, B. E.; Bau, R. *J. Am. Chem. Soc.*, **1980**, *102*, 7815.
(66) Dunbar, K. R.; Matonic, J. H.; Saharan, V. P.; Crawford, C. A.; Christou, G. *J. Am. Chem. Soc.*, **1994**, *116*, 2201.
(67) Lippert, B., to be published.
(68) See, e.g.: (a) Krentzien, H. J.; Clarke, M. J.; Taube, H. *Bioinorg. Chem.*, **1975**, *4*, 143. (b) Beck, W.; Kottmair, N. *Chem. Ber.*, **1976**, *109*, 970.
(69) Scheller, K. H.; Scheller-Krattiger, V.; Martin, R. B. *J. Am. Chem. Soc.*, **1981**, *103*, 6833.
(70) van der Veer, J. L.; van den Elst, H.; Reedijk, J. *Inorg. Chem.*, **1987**, *26*, 1536 .
(71) Jia, X.; Zon, G.; Marzilli, L. G. *Inorg. Chem.*, **1991**, *30*, 228.
(72) (a) Froystein, N. A.; Davis, J. T.; Reid, B. R.; Sletten, E. *Acta Chem. Scand.*, **1993**, *47*,649. (b)Froystein, N. A.;Sletten, E. *Acta Chem.Scand.*, **1991**,*45*, 219.
(73) Kim, S.-H.; Martin, R. B.; Inorg. Chim. Acta, **1984**, *91*, 19.
(74) Lönnberg, H.; Vihanto, P. *Inorg. Chim. Acta*, **1981**, *56*, 157.
(75) Reddy, P. R.; Rao, V. B. M. *J. Chem. Soc., Dalton Trans.*, **1986**, 2331.
(76) Shinoya, M.; Kimura, E.; Shiro, M. *J. Am. Chem. Soc.*, **1993**, *115*, 6730.
(77) Shinoya, M.; Ikeda, T.; Kimura, E.;Shiro, M. *J. Am. Chem. Soc.*, **1994**, *116*, 3848.
(78) (a) Fischer, B.; Lippert, B. *J. Inorg. Biochem.*, **1991**,*43*, 432. (b) Lippert, B., to be submitted.
(79) Lippert, B.; Sóvagó., I., to be published.
(80) (a) Guay, F.; Beauchamp, A. L. *J. Am. Chem. Soc.*, **1979**, *101*, 6260. (b) Aoki, K.; Saenger, W. *Acta Cryst.*, **1984**, *C 40*, 775.

(81) (a) Krumm. M.; Zangrando, E.; Randaccio, L.; Menzer, S.; Danzmann, A.; Holthenrich, D.; Lippert, B. *Inorg. Chem.*, **1993,** *32*, 2183. (b) Krumm, M.; Zangrando, E.; Randaccio, L.; Menzer, S.; Lippert, B. *Inorg. Chem.*, **1993,** *32*, 700.
(82) Longato, B., pers. commun.
(83) (a) Trovo, G.; Bandoli, G.; Nicolini, M.; Longato, B. *Inorg. Chim. Acta*, **1993,** *211*, 95. (b) Smith, D. P.; Baralt, E.; Morales, B.; Olmstead, M. M.; Maestre, M. F.; Fish, R. H. *J. Am. Chem. Soc.*, **1992,** *114*, 10647. (c) Kuo, L. Y.; Kanatzidis, M. G.; Sabat, M.; Tipton, A. L.; Marks, T. J*J. Am. Chem. Soc.*, . **1991,** *113*, 9027.
(84) Gagnon, C.; Beauchamp, A. L. *Acta Cryst.*, **1977,** *B 33*, 1448.
(85) Dieter, I.; Lippert, B.; Schöllhorn, H.; Thewalt, U. *Z. Naturforsch.*, **1990,** *45b*, 731.
(86) Lippert, B., to be published.
(87) Lippert, B.; Neugebauer, D. *Inorg. Chem.*, **1982,** *21*, 451.
(88) Renn, O.; Albinati, A.; Lippert, B. *Angew. Chem., Int. Ed. Engl.*, **1990,** *29*, 84.
(89) Neugebauer, D.; Lippert, B. *Inorg. Chim. Acta*, **1982,** *67*, 151.
(90) O'Halloran, T. V.; Mascharak, P. K.; Williams, I. D.; Roberts, M. M.; Lippard, S. J. *Inorg. Chem.*, **1987,** *26*, 1261.
(91) (a) Lippert, B.; Schöllhorn, H.; Thewalt, U. *Inorg. Chem.*, **1987,** *26*, 1736. (b) Schöllhorn, H.; Thewalt, U.; Lippert, B. *Inorg. Chim. Acta*, **1987,** *135*, 155.
(92) (a) Menzer, S.; Hillgeris, E. C.; Lippert, B. *Inorg. Chim. Acta*, **1993,** *211*, 221. (b) Quiros-Olozabal, M.; Salas-Peregrin, J. M.; Sanchez-Sanchez, M. P.; Faure, R. *An. Quim.*, **1990,** *86*, 518. (c) Authier-Martin, M.; Hubert, J.; Rivest, R.; Beauchamp, A. L. *Acta Cryst.*, **1978,** *B 34*, 273.
(93) Fusch, E. C.; Lippert, B., submitted to *J. Am. Chem. Soc.*.
(94) See, e.g.: (a) Rauter, H.; Hillgeris, E. C.; Erxleben, A.; Lippert, B. *J. Am. Chem. Soc.*, **1994,** *116*, 616. (b) Uchida, K.; Toyama, A.; Tamura, Y.; Sugimura, M.; Mitsumori, F.; Furukawa, Y.; Takeuchi, H.; Harada, I. *Inorg. Chem.*, **1989,** *28*, 2067.
(95) (a) Brown, S. J.; Kellet, P. J.; Lippard, S. J. *Science*, **1993,** *261*, 603. (b) Pil, P. M.; Lippard, S. J. *Science*, **1992,** *256*, 234.
(96) Wienken, M.; Zangrando, E.; Randaccio, L.; Menzer, S.; Lippert, B. *J. Chem. Soc., Dalton Trans.*, **1993,** 3349.
(97) Borch, R. F.; Pleasants, M. E. *Proc. Natl. Acad. Sci. U.S.A.*, **1979,** *76*, 6611.
(98) Eastman, A. *Chem. Biol. Interact.*, **1987,** *61*, 241.
(99) Van Houten, B.; Illenye, S.; Qu, Y.; Farrell, N. *Biochemistry*, *32*, 11794 (1993).
(100) See, e.g.: (a) Sigel, H. *J. Am. Chem. Soc.*, **1975,** *97*, 3209. (b) Clarke, M. J.; Taube, H. *J. Am. Chem. Soc.*, **1974,** *96*, 5413.
(101) Schöllhorn, H.; Thewalt, U.; Lippert, B. *J. Am. Chem. Soc.*, **1989,** *111*, 7213 (.
(102) See, e.g.: (a) Den Hartog, J. H. J.; Altona, C.; Chottard, J.-C.; Girault, J.-P.; Lallemand, J.-Y.; de Leeuw, F. A. M.; Marcelis, A. T. M.; Reedijk, J. *Nucl. Acids Res.*, **1982,** *10*, 4715. (b) Herman, F.; Kozelka, J.; Stoven, V.; Guittet, E.; Girault, J.-P.; Huynh-Dinh, T.; Igolen, J.; Lallemand, J.-Y.; Chottard, J.-C. *Eur. J. Biochem.*, **1990,** *194*, 119. (c) Berners-Price, S. J.; Frey, U.; Ranford, J. D.; Sadler, P. J. *J. Am. Chem. Soc.*, **1993,** *115*, 8649.
(103) (a) Kozelka, J.; Petsko, G. A.; Lippard, S. J. *J. Am. Chem. Soc.*, **1985,** *107*, 4079. (b) Kozelka, J.; Petsko, G. A.; Quigley, G. J.; Lippard, S. J. *Inorg. Chem.*, **1986,** *25*, 1075. (c) Kozelka, J.; Archer, S.; Petsko, G. A.; Lippard, S. J.; Quigley, G. J. *Biopolymers*, 1987, *26*, 1245.

(104) Bellon, S. F.; Coleman, J. H.; Lippard, S. J. *Biochemistry*, **1991**, *30*, 8026.
(105) Brabec, V.; Reedijk, J.; Leng, M. *Biochemistry*, **1992**, *31*, 12397.
(106) Wing, R. M.; Pjura, P.; Drew, H. R.; Dickerson, R. E. *EMBO J.*, **1984**, *3*, 1201.
(107) See, e.g.: (a) Reily, M. D.; Marzilli, L. G. *J. Am. Chem. Soc.*, **1986**, *108*, 6785. (b) Marcelis, A. T. M.; van der Veer, J. L.; Zwetsloot, J. C. M.; Reedijk, J. *Inorg. Chim. Acta*, **1983**, *78*, 195.
(108) Hambley, T. W. *Inorg. Chem.*, **1988**, *27*, 1073.
(109) (a) Frommer, G.; Lippert, B. *Inorg. Chem.*, **1990**, *29*, 2359 and references cited. (b) Schmülling, M.; Lippert, B.; van Eldik, R. *Inorg. Chem.*, in press.
(110) (a) Bressan, M.; Ettore, R.; Rigo, P. *J. Magn. Res.*, **1977**, *26*, 42. (b) Ettore, R. *J. Chem. Soc., Dalton Trans.*, **1983**, 2329. (c) Ettore, R.; Martelli, M. *Inorg. Chim. Acta*, **1985**, *108*, 73.
(111) Fischer, B.; Schimanski, A.; Lippert, B., to be submitted.
(112) Ishida, A.; Toki, S.; Takamuku, S. *J. Chem. Soc., Chem. Commun.*, **1985**, 1481.
(113) Matsuura, I.; Ueda, T.; Nagai, S.-I.; Nagatsu, A.; Sakakibara, J.; Kurono, Y.; Hatona, K. *J. Chem. Soc., Chem. Commun.*, **1992**, 1474.
(114) Gariepy, K. C.; Curtin, M. A.; Clarke, M. J. *J. Am. Chem. Soc.*, **1989**, *111*, 4949.
(115) Iverson, B. L.; Dervan, P. B. *Nucl. Acids Res.*, **1987**, *15*, 7823.
(116) (a) Arpalahti, J.; Jokilammi, A.; Hakala, H.; Lönnberg, H. *J. Phys. Org. Chem.*, **1991**, *4*, 301. (b) Arpalahti, J.; Käppi, R.; Hovinen, J.; Lönnberg, H.; Chattopadhyaya, J. *Tetrahedron Lett.*, **1989**, *45*, 3945.
(117) Suggs, J. W.; Dube, M. J.; Nichols, M. *J. Chem. Soc., Chem. Commun.*, **1993**, 307.
(118) Bergstrom, D.; Beal, P.; Husain, A.; Lind, R.; Jenson, J. *J. Am. Chem. Soc.*, **1989**, *111*, 374.
(119) Gehring, K.; Leroy, J.-L., Guéron, M. *Nature*, **1993**, *363*, 561and references cited.
(120) Fresco, J. R. *J. Mol. Biol.*, *1*, 106 (1959).
(121) (a) Arnott, S.; Selsing; E. *J. Mol. Biol.*,**1974**, *88*, 509. (b) Cheng, Y.-K.; Pettit, B. M. *J. Am. Chem. Soc.*, **1992**, *114*, 4456 and references cited.
(122) Chernyi, A. A.; Lysov, Yu. P.; Il'ychova, I. A.; Zibrov, A. S.; Shchyolkina, A. K.; Borisova, O. F.; Mamaeva, O. K.; Florentiev, V. L. *J. Biomol. Structure Dynam.*, **1990**, *8*, 513.
(123) (a) Topal, M. D.; Fresco, J. R. *Nature*, **1976**, *263*, 285. (b). Topal, M. D.; Fresco, J. R. *Nature*, **1976**, *263*, 289.
(124) Hunter, W. N.; Brown, T.; Anand, N. N.; Kennard, O. *Nature*, **1986**, *320*, 552.
(125) Patel, D. J.; Shapiro, L.; Hare, D. in ref, 1b, **1987**, Vol 1, p. 70.
(126) See, e.g.: Kennard, O. in ref. 1b, **1987**, Vol. 1, p. 25.
(127) See, e.g.: (a) Perahia, D.; Pullman, A.; Pullman, B. *Theoret. Chim. Acta*, **1977**, *43*, 207. (b) Anwander, E. H. S.; Probst, M. M.; Rode, B. M. *Inorg. Chim. Acta*, **1987**, *137*, 203 and references cited. (c) Barnett, G. *Mol. Pharmacol.*, **1986**, *29*, 378. (d) Kothekar, V.; Dutta, S. *Int. J. Quantum Chem.*, **1977**, *12*, 505. (e) Carsey, T. P.; Boudreaux, E. A. *Chem.-Biol. Interact.*, **1980**, *30*, 189.
(128) See, e.g.: Basch, H.; Krauss, M.; Stevens, W. J. *J. Am. Chem. Soc.*, **1985**, *107*, 7267.
(129) Faggiani, R.; Lippert, B.; Lock, C. J. L.; Speranzini, R. A. *Inorg. Chem.*, **1982**, *21*, 3216.

(130) Lippert, B. *J. Am. Chem. Soc.*, **1981,** *103*, 5691.
(131) Faggiani, R.; Lock, C. J. L.; Lippert, B. *J. Am. Chem. Soc.*, **1980,** *102*, 5418.
(132) Lippert, B.; Schöllhorn, H.; Thewalt, U. *Inorg. Chim. Acta*, **1992,** *198 - 200*, 723.
(133) (a) Lippert, B.; Schöllhorn, H.; Thewalt, U. *J. Am. Chem. Soc.*, **1986,** *108*, 6616. (b) Renn, O.; Lippert, B.; Albinati, A. *Inorg. Chim. Acta*, **1991,** *190*, 285.
(134) Clarke, M. J. *Inorg. Chem.*, **1980,** *19*, 1104.
(135) Schaaper, R. M.; Kunkel, T. A.; Loeb, L. A. *Proc. Natl. Acad. Sci. U.S.A.*, **1983,** *80*, 487.
(136) Dreyfus, M.; Dodin, G.; Bensaude, O.; Dubois, J. E. *J. Am. Chem. Soc.*, **1977,** *99*, 7027.
(137) See, e.g.: Poltev, V. I.; Teplukhin, A. V.; Kwiatkowski, J. S. *J. Biomol. Structure Dynam.*, **1992,** *9*, 747.
(138) Brabec, V.; Leng. M. *Proc. Natl. Acad. Sci. U.S.A.*, 1993, *90*, 5345 and references cited.
(139) Brabec, V.; Sip, M.; Leng, M. *Biochemistry*, **1993,** *32*, 11676.
(140) Froystein, N. A.; Sletten, E. *J. Am. Chem. Soc.*,**1994,** *116*, 3240.
(141) Krizanovic, O.; Sabat, M.; Beyerle-Pfnür, R.; Lippert, B. *J. Am. Chem. Soc.*, **1993,** *115*, 5538.
(142) Quiros, M.; Salas, J. M.; Sanchez, M. P.; Alabart, J. R.; Faure, R. *Inorg. Chem.*,**1991,** *30*, 2916.
(143) (a) Lippert, B.; Lock, C. J. L.; Speranzini, R. A. *Inorg. Chem.*, **1981,** *20*, 808. (b) Menzer, S.; Hillgeris, E. C.; Lippert, B. *Inorg. Chim. Acta*, **1993**, *210*, 167. (c) Schreiber, A.; Erxleben A.; Lippert, B., to be published.
(144) Hitchcock, A. P.; Lock, C. J. L.; Pratt, W. M. C.; Lippert, B. in: *Platinum, Gold, and Other Metal Chemotherapeutic Agents*, Lippard, S.J. (ed); ACS Symp. Ser. 209, ACS: Washington, D.C. **1983**, p. 209.
(145) Beyerle-Pfnür, R.; Brown, B.; Faggiani, R.; Lippert, B.; Lock, C. J. L. *Inorg. Chem.*, **1985,** *24*, 4001.
(146) Dieter-Wurm, I.; Sabat, M.; Lippert, B. *J. Am. Chem. Soc.*,**1992,** *114*, 357.
(147) Schreiber, A.; Hillgeris, E. C.; Lippert, B. *Z. Naturforsch.*, **1993,** *48b*, 1603.
(148) Menzer, S.; Sabat, M.; Lippert, B. *J. Am. Chem. Soc.*,**1992,** *114*, 4644.

DNA CLEAVAGE BY CATIONIC METALLOPORPHYRINS

B. MEUNIER, G. PRATVIEL AND J. BERNADOU
Laboratoire de Chimie de Coordination du CNRS,
205 route de Narbonne,
31077 Toulouse cedex, France

1. Introduction

Within the two last decades, much data has been published on chemical and biochemical aspects of structural damages generated by oxidative stress on cellular constituents (DNA, proteins, lipids and carbohydrates).[1] Oxidative damage to DNA can be initiated by several methods: ionizing radiation,[2] photooxidation (UV or visible light with or without photosentitizers),[3] hydroperoxides activated by traces of adventitious transition metals salts,[4] hydroxyl radicals[5] or various other oxidizing agents (for a recent review article on the oxidative degradation of DNA, see ref. 6). In this latter category, we find cytotoxic drugs like bleomycin or agents having an enediyne motif, and chemical nucleases mainly based on redox-active transition metal complexes (for recent review articles, see ref. 7,8). DNA damages can be produced by oxidation of nucleobases or sugar units. Damages on deoxyribose lead to the loss of one base information and/or a break on a DNA strand which might correspond to a lethal lesion, especially when an oxidation process produces a double-strand break (DSB), via a true DSB or via two near single-strand breaks (SSBs) on opposite strands.

The present review is focused on DNA cleavage by cationic metalloporphyrins, but it should be noted that many other transition metal complexes can also cleave DNA: iron-bleomycin is able to cleave DNA *via* H-abstraction at the 4' position of deoxyriboses[8] (this reaction might be mediated by an iron-oxo species[9]), Fe-EDTA alone[10a,b] or linked to a variety of vectors[10c,d,e], copper complexes[11] and several cobalt and ruthenium complexes can be used as DNA probes.[12] Porphyrin derivatives have been used in the diagnosis and treatment of malignant diseases. A hemin derivative such as HPD (hematoporphyrin derivative) tends to accumulate specifically in neoplastic tissues and produces irreversible damages *via* singlet oxygen when the dye is photoactivated by visible light.[13] Efforts have been made to prepare new porphyrin derivatives in cancer phototherapy.[14]

Cationic porphyrin molecules are able to bind to DNA[15] and RNA.[16] Most of the studies have been focused on free *meso*-tetrakis(4-*N*-methylpyridiniumyl)porphyrin (TMPyP) or on its metallated derivatives (iron, manganese, nickel, palladium, zinc; see Figure 1 for the structure of M-TMPyP). Several exhaustive review articles in this field are available.[15] The free porphyrin TMPyP intercalates between DNA base pairs, binds to chromatin *in vitro* and tends to localize in the cell nucleus.[17] For the metallated TMPyP derivatives three modes of binding have been recognized:

D.P. Kessissoglou (ed.), Bioinorganic Chemistry, 201-208

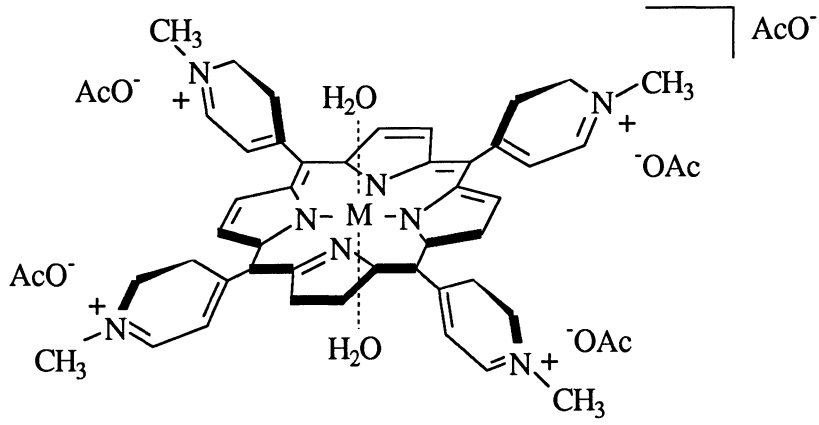

Figure 1. Structure of M-TMPyP pentaacetate (M stands for Mn or Fe).

(i) intercalation when metalloporphyrins do not have axial ligands,[15] (ii) outside DNA binding for complexes with axial ligand, and (iii) minor groove binding in the case of MnTMPyP (see below for arguments provided by studies on the molecular aspects of DNA cleavage by activated Mn-TMPyP). Spectroscopic studies of *N*-methylpyridiniumyl metalloporphyrin binding modes to DNA are not facilitated by the porphyrin-porphyrin stacking interactions.[18] Electrochemical or chemical activation of metalloporphyrins is an alternative approach to determine DNA binding constants.[19]

Cationic metalloporphyrins are able to generate DNA breaks by oxidation of sugars on both strands of *B*-DNA (for DNA structures, see ref. 20). More precisely, all these sugar degradation processes are initiated by H-abstractions, since the aliphatic nature of deoxyribose does not favor oxidation by electron abstraction. Hydrogen bonds of deoxyriboses have a well-defined stereochemistry and their orientations with respect to drugs or chemical nuclease are also controlled by DNA itself, via DNA-drug interactions. So, the homolysis of a C-H bond depends not only on the carbon substituents (removing a H-atom from a tertiary carbon is easier than from a secondary carbon, from a thermodynamic point of view), but also on the relative orientation of the drug/sugar C-H bonds. For drugs interacting within the minor groove of *B*-DNA, two tertiary C-H bonds are easily accessible: C4'-H and C1'-H. The third tertiary C-H bond (C3'-H) is only accessible from the major groove. Carbons C2' and C5' have two secondary C-H bonds. In both cases, only one C-H bond is accessible from the minor groove (the pro-R H-atom at C2' and the pro-S H-atom at C5'; for assignments of prochiral hydrogen atoms at C2' and C5' see ref. 21).

2. Cationic metalloporphyrins: mechanisms of potentiation and DNA cleavage

Synthetic metalloporphyrins are able to mimic heme-enzymes-mediated oxygenation and oxidation reactions.[22] Beside their use in P-450 or peroxidase modeling, iron or manganese porphyrins with peripheral positive charges, e.g. Fe- or Mn-*meso*-tetra(4-*N*-methylpyridiniumyl)porphyrins (Fe- or Mn-TMPyP, for crystallographic data see ref. 23), exhibit a strong interaction with DNA that brings into the vicinity of the target a powerful oxidizing species. The active oxidative species in the case of DNA cleavage is probably the same as that involved in catalytic oxygenation and oxidation reactions described for metallopor-

phyrins in general, namely a high-valent metal-oxo porphyrin complex able to hydroxylate a C-H bond or to epoxidize an olefin.[22] This active species is generated in the presence of oxygen atom donor compounds like iodosylbenzene,[24] hydrogen peroxide,[25a] potassium monopersulfate[25a-b,d] or magnesium monoperphthalate.[25c] Another way to generate an oxo-metalloporphyrin species is to use molecular oxygen associated with an electron source (a reducing agent or an electrode), as does cytochrome P-450.[19a, 24, 26-27] Among all these different methods, the most efficient for performing oxidative cleavage of DNA is the activation of cationic Mn-porphyrins by $KHSO_5$.[25, 28] Data on DNA cleavage by Mn^{III}-TMPyP/$KHSO_5$ suggest that diffusible radical species are not involved in the reaction (breaks are well-defined and H_2O_2 is at least three orders of magnitude less efficient in generating the active species[25a]). The high-valent TMPyP-Mn^{V}=O is a single-strand DNA cleaver. Catalytic activity can be observed only at low metalloporphyrin concentration to avoid self-oxidation, leading to the chromophore bleaching, (up to 5 SSBs per Mn-TMPyP molecule were observed[25a]). The high-valent TMPyP-Mn^{V}=O species responsible for DNA cleavage is too reactive to be directly characterized. An activation process for the generation and the reactivity of this manganese-oxo entities is proposed in Figure 2.

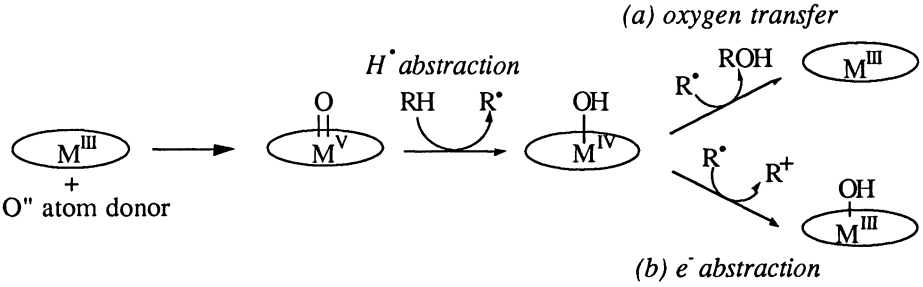

Figure 2. Two possible oxidative pathways for activated Mn-TMPyP: (a) P-450 route; (b) diverted P-450 route.

Mn-TMPyP belongs to a class of cationic metalloporphyrins that do not intercalate between DNA base-pairs but instead bind in the minor groove of AT-rich regions of DNA.[19a, 28, 29] Thus the ability of Mn-TMPyP to select AT-rich regions of DNA is apparently electrostatic/steric in origin. It has been proposed that this cationic metalloporphyrin is attracted by the high negative potential at the surface of the minor groove [31] of A·T-rich sequences. A close contact with the minor groove is necessary to enhance the cleaving efficiency of the metalloporphyrin, as deduced from studies on variations in total charge and in charge distribution at the macrocycle periphery.[18a, 29a-c, 31] At high ionic strength, the reagent is unable to bind and/or cleave DNA.[25a, 32] The preferred cleaving site of Mn-TMPyP on *B*-DNA consists of three consecutive A·T base-pairs creating a suitable "box" for highly selective DNA cleavage.[24, 25d-e, 29a,d] At this site Mn-TMPyP is strictly mediating hydroxylation at C5' on the nucleosides located on both 3'-sides of the "AT box"[33]: one single-strand break on each strand leads to double-strand cleavage with a 4 base-pair shift to the 3'-end of the opposite DNA strand. So far, there is no definite proof that such a cleavage pattern is the result of two SSBs by the same metalloporphyrin activated twice inside the minor groove, or whether it is effected by two different activated metalloporphyrins. On large DNA substrates, SSBs prevail [25a] and on oligonucleotides substrates (with one or two "AT boxes") DSBs are easily obtained.[33]

Mn-TMPyP is also able to degrade G·C-rich sequences with a reactivity reduced by two orders of magnitude relative to degradation of $(A{\cdot}T)_3$ sites. The mechanism of DNA lesions

at these regions of DNA is not fully understood and may involve sugar oxidation (C5' or C1') and/or base oxidations. Affinity constants of up to 10^7 M^{-1} have been published for Mn-TMPyP at the $(A{\cdot}T)_3$ binding site.[25e] Other values, 10^5 M^{-1} for A·T sequences and 10^3 M^{-1} for G·C sequences, have also been reported.[19b]

From different studies on DNA and oligonucleotides cleavage reactions with Mn-TMPyP/$KHSO_5$, different stable reaction products were identified: 5'- and 3'-phosphorylated termini, free bases and 5-methylene-2-furanone.[34] This furanone derivative results from the initial hydroxylation of the C1' carbon as indicated in the top of Figure 3. With Mn-TMPyP/$KHSO_5$ as cleaving reagent, C1' represents the main oxidation target for single-stranded or GC-rich double-stranded DNA, but only a minor target for AT-rich sequences containing DNA for which C5' then becomes the main target.[34b] In this case, HPLC analysis of the products released in solution after a heating step has allowed the observation and characterization of free bases, oxidized nucleosides[35] and furfural (Figure 3).[34] Using HPLC separation techniques or PAGE analyses, cleavage fragments from small oligonucleotides were analyzed [24, 25e, 32, 33, 36] and their transformation following chemical and/or enzymatic treatment allowed their identification (bottom of Figure 3): 3'-phosphate-ending fragments were subjected to alkaline phosphatase in order to obtain the corresponding oligonucleotides with 3'-OH ending; 5'-CHO ending fragments were heated (two consecutive β-eliminations give furfural as sugar residue, free base and 5'-phosphate ending fragment), or oxidized by I_2 in an alkaline medium (5'-COOH end) or reduced by $NaBH_4$ (5'-CH_2OH end).[36, 37]

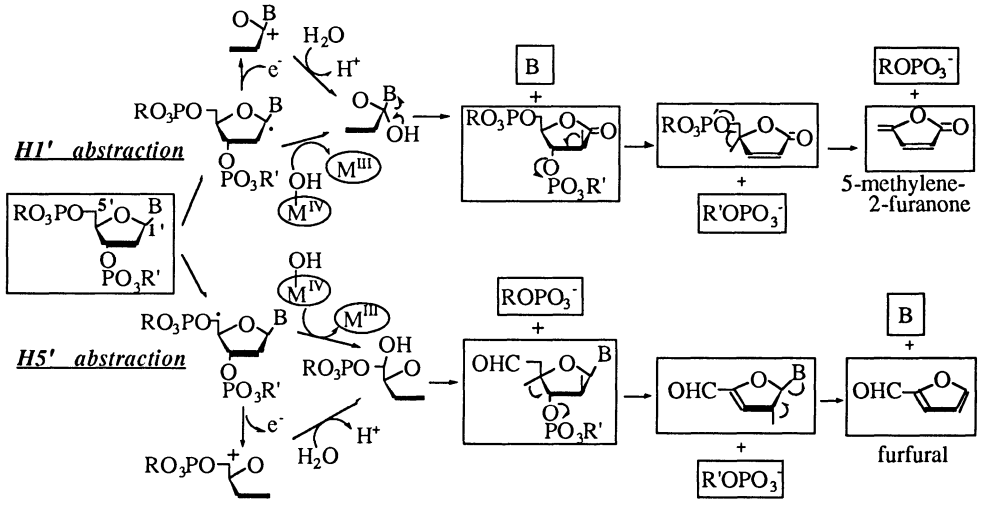

Figure 3. Proposed reaction mechanism when initial site of attack by Mn-TMPyP/$KHSO_5$ system is C1' (top) or C5' (bottom) of the deoxyribose.

The activated cationic metalloporphyrin initiates the oxidation of the deoxyribose by H5'-abstraction, giving a C5' centered radical which can reacts with the Mn^{IV}-OH complex (an alternative mechanism is the one-electron oxidation of this radical by Mn^{IV}-OH to generate a carbocation which is attacked by a water molecule to produce the 5'-OH derivative (see Figure 2 for the so-called P-450 diverted route). Spontaneous cleavage follows, with formation of a 3'-phosphate end and a 5'-aldehyde ending derivative (direct break of the DNA backbone). A first β-elimination produces a second break on the DNA backbone

with release of a 5'-phosphate end and a α, β-unsaturated aldehyde compound. Finally a second β-elimination gives rise to free base and furfural as sugar degradation product. The 5'-COOH ending fragments, sometimes observed,[36, 37] are probably due to a second oxidative reaction of the recycled activated Mn-TMPyP on the same site. Complete characterization of the α, β-unsaturated aldehyde intermediate was obtained by chemical methods.[35]

No efficient chemical model of restriction enzyme, able to hydrolyze a selected phosphodiester bond, is presently available. However, in an alternative pathway, hydroxylation of carbon 5' of deoxyribose immediately followed by reduction of the formed 5'-aldehyde may allow to mimic this hydrolysis step (oxidation step + reduction step = "pseudo-hydrolysis"). This was recently demonstrated using the Mn-TMPyP/$KHSO_5$ system and its specific hydroxylating activity at the C5' position of deoxyribose. The resulting fragments may be religated by chemical methods, so this system is able to mimick the well-know restriction endonuclease/ligase association.[37]

Hybrid molecules based on a metallotris(methylpyridiniumyl)porphyrin moiety attached to various vectors have been prepared allowing targeting of the nuclease activity. The vector can be an intercalating agent like 9-methoxyellipticine.[38] Such derivatives exhibit the essential properties of bleomycin. They are cytotoxic against leukemia cells *in vitro* and their nuclease activity, as well as their cytotoxicity, is metal-dependent.[38c,d] Mn-tris-pyridiniumylporphyrin[39] is also a suitable motif to be linked to various vectors like oligonucleotides.[40] The attachment of an efficient DNA cleaver to oligonucleotides might be useful in the development of new antitumoral or antiviral drugs. Recently, we have shown that the motif tris-methylpyridiniumylporphyrinatomanganese covalently linked to a 19-mer complementary to the initiation codon region of the *tat* gene of HIV-1 is able to cleave a 35-mer containing this intitiation codon zone, in the presence of a large excess of random double-stranded DNA, at very low concentrations (5 to 100 nM). Such a specificity cannot be observed with the free Mn-porphyrin because its reactivity is mainly directed to the large excess of random DNA.[41]

3. Conclusions

The DNA-cleavage route selected by Nature for cytotoxic drugs (bleomycin, enediyne) is a sugar oxidation and not a hydrolysis of phosphodiesters. So it is not surprising that synthetic transition metal complexes exhibiting redox properties and DNA affinity have been developed as "chemical nucleases". Development of these artificial and selective DNA cleavers, because of the need for highly efficient (quantitative cleavage of the target must be reached) and highly specific (sequence specificity on large DNA fragments) reagents, is a challenging area in the rational design of future antitumoral or antiviral agents as well as in the field of molecular biology.

4. Acknowledgments.

The authors are deeply indebted to the work of many co-workers and collaborators. We are also grateful to the CNRS, the 'Association pour la Recherche contre le Cancer' (ARC, Villejuif), the 'Agence Nationale de Recherches sur le Sida' (ANRS, Paris), the 'Région Midi-Pyrénées' and Genset (Paris) for financial support.

5. References

(1) H. Sies, *Angew. Chem. Int. Ed. Engl.* **1986**, *25*, 1058-1071. I. Fridovich, *Annu. Rev. Pharmacol. Toxicol.* **1983**, *23*, 239-257.

(2) J. Cadet, M. Berger, C. Decarroz, J.R. Wagner, J.E. van Lier, Y.M. Ginot, P. Vigny, *Biochimie* **1986**, *68*, 813-834. C. von Sonntag, *The Chemical Basis of Radiation Biology*, Taylor and Francis, Philadelphia, **1987**. C. von Sonntag, H-P. Schuchmann, *Methods in Enzymology* **1993**, in press.

(3) H. Urata, K. Yamamoto, M. Akagi, H. Hiroaki, S. Uesugi, *Biochemistry* **1989**, *28*, 9566-9569. J. Piette, *J. Photochem. Photobiol. B : Biol.* **1991**, *11*, 241-260; H. Kasai. Z. Yamaizumi, M. Berger, J. Cadet, *J. Am. Chem. Soc.* **1992**, *114*, 9692-9694. L.P. Candeias, S. Steenken, *ibid.* **1993**, *115*, 2437-2440. N. Paillous, P. Vicendo, *J. Photochem. Photobiol. B : Biol.* **1993**, *20*, 203-209.

(4) B. Demple, J. Halbrook, *Nature* **1983**, *304*, 466-468. J.F. Mouret, F. Odin, M. Polverelli, J. Cadet, *Chem. Res. Toxicol.* **1990**, *3*, 102-110.

(5) S. Steenken, *Chem. Rev.* **1989**, *89*, 503-520; A.J.S.C. Vieira, S. Steenken, *J. Am. Chem. Soc.* **1990**, *112*, 6986-6994.

(6) D.G. Knorre, O.S. Federova, E.I. Frolova, *Russ. Chemicals Rev.* **1993**, *62*, 65-86. G. Pratviel, J. Bernadou, B. Meunier, *Angew. Chem.*, submitted.

(7) I.H. Goldberg, *Acc. Chem. Res.* **1991**, *24*, 191-198. I.H. Goldberg, *Free Radical Biol. Med.* **1987**, *3*, 41-54. M.D. Lee, G.A. Ellestad, D.B. Borders, *Acc. Chem. Res.* **1991**, *24*, 235-243. K.C. Nicolaou, W.M. Dai, *Angew. Chem. Int. Ed. Engl.* **1991**, *30*, 1387-1416. K.C. Nicolaou, A.L. Smith, E.W. Yue, *Proc. Natl. Acad. Sci. USA* **1993**, *90*, 5881-5888. K.C. Nicolaou, A.L. Smith, *Acc. Chem. Res.* **1992**, *25*, 497-503. J.S. Taylor, P.G. Schultz, P.B. Dervan, *Tetrahedron* **1984**, *40*, 457-465. I. Lee, J.K. Barton, *Biochemistry* **1993**, *32*, 6121-6127 and references therein. D.S. Sigman, T.W. Bruice, A. Mazumder, C.L. Sutton, *Acc. Chem. Res.* **1993**, *26*, 98-104. T. Tanaka, M. Hirama, K.-I. Fujita, M. Ishiguro, *J. Chem. Soc., Chem. Commun.* **1993**, 1205-1207.

(8) S.M. Hecht, *Acc. Chem. Res.* **1986**, *19*, 383-391. J. Stubbe, J.W. Kozarich, *Chem. Rev.* **1987**, *87*, 1107-1136. D.H. Petering, R.W. Byrnes, W.E. Antholine, *Chem.-Biol. Interactions* **1990**, *73*, 133-182.

(9) (a) Y. Sugiura, T. Suzuki, J. Kuwahara, H. Tanaka, *Biochem. Biophys. Res. Commun.* **1981**, *105*, 1511-1518. (b) N. Murugesan, S.M. Hecht, *J. Am. Chem. Soc.* **1985**, *107*, 493-500. (c) G. Pratviel, J. Bernadou, B. Meunier, *Biochem. Pharmacol.* **1989**, *38*, 133-140. (d) E. Gajewski, O.I. Aruoma, M. Dizdaroglu, B. Halliwell, *Biochemistry* **1991**, *30*, 2444-2448.

(10) (a) M.E.A. Churchill, J.J. Hayes, T.D. Tullius, *Biochemistry* **1990**, *29*, 6043-6050. (b) T.D. Tullius, B.A. Dombroski, M.E.A. Churchill, L. Kam, *Methods in Enzymol.* **1987**, *155*, 537-558. (c) J.P. Sluka, J.H. Griffin, D.P. Mack, P.B. Dervan, *J. Am. Chem. Soc.* **1990**, *112*, 6369-6374. (d) S.A. Strobel, P.B. Dervan, *Science* **1990**, *249*, 73-75. (e) P.B. Dervan, *ibid.* **1986**, *232*, 464-471.

(11) D.S. Sigman, *Biochemistry* **1990**, *29*, 9097-9105 and references therein.

(12) A.E. Friedman, J.C. Chambron, J.P. Sauvage, N.J. Turro, J.K. Barton, *J. Am. Chem. Soc.* **1990**, *112*, 4960-4962. A.M. Pyle, J.K. Barton, *Prog. Inorg. Chem.* **1990**, *38*, 413-516.

(13) T.J. Dougherty, J.E. Kaufman, A. Goldfarb, K.R. Weishaupt, D. Boyle, A. Mittleman, *Cancer Res.* **1978**, *38*, 2628-2635. D. Kessel, *Biochem. Pharmacol.* **1984**, *33*, 1389-1393. D. Brault, C. Vever-Bizet, M. Dellinger, *Biochimie* **1986**, *68*, 913-921. E. Kvam, J. Moan, *Photochem. Photobiol.* **1990**, *52*, 769-773. *Photosensitizing Compounds: Their Chemistry, Biology and Clinical Use*; J. Wiley: Chichester, **1989**.

(14) R. Bonnett, R.D. White, U.J. Winfield, M.C. Berenbaum, *Biochem. J.* **1989**, *261*, 277-280. R.K. Pandey, K.M. Smith, T.J. Dougherty, *J. Med. Chem.* **1990**, *33*, 2032-2038. T. Ando, Y. Suzuki, R. Geka, K. Irie, K. Koshimizu, T. Takemura, S. Nakajima, I. Sakata, *Tetrahedron Lett.* **1991**, *32*, 5107-5110. C. Sentagne, B. Meunier, N. Paillous, *J. Photochem. Photobiol. B: Biol.* **1992**, *16*, 47-59.

(15) R.J. Fiel, *J. Biomol. Struc. Dynamics* **1989**, *6*, 1259-1274. R.F. Pasternak, E.J. Gibbs, *Metal-DNA Chemistry, ACS Sympos. Ser. 402* **1989**, 59-73. G. Raner, B. Ward, J.C. Dabrowiak, *J. Coord. Chem.* **1988**, *19*, 17-23. L.G. Marzilli, *New J. Chem.* **1990**, *14*, 409-420.

(16) N. Foster, A.K. Singhal, M.W. Smith, N. Marcos, K.J. Schray, *Biochim. Biophys. Acta* **1988**, *950*, 118-131.

(17) E.J. Gibbs, M.C. Maurer, J.H. Zhang, W.M. Reiff, D.T. Hill, M. Malicka-Blaszkiewicz, R.E. McKinnie, H.Q. Liu, R.F. Pasternak, *J. Inorg. Chem.* **1988**, *32*, 39-65.

(18) (a) M.A. Sari, J.P. Battioni, D. Dupré, D. Mansuy, J.B. Le Pecq, *Biochemistry* **1990**, *29*, 4205-4215. (b) K.T. Yue, M. Lin, T.A. Gray, L.G. Marzilli, *Inorg. Chem.* **1991**, *30*, 3214-3222. (c) X. Hui, N. Gresh, B. Pullman, *Nucleic Acids Res.* **1990**, *18*, 1109-1114. (d) U. Sehlstedt, S.K. Kim, P. Carter, J. Goodisman, J.F. Vollano, B. Nordén, J.C. Dabrowiak, *Biochemistry* **1994**, *33*, 417-426.

(19) (a) M. Rodriguez, T. Kodadek, M. Torres, A.J. Bard, *Bioconjugate Chem.* **1990**, *1*, 123-131. (b) L. Ding, J. Bernadou, B. Meunier, *ibid.* **1991**, *2*, 201-206.

(20) W. Saenger, *Principles of Nucleic Acid Structure*, Springer-Verlag, New-York, **1984**

(21) A. Mazumder, J.A. Gerlt, M.J. Absalon, J. Stubbe, R.P. Cummingham, J. Withka, P.H. Bolton, *Biochemistry* **1991**, *30*, 1119-1126. J.J. Hangeland, J.J. De Voss, J.A. Heath, C.A. Townsend, W.D. Ding, J.S. Ashcroft, G.A. Ellestad, *J. Am. Chem. Soc.* **1992**, *114*, 9200-9202.

(22) B. Meunier, *Chem. Rev.* **1992**, *92*, 1411-1456.

(23) S. Prince, F. Körber, *Acta Cryst.* **1993**, *C49*, 1158-1160.

(24) B. Ward, A. Skorobogaty, J.C. Dabrowiak, *Biochemistry* **1986**, *25*, 6875-6883.

(25) (a) J. Bernadou, G. Pratviel, F. Bennis, M. Girardet, B. Meunier, *Biochemistry* **1989**, *28*, 7268-7275. (b) E. Fouquet, G. Pratviel, J. Bernadou, B. Meunier, *J. Chem. Soc., Chem. Commun.* **1987**, 1169-1171. (c) G. Pratviel, J. Bernadou, M. Ricci, B. Meunier, *Biochem. Biophys. Res. Commun.* **1989**, *160*, 1212-1218. (d) B. Ward, R. Rehfuss, J.C. Dabrowiak, *J. of Biomol. Struct. & Dynamics* **1987**, *4*, 685-695. (e) J.C. Dabrowiak, B. Ward, J. Goodisman, *Biochemistry* **1989**, *28*, 3314-3322;

(26) (a) T.J. McMurry, J.T. Groves in *Cytochrome P-450: Structure, Mechanism and Biochemistry*, (Ed.: P. Ortiz de Montellano), Plenum Press, New-York, **1985**, pp. 1-28. (b) V. Ullrich, *Topics Curr. Chem.* **1979**, *83*, 67-104. (c) R.E. White, M.J .Coon, *Annu. Rev. Biochem.* **1980**, *49*, 315-356. (d) *Cytochrome P-450: Structure, Mechanism and Biochemistry*, (Ed.: P. Ortiz de Montellano), Plenum Press, New-York, **1985**. (e) A. Sorokin, A. Robert, B. Meunier, *J. Am. Chem. Soc.* **1993**, *115*, 7293-7299.

(27) R.J. Fiel, T.A. Beerman, E.H. Mark, N. Datta-Gupta, *Biochem. and Phys. Res. Commun.* **1982**, *107*, 1067-1074.

(28) R.W. Byrnes, R.J. Fiel, N. Datta-Gupta, *Chem.-Biol. Interactions* **1988**, *67*, 225-241.

(29) (a) S.D. Bromley, B.W. Ward, J.C. Dabrowiak, *Nucleic Acids Res.* **1986**, *14*, 9133-9148. (b) B. Ward, A. Skorobogaty, J.C. Dabrowiak, *Biochemistry* **1986**, *25*, 7827-7833. (c) G. Raner, B. Ward, J.C. Dabrowiak, *J. Coord. Chem.* **1988**, *19*, 17-23. (d) G. Raner, J. Goodisman, J.C: Dabrowiak, in *Porphyrins as Probes of DNA Structure and Drug-DNA Interactions , Chapter 5*, (Ed.: T.D. Tullius), ACS

Symposium Series 402, Washington, **1989**, pp. 74-89. (e) R.F. Pasternack, E.J. Gibbs, in *Metal-DNA Chemistry*, (Ed.: T.D. Tullius), ACS Symposium Series 402, **1989**, pp. 59-73. (f) R.F. Pasternack, E.J. Gibbs, J.J. Villafranca, *Biochemistry* **1983**, *22*, 5409-5417. (g) J.A. Strickland, L.G. Marzilli, K.M. Gay, W.D. Wilson, *ibid.* **1988**, *27*, 8870-8878. (h) R.J. Fiel, *J. of Biomol. Struct. & Dynamics* **1989**, *6*, 1259-1273. (i) L.G. Marzilli, *New J. Chem.* **1990**, *14*, 409-420.

(30) X. Hui, N. Gresh, B. Pullman, *Nucleic Acids Res.* **1990**, *18*, 1109-1114; R. Lavery, B. Pullman, *J. Biomol. Struct. & Dynamics* **1985**, *2*, 1021-1032. P.K. Weiner, R. Langeridge, J.M. Blaney, R. Schaefer, P.A. Kollman, *Proc. Natl. Acad. Sci. USA* **1982**, *79*, 3754-3758.

(31) L.G. Marzilli, G. Pethö, M. Lin, M.S. Kim, D.W. Dixon, *J. Am. Chem. Soc.* **1992**, *114*, 7575-7577.

(32) R.B. Van Atta, J. Bernadou, B. Meunier, S.M. Hecht, *Biochemistry* **1990**, *29*, 4783-4789.

(33) M. Pitié, G. Pratviel, J. Bernadou, B. Meunier, *Proc. Natl. Acad. Sci. USA* **1992**, *89*, 3967-3971.

(34) (a) J. Bernadou, B. Lauretta, G. Pratviel, B. Meunier, *C. R. Acad. Sci. Paris* **1989**, *309 III*, 409-414. (b) G. Pratviel, M. Pitié, J. Bernadou, B. Meunier, *Angew. Chem.* **1991**, *103*, 718; *Angew. Chem. Int. Ed. Engl.* **1991**, *30*, 702-704. (c) G. Pratviel, M. Pitié, J. Bernadou, B. Meunier, *Nucleic Acids Res.* **1991**, *19*, 6283-6288. (d) G. Gasmi, M. Pasdeloup, G. Pratviel, M. Pitié, J. Bernadou, B. Meunier, *ibid.* **1991**, *19*, 2835-2839.

(35) G. Pratviel, M. Pitié, C. Périgaud, G. Gosselin, J. Bernadou, B. Meunier, *J. Chem. Soc. Chem. Commun.* **1993**, 149-151.

(36) M. Pitié, G. Pratviel, J. Bernadou, B. Meunier in *The activation of Dioxygen and Homogeneous Catalytic Oxidation* (Eds.: D. H. R. Barton, A. E. Martell, D. T. Sawyer), Plenum, New-York, **1993**, pp. 333-346.

(37) G. Pratviel, V. Duarte, J. Bernadou, B. Meunier, *J. Am. Chem. Soc.* **1993**, *115*, 7939-7943.

(38) (a) F. Tadj, B. Meunier, B. *C. R. Acad. Sci. Paris* **1988**, *306 II*, 631-634. (b) L. Ding, G. Etemad-Moghadam, S. Cros, C. Auclair, B. Meunier, *J. Chem. Soc., Chem. Commun.* **1989**, 1711-1713. (c) L. Ding, G. Etemad-Moghadam, S. Cros, C. Auclair, B. Meunier, *J. Med. Chem.* **1991**, *34*, 900-906. (d) L. Ding, G. Etemad-Moghadam, B. Meunier, *Biochemistry* **1990**, *29*, 7868-7875.

(39) L. Ding, C. Casas, G. Etemad-Moghadam, B. Meunier *New J. Chem.* **1990**, *14*, 421-431.

(40) (a) A.S. Boutorine, T. Le Doan, J.P. Battioni, D. Mansuy, D. Dupré, C. Hélène, *Bioconjugate Chem.* **1990**, *1*, 350-356. See also (b) T. Le Doan, L. Perrouault, C. Hélène, M. Chassignol, N.T. Thuong, *Biochemistry* **1986**, *25*, 6736-6739. (c) E. Frolova, E.M. Ivanova, V.F. Zaytova, T.V. Abramova, V.V. Vlassov, *FEBS Lett.* **1990**, *269*, 101-104.

(41) C. Casas, C.J. Lacey, B. Meunier, *Bioconjugate Chem.* **1993**, *4*, 366-371. M. Pitié, C. Casas, C.J. Lacey, G. Pratviel, J. Bernadou, B. Meunier, *Angew. Chem. Int. Ed. Engl.* **1993**, *32*, 557-559.

THE ROLE OF METAL IONS IN BIOLOGICAL SYSTEMS AND MEDICINE

J. ANASTASSOPOULOU AND T. THEOPHANIDES
National Technical University of Athens, Chemical Engineering Department, Radiation Chemistry and Biospectroscopy, Zografou Campus, Zografou 15780, Athens, Greece.

ABSTRACT: Metals play crucial roles in life processes. It is increasingly recognized that metals are involved in cellular and subcellular functions. With the application of new and sophisticated machines to study biological and biochemical systems the true role of inorganic salts in living systems can be revealed. Inorganic chemistry is not the "Dead Chemistry" that some people may think. Today, it is known that metals are important ingredients in life, just as the organic molecules. For instance, the divalent magnesium and calcium ions play important regulatory roles in cells. Metallothionins are proteins rich in metal ions found in living systems. The divalent cations Zn^{2+}, Ca^{2+} and Mg^{2+} prevent cytotoxicity and *in vivo* antagonize Cd-induced carcinogenesis. Lack of body iron is common in cancer patients and it is associated with complications in surgery and in animal experiments. The transport of iron and other metal ions by the blood plasma is achieved through the formation of protein complexes. Copper is recognized as an essential metalloelement and is primarily associated with copper-dependent cellular enzymes. Metals are also used as inorganic drugs for many diseases.
The cisplatin (*cis*-$Pt(NH_3)_2Cl_2$) is the first member of a new class of potent antitumor drugs belonging to metal coordination complexes which are being introduced in Medicine. The emphasis in this chapter, however will mainly be on the metal-molecule interactions and the chemistry and structure of metal-complexes.

1. Introduction

There are a variety of naturally occurring metal complexes which are involved in some manner in life processes[1]. We all know that calcium builds strong bones and teeth. But calcium also helps to quell muscle cramps and trigger a number of reactions in the human body. Our cells in their activities depend on magnesium. In fact next to potassium, magnesium is the most abundant mineral inside each cell. Ca^{2+} and Mg^{2+}, as well as Zn^{2+}, Cu^{2+}, Fe^{2+} and Mn^{2+} are involved in biological processes in the nucleus and are present in detectable amounts (10^{-2} to 10^{-4} mol) and bound to DNA and RNA in the cells[2]. The active configuration of RNA is dependent on Mg^{2+} or Mn^{2+} concentration. Enzymes in both plants and animals depend on the energy to do their work delivered by magnesium. It is known that magnesium delivers the energy by activating the production of adenosine triphosphate (ATP) which provides energy to those billions of cells in our body. Magnesium is a catalyst or activator for this reaction and countless other physical activities.

D.P. Kessissoglou (ed.), Bioinorganic Chemistry, 209-218

The enzymatic activity, for instance in DNA-polymerase together with the effects of divalent ions, such as Mg^{2+}, Mn^{2+}, and Zn^{2+} on the rate of polymer synthesis has been reported[3].

Finally we will report on the developments of models for the metal ion sites found in metal complexes of single metal ions with organic ligands having as donor atoms, oxygen, nitrogen, sulfur or phosphorous donor atoms. Molecular models were originally developed for the conformational analysis of organic compounds. However, coordination compounds are less studied due to the presence of the metal ion which brings in a variety of geometries that the metals show in their compounds, and the lack of parameters for interactions with the metal ion. Most molecular mechanics programs treat metal-ligand interactions by defining a covalent bond between the metal ion and the ligand atom "bonded approach" or by using electrostatic and Van der Waals forces "non-bonded approach"[4]. This review will not analyze the methods, but it will report on the nature of the problems and the use of the methods that have been worked out to try to solve them.

2. Biological Effects

Metals are known since ancient times. The Egyptians is said to have used copper to sterilize water in 3000 BC, the Chinese used gold in medicine in 2500 BC and Hippocrates was using many metals, such as, Cu, Fe, Zn, Na, K to cure diseases[5].

The great majority of the elements of the Periodic Table are metals (about 80) and most of them are involved in life processes or have been used as drugs. The coordination chemistry of alkali, alkaline-earth and toxic cations and their complexation aspects for which stability constants and selectivities have been determined with some macrocyclic cryptates are illustrated on Figure 1.

The applications of the above cryptates for the elimination of the radioactive cations have been shown for cryptate 3, $^{85}Sr^{2+}$, $^{224}Ra^{2+}$, $^{140}Ba^{2+}$. The complexation selectivities were: $Sr^{2+}/Ca^{2+} = 4.10^3$, $Ra^{2+}/Ca^{2+} = 1.6.10^2$, $Ba^{2+}/Ca^{2+} = 1.3.10^5$ and $Sr^{2+}/K^+ = 4.10^2$, $Ra^{2+}/K^+ = 16$, $Ba^{2+}/K^+ = 1.3.10^4$. All in favor of the radionuclide. The experiments were performed in vivo (on rats) and the excretion of radioactive cations in faeces and urine were greatly enhanced in the presence of the cryptates[6].

As detoxification agents of heavy metals were also used several cryptates which formed strong binding with the toxic heavy metals (Cd^{2+}, Hg^{2+}, Pb^{2+}) and weak binding with biologically essential cations (Na^+, K^+, Mg^{2+}, Ca^{2+}, Zn^{2+}). For Ca^{2+} the cryptates 1-3, 6-8 were used successfully (selectivities Hg^{2+}/Ca^{2+} from 10^{13} to 10^{25}, Hg^{2+}/Zn^{2+} from 10^{11} to 10^{19} and for Pb^{2+} the cryptates 2,3,6-10 were found to be the best (selectivities Pb^{2+}/Ca^{2+} from 10^6 to 10^{14}, Pb^{2+}/Zn^{2+} from 10^5 to 10^{10}). Extraction and transport of cations were also possible with these cryptates[7] and they have found a large variety of applications in analytical chemistry.

The biological effects of occupational and environmental exposure to chromium have been reported recently[8]. In a report the occupational exposure to Cr compounds in industry of production of the metal and applications of the metals, such as chrome plating chromium chemicals and pigments and in various other industries, such as in leather tanning, production of Cr catalysts, paints textiles, corrosion inhibitors and others has been studied. In all these cases Cr exists in the bivalent and hexavalent state. Chromium is a human carcinogen. Lung cancers have been reported in chromate-exposed workers in the production of alizarin dyes in 1911 and 1935[9]. The latency period for Cr-associated lung cancers ranges between 10-15 years after the initial exposure. The main routes of

exposure to Cr are the skin, gastrointestinal tract and respiratory tract. The metabolism of Cr is greatly influenced by the routes of intake.

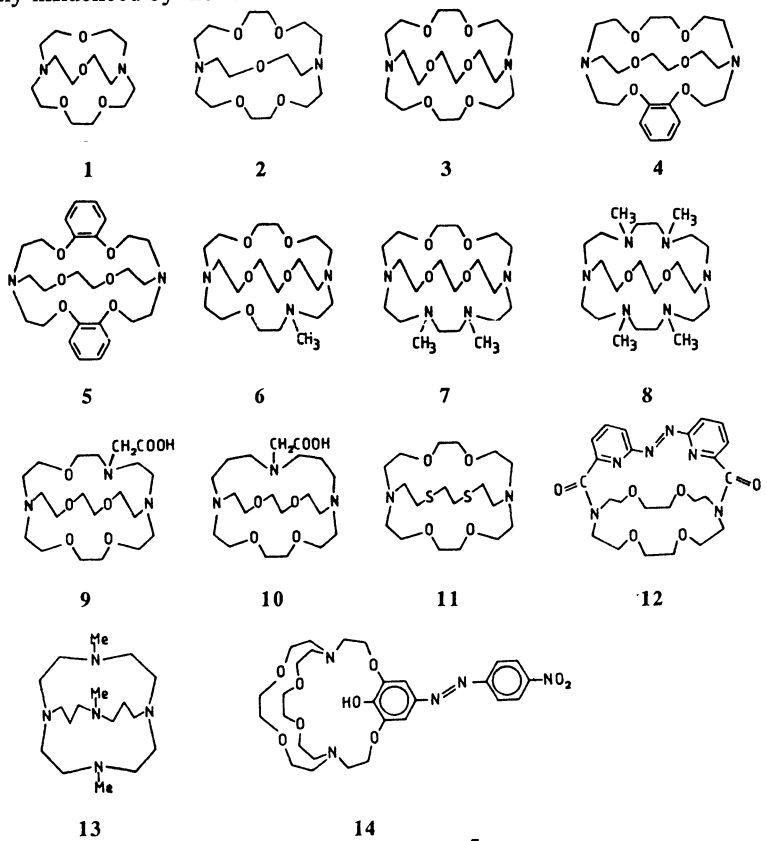

Figure 1. Cryptates[7]

The clinical aspects of aluminum metabolism and aluminum containing drugs, and links between aluminum neurotoxicity and cerebral atrophy in regular hemodialysis treatment patients are described in a report[10]. The main sings of beginning systematic aluminum intoxication are neurological symptoms accompanied by aggravation of an already existing renal anemia and/or osteopathy. Aluminum concentrations in blood plasma and different tissues are often found increased in patients with chronic intermittent hemodialysis treatment.

Copper (II) is recognized to be an essential trace element[11]. Its biological activity has been shown in electron transport processes as an integral enzyme co-factor, in antioxidant protection, pigment formation and hormone production[12].

It has also been shown that the perspective capacity of physiologically essential metals to antagonize DNA binding ($Zn^{2+} > Mg^{2+} > Ca^{2+}$) parallels their in vivo capacity to antagonize Cd-induced carcinogenesis[13]. This study concludes that magnesium is important in the maintenance of the general integrity of the biological system and that the prominent effect of magnesium in cancer systems may be its role in the control of immunity growth, or stabilization of the DNA structure[14].

3. Inorganic Drugs

The inorganic drug discoveries are many. Technetium, $^{99m}Tc(V)$ is used for radio imaging and other medical uses. Fe-complexes are present in metabolic processes in virtually all organisms and have been reported in the excellent work on siderophores (from the Greek: σίδηρος=iron , φορέας=carrier) by Kenneth Reymond et al[15]. There are many MRI contrast agents today, such as Gd(III) complexes, Mn(II) and Fe(III) as well. Gold(I) in colloid form or as a complex (Auranofin), $Au(I)(PEt_3)$acetylthioglucose is antiarthritic. Some gold complexes have been tested as anti-cancer agents. The anti-arthritis drugs based on gold complexes usually are compounds linked to thiosulfate (Sanochrysin) and sugar ligands such as auromycin. The mechanism of action of gold drugs is not known. There are of course the well known Pt anticancer drugs (see later). Polyoxymetallates have also been studied for anti-HIV[16]. Metals or metal coordination compounds may be used as macrocyclic antibiotics, radioisotopes with targeting agents such as antibodies ACE inhibitors. The current drug of choice for the treatment of iron overload is a siderophore[17].

Chelating agents are already in clinical use to remove toxic metals. Wilsons's disease is a genetic disorder due to Cu metabolism. Silver nitrate is still used today in some nurseries to treat/or prevent ophthalmic gonorrhea in the newborn, or as Ag(I) sulfadiazine as antibacterial but now in most places use modern penicillin derivatives. Trace element supplements are used in hospitals as hyperalimentation compounds taken intravenously. The most expensive clinical application of metals or organometallic complexes takes place in radiology. MRI has resurrected organometallics for radiologists. The Gadolinium complexes have already been mentioned above, but many other compounds are being attempted. Mn(II), and Fe(III) chelates are used for liver and tumor imaging[17]. Porphyrin derivatives are used to identify tumors, particularly radiologically undetectable lung tumors. They are also used as radiosensitizers of tumor cells prior to radiation therapy. The radiology literature is full of new metal compounds used in radiology.

The design of new drugs that contain metals is a new area of investigation and one can use computational chemistry to understand metalloproteins, metalloenzymes and haem proteins[18]. It is known that there are not many reported successes of drug design and even fewer with metal containing compounds and metalloenzymes. Pharmaceuticals and inorganic chemistry have been recently described in the review by Sadler[19]. The most important application of inorganic chemistry in pharmaceuticals is in antineoplastics, and nuclear medicine related to diagnostic radiology. Heavy metal chelates are used for imaging in nuclear medicine, for instance liver imaging was developed or modeled after similar agents in hepatobiliary imaging. There is a substitution of a radioactive metal with the paramagnetic metal ion. The role of thallium-201 chloride in brain tumor imaging has been used, since thallium-201 is a potassium substituted and it is widely used for myocardial imaging since 1971[20].

4. Screening of New Inorganic Antitumor Agents

Selecting and identifying novel agents for the treatment of neoplastic disease is a difficult job and it changes and evolves considering the empirical data available. Initially the strategy was predominantly based on in vivo rodent tumor models. The earliest rodent models used were the transplantable tumors, e.g. Yoshida ascites sarcoma, Sarcoma 180, and Erlich ascites carcinoma. These tumor models had limited successes and were

replaced in the 1950's by synergy transplantable murine tumors, e.g. L1210, P388, B16. These are then the backbone of the majority of screening programmes today. The prominent models have been the P388 and L1210 murine leukemias which have been extensively used by laboratories for the pre-clinical selection of new antitumor agents. One of the well prepared screening programmes is that of the NCI[21]. The screening between 1955-1982 indicated that from 600,000 compounds screened, only 50 drugs were in the clinic. A general conclusion that can be drawn from this reports is that very few solid tumors show successful response to chemotherapeutic agents in the clinic. The selection therefore based on cytostatic/cytotoxic agents must be changed to a new approach for screening for new anti-tumor agents. Single cell culture screening systems have been of little value and thus the development of new systems utilizing a range of cell lines was established from human solid tumors[22].

5. Platinum Anticancer Drugs

In 1969, Barnett Rosenberg and co-workers discovered accidentaly[23] that cis-diammine dichloroplatinum (II) (cisplatin) had antitumor activity. Today almost 25 years later this compound is one of the most widely used oncolytic drugs against a variety of cancers[24]. To date, well over 1000 analogues of cisplatin have been synthesized and examined for antitumor activity particularly against cancers of testicles, ovaries, head and neck, bladder and other carcinomas. However, the drug has a few side effects, such as, nephrotoxicity, cytotoxicity, vomiting, lost of hair, cross-resistance and lack of solubility and of course it kills the healthy cells as well.

The design and synthesis of the aldiol derived platinum complexes are analogues of cisplatin. The synthesis from D-manitol was performed by stereocontrolled manipulation of the hydroxyl groups. Unlike the hydroxyl substituted platinum complexes, the methoxy analogues appeared to lack cross-resistance in tissue culture trials using the P338 lines showing IC50 kg/mL resist/sens ratios close to unity, compared to cisplatin, which shows significant cross-resistance[25]. This chemotherapeutic agent has the DNA as a target for anticancer drug action. Platinum complexes, like nitrogen mustards and most other alkylating agents, react with the DNA primarily at the guanine-N7 position. Bifunctional compounds can react with two guanines on the same or on the opposite DNA strands to generate intrastrand or interstrand crosslinks[26] (Fig. 2). These drugs, produce DNA-protein crosslinks. However, it has often been difficult to determine, if either, of these lesions is the main cause of cell killing.

Cell killing could not be due simply to the presence of DNA lesions, but must involve an interaction with replication or mitosis. The number and persistence time of crosslinks in the genome could produce a lethal event. The molecular mechanism of action of cisplatin has been a fascinating subject of research[27] and still is. The binding at the N7 position of two adjacent guanines in DNA sequence results in a weakening of hydrogen bonding of the base pairs and the inevitable unwinding of the double helix[28,29].

The kinetics of crosslinks formation and repair[30] have been studied in some detail in L1210 cells treated with cisplatin by quenching DNA-cisplatin in L1210 cells and introducing mainly cisplatin monoadducts and selectively study the second coordinating position of the monoproduct to form crosslinks. It was concluded, however, by this study that sensitivity to alkylating agents and platinum complexes is not always fully explained by crosslink formation.

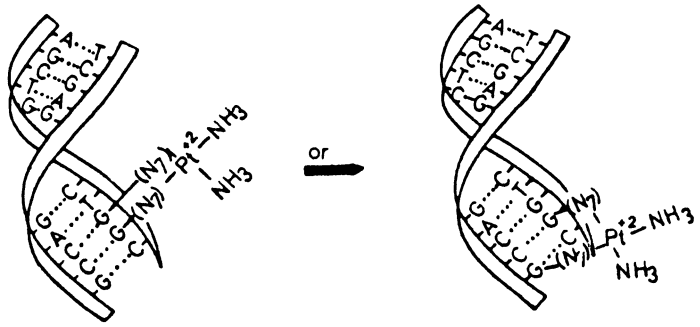

Figure 2. Intra- and interstrand crosslinks

We have recently reported[25] the synthesis and antitumor activity of a series of novel platinum complex analogues of cisplatin with the general formulae shown in Figure 3.

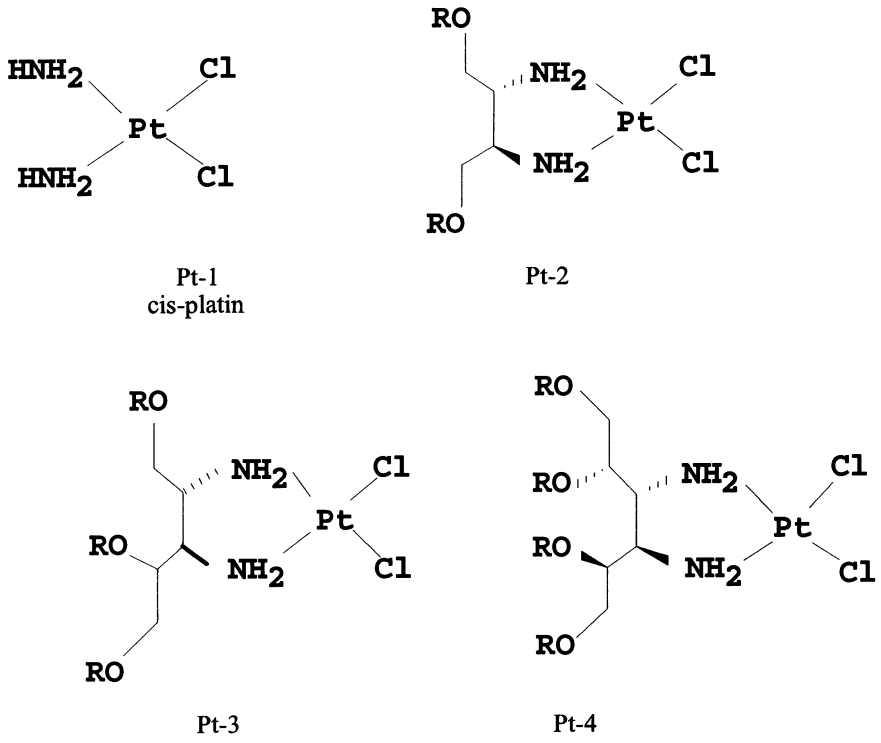

Figure 3. Novel platinum cisplatin analogues, R = H, alkyl

The antitumor activity of the hydroxy analogues showed significant in vitro activity against sensitive strains of L1210 leukemia and P388 with D50 values comparable to cisplatin. In vivo tests (subcutaneous and in- travenous) against PU-239 showed levels of activity approaching that of cisplatin and in vivo test results with M5076 sarcoma were inferior to cisplatin. The O-methyl analogs also showed significant in vitro and in vivo antitumor activity against several tumor lines. The same trends were observed in vivo with good resistant/sensitive ratios comparable or better from cisplatin. In all, promising antitumor activity is exhibited by these analogues.

6. Structure of Platinum-DNA Adducts and Spectroscopic Studies

The interactions of the above platinum aldiol complexes with nucleic acid compounds, such as guanosine, 5'-GMP, 3'-GMP, GpC, CpG have been studied by spectroscopic techniques like FT-IR, Raman and ^{1}H NMR as well as with Mass spectrometry[31,32]. These structural and spectroscopic studies with various nucleotides and DNA have shown that in all the above reactions the stable unit of *cis*-$Pt(NH_2R)^{2+}$ is chelated as intrastrand cross-linking moiety at two adjacent guanines, coordinated with the N7 nitrogen sites[33]. The reaction of *cis*-$Pt(NH_3)Cl_2$ or *cis*-$Pt(NH_2R)_2Cl_2$ analogues with a guanosine takes place through the N7 of guanine as follows[33] :

$$(diamine)_2PtCl_2 + 2G\text{-residue} \rightarrow (diamine)_2PtG_2\text{-residue}^{++} + 2Cl^-$$

The 2G-residues, may be two free guanines, guanosines, guanosine monophosphates or two guanines linked through sugar-phosphates as in DNA.
The above reaction is general and the assumption is made that it takes place also in vivo. The generality of this reaction is also deduced from the greater basicity of the N7 site of guanine. It has been observed in the solid FT-IR spectra of the complexes formed that a change from C2'-endo to C3'-endo conformation of the sugar, is accompanied by a shift of the sugar-phosphate characteristic band[34] from 825 cm^{-1} to 800 cm^{-1}. This conformational change has also been confirmed from ^{1}H NMR spectra of the complexes in aqueous solutions[35].

The secondary structure of DNA depends on the sugar-phosphate backbone vibrations. these "marker bands" of the furanose-phosphate backbone vibrations for the conformations C2'-endo/anti (B-DNA) C3'-endo/anti (A-DNA) and C3'-endo/syn (Z-DNA) have been observed in FT-IR of metal ion-nucleotide adducts and also in Raman spectra[36]. These vibrations reveal the conformational changes which take place in the secondary structure of double DNA helix upon metal fixation at the N7 site of guanine[37].

The primary structure of covalent bonds in DNA also changes upon metal complexation of the N7 site of guanine and this introduces changes in the "marker band" near 690 cm^{-1} due to the "breathing mode" of the purine ring, which shows considerable change upon coordination of a metal ion at the N7 site of guanine. These changes, however are general for all the metals that are bonded to N7 of guanine. An attempt to differentiate between the *cis*- and *trans*-$Pt(NH_3)_2Cl_2$ interactions with DNA the FT-IR spectra of the cis-Pt(DNA) and *trans*-Pt(DNA) adducts have been recorded and compared. The spectra are shown in Fig. 4. the FT-IR spectrum of *cis*-Pt(DNA) is different from that of the *trans*-Pt(DNA) adduct with respect to the marker bands[38]. These deferences are with respect to Pt-N7 mono adduct (*trans*-Pt) and Pt-(N7) bi-adduct (*cis*-Pt).

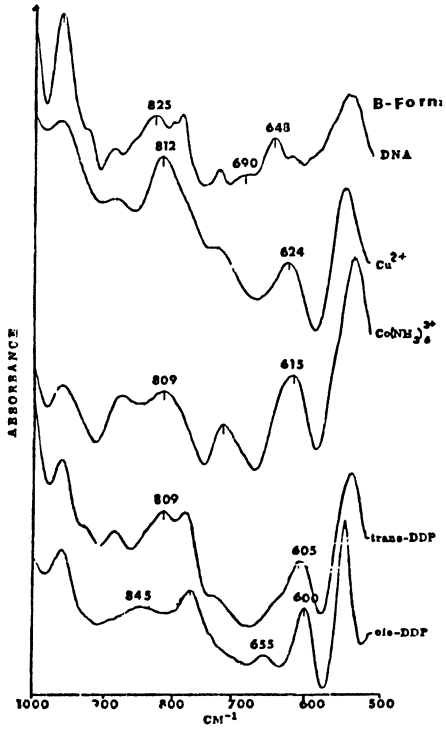

Figure 4. FT-IR spectra of DNA-metal complexes

7. Molecular Modeling of Coordination Compounds

Inorganic pharmaceuticals are a new challenge in modern pharmacology. This is helped by drug design based on molecular modeling of coordination compounds, and in particular modeling metal ion sites, in all the cases where metals play a role in living processes. The binding mode of metal ions in proteins, nucleic acids, membranes, etc. is complex. Metals do control the activity of enzymes and some of the most genetic processes in the replication of DNA and RNA. A great deal of effort is given in designing organic drugs, but very little in inorganic chemistry. This trend must change by showing how inorganic compounds are important for life. We think that this can be accomplished by exploring methods for molecular mechanics modeling of coordination compounds and inorganics in general[39]. We must develop molecular models for the metal complexes of single metal ions with organic ligands in order to find new approaches for the force fields of coordination compounds. A new force field for modeling metalloproteins has been developed by Vedani and Huhta[4]. This new force field for modeling metal-ligand separation, the symmetry and the energy expression has a function which includes as variables the metal-ligand separation, the symmetry at the metal center (metal site), the directionality of the metal-ligand bonds, the ligand-metal charge transfer and the ligand field stabilization (for transition metal ions). The program "YETI" incorporates the crystal

structure data, H-bonds, etc. in order to be used for modeling details of metal-coordination. It has been found that there is a clear preference for metal-bound ligand atoms to orient their lone pair towards the metal center just like a H-bond acceptor atom prefers to orient its lone pair towards the donor-H atom.

Results were described in a new analysis[4] of the center atom environments of Zn(II) and Co(II) in small-molecule crystal structures with data retrieved from Cambridge Structural Database (CSD). These results were used as a basis for an extended potential function to model metal centers in proteins. The new model has again been incorporated into the molecular mechanics program "YETI" (Version 4.5) and used to model biological complexes and Co(II)-substituted human carbonic anhydrase I. We think that this is an interesting new approach to study metal coordination complexes in bioinorganic chemistry.

8. References

(1) J.Anastassopoulou, Ph. Collery, J.-C.Etienne and T.Theophanides., *Metal Ions in Biology and Medicine,* John Libbey Eurotext, Paris, London, Vo 2, **1992**

(2) W.E.C. Waker and B.L. Vallee, *J.Biol. Chem,* **1959**, *234*, 3257.

(3) J.D. Slater, I. Tamir, L.A. Loeb, and A.S. Mildvan, *J. Biol. Chem.*,**1972**, *247,* 6784

(4) A. Vedani and D.W. Huhta, *J. Am. Chem. Soc.*,**1990**, *112*, 4759.

(5) J. Anastassopoulou and T. Theophanides, *in "Handbook on Metal Ligand Interactions in Biological Fluids",* (ed. Guy Berton), Vo 2. Part Five, Chap. 2., Section B, p.1, **1994.**

(6) J.-M. Lehn, *Angew. Chem, Int.. Ed. Engl.*,**1988**, *27*, 89.

(7) B. Dietrich, *J. Chem. Educ.,* **1985**, *62*, 954.

(8) S. Attila, Br. *J. Ind. Med.,* **1986**, *43*, 592.

9) S. Langard, *Int. J. Ind. Med.,* **1990**, *17*, 189.

(10) F. Gusamo and, T. Degasperi, *Clin. Nephrol.*,**1985**, *23*, 89.

(11) E.B.Hart, H.Steinbock, E.H.Griffith, E.L.Amma and J.Roberts, *Biochim. Biophys. Acta,* **1987**, *15*, 267.

(12) G.Arena, M.Bindone, V. Cardite, E. Conte, G.Maccorone, M.C.Riello and E. Rizarelli, in *"Metal Ions in Biology and Medicine",* (eds., J.Anastassopoulou, Ph. Collery, J-C. Etienne and T.Theophanides), John Libbey Eurotext, London, Paris, **1992**, Vo *2*, p. 32

(13) M.P. Waalkes and L.A. Poirier, *Toxicol. Appli. Pharm.*, **1984**, *75*, 539.

(14) T. Theophanides, *Int. J. Quantum Chem.,* **1984**, *26*, 933.

(15) K.N. Raymond, *J. Am. Chem. Soc.*, **1994**, *115*, 6758.

(16) C. Hill, *J. Med. Chem.,* **1992**, *35*, 1216

(17) K.N. Raymond, K.G. Muller, and B.F.Matsanke, in *"Current Chem.",* (ed., F.L. Boschke), Springer Verlag, New York, pp. 49-102, **1984.**

(18) H. Dutler and A.Ambar, *In "The Coordination Chemistry of Metalloenzymes",* (eds.,I.Bertini, S.R. Drago and C. Lucchinat) NATO Adv., Study Inst. Series, Reidel: Dordrecht, pp 135, **1991**

(19) P.J. Sadler, *Inorganic Chemistry and Drug Design, in Advances in Inorganic Chemistry,* **1991**, *36*, 1.

(20) E. Lebowitz, M.W. Greve, and R. Fairchild, J. Nucl. Med., **1974,** 151.

(21) J.M. Venditti, R.A. Wasley and J. Plowman, Advances in Pharmacology and Chemotherapy, (ed., S.Garattini, A. Goldin and F. Hawking), PP, F.L. Orlands,

Academic Press Inc., p. 20, **1984.**
(22) S.P. Fricker and R.G. Buckley, *Biochem. Soc., Trans.*, **1989**, *17,* 1049.
(23) B. Rosenberg, L. VanCamp, J.E. Troskov and V.H.Monsour, *Nature* (London) **1969,** *222*, 385.
(24) A.W. Pretsayko and S.T. Crooke, *"Cisplatin: Current Status and New Development"*, Academic Press, New York, **1980**
(25) S. Hanessian, J.Y. Gauthier, K. Okamoto, A.L. Beauchamp and T. Theophanides, *Can. J. Chem.*, **1993**, *71*, 880.
(26) T. Theophanides, *Chemistry in Canada*, **1980**, *32*, 30.
(27) T. Theophanides and J.Anastassopoulou, *in "Metal-Based Antitumor Drugs"*, (ed., M. Gielen), Tel Aviv, Israel, **1988**, Vo *2*, p. 151.
(28) T. Theophanides and J.Anastassopoulou, in *"Equilibri in Soluzione, Aspetti Theorici, Sperimentalied Applicanti"*, (eds., C. La Mesa, A. Napoli, N. Russo, and M. Toscano), Marra Editore, **1988.**
(29) P.K. Ganguli and T. Theophanides, *Inorg. chim. Acta*, **1981**, *55,* L43-L45.
(30) K. Micetich, L.A. Zwelling and K.W. Kohn, *Cancer Res.*, **1983**, *43*, 3609.
(31) K. Okamoto, V. Behnam, J.Y. Gautier, S. Hanessian and T. Theophanides, *Inorg. Chim. Acta*, **1986**, L1-L2.
(32) K. Okamoto, V. Behnam and T. Theophanides, *Inorg. Chim. Acta*, **1987,** *135,* 207.
(33) P.C. Kong and T. Theophanides, *Inorg. Chem.*,**1974,** *13,* 1167.
(34) T. Theophanides and J. Anastassopoulou, *in "Spectroscopy of Biological Molecules-New Advances"*, (eds., E.D.Schmid, F.W.Schneider and F.Siebert), Wiley, Chichester, **1987,** p. 433.
(35) T.Theophanides and J.Anastassopoulou, *in Handbook on Metal-Ligand Interactions of Biological Fluids,* ed., G. Berton, Published by M. Dekker, Inc., New York, Part 5, Ch. 2, sec. B, **1994,** p. 13
(36) T.Theophanides, in Spectroscopy of Inorganic Bioactivators. *Theory and Applications-Chemistry, Physics, Biology, and Medicine,* ed., T. Theophanides, Kluwer Academic Publishers, Dordrecht, Boston, London, **1989,** p. 265.
(37) T. Theophanides and J. Anastassopoulou, in *Metal-Based Antitumor Drugs*, ed., M. Gielen, Tel aviv, Israel, **1988,** Vo *2,* p. 151.
(38) T.Theophanides and J. Anastassopoulou, to be published.
(39) B.P. Hay, *Coord. Chem. Rev.* **1993**, *126*, 177.

THE INTERACTION OF HEAVY METAL IONS WITH DNA

N. KATSAROS
NCSR "Demokritos"
Institute of Physical Chemistry
153 10 Aghia Paraskevi Attikis
Greece

1. Introduction

The effect of metal ions upon conformation of DNA was realized early, when it became apparent that metal ions are involved in the stabilization of the Watson-Crick double helix[1,2]. Metal ions react with a variety of electron-donor sites on polynucleotides[3]. There are two main sites of interaction, the phosphate moieties of the ribose-phosphate backbone and the electron donor groups of the bases. The two types of interaction carry with them quite different effects upon the structure of polynucleotides. Reactions with the phosphate means stabilization of ordered structures but cleavage of phosphodiester bonds at high temperature. Whether the binding is non-specific, i.e., totally predictable on the basis of electrolyte theory, or whether specific bonds to the phosphate are produced, the result is to neutralize the array of negative charges on the double helix and thus to stabilize it. Such stabilization is accompanied by an increase in the "melting temperature" of DNA[4].

Reaction with the bases means destabilization of ordered structures, since metal ions can bind to the base stacking interactions that hold together the two strands of DNA. Destabilization is accompanied by a decrease in the melting temperature, Tm of DNA. The differences in behaviour of various metal ions with polynucleotides have made it apparent that some metal ions prefer the phosphate sites and other metal ions prefer the base sites. The difference was strikingly illustrated by the effect of magnesium(II) and cadmium(II) ions on the melting behaviour of DNA. However, metal ions cannot be placed into two categories of those that bind to phosphate and those that bind to the bases. Thus, copper(II) ions that are so effective in base binding, also bind to phosphate and are therefore capable of cleaving phosphodiester links in polyribonucleotides. On the other hand, zinc(II) ions which are so effective in degrading phosphodiester links due to phosphate binding have been demonstrated to bring about a temperature-reversible unwinding of DNA through binding to the bases. Also, DNA can be unwound at low ionic strength with copper(II) ions and subsequently rewound by cooling and then adding solid electrolyte. Evidence indicates that copper(II) forges intramolecular as well as intermolecular cross-links. Mercury(II) and silver(I) ions bind to the nucleoside bases in such a manner that the two chains become cross-linked, native double-stranded DNA can be regenerated from this structure by removal of these ions by complexing anions[5,6]

The antitumour drug *cis*-$Pt(NH_3)_2Cl_2$ shows a wide variety of biological activity and seems to act by causing a primary lesion on cellular DNA by binding to the bases. The

D.P. Kessissoglou (ed.), Bioinorganic Chemistry, 219-235

drug thus bound to native DNA causes both interstrand cross-linking and a partial destabilization of the DNA secondary structure.

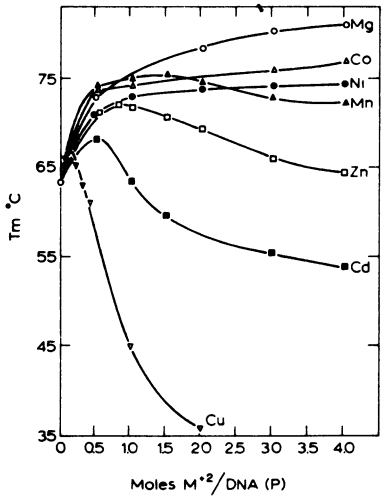

Figure 1. Variations of Tm of solutions of DNA as a function of divalent metal ion concentration.

The preference for phosphate over base association decreases in the order Mg(II)>Co(II)>Ni(II)>Mn(II)>Zn(II)>Cu(II) (Fig. 1). Also trivalent rare earth ions and hard metals in general stabilize ordered structures by binding to phosphates. The above series could be extended to include softer heavy metal ions. In the presence of Pb(II), Au(III), Pt(II), Pt(IV) or Rh(III), the melting temperature of DNA is substantially lowered. Heavy metal ions may therefore be placed to the right of the above series[7,8].

Several ruthenium complexes have been shown to inhibit cellular DNA synthesis in vitro at a level similar to that of *cis*-$Pt(NH_3)_2Cl_2$ and have shown antitumour activity in animal studies. Compounds containing pentammine-ruthenium(II) and (III) have been shown to inhibit DNA synthesis functioning, probably by binding to DNA. It has been observed that large complex cations that are strongly bound to phosphates stabilize the double helix very effectively[7]. The $[Co(NH_3)_6]^{3+}$ cation has been found to increase the Tm of poly(I-C) by about 50°C for high metal ion concentrations. However, a biphasic melting appears for low metal ion concentrations, attributed to cations moving from melted polynucleotide regions to double helix regions so that the uncomplexed helix melts at a lower temperature than the complexed[7,9]

A biphasic melting has also been observed in the case of $[Al(H_2O)_6]^{3+}$ interaction with DNA[8] and in the case of *cis,trans*-$[Pt(NH_3)_2Cl_2]$[10,11] interaction with poly(dA-dT). This has been explained by the subsequent melting of uncomplexed and complexed regions.

Of the various rhodium complexes studied for mutagenic activity, *cis*-$[Rh(en)_2Cl_2]Cl$ with a charge of +1 and two leaving groups of suitable lability has given positive results, while $[Rh(NH_3)_5Cl]Cl_2$ with one leaving group and a charge of +2 has given negative results[12]. Erck et al.[13] have studied the interaction of $Rh_2(acetate)_4$ with various polynucleotides for relatively short interaction times and have found that binding occurs with denatured DNA and poly-A, while there is no extensive binding with poly-G, poly-C and double helical DNA (A=adenine, G=Guanine, C=cytosine). The observed cytostatic

effect of this complex has been attributed to inhibition of DNA and RNA polymerases due to reaction with the -SH groups of the enzymes[14].

The interaction and conformational changes of various heavy metal ions among them Ru(II), Ru(III), Rh(II), Rh(III) systems with DNA is presented[15-19].

2. Results and discussion

2.1 THE INTERACTION OF RUTHENIUM(III)-CHLORIDE SYSTEM WITH DNA

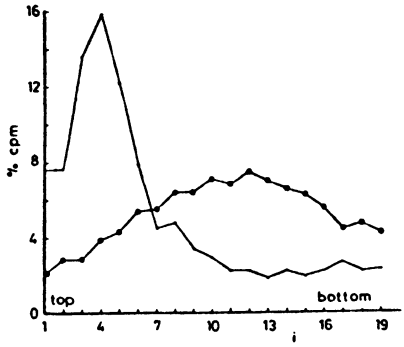

Figure 2. Density gradient from ultracentrifugation experiments. • DNA solution,° DNA -$RuCl_3$ solution.

2.1.1 *Sedimentation experiments.* In Figure 2 are presented the results of the sedimentation experiments. We observe for DNA solutions that DNA molecules with high molecular weight appear in the upper fractions of density gradients. On the contrary, DNA-$RuCl_3$ solutions indicate that the molecules with the higher molecular weight correspond to middle and lower fractions of the density gradients. Also, the ratio of the average molecular weight of DNA in $RuCl_3$ solution to the average molecular weight of DNA alone in solution is 2.2.

Thus from the distribution of molecular fractions in the sedimentation experiments and the increase of the average molecular weight of DNA in $RuCl_3$ solution, we conclude that the DNA is interacting with the Ru(III) ions.

2.1.2. *Electronic spectra.* $RuCl_3$ in the presence of chloride ions ($1x10^{-2}$ M NaCl) exhibits an absorption spectrum in the region 350 to 560 nm with maxima at 379, 460 and 552 nm characteristic of Ru(III) ions in water solution at concentrations between 5 x 10^{-4} and $1x10^{-3}$ M in the pH region 6.5 to 6.7. Several chlorohydroxy derivatives must exist in equilibrium in this pH region[20]. Spectra of unbuffered solutions or buffered citrate solutions exhibit no significant differences at these concentrations. The respective spectra in the presence of DNA at 25°C showed a decrease in absorption maxima and a shift of the bands in the visible spectrum. The observed changes are not very significant and indicate that Ru(III) does not interact with the bases at room temperature. The decrease in

absorbance observed could be interpreted as a decrease in effective metal ion concentration due to interaction with phosphates.

The conclusion that Ru(III) interacts with the phosphates at room temperature is further supported from the ultraviolet spectra of Ru(III)-DNA solutions. Ultraviolet spectra of Ru(III)-DNA solutions that were taken using in the reference cell concentration of the metal ion in the same as in the sample cell do not show any change in the 258 nm DNA band. The absorbance of these solutions is greater than in the respective DNA-NaCl solutions and is increasing with the r value.

The ultraviolet spectrum of DNA, as is well known, shows a maximum at 258 nm. The position of this maximum remains unchanged by the addition of Cu(II) ions at 25°C, but on increasing the temperature there was a small shift in the maximum towards longer wavelengths and an increase in the absorption due to decrease in hypochromicity.

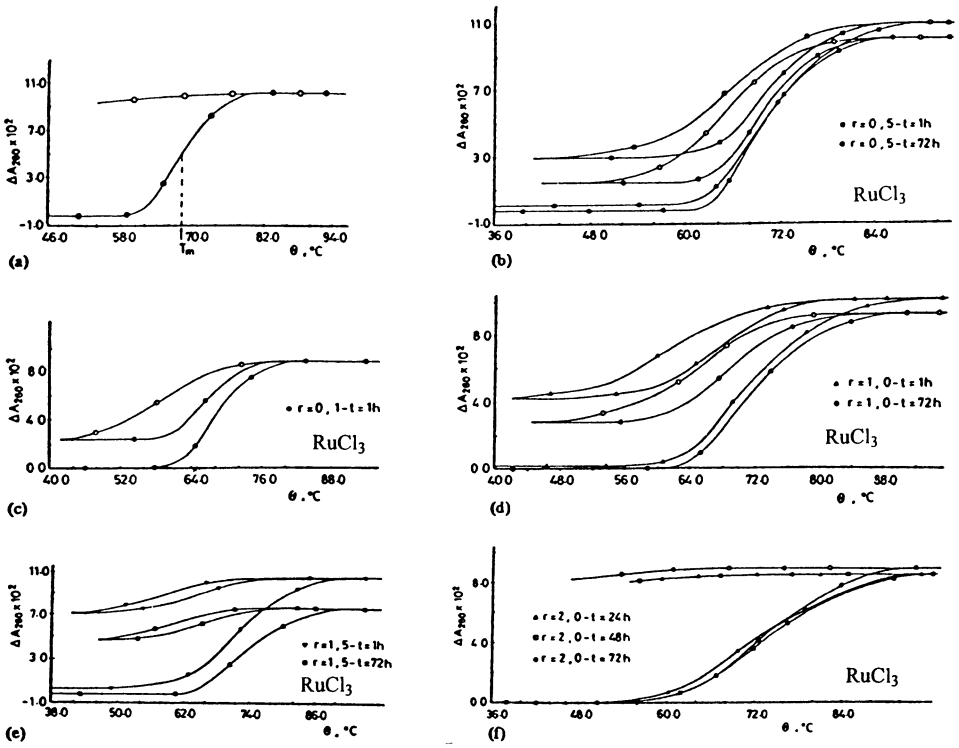

Figure 3. Melting behaviour of Ru(III)-DNA solutions. [DNA] = 5 x 10^{-5} M(P) in 1 x 10^{-2} M NaCl, r = Ru(III)/ [DNA], λ = 260 nm. •, Closed and o, open symbols are found on heating and cooling curves respectively.

It was concluded that Cu(II) ions at room temperature bind to phosphate sites only, but at higher temperatures when some relative motion of the two strands, in the DNA helix is possible, such as occurs at the "annealing temperature", penetration of the helix by the

Cu(II) ions can occur, which results in binding of the Cu(II) ions to nitrogen atoms of the bases[20].

This was further evidenced by the increased absorption and the blue shifting of the bands in the visible region of the spectrum caused by stronger ligand field of the nitrogen derivatives on coordination to Cu(II)[22,23] . Similar effects were observed in the ultraviolet and visible part of the spectrum with Au(III)[24] and cis-$Pt(NH_3)_2Cl_2$[25,26] and these changes were interpreted as being due to reduction of stacking interactions of the bases, disruption of hydrogen bonds between base pairs and interaction of the metal ions with the nitrogen of the bases.

The ultraviolet spectra of Ru(III)-DNA solutions that were heated up to 37°C remained unaltered, indicating that no observable reaction with the bases takes place up to this temperature. However, the ultraviolet spectra of dilute Ru(III)-DNA solutions that had been previously heated to 75°C and then cooled to room temperature exhibit an increased absorption and a shifting to longer wavelengths. Thus during thermal denaturation close to or at the "annealing temperature", some interaction takes place at an earlier stage of the denaturation process. This type of interaction, however, seems to be quite strong since it remains even after the solution is cooled. Ru(III) ions most probably form interstrand cross-links with the DNA at room temperature in a manner similar to that observed for cis-Pt(II) [25,26].

2.1.3. *Heating and cooling curves.* Figure 3a represents the well-known heating and cooling curves of DNA at low ionic strength (0.01 M NaCl). The melting temperature, Tm, is 67°C and the transition is relatively noncooperative. Cooling of the denatured DNA produces a slight decrease in absorbance due to randomized restacking. Figures 3b-3f represent the heating, cooling and reheating curves of DNA at different metal ion concentrations and in Table I are summarized the melting temperatures at various r values. We observe that the melting temperatures, Tm, of Ru(III)-DNA solutions are increased during the first heating with increasing concentration of the metal ion and in all cases are higher than the Tm of DNA alone. Thus, Ru(III) ions behave in the manner to be expected for metal ions that bind exclusively to phosphate[27]. The negative charges on the phosphate groups of native DNA repel each other and tend to unwind the molecule unless counterions are present. The more such counterions there are, the lower the tendency to unwind. Thus, the higher the Ru(III) concentration, the higher the melting temperature of DNA.

Figure 4 shows the change in Tm with increasing concentration of Ru(III) during the first heating at various times. We observed that in all cases equilibrium is attained rather quickly. This conclusion is also supported from the electronic spectra of these solutions at room temperature.

From the cooling curves of 3b-3f we observe a decrease in absorbance depending on the r value. The decrease in absorbance is greater for small values of r. At high r values the decrease in absorbance of the cooling curves is small and for r = 2 the decrease becomes minimal.

Eichhorn et al.[4] observed that Co(II) and Ni(II) increase the Tm with increasing metal ion concentration and the absorbance decreases for high values of r on cooling. It was suggested that Co(II) and Ni(II) interact with the phosphates for small values of r; however, at high r values Co(II) and Ni(II) also interact with the bases. Thus the addition of sufficient Co(II) or Ni(II) allows some of the metal to hold complementary bases in reverse during heating, so that rewinding can occur on cooling. The melting behaviour of Zn(II) and Mn(II) suggested that these ions bind to DNA both from the phosphate and from the bases.

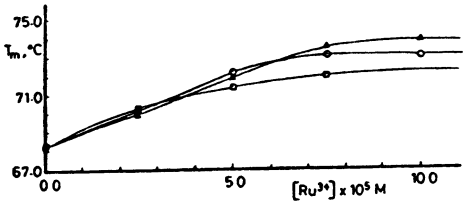

Figure 4. Tm dependence as a function of metal ion concentration at various times, during the first heating. □ t = 1 h, o t = 24 h, Δ t = 72 h.

Thus, Zn(II) and Mn(II) are capable of base interaction to such an extent that a large proportion of double-stranded DNA appears to be regenerated on cooling.

Table I. Melting temperatures of DNA-$RuCl_3$ solutions

t(h)	r				
	0.1	0.5	1.0	1.5	2.0
1	1st 68.0	1st 70.3	1st 71.4	1st 72.0	
	2nd 68.0	2nd 70.3	2nd 67.7	2nd 64.6	
24		1st 69.6	1st 72.2	1st 73.1	1st 73.0
		2nd 69.2	2nd 68.8	2nd 65.8	
48		1st 70.2	1st 70.7	1st 72.4	1st 73.7
		2nd 69.8	2nd 67.6	2nd 65.0	
72		1st 69.6	1st 71.9	1st 73.5	1st 73.9
		2nd 69.8	2nd 69.0	2nd 65.2	

From the melting curves (Figs. 3b-3f), we conclude that Ru(II) is interacting with the phosphate at room temperatures; however, at elevated temperatures it is also interacting with the bases of DNA. The phosphate interaction is dominant in all cases since the Tm is increasing for all values of r. However, for small values of r a portion of the metal ion during denaturation holds the two chains in close proximity so that the double helix is regenerated on cooling. This phenomenon is similar to that observed for high r values as opposed to our case in which this was observed for small values of r. Also, for Cu(II) and *cis*-Pt(II) the interaction of these metals with the bases of DNA starts about 37°C; for Ru(III), however, this interaction becomes apparent at much higher temperatures. most probably when most of the DNA is close to melting. These conclusions were also supported from the electronic spectra of Ru(III)-DNA solutions, which do not show any drastic changes when they were heated up to 40°C. Thus, it seems to be preferential binding of Ru(III) to the bases of single-stranded DNA versus double-stranded DNA; steric reasons most probably indice this preferential binding. For small values of r the metal ion concentration is enough to hold the two strands in close proximity and leave enough positions of the bases free to cause rewinding on cooling. Ru(III) ions interact strongly with the bases so that the bonds remain intact on cooling. These conclusions are strongly supported from the electronic spectra of Ru(III)-DNA solutions that had been previously melted and then cooled to room temperature. Thus, in these cases interstrand

cross-linking is proposed to be primarily responsible for the renaturation procedure. Also, an amount of the metal ion that is bound to phosphate is acting cooperatively on cooling in a manner similar to the addition of solid electrolyte observed for the rewinding of DNA in the presence of Cu(II) and Cd(II)[3].

In Table II is presented the percentage of renaturation of DNA as was calculated from the relative hypochromicity of the solutions on cooling[25,26]. We observe that the percentage of renaturation is increasing with time for a certain r value. This is may be due to increased interaction of the metal ion with the phosphate groups, thus leaving a greater number of free bases for renaturation. This is in accordance with our previous statement that Ru(III) ions are preferentially bound to phosphates.

Table II. Percentage renaturation of DNA-$RuCl_3$ solutions

t(h)	r			
	0.1	0.5	1.0	1.5
1	78	73	60	33
24		76	63	34
48		85	65	35
72		86	70	37

From Figures 3b-3f we observe that at high metal ion concentrations (r = 1, 1.5, 2) renaturation is reduced for steric reasons since quite a few positions of the bases are now blocked from Ru(III) ions, forming intrastrand crosslinks.

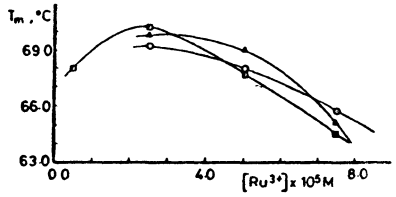

Figure 5. Tm dependence as a function of metal ion concentration at various times, during the second heating. □ t = 1 h, o t = 24 h, Δ t = 72 h.

Pascoe and Roberts[28] demonstrated that only 1 out every 400 reactions of cis-Pt(II) to Hela cell DNA was a cross-link and only 1 out of every 4000 reactions with trans Pt(II) was a cross-link. Thus, it is reasonable to assume that the single-stranded reactions of Ru(III) with the DNA bases dominate over cross-linking reactions. Renaturation at high r values is now inhibited because of the increased probability that the reaction with the opposite strand would be blocked due to the presence of another monofunctionally bound Ru(III) molecule at that site. In Table I and in Figures 3b-3f we observe that the Tm values during the second heating coincide with those of the first heating only for small values of r. In Figure 5 is presented the change in Tm with increasing metal ion concentration during the second heating.

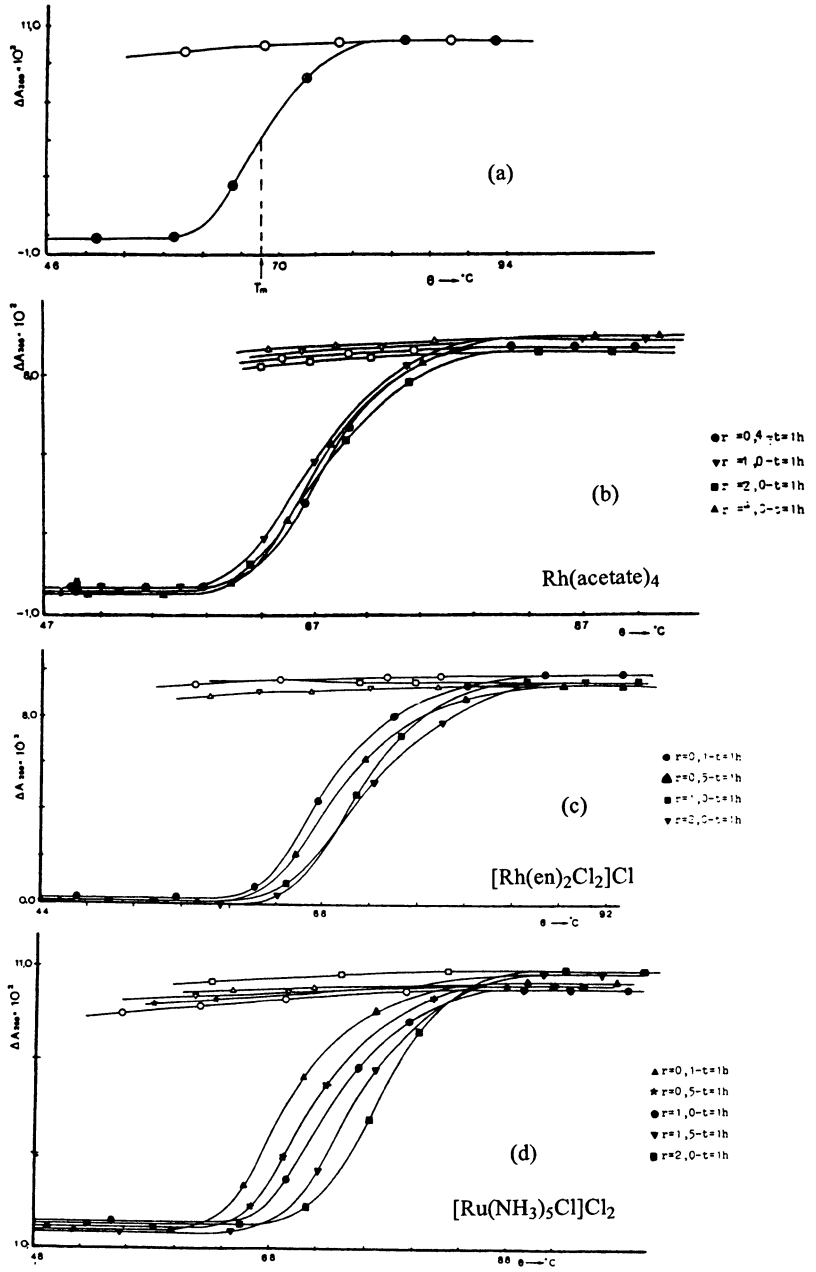

Figure 6. Melting behaviour of complex ions-DNA solutions. (a-d) DNA 5.0 x 10^{-5} M, NaCl 0.01 M, l=1.0 cm, λ=260 nm; (b-d) Rh(II), (III) in mole ratios to DNA shown. •Closed symbols are found on heating curves; _o open symbols are found on cooling curves.

The Tm is decreasing with increasing r value. This can be explained by the fact that during the second heating the cross-linked Ru(III)-DNA facilitates the interaction of Ru(III) ions with the bases of the DNA, thus decreasing the Tm with increasing r values.

In conclusion, Ru(III) is interacting with the phosphate moieties of DNA and only at denaturation temperatures starts to interact with the nitrogen of the bases forming interstrand cross-links responsible for the renaturation process. However, this occurs only for small values of r. Steric hindrance probably inhibits the renaturation procedure for high r values. The interstrand cross-links persist even at room temperature and are primarily responsible for the decrease in melting temperatures during the second heating.

2.2 THE INTERACTION OF Rh(II) AND Rh(III) WITH DNA

Electronic spectra of the complex ions $[Rh(en)_2Cl_2]Cl$ (en=ethylenediamine) and $[Rh(NH_3)_5Cl]Cl_2$ remain practically unchanged upon interaction with DNA. The initial bands of $[Rh(en)_2Cl_2]Cl$ at 353 and 293 nm and of $[Rh(NH_3)_5Cl]Cl_2$ at 345 and 270 nm change only slightly in intensity in the presence of DNA, while there is no shifting of the wavelength. The above observations are true for the r = 5.0, r = 10.0 values and for 1-24 h interaction times.

However in the case of $Rh_2(acetate)_4$ the initial bands of the complex at 585 and 445 nm are almost doubled in intensity in the presence of DNA after 24 h or longer interaction time. A similar observation has been made with Cu(II) which is known to interact with DNA through phosphate as well as base binding[29].

The absorption band of DNA at 285 nm which was attributed to electronic transitions on the nucleic acid bases[3] is not shifted in the presence of the two complex ions studied for the r values 0.2-2.0 and the r values 0.4-4.0 for $Rh_2(acetate)_4$ and for interaction times up to 24h. This implies that a possible interaction of the complexes with DNA does not include the bases of the double helix, at least under the above mentioned conditions.

Heating of the complexes solutions up to 90°C does not affect the 260 nm absorbance value of the solutions, thus showing stability of the complexes during the heating process of the Tm experiments (Fig. 6).

Characteristic heating and cooling curves of DNA in the presence of the complex ions studied are shown in Figures 6a-6d. The Tm values of $[Rh(en)_2Cl_2]^{+1}$, $[Rh(NH_3)_4Cl]^{+2}$-DNA solutions are higher than the Tm value of DNA in presence of Na^+ 1.0×10^{-2} M (Tm = 68.2°C) and increase with metal ion concentration. This fact is also clearly shown in Figures 7a and 7b which represent the Tm values as a function of metal ion concentration. This behaviour is consistent with metal ion interaction with the phosphate moieties of the double helix leading to stabilization of it[4,27,30,31], which is greater as the number of metal ions increase in solution.

The higher Tm values for longer interaction times, t = 24 or 48 h, (Fig. 6) are attributed to increased stability of the double helix due to rather slow equilibrium as well as to a possible conformational change of the helix after the binding of some metal ions on it, making the binding of additional ions easier. Several metal ions interacting rather slowly with DNA have already been mentioned as Au(III)[24], Rh(III)[32] while others interact faster as Hg(II)[33] and Ru(III) [15]. Cooling curves (Fig. 7) show no significant decrease in absorbance values, as expected by DNA in the presence of metal ions such as Mg^{+2} which interact only with the phosphate moieties[4], so that DNA is rewound upon cooling.

The Tm values for $[Rh(NH_3)_5Cl]^{+2}$ ion are higher than $[Rh(en)_2Cl_2]^{+1}$ for the same r value due to higher stabilization of the double helix in the presence of divalent as compared with monovalent cations.

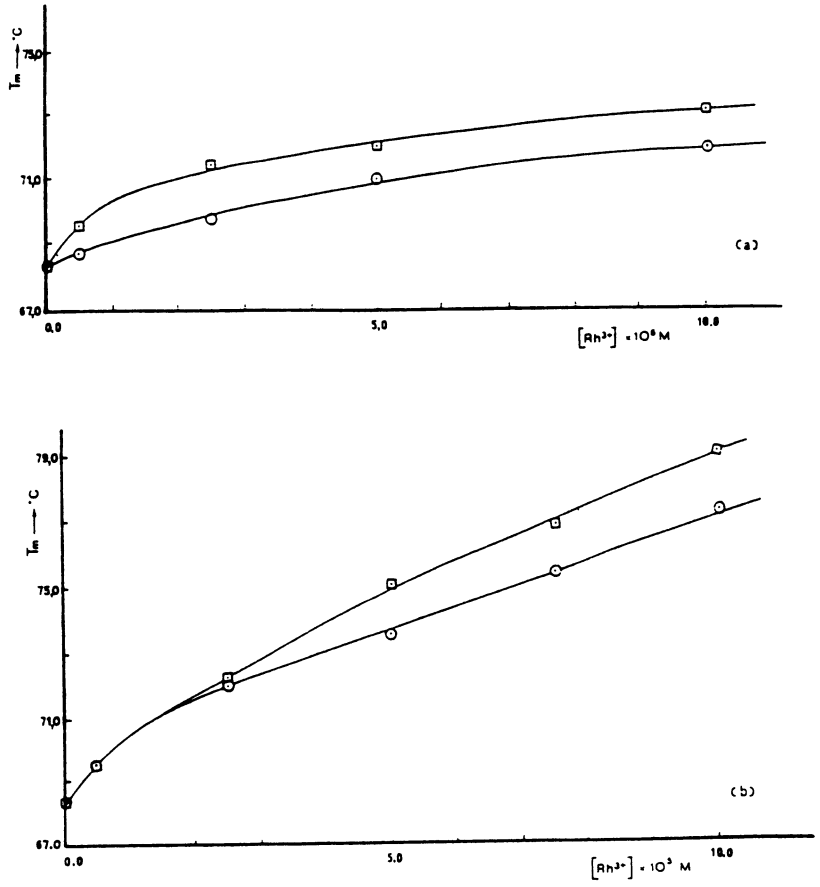

Figure 7. Tm dependence as a function of metal ion concentration. (a) cis-$[Rh(en)_2Cl_2]^{+1}$: o t = 1 h, □ t = 24 h; (b) $[Rh(NH3)_5Cl]^{+2}$: o t = 1 h, □ t = 24 h.

Tm values of DNA do not differ in absence or in presence of $Rh_2(acetate)_4$ for the various concentration values and interaction times with the exception of r = 4.0 at t = 48 h where there is a Tm value decrease. The above data imply that $Rh_2(acetate)_4$ does not change the Tm of DNA under the conditions studied. For relatively high r values and long interaction time the complex destabilizes the double helix, as concluded by the Tm value decrease, characterizing metal ion binding to nucleic acid bases which disrupts hydrogen bonding and stacking interactions[27,34]. It may be assumed that, as the temperature increases, even the small number of unpaired DNA bases present, makes possible the metal ion-nucleic acid base interaction which disrupts further hydrogen bonds

destabilizing the DNA structure and lowering the Tm value. A similar case has been observed with Cu(II) [29].

In order to elucidate the interaction of DNA with $Rh_2(acetate)_4$ sedimentation through an alkaline sucrose gradient was employed. The results showed that in presence of $Rh_2(acetate)_4$ the distribution is shifted to lower fractions of density gradient while the distribution for DNA lies on middle to upper fractions. This is attributed to an increase of the DNA average molecular weight due to interaction with the complex.

In conclusion, the complex ions *cis*-$[Rh(en)_2Cl_2]^{+1}$ and $[Rh(NH_3)_5Cl]^{+2}$, which have already been studied for mutagenicity[12], cause stabilization of the double helix after interaction with the phosphate groups. The complex $Rh_2(acetate)_4$ interacts with DNA bases for relatively high metal ion concentration and long interaction time, while under different conditions no interaction with DNA is observed. This conclusion is consistent with previous studies[13] explaining the cytostatic action of the complex by inhibition of DNA and RNA polymerases.

2.3 THE INTERACTION OF $[Ru(NH_3)_5Cl]^{+2}$ AND $[Ru(NH_3)_6]^{+3}$ IONS WITH DNA

2.3.1. *Electronic spectra.* Electronic spectra of the complex ions in solution change upon heating in the absence as well the presence of DNA, but the two modes of change differ. The absorption peak of $[Ru(NH_3)_5Cl]^{+2}$ ion at 328 nm moves to 297 nm after heating the solution to 85°C in 1 h and there appears a significant absorption at 258 nm. However, when DNA is present (r = 1.0), the initial absorption peaks at 328 and 258 nm (that are a "sum" of the peaks of metal ion and DNA) appear at 430, 350 and 258 nm after the heating process. A similar situation exists for $[Ru(NH_3)_6]^{+3}$ ion, which has an absorption peak at 267 nm before heating and at 538 and 297 nm after heating, also having a significant absorption at 258 nm, while in the presence of DNA (r = 1.0) the initial absorption peaks at 267 and 258 nm appear at 430, 350 and 258 nm after heating.

A solution obtained by mixing a metal ion solution heated to 85°C and cooled with a double-stranded DNA solution exhibits three absorption peaks after heating, namely at 430, 350 and 258 nm. However, when the preheated metal ion solution is mixed with a single-stranded DNA solution, the resulting solution (r = 1.0) has absorption peaks at 297 and 258 nm.

The spectral changes of complex ion solutions upon heating indicated a change of the absorbing complex ion. The absorption at 297 nm, which appears after heating the solutions up to 85°C, coincides with that of the $[Ru(NH_3)_5OH]^{+2}$ ion[35]. The formation of the above hydroxy complex is further supported by the pH value decrease for both complexes and by the conductivity values. Thus, the formation of the hydroxy complex from $[Ru(NH_3)_5Cl]^{+2}$ according to the reaction:

$$[Ru(NH_3)_5Cl]Cl_2 + H_2O \_\rightarrow [Ru(NH_3)_5OH]Cl_2 + Hcl$$

causes a pH decrease due to HCl formation, which is also responsible for the conductivity value increase, although the complex ion remains a 1:2 electrolyte. Also the formation of the hydroxy complex from $[Ru(NH_3)_6]^{+3}$ according to the reaction:

$$[Ru(NH_3)_6]Cl_3 + H_2O \rightarrow [Ru(NH_3)_5OH]Cl_2 + NH_4Cl$$

produces NH_4Cl, causing a pH decrease and practically no change in the conductivity value, although the initial 1:3 electrolyte gives a 1:2 electrolyte upon heating. The

formation of $[Ru(NH_3)_5OH]^{+2}$ ion, which absorbs at 297 nm, also explains the absorbance increase at 260 nm upon heating.

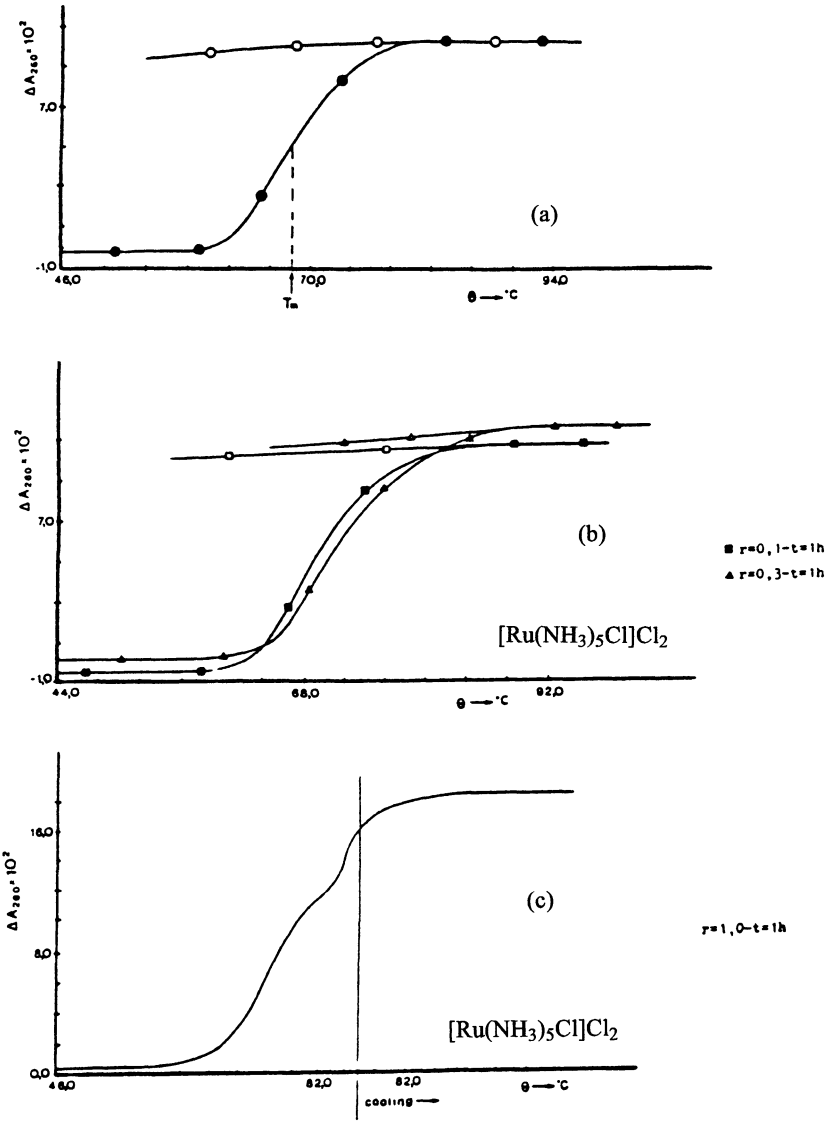

Figure 8. Melting behaviour of complex ion-DNA solutions. (a-f) [DNA] = $5x10^{-5}$ M, [NaCl] = 0.01 M; λ = 260 nm (b-f) Ru(III) in mole ratios to DNA shown. (d) Ru(III) complex preheated before addition.

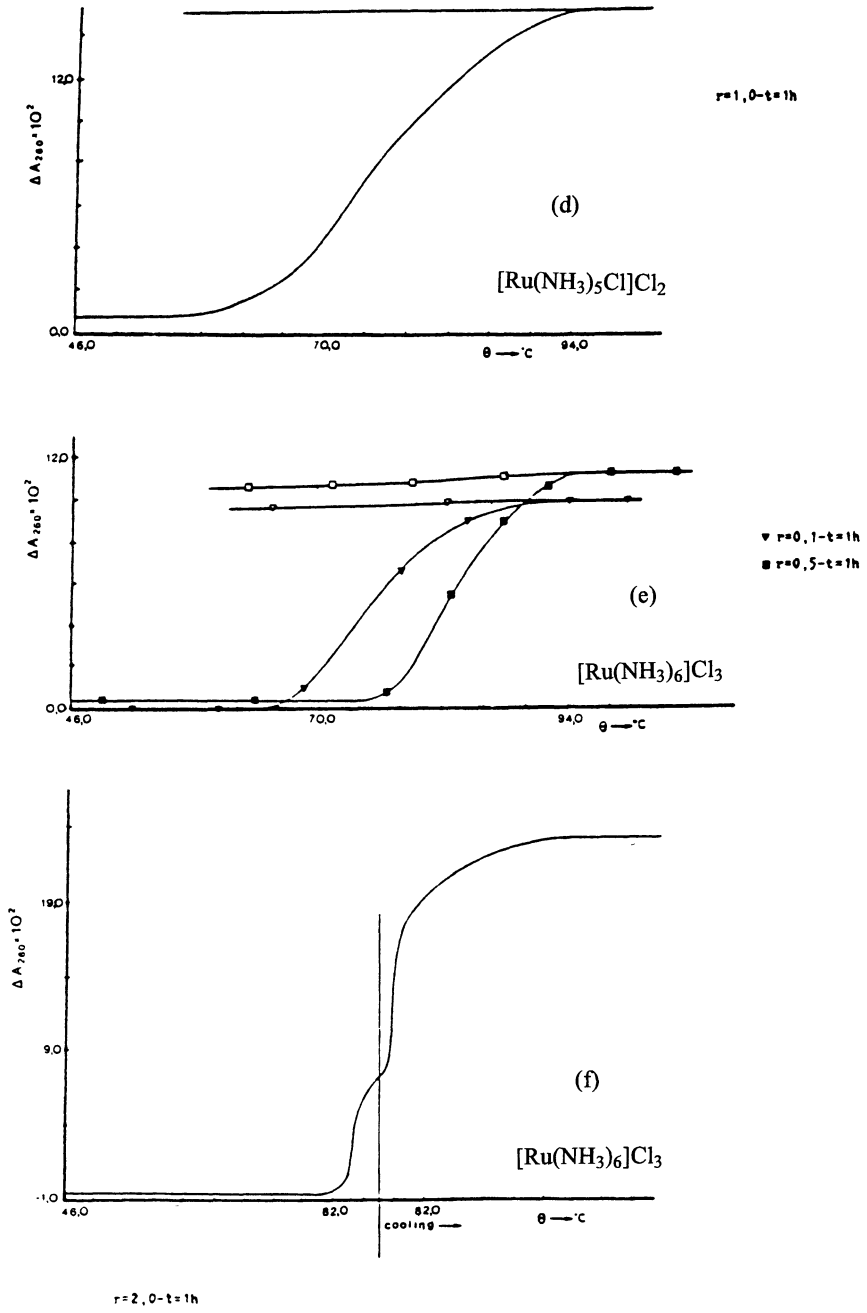

Figure 8. *Continued.* Closed symbols are found on heating curves; open symbols are found on cooling curves.

The above mentioned data indicate that the initial complex ions $[Ru(NH_3)_5Cl]^{+2}$ and $[Ru(NH_3)_6]^{+3}$ are transformed to the $Ru(NH_3)_5OH]^{+2}$ ion upon heating to 85°C. This hydroxy complex reacts preferentially with double-stranded DNA, resulting in absorptions at 430, 350 and 258 nm, as the interaction of the hydroxy complex with single-stranded DNA results in absorptions at 297 and 258 nm that correspond to the hydroxy complex and DNA, respectively and remain unchanged after reaction.

2.3.2. *Heating and cooling curves.* Figure 8a shows the heating and cooling curve of DNA at low ionic strength (0.01 M NaCl), with a Tm value of 68.2°C. Cooling causes only a slight decrease of absorbance, due to random stacking[3]. Figures 2b through 3g represent some of the heating and cooling curves of metal complex-DNA solutions at various r values and interaction times. The above data show a Tm value increase caused by $[Ru(NH_3)_5Cl]^{+2}$ in the r range 0.1-0.3 and by $[Ru(NH_3)_6]^{+3}$ in the r range 0.1-0.5 and the increase is greater as the concentration of metal ion increases. Also, cooling of the solutions does not cause any important absorbance decrease. The above are indicative of double-stranded DNA stabilization[2,30,31] due to metal ion-phosphate interaction.

A different situation exists at higher r values, namely r = 0.5 for $[Ru(NH_3)_5Cl]^{+2}$ and r = 1.0 for $[Ru(NH_3)_6]^{+3}$. where melting is biphasic. The first melting curve ends at 85°C and then the second melting curve begins; the second curve ends upon cooling the solutions. It should be noted that in Figure 8, the absorbance change due to hydroxylation reaction has been substracted by calculation at each temperature value. Figures 8c and 8f depict the biphasic melting for r = 1.0 and r = 2.0 in the presence of $[Ru(NH_3)_5Cl]^{+2}$ and $[Ru(NH_3)_6]^{+3}$, respectively, where biphasicity is more pronounced than for r = 0.5 and r = 1.0, where it first appears.

Because the solutions of the complex ions remain unchanged at temperature values lower than 85°C, it is concluded that the first melting curve in the Tm experiments may be considered to be caused by the initial complex ions $[Ru(NH_3)_5Cl]^{+2}$ and $[Ru(NH_3)_6]^{+3}$. The Tm values and the Tm representation as a function of metal ion concentration (Fig. 9) are explained by metal ion interaction with the phosphate groups of DNA. The higher Tm values for $[Ru(NH_3)_6]^{+3}$ ion than for $[Ru(NH_3)_5Cl]^{+2}$ ion are attributed to the first ion's higher charge[3]. Also, longer interaction times between metal ions and DNA do not greatly change the Tm values, so that a rather fast equilibrium may be suggested.

Regarding the second melting curve, the electronic data, pH values and conductivity measurements should be taken into consideration.

A few cases of biphasic melting have already been reported. In the case of cis, trans $[Pt(NH_3)_2Cl_2]$ interaction with poly(dA-Dt)[10,11], the first melting occurs at a low temperature identical to that of the free macromolecule, while the second melting occurs at a higher temperature. It is suggested that the macromolecule free-metal regions melt at a low temperature and that platinum-bound regions melt at a higher temperature, due to stabilization of the double helix. This explanation is not true for the $[Ru(NH_3)_5Cl]^{+2}$ and $[Ru(NH_3)_6]^{+3}$ complex ions, as there are two high-temperature melting curves in their case compared to the Tm of DNA in presence of Na^+ 10^{-2} M.

The $[Co(NH_3)_6]Cl_3$-DNA interaction[7] is another example of biphasic melting that has been attributed to metal ion binding preferentially to double- over single-stranded DNA, thus resulting in metal ion migration from single- to double-helix sites with subsequent increase of the "effective" r value and presentation of a biphasic melting curve. The appearance of the second melting curve for r = 0.5 and r = 1.0 for the complex ions $[Ru(NH_3)_5Cl]^{+2}$ and $[Ru(NH_3)_6]^{+3}$, respectively, is attributed to the formation of

$[Ru(NH_3)_5OH]^{+2}$ ion, as indicated by electronic spectra, pH values and conductivity measurements.

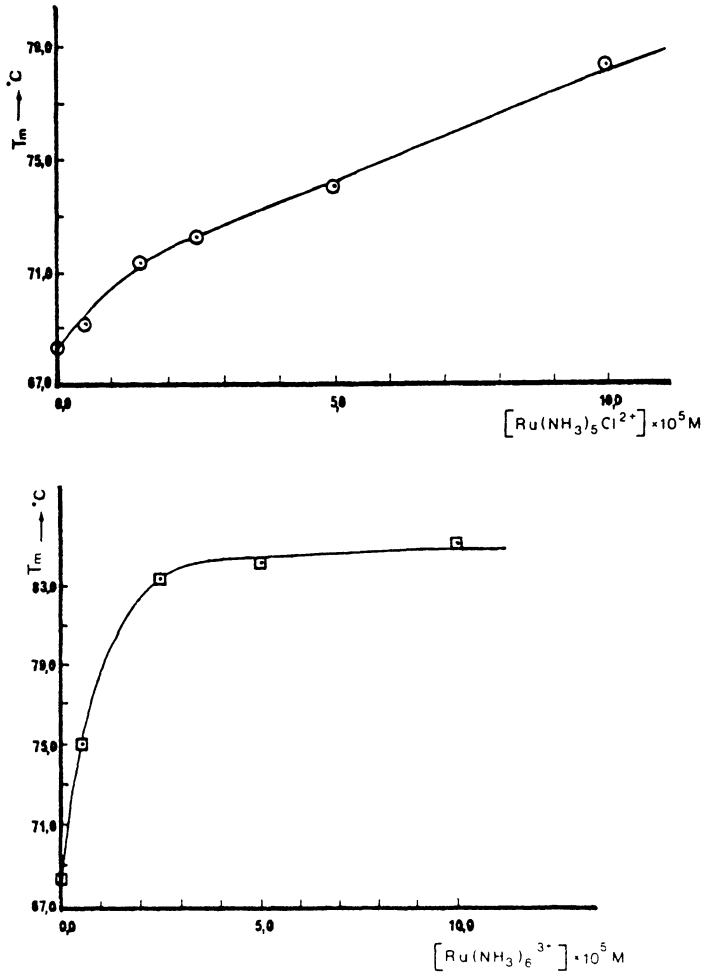

Figure 9. Tm dependence as a function of metal ion concentration at t = 1 h.

The complex ion formed binds preferentially to as-yet-unmelted double-stranded regions of the DNA, so that the respective sites of the macromolecule are stabilized and melt at a higher temperature, giving the second melting curve. The hydroxy complex that is formed at high temperatures attains an appreciable concentration at these temperatures and only then interacts with DNA, thus causing the biphasic melting.

The monophasic melting for low r values (r = 0.1-0.3 for $[Ru(NH_3)_5Cl]^{+2}$ and r = 0.1-0.5 for $[Ru(NH_3)_6]^{+3}$ at 24 and 48 h interaction time indicates that bound initial Ru complexes do not become hydroxylated.

The $[Ru(NH_3)_5OH]^{+2}$ preferential binding to double- rather than single-stranded DNA is confirmed by comparing the spectrum of the ion with single-stranded DNA with the spectrum of the ion with double-stranded DNA. The absorptions of the complex ion at 297 nm and of DNA at 258 nm remain unchanged after reaction in the first case, while in the second case they appear at 430, 350 and 258 nm.

The stabilization of DNA double helix upon interaction with $[Ru(NH_3)_5OH]^{+2}$ is shown by the heating and cooling curves (Fig. 8d) obtained when a solution of DNA is mixed with $[Ru(NH_3)_5OH]^{+2}$ solution that has been formed by heating solutions of the initial complexes to 85°C. The melting is monophasic. The increase in the Tm value of DNA is attributed ti the hydroxy complex-phosphate moieties interaction.

For low r values the melting is monophasic because the initial complex ion present interact almost completely with DNA and there is no hydroxy complex formed.

In conclusion $[Ru(NH_3)_5Cl]^{+2}$ and $[Ru(NH_3)_6]^{+3}$ interact at low r values with the phosphate groups of the DNA helix, causing stabilization of the helix. For relatively high values of r, biphasic melting occurs, the first phase of which is attributed to the initial complexes, while the second phase is attributed to the $[Ru(NH_3)_5OH]^{+2}$ ion, which is formed at high temperature from the amount of the initial complexes still not having interacted with DNA and interacts with DNA at this high temperature. Both phases of melting correspond to stabilization of the DNA helix, due to metal ions' interaction with the phosphate groups.

3. References

(1) Shack, J.;Jenkins, R.J. and Thompsett, J.M., *J.Biochem.,* **1953**,*203*,373.
(2) Thomas, R., *Trans.Faraday Soc.,* **1954**,*50*,304.
(3) Eichhorn, G.L., in "*Inorganic Biochemistry*", G.L. Eichhorn (ed.), Elsevier, New York, **1973**,p.1210.
(4) Eichhorn, G.L. and Shin, Y.A.,*J. Am.Chem.Soc.,* **1968**,*90*,7323.
(5) Rifkind, J.M.,Shin, Y.A., Heim J.M. and G.L. Eichhorn, G.L., *Biopolymers,* **1976**,*15*,1879.
(6) Shin, Y.A. and Eichhorn, G.L., *Biochemistry,* **1968**,*7*,1026.
(7) Karpel, R.L., Bertelsen, A.H. and Fresco, J.R., *Biochemistry,* **1980**,*19*,504.
(8) Karlic, S.J., Eichhorn, G.L., Lewis, P.N and Chapper, D.R.,*Biochemistry,* **1980**,*19*,5991.
(9) Ascoli, F., Branca, M., Mancini, C. and Bispisa, B., *Biopolymers,* **1973**,*12*,2431.
(10) Canuel, L.L., Boon-Keng Teo and Patel, D.J., *Inorg.Chem.,* **1981**,*20*,4003.
(11) In-Bok Paek, Snuder-Robinson, P.A. and Boon-Keng Teo, *Inorg.Chem.,* **1981**,*20*,4006.
(12) Warren, G., Abbott, E., Schultz, P., Bennett, K. and Rogers S., *Mutation Res.,* **1981**,*88*,165.
(13) Erck, A., Rinen, L., Whileyman, J., Chang, I.M., Kimball, A.P. and Bear, J., *Proc.Soc.Exp.Biol.Med.,* **1974**,*145*,1278.
(14) Howard, R.A., Spring, T.G. and Bear, J.L., *Cancer Res.,* **1976**,*36*,4402.
(15) Tselepi-Kalouli, E. and Katsaros, N., *Inorg.Chim.Acta,* **1986**,*124*,181.
(16) Sideris, E. and Katsaros, N., *Inorg.Chim.Acta.,* **1986**,*123*,1.
(17) Sideris, E.G. and Katsaros, N. in "*Nutrition, Growth and Cancer*", Tryfiates, G.F. (ed.), Alan R. Liss Inc., New York, **1988**,p.13.
(18) Tselepi-Kalouli, E. and Katsaros, N., *J.Inorg.Biochem.,* **1990**,*39*,170.

(19) Tselepi-Kalouli, E. and Katsaros, N., *J.Inorg.Biochem.*, **1990**,*37*,27.
(20) Connick, R.E. and Fine, D.A., *J.Am.Chem.Soc.*, **1960**,*82*,4187.
(21) Eichhorn, G.L. and Clark, P., *Proc.Natl.Acad.Sci.*, **1965**,*53*,586.
(22) Coates, J.H., Jordan, D.O. and Srivastava, Y.K., *Biochem.Biophys.Res.Commun.*, **1965**,*20*,611.
(23) Zimmer, C., Luck, G., Fritzsche, H. and Triebel, H., *Biopolymers*, **1971**,*10*,441.
(24) Pillai, C.K. and Nandi, U.S., *Biopolymers*,**1973**,*12*,1431.
(25) Hardr, H.C., *Chem.Biol.Inter.*, **1973**,*10*,27.
(26) Clear, M.J., *Coord.Chem.Rev.*, **1974**,*12*,349.
(27) Eichhorn, G.L. in "*Metal Ions in Genetic Information Transfer*, Eichhorn, G.L. and Marzilli, G.L. (eds.), Elsevier, New York, **1981**,Vol.3,p.12.
(28) Pascoe, J.M. and Roberts, J.J., *Biochem. Pharmacol.*, **1974**,*23*,1345.
(29) Richard, H., Schreiber, J.P. and Daune, M., *Biopolymers*, **1973**,*12*,1.
(30) Dove, W.F. and Davidson N., *J.Mol.Biol.*, **1962**,*5*,467.
(31) Steiner, R.F. and Beers, R.F., *Bioch.Bioph.Acta*, **1956**,*32*,166.
(32) Sasi, R. and Nandi, U.S., *Current Science*, **1978**,*47*,761.
(33) Yamane, T. and Davidson, N., *J.Am.Chem.Soc.*, **1961**,*83*,2599.
(34) Felsenfeld, G. and Miles, H.T., *Ann.Rev.Biochem.*, **1967**,*36*,407.
(35) Broomhead, J.A., Basolo, F. and Pearson, R.G, *Inorg.Chem.*, **1963**,*3*,826.

THERMODYNAMICS AND KINETICS OF COMPETING REDOX PROCESSES DURING DNA CLEAVAGE: REACTIVITY-BASED SELECTIVITY

C.-C. CHENG, GREGORY A. NEYHART, THOMAS W. WELCH, JAMES G. GOLL, AND H. HOLDEN THORP
Department of Chemistry
University of North Carolina at Chapel Hill
Chapel Hill, North Carolina 27599-3290

ABSTRACT. An understanding of the competition between competing redox processes that lead to the reduction of oxidants bound to DNA presents a new framework upon which to design selective cleavage agents and to interpret the results of structural studies based upon cleaving nucleic acids with small, transition-metal complexes.

1. Background

The oxidative damage of DNA by metal complexes is of interest in pharmaceutical applications and in developing probes for nucleic acid structure in solution.[1-3] Because of recent advances in experimental methodology, it has become possible to begin understanding the mechanisms of DNA cleavage on a fundamental level.[4,5] For example, cleavage of DNA by bleomycin (BLM) has been shown to occur via activation of oxygen by Fe(II)BLM to form a high-valent species (activated BLM) that is capable of abstracting the 4'-hydrogen atom from DNA sugars. Activated BLM is also capable of self-inactivation, as indicated by the fact that repeated electrochemical activation in the absence of DNA leads to a dramatic loss in the ability of BLM to degrade DNA.[6] The presence of DNA protects BLM from self-inactivation, leading to catalytic DNA damage; however, electrochemical experiments show a decrease in catalytic current during electrochemically activated DNA degradation,[6] indicating that self-inactivation does compete with DNA cleavage to some extent.

Recent studies have shown that sequence-specific isotope effects are observed for cleavage by FeBLM.[7,8] The isotope effects are observed by selective incorporation of 4'-deuterated nucleotides in restriction fragments and comparison of the extent of cleavage for the deuterated versus unlabeled sites. The observation of such a net isotope effect is revealing with regard to the cleavage mechanism. The first step in cleavage of DNA by activated FeBLM involves binding of the activated complex to DNA. As shown in Scheme 1, the bound complex can then either cleave DNA ($k_{cleavage}$), dissociate (k_{off}), or undergo other non-productive processes such as self-inactivation (k_X). The observation of a significant isotope effect on cleavage demonstrates that cleavage must be much slower than the other processes ($k_X + k_{off}$).[8] If this was not the case, then cleavage would be observed regardless of whether a hydrogen or deuterium was abstracted.

An important point brought out by Worth et al. is that the observed isotope effect $^D(V/K)$ is a net effect determined by the relative yields on a sequencing gel of cleavage of the protio and deuterio DNA.[8] This result must be considered in light of selection against

D.P. Kessissoglou (ed.), Bioinorganic Chemistry, 237-243

other processes, so the apparent isotope effect is equal to the true kinetic isotope effect scaled by the rates of competing processes:

$$^{D}(V/K) = (k_H/k_D)[(k_D + k_X + k_{off})/(k_H + k_X + k_{off})] \quad (1)$$

The observed isotope effects are sequence-specific, which could result either from different transition-state geometries for hydrogen abstraction at different sites (i.e. different k_H/k_D) or from a dependence of k_X on the DNA sequence. We report here on a system that exhibits such a sequence-specific k_X.

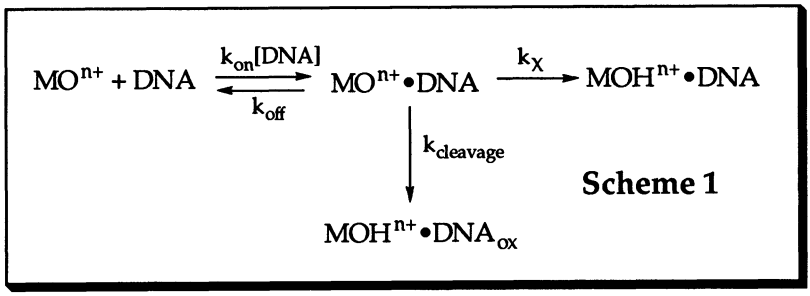

2. Oxometal Oxidants

In order to answer the questions enumerated above, a system is required where the extent and time-dependence of the reduction of the cleavage agent can be determined and correlated with an understanding of the extent and time-dependence of DNA oxidation. We have therefore chosen to study complexes based on $Ru(tpy)(bpy)O^{2+}$,[9] because this complex can be isolated in the active form and used as a stoichiometric cleavage agent (tpy = 2,2',2''-terpyridine, bpy = 2,2'-bipyridine).[10] In addition, the time-dependence of the reduction of the complex can be followed in a straightforward manner using optical spectroscopy.[11] We can therefore use existing methods to quantitate the extent of DNA oxidation by HPLC and gel electrophoresis, which we will describe below. These results can then be correlated with the known amount of oxidant that is consumed during the reaction, and in terms of Scheme 1, we can ascertain the quantity of cleavage agent that reacts via each of the $k_{cleavage}$ and k_X pathways. In this way, the efficiency with which the oxidizing equivalents are directed toward detectable DNA oxidation can be assessed. These experiments are difficult with existing catalytic cleavage agents, because the efficiency with which the catalyst is turned over by the sacrificial oxidant or activated by photolysis is difficult to quantitate. Finally, the kinetics of the metal reduction can be used to study the dynamics of the processes shown in Scheme 1 in real time.

Oxidation of $Ru(tpy)(bpy)OH_2^{2+}$ occurs in two one-electron/one-proton steps to generate ultimately the oxoruthenium(IV) species:[12]

$$Ru(II)OH_2^{2+} \rightarrow Ru(III)OH^{2+} + H^+ + e^- \quad (2)$$
$$Ru(III)OH^{2+} \rightarrow Ru(IV)O^{2+} + H^+ + e^- \quad (3)$$

The potentials for eq 2 and 3 are $E_{1/2}(III/II) = 0.49$ and $E_{1/2}(IV/III) = 0.62$ V vs SCE at pH 7. The cleavage reactions can therefore be performed stoichiometrically by isolation of $Ru(tpy)(bpy)O^{2+}$ or electrocatalytically by application of a potential of 0.8 V to a solution of $Ru(tpy)(bpy)OH_2^{2+}$.[9] Because of the proximity of the (IV/III) and (III/II) couples, the

$Ru(IV)O^{2+}$ complex is nearly as good a two-electron oxidant as a one-electron oxidant.[13] Therefore, C-H bond activation usually proceeds via hydride transfer,[14] and the complex is also reactive toward electron transfer and oxo transfer.[15] In addition, the $Ru(III)OH^{2+}$ state, which is present at long times during oxidation, reacts via hydrogen-atom transfer, although at a rate that is three orders of magnitude slower than hydride transfer by $Ru(IV)O^{2+}$.[14] Finally, the complex undergoes self-reduction analogous to that seen for FeBLM, where 10% of the ruthenium complexes are sacrificed to regenerate 90% of the original $Ru(II)OH_2^{2+}$.[16] Since all of the *reversible* redox potentials and pK_a's of the Ru(IV), Ru(III), and Ru(II) states are known, the thermodynamics of each redox pathway can be precisely determined. This is in contrast to many oxidants where, because of a catalytic mechanism involving an intermediate that cannot be isolated, the relevant thermodynamic parameters are not available.

3. DNA Cleavage Pathways

Analysis of HPLC and sequencing gels allows for the determination of the yields of the different redox pathways available to the $Ru(IV)O^{2+}$ oxidant during DNA cleavage. These reactions are best described using the model shown in Scheme 2. The sugar oxidation pathway, which probably proceeds via hydride abstraction,[5] liberates free base. Quantitation of the free base liberated shows that 10% of the total $Ru(IV)O^{2+}$ reacts via the k_{sugar} pathway.[10] However, 10% of the total $Ru(IV)O^{2+}$ represents a 20% yield based on a two-electron oxidation, because half of the $Ru(IV)O^{2+}$ is consumed via comproportionation to form $Ru(III)OH^{2+}$, which reacts on a much longer time scale than $Ru(IV)O^{2+}$.[14] On sequencing gels, the sugar oxidation pathway leads to about one-third frank scissions and two-thirds piperidine-labile scissions. Some frank scission products exhibit a metastable modified terminus. The sugar oxidation products and termini apparent on sequencing gels are consistent with oxidation at the 1' position, as seen for Cu-phenanthroline.[17]

Using the 20% yield of k_{sugar} as a basis, it is possible to calculate the yield of guanine oxidation, which occurs via an inner-sphere oxo transfer pathway. Guanine oxidation leads to piperidine-labile cleavage specifcally at guanine.[18] From the relative yields of guanine oxidation and oxidation at the other nucleotides, it can be shown that about 30% of the total $Ru(IV)O^{2+}$ is reduced via the k_G pathway. The remainder of the $Ru(IV)O^{2+}$ does not lead to detectable DNA oxidation products, implying that this fraction undergoes the characterized self-reduction pathway (k_X).

The relative yields of self-reduction, guanine oxidation, and sugar oxidation imply that $k_X > k_G > k_{cleavage}$. Two results support this ordering. First, sugar oxidation by $Ru(tpy)(bpy)O^{2+}$ yields an equal amount of all four nucleic acid bases, implying that there is no selectivity for a particular base. However, oxidants that are weaker by ~100 mV only release thymine from analogous oxidations.[10] This implies that there is a thermodynamic preference for oxidation of thymidine sugars, which also supports a 1' oxidation mechanism.

In addition, this result suggests that the k_{sugar} pathway is sufficiently demanding thermodynamically that tuning the potential leads to increased selectivity. Second, using an even weaker oxidant, $Ru(tpy)(bpy)OH^{2+}$, leads to guanine oxidation (only about 10% of that seen with $Ru(IV)O^{2+}$) and no sugar oxidation. Both the $Ru(IV)O^{2+}$ and $Ru(III)OH^{2+}$ are completely isostructural, so this effect must arise from a change in thermodynamics. This strongly supports the notion that $k_{sugar} > k_G$ and that these rates are thermodynamically controlled.

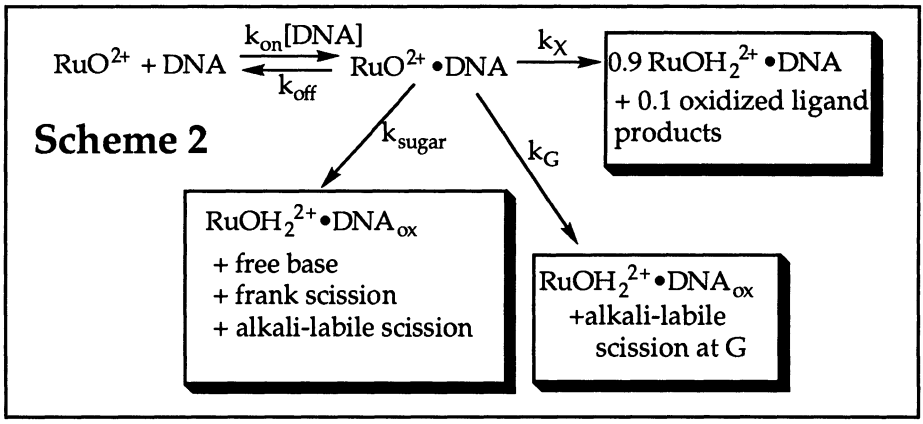

Finally, an even weaker oxidant, $Os(tpy)(bpy)O^{2+}$, can be prepared, and its crystal structure shows that it is isostructural with the ruthenium analogue. This complex is rapidly reduced in DNA but no DNA oxidation is apparent in sequencing gels or by HPLC. This implies that the complex reacts only via the k_X pathway. The kinetics of Os reduction therefore reflect directly the dynamics of k_X. The reduction dynamics are single exponential, first-order in DNA, and zero-order in osmium. These observations are consistent with the rate-limiting step being binding of osmium to the nucleic acid, which goes as k_{on}[DNA]. (The kinetics of $Ru(IV)O^{2+}$ reduction are much more complex, which is consistent with multiple reduction pathways.[11]) Furthermore, it can be shown using the kinetics that the rate of self-reduction of $Os(tpy)(bpy)O^{2+}$ is accelerated by a factor of five by the addition of DNA compared to that observed in homogeneous solution. Thus, *DNA catalyzes the self-reduction of the bound oxidant.* This result is consistent with the fact that polypyridyl oxidants undergo bimolecular self-reduction at neutral pH,[19] and binding of the oxidant to DNA leads to an increased local concentration of the bound oxidant. In addition, the catalysis is sequence-specific, with self-reduction in AT polymers proceeding twice as fast as that in GC polymers or calf thymus DNA. Thus, k_X can be catalyzed by DNA and can be sequence-specific, which has profound implications in terms of eq 1.

4. Oxidations of Model Nucleotides

A puzzling generality in nucleic acid oxidation by small molecules is the repeated observation that DNA oxidation generally gives more cleavages than RNA oxidation, even in structurally related analogues.[20] We have been interested in determining whether this observation might have an origin in the sugar reactivity rather than in structure. In addition, we reasoned that if our $Ru(tpy)(bpy)O^{2+}$ oxidations were under thermodynamic control, we would obtain the same products and relative reactivities in model nucleotides as in DNA. Indeed, oxidation of T, C, and A nucleotides gives the free base as the sole product, and in many cases where the rate is fast enough to permit a complete reaction, the yield of free base is nearly quantitative based both on $Ru(IV)O^{2+}$ and on the disappearance of the parent nucleotide, which stands in stark contrast to the studies of DNA polymers. We have not yet been able to determine the fate of the ribose carbon atoms; however, the kinetics of the reactions are of great interest.

Oxidation of mononucleotides under pseudo-first-order conditions occurs via saturation kinetics according to:

$$Ru(IV)O^{2+} + NMP^{2-} \rightleftharpoons Ru(IV)O^{2+}\bullet NMP^{2-} \rightarrow Ru(II)OH_2^{2+}\bullet NMP \quad (4)$$

Analysis by double-reciprocal plots therefore provides an equilbrium constant for the formation of the ion-pair (K_B) and the rate of oxidation (V_{max}) within the complex (Figure 1). As shown, the determined K_B values for AMP and dAMP are the nearly the same, as would be expected for a primarily electrostatic interaction. In addition, increasing the ionic strength lowers K_B and using ADP^{3-} in place of AMP^{2-} increases K_B. However, note that the rate of oxidation within the ion-pair is a factor of five faster for dAMP compared to AMP. We have made this same observation for oxidation of CMP and dCMP and for ribose and deoxyribose.

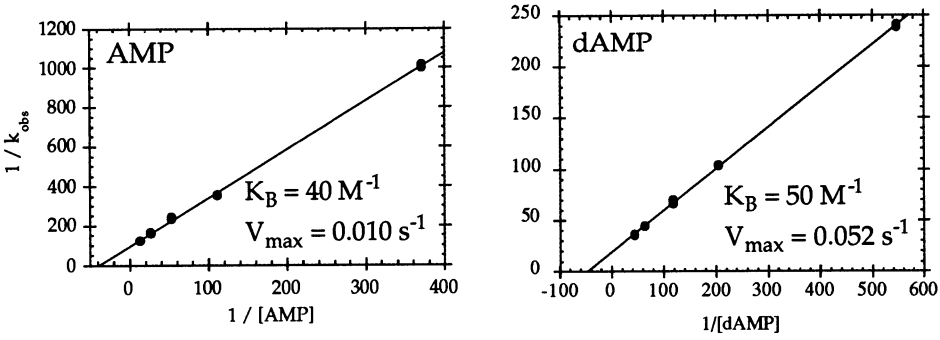

Figure 1. Kinetics of oxidation of AMP and dAMP by $Ru(tpy)(bpy)O^{2+}$.

Thus, even though ribonucleotides contain an extra hydroxyl group, oxidation of deoxynucleotides is always 5-8 times faster. We suspected that this result was consistent with oxidation at the 1' or 3' position to create a carbocation, which would be destabilized by the polar effect of the hydroxyl group on the adjacent carbon. To test this hypothesis, we determined the rate constant for the oxidation of 2-propanol and 1,2-dihydroxypropane and again observed a 5-fold faster rate with 2-propanol. Thus, our observation of a slower rate of oxidation of ribo- compared to deoxy-nucleotides is also consistent with 1' oxidation, as is the observation that nucleotide oxidations are considerably faster than oxidation of the sugars, even when corrections for ion-pair formation are made. The presence of the base instead of a hydroxyl group in the nucleotides would be expected to stabilize the 1' oxidation product. We have made some parallel observations for nucleotide oxidation by $Pt_2(pop)_4^{4-}$ ($pop = P_2O_5H_2^{2-}$).[21] These results imply that the increased reactivity of DNA to oxidation compared to RNA could have its origin in reactivity, although we certainly have not ruled out a structural effect in actual biopolymers.

5. Summary

In conlusion, we have developed a system for nucleic acid oxidation that allows two new aspects of these reactions to be determined. The first is the precise yield of DNA products based on the number of oxidizing equivalents delivered by the cleavage agent. The second

is the time dependence of the reduction of the cleavage agent. This new information can be used to understand how bound oxidants are directed toward different redox pathways. In particular, we have shown that nucleic acids are protected from oxidation by catalysis of self-reduction of bound oxidants. Furthermore, this catalysis is sequence-specific. These observations have profound implications in terms of understanding sequence-specific phenomena, such as kinetic isotope effects (eq 1). Thus, the extent of nucleic acid cleavage is related to the degree to which other redox pathways, such as sugar (k_{sugar}) and base oxidation (k_G), can compete with the catalyzed self-reduction (k_X).

By tuning the redox potential of the oxidant without changing the structure, the effect of changes in the rates of the competing processes shown in Scheme 2 can be assessed. The combined results support the general trend that $k_X > k_G > k_{sugar}$ and that the thermodynamic requirements for these steps fall in the same order. This notion is underlined by the observation that all three processes are observed with $Ru(IV)O^{2+}$, only guanine oxidation and self-reduction are observed with $Ru(III)OH^{2+}$, and only self-reduction is observed with $Os(IV)O^{2+}$. Thus, as oxidants become weaker, the two cleavage pathways are successively less able to compete with self-reduction.

We can now begin to use the information obtained to develop novel cleavage agents and to better understand nucleic acid oxidation in structurally complex biopolymers. For example, by lowering the driving force of the oxidant to between that of $Ru(tpy)(bpy)O^{2+}$ and $Ru(tpy)(bpy)OH^{2+}$, we have been able to develop a reagent where k_{sugar} is competent only for thymidine residues. This implies that the 1'-position in thymidine is easier to activate than in the other nucleotides. In addition, we have shown that 1' oxidation in deoxynucleotides is faster than in ribonucleotides, which is consistent with destabilization of the 1'-oxidized product by the polar effect of the 2'-hydroxyl. This information will be invaluable in understanding the cleavage of complex RNA's and in developing new reagents that are specific for RNA over DNA and vice versa.

6. Acknowledgment

H. H. T. thanks the David and Lucile Packard Foundation and the NSF.

7. References

(1) Sigman, D. S.; Bruice, T. W.; Mazumder, A.; Sutton, C. L. *Acc. Chem. Res.* **1993**, *26*, 98.
(2) Pyle, A. M.; Barton, J. K. *Prog. Inorg. Chem.* **1990**, *38*, 413.
(3) Burkhoff, A. M.; Tullius, T. D. *Nature (London)* **1988**, *331*, 455.
(4) Hecht, S. M. *Acc. Chem. Res.* **1986**, *19*, 83.
(5) Stubbe, J.; Kozarich, J. W. *Chem. Rev.* **1987**, *87*, 1107.
(6) Van Atta, R. B.; Long, E. C.; Hecht, S. M.; van der Marel, G. A.; van Boom, J. H. *J. Am. Chem. Soc.* **1989**, *111*, 2722.
(7) Kozarich, J. W.; Worth, L., Jr.; Frank, B. L.; Christner, D. F.; Vanderwall, D. E.; Stubbe, J. *Science* **1989**, *245*, 1396.
(8) Worth, J., L.; Frank, B. L.; Christner, D. F.; Absalon, M. J.; Stubbe, J.; Kozarich, J. W. *Biochemistry* **1993**, *32*, 2601.
(9) Grover, N.; Thorp, H. H. *J. Am. Chem. Soc.* **1991**, *113*, 7030.
(10) Welch, T. W.; Neyhart, G. A.; Goll, J. G.; Ciftan, S. A.; Thorp, H. H. *J. Am. Chem. Soc.* **1993**, *116*, 9311-9312.
(11) Neyhart, G. A.; Grover, N.; Smith, S. R.; Kalsbeck, W. A.; Fairley, T. A.; Cory, M.; Thorp, H. H. *J. Am. Chem. Soc.* **1993**, *115*, 4423.

(12) Takeuchi, K. J.; Thompson, M. S.; Pipes, D. W.; Meyer, T. J. *Inorg. Chem.* **1984**, *23*, 1845.
(13) Meyer, T. J. *J. Electrochem. Soc.* **1984**, *131*, 221C.
(14) Thompson, M. S.; Meyer, T. J. *J. Am. Chem. Soc.* **1982**, *104*, 4106.
(15) Dobson, J. C.; Seok, W. K.; Meyer, T. J. *Inorg. Chem.* **1986**, *25*, 1513-1514.
(16) Roecker, L.; Kutner, W.; Gilbert, J. A.; Simmons, M.; Murray, R. W.; Meyer, T. J. *Inorg. Chem.* **1985**, *24*, 3784-3791.
(17) Sigman, D. S. *Acc. Chem. Res.* **1986**, *19*, 180.
(18) Chen, X.; Burrows, C. J.; Rokita, S. E. *J. Am. Chem. Soc.* **1991**, *113*, 5884.
(19) Creutz, C.; Sutin, N. *Proc. Natl. Acad. Sci. USA* **1975**, *72*, 2858-2862.
(20) Holmes, C. E.; Hecht, S. M. *J. Mol. Biol.* **1993**, *268*, 25909-25913.
(21) Kalsbeck, W. A.; Gingell, D. M.; Malinsky, J. E. *Inorg. Chem.* **1994**, in press.

Modeling Active Sites

Mo/S CHEMISTRY AND ITS IMPORTANCE IN ENZYMATIC CATALYSIS
PART I. FUNCTIONAL GROUP CHEMISTRY OF THE Mo/S AND Mo/S/O COMPLEXES OF POSSIBLE RELEVANCE TO THE Mo-OXIDOREDUCTASES

DIMITRI COUCOUVANIS
Department of Chemistry
The University of Michigan,
Ann Arbor Michigan, 48109-1055 USA

1. Molybdenum in Biology

Molybdenum is an important trace element in biology and is found in a multitude of redox active enzymes as well as in the N_2 reducing nitrogenases. In nature molybdenum occurs mainly as molybdenite, MoS_2 , wulfenite, $PbMoO_4$ and as soluble salts of MoO_4^{2-} in the sea. The adaptation of Mo by bacteria, plants and animals as a metal of choice at first appears paradoxical given the perceived rarity of the element. The paradox is not there however if one realizes that in fact Mo is one of the more abundant elements on the planet and constitutes the most abundant redox active transition element in the oceans[1].

2. The Mo-Oxidoreductase Enzymes

A broad class of Mo containing enzymes are the oxidoreductases (oxotranferases) that catalyze the reaction

$$X + H_2O \longrightarrow XO + 2H^+ + 2e^- \qquad \textbf{eq.1}$$

This reaction is of general importance in the biological processing of:
a) nitrogen compounds, as in xanthine oxidase function[2] (xanthine $\longrightarrow$ uric acid), nitrite oxidase function[3] ($NO_2^- \longrightarrow NO_3^-$) or nitrate reductase function[4] ($NO_3^- \longrightarrow NO_2^-$).
b) sulfur compounds, as in sulfite oxidase function[5] ($SO_3^{2-} \longrightarrow SO_4^{2-}$) or sulfoxide reductase function[6] ($R_2SO \longrightarrow R_2S$).
c) carbon compounds, as in aldehyde oxidase[2] (RCHO $\longrightarrow$ RCOOH) or formate dehydrogenase[4] ($HCOO^- \longrightarrow CO_2$).

In addition to their common content of Mo the oxidoreductase enzymes also are characterized by the following unique features:
a) Water is used as the source of the oxygen atom incorporated into the substrate.
b) Reducing equivalents are generated rather than consumed.
c) In all cases the substrate reaction occurs at the Mo-cofactor (Mo-co) site whether it is oxidation (as in xanthine oxidase) or reduction (as in nitrate reductase).
d) The enzymatic systems can be described[1] as an enzymic electrical cell where the Mo-co serves as one electrode (anode in xanthine oxidase) and other prosthetic groups serve as the other electrode (flavin serves as the cathode in xanthine oxidase). The enzyme supplies the electrical connection. The xanthine oxidase system is shown schematically in Fig.1.

D.P. Kessissoglou (ed.), Bioinorganic Chemistry, 247-274

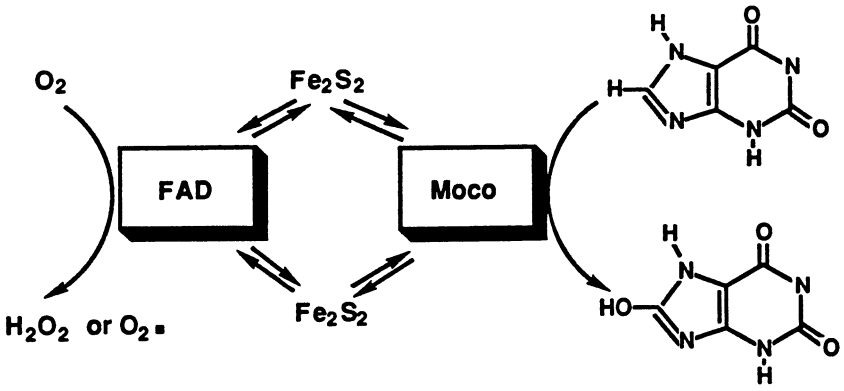

Figure 1. The Xanthine Oxidase System.

A number of Mo-X-ray absorption studies in these enzymes[7] have reached consensus in a general structural image of the Mo-co where the oxidized form contains a minimal $(L)_xMo^{VI}(O)_2(S\text{-}S)$ unit and in the reduced form contains a minimal $(L)_xMo^{IV}(O)(S\text{-}S)$ unit. The S-S ligand in the Mo-co is now recognized[8] to be the dithiolene functionalized pterin, molybdopterin, (Fig.2).

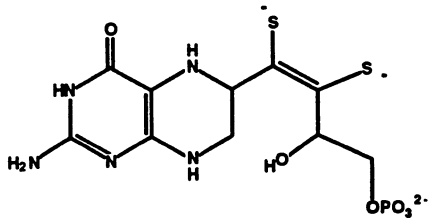

Fig.2. The Molybdopterin Ligand in the Mo-co of the Oxidoreductases (ref. 8).

The xanthine oxidase site is unique in that it contains both a Mo=S and Mo=O groups instead of two Mo=O groups. A quest for a synthetic analog for the Mo-co has been the subject of numerous studies by various groups[9,10]. On the basis of results that have been made available from elegant studies on either the enzymes[11] or model Mo complexes[9,10] the oxo-transfer hypothesis has been advanced by R.H.Holm[9a] (Fig.3) for the enzymic action of the oxidoreductases.

3. The Importance of Molybdenum Coordination Chemistry in Industrial Catalysis

3.1. HYDRODESULFURIZATION

The removal of sulfur from organosulfur compounds, present in crude petroleum, is carried out catalytically by the hydrodesulfurization (HDS) reaction[12] (eq.2).

$$RSH + H_2 \longrightarrow H_2S + RH \qquad \textbf{eq.2}$$

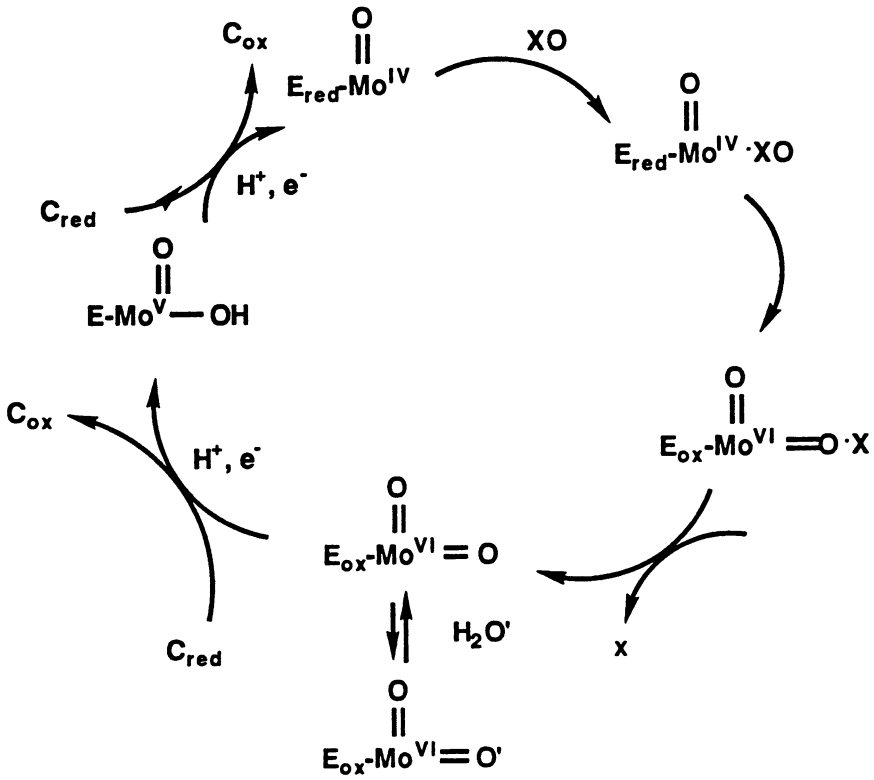

Figure 3. The Oxo-Transfer Hypothesis (Ref.9a)

The catalyst used industrially consists of "sulfided" molybdates supported on g-Al_2O_3, although many second and third row transition metal sulfides are active catalysts for the HDS reaction, with Ru, Os, Rh and Ir sulfides showing the highest activity[13]. Among the first row transition metal ions , Ni^{2+} and Co^{2+} ions serve as promoters in the MoS_2 HDS catalysis[12]. At present the sites that appear to be involved in the catalytic process are the edges of the MoS_2 microcrystals[14]. These edges very likely contain a multitude of Mo/S and Mo/S/O groups with various structural and reactivity characteristics. Some of the groups that may reside on the edges are outlined in Fig.4 .

3.2. THE OLEFIN METATHESIS REACTION.

The Industrially important olefin metathesis reaction is a reaction that involves the simultaneous cleavage of two olefin double bonds followed by the formation of the alternate double bonds. It is presently accepted that the catalyst is a metal alkylidene

$$C = C \; + \; C^* = {}^*C \longrightarrow 2\,{}^*C = C \qquad \text{eq.3}$$

complex that reacts with an olefin to form a metallacyclobutane intermediate (Fig.5) that decomposes to give the product olefin[16]. In this reaction the Mo = CH_2 is activated by the Mo = O "spectator" group and readily adds an olefin. This addition results in a change in the coordination geometry of the Mo atom from four coordinate, tetrahedral, to five

coordinate square-pyramidal. Associated with this change is a large negative free energy change that is attributed mainly to the transformation of the bond order of the Mo=O spectator group from double to triple[16].

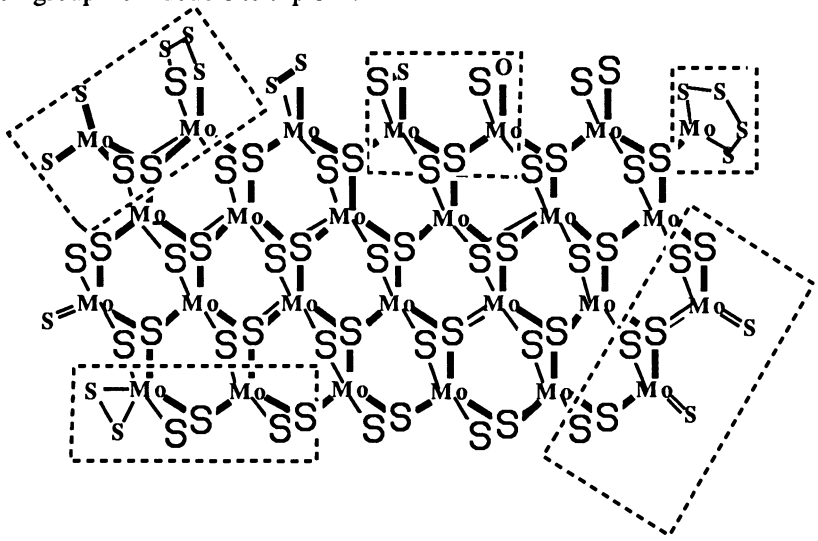

Possible Functional Groups on the Edges of MoS_2

Figure 4. Possible Functional groups on the edges of MoS_2

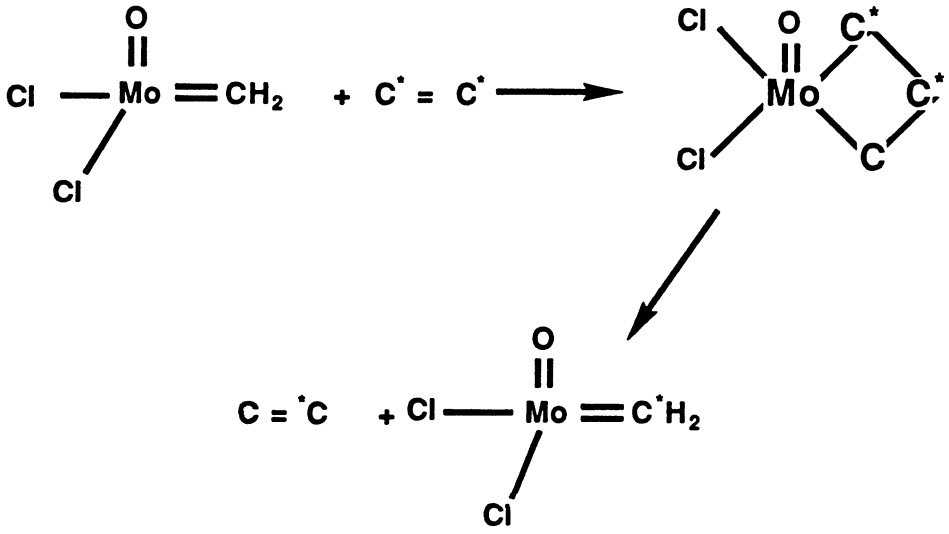

Figure 5. A Minimal Mechanism for the Olefin Metathesis Reaction, (ref. 16).

For nearly two decades we have been developing the concept of inorganic functional group chemistry in the Mo/S and Mo/S/O complexes and have focused[17] on the understanding of the rich chemistry of the $Mo(S)(S_x)$ and $Mo(O)(S_x)$ "functional groups" (x = 1,2 and 4). This chemistry is dominated by the nucleophilic character of the S_x ligands and their reactions toward alkynes, heteroallenes and SO_2.

The simplest among the S_x^{2-} ligands found in the thio- and oxothio-molybdate complexes is the S^{2-} ligand that exists mainly as: a) a terminal ligand in thiomolybdenyl units[18], (Mo^{+n}=S, n=4,5,6), b) a μ_2-bridging unit in cores such as $(Mo_2S_2)^{+6}$ [19] and c) a μ_3-bridging unit in $[Mo_3S_{13}]^{2-}$ [20] and in the Mo_4S_4 cores of the $[(L_3Mo)_4S_4]$ [21] and $[Mo_7S_8(H_2O)_{18}]^{8+}$ [22] complexes. Of particular interest from a reactivity point of view are the S^{2-} terminal ligands in oxo- and oxothiomolybdate complexes that contain the $Mo(S_t)(O_t)$ and $Mo(O_t)_2$ subunits. This interest stems from the presence of such units in the Mo cofactor of the oxidoreductase enzymes and (of the $Mo(S_t)(O_t)$ subunit) in xanthine oxidase[7] (vide infra).

4. Reactivity studies of synthetic Mo/S and Mo/S/O complexes

The reactivity of the Mo^{n+}=S group is evident in: a) sulfur addition reactions [18b] b) reactions with various transition metal ions [23] c) dimerization reactions[18a] d) reactions with unsaturated electrophilic organic molecules [18a,24,25] and reactions with SO_2. The implications of these studies in the enzymatic action or even in the inhibition of the oxidoreductase enzymes remains to be explored.

4.1. THE MO=S GROUP.

4.1.1. Sulfur Addition to the Mo=S Group in the Thiomolybdate Complexes. The addition of sulfur to terminal sulfido ligands, very likely is the end result of electrophilic attack on the Mo^{n+}=S, (n=4,5,6), sulfur, by the $^{+}S(S)_xS^{-}$ products of heterolytically cleaved S_8 molecules, and accounts for the synthesis of the $[(S_4)_2Mo^{IV}=E]^{2-}$ anions[26] (E=S,O) and various members of the $[Mo^{V}_2(S)_n(S_2)_{6-n}]^{2-}$, and $[Mo^{V}_2(O)(S)_n(S_2)_{5-n}]^{2-}$ series[2,27]. With transition metal ions, the thiomolybdenyl groups can serve as either electron pair donors, or as a source of sulfide ions for the eventual formation of highly insoluble, thermodynamically stable, transition metal sulfides. The former course of reactivity is represented in the multitude of heterometallic complexes where the MoS_4^{2-} anion serves as a ligand for transition metal ions[23].

4.1.2. Reactions of the Mo=S Group with Thiophilic Transition Metal Ions. The irreversible removal of sulfide ions from Mo=S units by the formation of insoluble transition metal sulfides allows for the introduction of non-sulfur terminal ligands in the thiomolybdate ions by metathetical reactions. An example of this reaction is available in the synthesis of the $[Mo_2O_2S_8X]^{-}$ anions[28] from the reaction of NiX_2 (X=Cl, I) with an isomeric form of the $[Mo^{VI}_2O_2S_9]^{2-}$ anion[29].

4.1.3. The Dimerization of Mo(V),4d^1 Complexes. The dimerization of Mo(V),$4d^1$ complexes to diamagnetic dimeric complexes with a formal Mo-Mo single bond is well documented[17b] and one electron oxidations of $(L)_nMo^{IV}$=S complexes invariably lead to dimerization with formation of the very stable di-m-sulfido, $[(L)_nMo^{V}\text{-}S]_2$ products[30]. Examples include the formation of $[(S_4)SMo^{V}=E]_2^{2-}$ from the air-oxidation of $[(S_4)_2Mo^{IV}=E]^{2-}$ and the formation of the $[(L)_2Mo^{V}=S]_2^{2-}$ dimer apparently from the oxidation of an unstable $[(L)_2Mo^{IV}=S]^{2-}$ intermediate (L= 1,2-dicarboethoxy-ethylene-1,2-dithiolate).

4.1.4. Reactions of the Mo=S Group with Electrophilic Molecules. Electrophilic attack on the Mo^{n+}=S sulfur occurs in reactions of various thiomolybdates with CS_2 [24] or activated alkynes, RC CR[25]. These reactions lead to the formation of perthiocarbonate or 1,2-dithiolene complexes as final products. Thus far, expected intermediates that contain vinyl sulfide or trithiocarbonate chelating ligands have not been detected in reactions with complexes that contain exclusively sulfur ligands. Apparently, the close proximity of Mo=S, Mo-S_2^{2-} or Mo-S_4^{2-} groups to the reactive vinyl sulfide or trithiocarbonate ligands in these intermediates allows for rapid intra- molecular sulfur transfer and rapid conversion to dithiolenes or perthiocarbonates. Replacement of neighboring Mo=S groups by the apparently less reactive Mo=O groups, in otherwise isostructural complexes, simplifies the reactivity patterns and eliminates some of the ambiguities inherent in the reactions of totally "sulfided" thiomolybdates.

The $[(MoS_4)Mo(E)(L)]^{2-}$ and $[(MoS_3O)Mo(E)(L)]^{2-}$complexes (E=S; L=S_4^{2-}, S_2^{2-}; E=O; L=S_4^{2-}, S_2^{2-} [17b]), (Fig.6), are structurally unique among the known plethora of dinuclear thio- and oxo-thio- molybdates. The asymmetric structures of the Mo-(m-S)2-Mo rhombic cores suggest that the mixed-valence, Mo^{IV}-Mo^{VI}, state is important for the description of the electronic structure of these anions.

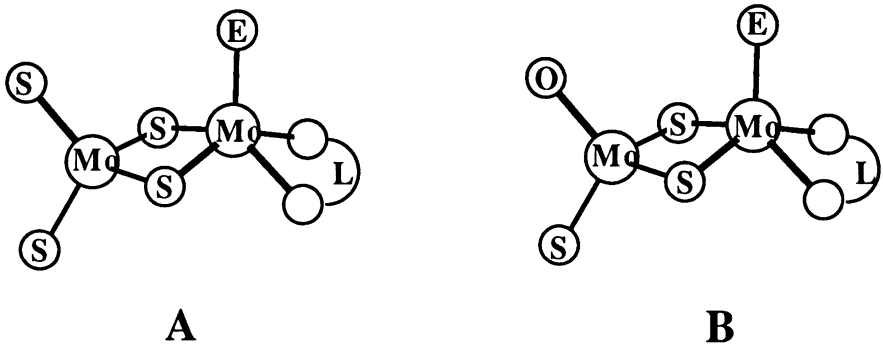

Figure 6. The $[(MoS_3E)Mo(E)(L)]^{2-}$ Complexes, (E = S, O; ref. 17b)

These complexes undergo dimerization equilibria (Fig. 7) and are reactive toward

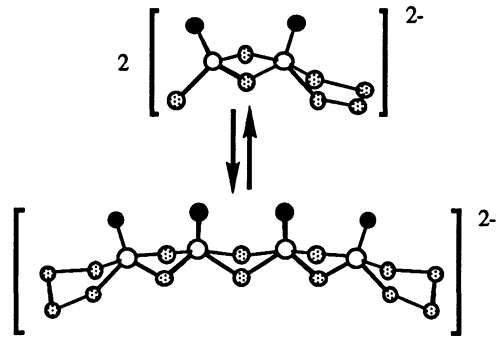

Figure 7. Reversible Dimerization of the $[(MoS_3O)Mo(O)(S_4)]^{2-}$ Complex, (ref. 17b).

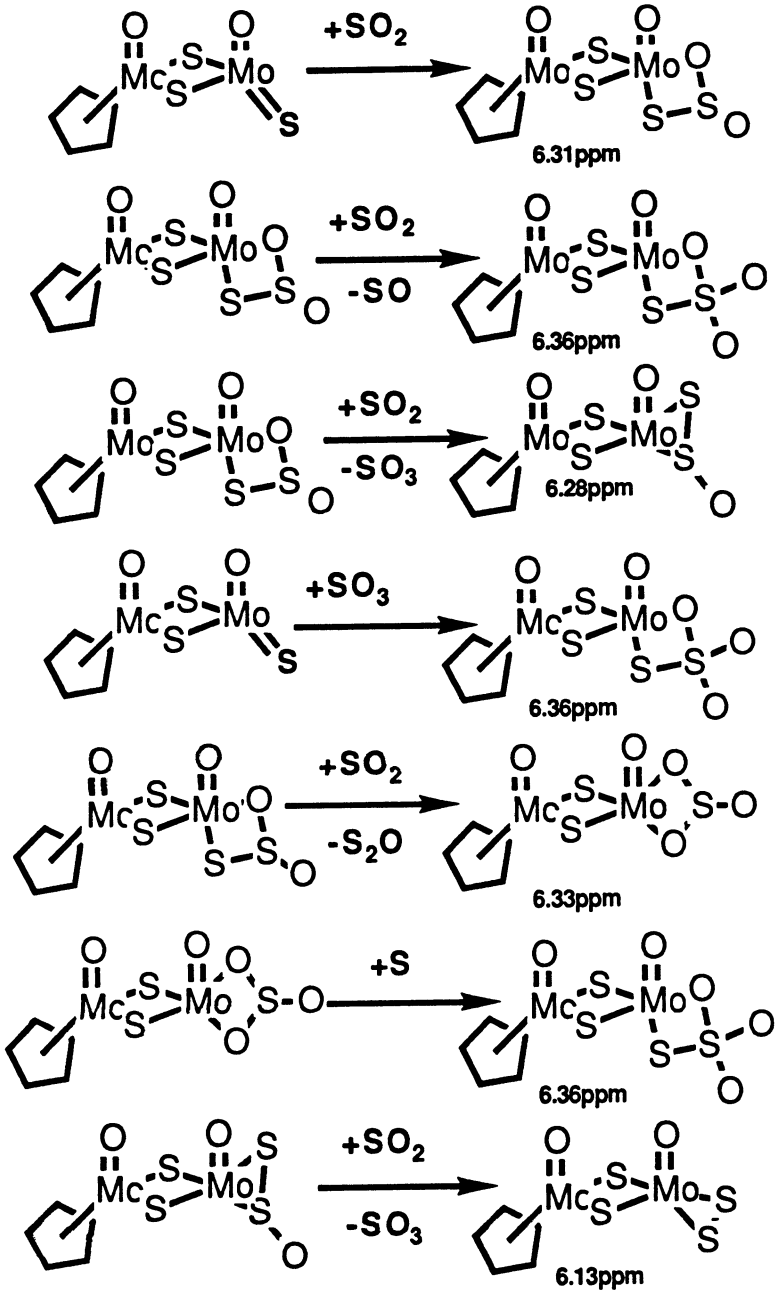

Figure 8. The Reactions of the $[(Cp)Mo(O)(\mu\text{–}S)_2Mo(O)(L)]^-$ Complexes with SO_2. (ref. 31b)

electrophilic reagents. ^{1}H–NMR studies of the reactions of the structurally similar $[(MoS_3O)Mo(O)(Cp)]^-$ complex, with such molecules as ROOC–C=C–COOR or CS_2 have made it possible to understand the reactivity patterns and propose reaction pathways that involve electrophilic attack at the Mo=S group and the initial formation of vinyl-sulfide or trithiocarbonate ligands respectively.

A significant outcome of these studies is the observation that: *the Mo=O bond is relatively inactive in these reactions and there exists no evidence to indicate that the Mo=O chromophore is directly involved in reactions with electrophilic reagents, it is quite clear however that this group as a neighboring spectator group enhances greatly the reactivity of the Mo=S group*

4.1.5 Reactions of the Mo=O activated Mo=S group with SO_2 The Mo=S bond of the Mo(O)(S) group in various Mo/S/O complexes readily inserts SO_2 [31] Depending on temperature these reactions afford a multitude of products. These products contain (as bidentate chelating ligands terminally bound to the Mo atom) a) thiosulfite or sulfite (reaction at 0° C), b) thiosulfate (reaction at 25° C), and c) sulfate (reaction at >100° C). The crystal structures of the $[(Cp)Mo(O)(\mu\text{–}S)_2Mo(O)(L)]^-$ complexes ($L=SO_3^{2-}$, $S_2O_3^{2-}$ and SO_4^{2-}) have been determined. The reaction of $[(MoS_3O)Mo(O)(Cp)]^-$ with SO_2 as monitored by ^{1}H NMR spectroscopy (Cp^-protons) in an SO_2–saturated DMF solution, in a sealed NMR tube over two days at probe temperature (37° C) shows complicated chemistry[31b]. A plausible scheme that may account for the formation and reactions of the $[(Cp)Mo(O)(\mu\text{–}S)_2Mo(O)(L)]^-$ complexes is shown in Fig. 8. The ^{1}H–NMR spectra of "authentic", structurally characterized, $[(Cp)Mo(O)(\mu\text{–}S)_2Mo(O)(L)]^-$ complexes has made it possible to unequivocally assign most of the NMR resonances shown in Fig. 8.

The reaction of $[O)(S)Mo(\mu 2\text{–}S)_2Mo(O)\ (S_4)]^{2-}$ with HSO_3^- to give the $[O)(S_2O_3)Mo(\mu 2\text{–}S)_2Mo(O)(S_2)]^{2-}$ complex[31c] (Fig. 9) with a coordinated thiosulfate ligand is relevant to the chemistry of xanthine oxidase. It supports an earlier suggestion that the reaction of xanthine oxidase with bisulfite involves the Mo=S unit in the Mo(S)(O) chromophore and affords Mo-bound thiosulfate[32].

4.2. THE REACTIVITY OF THE MO=O GROUP PROXIMAL TO ANOTHER MO=O GROUP.

The oxidative decoupling of the $[(Cl_4\text{–cat})MoFe_3S_4Cl_2]$ subunits in the $\{[(Cl_4\text{–cat})MoFe_3S_4\ Cl_2)2]2(S)(L)\}^{n-}$ doubly-bridged double-cubanes[33] gives the dimeric $[(Cl_2Fe)(\mu 2\text{–}S)_2Mo(O)(Cl_4\text{–cat})]^{2-}$ complex[34], (Fig. 10).

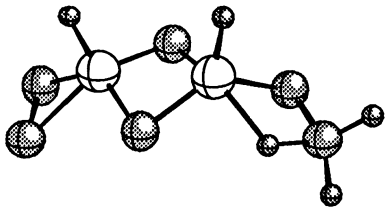

Figure 9. The molecular structure of the $[(S_2O_3)Mo(O)(\mu 2\text{–}S)_2Mo(O)(S_2)]^{2-}$ complex (ref. 31c).

This dimeric complex is readily obtained by a general reaction that appears "driven" by the Mo=O "spectator" effect[16]. This reaction employs thiomolybdate heterometallic

complexes and depends on the protonation (to H_2O) of one Mo=O group in the $(O)(O)Mo(\mu_2\text{–}S)_2FeCl_2$ complex by the acid form of bidentate ligands such as catechol, citric acid, oxalic acid etc[35]. The $(S_n)(O)Mo(\mu_2\text{–}S)_2FeCl_2$ complexes (n=1, 2) also undergo reactions at the Mo=S site driven by the Mo=O group. The addition of an activated alkyne to $(S_2)(O)Mo(\mu_2\text{–}S)_2FeCl_2$ leads to the $[(COOR)_2C{=}CS_2)$ $(O)Mo$ $(\mu_2\text{–}S)_2FeCl_2]^{2-}$ vinyl-disulfide complex (Fig. 11).

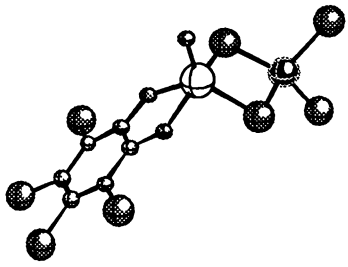

Figure 10. Molecular structure of the $[(Cl_2Fe)(\mu_2\text{–}S)_2Mo(O)(Cl_4\text{–cat})]^{2-}$ complex (ref. 34).

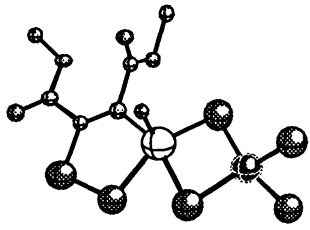

Figure 11. $[(COOR)_2C{=}CS_2)(O)Mo(\mu_2\text{–}S)_2FeCl_2]^{2-}$ (ref. 35).

The latter is quite stable, unlike the $[(COOR)_2C{=}CS_2)(O)Mo(\mu_2\text{–}S)]_2$ vinyl disulfide complex[36] that undergoes isomerization to the corresponding dithiolene[37].

5. The possible significance of basic functional group Mo/S/O chemistry in enzymatic catalysis by the Mo-Oxidoreductases

Our studies of the chemical properties of the $(O)Mo^{VI}(S)$ groups[17b] clearly show the superior reactivity of the $Mo^{VI}{=}S$ group relative to the $Mo^{VI}{=}O$ group and demonstrate the propensity of the Mo=S bond to undergo insertion reactions. These observations, *if applicable to the $(O)Mo^{VI}(S)$ chromophore in the active site of xanthine dehydrogenase*, suggest a possible modification of the first step in the proposed[9a] minimal mechanism for the oxidation of xanthine to uric acid. In this mechanism the C-8 position of xanthine appears to undergo nucleophilic attack by the Mo=O group to form Mo-O-C, with the Mo=S group serving as a proton acceptor, (Fig. 12A). As pointed out previously however [38], such a mechanism raises an interesting question: " .why replacing the Mo=S with a second Mo=O to give desulfo enzyme should necessarily lead to inactivation of the

enzyme,... ". This question may be answered if the Mo=O group is not involved in the initial step of the reaction. It is conceivable that xanthine (RH) initially inserts into the Mo^{VI}=S bond by an initial electrophilic attack by the Mo^{VI} at the C-8 position of xanthine. Subsequently the S atom accepts the C-8 proton to form R-Mo^{VI}(O)SH, (Fig. 12B). Subsequent events that may follow include: a) internal $2e^-$ reduction of the Mo and electrophilic attack by R^+ on the Mo=O group and b) hydroxylation of the Mo(IV) center to eventually form RO-Mo^{IV}(O)SH. The remaining steps (Fig.12) toward the formation of uric acid are the same as those proposed earlier[9a].

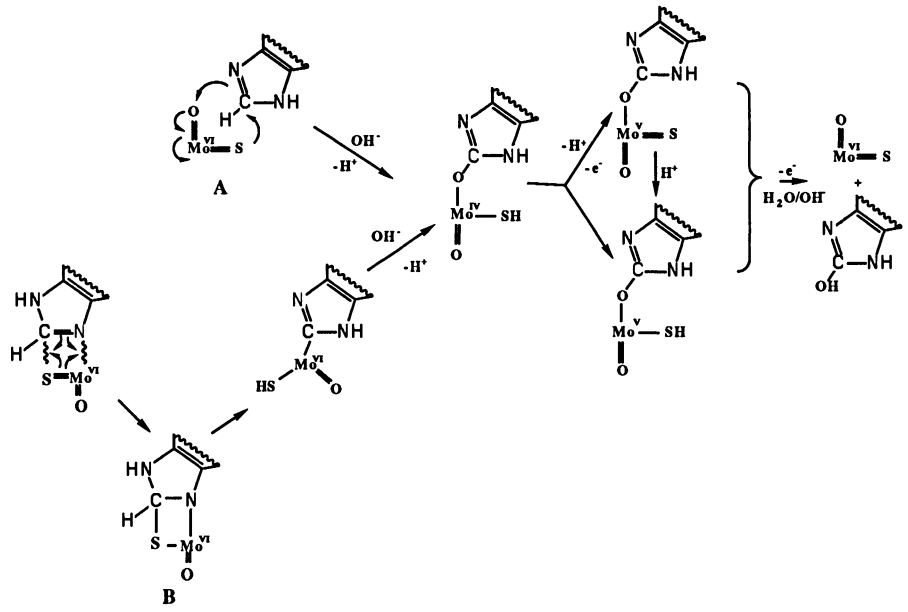

Figure 12. Possible Mechanisms for the Action of Xanthine Oxidase, (**A**, ref.9a, **B** ref. 17b)

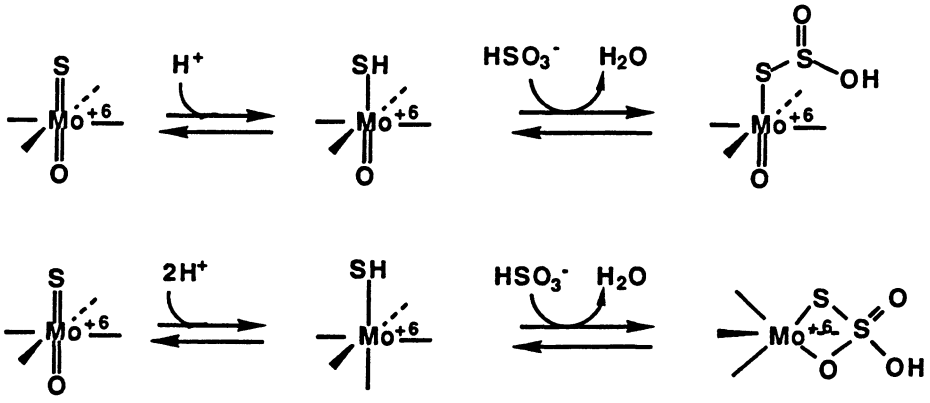

Figure 13. Proposed Mechanism of Xanthine Oxidase Inhibition by HSO_3^{2-} (ref. 32)

The reactivity of the Mo=S chromophore in the Mo center of xanthine oxidase also has been revealed in the reaction of this enzyme with bisulfite[32] (Fig.13). The HSO_3^- has been found to be a competitive inhibitor of xanthine oxidase and is a protector of the enzyme against cyanolysis. A 1:1 complex of the inhibitor and the enzyme has been isolated and the proposed mode of interaction has been suggested to involve the Mo=S group directly (Fig.13). The isolation of the $[O)(S_2O_3)Mo(\mu_2\text{-}S)_2Mo(O)(S_2)]^{2-}$ complex in our laboratory[31c] (Fig. 9) from the reaction of $[O)(S)Mo(\mu_2\text{-}S)_2Mo(O)(S_4)]^{2-}$ with HSO_3^- supports the direct involvement of the Mo=S group in the inhibition of xanthine oxidase with bisulfite (Fig.13).

Among the complexes isolated from the reactions of activated alkynes with the Mo=S group is included the $[(O)Mo^{IV}(L)_2]^{2-}$ complex[25a] (Fig.14; L= 1,2 dicarboethoxy 1,2-ethylene dithiolate). A similar complex as well as the cis-dioxo, $[(O)_2Mo^{VI}(L')_2]^{2-}$ complex also have been reported with L' = 1,2 toluene dithiolate[39]. Until recently these complexes were considered interesting curiosities but of marginal biological importance due to the presence of two rather than one dithiolene ligands. This attitude may change however if recent preliminary X-ray crystallographic results[40] for a tungsten oxidoreductase also forecast the structure of the Mo-co'c in other oxidoreductases. The structure of the W-co of aldehyde ferredoxin oxidoreductase, a tungsten containing oxotransferase, from *Pyrococcus Furiosus* shows the presence of two rather than one pterin molecules coordinated to the W atom. A reconstruction of the oxo-transfer hypothesis[9a] (Fig. 3) with Mo-cofactor containing two molybdopterins (Fig.15) includes a convenient intramolecular pathway for the release of H_2O and the regeneration of the catalyst.

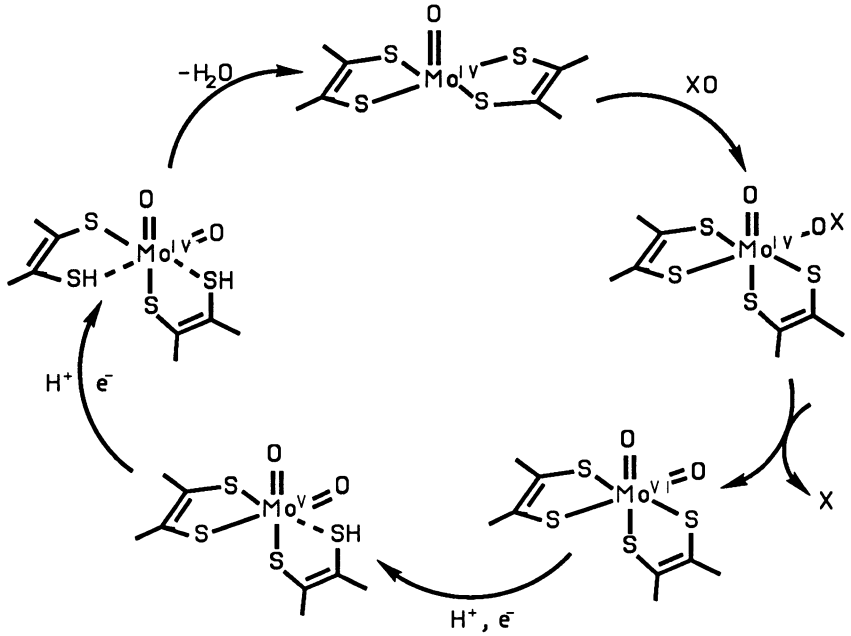

Figure 15. A modified oxo-transfer mechanism with a Mo-co that contains two molybdopterin units

In chemical catalysis the Mo=S bonds may play an important role as dipolar templates for the activation of substrate molecules. Of particular interest will be reactions with H_2

that may may under certain conditions result in heterolytic cleavage of the H_2 bond and formation of the Mo(H)(O)(SH) hydride-hydrosulfide units (Fig.16). In general

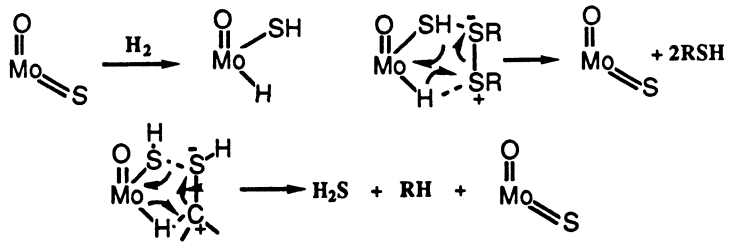

Figure 16. Possible role of the Mo(O)(S) unit in hydrotreating reactions.

M(H)(SR) units are rather rare. Notable exceptions include the one present in the [Mo(H)(tipt)$_3$(PMe$_2$Ph)$_2$] complex[41] (tipt = 2,4,6-SC$_6$H$_2$(^{i}Pr)$_3$) and the Rh(H)(SR) units obtained by the *reversible* addition of H_2 into the Rh-S bonds of the [(triphos)Rh(μ-S)$_2$Rh(triphos)]$^{2+}$ complex[42]. If the Mo(H)(O)(SH) units can be generated, they should be quite reactive and some of their reactions with disulfides, thiophenes, and thiols may result in S-S or C-S bond cleavage with direct relevance to HDS catalysis[12].

PART II. FUNCTIONAL CHEMISTRY OF SYNTHETIC FE/MO/S CLUSTERS OF POSSIBLE RELEVANCE TO NITROGENASE FUNCTION

1. The Fe/Mo/S Center in Nitrogenase

The Fe/Mo/S center in the nitrogenase enzymes is an extraordinary site where biological reduction of dinitrogen to ammonia occurs under ambient temperature and pressure[43-46]. Recent single crystal X-ray structure determinations of the Fe-Mo protein of nitrogenase from *A.vinelandii*[47] and *C. pasteurianum*[47,48] have revealed the structure of the Fe/Mo/S aggregate to near atomic resolution. The Fe/Mo/S cluster (Fig.17) consists of two cuboidal

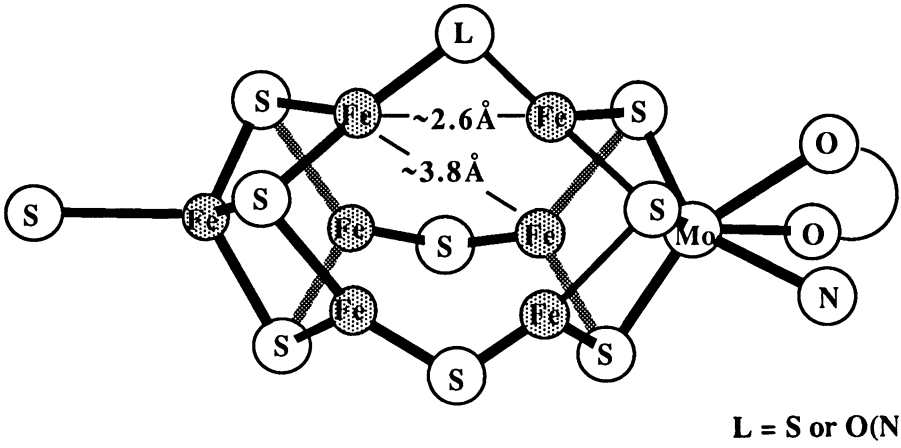

Figure 17. The Structure of the Fe/Mo/S Cofactor in the Fe/MoProtein of Nitrogenase (refs. 47,48)

subunits, Fe_4S_3 and $MoFe_3S_3$, bridged by two[47] or three[48] S^{2-} ions and anchored on the protein matrix by a Fe-coordinated cysteinyl residue and by a Mo-coordinated imidazole group from a histidine residue. The Mo atom also is coordinated by a homocitrate molecule that serves as a bidentate chelate. Unusual structural features include the unprecedented trigonal planar coordination geometry for the six μ-S-bridged iron atoms, and the unusually short Fe-Fe distances across the two subunits (2.5-2.6Å). The immense importance of this structure notwithstanding, a unique site for the activation and reduction of dinitrogen or other substrates still cannot be unequivocally identified and the location of the coordinatively saturated molybdenum atom in the periphery of the molecule has raised doubts concerning its direct involvement in catalysis.

2. Synthetic (Partial) Analogs for the Nitrogenase Fe/Mo/S Center

Prior to the Fe-Mo protein structure determinations, an abundance of speculative structural models[49] for the Fe/Mo/S center of nitrogenase had been proposed. Some of these models or their variants have been structurally and spectroscopically characterized in detail. *To our knowledge none of them has been directly identified as catalytically competent in the activation and reduction of nitrogenase substrates.* Indirectly, certain

synthetic Fe/Mo/S[49] and Fe/S clusters[50] (particularly $[Mo_2Fe_6S_8(SPh)_9]^{3-}$ and $[Fe_4S_4(SPh)_4]^{2-}$ in electrochemically reduced forms) have been associated with the reduction of nitrogenase substrates in the presence of proton sources[51]. These systems are mostly non-catalytic, heterogeneous and not well defined in terms of the actual nature of the reactant clusters. Whereas the Fe/Mo/S synthetic analog clusters until now have suffered from the drawback that they do not mediate chemistry related to dinitrogen reduction[52], various other complexes of molybdenum and tungsten undergo reactions that are of limited *direct* biological significance but are important from a fundamental chemical point of view. Among these reactions are included: a) the protonation-assisted reduction of dinitrogen complexes of low-valent molybdenum and tungsten to the hydrazido(-2) state[53], b) the catalytic reduction of N_2 to NH_3 with molybdocyanide catalysts[54], c) the proposed bimetallic activation of N-N bonds in protic environments and the reduction of N_2 to the hydrazine level[55], d) the catalytic reduction of hydrazine to ammonia on pentamethyl-cyclopentadienyl-trimethyl tungsten hydrazine complexes[56] and e) the catalytic reduction and disproportionation of hydrazine on certain Mo(IV) sulfur-ligated complexes.[57]

For these reactions, single metal atom site mechanisms have been proposed that outline: a) the stoichiometric reduction of N_2 to ammonia with $M{=}NNH_2$ as intermediates[53], b) the side-on (h^2) metal binding of N_2 followed by protonation and disproportionation[54] and c) reduction of N_2 by one electron one proton steps where an intermediate with coordinated hydrazine is proposed to lie on the pathway to ammonia[56]. Binuclear activation mechanisms also have been proposed for some of the model reactions[55,57] but are not as firmly supported as the single metal atom mechanisms. The possibility of binuclear activation of N_2 (and of other nitrogenase substrates) by the Fe/Mo/S center in nitrogenase has been considered previously[58].

3. The reduction of Nitrogenase Substrates with Fe/M/S Clusters (M = Mo, V)

3.1. THE CATALYTIC REDUCTION OF HYDRAZINE.

3.1.1. The $MoFe_3S_4$ Clusters. The syntheses in our laboratory of singly[59] (Fig.18-**II**) and doubly[33] (Fig.18-**III**) bridged "double-cubanes" have made available clusters that contain cuboidal subunits with $MoFe_3S_4$ cores and a N_2H_4 molecule in a bridging mode. The extent to which the hydrazine bridging units in the bridged clusters (Fig.18-**II,III**) are activated toward N-N bond cleavage was explored by allowing these "double cubanes" to react with reducing agents in the presence of protons[60].

Three different processes were investigated. a) stoichiometric reactions with cobaltocene as a reducing agent and 2,6-lutidine hydrochloride, Lut·HCl, as a source of protons, or *catalytic reductions* with various $N_2H_4/MoFe_3S_4$ cubane ratios in the presence of cobaltocene and Lut·HCl, (eq.4).

$$N_2H_4 + 2e^- + 4H^+ \longrightarrow 2NH_4^+ \qquad \text{(eq.4)}$$

and b) *catalytic disproportionation* reactions where N_2H_4 serves as both a reducing agent and a proton source (eq.5).

$$3N_2H_4 \longrightarrow 4NH_3 + N_2 \qquad \text{(eq.5)}$$

It was established that ammonia did not form in appreciable amounts from N_2H_4 in the presence of $Co(Cp)_2$ and Lut·HCl alone; it was also demonstrated that the CH_3CN (a poor substrate of nitrogenase[61]) that was used as a solvent did not undergo reduction under the reaction conditions. Of the Fe/Mo/S clusters studied the doubly-bridged double-cubane

(Fig.18, **III**) and the $[(Cl_4\text{-cat})Mo(O)(\mu\text{-}S)_2FeCl_2]^{2-}$ dimer[34] (one possible oxidative degradation product of the $[(Cl_4\text{-cat})MoFe_3S_4(Cl)_3\cdot CH_3CN]^{2-}$ cubane (Fig.18, **I**) did not promote the reduction or disproportionation of hydrazine to ammonia.

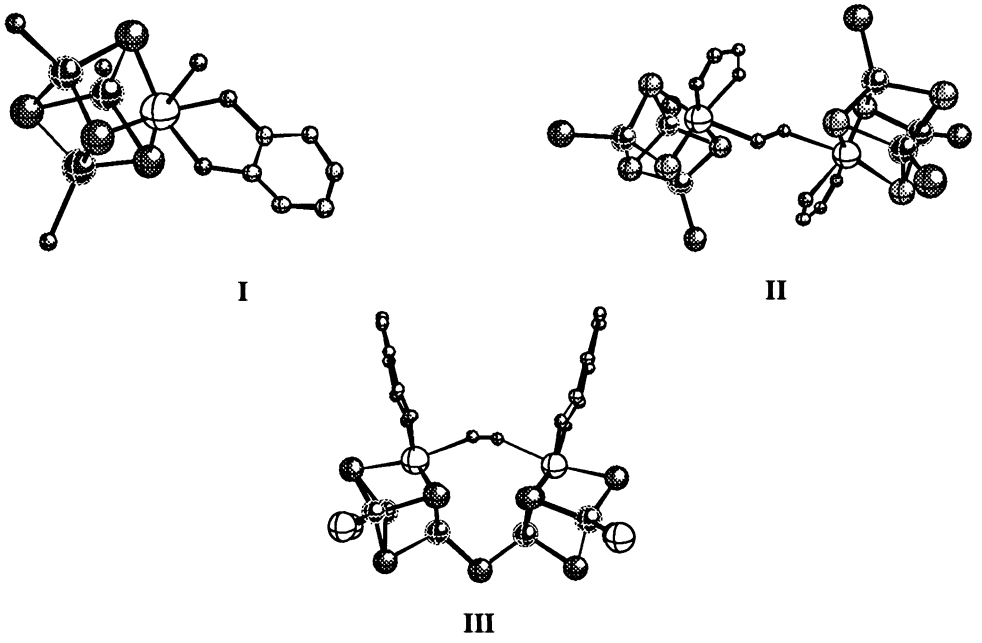

Figure 18. The Clusters tested as catalysts for the Reduction of Hydrazine to Ammonia (ref. 60)

Somewhat slow activity was detected when the singly-bridged double-cubane (Fig.18, **II**) was used as a catalyst. By far the most active catalysts in these reactions were the $[(L)MoFe_3S_4(Cl)_3\cdot L']^{n-}$ single cubanes (L = Cl_4-cat L' = CH_3CN, n = 2[62], **Ia**; L = citrate, n = 3[63], **Ib**; Fig. 18-**I**). The use of the latter in all of the reactions outlined above at ambient temperature resulted in the catalytic disproportionation and the stoichiometric or catalytic reduction, of N_2H_4 to NH_3 (Table I). The superior catalytic properties of **Ib** may be of relevance to the function of the homocitrate molecule in the nitrogenase cofactor (vide-infra). In all *catalytic disproportionation* reactions (in the absence of $Co(Cp)_2$ or Lut·HCl) the concentrations of either **Ia** or **Ib** after 12h of reaction time were found nearly the same as they were in the beginning of the reaction, the production of ammonia was reproducible and the yields of repetitive experiments fell within a relatively narrow range. In contrast the catalytic reduction of N_2H_4 with $Co(Cp)_2$ as a source of electrons and Lut·HCl as a source of protons stops before all of the hydrazine is reduced to ammonia. This may be attributed to the precipitation of the **Ia** or **Ib** anions by nascent counterions that include $LutH^+$, $[Co(Cp)_2]^+$, NH_4^+ and $N_2H_5^+$. The onset of precipitation within ~0.5h is not exactly predictable and as a result the yields of ammonia between successive runs show considerable variation (Table I). In DMF solution the onset of precipitation is longer (~12h) however the substitution of the DMF ligand by hydrazine in the coordination sphere of the molybdenum atom is not as facile as the substitution of CH_3CN and consequently the catalytic reduction is slower.

Table I. Production of NH_3[a] by the catalytic reduction of N_2H_4 by Ia: $[(Cl_4\text{-cat})MoFe_3S_4(Cl)_3(CH_3CN)]^{2-}$ or Ib: $[(Citr)MoFe_3S_4(Cl)_3]^{3-}$ in the presence of $Co(Cp)_2$ and Lut·HCl.

		NH_3 yield[b], equivalents[c,d]			% conversion			
Catalyst	$\frac{[N_2H_4]}{[catalyst]}$	1/2 h.	1h.	2h	NH_3 max[e]	1/2h.	1h.	2h
Ia[f]	1	1.4(2)	1.5(2)	1.6(2)	2	68	74	80
	10	13.2(2)	14.6(2)	19.2(2)	20	66	73	96
	20	32.8(3)	37.2(3)	40.0(3)	40	82	93	100
	40	61.6(3)	69.6(3)	73.9(3)	80	77	87	92
Ib[f]	10	20.0(2)	20.0(2)	20.0(2)	20	100	100	100
	20	38.0(2)	38.4(2)	N.Ag.	40	95	96	N.A.
	40	48.8(2)	56.8(2)	N.A.	80	61	71	N.A.
II[f]	1/2	0.6(2)	0.8(2)	1.0(2)	2	29	40	50
III[f]	1/2	h	h	h	2	--	--	--
IV[b]	1[i,j]	0.5(2)	0.7(2)	0.8(2)	1	50	67	80
	10[i,j]	4.5(1)	5.8(1)	10.0(1)	10	45	58	100

a) Reactions were carried out in CH_3CN, at ambient temperature under N_2 using the indicated catalyst and various amounts of N_2H_4 as shown in the second column. The initial concentrations of N_2H_4, $Co(Cp)_2$ and Lut·HCl were 1.25×10^{-3} M, 2.50×10^{-3} M and 5.00×10^{-3} M, respectively. The concentration of the catalyst was scaled accordingly to achieve the indicated ratios. A table with

results obtained with more concentrated solutions and data showing the catalytic but much slower N_2H_4 disproportionation reaction have been deposited with the supplementary material.

b) The NH_3 was quantified by the indophenol method. (A.L. Chaney, E.P. Marbach, *Clin. Chem.* (*Winston-Salem, NC*) **1962**, *8*, 130. and the N_2H_4 was quantified with p-(dimethylamino)benzaldehyde (G.W. Watt, J.D. Chrisp, *Anal. Chem.* **1952**, *24*, 2006. The protocol used in sample collection and treatment prior to analysis is identical to the one described in ref. 7.

c) The average of n independent experiments is reported where n is the number in parenthesis.

d) Analyses for N_2H_4 were carried out randomly for experiments where the yield of NH_3 indicated less than 100% conversion. In general there was a nitrogen atom balance to 100±5%. The results are included in a table deposited with the suppplementary material.

e) Maximum yield of NH_3 possible.

f) Abbreviations for the compounds are: Ia: $[(Cl_4\text{-cat})MoFe_3S_4(Cl)_3(CH_3CN)]^{2-}$; Ib: $[(Citr)MoFe_3S_4(Cl)_3]^{3-}$; II: $\{[(Cl_4\text{-cat})MoFe_3S_4(Cl)_3]_2(\mu_2\text{-}N_2H_4)\}^{4-}$; III: $\{[(Cl_4\text{-cat})MoFe_3S_4(Cl)_2]_2(\mu_2\text{-}N_2H_4)(\mu_2\text{-}S)\}^{4-}$; and IV: $\{[(Cl_4\text{-cat})MoFe_3S_4(Cl)_3(NH_2NHPh)\}^{2-}$.

g) N.A. = not available, due to the precipitation of the catalyst from solution.

h) No ammonia was detected and only a small trace was was found after 12 hours.

i) Phenyl hydrazine to cubane ratioj) Aniline was detected by a G.C.-mass spectroscopic measurement.

Qualitative comparative studies show that the rates of ammonia formation with **II** as a catalyst were considerably slower than those observed with **I** while **III** was totally ineffective as a catalyst (Table I). These results indicate that *the hydrazine molecule is activated by coordination to only one MoFe3S4 cubane and the addition of an additional equivalent of cubane (that is known to give II) inhibits the reduction.* In addition the results suggest that the availability of an uncoordinated NH_2 group (and the lone pair of electrons needed for protonation) is essential for the reduction of N_2H_4 to ammonia. The lack of reactivity of **III** almost certainly derives from the robust nature of the double cubane[33b] that precludes rupture of the N_2H_4 bridge and consequently prevents the generation of an available lone pair. The reactivity of **II** (Fig.18) may well be attributed to **I** that very likely exists in small amounts in equilibrium with **II**. Indeed addition of N_2H_4 to a solution of **II** leads to the formation of the $[(Cl_4\text{-cat})MoFe_3S_4(Cl)_3(N_2H_4)]^{2-}$ cubane. Additional evidence that the interaction of hydrazine with only one single cubane is necessary and sufficient for catalytic reduction is available in studies with phenyl hydrazine, $PhHNNH_2$. The replacement of the CH_3CN molecule in **I** by $PhHNNH_2$, by a known substitution reaction[62], occurs readily. The product (Fig.19) which for steric reasons does not interact further with another cubane molecule to form a bridged double cubane similar to **II**, has been structurally characterized[60] (Fig.19). The stoichiometric or catalytic reductions of the terminally coordinated $PhHNNH_2$ in this complex proceed with the formation of NH_3 and aniline (Table I)

3.1.2.Importance of the Mo atom. With the effectiveness of **I** in the catalytic reduction of hydrazine to NH_3 well established, the question regarding the identity of the metal site involved in catalysis remained to be answered. Toward this goal the reduction of N_2H_4 was attempted with the $[(Cl_4\text{-}cat)MoFe_3S_4(Cl)_3(PEt_3)]^{2-}$, **V**[64], and $[(Citr)MoFe_3S_4(Cl)_3]^{3-}$, **Ib**[63], clusters as potential catalysts. The PEt_3 ligand in **V** is known[66] to be substitutionally inert and so is the tridentate citrate ligand in **Ib**. The results

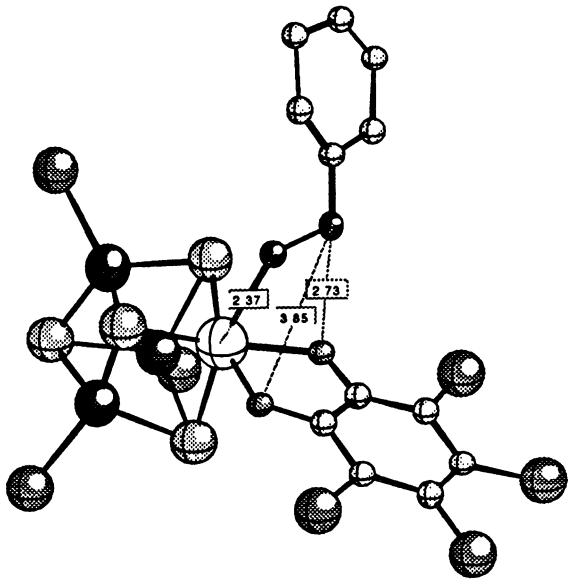

Figure 19. The Structure of the$[(Cl_4\text{-cat})MoFe_3S_4(Cl)_3(N_2H_3Ph)]^{2-}$ Cubane, (ref. 60).

show that under identical conditions the hydrazine *disproportionation* reactions (reactions not complicated by catalyst precipitation) catalyzed with either **V** or **Ib** are slower than the same reactions catalyzed with **Ia**. The importance of the Mo atom, rather than the Fe atoms, in catalysis is supported further by the observation that the $[Fe_4S_4Cl_4]^{2-}$ cluster is not active as a N_2H_4 reduction or disproportionation catalyst over a period of 12h. The structural similarity of the $MoFe_3S_4$ clusters to the Fe/Mo/S center in nitrogenase (Fig.1) and the competence of the former in the catalytic reduction of N_2H_4, a nitrogenase substrate[65], raise the question whether the activation and reduction of dinitrogen (or the derivative substrates, diazene and hydrazine) by the Fe/Mo/S center in nitrogenase could possibly take place ton the Mo atom by a single metal site mechanism.

3.1.3.Possible Mechanism. A simple proposed mechanism (Fig.20)

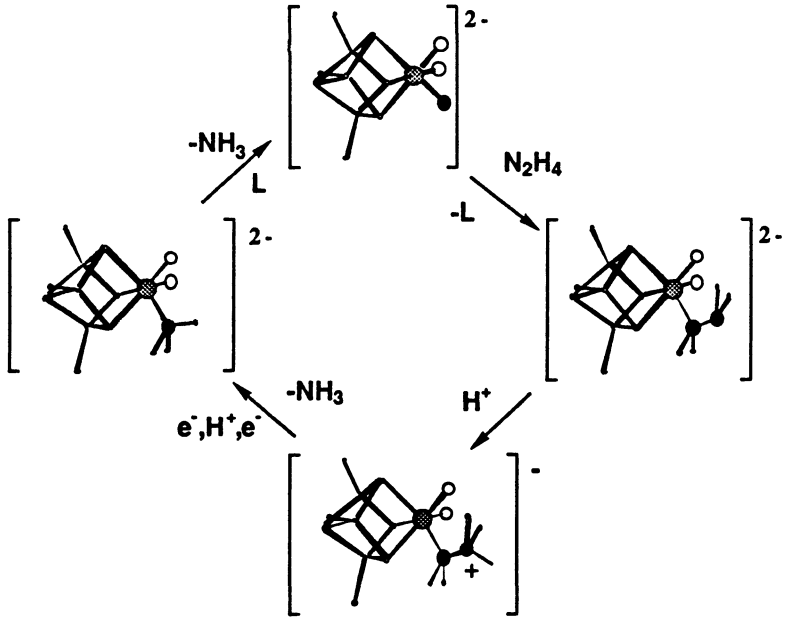

Figure 20. Proposed Mechanism for Hydrazine Reduction by the $MoFe_3S_4$ Cubanes (ref. 60)

for the catalytic reduction of N_2H_4 to ammonia by the Fe_3MoS_4 cluster is similar to a portion of the mechanism proposed previously for the reduction of NH_2NH_2 on the $(Me_5Cp)W(CH_3)_3$ fragment[56]. At present there is no evidence to support the sequence of events prior to N-N bond cleavage. An initial protonation step prior to reduction of the coordinated hydrazine molecule (Fig.20) is arbitrary and reflects our preference. For the action of nitrogenase a mathematical model has been derived by Thorneley and Lowe[66] and is based on detailed analyses of pre-steady state kinetics of hydrazine and ammonia formation and of hydrogen evolution as a function of various reagent concentrations and component ratios. The model is based on eight individual electron transfers on a mononuclear molybdenum species as required for the reduction of one N_2 molecule and two H^+ ions to H_2. Similar but less complete mechanisms also have been suggested by Cleland[67] and by Guth and Burris[68].

The apparent superior catalytic properties of the citrate derivative of the single cubane (18- **I**, Table I) is intriguing. A possibility for the role of carboxylate groups, in the reduction of substrates that also involves proton transfer is suggested (Fig. 21).

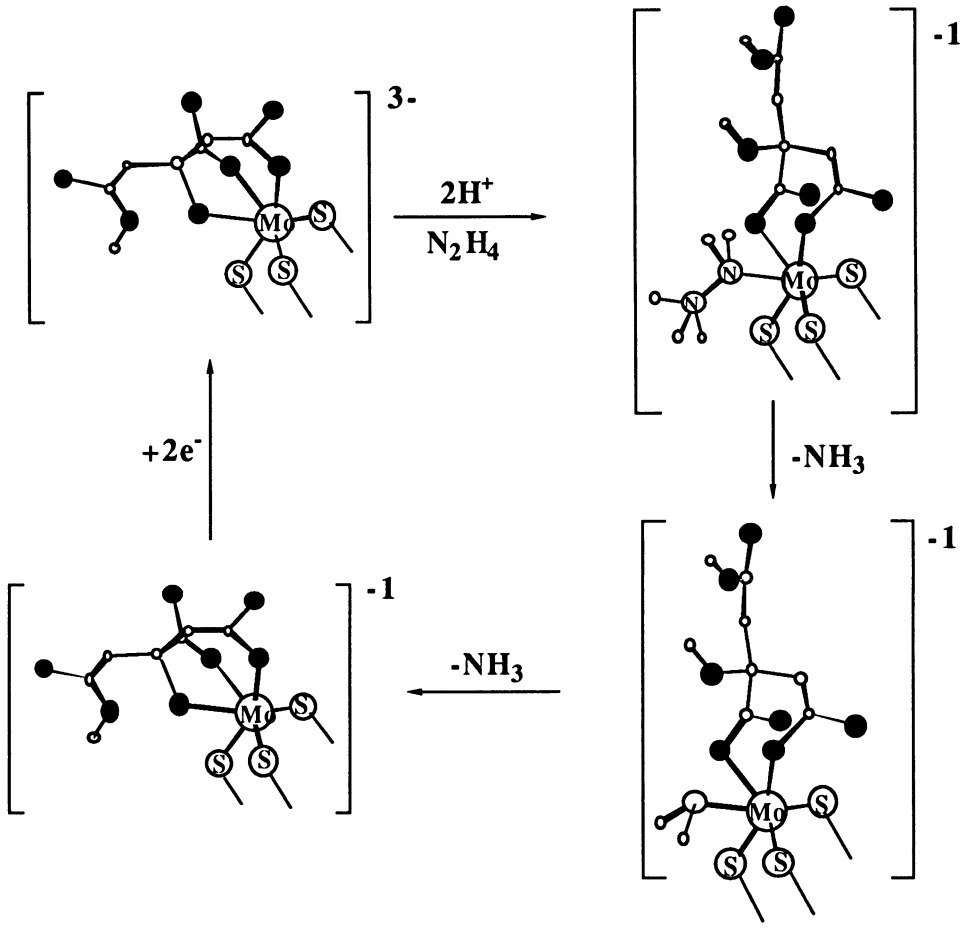

Figure 21. Possible Role of the Citrate Ligand as a proton "shuttle" in the Reduction of Hydrazine

3.1.4. Catalysis with a V/Fe/S cluster. Nitrogenase systems that contain V in place of Mo have been isolated from *A. vinelandii*[69a] and *A. chroococcum*[69b] and function under conditions of molybdenum deficiency. The structural similarity of the Fe/V/S center in the V-Fe protein from *A. chroococcum* to the Fe/Mo/S centers in the "conventional" Mo-nitrogenases has been established by a V-EXAFS analysis[70] and indicates that the vanadium is present as a removable FeV-cofactor[70] analogous to the FeMo-cofactor, with vanadium substituting for the molybdenum. The V-nitrogenase has been found to catalyze the reduction of N_2 and other nitrogenase substrates.

Catalytic reductions of N_2H_4 to NH_3 can be carried out using the $(Me_4N)[(DMF)_3VFe_3S_4Cl_3]\cdot 2DMF$ cluster[71] (Fig.22) as a catalyst in various hydrazine to cubane ratios (10:1, 20:1, and 40:1) in CH_3CN solutions at ambient temperature and pressure[72]. As

previously described, cobaltocene, $CoCp_2$, and lutidine hydrochloride, Lut·HCl, were used as the reducing agent and the proton source, respectively.

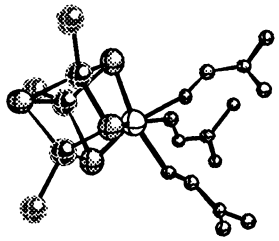

Figure 22. The Structure of the $(Me_4N)[(DMF)_3VFe_3S_4Cl_3]\cdot 2DMF$ cluster (ref. 71)

While preliminary results suggest that a structural intermediate containing N_2H_4 bound to the cubane is likely, coordination of hydrazine to the V atom prior to reduction can only be implied on the basis of the approximate relative rates for V-cubanes with different terminal ligands on the V atom. It is known[71a] that the reaction with $[(DMF)_3VFe_3S_4Cl_3]^-$ (**IV**) and between one and 30 equivalents of triethylphosphine (PEt_3) results in the formation of only the mono-substituted $[(DMF)_2(PEt_3)VFe_3S_4Cl_3]^-$ cluster (**V**). Typical catalytic reactions were carried out using 10 equivalents of hydrazine in the presence of **V**. The latter was formed *in situ* by stirring **IV** with a slight excess (1.1 equivalent) of PEt_3 for 15 minutes before the addition of additional reagents. The approximate rate of reduction of N_2H_4 by **V**, (Table II) was two-fold slower than the rate with **IV**. Additional experiments using $[(DMF)(bpy)VFe_3S_4Cl_3]^-$ [71a] (**VI**) as catalyst show that the rate of hydrazine reduction also decreased significantly (Table II). This difference in reactivity ,at least between **IV** and **VI**, is not due to a difference in redox potentials. The first reduction waves of **IV** and **VI** are detected by cyclic voltametric measurements in CH_3CN solution at -1.20V and -1.22V, respectively, (vs. Ag/AgCl). These results are consistent with those reported earlier[71a] for the same complexes in DMF solution vs. SCE. The profound effects of V-bound terminal ligands on the relative rates of hydrazine reduction are in agreement with those reported previously for the Mo system and suggest that the activation and reduction of the N_2H_4 molecule may occur on the V atom.

3.2 CATALYTIC REDUCTION OF ACETYLENE

The $[(Cl_4\text{-cat})(CH_3CN)MoFe_3S_4]^{2-}$ single cubane (Fig. 18-**I**) has been found effective in the slow catalytic reduction of acetylene to ethylene and a small amount of ethane.[73] As is the case for the reduction of acetylene by nitrogenase, the acetylene reduction by the model cubane gives *cis* ethylene as verified by isotopic substitution experiments. Preliminary results indicate that this reaction follows Michaelis/Menten kinetics with K_m = 6.2 mmol and a turnover of 0.11 mol of C_2H_4 (mol catalyst)$^{-1}$ (min)$^{-1}$. In nitrogenase, $K_m \sim 0.44$ mol and the turnover is 150-200 C_2H_4 (mol catalyst)$^{-1}$ (min)$^{-1}$.

3.3. THE STOICHIOMETRIC REDUCTION OF CN^-

The bridging CN^- ligand in the doubly-bridged double cubanes (Fig. 18 **III**) is reduced by cobaltocene in the presence of Lut·HCl to methane and ammonia[74]. The reduction of the CN^- ligand is not observed to any significant extent in the $[(Cl_4\text{-cat})MoFe_3S_4(Cl)_3(CN)]^{3-}$ single cubane or the μ-CN singly-bridged double-cubane (Fig.18-**II**). A proposed pathway for the stoichiometric reduction of the CN^- ligand in the

Table II. Comparative Catalytic Reduction of Hydrazines with the Mo and V cubanes in CH_3CN solution[a]

Catalyst	Sbstrt.	Sbstrt / Ctlst	NH_3 (Equiv.) 0.5 hr	1.0 hr	2.0 hr	NH_3 (Max)	Cnvrsn % 0.5 hr	1.0 hr	2.0 hr
Ia	N_2H_4	10	13.2 (2)	14.6 (2)	19.2 (2)	20	66	73	96
I	*N_2H_4*	*10*	*15.2 (3)*	*17.8 (3)*	*20.0(3)*	*20*	*76*	*89*	*100*
Ia	N_2H_4	20	32.8 (3)	37.2 (3)	40.0 (3)	40	82	93	100
I	*N_2H_4*	*20*	*23.2 (3)*	*28.8 (3)*	*35.6 (2)*	*40*	*58*	*72*	*89*
Ia	N_2H_4	40	61.6 (3)	69.6 (3)	73.9 (3)	80	77	87	92
I	*N_2H_4*	*40*	*36.8 (3)*	*48.0 (3)*	*64.8(2)*	*80*	*46*	*60*	*81*
Ia	N_2H_3Ph	10	4.5 (1)	5.8 (1)	10.0 (1)	10	45	58	100
I	*N_2H_3Ph*	*10*	*1.1(3)*	*1.5(3)*	*2.4(3)*	*20*	*11*	*15*	*24*

Ia ($MoFe_3S_4$ cubane, L = CH_3CN) *I (VFe_3S_4 cubane, 3L = 3DMF)*

a) For reaction conditions and protocols see footnotes in table I

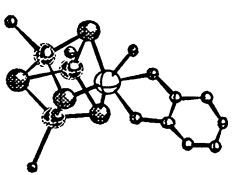

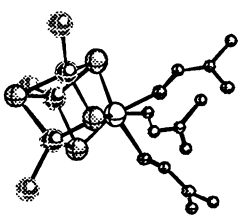

Possible Cyanide Activation and Reduction by the D-B-D-C

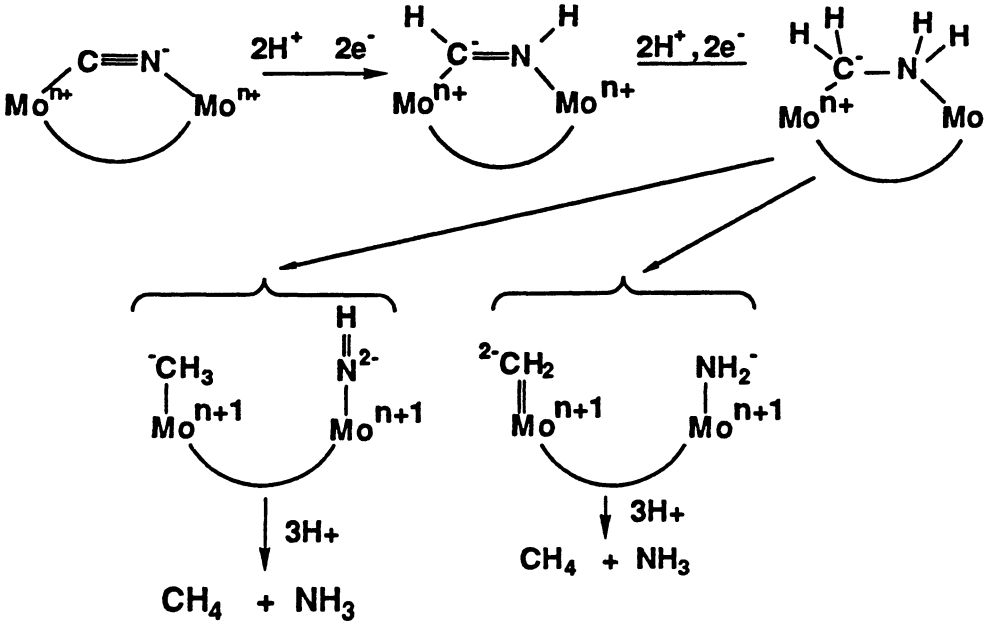

Oxidative Degradation of the NH_2OH DBDC

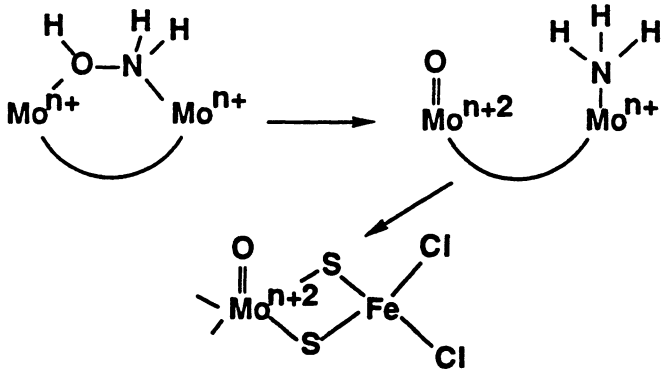

Figure 23

DBDC (Fig. 18 III) is shown below (Fig. 23). The reductive cleavage of the proposed μ_2-H_2C-NH_2^- bridge has a precedent in the reductive cleavage of the bridging

hydroxylamine·in the DBDC analogous to that shown in Fig. 18 **III.** Further, the possible formation of the $[(Cl_4\text{-cat})MoFe_3S_4(Cl)_3(CH_3)]^{3-}$ cluster prior to release of CH_4 is supported by the recent isolation of what appears to be this cluster. This black crystalline compound releases methane when treated with $Et_2O{\cdot}HCl$ in CH_3CN solution

4. Summary and conclusions

The results of the present study demonstrate that the molybdenum and vanadium atoms in the MFe_3S_4 clusters in environments very similar to those in the Fe/M/S centers of the nitrogenases, are catalytically active in the reduction of N_2H_4 to ammonia. It remains to be established whether the molybdenum atom in a specific $MoFe_3S_4$ cluster also is involved in the activation and reduction of N_2 to the hydrazine level. At present we have been unable to show any reactivity with N_2 and as reported earlier the CH_3CN ligand in $[(Cl_4\text{-cat})MoFe_3S_4(Cl)_3(CH_3CN)]^{2-}$ is not replaced by N_2 although the possibility still exists that a similar cluster may bind to N_2 through the Mo atom at a different (lower) oxidation level. It should be emphasized nevertheless that, as suggested recently[47a], the direct involvement of the unique coordinatively unsaturated Fe atoms cannot be ruled out. Indeed the early stages of N_2 reduction on the Fe/Mo/S center of nitrogenase may involve binuclear (Fe-Mo) activation prior to reduction to the hydrazine level. The binuclear activation of N_2 by initial binding to Fe and participation of the Mo atom in a Fe-μ-S-Mo bridging unit has been proposed previously· Earlier studies in our laboratory have shown that cuboidal subunits with the Fe_3S_4 core can serve as ligands for Mo(0) when the latter is stabilized by p acceptor ligands such as CO. At present we are exploring the possibility that the $[(CO)_3MoFe_3S_4(L)_3]^{3-}$·clusters[75] and derivatives will bind and activate N_2 and/or other nitrogenase substrates.

5. Acknowledgments

The studies reported in this account would not have been possible without the contributions of an extraordinary group of dedicated graduate students and research collaborators. I wish to acknowledge the immense contributions of all of my students. The solid state physics group (A.Kostikas, A Simopoulos and V.Papaefthymiou) in the Nuclear Research Center Demokritos in Athens Greece, and Dr. W.R. Dunham in the University of Michigan biophysics department, have been instrumental in conducting Mossbauer and EPR studies, very important for an in-depth understanding of the electronic structure of the Fe/Mo/S clusters. Financial support from the National Institutes of Health (GM-33080) and the National Science Foundation is gratefully acknowledged.

6. References

(1) Stiefel, E.I., In *Molybdenum Enzymes*. Stiefel, Coucouvanis, Newton, Eds. American Chemical Society, **1993**, pp. 1-19.

(2) a) Bray, R.C.; *Q. Rev. Biophys.*, **1988**, *21*, 299. b) Hille, R.; Sprecher, H.; *J. Biol. Chem.*, **1987**, *262*, 10914.

(3) Meincke, M.; Bock, E.; Kastrau, D.; Kroneck, P.M.H. *Arch. Microbiol.*, **1992**, *158*, 127.

(4) Adams, M.W.W.; Mortenson, L.E., In *Molybdenum Enzymes*, Spiro, T.G., Ed.; John Wiley & sons, New York, NY **1985**, pp 519-594.

(5) Rajagopalan, K.V., In *Molybdenum and Molybdenum Containing Enzymes*, Coughlan, M.P., Ed.; Pergamon Press, New York, NY **1980**, 241-272.
(6) Satoh, K.; Kurihara, F. N., *J. Biochem. Tokyo*, **1987**, *102*, 191.
(7) a) Hille, R., In *Molybdenum Enzymes*. Stiefel, Coucouvanis, Newton, Eds. American Chemical Society, **1993**, pp. 22-37 b) Hille, R.; George, G.N.; Eidsness, M. K.; Cramer, S. P., *Inorg. Chem,* **1989**, *28*, 4018 and references therein.
(8) Rajagopalan, K. V., In *Molybdenum Enzymes*. Stiefel, Coucouvanis, Newton, Eds. American Chemical Society, **1993**, pp. 38-49.
(9) a) Holm, R.H., *Coord. Chem. Rev.*, **1990**, *100*, 183. b) Berg, J.M.; Holm, R.H., *J.Am. Chem. Soc.* **1985**, *107*, 917.
(10) a) Roberts, S.A.; Young, C.G.; Kipke, C.A.;, Cleland, W.E.,Jr.; Yamanouchi, K.; Carducci, M.D.; Enemark, J.H., *Inorg. Chem.*, **1990**, *29*, 3650. b) Xiao, Z.; Young, C.G.; Enemark, J.H.; Wedd, A.G., *J.Am. Chem. Soc.* **1992**, *114*, 9194.
(11) Hille, R.; Sprecher, H., *J. Biol. Chem.*, **1987**, *262*, 10914.
(12) a) Massoth, F.E. *Adv. Cat,* **1978**, *27*, 265. b)Topsoe, J.; Clausen, B.S. *Catal. Rev.-Sci. Engineering,* **1984**, *26*, 395. c) Weisser, O.; and Landa, S.,*"Sulfide Catalysts: Their Properties and Applications"* Pergamon Press, London, **1973.**
(13) Pecoraro, T.; Chianelli, R., *J. Catal*, **1981**, *67*, 430.
(14) Stiefel, E.I.; Halbert, T.R.; Coyle, C.L.; Wei, L.; Pan, W.-H.; Ho, T.C.; Chianelli, R.R.; Daage, M. *Polyhedron,* **1989**, *8*, 1625.
(15) Parshall, G.W., "Homogeneous Catalysis"; Wiley, New York, **1980**, pp 174-176.
(16) Rappe, A.K.; Goddard, W.A. III, *J.Am. Chem. Soc.* **1980**, *102*, 5115. b) R A.K.; Goddard, W.A. III, *J.Am. Chem. Soc.* **1982**, *104*, 448.
(17) Coucouvanis, D.; Toupadakis, A.; Koo, Sang-Man; Hadjikyriacou, A. *Polyhedron,* **1989**, *8*, 1705. b) Coucouvanis, D.; Toupadakis, A.; Lane, J.D.; Koo, S.M.; Kim, C.G.; Hadjikyriacou, A.,*J. Am. Chem. Soc.*, **1991**, *113*, 5271.
(18) a) Coucouvanis D., Hadjikyriacou, A.I., Draganjac,M., Kanatzidis, M.G., Ileperuma, O., *Polyhedron,* **1986**, *5*, 349. b) Hadjikyriacou, A.I., Coucouvanis, D., *Inorg. Chem.,* **1987**, 26, 2400. c) Muller, A. *Polyhedron,* **1986**, *5*, 323.
(19) Harmer, M.A.; Halbert, T.R.; Pan, W.-H.; Coyle, C.L.; Cohen, S.A.; Stiefel, E.I. *Polyhedron,* **1986**, *5*, 341.
(20) Muller, A.; Bhattacharyya, R.G.; Pfefferkorn, B. *Chem. Ber.*, **1979**, *112*, 778.
(21) a) Martinez, M.; Ooi, B.-L.; Sykes A.G. *J.Amer. Chem. Soc.*, **1987**, *109*, 4615. b) Shibahara, T.; Kuroya, H.; Matsumoto, K.; Ooi, S. *J.Amer. Chem. Soc.*, **1984**, *106*, 789.
(22) Shibahara, T.;Yamamoto, T.; Kanadani, H.; Kuroya, H.,*J.Amer. Chem. Soc.*, **1987**, *109*, 3495.
(23) a) Coucouvanis, D.; Simhon, E.D.; Baenziger, N.C.; *J.Am. Chem. Soc.*, **1980**, *102*, 6644. b) McDonald, J.W.; Friesen, G.D.; Newton, W.E. *Inorg. Chim. Acta,* **1980**, *46*, L79. c) Muller, A.; Hellmann, W.; Romer, C.; Romer, M.; Bogge, H.; Jostes, R.; Schimanski, U., *Inorg. Chim. Acta* **1984**, *83*, L75. d) Coucouvanis, D.; Stremple, P.; Simhon, E.D.; Swenson, D.; Baenziger, N.C.; Draganjac, M.; Chan, L.T.; Simopoulos, A.; Papaefthymiou, V.; Kostikas, A.; Petrouleas, V. *Inorg. Chem.,* **1983**, *22*, 293. e) Coucouvanis, D., Baenziger, N.C.; Simhon, E.D.; Stremple, P.; Swenson, D.; Kostikas, A.; Simopoulos, A.; Petrouleas, V.; Papaefthymiou, V. *J.Amer. Chem. Soc.*,

1980, *102*, 1730. f) Coucouvanis, D.; Simhon, E.D.; Stremple, P.; Ryan, M.; Swenson, D.; Baenziger, N.C.; Simopoulos, A.; Papaefthymiou, V.; Kostikas, A.; Petrouleas, V., *Inorg.Chem*, **1984** ,*23*, 741. g) Coucouvanis, D. *Acc. Chem. Res.* **(1981)** *14*, 201.

(24) Coucouvanis, D.; Draganjac, M. *J.Amer. Chem. Soc.*, **1982**, *104*, 6820.

(25) a) Coucouvanis, D.; Hadjikyriacou, A.; Toupadakis, A.; Koo, Sang-Man; Ileperuma, O.; Draganjac, M.; Salifoglou, A. *Inorg. Chem.* **1991**, *30*, 754. b) Draganjac, M.; Coucouvanis, D. *J.Am. Chem. Soc.*, **1983**, *105*, 139.

(26) Draganjac, M.; Simhon, E.; Chan, L.T.; Kanatzidis, M.; Baenziger, N.C.; Coucouvanis, D. *Inorg. Chem.*,**1982**, *21*, 3321.

(27) a) Coucouvanis, D.; Koo, Sang-Man, *Inorg. Chem*, **1989**, *28*, 2.

(28) Hadjikyriacou, A.I; Coucouvanis, D. *Inorg. Chem*, **1989**, *28*, 2169.

(29) Coucouvanis, D.; Hadjikyriacou, A.I. *Inorg. Chem*, **1987**, *26*, 1.

(30) Bunzey, G.; Enemark, J.H.; *Inorg. Chem*, **1978**, *17*, 682.

(31) a) Kim, C. G.; Coucouvanis, D. *Inorg. Chem*, **1993**, *32*, 2232. b) Kim, C.G.; Coucouvanis, D., *Inorg. Chem*, **1993**, *32*, 1881. c) C.G. Kim, thesis, University of Michigan (1993).

(32) Fish, K.M.; Massey, V.; Sands, R.H.; Dunham, W.R., *J. Biol. Chem*,, **1990**, *265*, 19665-19671.

(33) a) PR. Challen, S.-M. Koo, C.G. Kim, W.R. Dunham, D. Coucouvanis, *J.Am.Chem. Soc.* **1990**, *112*, 8606. b) P.R. Challen, thesis, University of Michigan (1990). c) D. Coucouvanis, *et al.*, *Inorg. Chem.* **1989**, *28*, 4181.

(34) Coucouvanis, D.; Al-Ahmad, S.; Kim, C.G.; Mosier, P.E.; Kampf, J.W.; *Inorg. Chem*, **1993**, *32*, 1533.

(35) Coucouvanis, D.; Al-Ahmad, S. to be published.

(36) Halbert,T.R.; Pan, W.H.; Stiefel, E.I. *J. Am. Chem. Soc* , **1983**, *105*, 5476.

(37) Toupadakis, A., Ph. D. thesis, University of Michigan (1990).

(38) Hille, R.; Massey, V., In *Molybdenum Enzymes*, Spiro, T. G., Ed.; John Wiley & sons, New York, NY **1985**; pp 443.

(39) Ueyama, N.; Oku, H.; Nakamura, A., *J.Amer. Chem. Soc.*, **1992**, *114*, 7310.

(40) Rees, D., Personal communication.

(41) Burrow, T.E.; Lazarowych, N.J.; Morris, R.H.;Lane, J.; Richards, R.L., *Polyhedron*, **1989**, *8*, 1701.

(42) Bianchini, C.; Mealli, C.; Meli, A.; Sabat, M. *Inorg. Chem.* **1986**, *25*, 4617. b) Bianchini, C.; Meli, A., *Inorg. Chem.*, **1987**, *26*, 4268.

(43) W.H. Orme-Johnson, *Ann. Rev. Biophys. Chem.*, **1985**, *14*, 419.

(44) B.K. Burgess, *Advances in Nitrogen Fixation Research*, C. Veeger and W.E. Newton, Eds. (Martinus-Nijhoff, The Hague, **1983**), p. 103.

(45) R.H. Burris, *J. Biol. Chem.*, **1991**, *266*, 9339.

(46) a) B.E. Smith and R.R. Eady, *Eur. J. Biochem.*, **1992**, *205*, 1. b).W.E. Newton, *Biological Nitrogen Fixation*, G. Stacey, R.H. Burris, H.J. Evans, Eds. (Chapman Hall, New York, **1992**), p. 877.

(47) a) J. Kim and D.C. Rees, *Science* , **1992**, *257*, 1677. b) J. Kim and D.C. Rees, *Nature* , **1992**, *360*, 553. c) D.C. Rees, *et al.*, *New Horizons in Nitrogen Fixation*, R. Palacios, *et al.*, Eds. (Kluwer Academic Publishers, Dordrecht, **1993**), pp. 83-88.

(48) a) J.T. Bolin, *et al.*, *New Horizons in Nitrogen Fixation*, R. Palacios, *et al.*, Eds. (Kluwer Academic Publishers, Dordrecht, **1993**), pp. 89-94. b) J.T. Bolin, *et al.*, *Nitrogen Fixation: Achievements and Objectives*, P.M. Gresshoff, G. Stacey, L.E. Roth, W.E. Newton, Eds. (Chapman and Hall, New York,

1990), p. 117. c) J.T. Bolin, A.E. Ronco, T.V. Morgan, L.E. Mortenson, N.-H. Xuong, *Proc. Natl. Acad. Sci. U.S.A.*, in press.

(49) a) D. Coucouvanis, *Acc. Chem. Res.*, **1991**, *24*, 1. b) R.H. Holm, and E.D. Simhon, *Molybdenum Enzymes*, T.G. Spiro, Ed. (Wiley Interscience, New York, **1985**), chap. 1.

(50) J.M. Berg and R.H. Holm, *Iron Sulfur Proteins*, T. Spiro, Ed. (Wiley Interscience, New York, **1982**), p. 1.

(51) a) M. Tanaka, K. Tanaka, T. Tanaka, *Chem. Lett.*, **1982**, 767. b).K. Tanaka, Y. Hozumi, T. Tanaka, *Chem. Lett.*, **1982**, 1203. c)K. Tanaka, Y. Imasaka, M. Tanaka, M. Honjo, T. Tanaka, *J. Am. Chem. Soc.*, **1982**, *104*, 4258.

(52) G.J. Leigh, *J. Mol. Catal.*, **1988**, *47*, 363.

(53) a) J. Chatt, J.R. Dilworth, R.L. Richards, *Chem. Rev.*, **1978**, *78*, 589. b). T.A. George, L.M. Koczon, R.C. Tisdale, K. Gebreyes, L. Ma, *Inorg. Chem.*, **1991**, *30*, 883. c) T.A. George and B.B. Kaul, *Inorg. Chem.*, **1991**, *30*, 883. d) C.C. Cummins, S.M. Baxter, P.K. Wolczanski, *J. Am. Chem. Soc.*, **1988**, *110*, 8731.

(54) G.N. Schrauzer, P.R. Robinson, E.L. Moorehead, T.M. Vickrey, *J. Am. Chem. Soc.*, **1976**, *98*, 2815 (and references therein).

(55) A.E. Shilov, *J. Mol. Catal.*, **1987**, *41*, 221.

(56) R.R. Schrock, T.E. Glassman, M.G. Vale, M. Kol, *J. Am. Chem. Soc.* , **1993**, *115*, 1760.

(57) E. Block, G. Ofori-Okai, H. Kang, J. Zubieta, *J. Am. Chem. Soc.*, **1992**, *114*, 758.

(58) R.W.F. Hardy, R.C. Burns, G.W. Parshall, *Adv. Chem. Ser.* , **1971**, *100*, 219.

(59) P.E. Mosier, C.G. Kim, D. Coucouvanis, *Inorg. Chem.*, in press.

(60) Coucouvanis, D.; Mosier, P.E.; Demadis, K.D.; Patton, S.; Malinak, S.M.; Kim, C. G.; Tyson, M.A., *J. Am. Chem. Soc.*, **1993**, *115*, 12193.

(61) R.W.F. Hardy and E.K. Jackson, *Federation, Proc.*, **1967**, *26*, 725.

(62) R.E. Palermo, R. Singh, J.K. Bashkin, R.H. Holm, *J. Am. Chem. Soc.*, **1984**, *106*, 2600.

(63) D. Coucouvanis, K.D. Demadis, C.G. Kim, R.W. Dunham, J.W. Kampf, *J. Am. Chem. Soc.*, **1993**, *115*, 3344.

(64) R.E. Palermo and R.H. Holm, *J. Am. Chem. Soc.*, **1983**, *105*, 4310.

(65) a) R.N.F. Thorneley, R.R. Eady, D.J. Lowe, *Nature* , **1978**, *272*, 557. b) R.N.F. Thorneley and D.J. Lowe, *Biochem. J.*, **1984**, *224*, 887. c) L.C. Davis, *Arch. Biochem. Biophys.*, **1980**, *204*, 270.

(66) R.N.F. Thorneley and D.J. Lowe, *Biochem. J.*, **1983**, *215*, 393.

(67) W.W. Cleland, *Methods Enzymol.*, **1979**, *63*, 112.

(68) J.H. Guth and R.H. Burris, *Biochemistry* , **1983**, *22*, 5111.

(69) a) B.J. Hales, D.J. Langosch, E.E. Case, *J. Biol. Chem.*, **1987**, *261*, 15301.b) R.R. Eady, R.L. Robson, T.H. Richardson, R.W. Miller, M. Hawkins, *J. Biochem.* , **1987**, *244*, 197.

(70) a) G.N. George, C.L. Coyle, B.J. Hales, S.P. Cramer, *J. Am. Chem. Soc.*, **1988**, *110*, 4057. b) J.M. Arber *et al., Nature*, **1987**, *325*, 372.

(71) a) Kovacs, J.A.; Holm, R.H., *Inorg. Chem.*, **1987**, *26*, 702. b) Kovacs, J.A.; Holm, R.H., *Inorg. Chem.*, **1987**, *26*, 711. c) Ciurli, S.; Holm, R.H., *Inorg. Chem.*, **1989**, *28*,

(72) a) Steven M. Malinak and Dimitri Coucouvanis *J. Amer. Chem. Soc.* submitted b) In all cases, $[N_2H_4] = 1.4 \times 10^{-3}$ M and the concentrations of cubane, $CoCp_2$, and Lut·HCl were scaled accordingly. The total solution volume (CH_3CN) was 40.0 ml.

(73) Les Laughlin and D. Coucouvanis, Work in progress.
(74) P.E. Mosier and D. Coucouvanis, Work in progress.
(75) D. Coucouvanis, S. Al-Ahmad, A. Salifoglou, W.R. Dunham, R.H. Sands, *Angew. Chem. Int. Ed. Engl.*, **1988**, *27*, 1353.

USE OF *DE NOVO* DESIGNED PEPTIDES FOR THE STUDY OF METALLOPROTEINS AND ENZYMES

G. DIECKMANN[1], S. HEILMAN[1], D. McRORIE[2], W. DeGRADO[3], V.L.PECORARO[1]

[1]Department of Chemistry, University of Michigan, Ann Arbor, MI 48109, USA; [2]Department of Research & Applications, Beckman Instruments, Palo Alto, CA 94304, USA;[3]Biotechnology Department, DuPont-Merck Pharmaceutical Company Wilmington, DE 19880, USA.

ABSTRACT: *De novo* design of protein structure(s) is a useful technique for understanding the factors that influence metalloprotein structure and stability. We have designed a series of α-helical coiled coil proteins for the modelling of the trigonal Hg(II) site of the metalloregulatory protein mer R. The peptides Ac-G-(LKALEEK)$_4$-GCONH$_2$, and Ac-G-(LKALEEK)-(LKACEEK)-(LKALEEK)$_2$-GCONH$_2$ were designed to self-aggregate as three-helix bundles. These peptides have been shown to have pH dependent aggregation and stability characteristics. The cysteine substituted peptide converts to an exceptionally stable two-helix bundle when Hg(II) is bound. This example illustrates how metal ions may dictate peptide aggregation.

1. Introduction

De novo literally means anew or over again. *De novo* design refers to the process by which a protein sequence can be determined which will yield a desired secondary structure of a protein/(peptide) through observations of primary/secondary structural relationships in naturally occurring proteins. The ability to readily obtain a desired protein structure makes *de novo* design a technique which is amenable for use in the study of metalloproteins and enzymes. This is because the addition of a metal binding site, with a desired geometry and ligand donor set, can then be easily achieved. Use of *de novo* designed peptides for metalloprotein study offers several advantages over other techniques traditionally used to study such proteins such as site-directed mutagenesis and small molecule model chemistry. Some of these advantages include: 1) a smaller structure which is less complex than the naturally occurring protein of interest, 2) the ability to provide insight into the nature of the metal site (similar to small model chemistry), but with the addition of being able to study how the metal affects protein structure (or the protein the coordination chemistry of the metal), 3) use of truly biological ligand donor sets - amino acids, 4) ease in synthesis and variation of residues in the structure, and 5) ability to work in water at biological pH values because of the hydrophobic nature of the interior of proteins.

2. Protein Structure & a-Helical Coiled Coil Proteins

Despite the vast number of conformations available to the amino acids in proteins, many structural motifs occur over and over again[1]. One such recurring structural motif is that

D.P. Kessissoglou (ed.), Bioinorganic Chemistry, 275-285

of an α-helix. α-helical structures are characterized by hydrogen bonding from the carboxyl group of an amino acid to the amide proton four amino acid residues away in the sequence.

An α-helix is amphiphatic if one side of the helix structure contains predominately amino acid residues with hydrophobic side chains and the other side of the helix contains mainly residues with side chains which are neutral or charged. One type of protein characterized as amphiphatic is the α-helical coiled coil. The α-helices in these proteins come together, by means of hydrophobic interactions between helices, and coil about each other in a left-handed supercoil, hence the name coiled coil[2]. α-helical coiled coil proteins occur naturally in such proteins as tropomyosin and fibrinogen[2,3]. Coiled coil proteins have in common a heptad repeat substructure of residues within their sequence(2). These residues are generally given lower case letters **a** through **g**. As shown in Figure 1, positions **a** and **d** are occupied by hydrophobic residues, which serve to form

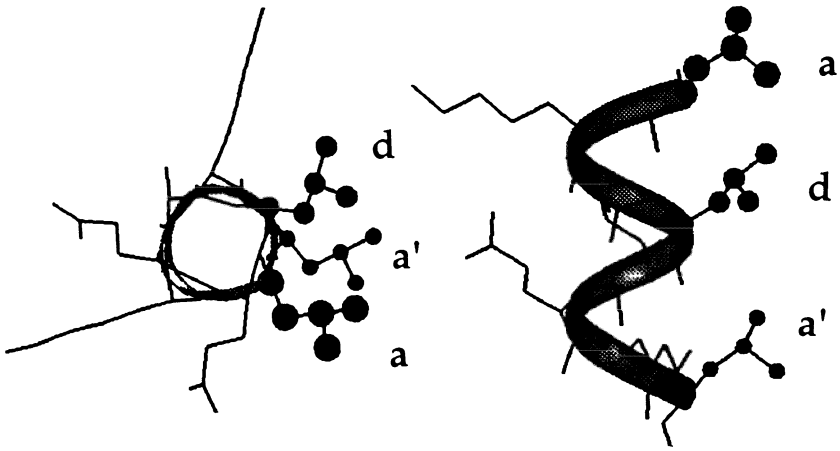

Figure 1. Views of an amphiphatic α-helix along the helical axis (left) and from the side (right). **a**=leucine in **a** position; **d**=leucine in **d** position; **a'**=leucine in **a** position of next heptad.

an interface of hydrophobic packing between aggregating helices. These hydrophobic packing layers are separated by a turn of the helix, which is equal to 5.4 A. Residues in positions **e** and **g** are charged and have the ability to form stabilizing interhelical salt bridges. The remaining residues, **b**, **c**, and **f** are solvent exposed and can be substituted with a variety of residues.

3. Construction of a Three-Helix Coiled Coil

Coiled coil proteins are well described structures[2,4] that can be modified to a number of helical aggregation states including two, three or four helix bundles[5]. Our group set out to obtain a three-helix bundle for future use in modelling the metalloregulatory protein

mer R, using the sequence Ac-G-(LAKLEEK)$_4$-GCONH$_2$. This peptide is called *Tri*, for its ability to from a three-helix bundle, and was modelled after the x-ray crystal structure of CoilSer, a known three-helix bundle[6]. See Figure 2.

Circular dichroism spectroscopy (CD) is a convenient method for assessing the α-helical nature of proteins. The CD spectrum of an α-helix is characterized by two negative peaks centered at λ=220 nm and 208 nm, coming from the $n \rightarrow p^*$ and $p \rightarrow p^*$ amide transitions, respectively.

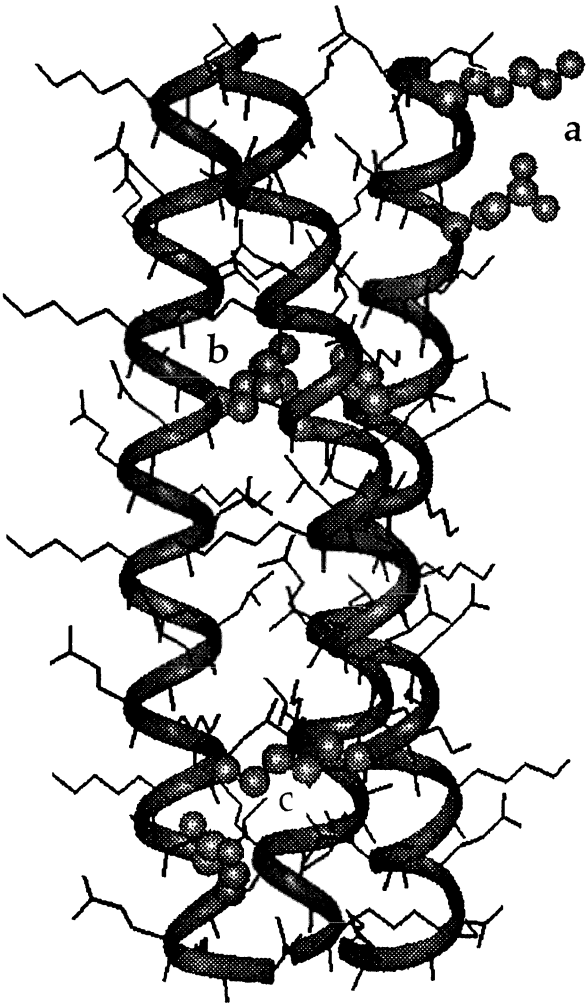

Figure 2. Model of the peptide Tri as a three-helix bundle at pH 5.5 showing important bundle stabilizing interactions. **a**= intrahelical salt bridging; **b**=hydrophobic packing layer in interior of bundle; **c**=interhelical salt bridging.

By monitoring the signal at λ=222 nm, the helicity of an α-helix can be assessed. This is achieved by converting the signal in mdegrees to a mean residue ellipticity, which is calculated using the following formula :

$$[\Theta]_{222} = \frac{\text{signal (degrees)} * 100}{\text{pathlength(cm)}*\text{number of residues}*\text{conc. of peptide(M)}}$$

A fully helical peptide (100% helicity) is given a value of -34,000 deg cm $dmol^{-1}$ for $[\Theta]_{222}$ [7].

As shown in Figure 3, the peptide *Tri* has significant α-helical content. The aggregation of *Tri* has been shown to be consistent with formation of a trimer at pH 5.5 by sedimentaion equilibrium, gel permeation chromatography and ESI-ms.

4. Affects of pH on Stability and Aggregation

Guanidine HCl can be used as a chemical denaturant of proteins. The stability of a helical structure can be determined by the amount of helical structure which remains in the presence of denaturants such as guanidine HCl. We undertook a study of observing the denaturation of the *Tri* family of peptides at varied pH's using circular dichroism spectroscopy, to determine if pH had any observable effect on the helical nature of these peptides. These titrations were carried out at pH values of 3.5, 4.5, 5.5, and 6.5. The midpoint of a denaturation curve provides the concentration of denaturant at which fifty percent of the helical structure remains. In Figure 3, it was found that the midpoint of the guanidine HCl denaturation curve of these peptides is shifted to higher values at pH 3.5 and 4.5 and to lower values at pH's 5.5 and 6.5.

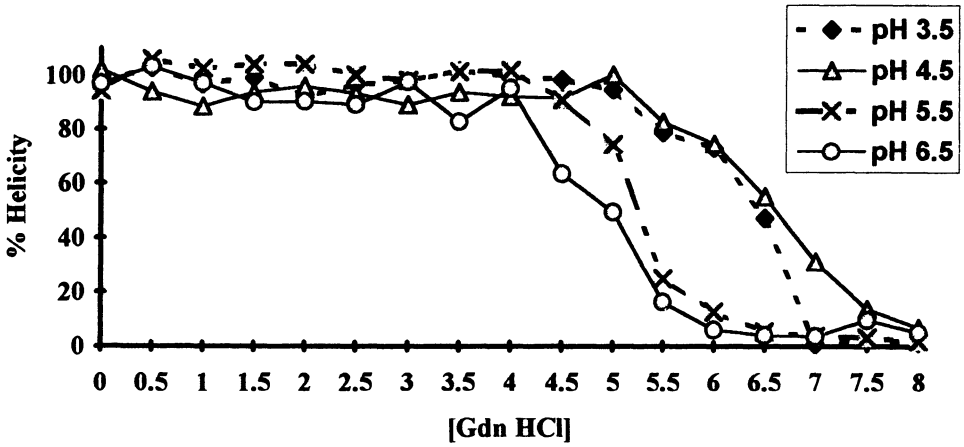

Figure 3. Guanidine HCl denaturation titration of *Tri* at various pH values.

Using sedimentation equilibrium studies, at varying proton concentrations, we have correlated a change in the aggregation state of these peptides with the stability changes seen at low pH values. At higher pH's the dominate species is that of the trimer, while at pH values lower than 5.0 the dimer predominates. This suggests that the salt bridging effects are of much greater importance to the aggregation state of these peptides than had previously been thought. Furthermore, the pH at which experiments are done is an important consideration for the overall structure present in solution.

5. Modelling of Peptide Structure

As discussed previously, it is important to know the likely structure of the designed protein before appropriate residues can be chosen to incorporate a specific metal binding site into the protein structure. This is achieved by building computer models of the peptide systems. All modelling work was performed on a Silicon Graphics Indigo 2 XZ with the Insight II and Discover programs (Biosym Technologies, Inc., San Diego, CA).

The secondary structure of a peptide is defined by the Φ and Ψ angles which represent the dihedral angles of the peptide backbone. Peptides with the Φ's and Ψ's appropriate for α-helices are built using hydrophobic residues (e.g. leucine, isoleucine, valine) in positions **a** and **d** and alanine in all other heptad positions. In this way hydrophobic packing is used initially to generate an aggregate model. Looking down the helical axis, it can be seen that consecutive **a** (and **d**) positions are rotated 20 degrees from one another (see Figure 1). In order to pack α-helices together, each helix is wound so that all heptad positions align along the length of the peptide. The helices are packed together using inter helical distances and side chain rotamers obtained from published protein crystal structures (Brookhaven **P**rotein **D**ata **B**ase). The helix bundle is than twisted to give a super-helical twist. Energy minimization are performed using a combination of steepest descent and conjugate gradient algorithms. The alanine residues are then replaced with appropriate hydrophilic residues (e.g. glutamate and lysine). One more round of energy minimizations is then requires to arrive at the final structure. Addition of a metal binding site involves replacement of specific positions in the bundle (typically **a** or **d** positions) to generate a desired ligand geometry and donor set for a metal.

6. Use of a Three-Helix Bundle to Study Metalloproteins

When designing a peptide for use in modelling a metal center, several aspects must be considered including: 1) the size and aggregation of the a-helices, 2) whether the overall structure will be covalently bound together or self aggregation will be important to the structure, 3) what coordination geometries can be achieved within the designed structure, and 4) if the metal is to be attached to the outside of the helices, placed at the bottom of a bundle of helices or located within the middle of the helices.

We are generally interested in the stability and structure of metallopeptides that may serve as models for complexation or catalysis in biological systems. A three-helix bundle is very desirable because of the number of metal coordination geometries which can be obtained using this aggregate. These geometries include linear, trigonal planar, tetrahedral, trigonal bipyramidal and octahedral, as shown in Figure 4 .

Mer R is the metalloregulatory protein responsible for regulating mercury resistance in bacteria [8]. Hg(II) is believed to be coordinated trigonally by three cysteine thiolates in

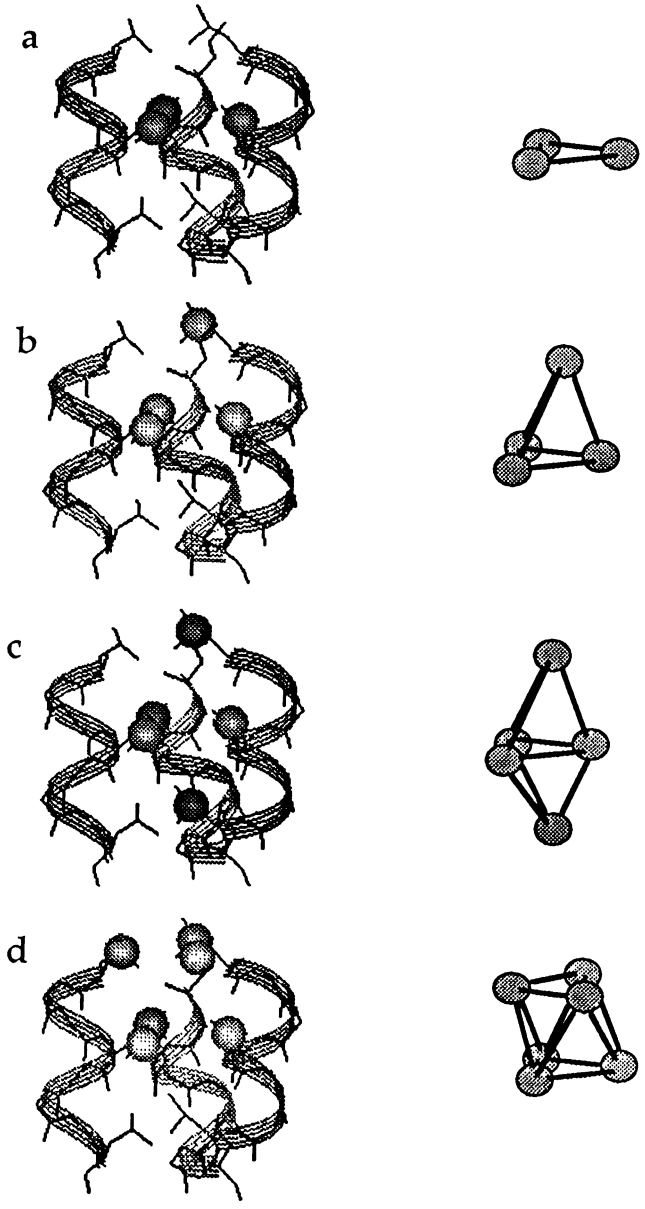

Figure 4. One turn of Tri showing the possible metal coordination geometries available in a three-helix bundle. The spheres are CPK surfaces on the b-methylene carbons of the leucine residues. **a** = trigonal; **b**=tetrahedral; **c**=trigonal bipyramidal; and **d**=octahedral.

Mer R [9], a geometry that is rather unusual for Hg(II). One approach for enforcing this uncommon Hg(II) coordination mode would be to take advantage of a peptide that aggregates into a three-helix bundle. Thus, the enthalpy inherent in the peptide assembly would outweigh the thermodynamic preference for a linear Hg(II) and force a trigonal coordination geometry. For this reason, *Tri*, was substituted at position twelve by a cysteine residue to form *Tri(L12C)*. This removes a single hydrophobic packing layer of the resultant three-helix bundle and provides three thiolate donors to create a trigonal binding site for Hg(II).

This substitution places the metal binding center directly within the protein bundle as shown in Figure 5.

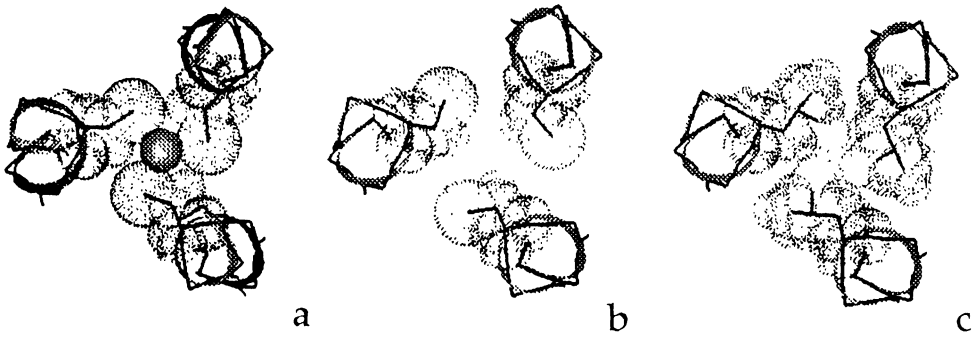

Figure 5. One layer of a three-helix bundle showing packing of the interior. **a** = three leucine residues, as in *Tri*; **b** = substitution of cysteine for leucine (*Tri(L12C)*); **c** = *Tri(L12C)* plus Hg(II).

Just as *Tri* was shown to exhibit a pH dependent aggregation state, *Tri(L12C)* has also shown similar behavior. Sedimentation equilibrium studies at pH 5.5 for *Tri(L12C)* exhibit characteristics of an equilibrium between a two and three-helix aggregation. At pH values lower than 5.5, sedimentation and gel permeation chromatography studies show increasing amounts of the dimer of *Tri(L12C)* dominate, while at pH values higher than 5.5 the trimer of *Tri(L12C)* increasingly becomes the major species.

To assess whether binding of Hg(II) is occurring at thiolate residues, all studies compared the interaction of Hg(II) with control peptide *Tri* and the metal binding peptide *Tri(L12C)*. Guanidine HCl denaturation titrations were used to determine if the helical nature of each of these peptides was changed upon the addition of Hg(II), and the helicity was monitored using CD. It was expected that no change in structure would be observed for *Tri* in the presence of Hg(II), unless Hg(II) is binding to the glutamate or lysine residues that form salt bridging interactions between the peptides. In contrast, the guanidine denaturation titration of *Tri(L12C)* would be significantly perturbed in the presence of Hg(II) since the stability of the three-helix bundle might be enhanced by metal complexation that would link the peptides together through mercury-sulfur bonds. Conversely, the stability of the structure might decrease because the addition of the metal within the bundle might serve to disrupt hydrophobic packing layers above and below the metal binding site. As predicted titrations of *Tri* in the presence of 0.33 equivalents of Hg(II) had no effect on the helical nature of the peptide, whereas the same ratio of Hg(II) profoundly affected the stability of *Tri(L12C)*. Titrations of *Tri(L12C)* in the presence of 0.33 equivalents Hg(II) were biphasic. As shown in Figure

6, the titration curve for Hg(II)/*Tri(L12C)* initially resembles that of *Tri(L12C)* in the absence of Hg(II). However, the denaturation curve leveled off at approximately sixty-six percent helicity (66% of the peptide remains helical, while 33% is denatured).

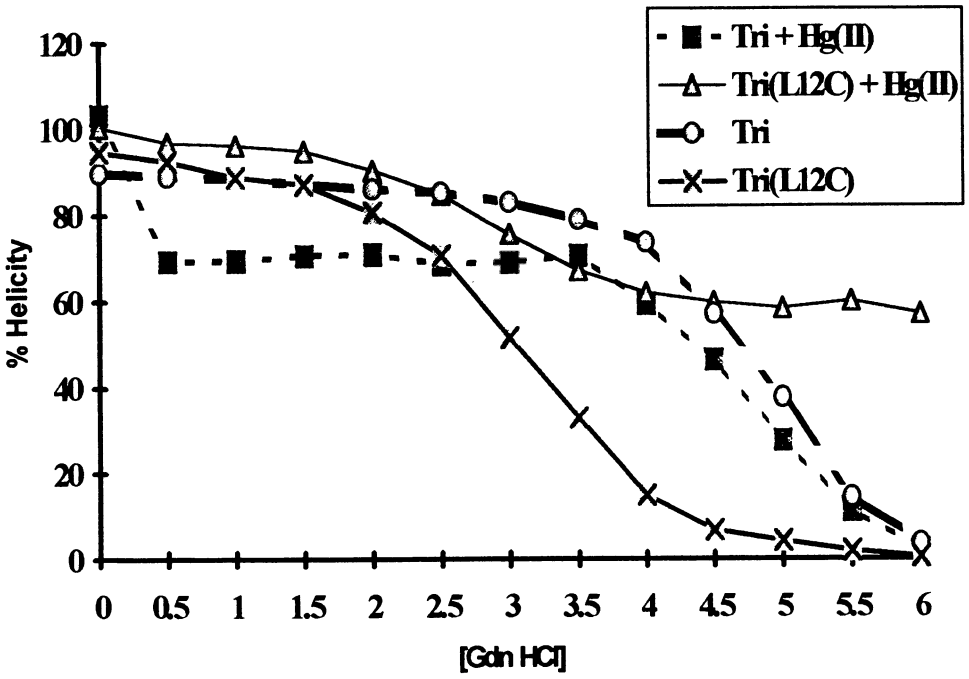

Figure 6. Guanidine HCl denaturation titrations of Tri and Tri(L12C) +/- Hg(II)

These results were interpreted according to a model where the binding of Hg(II) to *Tri(L12C)* occurred with a stiochiometry one Hg(II) to two *Tri(L12C)*. To test this hypothesis guanidine HCl denaturation titrations were performed using a variety of concentrations of Hg(II). The results shown in Figure 8 reflect a 2:1 peptide to Hg(II) stiochiometry. A 3:1 peptide to Hg(II) titration yielded a denaturation curve which levels of at 66% helicity, at 6:1 peptide to Hg(II) titration yielded a denaturation curve which leveled off at 33% helicity and at 2:1 peptide to Hg(II) titration showed no change in the helical nature of the peptide. See figure 7. The guanidine HCl titration of the Hg(II) to peptide species has greatly enhanced stability compared to a similar titration with the peptide alone. The Hg(II)[*Tri(L12C)*]$_2$ complex has been characterized by a number of methods in addition to CD (see Table 1 for summary). UV/vis titrations of Tri(L12C) to a solution containing Hg(II) show bands characteristic of a cysteine sulfur to Hg(II) LMCT. These absorbance bands continue to grow in with increasing equivalents of *Tri(L12C)* titrated until two equivalents are added, at which time the absorbance levels off. This results confirms ligation of Hg(II) to the cysteine thiolates and a stiochiometry of one equivalent Hg(II) to two equivalents of *Tri(L12C)*.

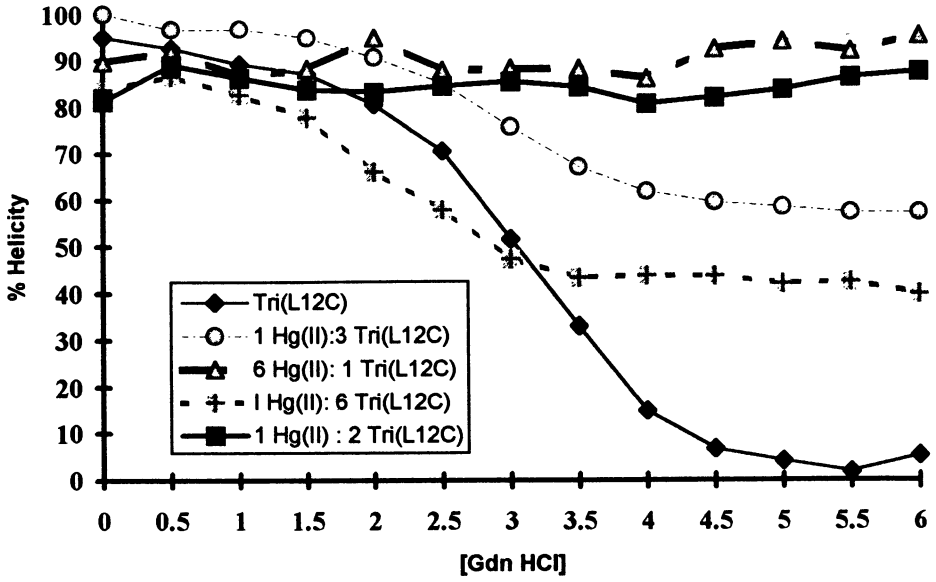

Figure 7. Determining Tri(L12C) to Hg(II) stiochiometry using Gdn HCl denaturation titrations

Gel permeation chromatography and ESI-ms of the Hg(II)[*Tri(L12C)*]$_2$ complex provides a molecular weight consistent with the formation of a one to two complex. EXAFS was used to determine the Hg(II)-S bond length of 2.32E (10), which is consistent with the formation of a linear two coordinate Hg(II) complex similar to that represented in Figure 8.

These results provide very interesting implications for metal constraints on protein structure. Clearly the energetic preference that defines helical aggregation when Hg(II) is coordinated to *Tri(L12C)* lies in favor of metal thiolate bonding. Thus, while a trigonal Hg(II) complex has not been formed we understand better the relative energies of metal binding versus hydrophobic association in these metallopeptide aggregates. Ag(I) shows similar behavior as Hg(II), however less thiolphilic metals do not perturb the native three-helix bundle stiochiometry. *Tri(L12C)*, similar to *Tri* has been shown to have a pH dependent aggregation state, existing as a dimer at low pH values and as a trimer at higher pH.

Future work in our group will focus on modifying the structure of *Tri* to achieve a trigonal site, by lengthening the peptide or moving the placement of the cysteine residue.

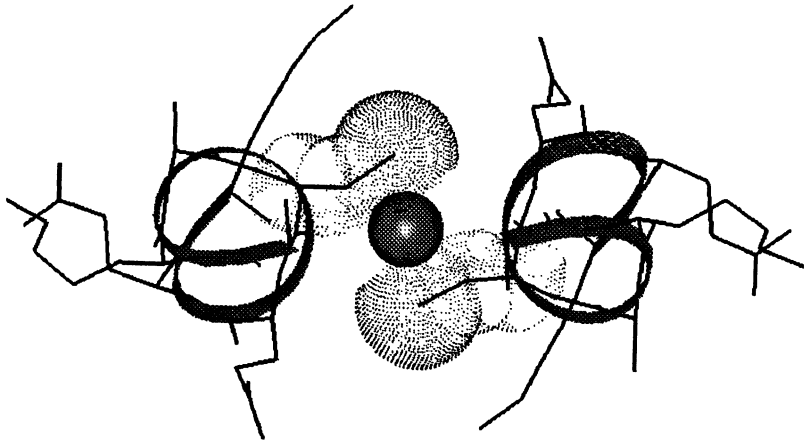

Figure 8. Model of Hg(II)[Tri(L12C)]$_2$ complex. Only one heptad of each helix is shown.

Table 1. Summary of Data Supporting Formation of a Hg(II)[*Tri(L12C)*]$_2$ Complex.

Experiment/ Technique	***Tri***	***Tri(L12C)***
Gdn HCl denaturations	no change in midpoint of titration upon addition of Hg(II)	midpoint shifts from 3M Gdn to 7.5 M Gdn with Hg(II)
^{1}H nmr	no change with Hg(II)	selective shifting or broadening of b-methylene protons upon Hg(II) addition
Gel Permeation chromatography	3-helix bundle	mixture of 2 & 3-helix bundles; 2-helix bundle with Hg(II)
UV/vis titrations	N/A	titration levels at 2 eq. *Tri(L12C)* per Hg(II)
UV/vis spectra	no LMCT	S-Hg(II) LMCT bands, ε=7500 cm^{-1}M^{-1}
EXAFS	N/A	2 sulfurs coordinated; Hg-S bond=2.32A
Sedimentation	3-helix bundle	mixture of 2 & 3-helix bundles; 2-helix bundle with Hg(II)

7. Conclusion

De novo design of protein structures provides a technique for the study of metalloprotein structure and stability. α-helical coiled coil proteins, are well characterized and provide for a number of helical aggregation states which makes this structure well suited for use in the study of metalloproteins.

Our studies have shown that these peptides must be well characterized before binding of metals, because of possible variations in stability and aggregation state which can occur with changes in pH. Using the peptide Ac-G-(LKALEEK)-(LKACEEK)-$(LKALEEK)_2$-$GCONH_2$, we have successfully bound Hg(II). It was desired that Hg(II) would be coordinated in a trigonal manner, however it seems that the thermodynamic preference of Hg(II) to be linearly coordinated is greater than the preference of this peptide to aggregate as a trimer. The linearly coordinated Hg(II)$[Tri(L12C)]_2$ complex is extremely stable to guanidine HCl denaturation, compared to the peptide alone. This provides an insight to the stability a coordinated metal can provide to a protein structure.

References

(1) Doolittle, R. *Science*,**1981**,*214*,148.
(2) Cohen, C. & Parry, D. *Proteins: Structure, Function & Genetics,* **1990**,*7*,1.
(3) Cohen, C. & Parry, D. *Science,* **1994**,*263*,488.
(4) Conway, J., and Parry, D. *Int. J. Bio Macromol,* **1991**,*13*,14.
(5) Harbury, P., Zhang, T., Kim, P. & Alber, T. *Science,* **1993**,*262*,1401.
(6) Lovejoy, B., Choe, S., Ciscio, D., McRorie, D., DeGrado, W., & Eisenberg, D., *Science,* **1993**,*259*,1288.
(7) Chen, Y., Yang, J., & Chau, K., *Biochemistry*,**1974**,*13*,3350.
(8) a)Helman, J., Ballard, B., & Walsh, C *Science*, **1990**, *247*,946; b)O'Halloran, T. In *Metals in Biological Systems* H. Sigel ed. Marcel Dekker:NY, **1989**,*25*,105.
(9) Wright, J., Tsang, H., Penner-Haahn, J., O'Halloran, T. *J.Am.Chem.Soc.,* **1990**, *112*,2434.
(10) EXAFS data unpublished results kindly obtained from D. Tierny and J. Penner-Hahn.

MODELING THE CHEMISTRY AND PROPERTIES OF MULTINUCLEAR MANGANESE ENZYMES

VINCENT L. PECORARO, ANDREW GELASCO &
MICHAEL J. BALDWIN
Department of Chemistry, University of Michigan,
Ann Arbor, MI 48109-1055 USA

ABSTRACT. Dinuclear manganese complexes have been prepared using two similar ligands 2-OHsalpn and salpn. These complexes span the Mn-oxidation states from II/II to IV/IV. The $[Mn(2\text{-}OHsalpn)]_2$ complexes have been demonstrated to be efficient functional models for the manganese catalases, and suggest a mechanism for inactivation of the enzymes. The high valent system $[Mn^{IV}(salpn)(\mu\text{-}O]_2$ can be successively protonated on the oxo bridges, which leads to changes in Mn-Mn distance, magnetic exchange and reaction chemistry. The second protonation leads to reductive decomposition of the dimer to Mn^{III} monomers, likely accompanied by oxidation of water.

1. Manganese Redox Enzymes

Manganese plays a versatile and often essential role in the biochemistry of many microorganisms, plants and animals, with numerous enzymes that exploit the redox capabilities of this element. Included in this group are the manganese catalases, superoxide dismutase, ribonucleotide reductase and the oxygen evolving complex (OEC). In this report we will describe how modeling chemistry provides insight into the structure, chemical properties and reactivity of the manganese catalases and the OEC.

1.1. MANGANESE CATALASES

Catalases catalyze the disproportionation of hydrogen peroxide into water and dioxygen. While the majority of the known catalases contain the heme prosthetic group, a class of non-heme catalases was isolated more than ten years ago.[1,2] These manganese enzymes contain a dinuclear center and are believed to cycle between the Mn^{II}/Mn^{II} and Mn^{III}/Mn^{III} oxidation level during catalysis.[3-6] The manganese centers are predominantly at the Mn^{III} oxidation state when isolated. Based on comparison to the visible spectra of model compounds an oxo (or hydroxo) bis-carboxylato bridged center has been proposed. To date three different manganese catalases have been identified.[1,7,8] A low resolution crystal structure of the *Thermus thermophilus* enzyme has indicated that two manganese ions are separated by 3.6Å in a reduced state of the enzyme.[9,10] Extended x-ray absorption fine structure (EXAFS) analysis on the superoxidized form of the enzyme from *Lactobacillus plantarum* has conclusively shown that the non-active Mn^{III}/Mn^{IV} state of the enzyme contains two manganese ions only 2.7Å apart.[11]

D.P. Kessissoglou (ed.), Bioinorganic Chemistry, 287-298

At least three epr active oxidation levels can be obtained for the manganese centers of the *T. thermophilus* enzymes.[12,13] Low temperature epr spectra indicate that in both the Mn^{II}/Mn^{II} and Mn^{II}/Mn^{III} states the manganese ions are weakly coupled while the superoxidized Mn^{III}/Mn^{IV} enzyme exhibits an epr spectrum consistent with manganese atoms that are very strongly coupled. This result coupled with the Mn–Mn distance from EXAFS has implicated a Mn_2O_2 core for this inactive species. In addition a third bridge between the Mn^{III} and Mn^{IV} has been suggested based on magnetic circular dichromism spectra.[14]

The inactive $Mn^{III/IV}$ enzyme is prepared by the addition of hydrogen peroxide to the reduced enzyme in the presence of hydroxylamine. The $Mn^{III/IV}$ is a dead species that forms rapidly, but activity can be recovered by anaerobic reduction with excess hydroxylamine.

While the mechanism of peroxide disproportionation is not known to the extent that it is for the heme catalases, kinetic studies on the *L. plantarum* enzyme have allowed Penner-Hahn to propose a scheme that accounts for the known steps of the reaction.[3] The $Mn^{II/II}$ enzyme first releases water as it binds hydrogen peroxide. The substrate is coordinated directly to one of the manganese ions as the hydroperoxide anion with the released proton being absorbed by an active site acid/base catalyst. The cluster is next oxidized by two electrons to generate a bis-μ-carboxylato, μ-oxo-bridged $Mn^{III/III}$ structure. Upon oxidation the enzyme releases the first equivalent of hydrogen peroxide derived water. A second equivalent of hydrogen peroxide is then bound (after deprotonation as hydroperoxide anion) and subsequently oxidized to dioxygen. The dioxygen that is released during catalysis has been shown from isotope experiments to come from only one molecule of hydrogen peroxide. In the last step of the reaction cycle dioxygen and the second equivalent of water are released, to give the $Mn^{II/II}$ enzyme ready for another cycle.

1.2. OXYGEN EVOLVING COMPLEX

Planetary dioxygen is almost exclusively derived from water oxidation that is coupled to non-cyclic photosynthesis in higher plants and algae. The oxygen evolving complex (OEC) that is responsible for this reaction is a multisubunit enzyme that contains a tetranuclear manganese site of undetermined structure. The OEC provides one reducing equivalent at a time to the reaction center chlorophyll through the redox active tyrosine, Y_Z, upon the photon driven charge separation of photosystem II. After the fourth oxidation of the OEC, the manganese site is reduced by the four-electron oxidation of two waters to molecular oxygen and four protons. The resultant protons provide a gradient for the production of ATP. The different oxidation states involved in the reaction cycle of the OEC are referred to as the S-states, S_0 through S_4 being the relevant states for the normal reactivity of the OEC, with the subscript referring to the number of stored oxidation equivalents. The S_1 state is the resting state of the dark-adapted site and is believed to have a $Mn(III)_2Mn(IV)_2$ oxidation state. Flashes of light advance the OEC through the S-states from S_0 through S_3, and a fourth flash brings the OEC to the transient S_4 which spontaneously oxidizes water by four electrons to return to S_0. The ability of the OEC to undergo four one-electron oxidations followed by a four-electron reduction, coupled to water oxidation, is remarkable but poorly understood.

Changes in the X-ray absorption edge energy indicate that each oxidation from S_0 through S_2 results in an increase in manganese oxidation state.[15-18] It is a matter of some controversy as to whether a manganese oxidation state change occurs with the higher S-state transitions since there is disagreement over the presence a significant shift in the X-

ray absorption edge upon advancement from S_2 to S_3.[18,19] Some workers have suggested that this oxidation occurs near but not on a manganese, perhaps on a nearby oxidizable protein residue.[20] Extended X-ray absorption fine structure (EXAFS) studies have shown that at least the S_1 and S_2 states of the OEC contain more than one Mn-Mn vector of 2.7Å and one Mn-Mn vector of 3.3Å.[17,21-25] The 2.7 E distances are generally agreed to correspond to high-valent $Mn_2(\mu\text{-}O)_2$ units, which have been shown to have similar Mn-Mn distances. The possible configurations of the manganese ions in the tetranuclear site are limited but not defined by the EXAFS data. The manganese connectivity has also been probed by studies of the changes in magnetic susceptibility in different S-states. An interesting result of the magnetic studies is the *increase* in magnetic moment upon advancing from S_1 to S_2,[26] which might be expected to correspond to a loss of one unpaired electron and a resulting decrease in magnetic moment. This is complicated somewhat, however, by the apparent existence of two different configurations of the manganese site in both S_1 and S_2. The S_1 state has different properties depending on whether it is in the "active" or dark-adapted "resting" state,[27] with the active state appearing to be paramagnetic while the resting state has been shown to be diamagnetic.[28,29] Two different configurations of the S_2 state are distinguished by different EPR features, either a multiline signal at $g = 2$ [30-33] or a broad derivative signal at $g = 4.1$,[21,34-36] that can be preferentially isolated by illumination of S_1 centers at different temperatures or by chemical manipulations of the reaction centers.

Although the overall reaction at the OEC requires the generation of four protons, the proton stoichiometry of each S-state is likely to be important in the reaction cycle. A number of attempts have been made to measure the proton uptake/release stoichiometry with S-state advancement using various methods.[37-39] Obtaining and interpreting these data are very difficult, and a variety of results have been reported depending on a number of factors. For some time, a 1:0:1:2 pattern for proton release upon the $S_0 \rightarrow S_1$: $S_1 \rightarrow S_2$: $S_2 \rightarrow S_3$: $S_3 \rightarrow S_4 \rightarrow S_0$ advancement had been accepted.[37] However, this stoichiometry has generally been rejected in favor of non-integer or 1:1:1:1 patterns, depending on the method of preparation and isolation of the OEC samples and on pH.[38,39]

Our recent activities in attempting to understand the issues discussed above better have centered around studying the protonation of the high-valent Mn_2O_2 core of $[Mn^{IV}(salpn)(\mu\text{-}O)]_2$. These studies, which we discuss in this chapter, explore the structural, magnetic, spectroscopic and chemical effects of successive protonations of one or both oxo bridges in this complex.

2. Mechanistic Model Studies

2.1. MANGANESE 2-OHSALPN CHEMISTRY

We have prepared dinuclear manganese complexes, spanning the oxidation state ranges from Mn^{II}/Mn^{II} to Mn^{III}/Mn^{IV}, utilizing the ligand 2-OHsalpn. These complexes all contain bis alkoxide bridges from the propane backbone of the ligand. This is the first manganese dimer series that has been isolated in four distinct oxidation states. The overall geometry of the compounds are very similar across the series, with bond length and angles consistent with the changes in manganese oxidation state. While a great many manganese model compounds have been prepared that have various oxidation levels, systems containing invariant ligands that span more than two isolatable oxidation states are rare.

The $[Mn^{II}(2\text{-}OHsalpn)]_2^{2-}$ dimer is prepared by adding 1 eq. of $Mn^{II}(ClO_4)_2$ to a degassed methanol solution containing 1 eq. of the ligand and three eq. of base. The dimer is insoluble in methanol and precipitates out of the reaction mixture. If the a nitro group is substituted at the 5-position on the salicylaldehyde rings and tetramethylammonium hydroxide is used as the base a similar complex can be isolated and crystallized from dmf/ether to give crystals suitable for X-ray diffraction. Structural analysis of this dimer shows two Mn^{II} ions each coordinated by two phenolate oxygens, two imine nitrogens and two alkoxide oxygen atoms. An ORTEP representation of the anion of $TMA_2[Mn^{II}(2\text{-}OH(5\text{-}NO_2sal)pn)]_2$ is shown in figure 1.[43]

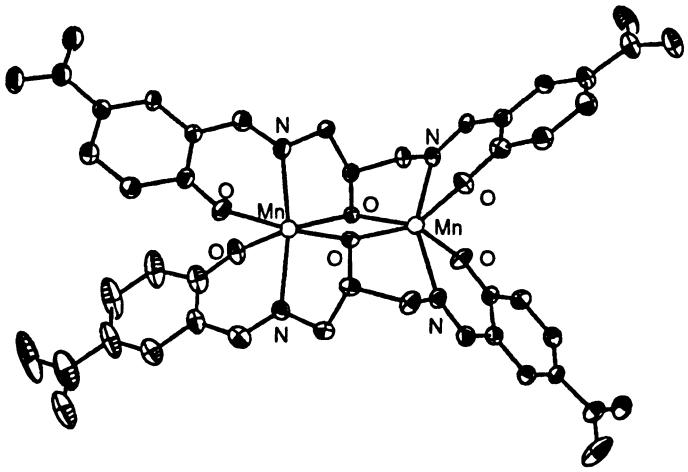

Figure 1. ORTEP drawing for anion of $TMA_2[Mn^{II}(2\text{-}OH(5\text{-}NO_2sal)pn)]_2$

If a solution of the sodium salt of the $[Mn^{II}(2\text{-}OH(5\text{-}NO_2sal)pn)]_2^{2-}$ dimer in acetonitrile is allowed to air oxidize the $[Mn^{III}(2\text{-}OH(5\text{-}NO_2sal)pn)]_2$ complex can be isolated. This complex has also been crystallographically characterized, containing a similar ligand environment to the Mn^{II} dimer. Previously we had reported a dramatically different structural geometry for a Mn^{III} dimer using 2-OHsalpn, having one backbone alkoxide atom bridging the two Mn ions, while the alkoxide from the other ligand backbone acts as a terminal ligand to one of the ions. The coordination sphere of the other Mn ion is completed by a donor solvent molecule. This asymmetric complex is formed in donor solvents. If the manganese dimer is prepared in a non-donating solvent such as dichloromethane or acetonitrile the symmetric species is isolated. These two types of dimers can be interchanged by solvation in donor vs. non-donor solvents.

The new geometry observed for this Mn^{III} dimer is important because it influences the reaction chemistry of the system. The symmetric Mn^{II} and Mn^{III} dimers disproportionate hydrogen peroxide in acetonitrile at similar rates to give dioxygen and water.[40] The asymmetric Mn^{III} dimer is not competent for this function. The symmetric systems are the first functional models for the manganese catalases that have been isolated and crystallographically characterized in both its oxidized and reduced forms. Studies comparing the rates of disproportionation for both dimers have indicated that the reaction is independent of the initial oxidation state of the complex. We have used the dimer

$[Mn^{III}(2\text{-}OH(5\text{-}Clsal)pn)]_2$ for most of our kinetic studies due to solubility of the different derivatives.

The addition of 1 equiv. of H_2O_2 to $[Mn^{III}(2\text{-}OH(5\text{-}Clsal)pn)]_2$ shows isosbestic conversion to $[Mn^{II}(2\text{-}OH(5\text{-}Clsal)pn)]_2$ by visible spectroscopy. Oxygen evolution experiments indicate that these complexes can complete the catalase reaction for at least 1000 turnovers without significant decomposition of the catalyst. Isolation of dioxygen after the addition of $H_2{}^{18}O_2$ yields exclusively $^{18}O_2$. If $H_2{}^{18}O_2$ and $H_2{}^{16}O_2$ are added simultaneously to either manganese complex, $^{18}O_2$ and $^{16}O_2$ are recovered but no $^{16,18}O_2$ is detected. This isotope labeling pattern follows the isotopic O_2 composition shown for the *L. plantarum* catalase.[*vide supra*]

When the disproportionation reaction is monitored under pseudo first-order conditions (i.e. $[H_2O_2]$ » [catalyst]) the complex exhibits saturation kinetics.[40] A plot of rate vs. $[H_2O_2]$ is shown in figure 2. The data is fit to the Michaelis-Menton equation for conditions of saturating levels of substrate. Based on this fit the k_{cat} for this reaction was determined to be 21.9 s^{-1} and the Michaelis constant K_M was found to be 72 mM. By comparison, the Mn catalase from *L. plantarum* [3]has a K_M= 200 mM and k_{cat}= 2 x 10^5 s^{-1} while $Mn^{II}(H_2O)_6$ has a k_{cat}= 6.3 x 10^{-3} s^{-1}. The catalytic efficiency of the enzyme and the model complex compare favorably with k_{cat}/K_M equal to 1.0 x 10^6 s^{-1} M for the *L. plantarum* enzyme,[3] and $[Mn^{III}(2\text{-}OH(5\text{-}Clsal)pn)]_2$ having a k_{cat}/K_M value of 3.0 x 10^2, indicating that the enzyme is only 3000 times more efficient than the synthetic $[Mn^{III}(2\text{-}OH(5\text{-}Clsal)pn)]_2$ dimer. This complex has proven to be the most efficient functional model for the manganese catalases.

If $[Mn^{III}(2\text{-}OH(5\text{-}Clsal)pn)]_2$ is added to solutions of deuterium peroxide in acetonitrile similar saturation kinetics are observed. The k_{cat} for this reaction drops by nearly one-half to 11.6 s^{-1}, however the K_M increases to 91 mM. The k_{cat}/K_M value is decreased to 130 s^{-1} M. Based on this experiment it is apparent that proton dissociation /association is an import-ant part of the rate-limit-ing step for the dispro-portionation reaction.[41] Penner-Hahn has proposed that an acid/base catalyst is necessary for enzymatic catalysis. It is possible that the alkoxide bridges could serve this function in this model system.

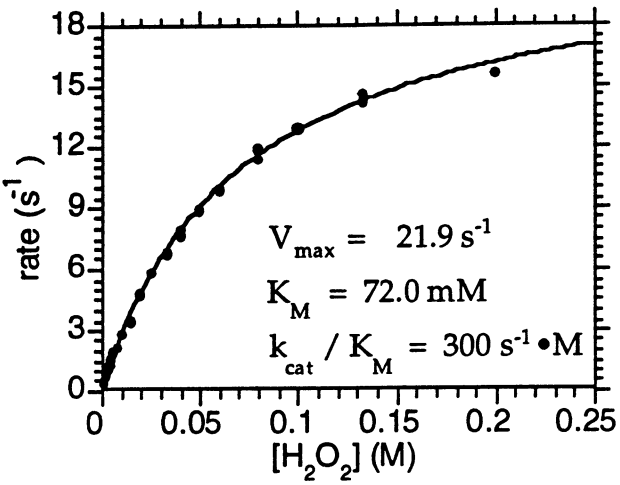

Figure 2. Plot of rate vs. Hydrogen peroxide concentration showing saturation kinetics

When warm acetonitrile solutions of $TEA_2[Mn^{II}(2\text{-}OH(5\text{-}Clsal)pn)]_2$ and $[Mn^{III}(2\text{-}OH(5\text{-}Clsal)pn)]_2$ are mixed in equilmolar ratios a new mixed valent species $TEA[Mn^{II/III}(2\text{-}OH(5\text{-}Clsal)pn)_2]$ forms upon cooling. This complex can also be prepared from the controlled air oxidation of the Mn^{II} dimer at low temperatures or by one-electron chemical reduction. This bis alkoxide bridged mixed-valent compound has interesting spectroscopic properties that allow the reaction chemistry in solution to be probed. Epr studies at 77 K of $TEA[Mn^{II/III}(2\text{-}OH(5\text{-}Clsal)pn)_2]$ in ethanol or dmf give spectra that have an absorptive feature in range of g = 5 -7 which is different from either the $Mn^{II/II}$ or the $Mn^{III/III}$ dimers. The $Mn^{III/III}$ is an integer spin system which is epr silent at conventional X-band spectroscopy, and the $Mn^{II/II}$ complex gives a classic spectrum for weakly coupled Mn^{II} dimeric complexes and enzymes.

If one equivalent of hydrogen peroxide is added to an ethanol solution of the ring substituted derivative $TEA[Mn^{II/III}(2\text{-}OH(3,5\text{-}Clsal)pn)_2]$ a new epr spectrum with sixteen lines centered at g = 2 appears. This spectrum is characteristic of $Mn^{III/IV}$ dioxo bridged dinuclear complexes. A related complex can be formed by the reaction of 2-3 equivalents of *t*-butylhydroperoxide with $TEA[Mn^{II/III}(2\text{-}OH(3,5\text{-}Clsal)pn)_2]$ which has a epr spectrum at 6 K containing both the g = 2 multiline and a broad derivative feature at g = 4-5. These complexes are different from the $Mn^{III/IV}$ dimer produced from the electrochemical oxidation of the symmetric $[Mn^{III}(2\text{-}OH(3,5\text{-}Clsal)pn)]_2$.

Bulk electrolysis of an acetonitrile solution of $[Mn^{III}(2\text{-}OH(3,5\text{-}Clsal)pn)]_2$ in the presence of $NaClO_4$ yields the crystalline precipitate $[Mn^{III/IV}(2\text{-}OH(3,5\text{-}Clsal)pn)_2]ClO_4$. This compound can be recrystallized from acetonitrile/toluene to give block crystals suitable for X-ray diffraction. This new complex contains the bis alkoxide bridges observed for the rest of the series, and has a very different geometry than its asymmetric derivative which can be isolated from THF.[42] The asymmetric dimer has a similar coordination environment to that observed for the asymmetric $[Mn^{III}_2(2\text{-}OHsalpn)_2(CH_3OH)]$ dimer.[*vide supra*]

The epr spectra of both the symmetric and asymmetric $Mn^{III/IV}$ dimers are similar. The temperature dependent spectra have a g = 4.3 feature at 77 K which converts to a 12 line g = 2 "multiline" on lowering the temperature to 5 K. This behavior is indicative of a weakly coupled dinuclear system, with a 12 line ground state spectrum and the g = 4.3 signal due to higher energy spin states. The weak coupling implied from the epr studies is confirmed by solid state variable-temperature magnetic susceptibility measurements. Both the symmetric and asymmetric $[Mn^{III/IV}(2\text{-}OH(3,5\text{-}Clsal)pn)_2]^+$ dimers are weakly antiferromagnetically coupled in the solid state, with the asymmetric dimer having a coupling constant $J = -10$ cm^{-1} and the symmetric dimer having a $J = -2$ cm^{-1}.[42,43] These low J values are unprecedented for $Mn^{III/IV}$ complexes which typically have coupling constants in the range of -100 to -150 cm^{-1}.

Variable temperature magnetic measurements on the $Mn^{II/II}$ and $Mn^{II/III}$ dimers indicated that the manganese ions are ferromagnetically coupled. This magnetic behavior is rare for manganese dinuclear complexes. $[Mn^{II}(2\text{-}OH(5\text{-}NO_2sal)pn)]_2^{2-}$ is the first example of a structurally characterized Mn^{II} dinuclear complex that is ferromagnetically coupled ($J = 0.6$ cm^{-1}), and $TEA[Mn^{II/III}(2\text{-}OH(5\text{-}Clsal)pn)_2]$ is only the second example for $Mn^{II/III}$ systems. The epr spectrum at 4.2 K of $TEA[Mn^{II/III}(2\text{-}OH(5\text{-}Clsal)pn)_2]$ in ethanol exhibits a feature at g = 5.8, consistent with an $S = {}^9/_2$ ground state arising from a ferromagnetically coupled dimer.[44]

Taken together the chemistry of the $Mn_2(2\text{-}OHsalpn)_2$ system gives some insight into the mechanism of the manganese catalases. If we combine some of the chemistry observed for the $Mn^{II/III}$ dimer and reexamine the Penner-Hahn mechanism, we can proposed a mechanism for inactivation of the enzyme. We have shown that a $Mn^{II/III}$

dimer can be oxidized by one equivalent of hydrogen peroxide to give a new species that is not the simple two-electron oxidation product but a compound that must have a new coordination environment.[*vide supra*] It is clear that a $Mn^{II/III}$ species can be prepared from either a one-electron oxidation of a Mn^{II}_2 dimer or a one-electron reduction of Mn^{III}_2 system, the latter being facilitated by hydroxylamine (a good one-electron reducing agent). If during the course of the catalytic cycle the enzyme in the Mn^{III} oxidation level is reduced by one electron by hydroxylamine, then there would be some transient level of $Mn^{II/III}$ species present. If the enzyme next reacts with another molecule of hydroxylamine the manganese center would be reduced to the Mn^{II}_2 level and the catalytic cycle would continue. If however the next substrate for the $Mn^{II/III}$ species is hydrogen peroxide the manganese core would be oxidized and then rearrange to give a $Mn^{III/IV}$ dioxo core that would inactivate the enzyme.

Although the Mn_2O_2 core of the manganese catalases is an inactive enzyme form, an understanding of such dimanganese units is required to explain the reactivity of the oxygen evolving complex. In previous contributions we have described the reactions of Mn^{III}(salpn) with H_2O_2 to form $[Mn^{IV}(salpn)(\mu\text{-}O)]_2$ and the subsequent catalase reaction catalyzed by this dimer. An interesting aspect of this disproportionation chemistry is that one equivalent of H^+ completely shuts off the reaction. To explain this observation we investigated the reactions of $[Mn^{IV}(salpn)(\mu\text{-}O)_2]$ in acidic solutions.

2.2. MANGANESE SALPN CHEMISTRY

The single protonation of $[Mn^{IV}(salpn)(\mu\text{-}O)]_2$ is facilitated by addition of a stoichiometric amount (or small excess) of a weak acid such as pyridinium triflate. This protonation significantly effects the dimer by: inhibiting the catalase-like activity, increasing the Mn-Mn distance, lowering the energy of the lowest energy charge transfer band (from 490 nm to 550 nm, with a change in color from red-brown to deep purple), and making the reduction potential more positive by > 600 mV.[45] Protonation occurs on one of the oxo bridges, as shown by the shift of the sharp O-H stretch in the IR spectrum upon labeling the oxo bridges with ^{18}O.

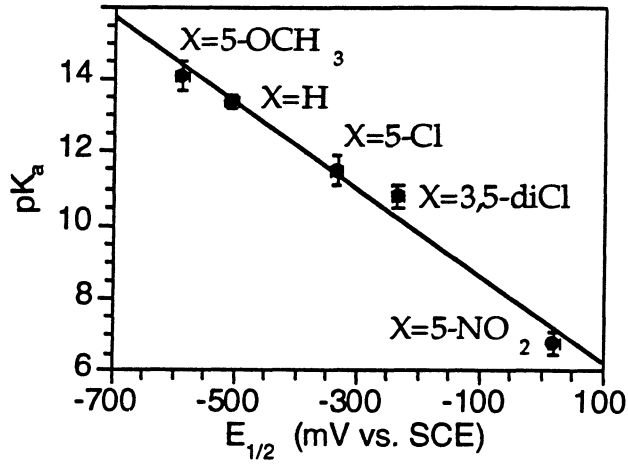

Figure 3. Reduction potential of $[Mn(X\text{-}salpn)(\mu\text{-}O)]_2$ vs. PK_a of $[Mn_2(salpn)_2(\mu\text{-}O, \mu\text{-}OH)]^+$

In order to understand the relationship between the protonation of the Mn_2O_2 core and its reduction potential, we prepared the series of complexes $[Mn^{IV}(X\text{-salpn})(\mu\text{-}O)]_2$, where the substituents X are electron donating or withdrawing groups on the phenolate rings of the salpn ligand (X = 5-OCH_3, H, 5-Cl, 3,5-diCl, or 5-NO_2). We obtained the reduction potentials of each of these complexes by cyclic voltammetry. We then obtained the pK_a values for the singly protonated derivatives by spectrophotometric titrations by acids of known pK_as in acetonitrile. When plotted as in figure 3 with the $E_{1/2}$ in mV vs. SCE for the unprotonated dimers on one axis and the pK_a for the corresponding singly protonated derivative on the other, a linear correlation is seen over a potential range of over 600 mV and a pK_a range of over 7 pK_a units. This correlation has a slope of 84 mV/pK_a unit. This indicates that the Mn_2O_2 core acts as one unit, such that the factors such as differences in ligation that affect the redox chemistry (by modifying the electron density on the manganese) affect the protonation chemistry in a related manner (by modifying the electron density on the oxo bridges).[46]

Addition of a second equivalent of pyridinium does not cause further protonation of the Mn_2O_2 unit. However addition of 2 equivalents of a strong acid, such as triflic acid, does cause further reaction. At room temperature, this reaction is marked by a loss of the deep red-brown color of $[Mn^{IV}(salpn)(\mu\text{-}O)]_2$, resulting in a light yellow-brown Mn^{III} product [*vide infra*]. At -50_°C, this decomposition reaction does not occur, and the doubly protonated complex $[Mn^{IV}(salpn)(\mu\text{-}OH)]_2(CF_3SO_3)_2$ is formed. Both the first and second protonation are reversible, and $[Mn^{IV}(salpn)(\mu\text{-}O)]_2$ is regenerated with stoichiometric addition of base. This protonation process is shown in the scheme below:

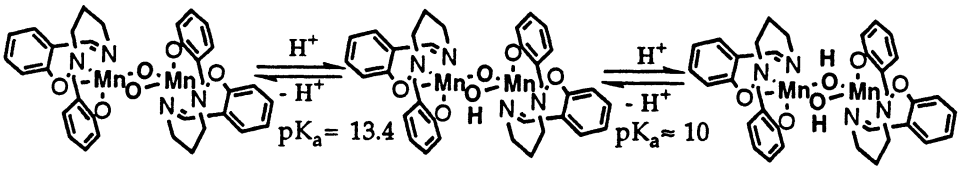

The complex $[Mn^{IV}(salpn)(\mu\text{-}OH)]_2(CF_3SO_3)_2$ can be isolated as a solid, and redissolved in cold acetonitrile to form a solution with an identical absorption spectrum (λ = 630 nm) to that produced *in situ*. The shift upon successive protonations of the Mn_2O_2 unit from 490 to 550 to 630 nm (each shift corresponding to about 2200 cm^{-1}) is consistent with a phenolate-to-manganese charge transfer from the salpn ligand being lowered in energy by a reduction in electron density on the Mn. The manganese edge energy in X-ray absorption experiments does not change upon these protonations (although the edge of Mn^{III}(salpn) complexes are observed at significantly lower energy) indicating that the oxidation state of the manganese ions remains at Mn^{IV} through the series of protonation states. The pK_a for each doubly protonated derivative, $[Mn^{IV}(X\text{-salpn})(\mu\text{-}OH)]_2$, was estimated by determining the strength of acid required to cause decomposition of the dimer in acetonitrile at room temperature, and while this provides only a rough estimate of the pK_a, it showed that the acidity of each doubly protonated derivative is 3-5 pK_a units greater than that of the corresponding singly protonated derivative.

The solid samples obtained for the series of complexes $[Mn^{IV}(salpn)(\mu\text{-}O)]_2$, $[Mn^{IV}{}_2(salpn)_2(\mu\text{-}O)(\mu\text{-}OH)](CF_3SO_3)$, and $[Mn^{IV}(salpn)(\mu\text{-}OH)]_2(CF_3SO_3)_2$ were used to probe the structural and magnetic effects of the successive protonations of the Mn_2O_2 unit. Extended X-ray absorption fine structure (EXAFS) experiments show that the Mn-Mn distances for these complexes increases from 2.73Å for the unprotonated dimer (as shown by both EXAFS and X-ray crystallography)[45,47,48] to 2.83 Å and 2.94 Å for the

singly[45,49] and doubly[49] protonated dimers, respectively. This indicates that changes in protonation state of the Mn_2O_2 units of the OEC should be detectable by observing changes in the Mn-Mn vectors found in the EXAFS experiments, although this may be complicated by changes in the oxidation states of the particular manganese ions involved.

Temperature dependent magnetic susceptibility measurements were made on this series of complexes using a superconducting quantum interference device (SQUID). The temperature dependence of the effective magnetic moment (μ_{eff} in Bohr magnetons) of each protonation state is shown in figure 4. Qualitatively, it can be seen that all of the complexes are antiferromagnetically coupled, although the coupling is decreased dramatically with each successive protonation. By fitting these data to an expression derived from the van Vleck equation, which incorporates a term to account for small amounts of a Mn^{III} impurity and fixes the g value at 2.00, we obtain coupling parameters, J [with $H = -2J(S_1 \cdot S_2)$], of -92 cm^{-1} (in agreement with the value reported by Gohdes and Armstrong),[47] -48 cm^{-1}, and -6 cm^{-1} for the unprotonated, singly protonated, and doubly protonated dimers, respectively.

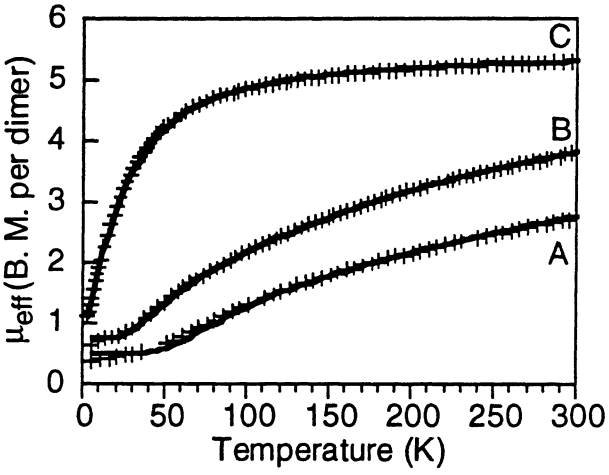

Figure 4. Temperature dependent magnetic moments of A) $[Mn(salpn)(\mu\text{-}O)]_2$, B)$[Mn_2(salpn)_2(\mu\text{-}O, \mu\text{-}OH)](CF_3SO_3)$, and C) $[Mn(salpn)(\mu\text{-}OH)]_2(CF_3SO_3)_2$

These large changes in the magnitude of anti-ferromagnetic coupling upon protonation of the oxo bridges should be considered in attempts to explain the complicated changes in magnetic properties of the OEC upon changes in S state or between different configurations which may be observed for the S_1 (resting and active) and S_2 (multiline and g=4.1) states.[28,29,33,50-53]

As mentioned above, addition of two equivalents of triflic acid to a solution of $[Mn^{IV}(salpn)(\mu\text{-}O)]_2$ at room temperature results in a bleaching of the solution due to loss of the low energy charge transfer band. The resulting solution has an absorption spectrum which is identical to that of the structurally characterized $Mn^{III}(salpn)(CH_3OH)^+$. The same absorption spectrum is obtained by dissolving the isolated solid $[Mn^{IV}(salpn)(\mu\text{-}OH)]_2(CF_3SO_3)_2$ in acetonitrile at room temperature. The product of this decomposition reaction has been obtained from the solution as a microcrystalline solid and has been shown to be $Mn^{III}(salpn)(H_2O)^+$. This reaction of the doubly protonated complex in solution occurs within seconds at room temperature, but is easily monitored

spectrophotometrically at -20_C, at which temperature the reaction nears completion in one to two hours. Subtraction of the spectrum of $[Mn^{IV}(salpn)(\mu\text{-}OH)]_2(CF_3SO_3)_2$ (scaled to the intensity of the 630 nm band) from the spectra collected at different times throughout the reaction indicate that the only observed product throughout the course of the reaction is $Mn^{III}(salpn)(H_2O)^+$.

This reactivity may be considered to be a proton-triggered redox reaction of the Mn_2O_2 center. While the identity of the reductant has not been deduced, one possibility is water, either from the oxo bridges or from trace amounts of water in the solvent. The overall change in Mn oxidation state is two electrons per dimer, which would produce either two hydroxyl radicals or H_2O_2 by bond formation between the hydroxide bridges of the dimer. This two-electron reaction, combined with the first half of the hydrogen peroxide disproportionation reaction which is catalyzed by the unprotonated dimer, $[Mn^{IV}(salpn)(\mu\text{-}O)]_2$, provides one possible scenario for the four-electron oxidation of water to dioxygen in the $S_0 \rightarrow S_4$ transition of the OEC. One $Mn^{IV}{}_2O_2$ unit would be protonated on both oxo bridges, perhaps by a nearby amino acid residue which is oxidized and thus made a strong acid (such as tyrosyl or histidyl), resulting in the proton triggered reduction of the manganese to Mn^{III} with production of hydrogen peroxide, followed by oxidation of the hydrogen peroxide by a second $Mn^{IV}{}_2O_2$ unit to O_2 with reduction of the Mn^{IV} to Mn^{III}. Reoxidation of one manganese ion by the oxidized amino acid would return the cluster to the S_0 state ($Mn^{III}{}_2Mn^{IV}$). While the details of this scenario are for the moment speculatory as applied to the OEC, it is clear that the structural, magnetic, and stability changes triggered by protonation of the Mn_2O_2 units are critical to understanding the chemistry of these high valent cores that are responsible for photosynthetic water oxidation.

3. Conclusions

We have demonstrated very different reaction chemistry for dinuclear manganese complexes using two similar ligands. The Mn(2-OHsalpn) models have allowed us to study the reaction of low valent dimers with oxygen and hydrogen peroxide. We have prepared the oxidation state series (II/II to III/IV) with invariant ligand coordination that is unprecedented in manganese chemistry. Two of these complexes are the most efficient functional models for the manganese catalases. In addition, this is the first system that the species at each end of the reaction have been isolated and crystallographically characterized. Oxidation from the $Mn^{II/III}$ species causes a rearrangement in geometry to presumably a $Mn^{III/IV}$ dioxo dimer which is in active toward hydrogen peroxide. These complexes suggest one pathway for the inactivation of the manganese catalases by hydroxylamine.

While the dioxo species for the Mn(2-OHsalpn) series is an inactive species toward hydrogen peroxide disproportionation chemistry, the $[Mn^{IV}(salpn)(\mu\text{-}O)]_2$ dimer is an efficient catalyst for the reaction, utilizing a high-valent cycle. This reaction can be turned off by a single protonation of the dioxo core. We have studied the $[Mn^{IV}(salpn)(\mu\text{-}O)]_2$ system in acidic environments to examine the effect of successive protonation chemistry on the structure, magnetic exchange and reaction chemistry of the dioxo dimers. This work will allow us to evaluate the small changes in tetramer conformation that have been proposed to cause spectroscopic perturbations.[54] In particular, a recent work has suggested that a slight elongation of the Mn - Mn distance in the OEC is responsible for the change from the g = 2 to the g = 4.1 epr signals,[55] this system can be used to examine this proposition.

4. References

(1) Kono, Y.; Fridovich, I. *J. Biol. Chem.* **1983**, *258*, 6015.
(2) Kono, Y.; Fridovich, I. *J. Biol. Chem.* **1983**, *258*, 13646.
(3) Penner-Hahn, J. E. In *Manganese Redox Enzymes*; V. L. Pecoraro, Ed.; VCH Publishers, Inc.: New York, 1992; pp 29-45.
(4) Waldo, G. S.; Fronko, R. M.; Penner-Hahn, J. E. *Biochemistry* **1991**, *30*, 10486.
(5) Waldo, G. S.; Fronko, R. M.; Penner-Hahn, J. E. *Biochemistry* **1991**, *30*, 10486.
(6) Khangulov, S. V.; Barynin, V. V.; Melik-Adamyan, V. R.; Grebenko, A. I.; Voevodskay, N. V.; Blumenfeld, L. A.; Dobrykov, S. N.; Il'ysova, V. B. *Bioorgan. Khim.* **1986**, *12*, 741.
(7) Vainshtein, B. K.; Melik-Adamyan, W. R.; Barynin, V. V.; Vagin, A. A. In *Progress in Bioorganic Chemistry and Molecular Biology*; Y. Ovchinnikov, Ed.; Elsevier. Publ.: Amsterdam, 1984; pp 117.
(8) Algood, G. S.; Perry, J. J. *J. Bacteriol.* **1986**, *168*, 563.
(9) Vainshtein, B. K.; Melik-Adamyan, W. R.; Barynin, V. V.; Vagin, A. A.; Grebenko, A. I. *Proc. Int. Symp. Biomol. Struct. Interactions Suppl. J. Biosci. (1&2)* **1985**, *8*, 471.
(10) Barynin, V. V.; Vagin, A. A.; Melik-Adamyan, V. R.; Grebenko, A. I.; Khangulov, S. V.; Popov, A. N.; Andrianova, M. E.; Vainshtein, B. K. *Dolk. Akad. Nauk. S.S.S.R (Crystallogr.)* **1986**, *288*, 877.
(11) Fronko, R. M.; Penner-Hahn, J. E.; Bender, C. J. *J. Am. Chem. Soc.* **1988**, *110*, 7554.
(12) Khangulov, S. V.; Voyevodskaya, N. V.; Barynin, V. V.; Grebenko, A. I.; Melik-Adamyan, V. R. *Biofizika* **1987**, *32*, 1044(Engl.).
(13) Khangulov, S. V.; Barynin, V. V.; Voevodskaya, N. V.; Grebenko, A. I. *Biochim. Biophys. Acta* **1990**, *1020*, 305.
(14) Gamelin, D. R.; Kirk, M. L.; Stemmler, T. L.; Pal, S.; Armstrong, W. H.; Penner-Hahn, J. E.; Solomon, E. I. *J. Am. Chem. Soc.* **1994**, *116*, 2392.
(15) Brudvig, G. W.; Crabtree, R. H. *Proc. Natl. Acad. Sci. USA* **1986**, *83*, 4586.
(16) Penner-Hahn, J. E.; Fronko, R. M.; Pecoraro, V. L.; Yocum, C. F.; Bowlby, N. R. *Physica B (Amsterdam)* **1989**, *158*, 107.
(17) Penner-Hahn, J. E.; Fronko, R. M.; Pecoraro, V. L.; Yocum, C. F.; Betts, S. D.; Bowlby, N. R. *J. Am. Chem. Soc.* **1990**, *112*, 2549.
(18) Ono, T.-a.; Noguchi, T.; Inoue, Y.; Kusunoki, M.; Matsushita, T.; Oyanagi, H. *Science* **1992**, *258*, 1335.
(19) Klein, M. P.; Sauer, K.; Yachandra, V. K. *Photosyn. Res.* **1993**, *38*, 265.
(20) Zimmermann, J.-L.; Rutherford, A. W.; Boussac, A. *Nature* **1990**, *347*, 303.
(21) Yachandra, V. K.; Guiles, R. D.; McDermott, A. E.; Cole, J. L.; Britt, R. D.; Dexheimer, S. L.; Sauer, K.; Klein, M. P. *Biochemistry* **1987**, *26*, 5974.
(22) Yachandra, V. K.; Guiles, R. D.; McDermott, A.; Britt, R. D.; Dexheimer, S. L.; Sauer, K.; Klein, M. P. *Biochim. Biophys. Acta* **1986**, *850*, 324.
(23) Penner-Hahn, J. E.; Fronko, R. M.; Waldo, G. S.; Yocum, C. F.; Bowlby, N. R.; Betts, S. D. In *Current Research in Photosynthesis*; M. Baltscheffsky, Ed.; Kluwer: Dordrecht, 1990; Vol. 1.
(24) George, G. N.; Prince, R. C.; Cramer, S. P. *Science* **1989**, *243*, 798-791.
(25) Prince, R. C.; Cramer, S. P.; George, G. N. In *Current Research in Photosynthesis*; M. Baltscheffsky, Ed.; Kluwer: Dordrecht, 1990; Vol. 1; pp 685.
(26) Sivaraja, M.; Philo, J. S.; Lary, J.; Dismukes, G. C. *J. Am. Chem. Soc.* **1989**, *111*, 3221.

(27) Beck, W. F.; de Paula, J. C.; Brudvig, G. W. *Biochemistry* **1985**, *24*, 3035.
(28) Dexheimer, S. L.; Klein, M. P. *J. Am. Chem. Soc.* **1992**, *114*, 2821.
(29) Koulougliotis, D.; Hirsh, D. J.; Brudvig, G. W. *J. Am. Chem. Soc.* **1992**, *114*, 8322.
(30) Dismukes, G. C.; Siderer, Y. *FEBS Lett* **1980**, *121*, 78.
(31) Dismukes, G. C.; Siderer, Y. *Proc. Natl. Acad. Sci. U.S.A.* **1981**, *78*, 274.
(32) Brudvig, G. W.; Casey, J. L.; Sauer, K. *Biochim. Biophys. Acta* **1983**, *723*, 366.
(33) Hansson, O.; Aasa, R.; Vaenngaard, T. *Biophys. J.* **1987**, *51*, 825.
(34) Zimmerman, J.-L.; Rutherford, A. W. *Biochim. Biophys. Acta* **1984**, *767*, 160.
(35) Casey, J. L.; Sauer, K. *Biochim. Biophys. Acta* **1984**, *767*, 21.
(36) Cole, J.; Yachandra, V. K.; Guiles, R. D.; McDermott, A. E.; Britt, R. D.; Dexheimer, S. L.; Sauer, K.; Klein, M. P. *Biochim. Biophys. Acta* **1987**, *890*, 395.
(37) Wille, B.; Lavergne, J. *Photobiochem. Photobiophys.* **1982**, *4*, 131.
(38) Jahns, P.; Lavergne, J.; Rappaport, F.; Junge, W. *Biochim. Biophys. Acta* **1991**, *1057*, 313.
(39) Jahns, P.; Haumann, M.; Bφgershausen, O.; Junge, W. In *Research in Photosynthesis, Vol II*; N. Murata, Ed.; Kluwer Academic Publishers: Netherlands, 1992; Vol. II; pp 333.
(40) Gelasco, A.; Pecoraro, V. L. *J. Am. Chem. Soc.* **1993**, *115*, 7928.
(41) Gelasco, A.; Pecoraro, V. L. **1994**, Manuscript in preparation.
(42) Larson, E.; Haddy, A.; Kirk, M. L.; Sands, R. H.; Hatfield, W. E.; Pecoraro, V. L. *J. Am. Chem. Soc.* **1992**, *114*, 6263.
(43) Gelasco, A.; Kampf, J. W.; Kirk, M. L.; Pecoraro, V. L. *submitted to J. Am. Chem. Soc* **1994**,
(44) Schake, A. R.; Schmitt, E. A.; Conti, A. J.; Streib, W. E.; Huffman, J. C.; Hendrickson, D. N.; Christou, G. *Inorg. Chem.* **1991**, *30*, 3192.
(45) Larson, E. J.; Riggs, P. J.; Penner-Hahn, J. E.; Pecoraro, V. L. *J. Chem. Soc., Chem. Commun.* **1992**, 102.
(46) Baldwin, M. J.; Gelasco, A.; Pecoraro, V. L. *Photosynth. Res.* **1993**, *38*, 303.
(47) Gohdes, J. W.; Armstrong, W. H. *Inorg. Chem.* **1992**, *31*, 368.
(48) Larson, E.; Lah, M. S.; Li, X.; Bonadies, J. A.; Pecoraro, V. L. *Inorg. Chem.* **1992**, *31*, 373.
(49) Baldwin, M. J.; Stemmler, T. L.; Riggs-Gelasco, P. J.; Kirk, M. L.; Penner-Hahn, J. E.; Pecoraro, V. L. *submitted to J. Am. Chem. Soc.* **1994**,
(50) de Paula, J. C.; Brudvig, G. W. *J. Am. Chem. Soc.* **1985**, *107*, 2643.
(51) de Paula, J. C.; Beck, W. F.; Brudvig, G. W. *J. Am. Chem. Soc.* **1986**, *108*, 4002.
(52) Kim, D. H.; Britt, R. D.; Klein, M. P.; Sauer, K. *J. Am. Chem. Soc.* **1990**, *112*, 9389.
(53) Haddy, A.; Aasa, R.; Andreasson, L. E. *Biochemistry* **1989**, *28*, 6954.
(54) de Paula, J. C.; Innes, J. B.; Brudvig, G. W. *Biochemisty* **1985**, *24*, 8114.
(55) Liang, W.; Latimer, M. J.; Dau, H.; Roelofs, T. A.; Yachandra, V. K.; Sauer, K.; Klein, M. P. *Biochemistry* **1994**, *33*, 4923.

MANGANESE-PROTEINS AND -ENZYMES AND RELEVANT TRINUCLEAR SYNTHETIC COMPLEXES

DIMITRIS P. KESSISSOGLOU
Department of General & Inorganic Chemistry,
Aristotle University of Thessaloniki,
Thessaloniki 54006, Greece

ABSTRACT. Manganese is an essential element in many biological processes. Two functional values can be distinguished; the Mn^{2+} as a Lewis acid, like divalent ions, *Magnesium, Calcium, Zinc* and in higher oxidation states(Mn^{3+}, Mn^{4+}) as an oxidation catalyst, like *Copper, Iron, Cobalt.* The most well known Mn(II) proteins are: *Arginase,* containing 4 Mn(II) ions per enzyme; *Concanavalin A,* a manganese-calcium metalloprotein; *Glutamine-Synthatase,* requiring two Mn(II) ions; *Phosphoenolpyruvate Carboxykinase*, converting irreversible cytoplasmic oxaloacetate to phosphoenolpyruvate; a *manganese ribonucleotide reductase* isolated from *B. ammoniagemes; Mn Thiosulfate Oxidase* containing a binuclear Mn(II) site; *Isopropylmalate Synthase,* with the Mn(II) bound to the S-H group near site; *Pyruvate carboxylase*, the first metalloenzyme shown to contain manganese. Manganese redox enzymes with manganese in oxidation states 3+ and 4+ are: *Manganese SOD* catalysing the dismutasion of superoxide radicals to oxygen and hydrogen peroxide with a single Mn(III) center; The *Manganese Peroxidase(MnP)* is one of the two known enzymes capable for the oxidative degradation of lignin containing protoporphyrin IX heme prosthetic group; non heme *manganese catalase* containing two manganese per subunit and the *Oxygen Evolving Complex,* catalysing one of the most important reactions occurring in the plants, the light driven oxidation of water to oxygen and protons, containing four manganese atoms while the presence of calcium and chloride ions is required for proper functioning. Open structure mixed valence trinuclear complexes with the formula $Mn(II)/Mn(III)_2(Schiff\text{-}base)_2(OOCR)_4(L)_2$ were prepared and structurally characterised in an attempt to mimic the active site of OEC.

1. Introduction

" Are there similarities between Manganese and Magnesium ?" of course not; you may say. Magnesium is a main element in the periodic table, Manganese is a transition metal, and only this difference is enough to imagine that there are many differences. But if we try to dig up the root of the name of Manganese we will find out that the name manganese is an anagram of magnesium(gn $\Leftrightarrow$ ng) and that is because this metal is so similar with magnesium that at the beginning it was thought that manganese and magnesium are the same element. Many years later when the role of Manganese in biological systems was established Prof. Cotzias* trying to explain the polyfunctional role of Manganese in biological systems claimed: "Mangania is the Greek word for magic or, in modern parlance,

D.P. Kessissoglou (ed.), Bioinorganic Chemistry, 299-320

for voodoism. If this is the root of the metal's name, it reflects some reality in the biology of manganese, which is rich in phenomena and lacking in adequate guiding principles"

Today we know that Manganese is an essential element in many biological processes e.g. Oxygen Evolving Complex of Photosystem II, Superoxide Dismutase etc. For human beings manganese is an essential trace element existing in quantities about 230 times lower than that of iron in the body. Plants and many microorganisms also require manganese and most of the proteins containing manganese studied to date are from these sources. We can distinguish two functional values, first the Mn^{2+} as a Lewis acid, like divalent ions, *Magnesium, Calcium, Zinc* and second in higher oxidation states(Mn^{3+}, Mn^{4+}) as an oxidation catalyst, like *Copper, Iron, Cobalt.*

2. Manganese(II)-proteins and -enzymes

The most obvious feature of the chemistry of Mn(II) in aqueous solution, which is the solution environment of manganese(II)-proteins and -enzymes , is the stability of Mn(II) in acid solution. Other characteristic features; the ionic radius of Mn^{2+}, 0.75 A, lies between that of Mg(II)(0.65 A) and Ca(II)(1.00 A) and the $3d^5$ electronic configuration of the Mn(II) makes it behave as a spherically polarizable ion, with no crystal-field stabilisation energy. Table 1 shows a list of enzymes and proteins[1] containing Mn(II) ion(s). The Mn(II) is pumped into vesicles where its competitive strength is enhanced. Mn(II) does not form metalloproteins but exchangeable metal complexes with proteins. Mn(II) concentration is close to or less than 10^{-8} M almost everywhere inside or outside cells.

Table I. Manganese(II) enzymes and proteins

Arginase(Mitochondria)
Concanavalin A(extracellular)
Galactosyl transferase(Golgi)
Glycosylaminase(mitochondria)
Glutamate synthetase (mitochondria)
Isopropylmalate synthase (mitochondria)
Isocitrate dehydrogenase (mitochondria)
Mn-ribonucleotide reductase (prokaryote)
Manganese-dioxygenase (prokaryote)
Phosphoenolpyruvate carboxykinase (mitochondria)
Proline dipeptidase(ubiquitous)
Pyruvate carboxylase (mitochondria)

2.1. ARGINASE

Arginase is the last enzyme in the urea cycle(Figure 1) and catalyses the hydrolytic cleavage of arginine to urea and ornithine according to the reaction shown below. *Arginase* contains 4 Mn(II) ions per enzyme molecule and is found in the mitochondria.

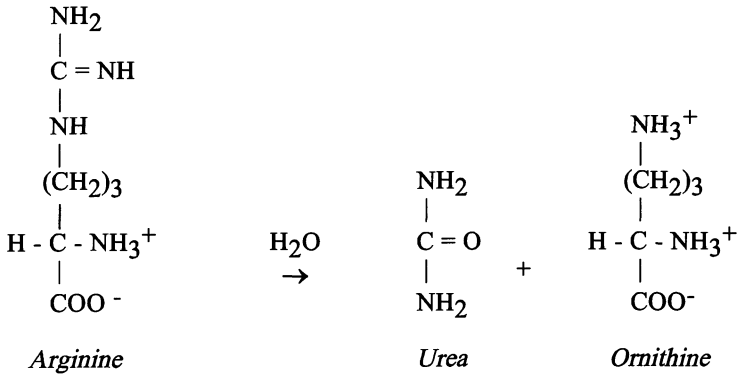

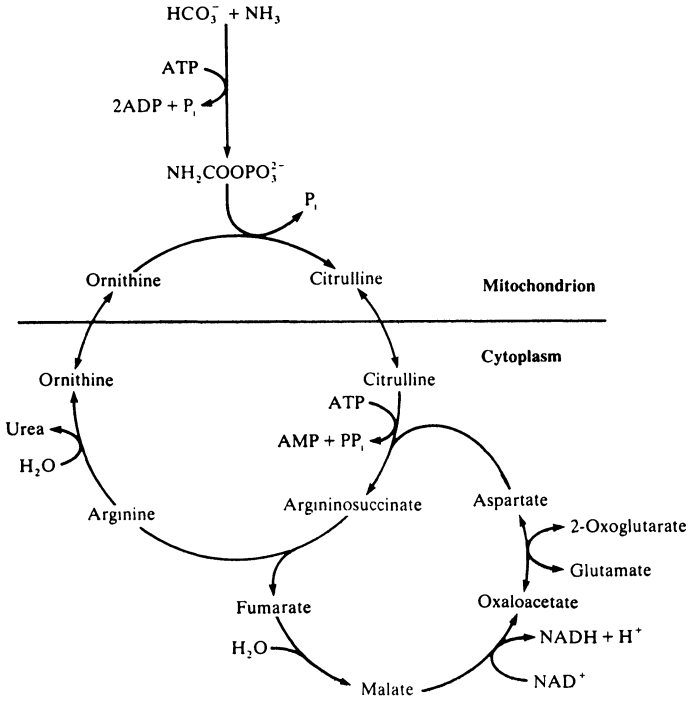

Figure 1. The Urea Cycle

2.2. CONCANAVALIN A

Concanavalin A is a manganese-calcium metalloprotein which has been structurally characterised[2,3]. *Concanavalin A* exists as a dimmer at pH=6 and a tetramer at pH>7.

Protomer has two binding sites a) a site S_1 for transition metal ions b) a site S_2 specific for calcium ions. Mn(II) is bound to the protein through *Glu, H_2O, H_2O, His, Asp* and *Asp* (Figure 2). The binding of the metal ions converts the apoprotein into a form that exhibits specific binding sites for small carbohydrates(a-d-glucopyranose, a-d-mannopyranose). Calcium can be replaced with another Mn(II) ion and subsequent EPR spectroscopy demonstrates weak antiferromagnetic coupling between the two manganese facilitated by a bridging carboxylate. The biological function associated with this activity remains uncertain.

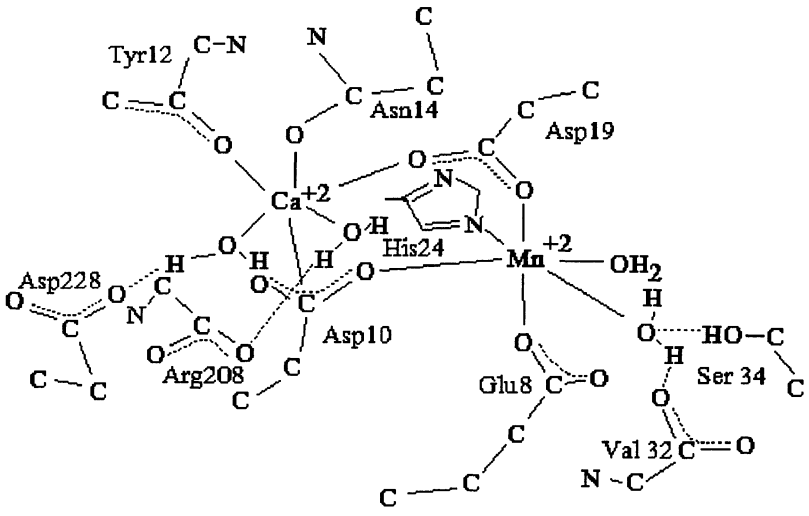

Figure 2. Structure of Concanavalin A

2.3. GLUTAMATE SYNTHETASE

Glutamine Synthetase and *Glutamate Synthetase* act together. The first one catalyses the synthesis of Glutamine in virtually all organisms

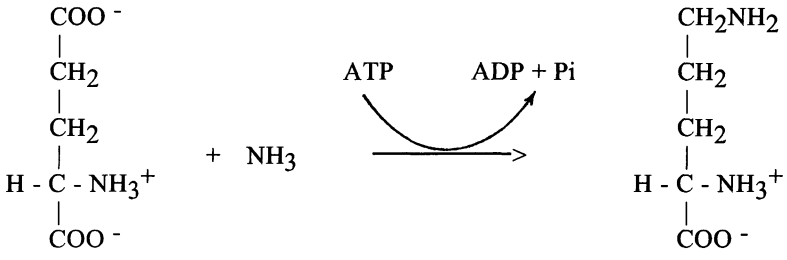

Glutamate *Glutamine*

while *glutamate synthatase* which is not present in humans but is found in bacteria catalyses the formation of glutamate.

This coupled enzyme system is used by the blue-green algae and is found in the mitochondria. *Glutamine-Synthatase* requires two Mn(II) ions associated with the active site of the enzyme. The distance between the Mn(II) sites is between 8-10 A and Mn(II) is bound to N or(and) O donor sites.

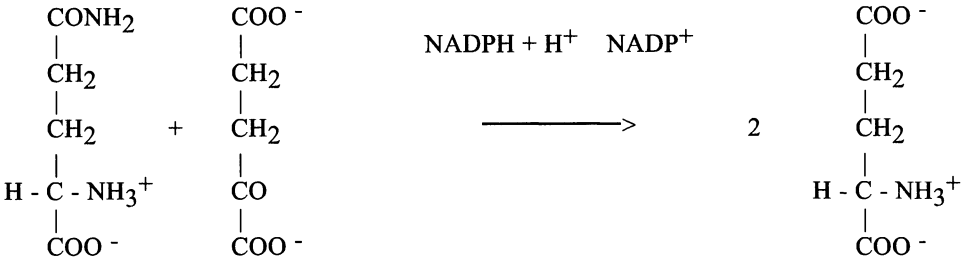

Glutamine *2-Oxoglutarate* *Glutamate*

2.4. MANGANESE RIBONUCLEOTIDE REDUCTASE

The synthesis of DNA is dependent on a ready supply of deoxyribonucleotides. The substrates for these are ribonucleoside diphosphates ADP, GDP, CDP and UDP. The enzyme responsible for the reduction to their corresponding deoxy derivatives is the *ribonucleotide diphosphate reductase* which uses thioredoxin as a cosubstrate. Recently a manganese-containing *ribonucleotide reductase*[4] was isolated from *B. ammoniagemes* consisting of a dimmer of MW=100,000 and a monomer of MW=80,000.

The presence of Mn(II) is suggested .

Antibodies that inhibit the iron enzymes were observed to be inactivated toward the Mn enzyme.

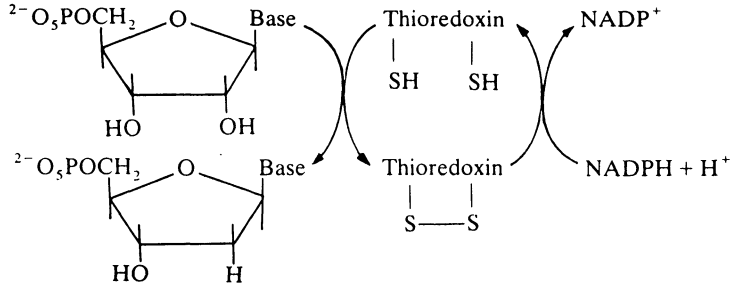

2.4. PHOSPHOENOLPYRUVATE CARBOXYKINASE

This enzyme converts irreversible cytoplasmic oxaloacetate to phosphoenolpyruvate only when the ATP concentration is high. The reaction type characterised as decarboxylation and phosphorylation

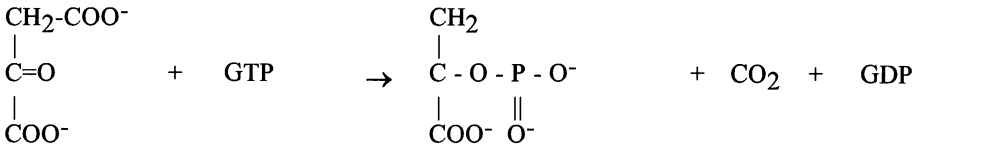

This reaction is a step in glucolysis(figure 4). In this enzyme manganese(II) may directly involved in interaction with substrate in the catalytic cycle and is bound to the protein through O.

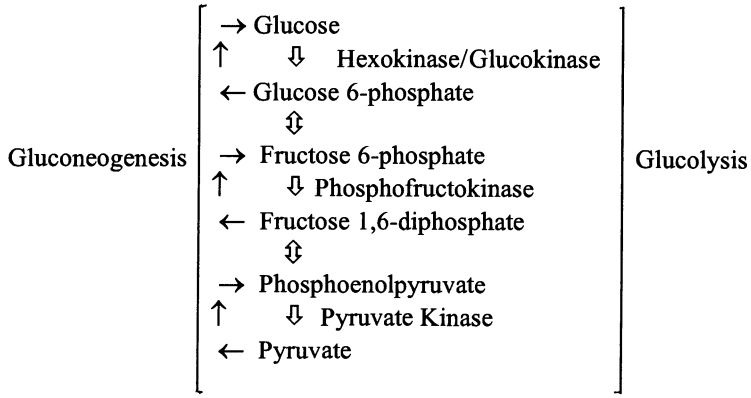

Figure 4. The gluconeogenesis and glucolysis

2.5. MANGANESE THIOSULFATE OXIDASE

It has been recently determined that *Thiobacillus versutus* specifically requires manganese for the oxidation of thiosulfate to sulfate[9]

$$5H_2O + S_2O_3^{2-} \rightarrow 2SO_4^{2-} + 4H^+, 10H^+$$

The enzyme appears to be part of a multienzyme system to utilise thiosulfate. EPR evidence seem to indicate a binuclear Mn(II) site.

2.6. ISOPROPYLMALATE SYNTHASE

The reaction catalysed by this enzyme is

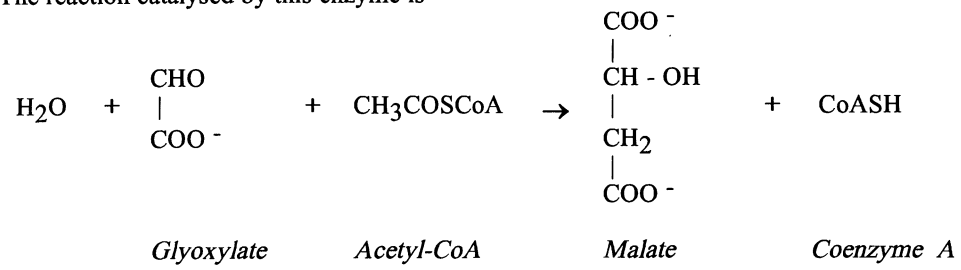

Mn(II) bound to the S-H group near site is involved in the reaction.

2.7. ISOCITRATE DEHYDROGENASE

This enzyme takes part at the 3rd step of the citric acid cycle and converts isocitrate to 2-oxoglutarate by an oxidative decarboxylation reaction

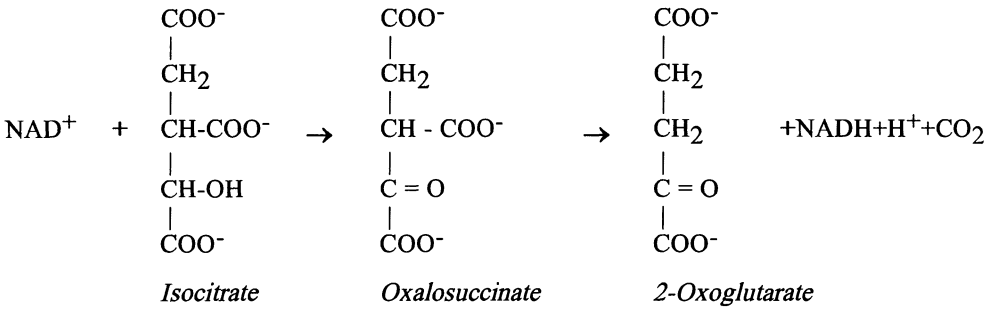

In this enzyme Mn(II) or Mg(II) is bound. ADP and NAD^+ activate and ATP or NADH inhibit the reaction.

2.8. PYRUVATE CARBOXYLASE

Pyruvate carboxylase, the first metalloenzyme shown to contain manganese[5], is a mitochondrial enzyme catalysing the conversion of pyruvate to oxaloacetate[6] and is in close association with citric acid cycle. The overall catalytic process is the sum of two reactions,

a) E-biotin + $MgATP^{2-}$ + HCO_3^- —> E-biotin-CO_2 + $MgADP^-$ + P_i^{2-}

b) $CH_3-C(=O)-COO^-$ + E-biotin-CO_2 → $CH_2COO^--C(=O)-COO^-$ + E-biotin

Pyruvate *Oxaloacetate*

This *biotin carboxylase* binds 4 Mn(II) very tightly without the Mn(II) to be involved directly in the catalytic cycle. The interatomic distances are too great[7] to allow direct coordination of pyruvate to metal ion. Is proposed that a molecule of water-buried in the protein-is tightly bound to Mn(II) and this coordinated water acts as an electrophile to activate pyruvate. Mn(II) is believed to have a role in maintaining the integrity of the active site and can be replaced with divalent magnesium with only a small decrease in activity.

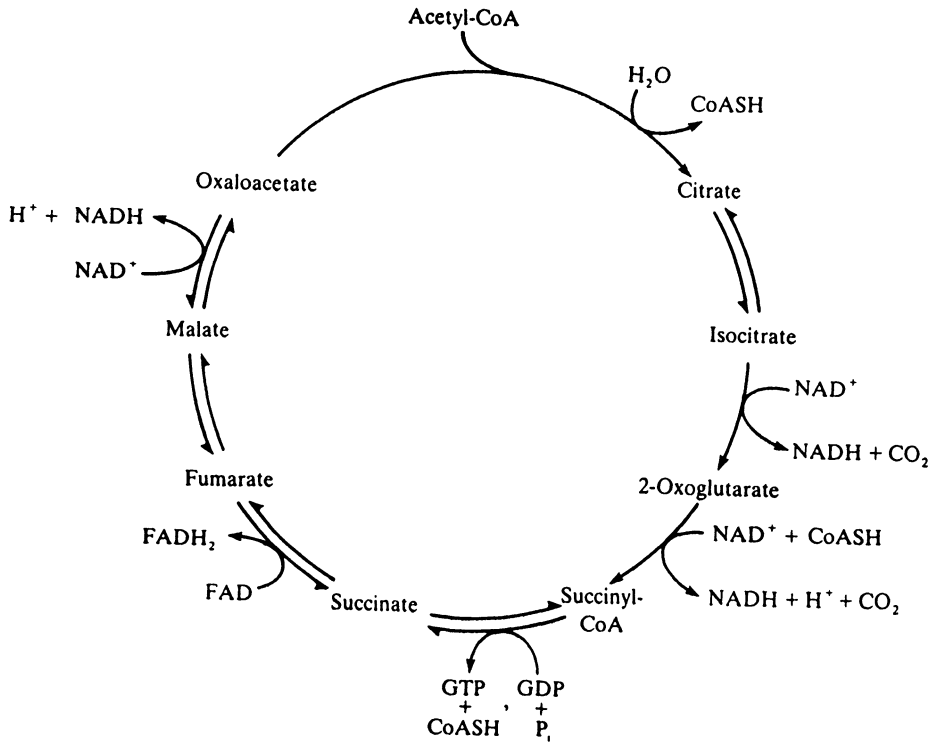

Figure 3. The citric acid cycle

3. Manganese Redox Enzymes

There are numerous enzymes that not only have a specific requirement for manganese but also utilise the redox capabilities of this element[8]. Table II shows a list of Manganese Redox Enzymes.

Table II. Manganese Redox Enzymes

Mn-ribonucleotide reductase (prokaryote)
Manganese Superoxide Dismutase(Mn SOD)
Manganese Peroxidase
Manganese Catalase
Mn Thiosulphate Oxidase
Oxygen Evolving Complex

3.1. MANGANESE SUPEROXIDE DISMUTASE(Mn SOD)

Manganese SOD catalyses the dismutasion of superoxide radicals to oxygen and hydrogen peroxide and presumably functions as a detoxification enzyme.

The enzyme is found in the mitochondria, Chloroplasts and prokaryotes. The Mn-SOD from *Thermus Thermophilus* has been crystallised and the X-ray structure[10] shows that it is a tetramer. The ligands bound to the single Mn(III) ion are three Histidines, one Aspartate and one Water/Hydroxide in a trigonal bipyramidal geometry(Figure 4).

$$2O_2^- + 2H^+ \rightarrow O_2 + H_2O_2$$

The manganese is believed to cycle between 3+ and 2+ oxidation states in a ping-pong type mechanism fact supported by the observation that the metal active center does not alter when the enzyme is reduced to the Mn(II) ion.

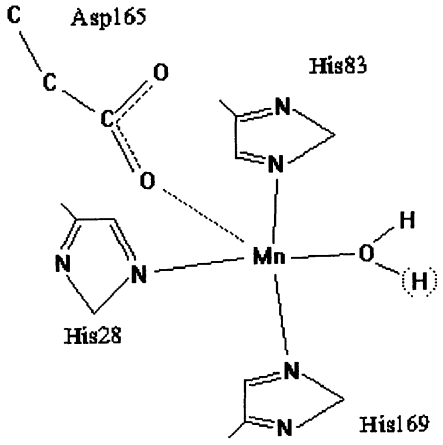

Figure 4. Structure of metal-active center of Mn-SOD

3.2. MANGANESE PEROXIDASE

The *Manganese Peroxidase(MnP)* is one of the two known enzymes capable of the oxidative degradation of lignin[11].

lignin(Phenolic polymer) → monomers
cinnamyl alcohol: $C_6H_5CH = CHCH_2OH$

Lignin is an amorphous, random, aromatic polymer synthesised from p-hydroxycinnamyl alcohol, 4-hydroxy-3-methoxycinnamyl alcohol and 3,5-dimethoxy-4-hydroxycinnamyl alcohol precursors by woody plants. The MnP is said to be associated with the strengthening of cross-linking in lignins - a function which can also be served by the haem peroxidases and Cu oxidases released from vesicles. Ligninase and MnP contain protoporphyrin IX heme prosthetic group, similar to the heme peroxidases with an L5-histidine. Also, they both utilise hydrogen peroxide to oxidatively decompose lignin. The MnP is unique in that it absolutely requires Mn(II) to complete its catalytic cycle[12]. The enzyme can be oxidised to an Fe(IV) porphyrin radical by H_2O_2. This radical is than reduced twice by Mn(II) giving two free Mn(III) species. Certain a-hydroxy acids promote this reaction through the chelation of Mn(III). In the absence of these acids manganese dioxide is formed. The resulting Mn(III) species are then proposed to be responsible for diffusion into the lignin matrix and initiation of phenolic radical decomposition of the polymer.

The following regulatory system has been found controlling the production of manganese peroxidases(ligninase) in *Phanerochaete Chrysosporium.*

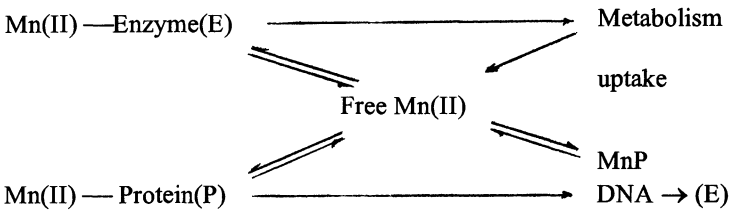

3.3. MANGANESE CATALASE

While the majority of known catalases utilise iron in the form of a heme prosthetic group to perform the disproportonation of hydrogen peroxide, non heme *manganese catalases* were isolated from *Lactobacillus plantarum, Thermoleophilum album and thermus thermophilus*[13]. These enzymes appear to exist as homoexamers or homotetramers containing two manganese per subunit.

Manganese catalase catalyses the reaction

$$2H_2O_2 \rightarrow O_2 + 2H_2O$$

A bis-μ-oxo bridged core has been proposed for the manganese dimmer in valent form, III/III, II/III or II/II. It is presently uncertain which oxidation states actually participate in the catalytic cycle. Penner-Hahn has proposed[8] a mechanism

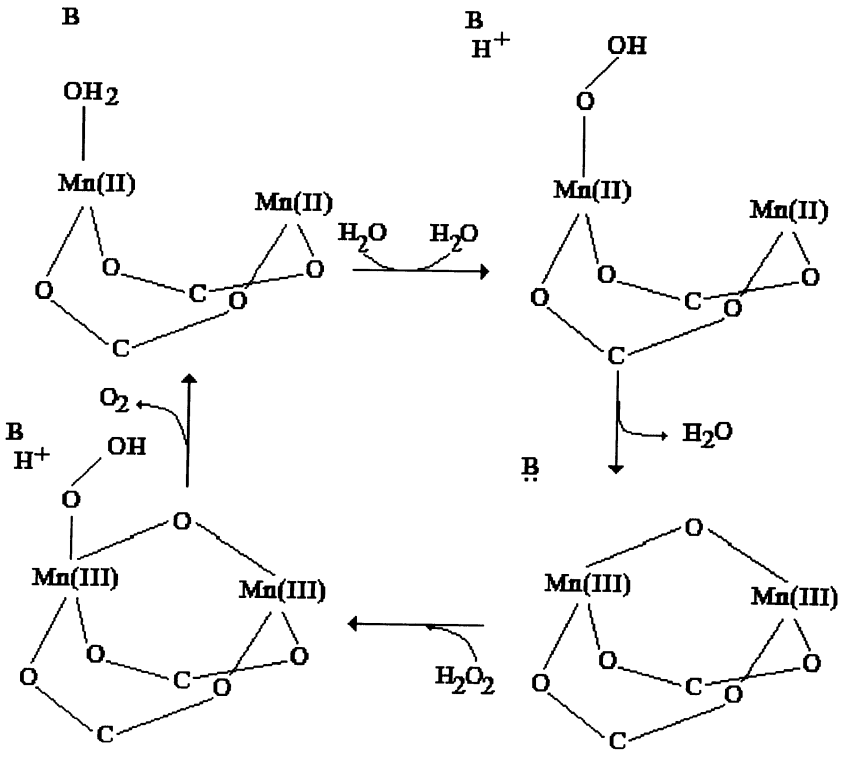

based on the presence of a bis-μ-carboxylato-μ-oxo bridged structure.

3.4. OXYGEN EVOLVING COMPLEX

One of the most important reactions occurring in the plants is the light driven oxidation of water to oxygen and protons.

$$2H_2O \rightarrow O_2 + 4H^+, 4e^-$$

Oxygen Evolving Complex is the name of the water oxidation center in Photosystem II and can be found in the thylakoid membranes of chloroplasts in plants. This manganese center[14] appears to contain four manganese atoms while the presence of calcium and chloride ions is required for proper functioning.

The OEC exhibits a periodicity in oxygen evolution corresponding to one molecule of molecular oxygen released every four quanta of light absorbed by the complex. Five states of the complex which have been called S states S_0-S_4 can be identified. The S_2 state is e.s.r. active showing a multiline signal at g=2 indicative of at least two coupled manganese atoms[15] and a broad signal at g=4.1. Extended X-ray absorption fine structure(EXAFS) studies[16] agree that at least two Mn-Mn vectors at 2.7 A and one 3.3 A vector are present. Every Mn atom is bound to either oxygen or nitrogen donors with distances 1.8 and 1.9 A. X-ray absorption near edge structure(XANES) measurements suggest 3.0 and 3.25 average oxidation state per manganese in the lower S states. Based on these data a number of structural proposals were addressed(*dimmer of dimmers, trimmer/monomer, distorted cubane, butterfly, dimmer/monomer*)

4. Relevant Trinuclear Synthetic Complexes

While the chemistry of mononuclear[17] and binuclear manganese[18,19] complexes has been well established, trinuclear manganese complexes have been only reported in the last 7-8 years. The trinuclear models could be distinguished into two structural features a)closed structure b)open structure, and two valence features a)homo valence b)mixed valence. In the following chapter there will be presented in more details the open structure and especially the mixed valence trinuclear complexes which are in the interest of authors research.

4.1. OPEN STRUCTURE HOMO VALENCE TRINUCLEAR COMPLEXES

The first example of the synthesis and characterisation of divalent linear, trinuclear complexes with the formula $Mn(II)_3(OAc)_6(biphme)_2$ {bipfme=methoxy-bis(1-methylimidazol-2-yl)phenylmetha-ne} appeared[20] in 1990. These complexes are comprised of a linear array of three Mn(II) ions in which a central hexacoordinate Mn(II) ion that resides on a crystallographic inversion center in the anti isomers is flanked by two metal ions that are essentially pentacoordinate. The metals are bridged by four bidentate and two monodentate μ-acetato ligands. The reaction used to prepare these trinuclear complexes is not restricted to biphme. Other bidentate, nitrogen-donating ligands may be employed, as evidenced by the synthesis of $Mn(II)_3(OAc)_6(phen)_2$, $Mn(II)_3(O_2CPh)_6(bpy)_2$, $Mn(II)_3(OAc)_6(bpy)_2$. These complexes may used as models for the metalloproteins concanavalin A and the reduced form of Ribonucleotide reductase.

4.2. OPEN STRUCTURE MIXED VALENCE TRINUCLEAR COMPLEXES

The first open structure trinuclear complex was the mixed valence compound[21] α-Mn(II)/Mn(III)$_2$(saladhp)$_2$(OAc)$_4$(CH$_3$OH)$_2$ as illustrated in figure 5,

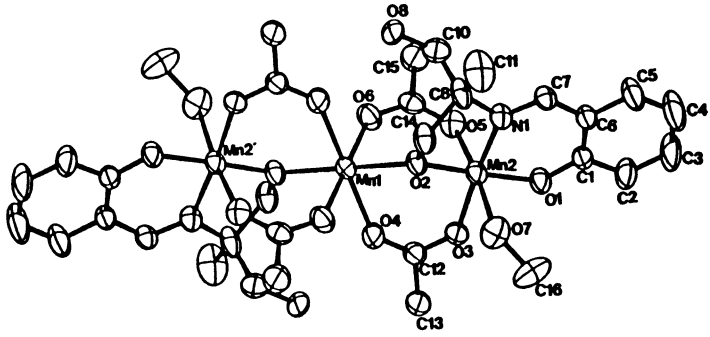

Figure 5. An ORTEP diagram of the mixed valence compound α-Mn(II)/Mn(III)$_2$(Hsaladhp)$_2$(OAc)$_4$(CH$_3$OH)$_2$

This linear compound includes a central, octahedral Mn(II) ion that is located on a crystallographic inversion center. It is flanked by two tetragonally distorted Mn(III) ions. The Mn(II) coordination sphere is composed of four syn bridging carboxylates and two μ-alkoxo oxygen atoms of the Schiff-base ligand. Each Mn(III) is six coordinate using two syn bridging acetates, a tridentate Schiff-base ligand and a neutral methanol molecule.

The Jahn-Teller distorted axes contain one carboxylate oxygen atom and the neutral monodentate ligand. In this complex the saladhp ligand is tridentate resulting in a meridional coordination geometry using an imine nitrogen and phenolate and alkoxide oxygen atoms to bind to the terminal Mn(III) ion. The Mn(III)-alkoxide oxygen distance is equivalent to the Mn(III)-phenolate oxygen distance. As expected there is a significant increase in the metal-alkoxide distance for Mn(II). The Mn(II) octahedron is regular in both distances and angles. The Mn(III)-Mn(II) atoms are separated by a distance of 3.511 A. Water can be substituted for methanol to give the isostructural α-Mn(II)/Mn(III)$_2$(Hsaladhp)$_2$(OAc)$_4$(H$_2$O)$_2$. While the Mn(III)-Mn(II)-Mn(III) angle remains linear[22], this simple modifications leads to a decrease in Mn(III)-Mn(II) separation(3.42 A). This illustrates how the simple expedient of water for an alcohol can cause a change in metal separation of greater than 0.1 A.

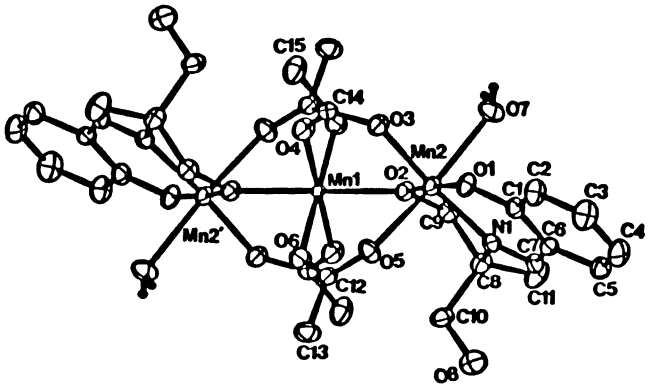

Figure 6. An ORTEP diagram of the mixed valence compound α-Mn(II)/Mn(III)$_2$(Hsaladhp)$_2$(OAc)$_4$(H$_2$O)$_2$

The neutral axial ligand can be substituted for 2-hydroxypyridine or dmf to generate the linear α-Mn(II)/Mn(III)$_2$(Hsaladhp)$_2$(OAc)$_4$(HpyrO)$_2$ (figure 7) and

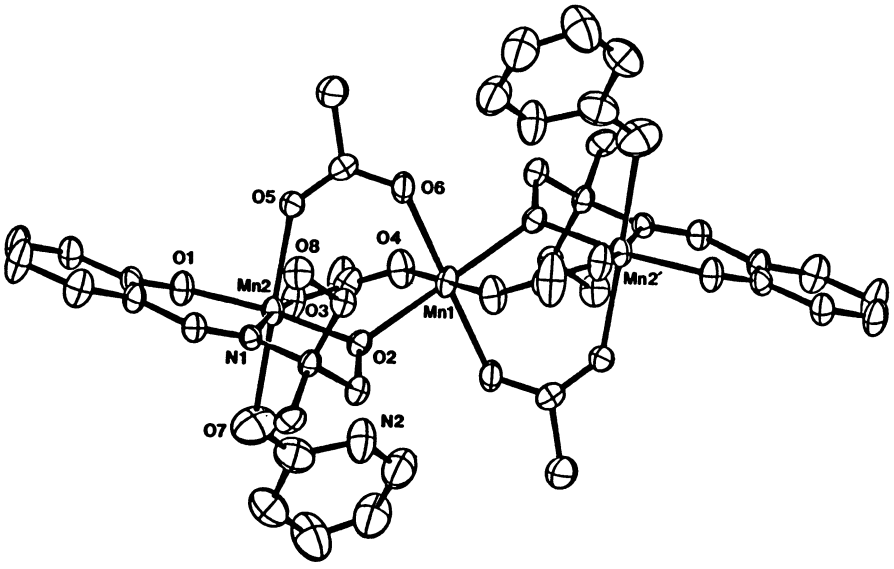

Figure 7. An ORTEP diagram of the mixed valence compound α-Mn(II)/Mn(III)$_2$(Hsaladhp)$_2$(OAc)$_4$(HpyrO)$_2$

α-Mn(II)/Mn(III)$_2$(5-Cl-Hsaladhp)$_2$ (OAc)$_2$(5-Cl-salac)$_2$(dmf)$_2$ (figure 8) respectively[23]

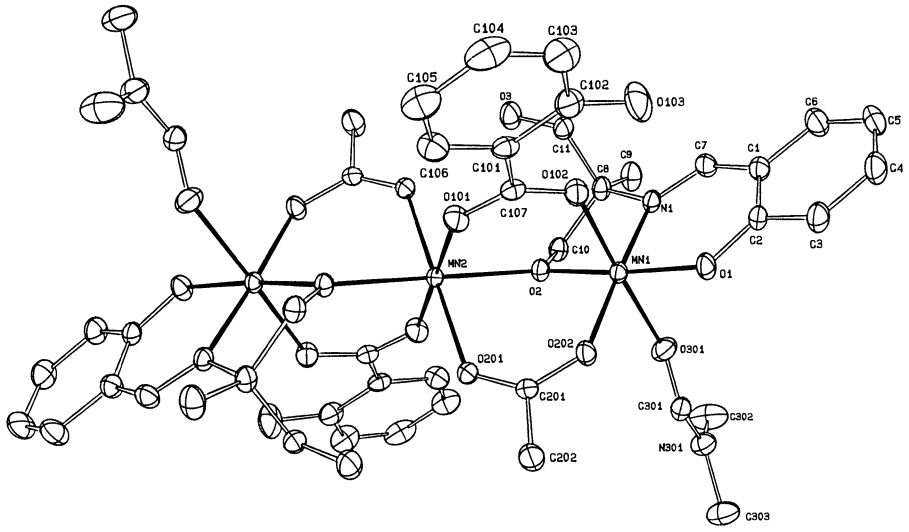

Figure 8. An ORTEP diagram of the mixed valence compound α-Mn(II)/Mn(III)$_2$(5-Cl-Hsaladhp)$_2$ (OAc)$_2$(5-Cl-salac)$_2$(dmf)$_2$

The b-Mn(II)/Mn(III)$_2$(Hsaladhp)$_2$(OAc)$_4$(CH_3OH)$_2$ which is also shown as figure 9, is a structural isomer of this trinuclear series[24]. Two-fold symmetry is restricted on this molecule leading to a bent form with an Mn(III) - Mn(II) - Mn(III) angle of 138^o . Quite interesting is the reorientation of solvent molecules so that they are situated on the *syn* face of the cluster. This isomer provided the first example of the orientation of solvent molecules onto the same face of a trinuclear cluster.

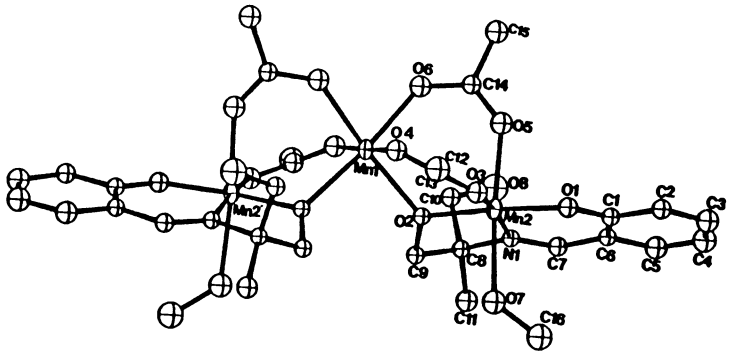

Figure 9. An ORTEP diagram of the mixed valence compound β-Mn(II)/Mn(III)$_2$(Hsaladhp)$_2$(OAc)$_4$(CH_3OH)$_2$

Recently, we have characterised a polymer containing a trimmeric mixed valence repeat unit with the formula [Mn(III)(Hsaladhp)(acetato)(5-Cl-salicylato)Mn(II)(acetato)(5-Cl-salicylato)(Hsaladhp)Mn(III)]$_n$. The X-ray structure(figure 10) of this polymeric compound[19] illustrates that the asymmetric unit comprises 2 Manganese atoms, Mn(III) in general position and Mn(II) which lies on a two fold axis. The alkoxide group acts as a bridge between the central Mn(II) and the terminal Mn(III) ions which are separated by 3.482(1) A. The trimmeric units are connected to each other by the phenolate bridging oxygen of the saladhp ligand creating a cation(2+) binuclear Mn(III)Mn(III) unit with an inversion center. The Mn(III) - Mn(III) separation of the terminal metal atoms is 6.491(1) A and the angle Mn(III)-Mn(II)-Mn(III) 137.5(4)^o. This angle is very similar with that observed in the β-Mn(II)/Mn(III)$_2$(Hsaladhp)$_2$(OAc)$_4$(CH$_3$OH)$_2$

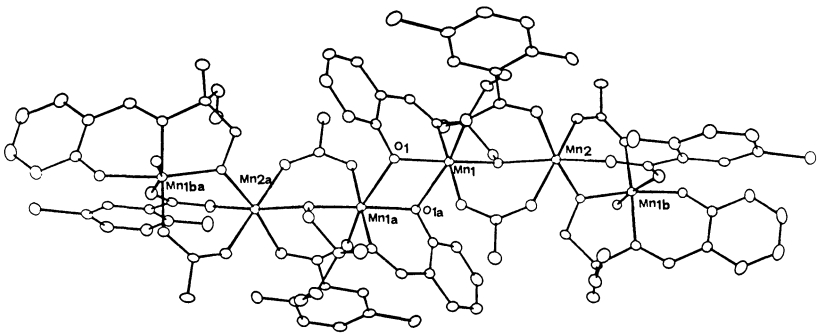

Figure 10. An ORTEP diagram of the mixed valence compound [Mn(III)(Hsaladhp)(acetato)(5-Cl-salicylato)Mn(II)(acetato)(5-Cl-salicylato)(Hsaladhp) Mn(III)]$_n$

The susceptibility data for α-Mn(II)/Mn(III)$_2$(Hsaladhp)$_2$(OAc)$_4$(CH$_3$OH)$_2$ can be fitted to a model with a terminal Mn(III) ion antiferromagnetically coupled to an Mn(II/III) spin system(Figure 11).

This model which predicted that the cluster had a quartet ground state was subsequently verified by magnetisation at 4.2 K(Figure 12). The J coupling constant is -7.1 cm-1 indicating that the manganese atoms are weakly antiferromagnetically coupled in this complex. The water exchanged complex shows an identical room temperature solid state moment, μ_{eff} = 8.1 MB, and variable temperature susceptibility curve. Therefor, even though there are significant changes in the Mn-Mn distance, the magnitude of the exchange coupling and the electronic ground state are unaltered. As a result of the obvious angular change, α and β forms of Mn(II)/Mn(III)$_2$(Hsaladhp)$_2$(OAc)$_4$(CH$_3$OH)$_2$ exhibit different terminal manganese separations, 6.5 and 7.1 A respectively but it appears to have little consequence for the magnetic properties(α-isomer: J=-7.1; β-isomer: J=-6.7 cm^{-1}).

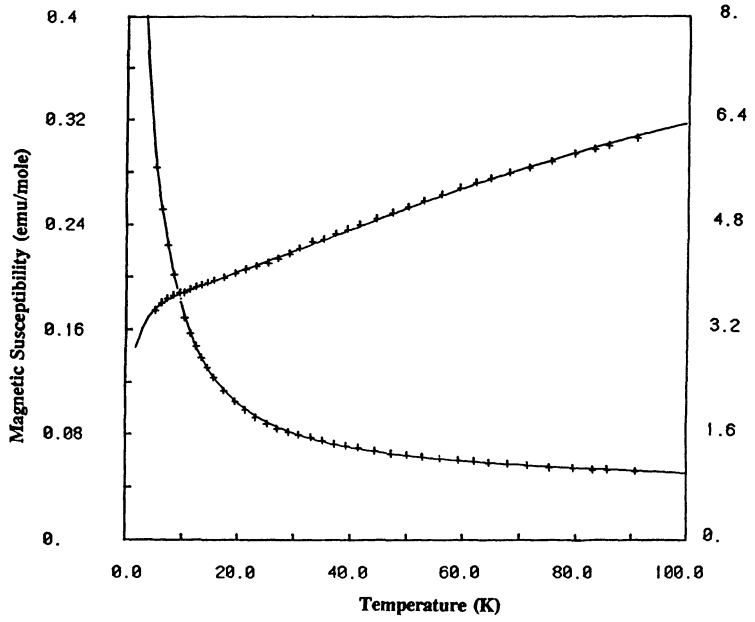

Figure 11. Variable temperature magnetic susceptibility data for α-Mn(II)/Mn(III)$_2$ (Hsaladhp)$_2$(OAc)$_4$(CH$_3$OH)$_2$

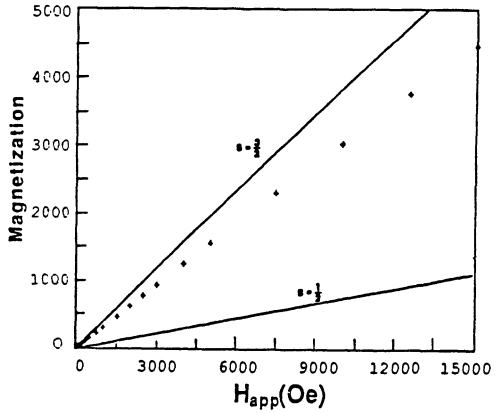

Figure 12. Magnetisation study for α-Mn(II)/Mn(III)$_2$(Hsaladhp)$_2$(OAc)$_4$(CH$_3$OH)$_2$ at 4.2 K over the field range 0-15000 G.

The insensitivity of the magnetochemistry to solvent exchange and isomer reorientation might be expected for two reasons. First, the Mn(III)-O(2)-Mn(II) distances and angles in the two α and β forms are very similar and second an analysis of the β form shows that the data can be fit quite well to a model assuming no exchange interaction between the terminal Mn(III) sites. Room temperature magnetic studies, 300 K, of the polymer cluster shows a

weak antifferomagnetic coupling with a magnetic moment μ_{eff}=8.06 MB, similar with that of the others trinuclear compounds.

The EPR spectra of the trinuclear complexes with only acetates bridges, in CH_2Cl_2, show a broad, low field component which arises from the ground state spin quartet. A classic six-line spectrum from uncomplexed Mn(II) is seen in MeOH due to dissociation to form monomeric units of Mn(II) and $[Mn(III)Hsaladhp]^+$. In dmf, a broad, low field component for the trinuclear complex, the sharp six-line of the uncomplexed Mn(II) and a multiline component centered at g=2 with approximately 19 lines spread over 1900 G appears(figure 13).

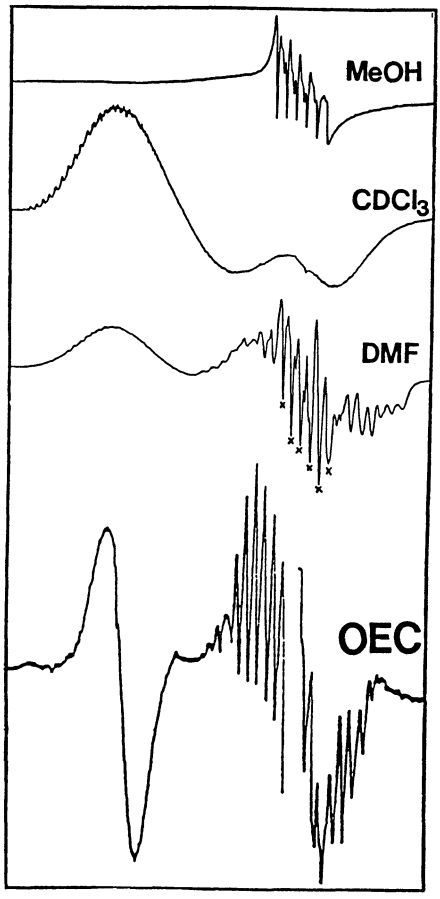

Figure 13. EPR spectra of trinuclear complexes in CH_2Cl_2, methanol and dmf

This trinuclear complex is more stable to dissociation in dmf than in methanol so that only a small portion of the complex dissociates completely. Some of the clusters remain intact giving the low field signal. The remaining material converts to a new species with changes in the distances/angles of the bridging atoms. This solvent dependent EPR spectroscopy illustrates how bond rupture or formation in a cluster can interchange two very different types of EPR spectral features.

The EPR powder spectra of the trinuclear complexes with two acetato and two salicylato bridging molecules, [Mn(III)(Hsaladhp)(acetato)(5-Cl-salicylato)Mn(II)(acetato)(5-Cl-salicylato)(Hsaladhp)Mn(III)]$_n$ or [Mn(III)(Hsaladhp)(acetato)(5-Cl-salicylato)Mn(II)(acetato)(5-Cl-salicylato)(Hsaladhp)Mn(III)](DMF)$_2$ show a broad low field signal at g=4.3 while as a dmf glass a six-line component arising from a dissociated Mn(II) at g=2.005(A=103 G; G=10^{-4} T) and a broad low field signal at g=4.3 but less intense appear. No any multiline signal centered at g=2, similar to that observed for the acetato-trinuclear cluster in dmf, has been detected(Figure 14).

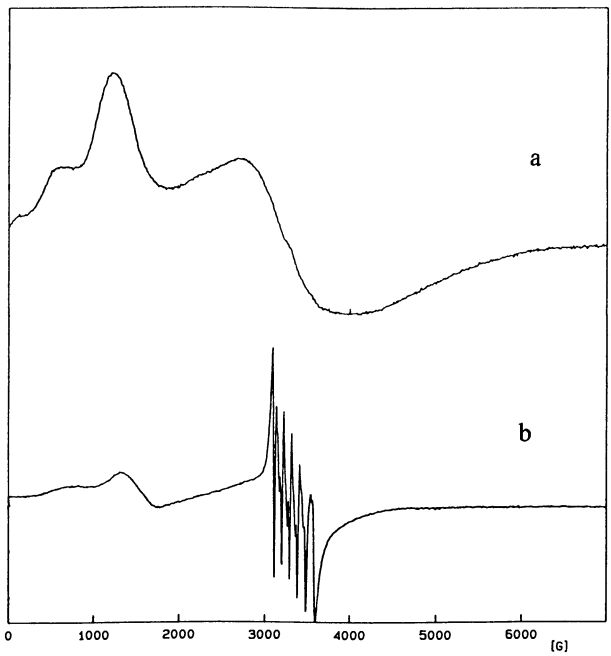

Figure 14. EPR spectra of polymer complex a) as powder and b) as dmf glass

The ^{1}H NMR spectrum obtained for Mn(II)/Mn(III)$_2$(Hsaladhp)$_2$(OAc)$_4$(CH$_3$OH)$_2$ in DCCl$_3$ contains five resonances that lie outside the diamagnetic region. Two relatively sharp

The ^1H NMR spectrum obtained for Mn(II)/Mn(III)$_2$(Hsaladhp)$_2$(OAc)$_4$(CH$_3$OH)$_2$ in DCCl$_3$ contains five resonances that lie outside the diamagnetic region. Two relatively sharp peaks are observed upfield(-20.7 and -24.0 ppm) and three peaks are observed downfield (+50.5, 38.5, and 25.6 ppm). It is possible to assign the upfield proton resonances at +50.5 and +38.5 ppm arise from the bridging acetate groups. This was confirmed by examining the spectrum of Mn(II)/Mn(III)$_2$(Hsaladhp)$_2$(d^3-OAc)$_4$(CH$_3$OH)$_2$. The resonance at 25.6 ppm is associated with the alkyl protons of the saladhp ligand. The trinuclear complex is a non electrolyte in HCCl$_3$ and has a room temperature solution μ_{eff}=8.1 μ_B. This is identical to the value for the complex in the solid state.

In CD$_3$OD, the two peaks assigned to acetato protons are missing while the peaks assigned to saladhp ligand are present suggesting a dissociation of the trinuclear complexes to monomeric units of [Mn(III)Hsaladhp]$^+$and Mn(II) in donor solvents.

The ^1H NMR spectrum obtained for Mn(II)/Mn(III)$_2$(Hsaladhp)$_2$(OAc)$_4$(CH$_3$OH)$_2$ in d^6-DMF is very complicated with peaks associated with the trinuclear complex and the dissociated [Mn(III)Hsaladhp]$^+$ species while there are also more intense features that are indicative of a third species.

The polymeric form of [Mn(III)(Hsaladhp)(acetato)(5-Cl-salicylato)Mn(II)(acetato)(5-Cl-salicylato)(Hsaladhp)Mn(III)]$_n$ cluster in dmf has a room temperature solution μ_{eff}=8.07 μ_B which is identical with that in solid state. The ^1H NMR spectrum shows a simple pattern with three resonances in the upfield region(+70, +50 and +34) and two in the downfield region(-24, -27) (figure 15).

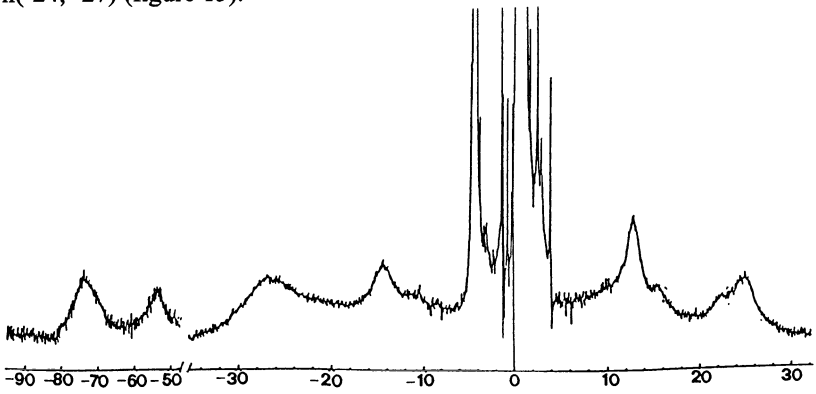

Figure 15. ^1H NMR spectrum of the polymer compound in d^6-dmf solution.

This polymeric form is not electrolyte in dmf consistent with the EPR results.

5. Acknowledgements

The author's special thanks go first of all to Prof. Vincent L. Pecoraro in whose lab the major part of this research work has been done and to the collaborators whose work has

been summarised in this article, Dr. Xinhua Li(University of Michigan), Dr. Myoung Soo Lah(University of Michigan), Prof. William Hatfield(Universiy of North Carolina, magnetochemistry), Prof. Martin Kirk(Universiy of North Carolina & University of New Mexico, magnetochemistry), Dr. Chris Bender(Michigan State University, EPR spectroscopy), Prof. Michael Maroney(University of Massachusetts, ^{1}H NMR), Dr. Catherine Raptopoulou(University of Thessaloniki), Ms. Dora Malamatari(University of Thessaloniki), Ms. Panagiota Hitou (University of Thessaloniki), Dr. Antonis Hatzidimitriou(CNRS, Toulouse France, X-ray structure determination), Dr. Andre Gourdon(CNRS, Toulouse France, X-ray structure determination), Prof. Loucia Banci and Prof. Ivano Bertini(University of Florence,Italy, ^{1}H NMR). Professor Kessissoglou also appreciates the financial support that he received from the Greek General Secretariat of Research and Technology.

6. **References**

(*) Cotzias, G.C. *Physiol. Rev.* **1958.**

(1) Frausto da Silva and Williams R.J.P., *"The Biological Chemistry of the Elements"* Clarendon Press, Oxford, **1991**

(2) Becher, J.W., Reeke, G.N., Wang, J.L., Cunningham, B.A., Edelman, G.M., *J.Biol.Chem.,* **1975**, 1513

(3) Reeke, G.N., Becher, J.W., & Edelman, G.M., *Proc. Nat. Acad. Scien. USA,* **1978**, *75*, 2286; Hardmann, K.D.; Agarwal, R.C., Freiser, M.J. *J.Mol.Biol.* **1982**, *157*, 69

(4) Stube, J. *J.Biol.Chem.* **1990**, *265*, 5329; Lynch, J.B., Juarez-Garcia C., Munck, E., Que, L. Jr., *J.Biol.Chem.* **1989**, *264*, 8091; Willing, A., Follmann, H., Auling, G. *Eur. J. Biochem.* **1990**, *265*, 2070.

(5) Schramm, V.L., Wedler, F.C. in *Manganese in Metabolism and Enzyme Function,* Academic Press, Orlando, FL, **1986.**

(6) Hansson, O., Aasa, R., Vanngard, T., *Biophys. J.* , **1987**, *51*, 825.

(7) Stadtman, E.R., Ginsburg, A, *Enzymes,* **1974**, *10*, 755; Balakrishman, M.S., Villafranka, J.J., *Biochemistry,* **1978**, *17,* 3531

(8) Pecoraro,V.L.,*Manganese Redox Enzymes,* VCH Publishers Inc, New York, **1992**

(9) Cammack, R., Chapman, A., Wei-Ping, Lu, Katagouni, A., Kelly, D.P. *Febs Lett.* **1989**, *253*, 239.

(10) Stallings, W.C., Pattridge, K.A., Strong, R.K., Ludwig, M.L. *J. Biol. Chem.* **1985**, *260*, 16424; Ludwig, M.L.; Metzger, A.L., Pattridge, K.A., Stallings, W.C., *J.Biol.Chem.* **1991**, *219*, 335.

(11) Gold, M.H., Wariishi, H., Valli, K., *Biocatalysis in Agricultural Biotechnology,* Chap. 9, Aer. Chem. Soc., Washington, D.C., **1989**, 127

(12) Wariishi, H., Khadar, V., Gold, M.H., *Biochemistry,* 1989,28,6017; Wariishi, H., Gold, M.H., *J.Biol.Chem.* **1990**, *265*, 2070.

(13) Kono, Y., Pridovich, I., *J.Biol.Chem.* **1983**, *258*, 6015; Algood, G.S., Perry, J.J., *J.Bacteriol,* **1986**, *168*, 563; Barynin, V.V.; Grebenko, A., *Dolk. Akad. Nauk. S.S.S.R.* **1986**, *286*, 461.

(14) Dismukes, G.C., *Photochem. Photobiol.* **1986**,*43*,99; Pecoraro,V.L., *Photochem. Photobiol.* **1988**,*48*,249

(15) Dismukes, G.C., Siderer, Y., *Proc. Natl. Acad. Sci.(USA),* **1981**,*78*,274; Casey, J., Sauer,K., *Biochem.Biophys.Acta,* **1984**,*767*,21; dePaula, J.C., Beck, W.F., Brudving,G.W., *J.Am.Chem.Soc.* **1986**,*108*,4002; Hansson,O.R.,Aasa, R., Vanngard, T., *Biophys.J.,* 1987,*51*,825; Zimmermann, J.-L., Rutherford, A.W., *Biochemistry,* **1986**,*25*,4609.

(16) Guiles,R.D., Yachandra,V.K., McDermott, A.E., Cole,J.L., Dexheimer, S.L., Britt,R.D. , Sauer, K., Klein, M.P. , *Biochemistry,* **1990**,*29*,486; George, G.N., Prince, R.C., Cramer,S.P., *Science,* **1989**,*243*,789; Penner-Hahn, J.E.,Fronko, R.M., Pecoraro,V.L., Yocum, C.F., Betts, S.D., Bowlby,N.R, *J.Am.Chem. Soc.* **1990**,*112*,2549; Tamura,N., Ikeuchi, M., Inoue, Y., *Biochim.Biophys.Acta,* **1989**,*973*,281; Andreasson,L.-e., *Biochim.Biophys.Acta,* **1989**,*973*,465

(17) Kessissoglou,D.P., Butler, W.M., Pecoraro,V.L., *J. Chem. Soc. Chem. Commun.* **1986,** 1253; Kessissoglou,D.P., Li,X.-h., Butler,W.M., Pecoraro, V.L., *Inorg. Chem.* **1987**, *26,* 2487; Bonadies,J.A., Kirk, M.L., Lah, M.S., Kessissoglou,D.P., Hatfield, W.E.; Pecoraro,V.L., *Inorg. Chem.*, **1989**, *28,* 2037;

(18) Gohdes J.W., Armstrong, W.H., *J.Am.Chem. Soc.*, **1989,** *111,* 802; Larson, E.J., Lah, M.S., Li,X-h., Bonadies , J.A., Pecoraro, V.L., *Inorg.Chem.* **1991,** *30,* 373; Larson, E.J., Pecoraro, V.L., *J.Am.Chem. Soc.* **1991,** *113,* 381; Goodson,P.A., Glerup,J., Hodgson,D.J., Michelsen, K., Weike, H. *Inorg. Chem.*,**1991**, *30*, 4309

(19) Christou,G., *Acc.Chem.Res.,* **1989,** *22,* 328; Shihaba,S., Onuma, S., Inoue, H., *Inorg.Chem.*, **1985**, *24*, 1723; Murray,B.D., Hope, H., Power, P.P., *J.Amer.Chem. Soc.,* **1985,** *107*, 169; Auger. N., Girerd,J.-J., Corbella, M.; Gleizes, A., Zimmerman, J.-L., *J.Am.Chem.Soc.,* **1990**, *112*, 448;

(20) Rardin,R.L., Bino,A., Poganiuch,P., Tolman, W.B., Liu, S., Lippard.S.J., *Angew. Chem. Int. Ed.Engl.,* **1990,** *29,* 812; Rardin,R.L., Poganiuch,P., Bino,A., Goldberg, D.P., Tolman, W.B., Liu, S., Lippard.S.J., *J.Am.Chem.Soc.* , **1992**, *114,* 5240.

(21) Li, X-h.; Kessissoglou, D.P., Kirk, M.L., Bender,C., Pecoraro,V.L., *Inorg. Chem.* **1988**, *27*, 1

(22) Kessissoglou, D.P., Kirk, M.L., Lah, M.S., Li,X.h., Raptopoulou, C.A., Hatfield,W.E., Pecoraro, V.L. , *Inorg. Chem.*, **1992**, *31,* 5424;

(23) Malamatari, D.A., Hitou, P., Hatzidimitriou,A.G., Gourdon, A., Kessissoglou, D.P. Kirk, M.L., manuscript in preparation

(24) Kessissoglou,D.P., Kirk, M.L., Bender,C.A., Lah, M.S., Pecoraro,V.L., *J. Chem. Soc.,Chem. Commun.,* **1989**, 84

CATALYTIC OXIDATION OF POLLUTANTS BY LIGNINASE MODELS BASED ON METALLOPORPHYRINS AND METALLOPHTHALOCYANINES

B. MEUNIER AND A. SOROKIN
Laboratoire de Chimie de Coordination du CNRS,
205 route de Narbonne, 31077 Toulouse cedex, France.

1. Introduction

A major problem in the cellulose industry is the expensive and polluting pretreatment of wood pulp to produce cellulose materials free of lignin. The currently used chlorine oxidation of lignin in white-paper manufacturing produces 4-5 kg of chlorinated and poorly biodegradable phenol residues per metric ton of treated wood pulp.[1,2] In the middle of the 1970s, several groups decided to investigate the possible industrial development of enzymatic degradation of lignin in order to avoid the release of large amounts of chlorinated organic molecules in the environment. Until now, no efficient enzymatic treatment was possible but the recent purification and characterization of two-heme containing peroxidases produced by a ligninolytic filamentous fungus, *Phanerochaete chrysosporium*, have stimulated modeling studies in the field. One of these peroxidases is ligninase or LiP [5] and the second one is manganese peroxidase or MnP.[6] The present review is organized as follows: after a short section on the biosynthesis of lignin and on the properties of the two peroxidases of *Phanerochaete chrysosporium*, LiP and MnP, recent advances on the modeling of these two heme-enzymes by synthetic metalloporphyrins are reported. The final section is focused on the use of these ligninase models in the catalytic oxidation of pollutants.

2. Lignin and peroxidases

Lignin is an essential component of the woody stems of arborescent plants where it is present in amounts ranging from 15 to 36%. Besides its structural role in plants (resistance towards impact, compression and bending), lignin has other functions essential for the life of plants: (i) to decrease of the water permeation across the cell walls, (ii) to distribute water, nutrients and metabolites, and (iii) to help in the plant defence against insects and microorganisms.[3,4]

Various microorganisms are able to degrade lignin by oxidation, the ultimate products being CO_2 and H_2O. Bacteria [7] play a minor role in delignification compared to that played by fungi.[8] One main class of fungi exhibits a high ligninolytic activity: "white rot fungi" (basidiomycetes) which are able to oxidize lignin with CO_2 and H_2O as ultimate degradation products. Among white rot fungi *Phanerochaete chrysosporium* [9-11] has the highest ligninolytic activity. Three main reactions mediated by the fungus are observed: (i) the cleavage of C_α-C_β bonds of phenylpropanoid units, (ii) the cleavage of C-O bonds in

D.P. Kessissoglou (ed.), Bioinorganic Chemistry, 321-331

the arylglycerol-b-arylether moieties and (iii) the demethoxylation of aromatic rings. This latter reaction was not well-documented for peroxidases prior to a study on the metabolism of 9-methoxyellipticine by horseradish peroxidase.[12] Two extra-cellular enzymes of *Phanerochaete chrysosporium* have been purified and identified as H_2O_2-dependent peroxidases: ligninase (LiP) and manganese peroxidase (MnP) ([5] and [6], respectively).

2. 1. LIGNINASE (or LiP)

The purification of ligninase by the groups of Kirk [5a] and Gold [5b] largely contributed to the understanding of the relationships between lignin degradation and reactions catalyzed by this enzyme.

Six isozymes of ligninase have been purified from the extracellular fluid of ligninolytic cultures of *Phanerochaete chrysosporium*. The main one (H8) has been used for physico-chemical analyses. This peroxidase, which has a molecular weight of 42, 000 Daltons, is composed of 15 % by weight of carbohydrates and contains one iron-protoporphyrin IX entity as the prosthetic group.[5] Hydrogen peroxide is the co-factor. Studies with $H_2{}^{18}O$ indicated the formation of labeled products were formed confirming the peroxidase nature of LiP, the crucial step catalyzed by ligninase being the formation of an initial radical-cation on methoxylated aromatic rings.[14,15] The resting state of the enzyme is a high-spin iron (III)-porphyrin with a histidine as proximal residue.[16,17] Single crystals of the enzyme have been obtained by T. L. Poulos[18] and co-workers and preliminary data confirmed the presence of a proximal histidine and a large pocket on the heme edge[19] cDNA of ligninase is now available.[20]

As for other peroxidases, a high-valent iron-oxo entity, compound I, is generated by the addition of hydrogen peroxide. This green compound (Soret band at 408 nm) has the same UV-visible characteristics as HRP-Compound I that contains an iron(IV)oxo species associated with a porphyrin π-radical-cation.[5c, 21] The addition of 0.5 equivalent of a 2 electron reducing agent like veratryl alcohol generates LiP-Compound II (Soret band at 420 nm) which corresponds to the iron(IV)oxo without an oxidized porphyrin ligand.[5c, 21] Unexpectedly, LiP is a fragile enzyme when exposed to more than 20 equivalents of hydrogen peroxide:[13] besides the two catalytically active forms (compounds I and II), two inactive forms LiP III* and LiP III have been obtained in the presence of an excess of hydrogen peroxide or by addition of molecular oxygen to the reduced form of LiP (ferrous state).[22] The fragility of LiP in the presence of an excess of hydrogen peroxide is the limiting factor for the industrial development of ligninase use in delignification or pollutant oxidation.

Veratryl alcohol is a secondary metabolite in delignification mediated by *Phanerochaete Chrysosporium* and is also a good substrate for ligninase and enhances the rate of oxidations catalyzed by LiP.[23,24] Many oxidation products generated from veratryl alcohol by LiP/H_2O_2 have been identified: veratraldehyde, two quinones (2-hydromethyl-5-methoxy-1,4-benzoquinone and 2-methoxy-1,4-benzoquinone) and three lactones have been isolated.[5d] Complete identification of the oxidation products of lignin model dimers with an arylglycerol-3-arylether moiety has also been performed.[25,26] The C_α-C_β bond cleavage is mediated by the initial formation of a radical-cation on one of the two aromatic rings. In the case of 1-(3,4-dimethoxyphenyl)-2-(2-methoxyphenoxy)propane-1,3-diol, the main oxidation products generated by LiP/H_2O_2 are veratraldehyde, guaiacol and glycolaldehyde.[27,28]

2. 2. MANGANESE PEROXIDASE (MnP)

The culture medium of *Phanerochaete chrysosporium* contains another extracellular peroxidase. This enzyme is manganese-dependent and is unable to catalyze the oxidation of

veratryl alcohol in the presence of H_2O_2.

Manganese peroxidase is a heme-glycoprotein of 46,000 Daltons and requires manganese(II) for its activity.[6] The primary amino acid sequence of MnP has been deduced from its cDNA.[29,30] This peroxidase exhibits a proximal histidine as well as distal histidine and arginine that assist the heterolytic cleavage of the peroxide O-O bond. The presence of the proximal histidine was confirmed by Raman resonance and EPR studies.[6a]

The native manganese peroxidase is oxidized by hydrogen peroxide to a compound I species similar to HRP-Compound I. Mn^{II} ion, which binds to the enzyme and reduces MnP-Compound I to MnP-Compound II. This latter oxidized form of MnP is only reduced to native MnP by manganese(II) but not by phenols. The oxidation of Mn^{II} to Mn^{III} by MnP is dependent on the presence of chelating agents in the reaction mixture. These chelating agents (a-hydroxyacids like lactate, succinate, malonate) have two different roles: they stimulate the catalytic activity by facilitating the dissociation of the enzyme-manganese complex by chelating Mn^{III} and they stabilize manganese at the oxidation state III. Mn^{III} salts can easily dismute to Mn^{II} and Mn^{IV}. Manganese ions cannot be replaced by iron(III), copper(II) or cobalt(II) salts.

Since Mn(III) chelates are only able to oxidize phenol derivatives, the main targets of MnP on lignin are the phenolic residues. 15% of the phenylpropane units in lignin have a hydroxyl group at the *para* position.[31]

A detailed study on a lignin model dimer with a phenol function, such as 1-(3,5-dimethoxy-4-hydroxyphenol)-2-(4-methoxy)propane-1,3-di ol, indicated that such a dimer was cleaved by $MnP/H_2O_2/Mn^{II}$ to the following monomers: 2,6-dimethoxybenzoquinone, 2-hydroxy-4'-methoxyacetophenone and 1-(4-methoxyphenyl)ethane-1,2-diol. Labeling experiments with $^{18}O_2$ and $H_2{}^{18}O$ confirmed that the key reaction was the initial formation of a phenoxy radical.[32] Partial depolymerization of lignin by MnP has been observed *in vitro* .[33]

2. 3. OXIDATION OF POLLUTANTS MEDIATED BY LIGNINASE

One of the most promising properties of ligninase is its capacity to oxidize various recalcitrant organic molecules. Microorganisms in soils and water convert many man-made chemicals into inorganic products.[34] However, some molecules are recalcitrant to biotransformation and are subject to accumulation in plants or animal tissues.

Among the compounds resisting microbial degradation, DDT and lindane are two classical examples.[35] Both are slowly transformed by microbial reduction and few extracellular enzymes are able to catalyze their oxidation. In order to be effective, these enzymes must have higher redox capabilities than horseradish peroxidase. Ligninase catalyzes the oxidation of chlorinated phenols. For example, 2,4,6-trichlorophenol, a major pollutant in paper mill effluents[37] is converted into 2,6-dichlorobenzoquinone.[36,37] 2,3,7,8-tetrachlorodibenzo-*p*-dioxine is also degraded by LiP.[38]

3. Model systems of ligninase

Early models of ligninase have been developed with iron protoporphyrin IX in combination with *tert*-butylhydroperoxide[39,40] or Fe(TPP)Cl in combination with O_2 and an electron source.[41] However, these metalloporphyrins are not water-soluble and are easily bleached in the reaction conditions.

3. 1. WATER-SOLUBLE METALLOPORPHYRIN COMPLEXES

Water-soluble sulfonated metalloporphyrins were found to be suitable catalysts in ligninase model studies.[42-45] In one case, sodium hypochlorite was used as oxygen donor.[42] However this oxidant only exists at elevated pH values and is an efficient oxygen atom donor in hydrophobic medium.[46] Aromatic chlorinations are the main reactions with hypochlorite solution below pH 8-9. Potassium monopersulfate seems to be a more suitable oxidant in ligninase modeling.[43-45] The best oxidant, *i.e.* the "clean oxidant", is of course hydrogen peroxide. However, the activation of H_2O_2 by synthetic metalloporphyrins in the absence of co-factors (imidazole derivatives) usually leads to the homolytic cleavage of the peroxide O-O bond[46a] (produced hydroxy radicals are strong inhibitors and/or bleaching agents of metalloporphyrin catalysts). The activity of the "$KHSO_5$/sulfonated metalloporphyrin" ligninase model has been checked with the usual lignin model molecules: veratryl alcohol and 1-(3,4-dimethoxyphenyl)-2-(2-methoxyphenoxy)propane-1,3-diol. We found that iron(III) tetrakis(4-sulfonatophenyl)porphyrin (FeTPPS) in combination with potassium monopersulfate is an efficient catalyst for veratryl alcohol oxidation to veratraldehyde and 2-hydroxymethyl-5-methoxy-1,4-benzoquinone, the same oxidation products generated by ligninase[45] (see Figure 1).

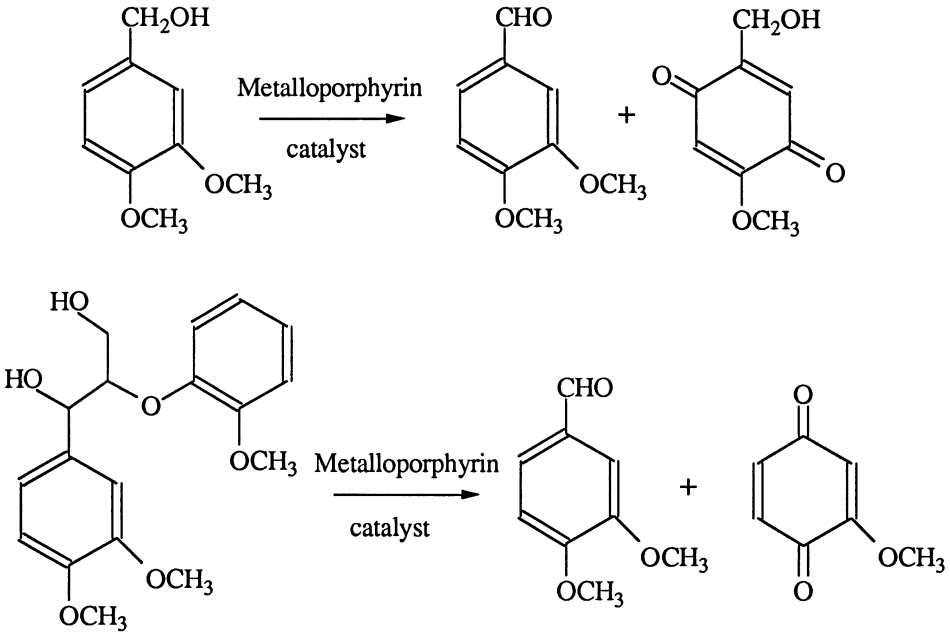

Figure 1. Product distribution in the catalytic oxidation of two lignin model molecules by the "$KHSO_5$/metalloporphyrin" system.

The dimer with one arylglycerol-b-arylether linkage was also cleaved at the C_α-C_β bond to generate veratraldehyde and 3-methoxy-1,4-benzoquinone. Catalytic activities ranged from 1 to 5 cycles per second.[44,45] The corresponding manganese complex, MnTPPS is slightly less active.[45]

Robust sulfonated iron and manganese porphyrins have also been used in ligninase modeling e.g., M-TMPS,[47] M-TDCPPS[48] and M-Br_8TMPS.[47] These sterically hindered

water-soluble complexes are the most promising catalysts. The degradation products of lignin models are similar to those obtained in ligninase-mediated oxidations. These iron catalysts are able to decolorize Poly B-411, a blue dye used to monitor the activity of ligninase.[48,49]

3. 2. SUPPORTED METALLOPORPHYRINS

These sulfonated metalloporphyrins are also efficient catalysts in ligninase modeling when supported on ion-exchange resins.[44,45] FeTPPS or MnTPPS strongly interact with the ammonium residues of Amberlite IRA 900, an ion-exchange resin derived from poly(vinylbenzene)[44,45] (see Figure 2). These supported catalysts can be recycled. The catalytic activity of MnTPPS-Amberlite used in a second run was still 95 % of that measured in the first run.[44]

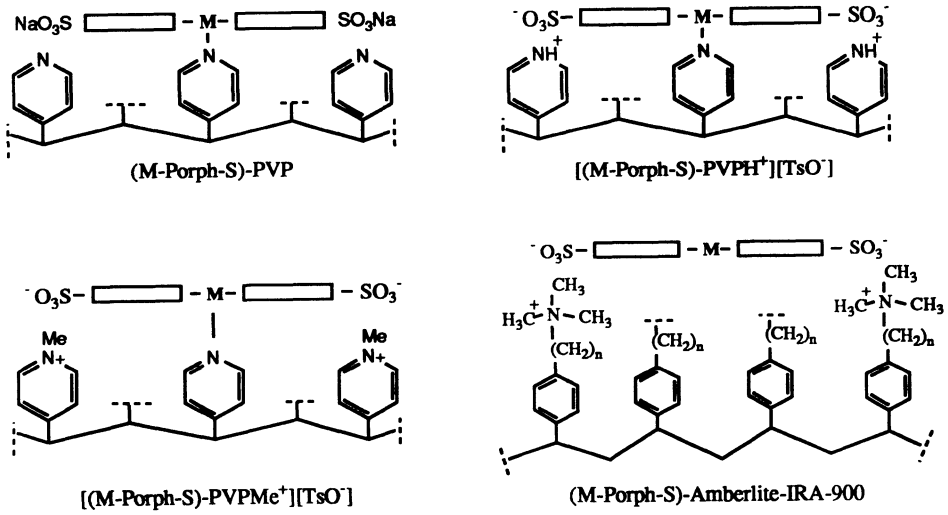

Figure 2. Schematic representation of supported sulfonated metalloporphyrins on cationic ion-exchange resins.

The main problem with the supported sulfonated manganese porphyrins is the necessary presence of pyridine in the reaction mixture in order to increase the catalyst activity (for the role of pyridine and imidazole derivatives to enhanced the catalytic activity of metalloporphyrins by proximal effect, see reference 46a. With a poly(vinylpyridine) (PVP) support, in contrast, it is possible to take advantage of the proximal effect of a pyridine ligand arising from the polymer itself. Such supported manganese catalysts are easily prepared from poly(4-vinylpyridinium) cross-linked with divinylbenzene[50] (see Figure 2 for a schematic representation of supported manganese porphyrin on PVP). The sulfonated manganese porphyrin is adsorbed on PVP via the coordination of pyridine as axial ligand.[51] The only axial interaction is not sufficient to avoid leaching of the MnTMPS from the PVP during catalytic oxidations. But an additional treatment of MnTMPS-PVP by an acid or a methylating agent regenerates the pyridinium units and reinforces the catalyst-polymer interactions by additional strong electrostatic interactions between peripheral sulfonato groups of the porphyrin ligand and pyridinium units of the cationized PVP. 90 %

of the initial run activity was found when MnTMPS-protonated PVP was recycled for the third time in the $KHSO_5$ oxidation of 1-(3,4-dimethoxyphenyl)-2-(2-methoxyphenoxyl)-propane-1,3-diol.[50] Such supported metalloporphyrins on poly(4-vinylpyridinium) polymers can also be used as catalysts in olefin epoxidation or alkane hydroxylation.[51] In addition, MnTMPS-protonated PVP was found to be a good biomimetic model of chloroperoxidase.[52]

3. 3. MANGANESE PEROXIDASE MODELS

The modeling of a non-specific peroxidase like ligninase is simple compared to the design of metalloporphyrin catalysts able to selectively oxidize manganese(II) salts, in the presence of chelating agents and of easily oxidized phenolic substrates. MnP has a manganese binding site, on the heme edge, able to control the selective oxidation of manganese(II) salts in the presence of phenols. How to reproduce the same selective oxidation with a synthetic metalloporphyrin without without having a selective binding to accomodate Mn(II) in the close vicinity of the catalytic site ? Modeling of MnP is more challenging than LiP modeling.

Dolphin reported in 1990 the role of manganese sulfate in the decolorization of a dye catalyzed by a sterically hindered sulfonated iron porphyrin in the presence of *m*-chloroperbenzoic acid.[55] The catalytic oxidation of Mn(II) chelates *i.e.* the key step performed by MnP, has been recently mimicked, using synthetic metalloporphyrins.[56] Oxidation of Mn(II)pyrophosphate to the corresponding Mn(III) chelate was performed with catalytic amounts (1-2 % based on Mn^{II}) of iron- or manganese sulfonated porphyrins. Sterically hindered iron complexes were the most active catalysts. We observed catalytic activities of 8 and 3 cycles/min for FeTDCPPS and FeTMPS, respectively.

A striking feature of these metalloporphyrin-catalyzed oxidations of manganese-pyrophosphate is the improvement of the catalytic activity by the presence of limited amounts of methoxylated benzene derivatives acting as co-substrates: 1,2-dimethoxybenzene, 3,4-dimethoxybenzyl alcohol (veratryl alcohol) or 1,2,4-trimethoxybenzene. The catalytic activity of FeTMPS is substantially increased by 2-5 % of one of these methoxylated benzenes.

Two possible explanations can be proposed for the improvement in the oxidations of Mn(II)pyrophosphate by these methoxylated aromatics: (i) an inhibition of the metalloporphyrin bleaching due to the presence of an easily oxidized substrate in the reaction mixture (80-90 % of the catalyst is still present after 10 min with 3 % of one of these di- or trimethoxylated benzene derivatives instead of 20 % of remaining catalyst in their absence) and, more important, (ii) a role of redox mediator for these methoxylated benzene derivatives, as reported in the oxidation of manganese salts by lignin peroxidase. The generation of the radical-cation form of veratrole, veratryl alcohol or 1,2,4-trimethoxybenzene by the high-valent oxo-metalloporphyrin complex might behave as a strong oxidant with respect to Mn(II)-pyrophosphate and contributing then to its oxidation. These results with a biomimetic model of manganese peroxidase is also an illustration of the key role of low molecular weight organic mediators in the oxidative degradation of lignin by fungus peroxidases.

3. 4. OXIDATION OF POLLUTANTS BY LIGNINASE MODELS

Sulfonated iron or manganese porphyrin catalysts in combination with $KHSO_5$ or H_2O_2, are highly efficient reagents for the oxidative dechlorination of 2,4,6-trichlorophenol to 2,6-dichlorobenzoquinone. Catalytic activities up to 20 cycles/sec have been observed.[53] In addition it should be noted that changing potassium monopersulfate for hydrogen

peroxide leads only to a small decrease in the catalytic activity. These biomimetic catalysts are also able to oxidize DDT. A classical peroxidase such as horseradish peroxidase is unable to catalyze the oxidation of such pollutant. By using various methoxylated aromatics it has been possible to establish a comparative scale for catalytic oxidations with HRP, LiP and FeTPPS.[53, 54] While HRP is unable to catalyze the oxidation of organic substrates having a $E_{1/2}$ potential value above 1.2 V (Ag/AgCl), LiP is active up to 1.4 V and the "FeTPPS/$KHSO_5$" system can oxidized recalcitrant molecules up to 1.7 V. These peroxidase models based on sulfonated metalloporphyrins are also efficient catalysts in pollutant oxidations when immobilized onto ion-exchange resins.

However, the main limitations of this catalytic system are the rather low activity when using hydrogen peroxide (a "clean oxidant", water being the only released by-product after oxidation) and the current absence of manufacturing of these biomimetic catalysts at the multi-hundred kilogramme scale. Since metal derivatives of phthalocyanines (Pc) are important industrial dye products, metallophthalocyanines are an attractive alternative as cheap and readily available oxidation catalysts.

The oxidative degradation of 2,4,6-trichlorophenol (TCP) is efficiently catalyzed by supported iron and manganese complexes of 2,9,16,23-tetrasulfophthalocyanine[57] (for structure of FePcS and MnPcS, see below).

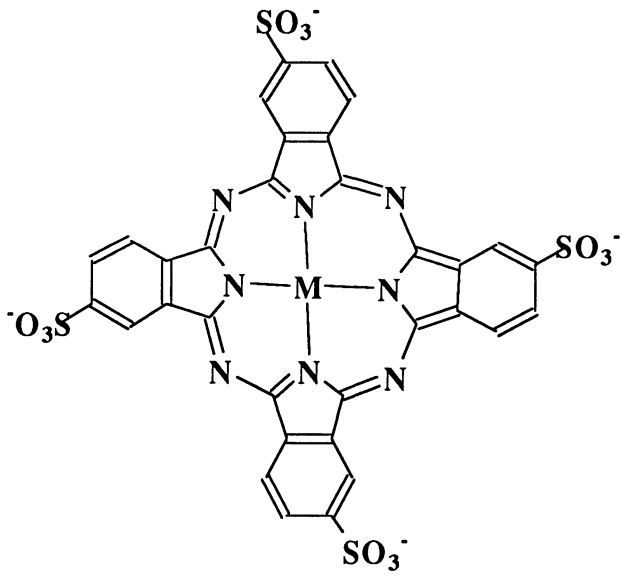

We assayed the catalytic activities of the soluble complexes FePcS and MnPcS in the oxidation of TCP by potassium monopersulfate or hydrogen peroxide (See Table 1).

In the $KHSO_5$ oxidation of TCP, at pH 7, both FePcS and MnPcS are highly efficient catalysts: full substrate conversion is observed within few minutes even with 0.1% of catalyst / TCP (runs 1 and 2 of Table 1). It should be noted that high turnover rates were obtained with $KHSO_5$, but it is also possible to use an environment-compatible oxidant such as H_2O_2 (runs 3 to 5). The initial oxidation product of TCP is the 2,6-dichloro-1,4-benzoquinone. But this quinone is only detected in the first 3 min of the catalytic reaction, as it then undergoes further catalytic transformations to more dechlorinated molecules. During the oxidative conversion of the polychlorinated phenol, the concomittant production of chloride anions was observed.

Highly attractive, in terms of possible industrial application, are the performances of these catalysts FePcS and MnPcS when they are fixed onto amberlite (FePcS-Amb and MnPcS-Amb, see Table 2 for data).

Table 1. Oxidation of 2,4,6-trichlorophenol by $KHSO_5$ and H_2O_2 mediated by iron and manganese phthalocyanine complexes, FePcS and MnPcS.

Run	Catalyst	% cat./sub.	pH	Oxidant	Conversion (%) 1 min.	5 min.
1	FePcS	0.1	7	$KHSO_5$	97	98
2	MnPcS	0.1	7	$KHSO_5$	100	-
3	FePcS	1	7	H_2O_2	6	38
4	FePcS	3.7	7	H_2O_2	68	100
5	MnPcS	1	8.5	H_2O_2	8	25

Table 2. Oxidation of 2,4,6-trichlorophenol by supported iron or manganese phthalocyanine catalysts onto amberlite.

Run	Catalyst	% cat./sub.	pH	Oxidant	Conversion (in %) 5 min	60 min
1	FePcS-Amb	1	2	$KHSO_5$	71	98
2	FePcS-Amb	1	7	$KHSO_5$	80	90
3	FePcS-Amb	1	7	H_2O_2	80	93
4	FePcS-Amb	3.7	7	H_2O_2	93	100
5	MnPcS-Amb	1	7	H_2O_2	45	63

As expected, supported metallophthalocyanine catalysts are slightly less efficient than the corresponding soluble catalysts in $KHSO_5$ oxidations. Full conversion of TCP mediated by FePcS-Amb is observed within 1 hour (runs 1, 2 of Table 2) as compared to 1 min for soluble FePcS. High catalytic activities are observed in H_2O_2 oxidations when these metallophthalocyanines are fixed onto amberlite. With the "clean oxidant" and 1% of FePcS-Amb catalyst, nearly full conversion of TCP is obtained in 1 h at pH 7 (run 3, Table 2).

Furthermore, the FePcS-Amb catalyst can be easily recycled by filtration and re-engaged in new H_2O_2 oxidations of TCP. The same conversion of TCP (95%) is observed in three successive TCP oxidations with FePcS-Amb as catalyst, confirming that this supported iron phthalocyanine complex is not degraded during the catalytic oxidation of the pollutant molecule. We are currently investigating the detailed mechanism of these catalytic oxidations by the FePcS-Amb-H_2O_2 system.

4. Conclusions

Iron and manganese complexes having a water-soluble sterically hindered porphyrin ligand in combination with potassium monopersulfate are efficient peroxidase models. Metalloporphyrin and metallophthalocyanine catalysts can be supported on regular ion-exchange resins. These catalysts are highly efficient catalysts for the oxidation of pollutants and

might have a future in the oxidation of micropollutants in water treatment.

5. Acknowledgments

One of the authors (B. M.) is indebted to Gilles Labat and Sabine Defrance whose work was cited in the reference list. Jean-Louis Séris (Elf-Aquitaine, Centre de Recherche de Lacq) is gratefully acknowledged for his constant participation and all fruitful discussions on peroxidase modeling and oxidation of pollutants over a period of seven years. Research work was supported by Elf-Aquitaine and CNRS. A. S. thanks EERO (European Environmental Research Organization) for 9-month postdoctoral fellowship.

6. References

(1) V.B. Huynh, H.M. Chang, T.W. Joyce, T.K. Kirk, *Tappi J.* **1985**, *68*, 98.
(2) H.M. Chang, T.W. Joyce, A.G. Campbell, E.D. Gerrard, V-B Huynh, T.K. Kirk, *Fungal decolorization of bleach plant effluents in recent advanes in lignin biodegradation research*, (T. Higuchi, H.M. Chang and T.K. Kirk, Eds.) UNI Publishing Tokyo, **1983**, p. 257.
(3) T.K. Kirk, T. Higuchi, H. M. Cheng (eds), *Lignin biodegradaion: microbiology, chemistry, and potential applications*, CRC Press, Vols 1-2, Boca Raton **1980**.
(4) W.A. Wood, S.T. Kellog (eds) *Methods in Enzymology*, Biomass, Part B, Lignin, Pectin, and Chitin , p. 3-328, Academic Press, New York, **1988**, 161.
(5) (a) M. Tien, T.K. Kirk, *Science* **1983**, *221*, 661. (b) J.K. Glenn, M.A. Morgan, M. B. Mayfield, M. Kuwahara, M.H. Gold, *Biochem. Biophys. Res. Commun.* **1983** *114*, 1077. (c) V. Renganathan, M.H. Gold, *Biochemistry* **1986**, *25*, 1626. (d) H. W.H. Schmidt, S.D. Haemmerli, H.E. Schoemaker, M.S.A. Leisola, *Biochemistry* **1989**, *28*, 1776.
(6) (a) Y. Mino, H. Wariishi, N.J. Blackburn, T.M. Loehr, M.H. Gold, *J. Biol. Chem.* **1988**, *263*, 7029. (b) M.D. Aitken, R.L. Irvine, *Arch. Biochem. Biophys.* **1990**, *276*, 405. (c) R.Z. Harris, H. Wariishi, M.H. Gold, P.R. Ortiz de Montellano, *J. Biol. Chem.* **1991**, *266*, 8751. (d) L. Banci, I. Bertini, A.E. Pease, M. Tien, P. Turano, *Biochemistry* **1992**, *31*, 10009.
(7) T.K. Kirk, R.L. Farrell, *Ann. Rev. Microbiol.* **1987**, *41*, 465.
(8) H. Janshekar, A. Fiechter, *Adv. in Biochemical Engineering/Biotechnology* **1983**, *27*, 119.
(9) K. Lundquist, T.K. Kirk, W. J. Connors, *Arch. Microbiol.* **1977**, *112*, 291.
(10) T.K. Kirk, E. Schultz, W.J. Connors, L.F. Lorentz, J.G. Zeikus, *Arch. Microbiol.* **1978**, *117*, 277.
(11) M. Tien, T.K. Kirk, *Methods in Enzymology* **1988**, *161*, 238.
(12) (a) G. Meunier, B. Meunier, *J. Am. Chem. Soc.* **1985**, *107*, 2558. (b) G. Meunier, B. Meunier, *J. Biol. Chem.* **1985**, *260*, 10576.
(13) (a) H. Wariishi, M.H. Gold, *FEBS Lett.* **1989**, *243*, 165. (b) Same authors, *J. Biol. Chem.* **1990**, *265*, 2070.
(14) P.J. Kersten, M. Tien, B. Kalyanaraman, T.K. Kirk, *J. Biol. Chem.* **1985**, *260*, 2609.
(15) H.E. Schoemaker, P.J. Harvey, R.M. Bowen, J.M. Palmer, *FEBS Lett.* **1985**, *183*, 7.
(16) A.L. Andersson, V. Renganathan, A.A. Chui, T.M. Loehr, M.H. Gold, *J. Biol. Chem.* **1985**, *260*, 6080.

(17) D. Kuila, M. Tien, J.A. Fee, M.R. Ondrias, *Biochemistry* **1985**, *24*, 3394.
(18) S.L. Edwards, R. Raag, H. Wariishi, M.H. Gold, T.L. Poulos, *Proc. Natl. Acad. Sci. USA* **1993**, *90*, 750.
(19) G.D. De Pillis, P.R. Ortiz de Montellano, *Biochemistry* **1989**, 28, 7947.
(20) (a) M. Tien, C.P.D. Tu, *Nature* **1987**, *326*, 520. (b) T.L. Smith, H. Schalch, J. Gaskell, S. Covert, D. Cullen, *Nucleic Acids Res.* **1988**, *16*, 1219.
(21) L.A. Andersson, V. Renganathan, T.M. Loehr, M.H. Gold, *Biochemistry* **1987**, *26*, 2258.
(22) M. Mylrajan, K. Valli, H. Wariishi, M.H. Gold, T.M. Loehr, *Biochemistry* **1990**, *29*, 9617.
(23) P.J. Harvey, H.E. Schoemaker, J.M. Palmer, *FEBS Lett.* **1986**, *195*, 242.
(24) S.D. Haemmerli, M.S.A. Leisola, D. Sanglard, A. Fiechter, *J. Biol. Chem.* **1986**, *261*, 6900.
(25) K. Miki, V. Renganathan, M.H. Gold, *Biochemistry* **1986**, *25*, 4790.
(26) K.E. Hammel, M. Tien, B. Kalyanaranam, T.K. Kirk, *J. Biol. Chem.* **1985**, *260*, 8348.
(27) T.K. Kirk, M. Tien, J.A. Fee, M.R. Ondias, *Biochem. J.* **1986**, *236*, 279.
(28) T. Higuchi, *Wood Res.* **1983**, *73*, 58.
(29) D. Pribnow, M.B. Mayfield, V.J. Nipper, J.A. Brown, M.H. Gold, *Biol. Chem.* **1989**, *264*, 5036.
(30) E.A. Pease, A. Andrawis, M. Tien, *J. Biol. Chem.* **1989**, *264*, 13531.
(31) K.V. Sarkanen, C.H. Ludwig (eds), *Lignins: Occurence, Formation, Structure and Reactions* , Wiley, New York **1971**.
(32) (a) H. Wariishi, K. Valli, M.H. Gold, *Biochemistry* **1989**, *28*, 6107. (b) U. Tuor, H. Wariishi, H.E. Schoemaker, M.H. Gold, *Biochemistry* **1992**, *31*, 4986.
(33) H. Wariishi, K. Valli, M.H. Gold, *Biochem. Biophys. Res. Commun.* **1991**, *176*, 269.
(34) (a) M. Alexander, *Science* **1981**, *211*, 132. (b) A.H. Neilson, *J. Appl. Bacteriol.* **1990**, *69*, 445. (c) R.A. Hites, *Acc. Chem. Res.* **1990**, *23*, 194.
(35) a) DDT and lindane are 1,1,1-trichloro-2,2-bis(*p*-chlorophenyl)ethane and 1a,2a,3b,4a,5a,6b-hexachlorocyclohexane, respectively.
(36) J.A. Bumpus, M. Tien, D. Wright, S.D. Aust, *Science* **1985**, *228*, 1434.
(37) K.E. Hammel, P.J. Tardone, *Biochemistry* **1988**, *27*, 6563.
(38) J.A. Bumpus, S.D. Aust, *BioEssays* **1987**, *6*, 166.
(39) T. Habe, M. Shimida, T. Okamoto, B. Panijpan, T. Higuchi, *J. Chem. Soc., Chem.Commun.* **1985**, 1323.
(40) A. Paszczynski, R.L. Crawford, R.A. Blanchette, *Appl. Environ. Microbiol.* **1988**, *54*, 62.
(41) T. Okamoto, K. Sasaki, S. Oka, *J. Am. Chem. Soc.* **1988**, *110*, 1187.
(42) D. Dolphin, T. Nakano, T.E. Maione, T.K. Kirk, R. Farrell, in *Lignin Enzymic and Microbiol. Degradation* (INRA Ed.) Paris, **1987**, *40*: 157 .*Chem. Abst.* **1988**, *109*, 69402u.
(43) B. Meunier, G. Labat, J.L. Seris, *French patent*, 88.09169 **1988**. *Chem. Abst.* **1990**, *113*, 152001r.
(44) G. Labat, B. Meunier, *New J. Chem.* **1989**, *13*, 801.
(45) G. Labat, B. Meunier, *J. Org. Chem.* **1989**, *54*, 5008.
(46) (a) B. Meunier,*Chem. Rev.* **1992**, *92*, 1411. (b) B. Meunier, E. Guilmet, M.E. De Carvalho, R. Poilblanc, *J. Am. Chem. Soc.* **1984**, *106*, 6668.
(47) P. Hoffmann, G. Labat, A. Robert, B. Meunier, *Tetrahedron Lett.* **1990**, *31*, 1991.
(48) F. Cui, D. Dolphin, *ACS Symp. Ser.* **1989**, *399*, 519.

(49) J.K. Glenn, M.H. Gold, *Appl. Environ. Microbiol.* **1983**, *45*, 1741.
(50) G. Labat, B. Meunier, *C. R. Acad. Sci. Paris, Part. II,* **1990**, *311*, 625.
(51) S. Campestrini, B. Meunier, *Inorg. Chem.* **1992**, *31*, 1999.
(52) G. Labat, B. Meunier, *J. Chem. Soc., Chem. Commun.* **1990**, 1414.
(53) G. Labat, J.L. Seris, B. Meunier, *Angew. Chem. Int. Ed. Engl.* **1990**, *29*, 1471.
(54) P.J. Kersten, B. Kalyanaraman, K.E. Hammel, B. Reinhammar, T.K. Kirk, *Biochem. J.* **1990**, *268*, 475.
(55) F. Cui, D. Dolphin, *Holzforschung* **1991**, *45*, 31.
(56) S. Defrance, J.L. Séris, B. Meunier, *New J. Chem.* **1992**, *16*, 1015.
(57) A.S. Sorokin, B. Meunier, manuscript in preparation.

NICKEL COORDINATION CHEMISTRY WITH OXOTHIOLATE LIGANDS AND ITS RELEVANCE TO HYDROGENASE ENZYMES

JUN-HONG CHOU, CONSTANTINOS VAROTSIS
and MERCOURI G. KANATZIDIS
Department of Chemistry, Michigan State University,
East Lansing MI 48824, USA

ABSTRACT. The coordination chemistry of several new nickel complexes with multidentate oxo/thiolate ligands, in relation with the active site problem of hydrogenase enzymes, is described. Structural, spectroscopic and electrochemical data are reported and discussed.

1. Introduction

The importance of nickel in biology has been increasingly realized in recent years because of the identification of nickel-sulfur active sites in numerous hydrogenase[1] enzymes and other metalloenzymes[2]. The detailed structures of the Ni centers in the hydrogenases are not well defined at the present time and may differ from enzyme to enzyme. Ni EXAFS studies on several hydrogenases[3-7] indicate the predominance of sulfur ligands (probably cysteinyl) in the first coordination sphere of nickel. The presence of additional nitrogen and/or oxygen donor ligands have also been detected[4]. The geometry of the Ni centers is believed be distorted octahedral, however five-coordinate sites or four-coordinate square planar structures could not be ruled out. Although the Ni coordination environment is not identical in all hydrogenases, in all cases, it is mononuclear and redox active.

An important property of the Ni centers in these enzymes is the stability of Ni^{3+} and the ability to shuttle between the 2+ and 3+ oxidation state. The redox potentials for the Ni^{3+}/Ni^{2+} couple of hydrogenases range from -0.390 to -0.640 V vs. SCE which is much lower compared to the more positive redox potentials for the redox couples of synthetic complexes[8] which are in the range of 0.5 to 0.150 V vs. SCE. The resting state of the enzyme appears to contain Ni^{3+}.

In order to understand the function and structure of Ni active sites in these enzymes, vigorous research activity is directed at the synthesis of appropriate model nickel-sulfur compounds. Ideally one desires pairs of model complexes that differ in nickel oxidation state while preserving the coordination sphere at the nickel site. However, nickel-thiolate complexes have the tendency to oligomerize[9], many of the nickel-thiolate exist as dimers[10], trimers[11] and higher polymers.[12] In the past two years many structurally related nickel complexes have been synthesized, but few possess redox potentials in the

D.P. Kessissoglou (ed.), Bioinorganic Chemistry, 333-348

biologically relevant region. The lowest potential, thus far, observed is that of [bis(norbornane-1,2-thiolate)Ni]$^{2-}$ [13] in which the Ni is coordinated with four sulfur atoms in a square planar geometry and $E_{1/2}$ = -0.76 V(in DMF) vs. SCE. Another series of nickel complexes with $E_{1/2}$ in the enzyme region, include [Ni(dapo)$_2$]$^{2-}$ [dapo=pyridine-2,6-bis(acetyloximate(2-)] and [Ni(emi)$_2$]$^{2-}$ [emi=N, N-ethylenebis(2-mercaptoisobutyramido)(2-)][14]. Several structurally interesting pentacoordinated nickel-thiolate complexes with nickel coordinated to three nitrogen and two sulfur atoms in trigonal bipyramidal geometry are also noteworthy.[15a] Recently, a number of interesting six-coordinate mononuclear complexes were reported.[16] The Ni(L-L)X where L-L=($H_2NC_2H_4SC_2H_4$)$_2$S, (H_2N-o-$C_6H_4SC_2H_4$)$_2$S and (-S-o-$C_2H_4SC_2H_4$)$_2$S and X=CH_3CN, Cl^-. These complexes possess either a "vacant" or labile coordination site, but they do not display reversible redox processes in solution. From these and other examples in the literature, it appears that one way to lower the Ni(III)/Ni(II) potentials is the incorporation of negative, and highly polarizable ligands such as thiolates in the coordination sphere of Ni.

Since the coordination of the Ni in the enzymes is not exclusively sulfidic, we are exploring mixed-donor oxothiolate ligands as coordination reagents to nickel. We decided to re-examine an old ligand, 2-mercaptophenol, and explore its coordination chemistry with nickel. This ligand is related to the well known class of 1,2-dithiolene ligands. Therefore, there are two important resonance forms that dominate the complexation chemistry and complicates the interpretation of the properties of the corresponding complexes. Particularly, the unequivocal assignment of metal oxidation states becomes ambiguous as two separate but equal possibilities exist, see Scheme I. Nevertheless, we reasoned that the presence of an oxygen donor and of an aromatic benzene ring may shift the balance toward one form, namely to the more desired (from the point of view of this work) species (iii) in Scheme I. This is based on the expectation that the more electronegative oxygen coupled with the need of the benzene ring to achieve aromaticity might stabilize species (iii) instead of (iv).

The synthesis, molecular structure, spectroscopic and electrochemical characterization of two nickel complexes with this ligand and the characterization of the Ni^{3+} state in this ligand environment. Electron paramagnetic resonance spectroscopy in combination with isotopic labeling, ^{61}Ni, was used to characterize the metal oxidation state.

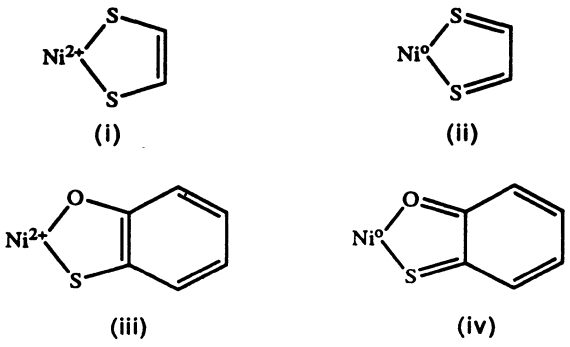

Scheme I

From a biological perspective one can argue that the 2-mercaptophenol as a ligand may not be entirely appropriate since sulfur ligands in proteins are either cysteines or methionines which contain -CH_2SH and -CH_2SCH_3 functionalities respectively. Therefore, we also choose a related but more biologically relevant oxothiolate, the ortho-hydroxy-benzylthiol (i.e. HO-o-C_6H_4-CH_2SH) as a ligand for investigation in Ni binding. This ligand is "innocent" since it has no resonance structures that could give rise to oxidation state ambiguities. We felt the similarity of this ligand to the all sulfur norbornane-1,2-thiolate[13] may give mononuclear nickel complexes with reversible redox processes.

2. Results and discussion

2.1 REACTIONS WITH THE 2-MERCAPTOPHENOLATE LIGAND

We began this work with the 2-mercaptophenolate ligand even though we were aware that it is not entirely biologically relevant. Our intention was to synthesize the monomeric complex shown in Scheme I, because it represents an example of a redox-active Ni center amidst anionic O- and S- environment.

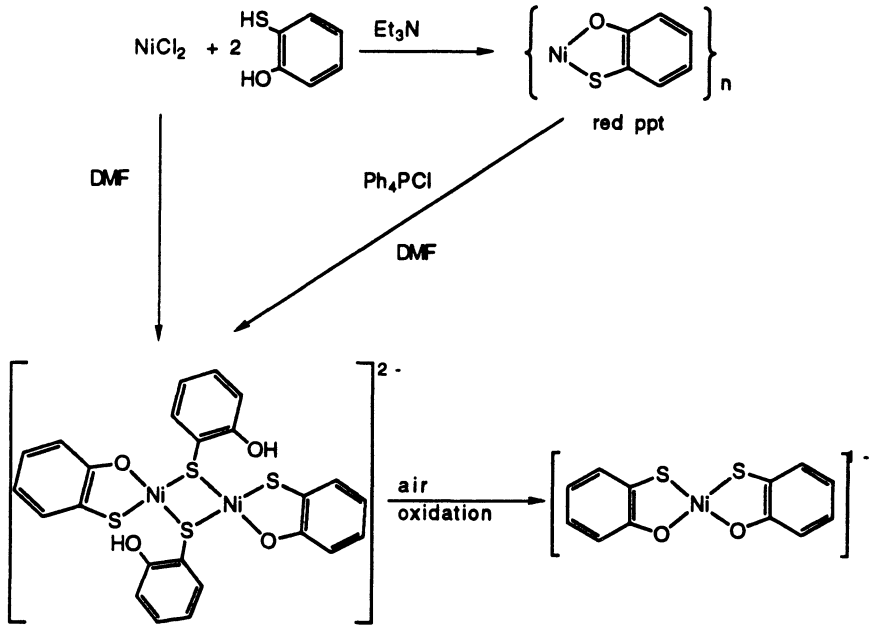

Scheme II

The complex was first reported by A. L. Balch[15b] et al as the Bu_4N^+ salt, without an X-ray structure determination, and was believed to be mononuclear, $[Ni\text{-}O_2S_2]^{2-}$, possessing a center of symmetry so that the sulfur atoms are disposed trans- to one another. Our interest centers in the exploration of the $Ni^{2+/3+}$ couple. However, the reaction of $NiCl_2$ with the mixture of 2-mercaptophenol and Ph_4PCl in CH_3CN with excess of Et_3N does not produce the desired complex. Instead, the latter turns out to be a very strong base, abstracting a proton back from Et_3NH^+ to form the dimeric diamagnetic compound $[Ni(C_6H_4SO)(C_6H_4SOH)]_2^{2-}$. (see Scheme II). During the preparation of this report, the Et_4N^+ salt of this complex was reported by a group from China.[17] The successful preparation of the target complex requires the complete absence of proton sources and absolute exclusion of air and water.

The $[Ni(C_6H_4SO)(C_6H_4SOH)]_2^{2-}$ is soluble in DMF but only slightly soluble in CH_3CN and MeOH. When exposed to air, the color of the solution changes within minutes from dark brown to dark green as monitored by UV-vis spectroscopy, see Figure 1. The presence of isosbestic points in the spectra suggests a clean conversion of the dimeric complex to the oxidized monomeric complex with no intermediates. The green, formally a Ni(III) complex, shows three new absorption peaks at 441(ε 4960) nm, 643(ε 5456) nm and a very intense peak at 1064(ε 29762) nm. The compound is very soluble in DMF, CH_3CN and CH_2Cl_2.

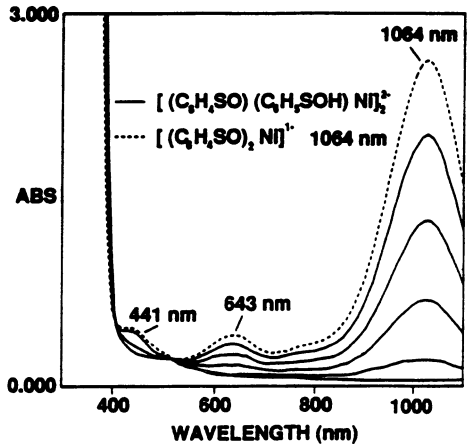

Figure 1. Electronic absorption spectra of $[(C_6H_4SO)(C_6H_4SOH)Ni]_2^{2-}$ (—) and $[(C_6H_4SO)_2Ni]^{1-}$ (--) in DMF solution; band maxima are indicated.

In addition to the air oxidation of $[Ni(C_6H_4SO)(C_6H_4SOH)]_2^{2-}$, the $[(C_6H_4SO)_2Ni]^-$ was readily synthesized as the Ph_4P^+ salt by the reaction of $NiCl_2$ with the mixture of $K_2(C_6H_4SO)$ and Ph_4PCl in methanol. The compound crystallized in triclinic space group P-1 (No. 2) with a = 9.998(3) Å, b = 10.230(3) Å, c = 16.134(4) Å, α = 92.07(2)°, β = 97.66(2)°, γ = 94.04(2)°, Z = 2. The complex was found to be disordered around a crystallographic inversion center and no accurate structural details could be obtained. An accurate structure for $[(C_6H_4SO)_2Ni]^-$ was obtained from the Bu_4N^+ salt. The crystallographic data for all compounds described here are given in Table 1.

Table 1. Crystallographic Data for $(Ph_4P)_2[(C_6H_4SO)(C_6H_4SOH)Ni]_2 \cdot 2DMF$ (1), $(Bu_4N)[(C_6H_4SO)_2Ni]$ (2), $(Ph_4P)K[(OC_6H_4CH_2S)_4Ni_3] \cdot CH_3OH$ (3), and $K_2[(OC_6H_4CH_2S)_2Ni] \cdot 5/2DMF$ (4)

	1	2	3	4
f. w.	1293.4	549.5	1138.2	1190.8
a, Å	14.421(2)	8.181(2)	12.038(5)	10.778(5)
b, Å	13.184(3)	22.069(8)	14.342(5)	25.01(1)
c, Å	20.710(4)	16.495(4)	16.063(4)	20.28(1)
α, deg.	90.00	90.00	82.41(4)	90.00
β, deg.	90.55(1)	97.59(2)	73.78(3)	93.36(2)
γ, deg.	90.00	90.00	66.69(2)	90.00
Z, V, Å^3	4, 3937(1)	4, 2952(2)	2, 2444(2)	4, 5458(4)
Space Group	$P2_1/n$ (No. 14)	$P2_1/n$ (No. 14)	P-1 (No. 2)	P21/n (No. 14)
D_{cal}, g/cm^3	1.091	1.236	1.548	1.450
μ(Cu Kα), cm^{-1}	20.99	8.177	14.78	11.91
$2\theta_{max.}$, deg.	120	45.8	45	40
No. of Data coll.	6495	4442	6890	5909
Data Used ($F_o^2 > 3\sigma(F_o^2)$)	3876	2042	4456	3534
No. of Variables	379	325	607	462
Final R/R_w, %	6.0/6.4	5.0/5.3	6.5/5.4	8.6/9.7

The structure of $[(C_6H_4SO)(C_6H_4SOH)Ni]_2^{2-}$ is shown in Figure 2 and selected bond distances and bond angles are given in Table 2. This complex is a dimer with a central Ni_2S_2 core and a crystallographically imposed center of symmetry. The geometry of each nickel is essentially square planar with nickel coordinated to three sulfur atoms and one oxygen atom. The mean Ni-S distance of 2.174 (4) Å is shorter than those found in the tetrahedral $[Ni(SPh)_4]^{2-}$ of 2.292 (5) Å[18] but comparable to those in $[Ni(ema)]^{2-}$ at 2.179 (1) Å[19]. In the latter complex, the Ni center also adopts a square planar geometry. The surprising feature in this complex is the protonation of one O atom which leaves a pendant OH group in the bridging 2-mercaptophenolate ligands. The distance between the hydrogen on O2 and O1 is 1.698Å indicates strong hydrogen-bonding. Similarly, the Ni-O distance of 1.857Å is also consistent with Ni-O distances in novel nickel complexes[20]. The long Ni-Ni distance of 3.26 Å precludes any metal-metal bonding. The Ni-S(2.160, 2.190Å), Ni-O(1.852Å) bond distances from the structure of the Et_4N^+ salt[17] are

essentially the same as in our structure, the difference being that the Et_4N^+ salt lacks a center of symmetry.

The structure of $[(C_6H_4SO)_2Ni]^-$ is shown in Figure 3. The surprising aspect of this structure is that it adopts the *cis-* conformation. Originally it was thought that the complex was in its *trans-* conformation. Here we parenthetically add that one may question the relative stability of the two different conformations. We tested whether the $[(C_6H_4SO)_2Ni]^-$ converted to its *trans-* isomer by prolonged boiling (two days) of an acetonitrile solution but found no evidence of such conversion. We conclude that the *cis-* geometry is the most stable form. It is unclear why this is so, but given the preference of Ni to form strong bonds with sulfur, it may be due to its desire to avoid using the same d-orbitals in forming two Ni-S bonds, thus resulting in stronger bonds than otherwise would be possible.

Comparative bond distances and angles with those of the dimer are also given in Table 2. The nickel is in a almost ideal square planar geometry with the angles S1-Ni-S2 = 91.0 (1)° and S1-Ni-O1 = 89.9 (2)°. The mean Ni-S distances in $[(C_6H_4SO)_2Ni]^-$ of 2.113 (6) Å is shorter than those found in $[(C_6H_4SO)(C_6H_5SO)Ni]_2^{2-}$ by 0.061 Å and the mean Ni-O distances is also shorter by 0.013 Å. The structural data reported here are not by themselves sufficient to distinguish the two possibilities shown in Scheme I.

Table 2. Selected Bond Distances (Å) and Bond Angles for $(Ph_4P)_2[(C_6H_4SO)(C_6H_4SOH)Ni]_2 \cdot 2DMF$(1) and $(Bu_4N)[(C_6H_4SO)_2Ni]$(2)

	(1)		(2)
Ni-S1	2.161(2)	Ni-S1	2.111(3)
Ni-S2	2.187(2)	Ni-S2	2.114(3)
Ni-O1	1.857(5)	Ni-O1	1.861(5)
S1-C25	1.751(7)	Ni-O2	1.829(4)
S2-C25	1.786(7)	S2-C23	1.733(8)
O1-C26	1.351(9)	O2-C24	1.317(9)
S2-Ni-O1	175.6(2)	S1-N1-O2	178.4(2)
S1-Ni-S2	96.34(8)	S2-Ni-O1	179.0(2)
S1-Ni-O1	89.6(2)	S1-Ni-S2	91 0(1)
Ni-S1-C25	97.0(3)	S1-Ni-O1	89.9(2)
Ni-S2-C31	108.5(2)	S2-Ni-O2	90.3(2)
Ni-O1-C26	118.7(4)	O1-Ni-O2	88.9(2)
S1-C25-C26	115.6(5)	Ni-S2-C23	97.0(3)
S1-C25-C30	125.5(6)	Ni-O2-C24	117.4(4)

Whether the hole is localized on Ni or delocalized on the ligand can be better addressed with EPR spectroscopy, in combination with isotopic labeling of the Ni center with ^{61}Ni. This can be achieved by determining the ^{61}Ni-hyperfine splitting magnitude on the observed signal. If the oxidation is centered on the ligand, little or not such hyperfine splitting may be observed, while localization primarily on the Ni center (i. e. Ni^{3+}) is expected to give rise to a large splitting.

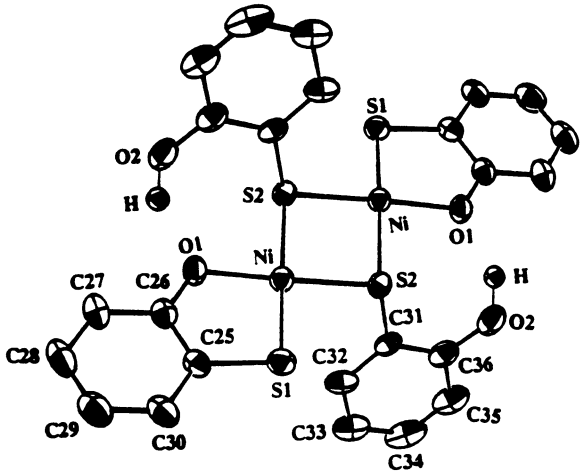

Figure 2. The structure of $[(C_6H_4SO)(C_6H_4SOH)Ni]_2^{2-}$ showing overall stereochemistry with 25% probability ellipsoids and atom numbering scheme. H atoms omitted.

One can evaluate the relative magnitude of the ^{61}Ni-hyperfine splitting by comparison with well known examples of Ni^{3+} complexes. The EPR spectra of $[(C_6H_4SO)_2Ni]^-$, in DMF solution, show an isotropic signal at room temperature with g value of 2.134, see Figure 4. However, at 77 K three g values of 2.188, 2.033, 2.014 which is consistent with Ni(III) in $[Ni(TAAB)]^{1+}$ and Ni-O-phenylene bisdimethylarsine[21-23].

We have also made the ^{61}Ni analog of $[(C_6H_4SO)Ni]^{1-}$ in methanol. The EPR spectra of the green methanol solution in the temperature range from 4.3K to 77K showed essentially the same spectra with insignificant hyperfine splitting. The values of <g> together with the anisotropy of the signals all suggest that it is a Ni^{3+} complex, yet the isotope experiment indicates that the single electron is significantly delocalized throughout the ligand. The EPR studies performed on the hydrogenases revealed much larger hyperfine pattern on substitution with ^{61}Ni indicating that it arises from a single Ni^{3+} ion in which there is significant localization of spin density.[24]

The magnetic susceptibility of $[(C_6H_4SO)_2Ni]^{1-}$ was measured as a function of temperature (5-300 K) under constant magnetic field (5000 G). The complex is paramagnetic obeying Curie-Weiss Law, as shown in Figure 5. The paramagnetism of the complex makes it difficult to obtain ^{13}C and ^{1}H NMR spectra. The calculated μ_{eff} of this

complex calculated from the slope of the linear $1/\chi_m$ vs. T dependence gives a value of 1.72 BM, consistent with a formal high spin d^7 configuration.

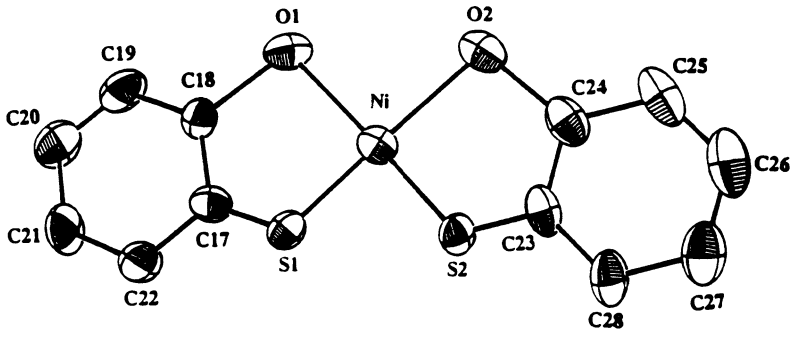

Figure 3. The structure of $[(C_6H_4SO)_2Ni]^{1-}$. H atoms omitted.

The reversible redox couple of $[(C_6H_4SO)_2Ni]^{1-}$ is revealed by the cyclic voltammogram in Figure 6. The complex shows a reversible one electron reduction process with the $E_{1/2}$ =-0.525V vs. SCE which is the second lowest $E_{1/2}$ ever observed in a well characterized Ni-S complex and falls in the biologically relevant range of -0.39 to -0.64 V. From the recent literature, we learn that all the model complexes synthesized with $E_{1/2}$ in the biological region possess a square planar metal center with Ni coordinated to different combinations of sulfur, oxygen, and nitrogen atoms except $[Ni(dapo)_2]^{1-}$ which has a octahedral geometry[5]. There does not seem to have any particular pattern emerging about the relationship between the $E_{1/2}$ and the geometry of the metal and thus more data are needed to be able to draw any significant conclusions.

2.2 RESONANCE RAMAN SPECTRA

Representative resonance Raman (RR) spectra of the monomeric Ni^{3+} complex are shown in Figure 7. The excitation wavelength 441.6 nm is near the maximum of the 444 nm absorption band. The RR spectra of the Ni^{3+} complex shows only three bands between 220 and 450 cm^{-1}. This may be due to the relatively high symmetry of the monomeric structure. The Ni^{3+} compound exhibits two bands at 412 cm^{-1} and 335 cm^{-1} which give isotopic shifts of more than 6 cm^{-1} by the ^{58}Ni-^{61}Ni substitution.

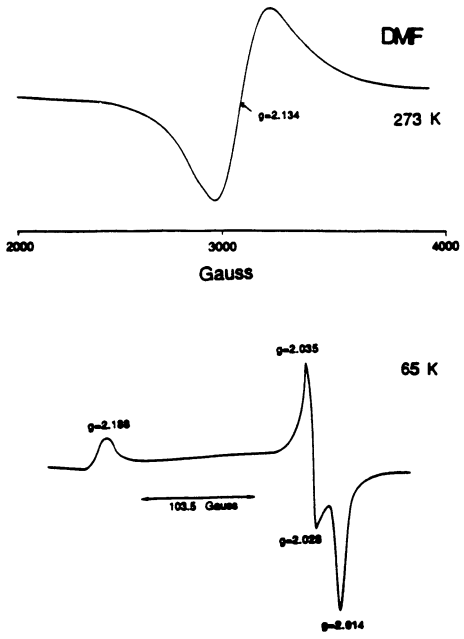

Figure 4. X-band EPR spectra of $[(C_6H_4SO)_2Ni]^{1-}$ at 273K and 77K in DMF solution, apparent g values are indicated.

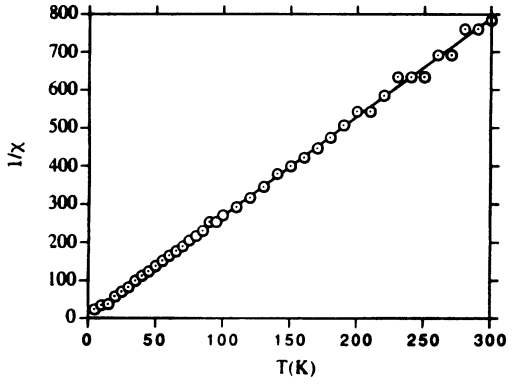

Figure 5. Magnetic susceptibility of $[(C_6H_4SO)_2Ni]^{1-}$. $1/\chi_m$ vs. Temperature. (χ_m in emu/mole)

The latter band is due to the Ni-S stretching mode since the same mode is assigned at 350 cm^{1-} in several $[Ni(S_2C_2O_2)_2(S_nX_4)_2]^{2-}$ complexes[25]. The 412 cm^{-1} band is assigned to a Ni-O stretching mode of the monomeric species. The observed Ni isotope shifts are in satisfactory agreement with those observed in other Ni containing acetylacetonato complexes. When 351.1 nm excitation was used, the RR spectrum (not shown) displays overtones of the Ni-O and Ni-S modes. A complete analysis of the 351.7 nm spectrum as well as that observed with 647.1 nm excitation will be presented elsewhere.

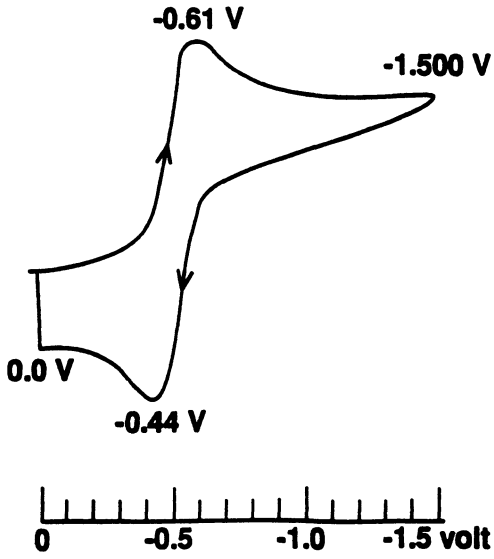

Figure 6. Cyclic voltammogram of $[(C_6H_4SO)_2Ni]^{2-/1-}$ at a Pt foil electrode in CH_3CN solution. Peak and half wave potentials vs. SCE are indicated.

Figure 8 shows room temperature RR spectra of $[(C_6H_4SO)(C_6H_4SOH)Ni]_2^{2-}$ obtained with 406.7 nm excitation, at the center of the blue absorption band. The Raman spectrum is characterized by three bands of moderate intensity at 397, 386 and 285 cm^{-1} and three weak bands at 438, 412 and 246 cm^{-1}. Assignments of infrared and Raman spectra of several Ni(II) metal complexes with sulfur and oxygen-containing ligands have been reported by several workers.[25] On the basis of this earlier work, the bands at 397 and 386 cm^{1} are assigned to the symmetric and asymmetric Ni-S stretching mode, respectively.The 285 cm^{-1} vibration in our spectra is assigned to a purer Ni-O stretching

mode than the 438 cm^{-1} band[25e] while the 246 cm^{-1} vibration is probably due to a ring deformation mode.

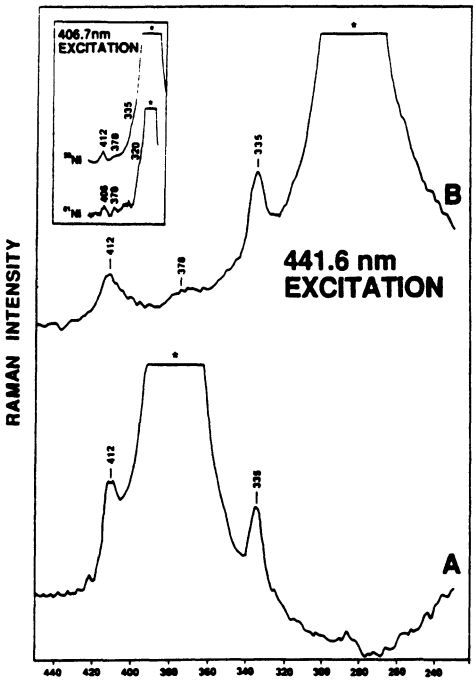

Figure 7. Resonance Raman spectra of $[(C_6H_4SO)_2Ni]^{1-}$ in (A) CH_3CN and (B) CH_2Cl_2 solution at room temperature. Insert : Raman spectra of $[(C_6H_4SO)_2Ni]^{1-}$ with ^{58}Ni and ^{61}Ni in CH_2Cl_2 at room temperature.

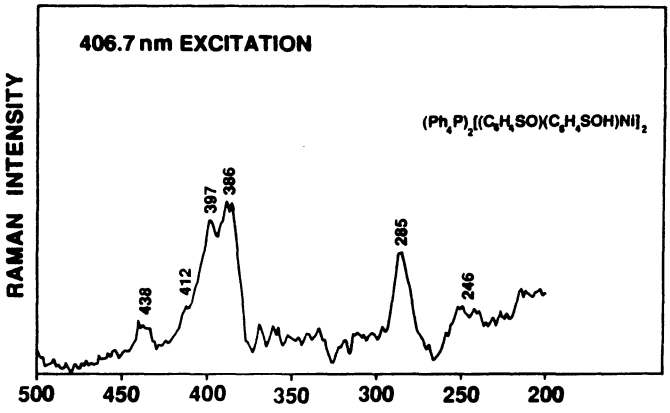

Figure 8 Room temperature RR spectra of $[(C_6H_4SO)(C_6H_4SOH)Ni]_2^{2-}$ in CH_3CN solution (excited at 406.7 nm). The spectrum of CH_3CN was subtracted from the spectra.

Attempts to make the $[(C_6H_4SO)_2Ni]^{2-}$ is currently underway, but the thiolato nickelates have a tendency to form high nuclearity aggregates. The oxo/thiolato ligands seem to be a good choice to achieving biologiacally relevant $E_{1/2}$ redox potentials for a $Ni^{2+/3+}$ couple, but since the unpaired electron in $[(C_6H_4SO)_2Ni]^{2-}$ is substantially delocalized onto the ligands through the conjugate system, the utility of this complex as proper model for Ni enzymes is limited. To avoid the delocalization and achieve a pure Ni^{3+} state other oxo/thiolato ligands are needed.

2.3 REACTIONS WITH THE 2-HYDROXY-BENZYLTHIOLATE LIGAND.

We employed the 2-hydroxy-benzylthiolate anion because it limit spin delocalization onto itself. The conjugated system is interrupted by the insertion of a CH_2 group between the aromatic ring and the sulfur atom. Based on the Ni^{2+}/ligand ratio, two nickel complexes can be isolated from this system, a very stable trinuclear species and a mononuclear species. The trinuclear complex has the formula $[Ni_3(O\text{-}o\text{-}C_6H_4\text{-}CH_2S)_4]^{2-}$ and it forms readily even when the ligand to metal ratio is 2:1. The crystal data for this material are summarized in Table 1, and its structure is shown in Figure 9.

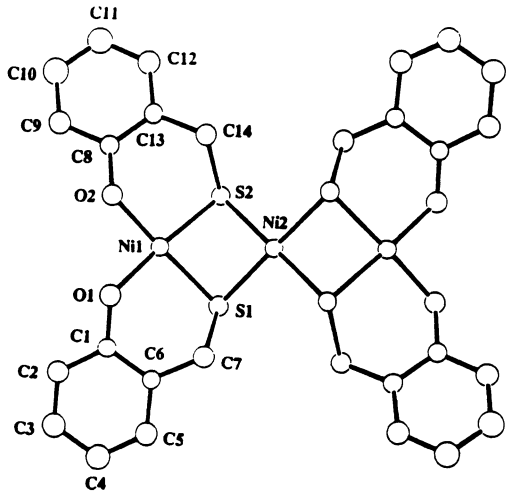

Figure 9. The structure of the $[Ni_3(O\text{-}o\text{-}C_6H_4\text{-}CH_2S)_4]^{2-}$ anion. This complex was isolated as a mixed K, Ph_4P^+ salt. The average Ni-S and Ni-O bond is 2.167 Å and 1.910 Å respectively.

Unfortunately, the cluster like character of this compound makes it unsuitable for consideration as a model for a biological Ni site. However, we were able to "break-up" the trimer by further addition of several more equivalents of ligand. From a ligand to metal ratio of 5:1 the blue air-sensitive $[Ni(O\text{-}o\text{-}C_6H_4\text{-}CH_2S)_2]^{2-}$ complex is formed which can

be isolated in crystalline form as the K^+ salt. In acetonitrile solution the complex absorbs at 538 and 643 nm, see Figure 11.

The structure of $[Ni(O\text{-}o\text{-}C_6H_4\text{-}CH_2S)_2]^{2-}$, shown in Figure 10, is quite interesting since this chelating ligand also adopts a *cis*-configuration around the square-planar nickel. Although it is possible that in both cases, the O-o-C_6H_4-S and the O-o-C_6H_4-CH_2S ligand, the corresponding complexes are kinetic products, this seems unlikely in view of the fact that they do not convert to the more aesthetically pleasing *trans*-isomer, either upon prolonged standing or heating. The average Ni-S and Ni-O bond distance in this complex is 2.156 Å and 1.935 Å respectively. Table 3 summarizes the most important distances and angles for these two complexes.

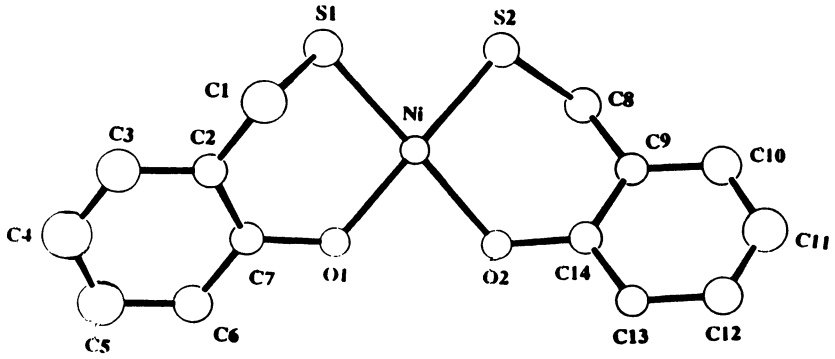

Figure 10. The structure of the $[Ni(O\text{-}o\text{-}C_6H_4\text{-}CH_2S)_2]^{2-}$ anion.

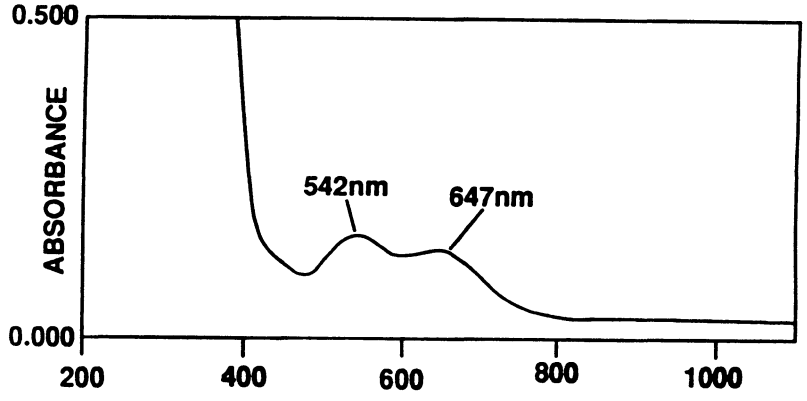

Figure 11. Optical absorption spectrum of $[Ni(O\text{-}o\text{-}C_6H_4\text{-}CH_2S)_2]^{2-}$ in DMF.

The *cis*- sulfur arrangement in $[Ni(O\text{-}o\text{-}C_6H_4\text{-}CH_2S)_2]^{2-}$ renders the molecule extremely basic, which is probably responsible for the strong trimerization tendency in these systems. Thus, the $[Ni_3(O\text{-}o\text{-}C_6H_4\text{-}CH_2S)_4]^{2-}$ anion can be viewed as the coordination complex of two $[Ni(O\text{-}o\text{-}C_6H_4\text{-}CH_2S)_2]^{2-}$ "ligands" and a nickel atom. This high basicity suggests that these sulfur sites would be strong proton acceptors, suggesting it is plausible that in hydrogenase the sulfur atoms in the immediate coordination sphere of nickel can act as proton storage sites or play an active role in helping cleave heterolytically the hydrogen molecule. If this contention is valid, it implies that the hydride generated by the heterolytic cleavage binds to the nickel atom.

The redox properties of the $[Ni(O\text{-}o\text{-}C_6H_4\text{-}CH_2S)_2]^{2-}$ complex were explored with cyclic voltammetry (in acetonitrile) but unfortunately no reversible redox potential was found. An irreversible oxidation wave at -0.24 V vs SCE is due to ligand oxidation. This lack of reversible oxidation is somewhat surprising in view of the very encouraging behavior (facile reversible oxidation) observed in the [bis(norbornane-1,2-thiolate)Ni]$^{2-}$ reported by Millar[13] et al which contains a similar ligand and a square planar Ni center.

Table 3. Selected Bond Distances (Å) and Bond Angles for $(Ph_4P)K[(OC_6H_4CH_2S)_4Ni_3]$. CH_3OH (**3**), and $K_2[(OC_6H_4CH_2S)_2Ni]$. 5/2DMF (**4**)

$(Ph_4P)K[(OC_6H_4CH_2S)_4Ni_3]$		$K_2[(OC_6H_4CH_2S)_2Ni]$. 5/2DMF	
Ni - S1	2.143(5)	Ni1 - S1	2.162(3)
Ni - S2	2.173(5)	Ni1 - S2	2.152(3)
Ni - O1	1.96(1)	Ni1 - O1	1.891(6)
Ni - O2	1.91(1)	Ni1 - O2	1.883(6)
S1 - C14	1.83(2)	Ni2 - S1	2.197(3)
S2 - C7	1.86(2)	Ni2 - S2	2.183(3)
S1 - Ni - S2	84.9(2)	S1 - Ni1 - S2	81.3(1)
S1 - Ni - O1	(6.7(3)	S1 - Ni1 - O1	96.1(2)
S1 - Ni - O2	175.8(3)	S1 - Ni1 - O2	176.7(2)
S2 - Ni - O1	175.8(3)	S2 - Ni1 - O1	176.1(2)
S2 - Ni - O2	96.2(4)	S2 - Ni1 - O2	97.0(2)
O1 - Ni - O2	82.6(4,	O1 - Ni1 - O2	85.6(3)
Ni - S1 - C14	91.1(6)	S1 - Ni2 - S1	180.00

There is recent spectroscopic evidence that the Ni center in hydrogenases in the inactive form is in an elongated octahedral environment, which essentially is very close to square planar. In the reduced state the Ni ion appears to be 5-coordinate.[26] Whether this is true or not, there are several factors that have to be satisfied in trying to model the hydrogenase site, some of them conflicting. For example, in any model compound the redox potentials for both redox couples must lie within 400 mV of one another. It is well known from the coordination chemistry of nickel that the ligand conditions that favor a $Ni^{2+/3+}$ couple are incompatible with the $Ni^{2+/1+}$ couple. One way that this may be achieved is if the redox process is accompanied by proton transfer reactions. For example, protonation may lower the reduction potential of the site significantly to allow for an additional electron to hop on

the nickel center. Protons may also be part of the activation process of hydrogen which is thought to be heterolytically cleaved. Although a fair amount of work has been carried out in trying to model the Ni centers in various enzymes, still a structural and functional model is not available. Future work must focus on redox active compounds with biologically relevant ligands. This presents an excellent opportunity but also a great challenge for the synthetic inorganic chemist.

3. Acknowledgment

Financial support from the National Institutes of Health for a BRSG grant is gratefully acknowledged. MGK is a Camille and Henry Dreyfus Foundation Fellow 1993-1995.

4. References

(1) Lancaster, J. in *Bioinorganic Chemistry of Nickel*, VCH, New York, **1988**, and ref. therein.

(2) (a) Christians, S. and Haltwasser, H. *Arch. Microbiol.* **1986**, *145*, 51. (b) Ragsdale, S. W.; Ljungdahl, L. G.; DerVartanian, D. V. *Biochem. Biophys. Rev. Commun.*, **1983**, *115*, 658. (c) Rasdale, S. W.; Wood, H. G.; Anthioline, W. E. Proc. *Natl. Acad. Sci.* U. S. A., **1985**, *82*, 6811.

(3) (a) Lindahl, P. A.; Kojima, N.; Hausinger, R. P.; Fox, J. A.; Teo, P. K.;Walsh, C. T.; Orme-Johnson, W. H. *J. Am. Chem. Soc.* **1984**, *106*, 3262. (b) Scott, R. A.; Wallin, S. A.; Czechowski, M.; DerVartanian, D. V.;LeGall, J.; Peck, H. D., Jr.; Moura, I. *J. Am. Chem. Soc.* **1984**, *106*, 6864. (c) Scott, R. A.; Czechowski, M.; DerVartanian, D. V.; LeGall, J.; Peck, H. D., Jr.; Moura, I. *Rev. Dort. Quim.* **1985**, *27*, 67. (d) Cramer, S. P.; Eidsness, M. K.; Pan, W. -H.; Morton, T. A.; Ragsdale, S. W.;DerVartanian, D. V.; Ljundgahl, L. G.; Scott, R. A. *Inorg. Chem.* **1987**, *26*, 2477.

(4) (a) Cammack, R.; Bagyinka, C.; Kovacs, K. *Eur. J. Biochem.* **1989**, 182, 357. (b) Tan, S. L.; Fox, J. A.; Kojima, N.; Walsh, C. T.; Orme-Johnson, W. H. *J. Am. Chem. Soc.* **1984**, *106*, 3064.

(5) Hausinger, R. P. *Mircobiol. Rev.* **1987**, *51*, 22.

(6) Maroney, M. J.; Colpas, G. J.; Bagyinka, C. *J. Am. Chem. Soc.* **1990**, *112*, 7076.

(7) Albracht. S. P. J.; Kruger, A.; van der Zwann, J. W.; Unden, G.; Bocher, R.; Mell, H.; Fontijn, R. D. *Biochim. Biophys. Acta.* **1986**, *874*, 116.

(8) (a) Nag. K.; Chakravorty, A. *Coord. Chem. Rev.* **1980**, 33, 87. (b) Hains, R. J.; Mcauley, *A. Coor. Chem. Rev.* **1981**, *39*, 77. (c) Lappin, A. G.; Mcauley, A. *Adv. Ing. Chem.* **1988**, *32*, 241.

(9) Tremel, W.; Kriege, M.; Krebs, B.; Henkel, G. *Inorg. Chem.* **1988**, *27*, 3886 and freferences therein.

(10) (a) Watson, A. D.; Rao, Ch. P.; Dorfman, J. R.; Holm, R. H. *Inorg. Chem.* **1985**, *24*, 2820. (b) Nicholson, J. R.; Christou, G.; Huffman, J. C.; Folting, K. *Polyhedron* **1987**, *6*, 863. (c) Synder, B. S.; Rao, Ch. P.; Holm, R. H.

Aust. J. Chem. **1986**, *39*, 963. (d) Barclay, G. A.; McPartlin, E. M.; Stephenson, N. C.; Moss, D. S. *Chem. Commun.* **1969**, 325. (f) Villa, A. C.; Manfredotti, A. G.; Nardell, M.; Delizzi, C. *Chem. Commun.* **1970**, 1322.

(11) (a) Tremel, W.; Kriege, M.; Kreb, B.; Henkel, G. *Inorg. Chem.* **1988**, *27*, 3886. (b) Tremel, W.; Kreb, B.; Henkel, G. Chem. Commun. **1986**, 1527. (c) White, G. S.; Stephen, D. W. *Organometallics* **1988**, *7*, 903.

(12) (a) Kriege, M.; Henkel, G. *Z. Naturforsch. B* **1987**, *42B*, 1121. (b) Woodward, P.; Dahl, L. F.; Abel, E. W.; Cross, B. C. *J. Am. Chem. Soc.* **1965**, *87*, 5251. (c) Dance, I. G.; Scudder, M. L.; Secomb. R. *Inorg. Chem.* **1985**, *24*, 1201. (d) Wark, T. A.; Stephan, D. W. *Organometallics* **1989**, *8*, 2836.

(13) Fox, S.; Wang, Y.; Sliver, A.; Millar, M. *J. Am. Chem. Soc.* **1990**, *112*, 3218.

(14) (a) Kruger H. -J.; Holm, R. H. *J. Am. Chem. Soc.* **1990**, *112*, 2955. (b) Kruger H. -J.; Gang Peng; Holm, R. H. *Inorg. Chem.* **1991**, *30*, 734.

(15) (a) Baidya, N.; Olmstead, M.; Mascharak, P. K. *Inorg. Chem.* **1991**, *30*, 929. (b) Balch, A. L.; Rohr-scheid, F.; Holm, R. H. *J. Am. Chem. Soc.* **1965**, *87*, 2301.

(16) Cha, M.; Gatlin, C. L.; Critchlow, S. C.; Kovacs, J. A. *Inorg. Chem.* **1993**, *32*, 5868

(17) Kang, B.; Weng, J.; Liu, H.; Wu, D.; Huang, L.; Lu, C.; Cai, J.; Chen, X.; Lu, J. *Inorg. Chem.* **1990**, *29*, 4873.

(18) Swenson, D.; Baenziger, N. C.; Coucouvanis, D. *J. Am. Chem. Soc.* **1978**, *100*, 1933.

(19) Kruger, H. -J.; Holm, R. H. *Inorg. Chem.* **1989**, *28*, 1148.

(20) Snyder, B. S.; Rao, Ch. P.; Holm. R. H. *Aust. J. Chem.* **1986**, *39*, 963.

(21) Tremel, W.; Kriege, M.; Krebs, B.; Henkel, G. *Inorg. Chem.* **1988**, *27*, 3886 and freferences therein.

(22) Yamamura, T.; Tadokoro, M.; Kuroda, R. *Chem. Lett.* **1989**, 1245.

(23) Yamamura, T.; Tarokoro, M.; Hamaguchi, M.; Kuroda, R. *Chem. Lett.* **1989**, 1481.

(24) Lancaster, J. R., Jr. FEBS *lett.* **1980**, *115*, 185.

(25) (a) Nakamoto, K.; Vdovich, C.; Takemoto, J. *J. Am. Chem. Soc.* **1970**, *92*, 3973. (b) Muller, A.; heinsen, H. H.; Vandrish, G. *Inorg. Chem.* **1974**, *13*, 1001. (c) Burke, J. M.; Fackler, J. P. *Inorg. Chem.* **1972**, *11*, 2744. (d) Cormier, A.; Nakamoto, K. *Spectrochimica Acta.* **1974**, *30A*, 1059. (e) Nakamura, Y.; Nakamoto, K. *Inorg. Chem.* **1975**, *14*, 63. (f) Coucounanis, D.; Benziger, N. C.; Johnson, S. M. *J. Am. Chem. Soc.* **1972**, *95*, 3875. (g) Müller A, Diemann, E.; Jostes, R.; Bögge, H. *Angew. Chem. Int. Ed. Eng.* **1981**, *20*, 934.

(26) Wang, C.-P.; Franco, R.; Moura, J. J.; Moura, I.; Day, E. P. *J. Biol. Chem.* **1992**, *267*, 7378

ARTIFICIAL BATTERIES WITH LANTHANIDE PORPHYRINS?

A. G. COUTSOLELOS
University of Crete, Department of Chemistry, Laboratory of Bioinorganic Coordination Chemistry University of Crete, P.O.Box 1470, 71409-Heraklion, Crete, Greece.

ABSTRACT: This work discusses the synthesis, physicochemical properties, and X-ray data of lanthanide porphyrins. Complexes of the type Ln(por)(acac), Ln(por)$_2$, Ln(H)(por)$_2$ and Ln$_2$(por)$_3$ have been synthesized with all lanthanide ions. Also complexes of type Ln(H)(por)(por)' or Ln(por)(por)' have been recently reported. These complexes are of interest as models for biological systems. The review attempts to show the fundamental importance of the lanthanide porphyrins, and it is focused on the following points: i) The original synthetic routes of lanthanide porphyrins. ii) The physicochemical properties of these complexes. These types of complexes are present in the nature in several bacteria, as the *Rhodopseudomonas virides.*

1. Introduction

Lanthanide and actinide porphyrin sandwich complexes of the type $[M^{III}(Por)_2]^-$, $M^{IV}(Por)_2$ and $M^{III}_2(Por)_3$ have provided an ideal series of molecules for studying the electronic structure and dynamics of interacting porphyrin macrocycles[1-27]. These double-[1-24] and triple-decker complexes[1-5,25-27] have been synthesized mainly with identical, symmetrical macrocycles, but complexes with dissimilar, asymmetrical macrocycles are also known and have been studied in large part for derivatives of Ce^{IV}, [19-21,28,29] Th^{IV} [22], Eu^{III} [14,30] or La^{III}.[24]

Many singly oxidized double-decker complexes exhibit a π - π interaction between the two macrocycles.[2,3,10-1 5.18.20,28] This most often occurs for the bis-(oep) derivatives and results in a formation of the porphyrin π-cation radical as compared to a single macrocyclic species. The oxidized double-decker porphyrins exhibit a near IR absorption band which does not appear in the neutral complex,[3, 6-8, 13,14,17,21,22] and may also have diagnostic infrared marker bands indicative of a porphyrin π-cation radical.[31-33] These bands generally appear between 1270 and 1295cm^{-1} for tetraphenyl porphyrins (tpp)[32,33] or between 1520 and 1570cm^{-1} for octaethylporhyrins (oep).[31,33] Similar bands have also been reported for singly oxidized $[M^{III}(tpp)_2]^+$ (M^{IV}=Th or U)[17] and $[M^{III}(oep)(tpp)]^+$ (M=Eu[14] or Ce[20]). The latter two cationic complexes have bands characteristic of an oep rather than a tpp π- cation radical, implying that localization of the hole is note on the oep than on the tpp macrocycle.[14,20] On the other hand, resonance Raman spectra of $[Ce^{IV}(oep)(tpp)]^+$ are consistent with the aspect that the electron have been abstracted from a mixed orbital involving both the oep and tpp macrocycles.[21] This point might be

D.P. Kessissoglou (ed.), Bioinorganic Chemistry, 349-357

resolved by a spectroscopic study of higher oxidized or reduced forms of double-decker complexes, but an analysis of this type has non yet appear in the literature.

2. Synthetic routes

Two different methods have been described in the literature for the metallation of porphyrin rings by lanthanide ions. The first one, developed for the metallation of the ytterbium ion into the meso-porphyrin IX for water-soluble lanthanide porphyrins[34,35], involved heating the free base and lanthanide acetylacetonate in molten imidazole. The second method for the preparation, specifically for the lanthanide bisporphyrinates entailed the reaction of free base and $Ln^{III}(acac)_3.xH_2O$ in boiling 1,2,4-trichlorobenzene.[4]

The most extensively discussed and employed method was the acetylacetonate method for the majority of the lanthanide ion, leading to the formation of bis-and tris-(porphyrinates). These complexes may serve as structural and spectroscopic models for the "special pair" of the bacteriochlorophyl *b* dimmer $[Mg(Bchl)]_2$ (representing the reaction center of bacterial Photosystem) as well as in artificial batteries.[36]

The total reaction scheme of the above method is presented in Figure 1. The double-deckers of the "lighter" lanthanide ions La to Gd, were synthesized as follows: $Ln^{III}(acac)_3.xH_2O$ and $(por)H_2$ were heated to reflux in Tcb. The reaction was monitored by UV-visible spectroscopy. The monoporphyrinate is formed first while the double-decker is formed via two pathways under prolonged heating. In the case of La^{III} and Pr^{III} the "life time" of the monoporphyrinate complex is very short and it is transformed quickly to the more stable $Ln^{III}(por)_2$. That is the reason why no data for these two monoporphyrinates are available. However our group has isolated traces of these monoporphyrinates representatives[37] which have been characterized by UV-visible spectroscopy, only when the reaction time of the metallation procedure is inferior to 30 minutes. The triple-decker complexes have been obtained only with octaethyl porphyrin[24] and this is because the low steric effect of the substitutent groups of this macrocycle. The symmetrical double-decker complexes of the "heavier" lanthanide ions, from Gd to Lu, have been synthesized by addition of the dilithium salt, $Li_2(por)$, to the $Ln^{III}(por)(acac)$.

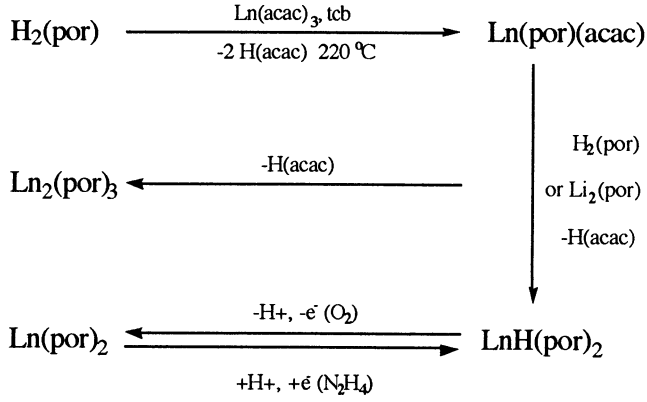

Figure 1. Formation of double- and triple-deckers.

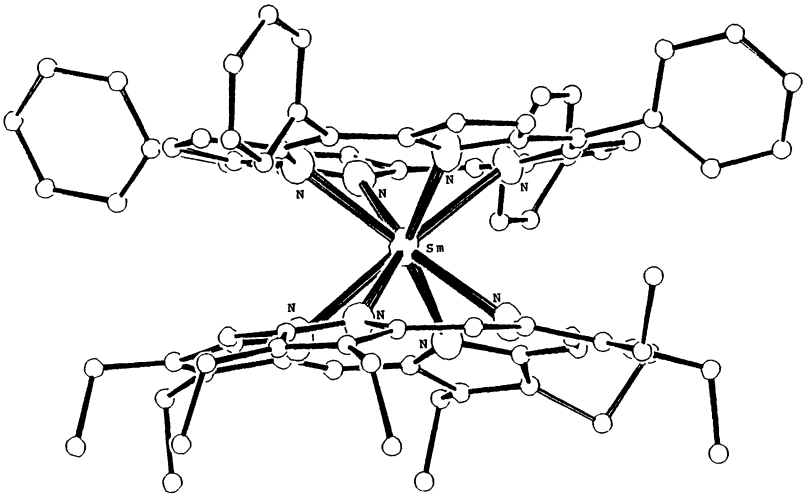

Figure 2. X-ray structure for Sm^{III} asymmetric double-decker.

An interesting new family of the so called double-decker complexes are the compounds of the type $Ln^{III}(por)(por)'$. Buchler and coworkers[20] have provided the synthesis and the X-ray characterization of the $Ce^{IV}(tpp)(oep)$ complex which has been isolated after the reaction of $(tpp)H_2$, and $(oep)H_2$ with the cerium acetylacetonate. This complex has been extracted from a mixture of two symmetrical double-decker and the free bases. Our group has proposed the synthesis of the asymmetrical double-decker $Sm^{III}(oep)(tpp)$ by an easier way; addition of $Li_2(oep)$ to the isolated $Sm^{III}(tpp)(acac)$.[38] We must notice at this point that the Cerium is at the oxidation state +4 while the Samarium at the oxidation state +3 (Figure 2). The corresponding Gadolinium one, $Gd^{III}(tpp)(oep)$, has been studied by X-ray diffraction at liquid Helium temperature. So it became possible to identify the presence of an hydrogen atom on one of the two porphyrin rings[39].

3. Discussion

3.1. MONOPORPHYRINATES: $Ln^{III}(por)(acac)$

As it has been mentioned above the complexes of type $Ln^{III}(por)(acac)$ are the first formed complexes after the metallation reaction. Their yield and their stability increase from lanthanum to Lutetium and this is probably due to the "lanthanide contraction".[40-43] The great interest of these complexes is the fact that can be used as precursors for the synthesis of asymmetrical double-deckers.[39]

In order to draw more attention to the problem concerning the metallation reactions of the lanthanide ions, we have studied[36] the metallation reaction of Cerium (III) ion, ion

from the so called "light lanthanides" with substituted tetraphenyl porphyrin ring (ortho-, meta-, and para- substituted).

Only the formation of double-decker compounds was observed except from the case of ortho-substituted where no metallation reaction was observed. In the above mentioned work no traces of monoporphyrin complexes were observed. From the existed data in literature it is obvious that generally the insertion of lanthanide ions to the porphyrin ring depend on the size, the electronic configuration of the metal ion, the porphyrin ring (donor, acceptor, steric effects) and the final oxidation state of the metal ion. No X-ray data are available for the moment for any $Ln^{III}(por)(acac)$ complex and this is probably due to their water-sensitivity and to the recrystallization solvent which always is present in the molecules of these compounds.

3.2. DOUBLE-DECKERS

The complexes $Ln^{III}(por)_2$ and $Ln^{III}(por)(por)'$ as it has been already mentioned are of particular interest because the two macrocycles are in a very close proximity and can be used as models to study the interaction of the two rings. This modeling is more focused on imitating the "special pair" than understanding the well known structure of the "active center" in photosynthetic bacteria. At this point it is useful to remind that the two bacteriochlorophyll chromophores in the photosynthetic bacteria of *Rhodopseudomonas virides* have as main feature a ~3.3Ä van der Waals distance between them.[44]

The only existed X-ray studies data of synthetic double-deckers with lanthanide ions concern the $(oep)_2Ce^{IV}$,[1] $Eu^{III}(oep)_2$[3], $Ce^{IV}(oep)(tpp)$[20] and $Sm^{III}(oep)(tpp)$ complexes. The corresponding $Gd^{III}(tpp)(oep)$ is under investigation.[39]

From Lanthanum to Lutetium the lanthanide ions posed an oxidation state +3 except from the Cerium which is at an oxidation state +4. The general formula $Ln^{III}(por)_2$ has been proposed for the total number of the above complexes except from Praseodymium in which the $Pr^{III}H(por)_2$ and $Pr^{III}(Por)_2$ forms has been observed[13]. The presence of the above mentioned hydrogen atom is still a problem to be solved by the various spectroscopic methods. Two formulas can be postulated concerning the charge distribution of the complexes with and without hydrogen atom (Figure 3).

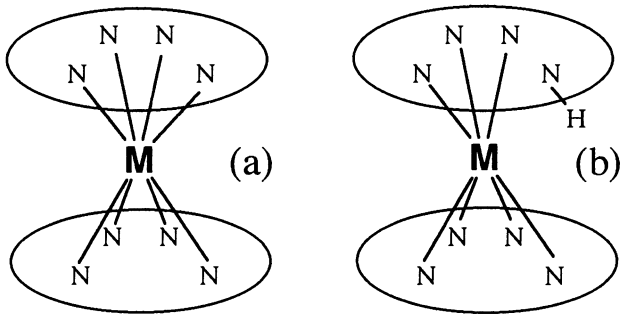

Figure 3. Charge distribution for $Ln^{III}(por)_2$: -2/+3/-1˙ (a) and $Ln^{III}H(por)_2$: -2/+3/-2 (b) [por/M/por].

The formula **a**, $Ln^{III}(Por)_2$ can be detected and distinguished from **b** essentially by e.s.r. and near-i.r spectroscopes. The difficulty was how and when we can assume the formula **a** or **b** as it depends from the synthetic route or the treatment of the complex with various

solvents. Of course there is not any ambiguity when a π- radical and/or a near-IR band can be detected; in this case the form **a** is the right one.

A more specific and detailed presentation, may be useful to understand the behavior of the double-decker complexes. In the neutral dimmer sandwiches which contain a Lu^{III} ion, a single hole resides in the porphyrin π-system.[15,16,21,27,45,46] Consequently, these complexes are electronically similar to π- cation radicals. Studies have shown that in all of the single-hole complexes (with the exception of the asymmetrical Ce^{IV}(oep)(tpp) sandwich), the hole is delocalized on the electronic time scale[15]. On the basis of this result, the molecular orbital (MO) diagram (Scheme 4) has been proposed, which qualitatively accounts for the electrochemical and spectroscopic properties of the double-decker sandwich complexes. As it can be observed at this MO diagram, removal of a second electron from the porphyrin π-system should lead to an enhanced π-π interaction in the ground state of the sandwich complexes. The case of Eu^{III} and Ce^{IV} has been investigated but in this work only that of Eu^{III} is presented as the oxidation state 3+ is common to all lanthanide double-decker complexes. The room-temperature absorption spectra of Eu^{III}(oep) and $Eu^{III}(oep)_2^+$ have been compared[46] to $Eu^{III}(TPnP)_2$ and $Eu^{III}(TPnP)_2^+$compounds. The positions of the Soret maxima of the oxidized sandwich complexes are blue-shifted relative to those of the neutral species. This behavior is typically observed upon oxidation of porphyrinic macrocycles[47]. Furthermore, the UV-Vis spectra of the cations show a set of bands which indicates that the equivalent of the one hole resides on each of the two rings of the sandwich. The most noteworthy result of the oxidation, is the extremely large blue shift of the near-IR absorption feature (e.g. 1228 $\rightarrow$861 nm for oep). This oxidation-induced shift to higher energy is consistent with an enhanced π-π interaction in the two-hole complexes relative to that present in the one-hole species.

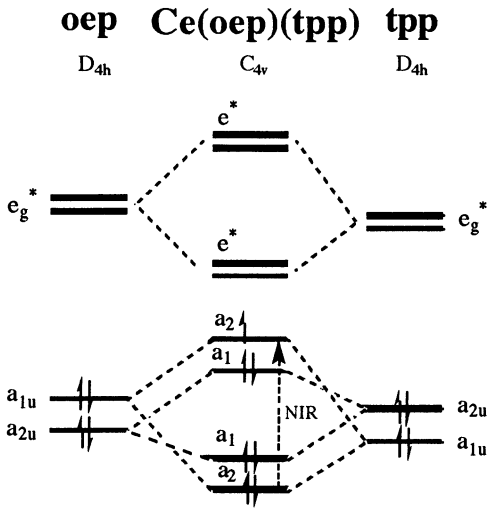

Figure 4. Molecular orbital (MO) diagram for Ce^{IV}(oep)(tpp).

The general features observed in the UV-Vis and RR spectra for these two-hole complexes, are consistent with the second hole residing on the same MO on which the hole resides on the single hole complexes [e.g.: a_{1u}-derived for $Eu^{III}(oep)_2$; a_{2u}-derived for $Eu^{III}(tpp)_2$]. E.s.r. spectra of the two-hole complexes also suggest that no unpaired electron resides on the porphyrin π-π system at room or low temperature, according also to the same authors.

Studies from our laboratory, have shown that for the symmetric or asymmetric double decker the following equilibrium is possible in solution:

$$\mathbf{LnH(por)_2} \underset{}{\overset{-H^+/O_2}{\rightleftharpoons}} \mathbf{Ln(por)_2}$$

or

$$\mathbf{LnH(por)(por)'} \overset{-H^+/O_2}{\rightleftharpoons} \mathbf{LnH(por)(por)'}$$

For the complex $Sm^{III}H(oep)(tpp)$, in CH_2Cl_2 solution the UV-Visible spectrum exhibits intermediates features of the two symmetrical double-deckers [$Sm^{III}(oep)_2$ and $Sm^{III}(tpp)_2$] with the Soret band at 400nm (Figure 5). This band is blue-shifted (9nm) compared to the $Sm^{III}(tpp)_2$ and red-shifted (21 nm) compared to $Sm^{III}(oep)_2$. In the same figure 5 we observe in details the differences of this double-decker, $Sm^{III}H(oep)(tpp)$ in CH_2Cl_2 and DMF solutions respectively. The changes at the spectra may be attributed to an equilibrium between the protonated and deprotonated form of the complex. The protonation process is solvent-dependent; in CH_2Cl_2 the protonated form is present, while in DMF the deprotonated form becomes dominant. In contrast no near-IR band at the region 1200-1600nm has been observed for both solutions. $Sm^{III}H(oep)(tpp)$ complex is e.s.r. active at the solid state and as CH_2Cl_2 solution but inactive in DMF solution. At this point we must stress the following: The UV-Visible spectra in DMF is identical to the corresponding $Ln^{III}(por)_2^-$ X^+ and $Ac^{IV}(por)_2$.This might drive us to postulate the formulas $[Sm^{III}(oep)(tpp)]^-$ or $Sm^{IV}(oep)(tpp)$ in DMF. The first one could also be supported by the UV-visible data of the whole series of the $Ln^{III}(oep)(tpp)$ complexes in DMF. In the region 600-650nm we observe a band for La and Lu compounds. This band has been supposed as a charge transfer originated. (La and Lu has zero electronic configuration or 14 electrons). The band is split in two of progression from Praseodymium to Ytterbium. In respect to the proposed molecular orbital (MO) diagram it might means that going from Pr to Yb we can distinguish better a metal to ligand (porphyrin) charge transfer which leads to a formal oxidation state +4.

This result should be examined better with more experimental and theoretical work. Also the presence of an hydrogen atom must be studied by a complete study of the $La^{III}H(por)_2$, $Lu^{III}H(por)_2$ in CH_2Cl_2 and DMF and the corresponding asymmetric one's in CH_2Cl_2 and DMF.

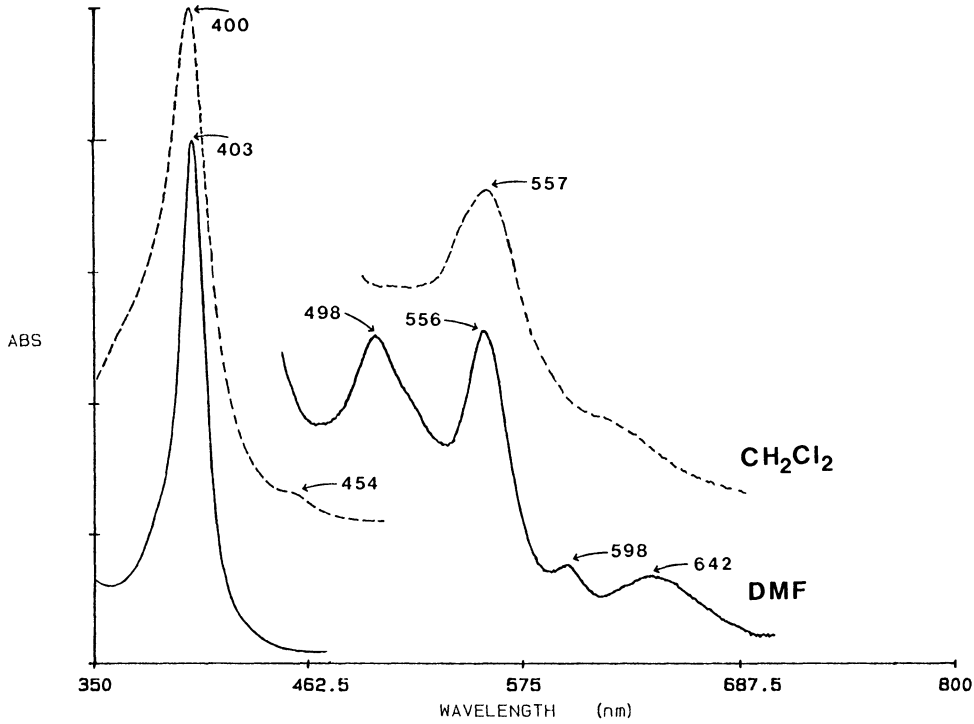

Figure 5. UV-Visible spectra of Sm(oep)(tpp) in CH_2Cl_2 and DMF.

4. Abbreviations

Por=unspecified porphyrinate(2^-)
tpp=meso-5,10,15,20-tetraphenyl porphyrinate (2^-)
(oep)H_2 = 2,3,7,8,12,13,17,18 octaethylporphyrin
Ln^{III}(por)acac=the general formula of lanthanide porphyrinate acatylacetonato
DMF= N,N-dimethyl formamide; 1,2,4-Tcb, 1,2,4-trichlorobenzene

5. References

(1) Buchler, J. W.; De Cian, A.; Fischer, J.; Kihn-Botulinski, M.; Paulus, H.; Weiss, R. *J. Am. Chem. Soc.* **1986**, *108*, 3652.
(2) Buchler, J. W.; Scharbert, B. *J. Am. Chem. Soc.* **1988**, *110*, 4272.

(3) Buchler, J.W.; De Cian, A.; Fischer, J.; Kihn-Botulinski, M.; Weiss, R. *Inorg. Chem.* **1988**, *27*, 339.
(4) Buchler, J. W.; Kapellmann, H.G.; Knoff, M.; Lay, K.-L.; Pfeifer, S. *Z. Naturforsch.* **1983**, *38b*, 1339.
(5) Buchler, J. W.; Elsässer, K.; Kihn-Botulinski, M.; Scharbert, B. *Angew. Chem. Int. Ed. Engl.* **1986**, *25*, 286.
(6) Duchowski, J. K.; Bocian, D. F. *J. Am. Chem. Soc.* **1990**, *112*, 3312.
(7) Yau, X.; Holten, D. *J. Phys. Chem.* **1988**, *92*, 409.
(8) Bilsel, O.; Rodriguez, J.; Holten, D.; Girolami, G. S.; Milam, S. N.; Suslick, K. S. *J. Am. Chem. Soc.*, **1990**, *112*, 4075.
(9) Girolami, G. S.; Milam, S. N.; Suslick, K. S. *Inorg. Chem.* **1987**, *26*, 343.
(10) Buchler, J. W.; Hammeschmitt, P.; Kaufeld, I.; Löffler, J. *Chem. Ber.* **1991**, *124*, 2151.
(11) Buchler, J. W.; De Cian, A.; Fischer, J.; Hammerschmitt, P.; Weiss R. *Chem. Ber.* **1991**, *124*, 1051.
(12) Buchler, J. W.; Hüttermann, J.; Löffler, J. *Bull. Chem. Soc. Jpn.* **1988**, *61*, 71.
(13) Buchler, J. W.; Kihn-Botulinski, M.; Scharbert, B. *Z. Naturforsch.* **1988**, *43b*, 1371.
(14) Buchler, J. W.; Löffler, J. *Z. Naturforsch.* **1990**, *45b*, 531-542.
(15) Donohoe, R. J.; Duchowski, J. K.; Bocian, D. F. *J. Am. Chem. Soc.* **1988**, *110*, 6119-6124.
(16) Perng, J.-H.; Duchowski, J. K.; Bocian, D. F. *J. Phys. Chem.* **1990**, *94*, 6684-6691.
(17) Girolami, G. S.; Milam, S. N.; Suslick, K. S. *J. Am. Chem. Soc.* **1988**, *110*, 2011-2012.
(18) Kim, K.; Lee, W. S.; Kim, H. J.; Cho, S. H.; Girolami, G. S.; Gorlin, P. A.; Suslick, K. S. *Inorg. Chem.* **1991**, *30*, 2652-2656.
(19) Bilsel, O.; Rodriguez, J.; Holten, D. *J. Phys. Chem.* **1990**, *94*, 3508-3512.
(20) Buchler, J. W.; De Cian, A.; Fischer, J.; Hammerschmitt, P.; Löffler, J.; Scharbert, B.; Weiss, R. *Chem. Ber.* **1989**, *122*, 2219-2228.
(21) Duchowski, J. K.; Bocian, D. F. *Inorg. Chem.* **1990**, *29*, 4158-4160.
(22) Bilsel, O.; Rodriguez, J.; Milam, S. N.; Gorlin, P. A.; Girolami, G. S.; Suslick, K. S.; Holten, D. *J. Am. Chem. Soc.* **1992**, *114*, 6528-6538.
(23) Radzki, S.; Mack, J.; Stillman, M. J. *New J. Chem.* **1992**, *16*, 583-589.
(24) Buchler, J. W.; Kihn-Botulinski, M.; Löffler, J.; Scharbert, B. *New J. Chem.* **1992**, *16*, 545-553.
(25) Buchler, J. W.; Löffler, J.; Wicholas, M. *Inorg. Chem.* **1992**, *31*, 524-526.
(26) Buchler, J. W.; Kihn-Botulinski, M.; Löffler, J.; Wicholas, M. *Inorg. Chem.* **1989**, 28, 3770-3772.
(27) Duchowski, J. K.; Bocian, D. F. *J. Am. Chem. Soc.* **1990**, *112*, 8807-8811.
(28) Lachkar, M.; De Cian, A.; Fischer, J.; Weiss, R. *New J. Chem.* **1988**, *12*, 729-731.
(29) Chabach, D.; Lachkar, M.; De Cian, A.; Fischer, J.; Weiss, R. *New J. Chem.* **1992**, *16*, 431-433.
(30) Moussavi, M.; De Cian, A.; Fischer, J.; Weiss, R. *Inorg. Chem.* **1986**, *25*, 2107-2108.
(31) Kadish, K. M.; Mu, X.H. *Pur. Appl. Chem.* **1990**, *62*, 1051.
(32) Scholz, W. F.; Reed, C. A.; Lee, Y. J.; Scheidt, W. R.; Lang, G. *J. Am. Chem. Soc.* **1992**, *104*, 6791-6793.

(33) Shimomura, E. T.; Phillipi, M. A.; Goff, H. M.; *J. Am. Chem. Soc.* **1982**, *104*, 6791-6793.
(34) Adler, A. D.; Longo, F. R.; Finarelli, J. D.; Goldmacher, J.; Assour, J.; Korsakoff, *Org. Chem.* **1987**, *32*, 476.
(35) Horrocks, Jr, W. Dew.; Hove, E. G. *J. Am. Chem. Soc.* **1978**, *100*, 4386.
(36) Davoras, E.; Spyroulias, G. A.; Mikros, E.; Coutsolelos, A. G. *Inorg. Chem.* **1994**, *33*, 3430 and references therein.
(37) Coutsolelos, A.G. unpublished results.
(38) Coutsolelos, A. G.; Spyroulias, G. A.; Raptopoulou, C.; Terzis, A. submitted for publication.
(39) Coutsolelos, A. G.; Spyroulias, G. A.; Raptopoulou, C.; Terzis, A. in preparation.
(40) A.G.Coutsolelos and G.A. Spyroulias, Polyhedron, 1994, *13*, 647.
(41) Wong, C.P.; Wenteicher, R.F.; Horrocks ,W.Dew *J. Am. Chem. Soc.* **1974**, *96*, 7149.
(42) Wong, C. P. in Inorganic Synthesis (Edited by S.L. Holt Jr), Wiley, New York **1983**, Vol.22 p. 156
(43) T.S. Srivastava, *Bioinorg. Chem.* **1978**, *8*, 61.
(44) Norris, J. R.; Schiffer, M. *Chem & Eng. News*, **1990**, July 30. 22-37.
(45) Duchowski, J. K.; Bocian, D. F. *J. Am. Chem. Soc.* **1990**, *112*, 3312.
(46) Perng, J.-H.; Duchowski, J. K.; Bocian, D. F. *J. Phys. Chem.* **1991**, *95*, 1319.
(47) Felton, R.M. In the porphyrins; Dolphin, D., Ed.; Academic Press: New York, **1978**, Vol.V, pp53-125.

NOVEL TRANSITION METAL HETEROPOLYMETALATES AND DERIVATIVES: STRUCTURAL CHEMISTRY, BIOLOGICAL AND CATALYTIC RELEVANCE

BERNT KREBS
Institute of Inorganic Chemistry
University of Mónster
Wilhelm-Klemm-Strasse 8
D-48149 Mónster, Germany

ABSTRACT. An account is given on some new developments in the field of polynuclear iso- and heteropolymolybdates and -tungstates. This class of compounds attracts special attention because of their extremely variable range of applications reaching from the well-known analytical ones to important industrial oxidation catalysts, and, most importantly in the present context of biological applications, extending to possible significance in the fields of antitumor reagents and of anti-HIV and anti-retroviral agents. Starting with the synthesis and structural properties of some typical novel examples of polynuclear heteropolymolybdates and -tungstates, a brief review is given on some most recent results in the latter field of biomedical and pre-clinical research in the field of their biological action.

1. Introduction

The chemistry of polynuclear oxometalate anions is dominated by molybdenum, tungsten, and vanadium in their highest oxidation states or in certain reduced states[1-5]. Since the discovery of the first members of this class in the mid-19th century the field has evolved to produce one of the chemically and structurally most variable classes of inorganic compounds. As is well known, the most spectacular development is observed, besides the large class of isopolyanions, $[M_mO_y]^{p-}$, for the even more variable heteropolymetalates, $[X_xM_mO_y]^{q-}$, with X representing one of 68 elements from all parts of the periodic table except the noble gases. Recent experimental research shows the wide variety of discrete oxoanions with different degrees of complexity. They range in the series of isopolymetalates from mononuclear to highly aggregated species such as $[Mo_{36}O_{112}(H_2O)_{16}]^{8-}$ [6,7] and to even higher nuclearities for the heteropolymetalates[1-4].

During the past two decades transition metal polyoxoanions have attracted much attention because of their extremely variable applications which are by far not yet evaluated by experimental research. They range from their well-known role as reagents in analytical applications to the wide field of homogeneous and especially heterogeneous industrial catalysis and, more recently, to biological and clinical applications. Functionalized derivatives using organometallic and other groups attached to the oxide surface of the polyoxometalates are prepared for the investigation of catalytic properties, and systematic investigations were started to probe the cytostatic properties for cancer therapy, or their possible application in the treatment of AIDS.

Besides a review on some recent interesting development of the chemistry and structural chemistry of oxomolybdates and -tungstates and derivatives as well as on the application

D.P. Kessissoglou (ed.), Bioinorganic Chemistry, 359-370

of modern investigational methods in their characterization[5], attention will be focussed on these possible applications of iso- and especially heteropolymolybdates in the field of their relevance for biological systems and life processes. Especially, the attention of the community of bioinorganic chemists should be more directed to this field, and it should take benefit of this vast area of potential original research. A few examples of recent biological applications will be briefly reviewed.

2. Novel Heteropolymolybdates and -Heteropolytungstates

2.1. ORGANOSUBSTITUTED POLYOXOMETALATES

2.1.1. *(n-$Bu_4N)_2[(Ph_2Sn)_2(\mu$-OH)$_2(\mu$-$MoO_4)_2]\cdot 4CH_2Cl_2$* (**1**). For the preparation of **1** Ph_2SnCl_2, (n-$Bu_4N)_2[Mo_2O_7]$ and (n-Bu_4N)OH are reacted in acetonitrile[8].

The anion of **1** contains two MoO_4 tetrahedra bonded to two octahedrally coordinated tin atoms (Fig. 1). In detail the structure is composed of a four-membered [Sn-O(H)-Sn-O(H)] ring which is capped on both sides by a tetrahedral MoO_4 unit. In addition to two bonds to bridging molybdate ligands and two bonds to bridging OH groups, each tin atom has two Sn-C bonds to phenyl rings to complete a distorted octahedral cis-Ph_2SnO_4 coordination. The two coordinated hydroxyl groups are also in *cis* configuration to each other. The structural motif [Sn-O(H)-Sn-O(H)] has been observed previously for hexacoordinated tin, but apparently the only four-membered [Sn-O(H)-Sn-O(H)] ring reported yet is in the compound [n-BuSn-(OH)($O_2P(C_6H_{11})_2)_2]_2$ [9]. $[(Ph_2Sn)_2(\mu$-OH$)_2(\mu$-$MoO_4)_2]^{2-}$ is the first known molecular diorganotin molybdate. A similar anion of this type, $[(Ph_2Sb)_2(\mu$-O$)_2(\mu$-$MoO_4)_2]^{2-}$, has been characterized in 1989[10]. The only structurally known diorganotin molybdate , $[Me_2SnMoO_4]$, is three-dimensionally polymeric and is composed of corner-sharing MoO_4 tetrahedra and trans-Me_2SnO_4 octahedra[11].

2.1.2. *(n-$Bu_4N)_2[PhSeMo_4O_{14}(OH)]$* (**2**). **2** can be obtained by reacting $Na_2MoO_4\cdot 2H_2O$ with $PhSeO_2H$ in hot water and addition of (n-Bu_4N)Cl [12]. The structure of the anion (Fig. 2) contains four distorted MoO_6 octahedra connected by common edges and faces to form a four-membered ring. On one side the ring is

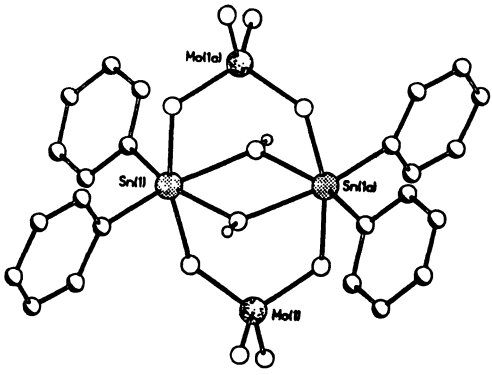

Figure 1. Structure of $[(Ph_2Sn)_2(\text{l-OH})_2(\text{l-}MoO_4)_2]^{2-}$ in **1**

capped by one OH group as a common corner of all octahedra. On the opposite side a w-tetrahedral $PhSeO_2$ group is bonded, the lone pair of Se(IV) completes the tetrahedron. The anion can be regarded to be a fragment of the NiAs structure, since the oxygen atoms show approximately hexagonal packing.

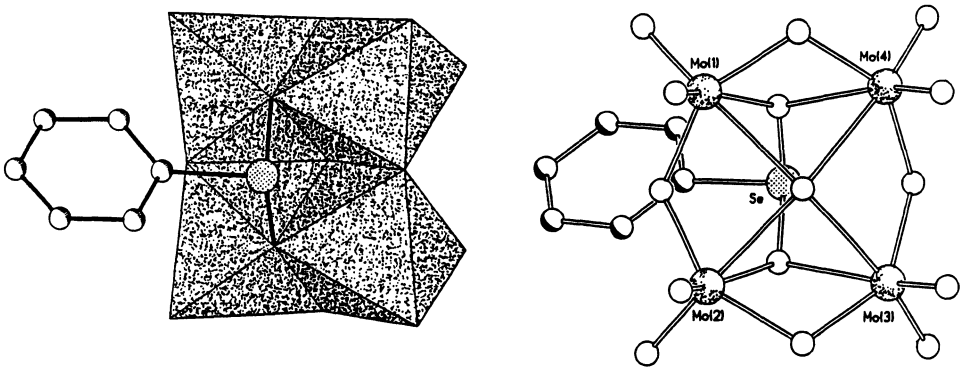

Figure 2. Structure of $[PhSeMo_4O_{14}(OH)]^{2-}$ in 2

2 represents the first organoselenopolyoxomolybdate. Its structure is similar to the well known anions $[Me_2AsMo_4O_{14}(OH)]^{2-}$ [13] and $[H_2CMo_4O_{14}(OH)]^{3-}$ [14]. In these complexes the $PhSeO_2$ group with the unshared electron pair is substituted by an isoelectronic Me_2AsO_2 unit or an H_2CO_2 group. A comparison of the structure of $[PhSeMo_4O_{14}(OH)]^{2-}$ with those of the latter two compounds indicates that the influence of the different organic and organometallic substituents on the details of the bonding pattern in the $Mo_4O_{14}(OH)$ framework is quite small.

2.2. NOVEL Sb(III)-CONTAINING HETEROPOLYMETALATES

2.2.1. *$Na_9[SbW_9O_{33}]\cdot 19.5H_2O$* (3). This compound is synthesized by dissolving Sb_2O_3 in concentrated hydrochloric acid and adding to a solution of $Na_2WO_4\cdot 2H_2O$ in water[15]. The crystal structure of 3 consists of discrete $[SbW_9O_{33}]^{9-}$ anions, sodium cations and water molecules. Fig. 3 gives a view of the anion in two different representations. The anion structure is closely related to the α-Keggin structure $[XM_{12}O_{40}]^{n-}$ by removal of one W_3O_{13} group of edge-sharing WO_6 octahedra, the remaining complex having the a-B-XM_9 fragment structure. In detail each anion contains nine WO_6 octahedra arranged in three W_3O_{13} groups of three edge-shared octahedra. These groups are linked to each other by shared corners.

The Sb(III) atom is linked to the triply bridging oxygen atoms of the W_3O_{13} groups, to build a SbO_3 pyramid in the center of the tungsten oxygen cage. The nonbonding nature of the unshared pair of electrons at the Sb(III) atom prevents further condensation to complete the Keggin structure.

2.2.2. *$K_{12}[Sb_2W_{22}O_{74}(OH)_2]\cdot 27H_2O$* (4). An acidified solution of the $[SbW_9O_{33}]^{9-}$ anion and $Na_2WO_4\cdot 2H_2O$ in water leads to the novel 22-nuclear heteropolytungstate 4. The two identical β-B-SbW_9-subunits in $[Sb_2W_{22}O_{74}(OH)_2]^{12-}$ are connected to each

other by four WO_6 octahedra. In comparision to the α-B-$[SbW_9O_{33}]^{9-}$ anion one W_3O_{13} group in the subunit has been rotated by 60° along the Sb-O vector.

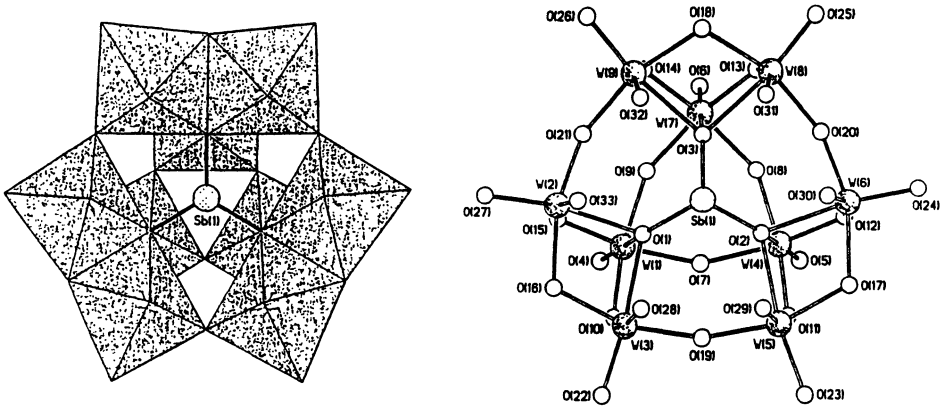

Figure 3. Structure of $[SbW_9O_{33}]^{9-}$ in **3**

An unusual feature of this anion is the presence, besides the usual WO_6 octahedra with one or two terminal oxygen atoms, of WO_6 octahedra with none or with three terminal oxygen ligand atoms (see Fig. 4: W(1) and W(11)). WO_6 octahedra with three facial terminal oxygen atoms have never been reported for polyoxotungstates so far.

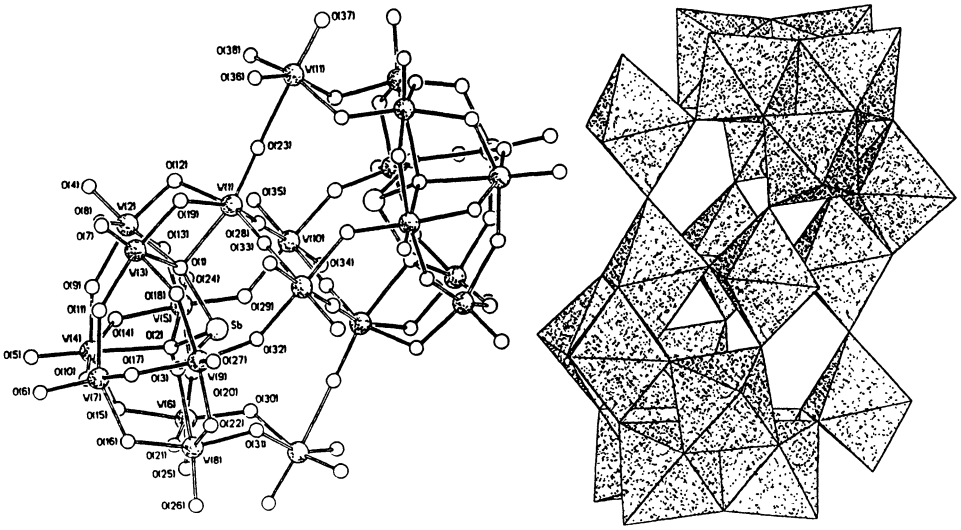

Figure 4. Structure of $[Sb_2W_{22}O_{74}(OH)_2]^{12-}$ in **4**

According to the chemical analysis and for establishing electroneutrality, each anion must contain two protons. Therefore it is suggested that each *fac*-WO_3 group has one protonated terminal oxygen atom. The presence of terminal OH groups in polytungstates is a rare bonding situation; so far only bridging ones have been identified[16]. Another special feature of the anion structure in **4** is the coordination of W(1) exclusively by bridging oxygen atoms (to five doubly and one quadruply bridging oxygen, see Fig. 4). This anion is the first known heteropolytungstate completely built up by β-B-XW_9 subunits.

2.2.3. *$[Me_4N]_{10}Na_{12}[Na_2Sb_8W_{36}O_{132}(H_2O)_4]\cdot 19.5H_2O$* (**5**). This compound can be obtained by adding solid $SbCl_3$ to a solution of $Na_9[SbW_9O_{33}]\cdot 19.5H_2O$.

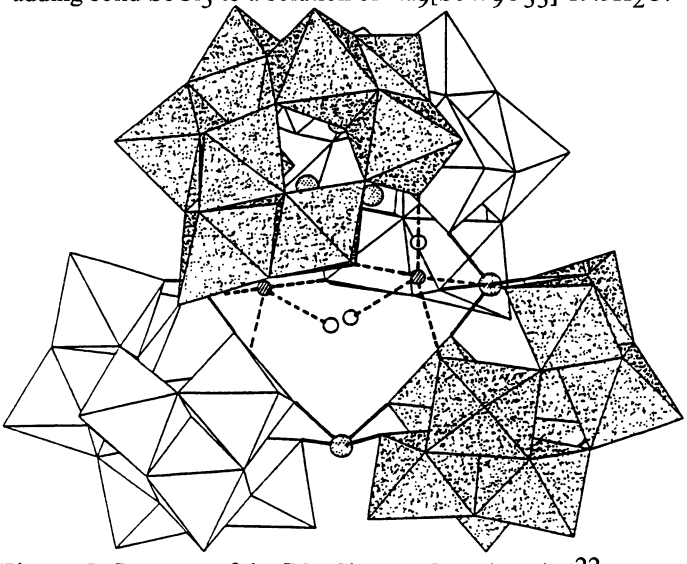

Figure 5. Structure of the $[Na_2Sb_8W_{36}O_{132}(H_2O)_4]^{22-}$ anion in **5**

The structure contains discrete $[Na_2Sb_8W_{36}O_{132}(H_2O)_4]^{22-}$ anions (Fig. 5). Each anion is built of four identical β-B-SbW_9-Keggin fragments with sodium and Sb(III) atoms bonded to them. In detail four SbO_4-groups with ψ-trigonal bipyramidal coordinated Sb(III) atoms share two oxygen atoms with different XW_9 units to connect them. In the center of the SbW_9 units the Sb(III) atoms are bonded to the triply bridging oxygen atoms to form a SbO_3 pyramid. Remarkably, two sodium ions are incorporated in the tungsten-oxygen cluster, effecting an additional connection of the four subunits. **5** is another new Sb(III) heteropolytungstate only consisting of β-B-XW_9 subunits. It is one of the largest heteropolytungstates known so far[17-19].

2.2.4. *$[Me_4N]_7[H_2SbW_{18}O_{60}]\cdot 3H_2O$* (**6**). For the synthesis of **6**, Sb_2O_3 is dissolved in hydrochloric acid and added to a $Na_2WO_4\cdot 2H_2O$ solution in water, followed by addition of $(CH_3)_4NBr$ in water.

The interesting novel anion consists of one W_9O_{33} unit and one SbW_9O_{33} group linked together by six oxygen atoms (Fig. 6). The SbW_9O_{33} group is an α-B-Keggin fragment, with a tri-coordinated Sb(III) atom in the center, disordered in the crystal structure between both half-units. For establishing electroneutrality two protons must be bonded inside the cavity in one half of the anion, which has also been suggested by Jeannin and Martin-Frère[20] for the comparable As(III) compound.

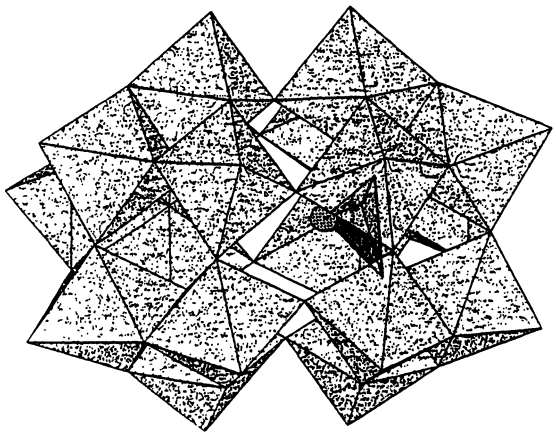

Figure 6. Structure of $[H_2SbW_{18}O_{60}]^{7-}$ in **6**

3. Iso- and Heteropolymetalates in Catalysis: Novel Developments

The extensive use of iso- and heteropolymetalates, especially those of vanadium, molybdenum and tungsten, and the most recent research results in this field are addressed only shortly in this brief report. A wide variety of reactions is catalyzed by this class of compounds. They include, in the field of acid catalysis, aromatic alkylation and trans-alkylation, acetalization, esterification, hydration and dehydration, isomerization as well as poly- and oligomerization. Catalytic oxidation reactions are able to activate various substrates, ranging from alkanes, alkenes, and alkines to alkohols and aldehydes as well as to inorganic reactands. An excellent and comprehensive review on the most recent development in heteropoly acid catalysts in acid catalyzed reactions and oxidation catalysis has been given very recently by Schwegler et al. [21], and the reader interested in these technical aspects is referred to this account for details.

4. Antitumor and Antiviral Activity of Iso- and Heteropolymetalates

In addition to their great importance and widespread use as industrial oxidation catalysts in a variety of applications, polyoxomolybdates and -tungstates have proven to be a very promising class of candidates for anticancer and antiviral action. In fact, besides the well-known cis-platinum and its analogues, and maybe besides some titanocene and ruthenium compounds with proven antitumor properties, the present class of polyoxo compounds seems to develop, in the field of metal-containing antitumor and antiviral agents, towards the most interesting compounds of the future. Of course, very little is yet known on the possible modes of action in the cell, on the transport mechanisms to enter the cell, even on the question of possible decomposition reactions towards smaller units within the biological systems. Before any general judgement on the value of specific compounds and on the differentiation according to nuclearity, to oxidation states, or to the nature of heteroatoms or other hetero-substituents can be given, detailed mechanistic investigations *in vitro* and *in vivo* are necessary.

Among the more active and successful research groups in the fields of antitumor and anti-HIV activity of polyoxometalates, those of C.L. Hill, T. Yamase, J.W. Blasecki, and P. Clayette and D. Dormont have contributed significantly to the present state of the field, and they have reviewed some aspects of its development recently, including a list of the important references[22].

In a systematic study by T. Yamase et al. [22b] on the antitumor properties of normal heptamolybdate, $[NH_3Pr^i]_6[Mo_7O_{24}]\cdot 3H_2O$ has been found to be a potent antitumor agent with low toxicity *in vivo* against Meth-A sarcoma, MM-46 adenocarcinoma, and MX-I human breast, OAT human lung, and CO-4 human colon cancer xenografts. If the heptamolybdate(VI) is reduced to its one-electron reduction product, the $Mo^VO_5(OH)$ site in the Mo_7O_{24} framework induces rather strong toxicity. This is in contrast to the d^0-$Mo^{VI}O_6$ site in the oxidized form but the antitumor properties of the former is similar to the latter.

The tumor growth suppression of heptamolybdate is superior to that of 5-fluorouracil (5-FU) and of 1-(4-amino-2-methylpyrimidin-5-yl)methyl-3-(2-chloro-ethyl)-3-nitrosourea (ACNU) which are clinically applied drugs showing a good activity against breast, gastrointestinal, and intracranial tumors[23]. In addition, two new antiviral polyoxometalates, $K_7[PTi_2W_{10}O_{40}]\cdot 7H_2O$ and $[NH_4]_{12}H_2$-$[Eu_4(H_2O)_{16}(MoO_4)(Mo_7O_{24})_4]\cdot 13H_2O$ have been recognized against a broad spectrum of DNA and RNA viruses such as herpes simplex, human cytomegalovirus, coxsackievirus type B5, influenza B, and human immunodeficiency virus HTLV-111_b [24-26]. They seem to compare favourably to the activity of other polyoxometalates such as $[SiW_{12}O_{40}]^{4-}$, $[Sb_9W_{21}O_{86}]^{19-}$, $[As_4W_{40}O_{140}]^{28-}$, and their lacunary compounds against oncogenic and HIV viruses[27-30]. Although these compounds inhibit viral and bacterial DNA and RNA polymerases, the compounds seem to lack significant *in vivo* anti-HIV activity[31,32].

On the basis of the one-electron reduction of heptamolybdate, Yamase[22b] presents a remarkable proposal for the mechanism of the antitumor activity of the $[Mo_7O_{24}]^{6-}$ anion, suggesting the reduction product $[Mo_7O_{23}(OH)]^{6-}$ being involved in the antitumor reaction, with repeated cycles of the reaction of equ.(1) in the tumor cells:

$$[Mo_7O_{24}]^{6-} + e^- + H^+ \Leftrightarrow [Mo_7O_{23}(OH)]^{6-} \qquad (1)$$

The mechanism is based on the hypothesis that the tumor cells possess electron-donating sites with a redox potential negative enough to reduce the heptamolybdate(VI). The reoxidation of $[Mo_7O_{23}(OH)]^{6-}$ with the oxidation potential of -0.50 V vs. Ag/AgCl at pH 7 is probably coupled with the reduction of the tumor cell, leading to the observed cell death. The strong toxicity of $[Mo_7O_{23}(OH)]^{6-}$ is suggested to be linked with the electrochemical reduction of the host cells. Regarding the interaction of the polymolybdate with DNA being nonspecific and weak[33], the antitumor mechanism based on the reversible redox reaction is characteristically different from the mechanism of cis-$Pt(NH_3)_2Cl_2$ which is based on the dissociation of choride ligands followed by binding to N-7 atoms of guanine bases in DNA with a resultant formation of DNA intrastrand cross-links. As $[Mo_7O_{24}]^{6-}$ interacts with flavin mononucleotide (FMN) to yield a 1:1 complex which gives a redox potential 0.1 V more positive than FMN, Yamase suggests that the antitumor activity due to the repeated redox cycles of $[Mo_7O_{24}]^{6-}$ in tumor cells, would inhibit the ATP generation coupled with the electron transfer from NADH to coenzyme Q in/on the mitochondria[22b].

A rather instructive report on the development of research in the field of anti-HIV activity of polyoxometalates is given in the article by Hill et al. in the above-mentioned book[22a]. After the detection of significant antiviral activity of polyoxometalates more than

20 years ago[34] a first development in the field lead to some research with cell cultures using a few basic polyoxotungstates (for a more detailed account of the historical development of the field see[22a,22b]. The antimony-containing heteropolytungstate, $(NH_4)_7Na[NaW_{21}Sb_9O_{86}]$ (called HPA-23 by the French investigators) reached limited clinical treatment of HIV infections. Unfortunately HPA-23 proved to be too toxic to be effective in both the French clinical trial and a subsequent one conducted by Moskovitz et al.[29,32,35].

In the mid to late 1980's vigorous new efforts by the groups of Hill, Schinazi et al. and of Yamase et al. who could bring in their great chemical experience into the field of polyoxometalates resulted in a chemically more systematic investigation of the many aspects of the potential antiviral, and in general, physiological behavior of these compounds[26,30,36-41]. The first of the groups first noticed in 1985, upon evaluating several polyoxometalates against HIV in cell culture, that several polyoxotungstates might be less toxic and more effective than HPA-23 [36]. Parallel to it, and partially stimulated by the success of the American group the Japanese group also reported results on their productive program in polyoxometalate anti-HIV chemotherapy [26,39,40]. Shortly after, industrial firms entered this reearch (Johnson Matthey Corporation in collaboration with the Hill and Schinazi groups and Du Pont with J. Blasecki[22c]. Also, the French group of J. Dormont et al. has successfully continued their polyoxometalate antiviral work with some significant results being reviewed in l.c.[22d].

At present, cell culture studies have been performed on as many as more than two hundred polyoxometalates. A review on the current status of HIV chemotherapy[42] has appeared recently. Much of this work has been and is performed in the group of Hill, Schinazi et al., and a comprehensive list of activities and toxicities of various polyoxometalate spezies investigated is given in the review cited above[22a] where a number of additional references is cited. The list includes isopoly compounds like $[Mo_6O_{19}]^{n-}$ (n = 2 to 8) as well as a large number of heteropoly spezies which include, besides the Keggin, lacunary Keggin, Wells-Dawson and defect Wells-Dawson type anions, sandwiched $[Y_{34}(XM_9O_{34})_2]^{n-}$ (n = 10 to 12) and $[Y_4(X_2M_{15}O_{56})_2]^{16-}$ anions as well as anions of the types $[X_2W_{18}Nb_6O_{77}]^{8-}$, $[YXM_{11}O_{40}]^{n-}$ (n = 4 to 8), $[YXM_{11}O_{39}]^{n-}$ (n = 5 to 8), $[NaW_{21}Sb_9O_{86}]^{18-}$ (HPA-23), and organo-substituted anions such as $[XW_{11}O_{39-41}R_m]^{n-}$ (n = 3 to 6, m = 1 or 2). In order to establish relationships between the structural, electronic, and chemical properties of the polyoxometalate drugs and their biological activities current experimental investigations must include studies of (a) the anti-HIV efficacy and toxicity in cell culture, (b) the selectivity in cell culture, (c) the toxicity in mammals, (d) the efficacy in virally infected mammals, and (e) the pharmacokinetics in mammals. The first of these issues has been investigated rather successfully, and a number of compounds with promising antiviral activity and low toxicity were discovered [22(a)] whereas only limited knowledge is available concerning issues (b) to (e).

Some of the results obtained in the group of Hill et al. up to now [22(a)] can be summarized as follows:

(a) Polyoxo*tungstates* appear to be the most effective anti-HIV polyoxometalates, as compared to others. Although this cannot yet be correlated to its specific chemistry, polyoxotungstates as a class prove to be rather efficient in cell culture. According to Hill et al. [22a] more than 70% of the polyoxotungstates of all structural classes evaluated to date have high levels of activity (low EC_{50} values) and low toxicity (high IC_{50} values). (b) The derivatization of polyoxometalate surfaces with some organic group does not greatly diminish the anti-HIV activity nor increase the toxicity of the compounds[41]. (c) Remarkably, anti-HIV activity and toxicity of polyoxometalates are dependent on the

cation, as, e.g., indicated by the ammonium ion and protonated basic amino acid forms of the polyoxometalate drugs being significantly less toxic than the free acid forms[38]. Within the range of Keggin-type polyoxotungstates, changing the cation from proton to ammonium alters the toxicity by two orders of magnitude. (d) The toxicicity of polyoxotungstates to human bone marrow cells varies over five orders of magnitude from HPA-23, which is the most toxic compound yet tested against such cells, to $(NH_4)_5[BW_{12}O_{40}]$, which is virtually non-toxic and far less toxic than AZT (3'-azido-3'-deoxythymidine) to these cells[22a,38]. (e) The toxicity of polyoxometalates in rats and mice is highly variable and does not yet correlate in a clear way with the molecular properties of the complexes.

In some recent investigations, Hill et al.[41,43,44] reported some significant novel findings concerning the screening of some specifically substituted heteropolytungstates with respect to their anti-human immunodeficiency virus activities. In the first[41], novel water-soluble cesium and tetramethylammonium salts of polyoxotungstate anions with covalently attached organosilyl groups of formula $[(RSi)_2O]$-$[SiW_{11}O_{39}]^{4-}$ with R = $CH_2CH_2COCH_3$, $(CH_2)CN$, and $CH{=}CH_2$ were shown to have activities (EC_{50}) against human immunodeficiency virus in primary human lymphocytes from 3.3 μM to 39.0 μM. With toxicities (IC_{50}) greater than 100 μM, their inhibition constants against purified virion-derived HIV-1 reverse transcriptase are in the range of 1 to 10 μM. In the second paper[43], peroxoniobium-substituted heteropolytungstates of the types $[Si(NbO_2)_3W_9O_{37}]^{7-}$ and $[Si(NbO_2)W_{11}O_{39}]^{5-}$ (isolated as their cesium, potassium and trimethylammonium salts) were discovered to be a remarkable new class of potent anti-HIV agents. The anti-HIV activities in human peripheral blood mononuclear cells (PBMC) acutely infected with HIV-1 are low in precursor complexes like $K_7H[Nb_6O_{19}]$, but are impressive for the above compounds, with one of the most effective agents being $Cs_7[Si(NbO_2)_3W_9O_{37}]$, showing an EC_{50} of 1.0 μM. Toxicities to uninfected PBMC are negligible. The activities and selectivities against HIV-1 reverse transcriptase are rather high with IC_{50} values from 0.03 to 0.06 μM. Using a cell-free system, $[(CH_3)_3NH]_7[Si(NbO_2)_3$-$W_9O_{37}]$ inhibits the interaction between gp120 and CD4 by 70% at 25 μM.

Preclinical studies[44] on the pharmacokinetics in rats of the antiviral polytungstates $K_{12}H_2[P_2W_{12}O_{48}]{\cdot}24H_2O$, $K_{10}[P_2W_{18}Zn_4(H_2O)_2O_{68}]{\cdot}20H_2O$, and $[(CH_3)_3NH]_8[Si_2W_{18}Nb_6O_{77}]$, which show potent antiviral activity against HIV types 1 and 2, herpes simplex virus, and cytomegalovirus in vitro, indicate strong bonding to serum proteins and structure-dependent moderate to wide distribution throughout the body. One week after single-dose administration high concentration levels of the agents were detected in the kidneys and liver.

According to extensive cell culture studies there appear to be at least two different molecular modes of action: (a) inhibition of HIV reverse transcriptase (RT) (the predominant mode of action of AZT and the other nucleoside drugs), and (b) inhibition of the fusion of infected cells to uninfected ones (syncytium formation)[26,45]. The latter activity is of considerable interest and will continue to be one of the focal points of research on these complexes in the near future[22a].

Our knowledge concerning the efficiacy of polyoxometalates in virally infected mammals and the pharmacokinetics in mammals is still limited. Activity of HPA-23 *in vivo* against some viruses is documented[29,32,34,35] and more recently several other compounds have shown activity against other viruses *in vivo* [422c,29,32,45-48].

First pharmacokinetic studies by Hill, Schinazi et al. indicate that some otherwise promising polyoxometalate drugs do not clear readily from the body, whereas, other complexes do. Some polyoxometalates have measurable levels of oral bioavailability and

some appear to cross the blood brain barrier[45]. Finally, one of the most important questions remaining to be answered by the *in vivo* studies is the uncertainty as to whether the complexes are staying intact or not in the mammalian body, or if they dissociate or hydrolyze in the neutral pH regime to lower molecular mass species. Some authors have addressed this question[22a] but, in spite of the difficulties in analyzing polyoxometalates under *in vivo* conditions, a great deal of research needs to be done in this area.

5. Acknowledgements

The important contributions of the doctoral students Rainer Böhner, Rita Klein, Bernhard Lettmann, Heinrich Pohlmann, and Christian Thülig to our own work reported in this account are gratefully acknowledged. Our research was supported by the Deutsche Forschungsgemeinschaft and the Fonds der Chemischen Industrie.

5. References

(1) Pope, M.T. *Heteropoly and Isopoly Oxometalates*; Springer-Verlag: Berlin, Heidelberg, New York, Tokyo, 1983.
(2) Pope, M.T. In: *Comprehensive Coordination Chemistry* (G. Wilkinson, Ed.); Pergamon Press: Oxford, 1987; Vol. 3, pp 1023-1058.
(3) Pope, M.T.; Müller, A. *Angew. Chem. Int. Ed. Engl.* **1991**, *30*, 34.
(4) Pope, M.T. *Progr. Inorg. Chem.* **1991**, *39*, 181.
(5) Krebs, B.; Klein, R. In: *Polyoxometalates - From Platonic Solids to Anti-Retroviral Activity* (M.T. Pope and A. Müller, Eds.); Kluwer Acad. Publ.: Dordrecht, 1993, pp 41-57.
(6) Krebs, B.; Paulat-Böschen, I. *Acta Crystallogr.* **1982**, *B38*, 1710.
(7) Krebs, B.; Stiller, S.; Tytko, K.H.; Mehmke, J. *Eur. J. Solid State Inorg. Chem.* **1991**, *28*, 883.
(8) Krebs, B.; Lettmann, B.; Pohlmann, H.; Fröhlich, R. *Z. Kristallogr.* **1991**, *196*, 231
(9) Holmes, R.R.; Swamy, K.C.K.; Schmid, C.G.; Day, R.O. *J. Am. Chem. Soc.* **1988**, *110*,7060
(10) Liu, B.; Ku, Y.; Wang, M.; Wang, B.; Zheng, P. *J. Chem. Soc., Chem. Comm.* **1989**, 651
(11) Sasaki, Y.; Imoto, H.; Nagano, O. *Bull. Chem. Soc. Jpn.* **1984**, *57*, 1417
(12) Krebs, B.; Lettmann, B.; Pohlmann, H. *Z. Kristallogr.* **1989**, *186*, 233
(13) (a) Matsumoto, K.Y. *Bull. Chem. Soc. Jpn.* **1979**, *52*, 3284, (b) Barkigia, K.M.; Rajkovic-Blazer, L.M.; Pope, M.T.; Prince, E.; Quicksall, C.O. *Inorg. Chem.* **1980**, *19*, 2531
(14) Day, V.W.; Fredrich, M.F.; Klemperer, W.G.; Liu, R.-S., *J. Am. Chem. Soc.* **1979**, *101*, 491
(15) Krebs, B.; Pohlmann, H. to be published
(16) Wasfi, S.H.; Pope, M.T.; Barkigia, K.; Butcher, R.; Quicksall, C.O. *J. Am. Chem. Soc.***1978**, *100*, 7786
(17) Alizadeh, M.H.; Harmalker, S.P.; Jeannin, Y.; Martin-Frère, J.; Pope, M.T., *J. Am. Chem. Soc.***1985**, *107*, 2662
(18) Robert, F.; Leyrie, M.; Hervé, G.; Tézé, A.; Jeannin, Y. *Inorg. Chem.* **1980**, *19*, 1746

(19) Contant, R.; Tézé, A. *Inorg. Chem.* **1985**, *24*, 4610
(20) Jeannin, Y.; Martin-Frère, J. *Inorg. Chem.* **1979**, *18*, 3010
(21) Jansen, R.J.J.; van Veldhuizen, H.M.; Schwegler, M.A.; van Bekkum, H. *Rec. Trav. Chim. Pays-Bas* **1994**, *113*, 115.
(22) (a) Hill, C.L.; Kim, G.-S.; Prosser-McCartha, C.M.; Judd, D. In: *Polyoxometalates - From Platonic Solids to Anti-Retroviral Activity* (M.T. Pope and A. Müller, Eds.); Kluwer Acad. Publ.: Dordrecht, 1993, pp 359-371; (b) Yamase, T. *ibid.*, pp 337-358; (c) Blasecki, J.W. *ibid.*, pp 373-385; (d) Clayette, P.; Dormont, D. *ibid.*, pp 387-400; (e) Crans, D.C. *ibid.*, pp 401-408.
(23) Yamase, T.; Fujita, H.; Fukushima, K. *Inorg. Chim. Acta* **1988**, *151*, 15.
(24) Inouye, T.; Tokutake, Y.; Yoshida, Y.; Yamamoto, A.; Yamase, T.; Nakamura, S. *Chem. Pharm. Bull.* **1991**, *39*, 1638.
(25) Fukuma, M.; Seto, Y.; Yamase, T. *Antiviral Res.* **1991**, *16*, 327.
(26) Take, Y.; Tokutake, Y.; Inouye, Y.; Yoshida, T.; Yamamoto, A.; Yamase, T.; Nakamura, S. *Antiviral Res.* **1991**, *15*, 113.
(27) (a) Jasmin, C.; Raybaud, N.; Chermann, J.C.; Haapala, D.; Sinoussi, F.; Boy-Loustau, C.; Bonissol, C.; Kona, P.; Raynaud, M. *Biomedicine* **1973**, *18*, 319; (b) Jasmin, C.; Chermann, J.C.; Hervé, G.; Tézé, A.; Souchay, P.; Boy-Loustau, C.; Raybaud, N.; Sinoussi, F.; Raynaud, M. *J. Natl. Cancer Inst.* **1974**, *53*, 469; (c) Larnicol, N.; Augery, Y.; Le Bousse-Kerdiles, C.; Degiorgis, V.; Chermann, J.C.; Tézé, A., Jasmin, C. J. *Gen. Virol.* 1981, 55, 17.
(28) Vittecoq, D.; Woerle, R.; Barre-Sinoussi, F.; Chermann, J.C. *Biomed. Pharmacother.* **1988**, *42*, 35.
(29) Rozenbaum, W.; Dormont, D.; Spire, B.; Vilmer, E.; Gentilini, M.; Griscelli, C.; Montagnier, L.; Barre-Sinoussi, F.; Chermann, J.C. *Lancet* **1985**, 450.
(30) Hill, C.L.; Weeks, M.; Schinazi, R.F. *J. Med. Chem.* **1990**, *33*, 2767.
(31) Balzarini, J.; Mitsuya, H.; De Clercq, E.; Broder, S. *Int. J. Cancer* **1986**, *37*, 451.
(32) Moskovitz, B.L.; the HPA-23 cooperative study group. *Antimicrob. Agents Chemother.* **1988**, *32*, 1300.
(33) Tomita, K.; Yamase, T.; Shishido, K. *Inorg. Chim. Acta* **1989**, *157*, 167.
(34) Raynaud, M.; Chermann, J.C.; Plata, F.; Jasmin, C.; Mathé, G. *C. R. Acad. Sci. Paris*, **1971**, *272*, 347.
(35) Burgard, M.; Sansonetti, P.; Vittecoq, D.; Descamps, P.; Guetard, D.; Herson, S.; Rozenbaum, W.; Rouzioux, C. *AIDS* **1989**, *3*, 665.
(36) Schinazi, R.F.; Hill, C.L. 26th ICAAC, New Orleans, La.; Abstract 2; Dagani, R. *Chem. Engng. News* **1986**, *64*, 7.
(37) Hill, C.; Weeks, M.; Hartnup, M.; Sommadossi, J.-P.; Schinazi, R. Ann. *N. Y. Acad. Sci.* **1990**, *616*, 528.
(38) Hill, C.L.; Hartnup, M.; Faraj, M.; Weeks, M.; Prosser-McCartha, C.M.; Brown, R.B.; Schinazi, R.F.; Sommadossi, J.-P. In: *Advances in Chemotherapy of AIDS, Pharmacology and Therapeutics* (R. Diasio, J.-P. Sommadossi, Eds.); Pergamon Press, New York, 1990, pp 331 ff.
(39) Inouye, Y.; Take, Y.; Tokutake, Y.; Yoshida, Y.; Yamamoto, A.; Yamase, T.; Nakamura, S. *Chem. Pharm. Bull.* **1990**, *38*, 285.
(40) Inouye, Y.; Tokutake, Y.; Kunihara, J.; Yoshida, T.; Yamase, T.; Nakata, A.; Nakamura, S. *Chem. Pharm. Bull.* **1992**, *40*, 805.
(41) Weeks, M.S.; Hill, C.L.; Schinazi, R.F. *J. Med. Chem.* **1992**, *35*, 1216.
(42) Schinazi, R.F.; Mead, J.R.; Feorino, P.M. *AIDS Resarch and Human Retroviruses* **1992**, *8*, 963.
(43) Kim, G.-S.; Judd, D.A.; Hill, C.L.; Schinazi, R.F. *J. Med. Chem.* **1994**, *37*, 816.

(44) Ni, L.; Boudinot, F.D.; Boudinot, S.G.; Henson, G.W.; Bossard, G.E.; Martellucci, S.A.; Ash, P.W.; Fricker, S.P.; Darkes, M.C.; Theobald, B.R.C.; Hill, C.L.; Schinazi, R.F. *Antimicrob. Agents Chemother.* **1994**, *38*, 504.
(45) l.c.. [22(a)], ref. 56.
(46) Werner, G.H.; Jasmin, C.; Chermann, J.C. *J. Gen. Virol.* **1976**, *31*, 59.
(47) Kimberlin, R.H.; Walker, C.A. *Arch. Vir.* **1983**, *78*, 9; *AAC* **1986**, *30*, 409.
(48) Pepin, M.; Blancou, J. *Arch. Vir.* **1985**, *83*, 327.

PURPLE ACID PHOSPHATASES AND CATECHOL OXIDASE AND THEIR MODEL COMPOUNDS. CRYSTAL STRUCTURE STUDIES OF PURPLE ACID PHOSPHATASE FROM RED KIDNEY BEANS

BERNT KREBS
Institute of Inorganic Chemistry
University of Münster
Wilhelm-Klemm-Strasse 8
D-48149 Münster, Germany

ABSTRACT. Recent results on the structures and functions of purple acid phosphatases and catechol oxidases as well as on their model compounds are reviewed and discussed. Purple acid phosphatase from kidney beans (KBPAP) was crystallized in two modifications, and the structure is being refined at 2.8 E resolution by X-ray diffraction. The enzyme is a dimer of quasi-identical subunits connected by a disulfide bridge. The sequence could be determined using MALDI mass spectrometry. Structural and functional model complexes for Fe-Fe and Zn-Fe PAP's were prepared with new dinucleating ligands, partly with bridging and terminal phosphate ligands. Some of them show considerable phosphatase activity and, like the enzyme itself, also appear to have oxygen-activating properties. EXAFS and XANES on KBPAP indicate rather long metal-metal distances as compared to the values proposed for uteroferrin. The rather weak antiferromagnetic coupling in the beef spleen phosphatase (as well as in the model compounds) and the X-ray diffraction data suggest hydroxo bridging of the metals in the enzyme rather than oxo bridging.

Two catechol oxidases with Cu(II)-Cu(II) active centers were isolated, purified, and characterized. Dinuclear and tetranuclear model complexes were synthesized with tri-, penta- and heptadentate dinucleating ligands containing bridging phenolate or alcoholate groups. Correlations are obtained between the coordination numbers, properties of the donor groups and catalytic activity, dinuclear Cu(II) complexes with tridentate ligands like 2,6-bis(morpholinyl-N-methyl)-4-methylphenol being the most active. Catechol oxidase as well as its biomimetic model complexes are investigated as possible active elements in bio- and chemosensors for the analysis of hormones and neurotransmitters like adrenaline in medical diagnosis. Molecular modeling methods are employed favourably during these investigations.

1. Introduction

Purple acid phosphatases (PAPs) have been isolated from mammals as well as from plants. They are a group of glycoproteins which are active at pH 4-6 towards activated phosphoric acid esters and anhydrides. Besides hemerythrin, ribonucleotide reductase, and methane monooxygenase, the purple acid phosphatases belong to the highly important class of metalloenzymes with iron-containing dinuclear active sites. The intensive current reasearch in this field is concentrated on the properties of the protein as well as on the synthesis of model complexes. Among the active groups are those of L. Que, Jr., S.J. Lippard, B.A.

D.P. Kessissoglou (ed.), Bioinorganic Chemistry, 371-384

Averill, G.A. Sykes, J.-M. Latour, and H. Witzel. We have concentrated our attention on the mammalian enzymes from bovine spleen and from porcine uteri (uteroferrin), containing an antiferromagnetically coupled Fe^{II}-Fe^{III} diiron center in the active state and, especially, on the plant metalloenzyme from red kidney beans *Phaseolus vulgaris*, containing a Zn^{II}-Fe^{III} center in the active site.

Catechol oxidase from *Lycopus europaeus* (or from other sources such as black poplar and other plants) is classified as an o-diphenoloxidase which catalyzes the oxidation of o-diphenols to o-quinones with a concomitant reduction of O_2 to H_2O. According to present knowledge, the active site of catechol oxidase consists of a dinuclear copper moiety (type 3 copper, ESR silent). Systematic EXAFS, XANES, ESR and other spectroscopic investigations on the native *Lycopus* metalloprotein indicate the Cu^{II}-Cu^{II} centers in the protein to have in the *met* form a short CuKKKCu distance with an ESR signal appearing only after denaturing. The details of the structure and function of this interesting copper enzyme remain to be understood. Besides the work on the protein itself, various activities are underway to prepare significant structural and functional model complexes. Especially helpful in this field are the recent results reported, among others, by the groups of N. Kitajima, K.D. Karlin, and E.I. Solomon on relevant novel peroxo copper complexes.

In the present brief review we wish to report on some recent own results in both fields of purple acid phosphatases and catechol oxidase as well as on their model chemistry.

2. Purple Acid Phosphatases

Purple acid phosphatases (PAPs) hydrolyzing activated phosphoric acid esters and anhydrides have in common a two-metal center with a tyrosine σ Fe(III) charge transfer transition which is responsible for a broad absorption band in the range of 500 - 600 nm and a typical resonance Raman spectrum. PAPs have been isolated from several mammalian, plant, and microbial sources. The widespread appearance in nature implies an important and general role in all living organisms. In the mammalian enzymes from spleen, macrophages, osteoclasts and from uterine fluids (uteroferrin) the second metal ion in the active site is Fe(II). They all are monomeric glycoproteins and have a molecular mass of around 35 kDa. The physical data of these intensively studied enzymes are reviewed in[1-3]. Evidences for the ligands of the mammalian enzymes could be obtained by analysis of the paramagnetic shifts in NMR measurements[4-6] and by EXAFS data[7], also available for kidney bean purple acid phosphatase (KBPAP)[8]. From the pH-dependence of spectroscopic and kinetic data[9] it is postulated that an aqua ligand at the Fe(III) site is deprotonated with a pK value around 4.5 to a hydroxo ligand, which attacks the Me(II) bonded ester in an S_N2-reaction. This mechanism for ester hydrolysis is supported by kinetic investigations[10-11], demonstrating that substrates and substrate analogous inhibitors interact first with the Me(II) site. Furthermore the inversion of the absolute configuration at the phosphorus after hydrolysis reported by Averill, Knowles et al. [12] is in agreement with the postulated reaction path.

The PAPs have attracted great interest because of the dinuclear Fe(III)-Fe(II)-center in the active site of the mammalian species. With respect to the structure of the active site these phosphatases can be compared to the two-iron centers in hemerythrin[13], ribonucleotide reductase[14] and methane monooxygenase[15], whose structures are already known. In analogy to these dinuclear iron proteins and on the basis of experimental results a role of the mammalian Fe(III)-Fe(II) PAPs in the activation of dioxygen and in the generation of free radical species involving Fenton chemistry is under discussion[16,19].

Purple acid phosphatase of the common bean *Phaseolus vulgaris* is a homodimeric 110-kDa glycoprotein with a Fe(III)-Zn(II) center in the active site of each monomer, which

can be crystallized[17]. Zn(II) can be exchanged by Fe(II) without affecting the activity. The similarity of the reaction with substrates and of the interactions with inhibitors as well as of the spectroscopic data between the mammalian Fe(III)-Fe(II) enzymes and the corresponding Fe(III)-Fe(II) species of the kidney bean enzyme requires a high degree of conformity in the active site. This can be demonstrated in the EPR spectra, showing antiferromagnetic coupling[18] and in the Mφssbauer spectra[19]. The X-ray structure of KBPAP is expected to provide new insights into the structure and function of this enzyme class in order to correct and confirm previous inferences and speculations.

2.1. CRYSTAL STRUCTURE OF PURPLE ACID PHOSPHATASE FROM RED KIDNEY BEANS

Kidney bean PAP contains 432 amino acid residues and 5 heterogeneous glycosylation sites per monomer[20,21]. The structure of the enzyme was solved using multiple isomorphous replacement methods combined with density modification techniques. A tetragonal crystal form of space group $P4_32_12$ and cell parameters a = b = 104.4 Å and c = 309.9 Å, and an orthorhombic crystal form of space group $C222_1$ with a = 132.7 Å, b = 347.3 Å, and c = 128.7 Å have been used for structure determination. The KBPAP dimer has the shape of a twisted heart with overall dimensions 40 x 60 x 75 Å (Fig. 1). The two dinuclear metal centers are 35 Å apart. They are at the bottom of a small, broad cavity formed by both monomers. Access to the active site is not under the control of any channels or deep canyons in the native protein conformation. The two monomers are linked by a disulfide bridge between the two long loops in the upper part of the dimer in Fig. 1.

The secondary structure of KBPase is dominated by β-sheets. Fig. 2 shows the secondary structure of one monomer and Fig. 3 the topology diagram of the KBPAP fold. The monomer consists of two domains. The smaller N-terminal domain is

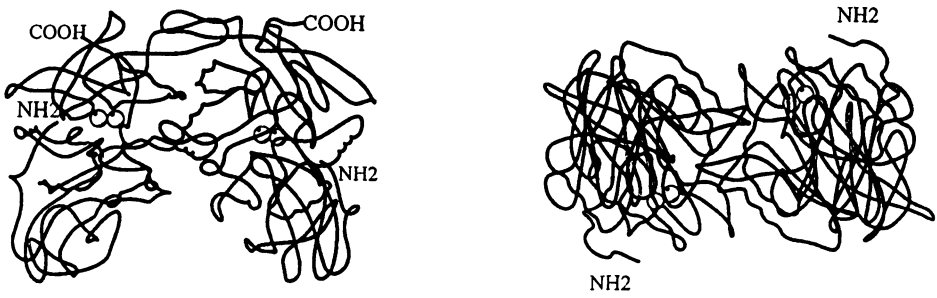

Figure 1. KBPAP dimer represented as coil (left: viewed onto twofold-axes; right: viewed along twofold-axes)

located in the lower part (see Fig. 1) and does not participate in any interactions between the two monomers. It is ~ 120 amino acid residues long and is built up by two sandwiched β-sheets of three antiparallel strands. A long curved β-strand (B4) shields one edge of the sandwich. The C-terminal or catalytic domain comprises the amino acid residues 120 to 432 and can be classified as an a/b-domain. It is dominated by two large sandwiched β-sheets of 6 and 7 β-strands. The smaller sheet has 3 parallel strands (B8 - B10), whereas in the larger sheet 4 strands are parallel (B12 - B14, B18).

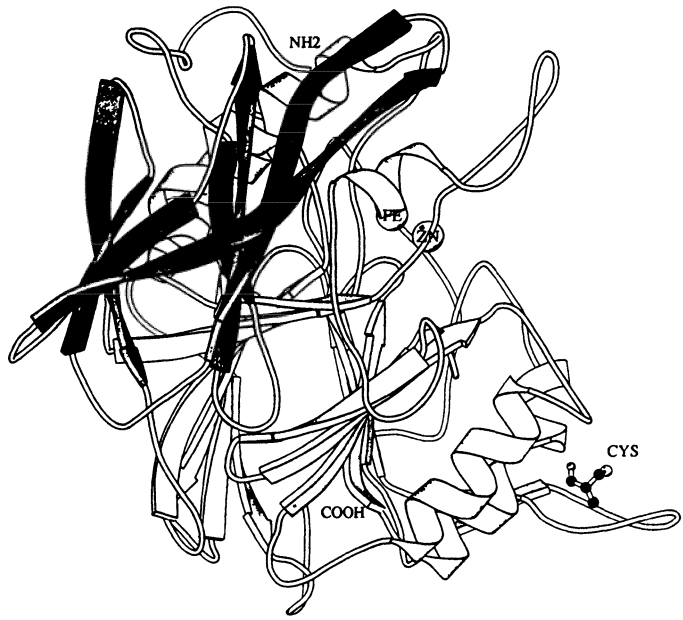

Figure 2. Secondary structure of a KBPAP monomer (N-terminal domain shaded; represented cysteine indicates the position of the disulfide bridge)

The four α-helices A1, A2, A4, and A5 build the connections between the parallel strands. The two sandwiched motifs, each comprising 3 parallel strands and 2 helices, are connected by helix A3 und strand B13. Each of these motifs may be compared to a mononucleotide binding motif of the NAD-binding domains of dehydrogenases[22].

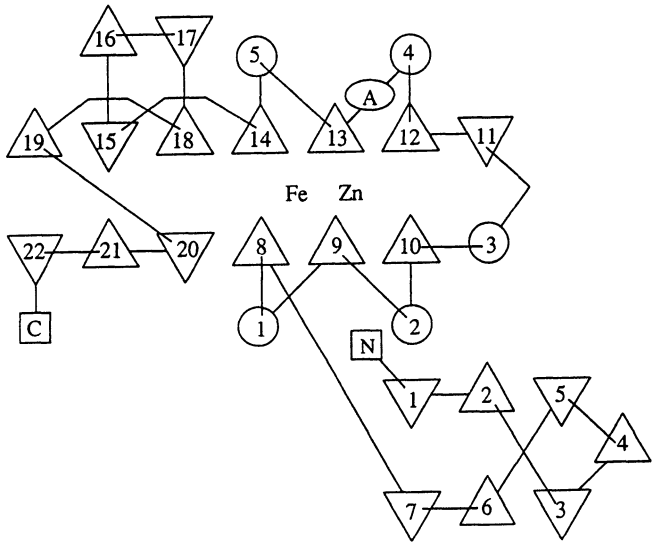

Figure 3. Schematic drawing of the folding of KBPAP (β-strands represented as triangles, α-helices shown as circles)

Whereas in the dehydrogenases two mononucleotide binding domains are arranged parallel to form one β-sheet of six parallel β-strands, the two motifs are sandwiched atop of each other in the KBPAP structure. The four helices A1, A2, A4, and A5 are arranged parallel to each other and shield symmetrically both sides of the sandwiched β-sheets. The active site is located at the carboxy end of the sandwiched parallel β-strands, which is a characteristic feature of this domain type[22].

The secondary structure of KBPAP represents a new fold. The catalytic domain of KBPAP is perfectly different as compared to the secondary structures of the dinuclear iron proteins hemerythrin, ribonucleotide reductase, and methane monooxygenase that are involved in transport and activation of dioxygen. The catalytic domains of these metalloproteins are strongly dominated by α-helices and the active sites are located in a pocket between the α-helices of a four-helix bundle. Further refinement of the current KBPAP model will show the degree of similarity of the two metal cluster of the Fe(III)-Zn(II) purple acid phosphatase with the catalytic centers of these dinuclear iron enzymes.

2.2. MODEL COMPLEXES

In terms of the synthesis of PAP active site model compounds phosphate or phosphoric acid ester coordination is of extraordinary importance. The active sites from bovine spleen and uteroferrin contain homodinuclear Fe(III)-Fe(III) centers in their inactive purple forms and Fe(II)-Fe(III) units in their active pink forms. In contrast the PAP from kidney beans has a heterodinuclear Fe(III)-Zn(II) dinuclear unit in its active center. The iron(III) ions for the mammalian PAP are high spin and antiferromagnetically coupled via proposed bridging ligands. So far it is unclear whether the tightly bonded phosphate group which was detected in the purple form of PAP is bridging or terminally coordinated[7,23]. New EXAFS studies favour the O,O'-bridging mode[7].

In recent years diiron(II,III), diiron(III,III) and iron(III)-zinc(II) model compounds containing coordinated phosphate and phosphoric acid esters[24-31] have been synthesized and characterized. Recently an attempt to synthesize a diiron complex with a terminally coordinated phosphato ligand was successful[24]. The ligand N,N,N',N'-tetrakis(2-benzimidazolylmethyl)-2-hydroxy-1,3-diaminopropane (Htbpo) which has proven to be suitable for the synthesis of dinuclear metal complexes was used. The structure of the cation of $[Fe_2Cl_2(tbpo)\{O_2P(OPh)_2\}(CH_3OH)](ClO_4)_2 \cdot 3CH_3OH$ (**1**) is shown in Fig. 4.

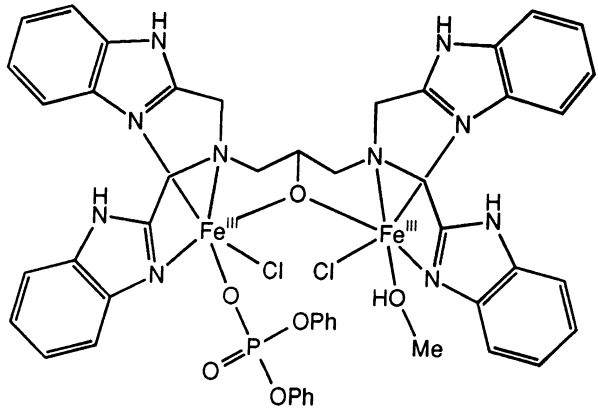

Figure 4. Molecular structure of $[Fe_2Cl_2(tbpo)\{O_2P(OPh)_2\}(CH_3OH)]^{2+}$ in **1**

The Fe^{III} atoms in this compound are coordinated by the heptadentate ligand tbpo$^-$. Each metal atom is bonded to two benzimidazole moieties, to one tertiary nitrogen atom as well as to the bridging alkoxo oxygen atom. The distorted octahedral environment of Fe(1) is completed by a chloro and a diphenylphosphato ligand. In contrast Fe(2) is coordinated by a chloro and a methanol ligand. Recently novel dinucleating ligands containing mixed phenolate and pyridine donors have been synthesized. Their compounds containing novel (μ-alkoxo)bis(μ-diphenylphosphato) and (μ-phenoxo)bis(μ-diphenylphosphato) bridges were crystallized and the spectroscopic, magnetic and bonding properties of the Fe(III)-Fe(III) pairs were studied[25].

The first heterodinuclear phosphate bridged iron(III)-zinc(II) model compound for the active site of PAP from kidney beans could be obtained by using the ligand 2,6-bis[bis(2-pyridylmethyl)aminomethyl]-4-methylphenol (Hbpmp)[26]. Fig. 5 shows the structure of the cation of $[Zn^{II}Fe^{III}(bpmp)(O_2P(OPh)_2)](ClO_4)_2 \cdot 1.5CH_3OH \cdot H_2O$ (2).

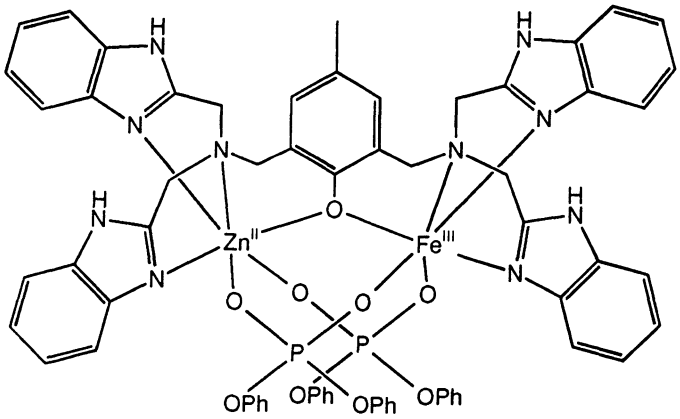

Figure 5. Molecular structure of the cation $[Zn^{II}Fe^{III}(bpmp)(O_2P(OPh)_2)]^{2+}$ in 2

The molecule contains a μ-phenoxo-bridged $Zn^{II}Fe^{III}$ unit in which the metal centers are additionally linked by two l-diphenylphosphato bridges. The nitrogen donors of the ligand bpmp$^-$ complete the octahedral environment of the two metal centers by facial coordination. The ZnKKKFe distance of 3.695 Å is significantly larger than in the carboxylate-bridged Zn^{II}-Fe^{III} (3.428 Å) complex [32], presumably as a result of the larger bite distance of phosphate. The ZnKKKFe distance resembles the value of 3.65 Å determined by EXAFS measurements on the kidney bean phosphatase in the presence of phosphate[8].

Based on these structural and spectroscopic results, we synthesized a whole series of Fe(II)-Fe(III), Fe(III)-Fe(III) and Fe(III)-Zn(II) model compounds containing pentadentate and heptadentate ligands with benzimidazole, methylimidazole and pyridine moieties and examined them for their dioxygen-activating properties and their phosphatase activity. Besides specific reactions with dioxygen, some of the diiron complexes with heptadentate pyridine and benzimidazole groups show peroxidase activity. Selective catalytic oxidation reactions with H_2O_2 show promising performances for the oxidation of alkanes to alcohols as well as to ketones, or of alcohols to aldehydes and ketones. For a review on previous work see[33].

3. Catechol Oxidases

Among the copper proteins hemocyanin and tyrosinase are the two prominent members with a single type 3 active site[34-36]. They are characterized by an antiferromagnetically coupled EPR-silent Cu(II) pair. A typical Cu(II) signal only appears after denaturation of the protein.

Hemocyanin is an oligomeric oxygen transport protein of molluscs and arthropods with a Cu(I) pair in the deoxy form first isolated and crystallized by Kubowitz[37]. In the X-ray structure of deoxyhemocyanin a CuKKKCu distance of 360 pm is found[38]. A distance of 340 pm is reported for oxyhemocyanin crystals, which are produced after binding of oxygen[39]. The oxygen is bonded as a Cu(II) peroxo complex, side-on in the μ-η^2:η^2-form[35,39]. The ligands of the two copper ions are two histidines at a short distance with a third histidine at a longer distance in a three-coordinate complex[38]. Apart from the protein absorption feature at 280 nm a relatively strong absorption at 350 nm (ε = 20.000) is observed in oxyhemocyanin which is assigned to a peroxo $\rightarrow$ Cu(II) CT band[43]. In the deoxy form the band disappears. Another absorption band is seen at 570 nm. It is also assigned to a peroxo $\rightarrow$Cu(II) CT transition, since it is only found in the oxy-form but not in the Cu(II) oxygen-depleted *met* form[40,41].

Here we report on two catechol oxidases from *Populus nigra*, first described by Trémolière and Bieth[42] and from *Lycopus europaeus*[43], which convert caffeic acid to quinones and melanines at injured cells. They are different enzymes in terms of molecular mass and amino acid composition, but with an identical reaction path involving a single type 3 copper center. We also report on model complexes which very convincingly support our view on the reaction path.

3.1. PREPARATION OF CATECHOL OXIDASES

The catechol oxidases were isolated according to a modified procedure developed by Fischer for the *Lycopus* enzyme[43]. All operations were performed at 4 °C. A typical preparation started with 40 g lyophilized leaves. The lyophilized leaves were suspended in 1.4 l buffer (0.05 M imidazole, 0.1 M sodium ascorbate, 0.3 % triton X -100) pH = 6.0 and homogenized with an Ultra-Turrax (6000 rpm) in the presence of 60 g polyvinylpyrrolidone (PVP, Sigma), in order to absorb low molecular mass phenolic compounds like caffeic acid, the natural substrate. The homogenate was centrifuged at 10000 x g for 1 h and the supernatant liquid was filtered through glass wool. A 1.5 fold volume of ethanol was slowly added to the solution and stirred for another 2 h. After 30 min of centrifugation at 10000 x g the precipitate was resuspended two times in 400 ml 0.05 M triethanolamine acetate at pH = 5.8 with 0.025 M sodium ascorbate under stirring for several hours. The solution was again centrifuged at 10000 x g. The clear supernatant was loaded onto a DEAE cellulose column (2 x 30 cm) at 40 ml/h. Catechol oxidase passed through and the active fractions were pooled, buffered to 0.05 M triethanolamine acetate (pH = 6.8) and loaded onto a column (2 x 20 cm) of Q sepharose FF (Pharmacia). The absorbed enzyme was eluted with a 0 - 0.8 M NaCl gradient at 40 ml/h. The active fractions were pooled and concentrated by ultrafiltration, (Amicon PM 10) to 10 ml. This enzyme solution was buffered to 0.05 M sodium phosphate at pH = 7.0 and subjected to gel permeation chromatography on a Sephadex G-100 superfine column (Pharmacia, 2 x 100 cm) with either 0.05 M sodium phosphate or triethanolamine acetate at pH 7.0. The slightly yellowish fractions were pooled and stored at 4 °C without loss of activity for several months.

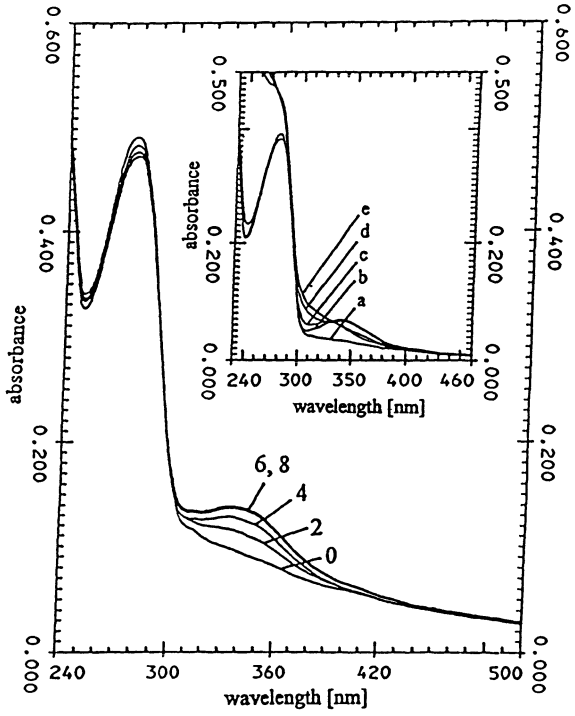

Figure 6. UV-Vis spectrum of catechol oxidase from *Lycopus* at pH 7 before and after addition of H_2O_2

3.2. PROPERTIES OF THE ENZYMES

The catechol oxidases of *Lycopus* (M_r = 40 kDa) and *Populus* (M_r = 56 kDa) are copper enzymes of type 3 which only catalyze the oxidation of catechols to quinones without acting on tyrosine. They are isolated in the antiferromagnetically coupled Cu(II)-Cu(II) *met* form and exhibit after addition of H_2O_2 an absorption band at 345 nm with ε-values of 3500 M^{-1} cm^{-1} and 3000 $M^{-1}cm^{-1}$. Saturation of the *Lycopus* enzyme is reached with 6 equivalents of H_2O_2, of the *Populus* enzyme with 80 equivalents.The new absorption band has to be assigned to a peroxo Cu(II) charge transfer transition and corresponds to that of the peroxo complexes of hemocyanin and tyrosinase, but with a much lower intensity comparable to that of laccase or ascorbate oxidase.

MALDI spectra of the catechol oxidases from *Lycopus* and black poplar display singly charged molecular ions with M_r of 39800 for the *Lycopus* monomer (M^+). They are detected as well as the multiply charged molecular ions $M^{2+}$and M^{3+} with signals at 20000 and 14000 Da, respectively. For the black poplar enzyme a M_r of 56000 Da is found. The multiply charged monomer molecular ions at 28000 and 18700 Da are also seen.

The electronic spectrum of the native enzyme from *Lycopus* in 0.05 M sodium phosphate buffer, pH 7.0 without and after addition of H_2O_2 is presented in Fig. 6. The protein part of the UV spectrum with the maximum at 280 nm depends on the presence of tyrosines, but there is no significant shoulder at 288 nm which would be expected in the

presence of higher amounts of tryptophan. The absence of a shoulder in the range of 345 nm in both native enzymes indicates that they are in the *met* form after preparation.

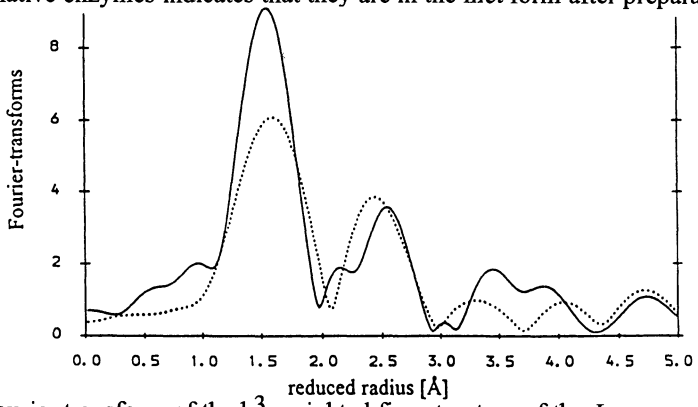

Figure 7. Fourier transform of the k^3-weighted fine structure of the *Lycopus* enzyme. Solid line: Fourier transform range $28 < k < 115$ nm^{-1}; dotted line: Fourier transform range $50 < k < 115$ nm^{-1}

Addition of H_2O_2 leads to a new absorption band at 345 nm with an ε-value of 3000 mol^{-1} cm^{-1} . Saturation is reached with 6 equivalents of H_2O_2. For the poplar enzyme 100 equivalents are needed. According to Solomonn et al. [40] the new absorption band at 345 nm has to be attributed to the oxy form of the catechol oxidase, caused by an O_2^{2-} →Cu(II) charge transfer transition. Such a CT band, however with a relatively high ε-value of 20000 mol^{-1}cm^{-1} after addition of H_2O_2, is also reported for hemocyanin and tyrosinase[35,41,44]. The insert shows that higher concentrations of H_2O_2 lead to a time dependent reaction with an isosbestic point and to inactivation indicating destruction of the peroxo complex. The band also disappears after gel filtration on Sephadex G 75. The original spectrum of the native *met* enzyme is obtained. Further addition of 2, 4, 6 and 8 equivalents of catechol (c - f) results in the appearance of a new absorption band at 390 nm belonging to the reaction product o-benzoquinone. The 345 nm absorption band disappears. Obviously all the H_2O_2 is reduced to H_2O.

The EXAFS data (Fig. 7) for both catechol oxidases[45] in the *met* form show a very short CuKKKCu distance of 293 pm as compared to 340 - 360 pm for the other type 3 Cu proteins, indicating μ-hydroxo bridges at the *met* enzymes.

3.3. MODEL COMPLEXES

Model complexes with CuKKKCu distances of 300 pm with two, three or four coordinating ligands (Fig. 8), one of them a bridging phenoxo group, show phenoxo σ Cu(II) charge transfer bands in the range of 400 to 460 nm. Those with 4 and 3 ligands do not exhibit an increased absorption in the range of 350 nm after addition of H_2O_2. In contrast, dinuclear complexes with only two ligands besides weakly bonded μ-aqua or μ-hydroxo ligands show a new absorption band at 345 nm. At the same time, a μ-hydroxo absorption band disappears at 315 nm. Catechol is oxidized by H_2O_2 as well as with O_2 in presence of the complex. The spectroscopic data indicate that two different bidentate binding sites exist for catechol and H_2O_2 resp. O_2. The electron transfer from catechol to oxygen requires simultaneous binding of both substrates and should occur without formation of a stable Cu(I) intermediate.

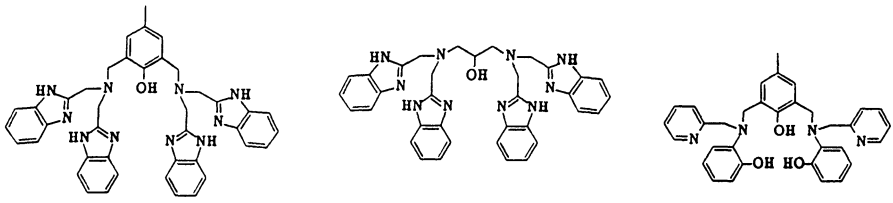

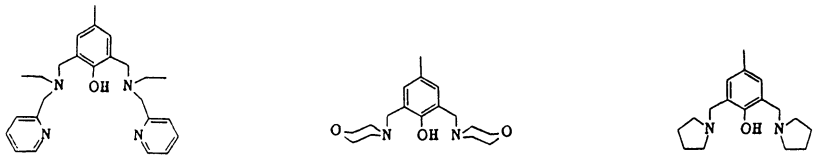

Figure 8. Ligands employed in the preparation of model complexes

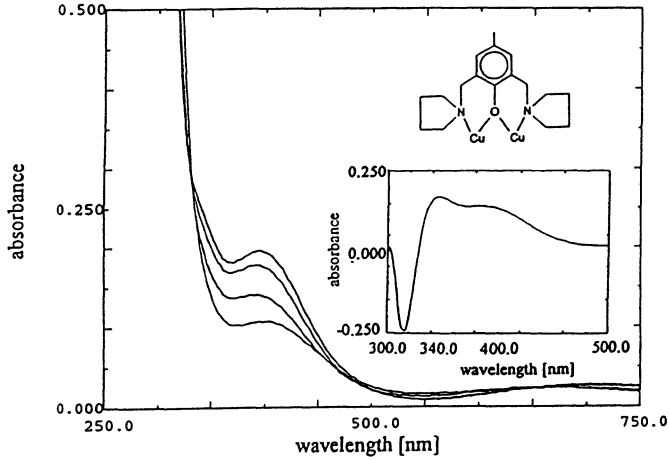

Figure 9. Absorption spectrum of the dipodal complex I (see insert; coord. sphere completed by water ligands) with and without 1, 2 and 3 equivalents of H_2O_2. Insert: Difference spectrum proving the new band at 345 nm and the increase of the absorption at 397 nm

The unexpectedly short CuKKKCu distance obtained from the EXAFS data induced studies on the spectral behaviour of dinuclear model complexes with CuKKKCu distances in the same range of 300 pm. Therefore we chose to prepare complexes containing dinucleating ligands with phenoxo or alkoxo bridges. In one of these compounds, $[Cu_4OCl_4(bpyrk)_2]\cdot 2CH_3OH$, a CuKKKCu distance of 298 pm is observed in the

$[Cu_2bpyrk]^{3+}$ subunit from X-ray crystal structure analysis. If H_2O_2 binds to these complexes in a similar way as in the enzyme, we should also expect a peroxo σ Cu(II) CT band (synthesis of the ligand hbpyrk see[46].

A series of dinuclear and tetranuclear model complexes were synthesized with various types of tri- penta- and heptadentate dinucleating ligands (Fig. 8), primarily with bridging phenolate or alcoholate.

Only the complex of copper(II) with the ligand hbpyrk (Fig. 9) with a μ-phenoxo → Cu(II) CT band at 403 nm and a μ-hydroxo → Cu(II) CT band at 315 nm shows a new band after addition of H_2O_2 and an increase in intensity of the phenoxo → Cu(II) CT transition which shifts from 403 nm to 396 nm. Saturation is reached at five equivalents, nearly identical with the saturation in the case of the *Lycopus* enzyme (Fig. 6). The insert demonstrates the maximum of the new band at 346 nm which should be the μ-peroxo → Cu(II) CT transition. Furthermore the μ-hydroxo → Cu(II) CT band, which is in the complex at 315 nm, disappears after addition of H_2O_2, as shown in Fig. 10. These results indicate that the peroxo complex is only formed, if besides the two complex ligands further coordination sites are occupied by weakly binding aqua or μ-hydroxo ligands. At least one μ-hydroxo ligand is displaced by the peroxo group.

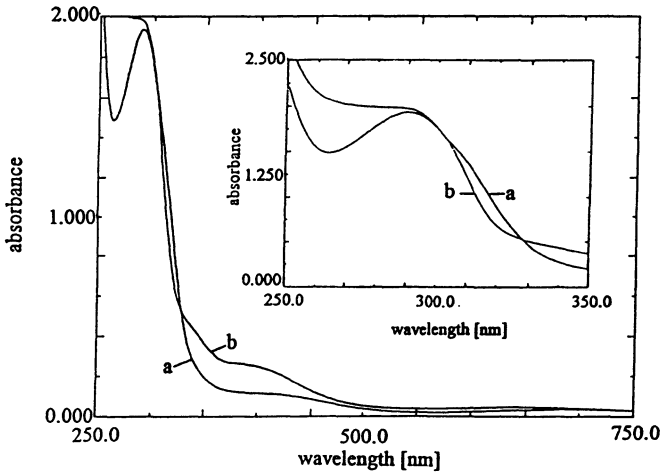

Figure 10. Absorption spectrum of complex I without (a) and after addition of 5 equivalents of H_2O_2 (b). Insert: Disappearance of the band at 315 nm after H_2O_2 addition

Fig. 11 shows that addition of one equivalent of catechol in the absense of H_2O_2 reduces the intensity of the phenoxo → Cu(II) band and also that of the μ-hydroxo CT band in the 305 - 315 nm range, indicating interaction with the complex. However, we do not see reduction of Cu(II) to Cu(I) which should cause complete loss the phenoxo CT band, nor do we see reduction of oxygen which should result in the formation of the peroxo complex with its increased intensity at 345 nm. In order to decide whether it is the same μ-hydroxo CT band which disappeared after addition of H_2O_2 we first added one equivalent of catechol. The difference spectrum (insert of Fig. 11) demonstrates a further reduction of the absorption in the 305 - 315 nm range and a shift of the maximum which let us suggest that a different group is replaced by catechol.

We investigated the time dependence of the oxidation of 5 equivalents catechol in the presence of 5 equivalents of H_2O_2 by the complex. The colour changes to brown; according to our investigations the melanine products (not identified) are obviously the same as those obtained without H_2O_2 in the presence of oxygen. Similar results are found with the complex of Teipel[47,48] in which the pyrrolidine is replaced by morpholine, synthesized in analogy to complex I.

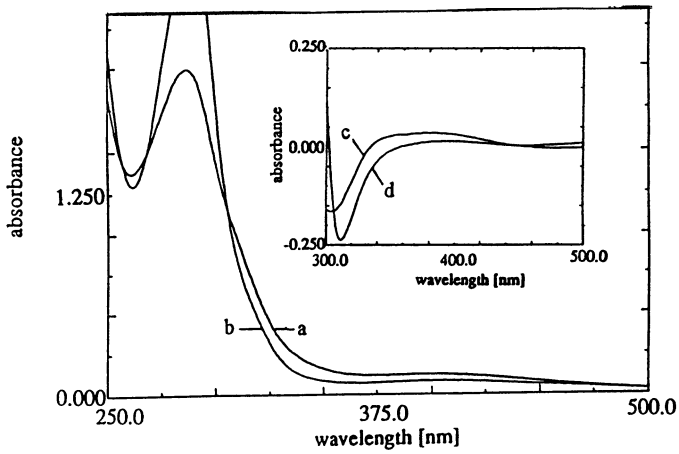

Figure 11. Absorption spectrum of complex I without (a) and after addition of 1 equivalent of catechol (b). Insert: The difference spectrum after addition of 1 equivalent of H_2O_2 (c) and after an additional equivalent of catechol (d)

It is remarkable that only those interact with H_2O_2 which have two coordination sites occupied by donor atoms of the dinucleating ligands and two coordination sites unoccupied, thus supplying additional binding sites for solvent molecules or substrates. The H_2O_2 uptake is connected with the appearence of the 345nm μ-peroxo → Cu(II) CT band and disappearance of a 315 nm μ-hydroxo → Cu(II) CT-band (s. insert of Fig. 10). This strongly indicates displacement of a μ-hydroxo group by a μ-peroxo group. For the reduction of the peroxo complex the enzyme as well as our model compound use catechol. This requires an additional binding site for catechol which transfers two electrons to the peroxo group. In order to examine the mechanisms of the activity of copper enzymes and copper complexes we have used and refined the method of molecular modeling[49]. For a recent review on copper-dioxygen complexes see[50].

4. Acknowledgements

The work reported in this account has been done in close cooperation with Prof. Herbert Witzel (Institute of Biochemistry, University of Münster) who was substantial for its biochemical part. The contributions of the doctoral students involved in this work are gratefully acknowledged. Among them are especially Friedhelm Ahlers, Bernd Bremer, Burkhard Eulering, Thomas Klabunde, Rainer Kruth, Michael Körner, Cetin Nazikkol, Stefan Priggemeyer, Jörg Reim, Annette Rompel, Klaus Schepers, Michael Schmidt, Norbert Sträter, Hildegard Suerbaum, Stephan Teipel, Frank Wiesemann, Frank Zippel.

Fruitful cooperation with the groups of Dr. H.-F. Nolting, Hamburg (EXAFS), Prof. F. Hillenkamp, Münster (MALDI), Prof. W. Haase, Darmstadt (magnetochemistry), and Prof. W. Müller-Warmuth (Mφssbauer) is gratefully acknowledged. The work was supported by the Deutsche Forschungsgemeinschaft and the Fonds der Chemischen Industrie.

4. References

(1) Doi, K.; Antanaitis, B.L.; Aisen, P. *Struct. Bonding* **1988**, *70*, 1.
(2) Que Jr., L.; True, A.E. *Prog. Inorg. Chem.* **1990**, *38*, 97.
(3) Vincent, J.-B.; Olivier-Lilley, G.L.; Averill, B.A. *Chem. Rev.* **1990**, *90*, 1447.
(4) Scarrow, R.C.; Pyrz, J.W.; Que Jr., L. *J. Am. Chem. Soc.* **1990**, *112*, 657.
(5) Holz, R.C.; Que Jr., L.; Ming, L.-J. *J. Am. Chem. Soc.* **1991**, *114*, 4434.
(6) Wang, Z.; Ming, L.-J.; Que Jr., L.; Vincent, J.B.; Crowder, M.W.; Averill, B.A. *Biochemistry* **1992**, *31*, 5263.
(7) True, A.E.; Scarrow, R.C.; Randall, C.R.; Holz, R.C.; Que Jr., L. *J. Am. Chem. Soc.* **1993**, *115*, 4246.
(8) Priggemeyer, S.; Eggers-Borkenstein, P.; Ahlers, F.; Krebs, B.; Henkel, G.; Körner, M.; Witzel, H.; Nolting, H.-F.; Hermes, C. *Inorg. Chem.* **1994**, *33*, in press.
(9) Aquino, M.A.S.; Lim, J.-S.; Sykes, A.G. *J. Chem. Soc. Dalton Trans.* **1992**, 2135.
(10) Aquino, M.A.S.; Lim, J.-S.; Sykes, A.G. *J. Chem. Soc. Dalton Trans.* **1994**, 429.
(11) Dietrich, M.; Münstermann, D.; Suerbaum, H.; Witzel, H. *Eur. J. Biochem.* **1991**, *199*, 105.
(12) Mueller, E.G.; Crowder, M.W.; Averill, B.A.; Knowles, J.R. *J. Am. Chem. Soc.* **1993**, *115*, 2974.
(13) Holmes, M.A.; Trong, I.L.; Turley, S.; Sieker, L.C.; Stenkamp, R.E. *J. Mol. Biol.* **1991**, *218*, 583.
(14) Nordlund, P.; Eklund, H. *J. Mol. Biol.* **1993**, *232*, 123.
(15) Rosenzweig, A.C.; Frederick, C.A.; Lippard, S.J.; Nordlund, P. *Nature* **1993**, *366*, 537.
(16) Hayman, A.R.; Cox, T.M. *J. Biol. Chem.* **1994**, *269*, 1294.
(17) Sträter, N.; Fröhlich, R.; Schiemann, A.; Krebs, B.; Körner, M.; Suerbaum, M.; Witzel, H. *J. Mol. Biol.* **1992**, *224*, 511.
(18) Beck, J.L.; De Jersey, J.; Zerner, B.; Hendrich, M.P.; Debrunner, P.G. *J. Am. Chem. Soc.* **1988**, *110*, 3317.
(19) Suerbaum, H.; Körner, M.; Witzel, H.; Althaus, E.; Mosel, B.-D.; Müller-Warmuth, W. *Eur. J. Biochem.* **1993**, *214*, 313.
(20) Stahl, B.; Klabunde, T.; Witzel, H.; Krebs, B.; Steup, M.; Karas, M.; Hillenkamp, F. *Eur. J. Biochem.* **1994**, *220*, 321.
(21) Klabunde, T.; Stahl, B.; Suerbaum, H.; Hahner, S.; Karas, M.; Hillenkamp, F.; Krebs, B.; Witzel, H. *Eur. J. Biochem.* **1994**, *220*, in press.
(22) Bränden, C.-I. **1980** *Quart. Rev. Biophys.*, *13*, 317.
(23) Kauzlarich, S.M.; Teo, B.K; Zirino, T.; Burmann, S.; Davis, J.C.; Averill, B.A. *Inorg. Chem.* **1986**, *25*, 2781.
(24) Bremer, B.; Schepers, K.; Fleischhauer, P.; Haase, W.; Henkel, G.; Krebs, B. *J. Chem. Soc., Chem. Commun.* **1991**, 510.
(25) Krebs, B.; Schepers, K.; Bremer, B.; Henkel, G.; Althaus, E.; Müller-Warmuth, W.; Griesar, K.; Haase, W. *Inorg. Chem* **1994**, *33*, 1907.

(26) Schepers, K.; Bremer, B.; Krebs, B.; Henkel, G.; Althaus, E.; Mosel, B.; Müller-Warmuth, W. *Angew. Chem.* **1990**, *102,* 582; *Angew. Chem., Int. Ed. Engl.* **1990**, *29*, 531.
(27) Drüeke, S.; Wieghardt, K.; Nuber, B.; Weiss, J.; Fleischhauer, H.P.; Gehring, S.; Haase, W. *J. Am. Chem. Soc.* **1989**, *111*, 8622.
(28) Armstrong, W.H.; Lippard, S.J. *J. Am. Chem. Soc.* **1985**, *107*, 3730.
(29) Turowski, P.N.; Armstrong, W.H.; Roth, M.E.; Lippard, S.J. *J. Am. Chem. Soc.* **1990**, *112*, 681.
(30) Yan, S.; Cox, D.D.; Pearce, L.L.; Juarez-Garcia, C.; Que Jr., L.; Zhang, J.H.; Connor, C.J. *Inorg. Chem.* **1989**, *28*, 2507.
(31) Norman, R.E.; Yan, S.; Que Jr., L.; Backes, G.; Ling, J.; Sanders-Loehr, J.; Zhang, J.H.; O'Connor, C.J. *J. Am. Chem. Soc.* **1990**, *112*, 1554.
(32) Borovik, A.S.; Papaefthymiou, V.; Taylor,L.F.; Anderson, O.P.; Que Jr., L. *J. Am. Chem. Soc.* **1989**, *111*, 6183.
(33) Feig, A.L.; Lippard, S.J. *Chem. Rev.* **1994**, *94*, 759.
(34) Malmström, B.G. *Annu. Rev. Biochem.***1982**, *51*, 21.
(35) Solomon, E.I.; Baldwin, M.J.; Lowery, M.D. *Chem. Rev.* **1992**, *92*, 521.
(36) Feiters, M.C. *Comments Inorg. Chem.* **1990**, *11*, 131.
(37) Kubowitz, F. *Biochem. Z.* **1938**, *299*, 32.
(38) Volbeda, A.; Hol, W. G. J. *J. Mol. Biol.* **1989**, *209*, 249.
(39) Magnus, K.; Ton-That, H. *J. Inorg. Biochem.* **1992**, *47*, 20.
(40) Eickman, N.C.; Himmelwright, R.S.; Solomon, E.I. *Proc. Natl. Acad. Sci. USA* **1979**, *76*, 2094.
(41) Himmelwright, R.S.; Eickman, N.C.; LuBien, C.D.; Lerch, K.; Solomon, E.I. *J. Am. Chem. Soc.* **1980**, *102*, 7339.
(42) Trémolère, M.; Bieth, J.B. *Phytochemistry* **1984**, *23*, 501.
(43) Fischer, H. *Ph.D. Thesis*, University of Münster, 1991.
(44) Jolley, R.J. Jr.; Evans, L.H.; Makino, N.; Mason, H.S. *J. Biol. Chem* .**1974**, *249*, 335.
(45) Rompel, A.; Fischer, H.; Meiwes, D.; Büldt, K.; Nolting H.-F.; Hermes, C.; Krebs, B.; Witzel, H. *Eur. J. Biochem.*, in press.
(46) Reim, J.; Krebs, B. *Angew. Chem.* **1994**, *106*, 2040; *Angew. Chem. Int. Ed. Engl.* **1994**, *33*, 1969.
(47) Teipel, S. *Ph.D. Thesis*, University of Mónster, 1993.
(48) Bremer, B.; Schepers, K.; Teipel, S.; Krebs, B. *J. Inorg. Biochem* .**1991**, *43*, 544.
(49) Wiesemann, F.; Teipel, S.; Krebs, B.; Höweler U. *Inorg. Chem.* **1994**, *33*, 1891.
(50) Kitajima, N.; Moro-oka, Y. *Chem. Rev.* **1994**, *94*, 737.

MOLYBDENUM - COPPER ANTAGONISM

DIMITRIS P. KESSISSOGLOU
Department of General & Inorganic Chemistry,
Aristotle University of Thessaloniki,
54006 Thessaloniki, GREECE

1. Indroduction

Antagonism is the Greek word which best describes the struggle between two opposite sites both wanting to overrule. Many scientists use the synonymous word competition but if we try to analyse the two words I think the distinct difference is on the results. The *Antagonism* stresses who is the winner and who is the loser. In the competition the rank of the competitors is also of interest and more related with the Greek word *Synagonism.*

Table 1. Oxidation States of some metals at pH=7 taking into account the formation of Hydroxides

V	>-3	-2 - -3	-1 - -2	0 - -1	0	0 - 1	1 - 2	2 - 3	>3
	Ca^{2+}				Ca				
					Cu	Cu^{+}	Cu^{2+}		
	Mg^{2+}				Mg				
				Mo^{3+} MoO_2	Mo	$MoO_2^{=}$			
			Mn^{2+}	Mn^{3+}	Mn	MnO_2		MnO_3	$MnO_4^{=}$ MnO_4^{-}
					Ni	Ni^{2+}			Ni^{3+}
				Fe^{2+}	Fe	Fe^{3+}			FeO_4
			Cr^{3+}	Cr^{2+}	Cr		$CrO_4^{=}$		
		V^{3+}	V^{2+} VO^{2+}	HVO_4^{-}	V				
					Co	Ni^{2+}	Co^{3+}		CoO_2
				Zn^{2+}	Zn				

This truth is quite obvious in everyday life and chemistry maybe is the science where *antagonism* is an essential procedure. Electrochemical series is based on the *antagonism* of metals to kick out other metals from their compounds but the same time the competition of the elements allow us to regulate an electrochemical reaction. In biology *antagonism* is so important making the whole procedure the crucial point for the existence of the life.

D.P. Kessissoglou (ed.), Bioinorganic Chemistry, 385-400

In this report the interest is focused on the *antagonism* between two metal ions, molybdenum and copper but before we try to frame this particular procedure it is of interest to give some principal informations on metal ions *antagonism* of biological interest.

The elements, except of C, H, N and O, essential for the synthesis of biological macromolecules, which have essential functional potential are: i) Na, K, Ca for the transmission of information, ii) Fe, Cu, Zn, Mo for catalysis, iii) Fe, Mn, Cu for transfer of electrons and iv) Ca, P, Si for the building of solid structures. Of course there is the question why living systems use only these metal ions and reject the rest ones as toxic. One restriction is the redox potential in water at pH=7 which range from -0.42 to +0.78 V and so a transition metal ion has a small range of stable oxidation states e.g. Fe(+2, +3), Cu(+1, +2) etc. (Table 1)

2. Effective stability constant

A genaral mechanism describing the uptake of a certain metal ion M^{n+} involves a series of reactions which are interrelated, as it is obvious at the following scheme for plants.

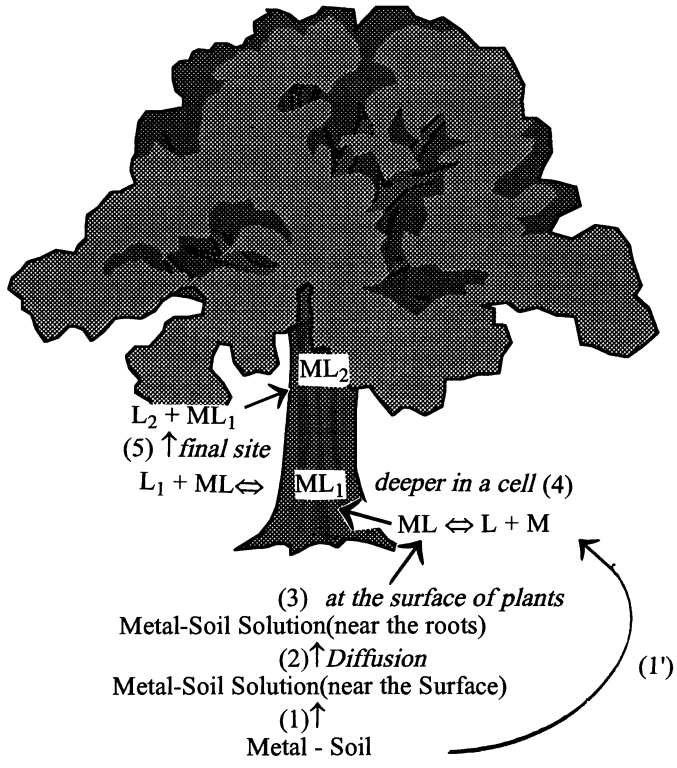

Scheme 1. Some pathways for the uptake and incorporation of metals and ligands in soil.

Step 1 describes the presence and then the solubility in water of metal ions in the soil. In some cases is activ also step 1' when the plant sends out a ligand L which interact with metal ion giving a soluble complex. Step 2 is related with a diffusional procedure and depends on the nature of metal salt, on the distance to the roots and on the nature of the soils. Steps 1', 3, 4, and 5 are complexing reactions under thermodinamic or kinetic biological control. In some of these steps may occur redox reactions as is the case of MoO_4^{2-} and many of these redox steps are irreversible. Many of the uptake mechanism are not specific, given the possibility of *antagonism.* The affinity of the alkaline-earth and first-series transition metal ions towards organic carboxylates, phosphates, sulphates etc represented by the stability constants of their complexes shows little selectivity. For istance, leaves from sugar cane bind Cu^{2+} , Zn^{2+}, and Mn^{2+} with a logK 1.87, 1.95 and 1.79 respectively. Many plants concetrate ions on their surfaces some essential and some biological toxic. The overall process explains why non-essential elements may antagonise with the essential elements and may preferentially captured.

In order to understand what affect the selective uptake of metal ions and consequently the antagonism of metal ions is necessary to examine the terms which involve into these processes.

To a first approximation we can consider that when any organic surface is immersed in an aqueous media, e.g. roots in soil the uptake is based upon equilibrium considerations, i.e.

Amount bound varies as $K_{ML}x$ [concentration of free ion] where K_{ML} is the *effective stability constant* of the 1:1 complex of each metal ion with the ligands at the surface.

The *effective stability constants* (K_{ML}^{eff}) are the critical values which control the amount of metal ions bound to biological systems. The *effective stability constant* (K_{ML}^{eff}) is related to convetional stability constant by the equation

$$\log K_{M1L1}^{eff} = \log K_{M1L1} - \log a_L - \log a_M$$

considering competitive complex formation for two metals M_1 and M_2 and two ligands L_1 and L_2 and when only M_1L_1 and M_2L_1 complexes are formed.

$$\{\log K_{M1L1}^{eff} = \log K_{M1L1} - \log[\,1 + \sum_{i=1}^{i=n} K_{M1L2}\,[L_2]^i\,\} - \log\{\,1 + \sum_{i=1}^{i=n} K_{L1}\,[H^+]^i\,] +$$

$$+ K_{M2L1}\,[M_2]\}$$ and for a protic acid(LH)

$$\log K_{M1L1}^{eff} = \log K_{M1L1} - \log\{\,1 + K_{L1H}\,[H^+]^+\,\} - \log\{\,1 + \Sigma K_{L1}\,[H^+] +$$

$$K_{M2L1}[M_2]\} - \log[1 + K_{M1L2}\,[L_2]\}$$

Disregarding acidity effects assuming that the proton does not complete for the site then

$M_1 + M_2 + L_1 + L_2 \rightarrow M_1L_1 + M_2L_2$

when M_1L_2 excluded by lack of M_1, removed by L_1

M_2L_1 excluded by lack of L_1 , removed by M_1

The generation of this circumnstance can be approached in terms of effective stability constants

$\log K_{M1L1}^{eff} = [M_1L_1] / [M_1]^* \times [L_1]^*$

where $[M_1]^*$ is the concentration of M_1 not bound to L_1 and $[L_1]^*$ is the concetration of L_1 not bound to M_1, i.e. in each case it is a sum which one can easily derive as
$[M_1]^* = [M_1]\{ 1 + K_{M1L2} [L_2]\}$

$[L_1]^* = [L_1]\{ 1 + K_{M2L1}[M_2]\}$

if binding of M_2 and L_1 is to be avoided we have to decrease $[M_2]$ to such an extent that $K_{M2L1}[M_2]$ becomes smaller than say 1% to be negleted in the expression for $[L_1]^*$. This can be done by preferential binding of M_2 to L_2. In this case $M_2 = [M_2L_2] / [L_2] \times K_{M2L2}$ one obtains $K_{M2L1} [M_2L_2] / K_{M2L2} [L_2] < 10^{-2}$

3. Selectivity of the Uptake

The different ways of achieving selective binding based on:

3.1.1 *Charge Type:* In aqueous media V, Cr, Mn and Fe normaly found in oxidation states +3, Mn, Fe, Co, Ni, Cu and Zn in oxidation states +2. Appropriate biological ligands for the M^{3+} ions are small anoins such as R_2N^-, RO^-. Highly negative charged ligands having RO^- donors, which occurs in hydroximates, enolates, phenolates are useful in the selective uptake of Fe^{3+} and Mn^{3+}. Vanadium and Molybdenum in the second row are probably handled initially as oxoanions, VO_4^{3-} and MoO_4^-.
3.1.2 *Ion Size.* Selection by complexation based on size is used by biological systems. The ligands are often cyclic and create a central cavity which fits most closely a particular cation size. Recently of so-called *crown-ethers* and other macrocyclic ligands strongly favour the complexation of one particular ion. Magnesium is taken up in a porphyrin-type cyclic ligand of fixed geometry and cavity size, chlorophyll in contrast with calcium which is excluded due to its large size. Another method to have size selectivity based on covalent ligand design is by protein folding. Size selectivity is sensitive and affect ions of quite similar size e.g. Mn^{2+}(0.75 Ä radius) $\log K_{[MnEDTA]}$=14.1, Zn^{2+}(0.60 Ä radius) $\log K_{[ZnEDTA]}$=16.2.
3.1.3 *Liganding Atom.* This mechanism is based on the affinity of the hard ions for oxygen-donor ligands, while the soft ions prefer to coordinate to sulfur or nitrogen donors. The Irving-Williams order of stability shows that the divalent transition metals form complexes that may differ in their thermodynamic stability by several orders of magnitude if the liganding atoms are appropriately chosen. It is known that outside the cell most donors are of the O-donor variety and RSH ligands are oxidized away. This means that uptake inside/outside selectivity can be based on soft/hard discrimination Cu/Zn *antagonism.* Copper is bound by 4 nitrogen as in superoxide dismutase in the inside cells or 4(N/S) sites as in plastocyanin-like proteins outside cells, overcoming *antagonism* with zinc which is more available. Selectivity by donor atom type is very powerfull if the concentrations of ligands and metal are controlled.
3.1.4 *Preferential Coordination Geometry.* The most characteristic example describing the preference of certain metal ions for coordinating sites of particular geometry is the metalloenzyme *superoxide-dismutase.* In the blue-green *superoxide Dismutase* there is simultaneous zinc and copper selectivity, the zinc site is close to tetrahedral and the copper site shows a distorted tetragonal geometry. In the wine-red Mn(III)-SOD the manganese ion prefers tetragonal geometry, while in yellow Fe(III)-SOD the iron prefers tertrahedral or octahedral coordination geometries. We have to notice that while the metal ions have

preferred geometries, it is the organic ligands which generate holes of perticular sizes and shapes.

3.1.5 *Spin-pairing stabilization.* For transition metal ions there is a possibility to increase selectivity based on a spin-state change of a metal on binding to some ligands.. The selection of iron in preference to copper in porphyrins could perhaps be based on the low-spin stabilisation of Fe(II). It is expected that strong N/S-donor ligands will bind to low-spin Co(III)>Mn(III)>Fe(III) while the order for low-spin divalent ions will be Fe(II)>Co(II)>Mn(II).

3.1.6 *Binding in clusters.* Generally, clusters are stabilised by highly charged cations since they involve highly charged anions, O^{2-} and S^{2-} and in biology are only observed in proteins. Clusters are usually found to anion protein sidechains

4. Molybdenum-Copper Antagonism

4.1. Mo, Cu, S CHEMISTRY

The antagonistic function of the molybdenum ion with regard to copper in humans and animals[3] has raised the interest in the interaction of Cu ions with ligated molybdenum species. Most of the Mo-Cu mixed-metal complexes reported till now(apo ergasia 12) employ mainly $[MoS_4]^{2-}$ as the source of the molybdenum component. The so called *Molybdenum-Copper Antagonism* is probably enhanced by the synergic effect of sulfur as sulfate or thioamino acids(απο εργασια Inorg Chim. Acta 1992,493). The compounds having a $[MoO_4]^{2-}$ moiety, the major source for free molybdenum in biological systems at pH=7, interacting with Cu(II) ions could give a new insight in the understanding the metabolic disturbances and diseases in humans and animals caused by deficiency(Growth depression; defective keratinization; hyperocipurinaemia) or excess[Anaemia; persistent dysentery(grazing animals); gout-like syndrome(USSR)] of molybdenum due to interference with Cu(II) absorption. Studies for understanding this Mo-Cu interaction a series of compounds with $[MoS_4]^{2-}$ and Cu(I) have been prepared and can be classified according to their Mo:Cu ratio.

4.1.2. Binuclear Complexes with Mo:Cu 1:1 Ratio: The complexes have the core

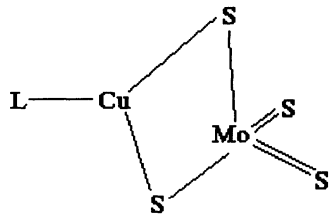

with the Mo ion in an oxidation state 6+, while the Cu(I) atom is also coordinated to thio containing ligands or cyano-ions[5,6](e.g. $CuSR(MoS_4)]^{2-}$ or $CuCN(MoS_4)]^{2-}$. The crystal structure of $(t\text{-}BuNC)_4Mo(\mu\text{-}t\text{-}BuS)_2CuBr$ have shown a distorted octahedral geometry around Mo(II) and an almost exact trigonal-planar coordination environment around Cu(I) ion[7].

4.1.3. Trinuclear Complexes with Cu:Mo 2:1 Ratio: For this ratio two types of metal arrangments have been observed, the a) "linear" [6-8] and the b) "bent" [9]. In the linear arrangment Mo occupies the cetral position with an tetrahedral geometry around Mo atom

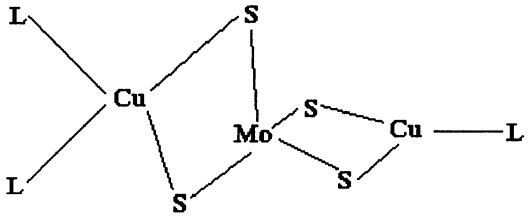

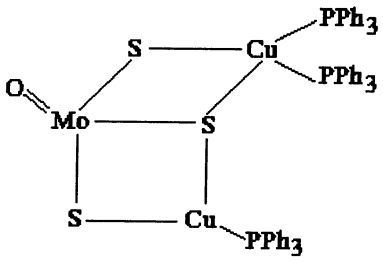

while the Cu atoms adopt trigonal planar or tetrahedral environment. In the compound $[Cu_2Br_2(MoS_4)]^{2-}$ the two Br atoms can be substituded with CN groups forming a zig-zag polymer with $Cu(\mu_2\text{-}CN)_2Cu$ bridges. For the "bent" arrangment the compounds reported[9] contain the $[MoOS_3]_2$ core.

4.1.4. Tetranuclear Complexes with Cu:Mo 2:2, 3:1 and 1:3 Ratio: The only known tetranuclear geometry with 2:2 ratio is the linear observed in the structure of $[\{(C_5H_{10}NO)_2Mo(\mu_2\text{-}S)_2Cu\text{-}\mu_2\text{-}Cl\}_2]$ compound[10].

The 3:1 ratio propably is the most favour for more than one arrangements. In the "open" arragment[11,12] the thimolybdate moiety $[MoS_4]^{2-}$ acts as tetradentate ligand with Cu-Mo-Cu angle of 90°.

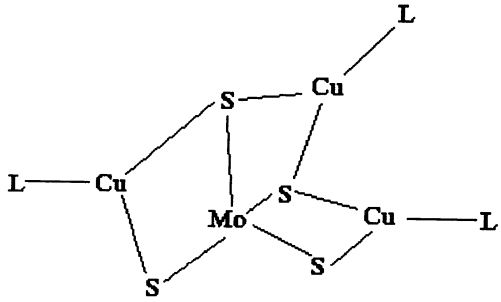

The compound $[Cu_3Cl_3(MoS_4)]^{2-}$ is the most characteristic compound. Going from the "open" to the "bent" structure we observe a distinct difference. Only compounds having the $[MoS_3O]^{2-}$ moiety have been reported[9,13] in which the terminal oxygen remain unbound

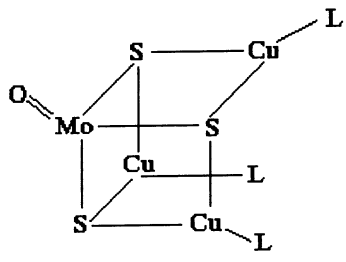

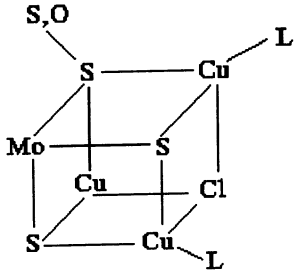

Finally for the "closed" structure -the cubane-like core- having 3 Cu and 1 Mo atoms both species $[MoOS_3]^{2-}$ and $[MoS_4]^{2-}$ have been reported[14] e.g. $[Cu_3Cl_3MoS_3O]^{2-}$, $[Cu_3MoS_3Cl](PPh_3)_3O$.

For the Cu:Mo 1:3 ratio the only compound reported up today is this having the $[Mo_3CuS_4]$ core[15]

4.1.5. Pentanuclear Complexes with Cu:Mo 4:1 Ratio: Only "open" structures were isolated with the thiomolybdate species $[MoS_4]^{2-}$ acting as tetradentate ligand

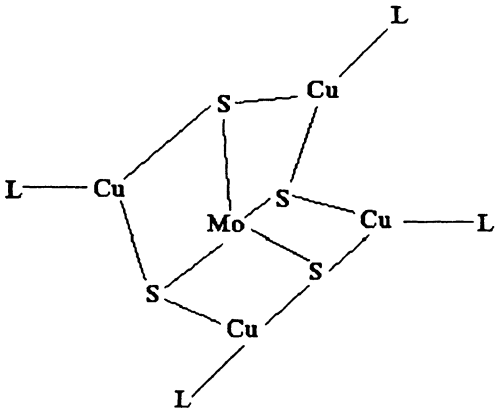

and in which the presence of Cl, or Br ligands leads to the formation of a polymeric linear chain[16] e.g. $[Cu_4Br_4MoS_4]^{2-}$

4.1.6. Hexanuclear and Heptanuclear Complexes with Cu:Mo 5:1 or 6:1 Ratio: Only one example for each ratio have been reported[17,18]. For the ratio 5:1 the compound $[Cu_5Cl_7MoS_4]^{4-}$ shows a double cubane-like structrure

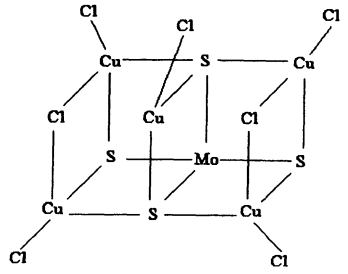

while for the compound $[Cu_6Cl_9MoS_4]^{5-}$ the overall geometry could be described as a distorted octahedron of coppers encapsulating the tetrahedral thiomolybdate

4.2. Mo, Cu, O CHEMISTRY

While the chemistry of Mo(VI) thiometallates in interaction with Cu(I) and Cu(II) ions has been well established no reports about Mo(VI)-Cu(II) complexes with rich in oxygen environment there are in the literature. Taking this challange to explore this interaction we have chosen as ligands rich hydroxy schiff-bases.

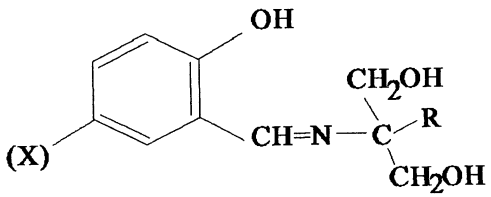

Mo and Cu Schiff-bases complexes represent an important and interesting class of coordination compounds. Schiff-bases containing polyfunctional groups have not only produced stable metal complexes but these ligands and their metal complexes have played a significant role in the domain of model systems of biological interest. Mo(VI) and Cu(II) metal ions have more or less a significant role in many metalloenzymes.

The higher oxidation states of molybdenum complexes contain the molybdenum oxo group $[MoO_2]^{2+}$. It is well known[18-20] that catalytic reactions of the molybdenoenzymes involve oxidation states Mo(VI), Mo(V) and Mo(IV) during the process of electron transfer to or from the redox centers. Simple molybdenum(VI) coordination compounds contain the *cis*-dioxo $[MoO_2]^{2+}$ cation. Bidentate, tridentate and tetradentate Schiff-base-$[MoO_2]^{2+}$ complexes with six-coordinate environment have been reported[21] The monomeric form of $MoO_2L{\cdot}A$(L=Schiff-base, A=monodentate ligand) is the dominant for tridentate Schiff-bases.

4.2.1. Synthesis. The synthesis of molybdenum compounds can be achieved via the pseudo template reaction of Mo(VI) acetylacetonate with salicylaldehyde, 5-Bromo-Salicylaldehyde or 5-chloro-salicylaldehyde and 2-amino-2-methyl-1,3-propanediol or 2-amino-2-ethyl-1,3-propanediol, in methanol. The reactions involve deprotonation of the ligand by the MoO_2 $(acac)_2$ without using a base, e.g.,

$$XC_6H_3(OH)CHO + H_2NC(R)(CH_2OH)_2 + MoO_2(acac)_2 \xrightarrow{MeOH} MoO_2[XC_6H_3(O)CH{=}NC(R)(CH_2O)(CH_2OH)(CH_3OH) \quad (1)$$

The molybdenum compounds are yellow crystalline solids that appear to be air and moisture stable. Reaction of MoO_2(5-Cl-Hsaladhp)(MeOH)[H_3saladhp=1,3-Dihydroxy-2-methyl-2-(salicylideneamino)propane] with $Cu(CH_3COO)_2$ in methanol/acetonitrile 1:1, yields the mixed metal $Cu_2Mo_2O_4$[5-Cl-Ph(O)CH=NC$(CH_3)(CH_2O)_2]_2(CH_3O)_2$ **(1)** cluster with a $Mo_2Cu_2O_4$ cubane like core[22]. (Figure 1)

$$2\ MoO_2[5\text{-}Cl\text{-}Ph(O)CH{=}NC(CH_3)(CH_2O)(CH_2OH)](CH_3OH) + 2Cu(CH_3COO)_2$$

$$\xrightarrow{MeOH} Cu_2Mo_2O_4[5\text{-}Cl\text{-}Ph(O)CH{=}NC(CH_3)(CH_2O)_2]_2(CH_3O)_2 + 4CH_3COOH$$

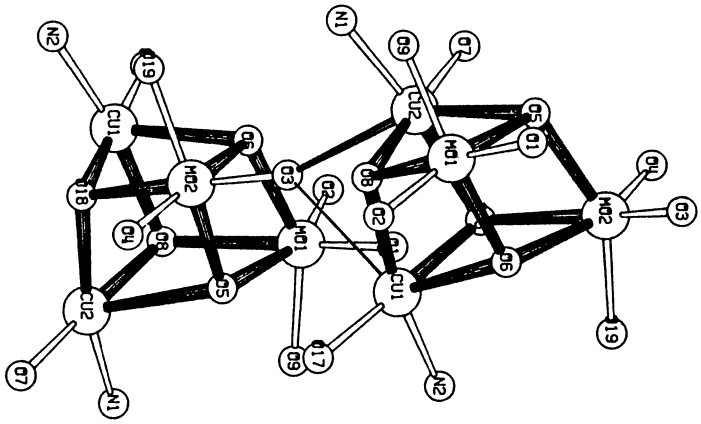

Figure 1. The crystal structure of **(1)**

4.2.2. Structure. The $Mo_2Cu_2O_4$ core can be described as a strongly distorted cube in which four corners are occupied by two copper and two molybdenum atoms. The cube is completed by four oxygen atoms from the two Schiff-base and two methoxy ligands. The copper atoms are bridged by the alkoxy oxygen atoms of the saladhp ligand with a Cu...Cu distance 2.951 Å and the molybdenum atoms, by the methoxy oxygen atoms with a Mo....Mo distance of 3.528 Å; the Mo and Cu atoms are connected by one methoxy and one alkoxy oxygen atom with an average Mo....Cu distance of 3.429 Å. In mixed Mo-Cu compounds with a Cu_3MoS_3Cl cubane like core the Cu...Cu distances are quite longer(3.10 -3.19 Å) whereas the Mo....Cu distances are quite shorter(2.68-2.74 Å). The Mo...Mo distances of 3.528 Å is more than 0.6 Å longr than those observed in complexes with Mo_3CuS_4 or Mo_4S_4 cubane like core. One of the most intersting and unsual features of this structure is the dihedral angle of 150.8 ° between the two O(8) - Cu- O(18) planes; this is the first example of a cubane-like complex containing a triply alkoxo-bridged roof-shaped Cu(II) dimmer with a dihedral angle differing so greatly from 180 °. Moreover, the dihedral angle of the two O(5)-Mo-O(6) planes was found to be 168.1 °. The O(3)atom of the Mo=O moiety has a contact to a neighboring cube through the Cu(2)[Cu(2)-O(3) =2.640 Å] atom, affording an infinite-chain arrangement.

Reflux of **(1)** with excess of bipyridyl in acetonitrile yields pale blue-green crystals of the tetranuclear cluster, $CuMo_3O_8[5\text{-}Cl\text{-}Ph(O)CH{=}NC(CH_3)(CH_2O)(CH_2OH)]_2(bpy)_2$. This procedure was successful only with the 5-Cl and 5-Br saladhp analogue. The X-ray structure of **(2)** confirms the presence of a trinuclear unit $[Mo_3O_8]^{2-}$ coordinatively bound to $[Cu(bpy)]^{2+}$ ion(Figure 2).

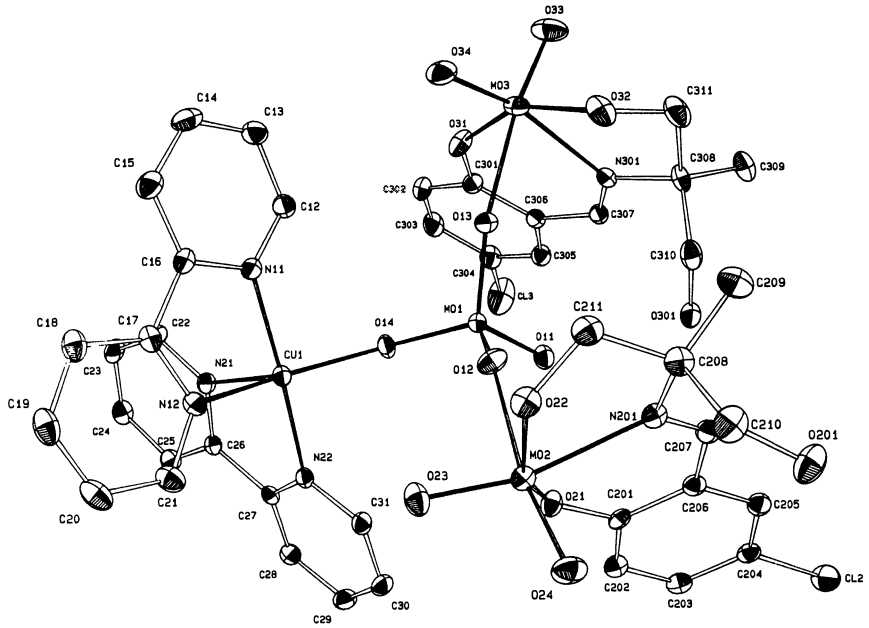

Figure 2. The crystal structure of **(2)**

The molybdenum part of the structure may be described in terms of three oxo-bridged molybdenum centers, alternating one tetraoxomolybdate center $[MoO_4]^{2-}$, and two six co-ordinated $[MoO_2$(schiff-base)] moieties. The two oxo-groups of the capping $[MoO_4]^{2-}$ unit interact with the schiff-base co-ordinated Mo atoms at an average distance of 2.22 Å. The third oxo group of the tripodal $[MoO_4]^{2-}$ tetrahedron bridges the $[Mo_3O_8]^{2-}$ unit with the $[Cu(Bpy)]^{2+}$ ion, possessing one site in the equatorial plane of the trigonal bipyramidal Cu^{2+} coordination environment. The Mo-O(alkoxy) 1.915 Å, Mo-O(phenoxy) 1.971 Å(average) and Mo-N, 2.229 Å(average) distances of the schiff-base are consistent with the Mo-O and Mo-N distances of the monomer analogue. It is noteworthy that the sum of the trans Mo-O distances of the $[MoO_2$(saladhp)] units are almost identical (3.876-3.998 Å) with a mean value of 3.933 Å. While the octahedrons around each Mo(schiff-base) units show a strong *cis*-distortion the lack of any elongation or depression along one of the axis of the octahedron is a strong evidence that Mo keep a d^0 configuration with a Mo(VI) oxidation state. The phenolate and the coordinated aliphatic oxygens occupy *trans* positions of the octahedron. The O(14) bridging the Mo and Cu unit forms an angle of 140.6(2) ° while the angles for the oxygens connecting the Mo(1) with Mo(2) and Mo(3) are 145.5(2)° and 161.2(2)° respectively. The $[MoO_4]^{2-}$ moiety shows an almost ideal tetrahedral geometry with the O(i) - Mo(1) - O(j) angles around Mo(1) varying from 107.8° to 111.3° with an average value of 109.4°. The copper unit shows a distorted trigonal bipyramidal geometry in which each bpy molecule occupies one axial and one equatorial position. The axial distances Cu(1) - N(22) = 1.990 Å and Cu(1) - N(11) = 1.978 Å are shorter than those on the equatorial plane Cu(1) - N(21) = 2.161 Å Cu(1) - N(12) = 2.047 Å consistent with a local molecular d_z^2 ground state[23].

The co-ordination mode of the Schiff-base is also quite interesting. In the starting material MoO_2(5-Cl-Hsaladhp)(MeOH), it acts as tridentate ligand, possessing three sites

in the equatorial plane of the molybdenum octahedron. In the compound **(1)** the schiff base is transferred from the molybdenum to copper ion and acts as tetradentate ligand with two oxygens and one nitrogen bound to Cu^{2+} ion, occupying the three sites in the basal plane of the square pyramid and one oxygen bound to Mo(VI) ion, while in compound **(2)** the schiff base returns to Mo atom acting again as tridentate ligand and possessing the three sites in the equatorial plane of the molybdenum octahedron.

4.2.3. Spectroscopic Properties. The MoO_2(schiff-base)(CH_3OH) complexes exhibit two ν(O=Mo=O) vibrations at about 930 cm^{-1}(ν_{asym}) and 880-890 cm^{-1}(ν_{sym}) confirming the presence of a *cis*-MoO_2 structure; in the case of a *trans*-MoO_2 group, only one band is expected. Dioxomolybdenum(VI) prefers the *cis*-MoO_2 structure for maximum utilisation of the $Mo_{d\pi}$ - $O_{p\pi}$ orbitals for chemical bonding. The corresponding $Cu_2Mo_2O_4$(schiff-base)$_2$($MeO)_2$ complexes show three ν(O=Mo=O) vibrations in the region 940-950, 910-920 and 885-890 cm^{-1}. The IR spectrum of the compound **(2)** displays a complex pattern of bands in the 770-920 cm^{-1} range attributable to Mo-O modes. The bands at 920 and 890 cm^{-1} may be assigned to the *cis*-MoO_2 moieties of the molybdenum atoms bound to schiff-base ligand*(supra infra)* while the bands at 770, 805 and 825 cm^{-1} and that at 860 cm^{-1} may be attributed to the bridged and terminal Mo=O group of the MoO_4 moiety[24], respectively. This assignment show a linear relation with the bond-lengths observed for the **(2)** complex.

In the region 3000-3400 cm^{-1} the monomer complexes show two broad bands due to the ν(O-H) of the coordinated methanol and the uncoordinated CH_2OH group of the ligand. The ν(C=N) and ν(C=O) bands of the schiff-bases appear at about 1630 and 1530 cm^{-1} respectively, characteristic of the five member ring Mo-O-C-C-C-N. At the corresponding $Cu_2Mo_2O_4$(schiff-base)$_2$($MeO)_2$ complexes ,the Δν of ν(C=N) - ν(C=O) is smaller by 20-30 cm^{-1} reflecting the substitution of Mo by Cu. For the **(2)** compounds the ν(C=N) and ν(C=O) bands are observed at frequencies expected for the MoO_2(schiff-base) species.

The room-temperature powder X-band EPR spectrum of $Cu_2Mo_2O_4$[5-Cl-Ph(O)CH=NC(CH_3)($CH_2O)_2$]$_2$($CH_3O)_2$ presents two features at ca. 800 and 7500 G, (figure 4)

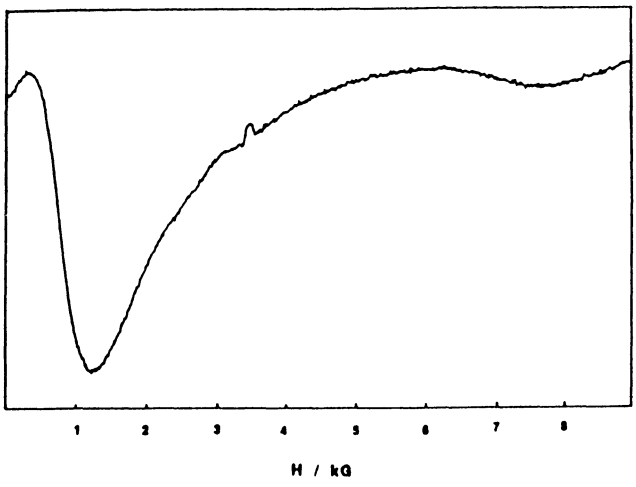

Figure 4. Room-temperature EPR powder spectrum of **(1)**

which is in accordance with a dimmer with an S=1 ground state,in good agreement with the magnetic susceptibility results. Moreover, the existence of only two lines is indicative of D>hv and of a strongly unaxial D tensor. As a matter of fact, D and E values of 0.45±0.05 cm^{-1} and 0.15±0.05 cm^{-1} respectively, could be estimated[31] by assuming a g value of 2.08. The observed lined are due to the 1↔0 transitions in the perpendicular orientations: from the y axis(800 G) and from the x axis(7500 G). The room-temperature powder and the low temperature(T=95 °C) DMSO-glass X-band EPR spectrum of **(2)** is typical of a Cu(II) ion with no interaction with the $[MoO_4]^{2-}$ moiety. The EPR powder spectrum shows only a broad band with g=2.12, while in the EPR DMSO-glass spectrum at 95 K, four copper hyperfine components (I=3/2) appear in the low field $g_{||}$ signal, with $g_{||}$= 2.26, $g_{\perp}$ = 2.06 and $A_{||}$ = 165.4.104 cm^{-1}. This clearly shows that the unpaired electron is located on Cu(II) ion and the oxidation states for copper and molybdenum are 2+ and 6+ respectively. No super hyperfine structure of the EPR signal due to copper-nitrogen interaction has been detected.

4.2.4. Magnetic Properties. All the monomer Mo complexes are diamagnetic. The magnetic behaviour of **(1)** and **(2)** in the form of a $\chi_M T$ vs T plot, χ_M being the magnetic susceptibility per copper(II) ion and T the temperature, is shown in figure 5.

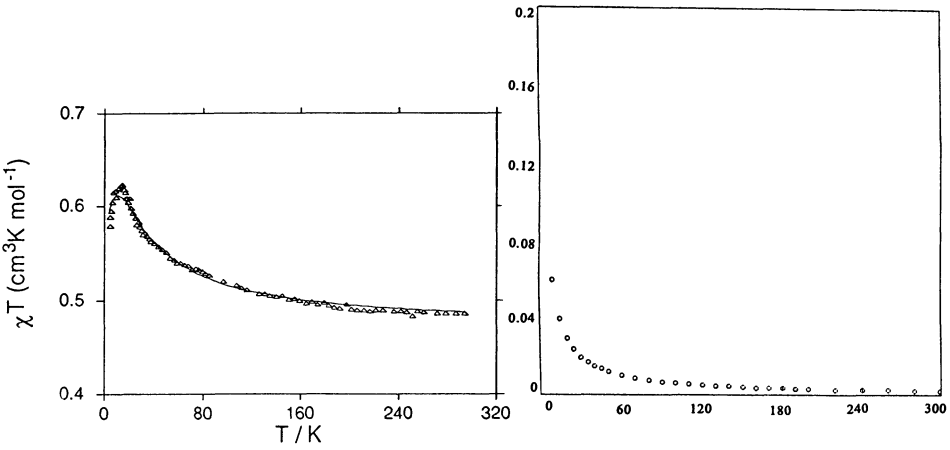

Figure 5. Magnetic data of (1) and (2) in a temperature range 4-300 K

For **(2)** at room temperature $\chi_M T$ is equal to 0.375 cm^3 $K{\cdot}mol^{-1}$ and the μ_{eff}=2.184 MB while at 5.00 K, it is equal to 0.464 $cm^3{\cdot}K{\cdot}mol^{-1}$ and the μ_{eff}=2.179 MB. Each cluster is composed of one Cu(II) and three Mo(VI) ions. However, the three Mo(VI) ions are diamagnetic: hence, the only paramagnetic center in the cluster is the Cu(II) ion. All the values of magnetic susceptibility follow the so-called Curie-Weiss law showing an idealised for S=1/2 system behaviour.

For **(1)** the interpretation of the magnetic behaviour in the 4.2-290 K temperature range is straightforward. Each cubane-like core of the complex is composed of two pairs of Cu(II) and Mo(VI) ions. However, the two Mo(VI) ions are diamagnetic; hence, only the exchange parameter for the two Cu(II) interacting between the two single ion spin doublets

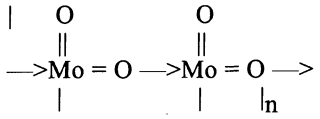

linkages. Recently *Holm at al* [28] have reported the structures of two dimmers Mo_2O_3(3-t-Bussp)$_2$(DMF)$_2$ and Mo_2O_3(3-t-Bussp)$_2$(DMF)$_2$ which are the products of the reaction of the Mo(VI)O_2(schiff-base)(DMF) with $PMePh_2$ as well as the structure of the mononuclear MoO(3-t-Bussp)(bpy). All these complexes reported are diamagnetic, while the compounds presented here, show a μ_{eff} of about 1.6 - 1.7 MB which is consistent with the presence of one unpaired electron per molybdenum ion. Powder EPR spectra are characterised by a single broad signal with g=1.900, agreeing for 5+ oxidation state of the central atom[29]. The paramagnetism of these compounds may be explained if we accept a monomeric form, with a Mo(V) having a square pyramidal environment. Further support for this assessment is that all these complexes exhibit only one ν(Mo=O) band at 940 - 950cm^{-1} consistent with a five coordinate geometry[7]. The absence of any band characteristic for Mo=O→Mo bridge and the presence of a new strong band at 1100 cm^{-1} due to the aliphatic C-O group bound to a Mo atom leads to the conclusion for a polymeric structure(scheme 2). The most characteristic evidence for the deprotonation of the -CH_2OH group is the absence of any ν(O-H) in the region 3100-3400 cm^{-1}.

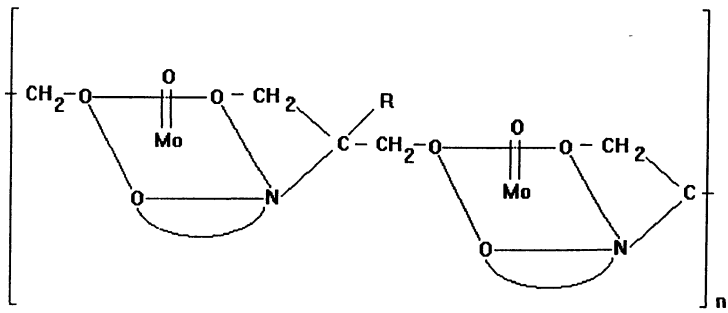

Scheme 2. Proposed Structure for the [Mo(V)O(Schiff-base)]$_n$ compounds.

The reactivity of $Cu_2Mo_2O_4$[5-Cl-Ph(O)CH=NC(CH_3)(CH_2O)$_2$]$_2$(CH_3O)$_2$ **(1)** cluster with Pbu_3 or dppm has been studied by UV-Vis in DMF. The deep green solution slowly turns to yellow. As seen in figure 5 a new intense band appears at 315 nm and two isosbestic points at 350 and 420 nm were found. The reaction was considerably slow and temperature dependent. At 25 °C the reaction proceeded to completion in 24 h while at 60 °C required 8 h. The reaction products have λ_{max} = 315 nm. The band at 650 and 370 nm of the starting solution may be assigned to d-d, and LMCT transition of the copper unit as has been showed for the mononuclear and binuclear[29,30] analogous Copper-schiff-base complexes. The absence of any absorption at 345 nm or higher but on the other hand the appearance of an isosbestic point at this λ, reflects the neutrality of Mo(VI) site towards the schiff-bases(all the analogous Mo(VI)O_2(schiff-base)(DMF) compounds show a band at 345 nm) and towards the PBu_3 or dppm (the Mo(V)(schiff-base) show a band at 405

leads to two molecular levels characterised by S=0 and S=1, respectively, and separated by J. J is positive if the spin triplet is the lowest level. At room temperature, the $\chi_M T$ value is already higher than that expected (ca. 0.40 cm^3 $Kmol^{-1}$) for a non coupled copper(II) ion. The increase in $\chi_M T$ upon cooling shows that the S=1 level is actually the lowest in energy. The decrease in $\chi_M T$ below ca.14 K is most likely due to the superimposition of a very weak interdimmer antiferromagetic coupling between the S=1 molecular spins on the intramolecular ferromagnetic coupling.

Considering the structure, two exchange path ways are possible: one through the O(8) and O(18) atoms bridging the two neighbouring Cu(1) and Cu (2) atoms of the same cubane-like unit and the other one through the O(3) bridging two subsequent cubane-like cores. Although the crystal structure suggests a one-dimensional chain structure, the magnetic data indicate that the compound rather behaves magnetically as a chain of weakly interacting binuclear units. Therefore, a least-squares fit of the experimental data from room temperature down to 4.2 K was attempted first in terms of a binuclear formulation via a simple Bleaney-Bowers equation[32] The energy gap J between the triplet and the single state was deducted from the magnetic data through the theoretical equation

$$\chi_M = \frac{N\beta^2 g^2}{kT}[3+\exp(-J/kT)]^{-1}$$

where N,β,k, and g have their usual meanings. J and g values were determined by minimising the reliability factor $R=\Sigma_i[(\chi_{obsd})_i - (\chi_{theor})_i]^2 / \Sigma_i(\chi_{obsd})_i^2]$, giving J=+38 cm^{-1} and g=2.215. R was then equal to 1.74×10^{-4}, showing that a good fit was obtained when only interaction within the Cu(II) dimmers inside each cubane-like core was considered. The absence of a line at ca. 3000 G in the EPR spectrum of **(1)** (vide infra) is in line with the absence of Cu(II) monomeric impurities , confirming further our choice concerning the dimmer law used in the fitting procedure. In a second approach, the possible interaction between the Cu(II) dimmers inside each cubane-like core was considered by using the molecular field approximation model[33]. In the frame of this approximation, values of +30.5 cm^{-1}, 2.241 cm^{-1}, and -0.2342 cm^{-1} were obtained for J,g, and zJ′, respectively, with a better R value ($R=8.44\times10^{-5}$) than that in the previous calculation. In the three-parameter fitting with J, g, and zJ′ variables, the quality of the fit was improved, confirming both the ferromagnetic nature of the intrabinuclear interaction and the antiferromagnetic one of the interdimer interaction. Consequently, it seems quite appropriate to employ in our case the molecular field approximation, with a J′ value of -0.167 cm^{-1} (for z=2) proposed for **(1)**.

4.2.5. Reactivity with dppm. The reaction of the monomer complexes with dppm in methanol or acetonitrile leads to the synthesis of five-coordinate complexes of the type MoO(Schiff-base) in which the fifth position of a distorted square pyramidal geometry is occupied by the deprotonated uncoordinated $-CH_2O^-$ moiety of a neighbouring molecule. Oxygen transfer reactions have been reported by *Topich and Lyon* [25] .According to their results this type of reactions leads to the formation of an oxo-molybdenum(IV) complex with a $4d_{xy}^2$ electron configuration. *Boyd and Spence* have synthesised also Mo(IV)O(Schiff-base) from the corresponding Mo(VI) complexes using $PEtPh_2$ as the reducing agent but only μ-oxo Mo(V) dimmers Mo_2O_3(schiff-base)$_2$ were obtained from some MoO_2(schiff-base) complexes[26]. *Chakravorty at al* [27] have assigned the presence of only a single stretch at 930 cm^{-1} and a broad band at 800 cm^{-1} for MoO_2(schiff-base) complexes to the formation of a polymer. The polymerisation most likely takes place via

nm and a shoulder at 510 nm). Considering all these data we may accept that only reduction of the Cu(II) to Cu(I) take place during this reaction(figure 6).

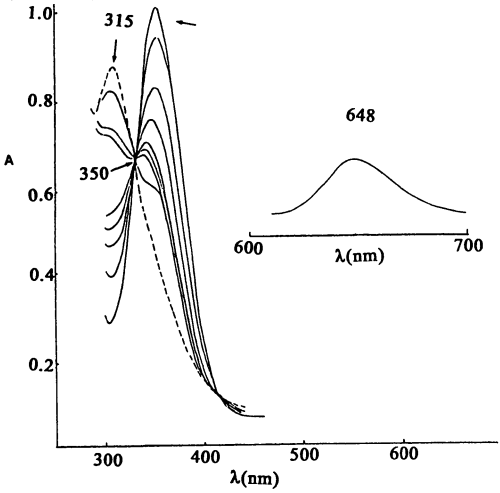

Figure 6. UV-Vis spectra of (1) in the presence of dppm.

5. Acknowledgement.

The author's special thanks go to the collaborators whose work has been summarised in this article, G.Bakalbassis, A.N.Papadopoulos, C.P.Raptopoulou, A.G.Hatzidimitriou (University of Thessaloniki), A.Gourdon (CNRS Toulouse, France), A.Terzis (C.N.R. "Demokritos"), J.Mrozinski(University of Wroclaw). The author also appreciates the financial support that he has received from the Greek Ministry of Industry, Energy and Technology, General Secretariat of Research and Technology.

6. References

(1) *Comprehensive Inorganic Chemistry* Pergamon, Oxford, 1973, vol. 6

(2) Frausto da Silva and R.J.P. Williams , *The Biological Chemistry of the Elements* Clarendon Press, Oxford **1991,** p. 417 & 540.

(3) C.F. Mills, *Chem.Br.*,1979,**15**,512; C.F. Mills, *Philos.Trans.R.Soc.London, Ser B,* 1979,**B288**,1; J.C. Bailar, H.J. Emeleus, R.Nyholm, and R.N. Trotman-Dickenson, in *Comprehensive Inorganic Chemistry* Pergamon, Oxford, 1973, vol. 3, chap. 36;

(4) A.Muller, H.Bogge and U. Schimanski, *J.Chem.Soc.,Chem.Commun.,* **1980**,91; T. Shihabara, H. Akashi and H. Kuroya, *J.Am.Chem.Soc.,* **1988**,*110*,3313; M. Minelli, J.H. Enemark, J.R. Nicholson,and C.D.Garner, *Inorg. Chem.* **1984**,*23*,4386; Y. Jeannin, F. Secheresse, S. Bernes and F. Robert, *Inorg. Chim. Acta,* **1992**,*198-200*,493S. Bernes, F. Secheresse, and Y. Jeannin, *Inorg. Chim. Acta,* **1992**, *191*,11

(5) *a)* Müller, A.; Dartmann, M. ; Romer, C. ; Clegg, W. & Sheldrick, G.M. *Angew. Chem. Int. Ed. Engl.,* **1981**, *20,* 1060; b)Gheller, S.F.; Gazzana, P.A.; Masters,

A.F.; Brownlee, R.T.C.; O'Connor, M.J.; Wedd, A.G.; Rodgers, J.R. & Snow, M.R. *Inorg. Chim. Acta,* **1981,** *54,* 131

(6) Acott, S.R. ; Garner, C.D. ; Nicholson, J.R. & Clegg, W., *J.Chem.Soc., Dalton Trans.,* **1983**, 713;

(7) Payne, N.C.; Okura, N.; Otsuka, S., *J.Am.Chem.Soc.,* **1983,***105,* 245

(8) a)Secheresse, F.; Salis, M; Potvin, C. & Manoli, J.M., *Inorg. Chim. Acta,***1986,** *114,* 19; b) Potvin, C. : Manoli, J.M.: Secheresse, F. & Marzak, S.. *Inorg. Chim. Acta,* 1987, **134,** 9; c) Müller, A.; Bögge, H. & Schimanski, U., *Inorg.Chim.Acta,* **1980,***45,* L249

(9) Müller, A.; Schimanski, U. & Schimanski, J., *Inorg.Chim.Acta,* 1983,***76,*** L245

(10) Bristow, S.; Garner, C.D. & Clegg, W., *Inorg.Chim.Acta,* **1983,** *76,* L261

(11) Clegg, W.; Garner C.D. & Nicholson, J.R., *Acta Crystallogr., Sect. C,* **1983,** *39,*552.

(12) Huang, Z.; Lei, X.; Liu, H.; Kang, B.; Liu, Q; Hong M.; Liu, H, *J.Inorg. Chim. Acta* **1990,***169,*25; Liu, H., Cao, R., Lei, X.; Wu, D.; Wei, G.; Huang, Z.; Hong M. & Kang, B., *J. Chem. Soc., Dalton Trans.,* **1990**, 1023

(13) Clegg, W.; Beheshti, A. & Garner C.D., *Acta Crystallogr., Sect. C,* **1988,** *44,* 170.

(14) Müller, A.; Bögge, H. & Schimanski, U., *Inorg.Chim.Acta,* **1983,***69,*5; Müller, A.; Bögge, H.; Tölle; Jostes, R.; Schimanski, U.; Dartmann, M. *Angew. Chem. Int. Ed. Engl.,* **1980,***19,* 654.

(15) Xintao, W.; Shaofeng, L.; Lianyong, Z.; Ojangjin, W. & Jiaxi, L., *Inorg. Chim. Acta,* **1987,***133,*39.

(16) Nicholson, J.R.; Flood, A.C.; Garner, C.D. & Clegg, W., *J.Chem. Soc., Chem. Commun,* **1983**, 1179

(17) Secheresse, F. ; Robert, F. ; Marzak, S.; Manoli, J.M. & Potvin, C., *Inorg. Chim. Acta,* 1991, **182,** 221;

(18) Bray, R.C., *Enzymes,* **1975,***12,*299; Bray, R.C., in *Molybdenum Chemistry of Biological Significance,* Eds. W.E. Newton, S. Otsuka, Plenum Press, New York, **1980**, p. 117; E.I. Stiefel, *Prog. Inorg. Chem.,* **1977,***22,*1.

(19) Coucouvanis, D. *Acc. Chem. Rev.*, 1981,**14**,201.

(20) Bray,R.C.; Vincent,S.P.; Lowe,D.J.; Clegg,R.A. & Garland,P.B., *Biochem.J.* 1976,**155**,201.

(21) Syamal, A. & Maurya, M.R., *Coord. Chem. Rev.* **1989,***95,* 183

(22) Kessissoglou, D.P.; Raptopoulou, C.P. ; Bakalbasis, E.G. ; Terzis, A. & Mrozinski, J., *Inorg. Chem.,* **1992,***31,*4339

(23) Hathaway, B.J. *Struct. & Bonding* ,**1984**,*57,*55

(24) Hsich, T.C.; Shaikh, S.N. & Zubieta, J. ,*Inorg.Chem.*, **1987**,*26,*4079

(25) Topich, J. & Lyon, J.T. III, *Inorg. Chem.* **1984,***23,*3202

(26) Boyd, I.W. & Spence, J.T., *Inorg. Chem.* **1982,***21,*1602.

(27) Rajan O.A. & Chakravorty, A., *Inorg. Chem.* **1981**,*20,*660; Rajan O.A. & Chakravorty, A. , *Inorg. Chim. Acta* **1979**,*37,*L503; Ghosh, P. & Chakravorty, A. *Inorg. Chem.* **1983**,*22,*1322

(28) Craig, J.A.; Harlan, E.W.; Snyder, B.S.; Whitener, M.A.; Holm, R.H., *Inorg. Chem.* **1989**,*28,*2082

(29) Purohit, S.; Koley, A.P.; Prasad, L.S. & Manoharan, P.T., *Inorg. Chem.* **1989,** *28,* 3735

(30) Topich J. III & Lyon, J.T., *Polyhedron,* **1984,***3,*55

(31) Gade, S.; Strand, D.; Knispel, R., *J.Magn,Reson.* **1985,** *64,* 395

(32) Bleaney, B, & Bowers, K.D., *Proc. R. Soc. London,* **A1952,** *250,* 451

(33) Ginberg, A.P.; Lines, M.E., *Inorg. Chem.,* **1972,** *11,*2289

SUBJECT INDEX

—A—

—B—

—C—

—D—

—E—

—F—

—G—

—H—

—I—

—K—

—L—

—M—

—N—

—O—

—P—

—R—

—S—

—T—

—U—

—V—

—W—

—X—

—Y—

—Z—